Springer Protocols

Guangpu Li   *Editor*

Rab GTPases

Methods and Protocols

Humana Press

Methods in Molecular Biology

Rab GTPases

Methods and Protocols

Edited by

Guangpu Li

Department of Biochemistry and Molecular Biology, University of Oklahoma Health Sciences Center, Oklahoma City, OK, USA; Peggy and Charles Stephenson Cancer Center, University of Oklahoma Health Sciences Center, Oklahoma City, OK, USA

✸ Humana Press

Editor
Guangpu Li
Department of Biochemistry and Molecular Biology
University of Oklahoma Health Sciences Center
Oklahoma City, OK, USA

Peggy and Charles Stephenson Cancer Center
University of Oklahoma Health Sciences Center
Oklahoma City, OK, USA

Printed on acid-free paper

Preface

Rab GTPases are master regulators of intracellular membrane trafficking in all eukaryotes from the last eukaryotic common ancestor (LECA) to human. In the human genome, there are 66 Rab genes some of which are ubiquitously expressed in all tissues, while others are expressed only in specific tissues. Individual Rabs target to distinct organelles and vesicles to promote vesicular transport through the exocytic and endocytic pathways, which are fundamental to cell physiology and have great impact on other cellular processes, such as hormone secretion, signal transduction, cell migration, and cell growth/differentiation. Indeed, mutations and/or altered expression of Rabs has been implicated in various human diseases ranging from neurodegenerative diseases, diabetes to cancer.

This book covers the latest technological advances in the characterization of the biosynthesis and functions of Rab GTPases and their regulation by guanine nucleotide exchange factors (GEFs) and GTPase-activating proteins (GAPs). The methods are described in detail so that beginners and experts alike can explore the general biochemical principles of Rab GTPase cycle and membrane targeting in vesicular transport and the specific functions of individual Rabs in different cell types. As such, this book should provide a valuable resource for researchers and students interested in the field.

The book consists of 28 chapters, starting with an overview of the Rab GTPase family, which represents the largest branch of the Ras superfamily of small GTPases that are essentially everywhere in the cell and function as molecular switches in regulation of diverse cellular functions by alternating between active GTP-bound and inactive GDP-bound conformations. The next group of chapters describes systematic approaches to the identification and classification of Rabs and Rab GAPs as well as the detection of Rab isoprenylation and membrane distribution. The following chapters examine the biochemical and functional properties of individual Rabs in the order of exocytic, recycling, and endocytic Rabs. The techniques range from in vitro approaches using reconstituted systems to in vivo studies in yeast, *Drosophila*, and mammalian cells. These techniques may also be useful for the study of Rabs in other organisms, especially the large number of uncharacterized Rabs identified through genome sequencing projects.

Oklahoma City, OK, USA   *Guangpu Li*

Contents

Contributors

DANIEL ABANKWA • *Turku Centre for Biotechnology, Åbo Akademi University, Turku, Finland*

JACOB O. AGOLA • *Department of Pathology, University of New Mexico HSC, Albuquerque, NM, USA; Cancer Center, University of New Mexico School of Medicine, Albuquerque, NM, USA; Department of Chemical and Biological Engineering, Center for Micro-Engineered Materials, School of Engineering, University of New Mexico, Albuquerque, NM, USA*

PATRICK D. ALLAIRE • *Department of Biology, University of Utah, Salt Lake City, UT, USA*

JONTHAN M. BACKER • *Department of Molecular Pharmacology, Albert Einstein College of Medicine, Bronx, NY, USA; Department of Biochemistry, Albert Einstein College of Medicine, Bronx, NY, USA*

ANNE R. BRESNICK • *Department of Biochemistry, Albert Einstein College of Medicine, Bronx, NY, USA*

TIONE BURANDA • *Department of Pathology, University of New Mexico HSC, Albuquerque, NM, USA; Cancer Center, University of New Mexico School of Medicine, Albuquerque, NM, USA*

MATIAS A. BUSTOS • *Instituto de Histología y Embriología (IHEM, CONICET/UNCuyo), Facultad de Ciencias Médicas, CC56, Universidad Nacional de Cuyo, Mendoza, Argentina*

BRIAN P. CERESA • *Department of Pharmacology and Toxicology, University of Louisville, Louisville, KY, USA*

SERENA CERVANTES • *Department of Cellular and Molecular Medicine, Howard Hughes Medical Institute, University of California at San Diego, La Jolla, CA, USA*

YU CHEN • *Cell Biology and Metabolism Program, NICHD, NIH, Bethesda, MD, USA*

PRAVEEN D. CHOWDARY • *Department of Chemistry, Stanford University, Stanford, CA, USA*

DANIEL F. CIMINO • *Department of Cell Biology and Physiology, University of New Mexico, Albuquerque, NM, USA; Cancer Center, University of New Mexico School of Medicine, Albuquerque, NM, USA*

DENISE COLLADO • *Department of Molecular Pharmacology, Albert Einstein College of Medicine, Bronx, NY, USA*

BIANXIAO CUI • *Department of Chemistry, Stanford University, Stanford, CA, USA*

SARALIN DAVIS • *Department of Cellular and Molecular Medicine, Howard Hughes Medical Institute, University of California at San Diego, La Jolla, CA, USA*

HASHEM A. DBOUK • *Department of Molecular Pharmacology, Albert Einstein College of Medicine, Bronx, NY, USA*

JENNIFER B. DENNISON • *Department of Systems Biology, UT MD Anderson Cancer Center, Houston, TX, USA*

YOAN DIEKMANN • *Research Department of Genetics, Evolution and Environment, University College London, London, UK*

GREGORY EMERY • *Department of Pathology and Cell Biology, Faculty of Medicine, University of Montréal, Montréal, QC, Canada; Institute for Research in Immunology and Cancer, University of Montréal, Montréal, QC, Canada*

Kan Etoh • *Laboratory of Membrane Trafficking Mechanisms, Department of Developmental Biology and Neurosciences, Graduate School of Life Sciences, Tohoku University, Sendai, Miyagi, Japan*

Shanshan Feng • *Department of Biology, University of Pennsylvania, Philadelphia, PA, USA*

Susan Ferro-Novick • *Department of Cellular and Molecular Medicine, Howard Hughes Medical Institute, University of California at San Diego, La Jolla, CA, USA*

Mitsunori Fukuda • *Laboratory of Membrane Trafficking Mechanisms, Department of Developmental Biology and Neurosciences, Graduate School of Life Sciences, Tohoku University, Sendai, Miyagi, Japan*

Bruno Goud • *Molecular Mechanisms of Intracellular Transport, Centre National de la Recherche Scientifique, Institut Curie, Paris, France*

Wei Guo • *Department of Biology, University of Pennsylvania, Philadelphia, PA, USA*

Camilo Guzmán • *Turku Centre for Biotechnology, Åbo Akademi University, Turku, Finland*

Viorica Ivan • *Department of Molecular Cell Biology, Institute of Biochemistry of the Romanian Academy, Bucharest, Romania*

Jane J. Kim • *Department of Biochemistry and Molecular Genetics, University of Illinois at Chicago, Chicago, IL, USA; Department of Biological Sciences, University of Illinois at Chicago, Chicago, IL, USA*

Hotaka Kobayashi • *Laboratory of Membrane Trafficking Mechanisms, Department of Developmental Biology and Neurosciences, Graduate School of Life Sciences, Tohoku University, Sendai, Miyagi, Japan*

Carl Laflamme • *Department of Pathology and Cell Biology, Faculty of Medicine, University of Montréal, Montréal, QC, Canada; Institute for Research in Immunology and Cancer, University of Montréal, Montréal, QC, Canada*

David G. Lambright • *Program in Molecular Medicine, University of Massachusetts Medical School, Worcester, MA, USA*

Guangpu Li • *Department of Biochemistry and Molecular Biology, University of Oklahoma Health Sciences Center, Oklahoma City, OK, USA; Peggy and Charles Stephenson Cancer Center, University of Oklahoma Health Sciences Center, Oklahoma City, OK, USA*

Zhimin Liang • *Department of Biochemistry and Molecular Biology, University of Oklahoma Health Sciences Center, Oklahoma City, OK, USA*

Andrew J. Lindsay • *Molecular Cell Biology Laboratory, School of Biochemistry and Cell Biology, Biosciences Institute, University College Cork, Cork, Ireland*

Zhanna Lipatova • *Department of Biochemistry and Molecular Genetics, College of Medicine, University of Illinois at Chicago, Chicago, IL, USA*

Jennifer Lippincott-Schwartz • *Cell Biology and Metabolism Program, NICHD, NIH, Bethesda, MD, USA*

Jaclyn Lopiccolo • *Department of Molecular Pharmacology, Albert Einstein College of Medicine, Bronx, NY, USA*

Guodong Lu • *Key Laboratory of Biopesticide and Chemical Biology, Ministry of Education, Fujian Agriculture and Forestry University, Fuzhou, China*

Ornella Lucchesi • *Instituto de Histología y Embriología (IHEM, CONICET/UNCuyo), Facultad de Ciencias Médicas, CC56, Universidad Nacional de Cuyo, Mendoza, Argentina*

Anthony Mangan • *Department of Cell and Developmental Biology, School of Medicine, University of Colorado Denver, Aurora, CO, USA*

M. Caleb Marlin • *Department of Biochemistry and Molecular Biology, University of Oklahoma Health Sciences Center, Oklahoma City, OK, USA*

Soujiro Marubashi • *Laboratory of Membrane Trafficking Mechanisms, Department of Developmental Biology and Neurosciences, Graduate School of Life Sciences, Tohoku University, Sendai, Miyagi, Japan*

Luis S. Mayorga • *Instituto de Histología y Embriología (IHEM, CONICET/UNCuyo), Facultad de Ciencias Médicas, CC56, Universidad Nacional de Cuyo, Mendoza, Argentina*

Mary W. McCaffrey • *Molecular Cell Biology Laboratory, School of Biochemistry and Cell Biology, Biosciences Institute, University College Cork, Cork, Ireland*

Peter S. McPherson • *Department of Neurology and Neurosurgery, Montréal Neurological Institute, McGill University, Montréal, QC, Canada*

Gordon B. Mills • *Department of Systems Biology, UT MD Anderson Cancer Center, Houston, TX, USA*

Stéphanie Miserey-Lenkei • *Molecular Mechanisms of Intracellular Transport, Centre National de la Recherche Scientifique, Institut Curie, Paris, France*

Ashwini K. Mishra • *Program in Molecular Medicine, University of Massachusetts Medical School, Worcester, MA, USA*

Shreya Mitra • *Department of Systems Biology, UT MD Anderson Cancer Center, Houston, TX, USA*

Jennifer Molina • *Department of Systems Biology, UT MD Anderson Cancer Center, Houston, TX, USA*

Yasunori Mori • *Laboratory of Membrane Trafficking Mechanisms, Department of Developmental Biology and Neurosciences, Graduate School of Life Sciences, Tohoku University, Sendai, Miyagi, Japan*

Paulina S. Mrozowska • *Laboratory of Membrane Trafficking Mechanisms, Department of Developmental Biology and Neurosciences, Graduate School of Life Sciences, Tohoku University, Sendai, Miyagi, Japan*

Arafath Kaja Najumudeen • *Turku Centre for Biotechnology, Åbo Akademi University, Turku, Finland*

Ryan M. Nottingham • *Department of Biochemistry, Stanford University School of Medicine, Stanford, CA, USA*

Peter J. Novick • *Department of Cellular and Molecular Medicine, University of California San Diego, La Jolla, CA, USA*

Norihiko Ohbayashi • *Laboratory of Membrane Trafficking Mechanisms, Department of Developmental Biology and Neurosciences, Graduate School of Life Sciences, Tohoku University, Sendai, Miyagi, Japan*

Johan Peränen • *Institute of Biotechnology, University of Helsinki, Viikinkaari, Finland*

José B. Pereira-Leal • *Instituto Gulbenkian de Ciência, Oeiras, Portugal*

Suzanne R. Pfeffer • *Department of Biochemistry, Stanford University School of Medicine, Stanford, CA, USA*

Itziar M.D. Posada • *Turku Centre for Biotechnology, Åbo Akademi University, Turku, Finland*

Rytis Prekeris • *Department of Cell and Developmental Biology, School of Medicine, University of Colorado Denver, Aurora, CO, USA*

Yaoyao Qi • *Department of Biochemistry and Molecular Biology, University of Oklahoma Health Sciences Center, Oklahoma City, OK, USA; Key Laboratory of Biopesticide and Chemical Biology, Ministry of Education, Fujian Agriculture and Forestry University, Fuzhou, China*

BRIGITTE RITTER • *Department of Biochemistry, Boston University School of Medicine, Boston, MA, USA*

MARIA C. RUETE • *Instituto de Histología y Embriología (IHEM, CONICET/UNCuyo), Facultad de Ciencias Médicas, CC56, Universidad Nacional de Cuyo, Mendoza, Argentina*

RACHEL S. SALAMON • *Department of Molecular Pharmacology, Albert Einstein College of Medicine, Bronx, NY, USA*

NAVA SEGEV • *Department of Biochemistry and Molecular Genetics, College of Medicine, University of Illinois at Chicago, Chicago, IL, USA*

PETER C. SIMONS • *Department of Pathology, Center for Molecular Discovery, University of New Mexico, Albuquerque, NM, USA; Cancer Center, University of New Mexico School of Medicine, Albuquerque, NM, USA*

DANIEL SIVALINGAM • *Department of Biology, California State University, Northridge, CA, USA; Department of Neurobiology, David Geffen School of Medicine, University of California, Los Angele, CA, USA*

LARRY A. SKLAR • *Department of Pathology, Center for Molecular Discovery, University of New Mexico, Albuquerque, NM, USA; Cancer Center, University of New Mexico School of Medicine, Albuquerque, NM, USA*

PETER VAN DER SLUIJS • *Department of Cell Biology, University Medical Center Utrecht, Utrecht, The Netherlands*

ELIZABETH SMYTHE • *Department of Biomedical Science, Centre for Membrane Interactions and Dynamics, University of Sheffield, Sheffield, UK*

DANIÈLE STALDER • *Department of Cellular and Molecular Medicine, University of California San Diego, La Jolla, CA, USA*

CLAUDIA N. TOMES • *Instituto de Histología y Embriología (IHEM, CONICET/UNCuyo), Facultad de Ciencias Médicas, CC56, Universidad Nacional de Cuyo, Mendoza, Argentina*

ANGELA WANDINGER-NESS • *Department of Pathology, University of New Mexico, Albuquerque, NM, USA; Cancer Center, University of New Mexico School of Medicine, Albuquerque, NM, USA*

JUAN WANG • *Department of Cellular and Molecular Medicine, Howard Hughes Medical Institute, University of California at San Diego, La Jolla, CA, USA*

ZONGHUA WANG • *Key Laboratory of Biopesticide and Chemical Biology, Ministry of Education, Fujian Agriculture and Forestry University, Fuzhou, China*

BIN WU • *Department of Biology, University of Pennsylvania, Philadelphia, PA, USA*

TAKAO YASUDA • *Laboratory of Membrane Trafficking Mechanisms, Department of Developmental Biology and Neurosciences, Graduate School of Life Sciences, Tohoku University, Sendai, Miyagi, Japan*

KAI ZHANG • *Department of Biochemistry, University of Illinois at Urbana-Champaign, Urbana, IL, USA*

Chapter 1

Rab Family of GTPases

Guangpu Li and M. Caleb Marlin

Abstract

Rab proteins represent the largest branch of the Ras-like small GTPase superfamily and there are 66 Rab genes in the human genome. They alternate between GTP- and GDP-bound states, which are facilitated by guanine nucleotide exchange factors (GEFs) and GTPase-activating proteins (GAPs), and function as molecular switches in regulation of intracellular membrane trafficking in all eukaryotic cells. Each Rab targets to an organelle and specify a transport step along exocytic, endocytic, and recycling pathways as well as the crosstalk between these pathways. Through interactions with multiple effectors temporally, a Rab can control membrane budding and formation of transport vesicles, vesicle movement along cytoskeleton, and membrane fusion at the target compartment. The large number of Rab proteins reflects the complexity of the intracellular transport system, which is essential for the localization and function of membrane and secretory proteins such as hormones, growth factors, and their membrane receptors. As such, Rab proteins have emerged as important regulators for signal transduction, cell growth, and differentiation. Altered Rab expression and/or activity have been implicated in diseases ranging from neurological disorders, diabetes to cancer.

Key words Rab, GTPase, GTP-binding protein, Membrane trafficking, Vesicular transport, GAP, GEF, Effector

1 Introduction

Rab GTPases play an important role in specifying transport pathways in the intracellular membrane trafficking system of all eukaryotes from the last eukaryotic common ancestor (LECA) to mammals. In the LECA, there are at least 20 prototype Rabs forming six groups, e.g., Rab1/Ypt1 and Rab8/Sec4 in group I, Rab5/Ypt51 in group II, Rab7/Ypt7 and Rab9/Ypt9 in group III, Rab11/Ypt31 and Rab4/Ypt4 in group IV, Rab6/Ypt6 in group V, and Rab28 in group VI [1, 2] (Fig. 1). Most of these ancient Rabs are conserved throughout evolution while some are lost in certain species. There is significant expansion of the Rab family in mammalian cells to accommodate increasing complexity of the intracellular trafficking system, with 66 Rab genes in the human genome. Historically Rab GTPases are best characterized in the

	Mammalian	Yeast
I	Rab1	Ypt1
	Rab8	Sec4
II	Rab5	Ypt51 / Ypt52 / Ypt53 / Ypt10
	-	RabX1
III	Rab7	Ypt7
	Rab9	Ypt9
	Rab2	Ypt2
IV	Rab4	Ypt4
	Rab11	Ypt31 / Ypt32
V	Rab6	Ypt6
VI	Rab28	-

Fig. 1 The mammalian and yeast Rab/Ypt homologs. Data from Diekmann et al. and Klöpper et al. [1, 2] reveal six major groups of Rab GTPases from the LECA to mammals. Shown are only the mammalian Rabs with yeast Rab/Ypt homologs. RabX1 is not present in mammalian cells, while there are no members of group VI, including Rab28, found in yeast

budding yeast *Saccharomyces cerevisiae* (*S. cerevisiae*) and in mammalian cells [3], and evolutionarily older Rabs tend to be more highly and widely expressed and more intensively studied [4]. This volume focuses on the techniques used for biochemical and functional characterizations of these *S. cerevisiae* and mammalian Rabs.

The intracellular membrane trafficking system governs protein secretion during exocytosis and uptake of extracellular nutrients during endocytosis in eukaryotic cells. It is also a fundamental transport system for targeting newly synthesized enzymes to correct membrane compartments/organelles, e.g., the lysosomal hydrolases. As such, it is essential for cell physiology. Intracellular membrane trafficking is mediated by vesicular carriers from donor to acceptor compartments and Rab GTPases are involved in every facet of the vesicular transport process via temporal and spatial interactions with a series of effectors [5, 3, 6]. These effectors include cargo proteins to be packaged into the vesicles, motor proteins that facilitate the movement of vesicles along actin and microtubule cytoskeletons, and tethering factors that dock vesicles to target compartments for membrane fusion.

Each Rab specifically targets to a distinct membrane compartment [7], e.g., Rab2 to the transport vesicles between the endoplasmic reticulum (ER) and the Golgi, Rab5 to early endosomes, Rab7 to late endosomes, etc. (Fig. 2). This membrane targeting process requires posttranslational isoprenylation (geranylgeranylation) of the two Cys residues at or near the C-terminus of each

AP – Autophagosome	**EE** – Early Endosome	**GSV** – GLUT4 Storage Vesicle
IM – Isolation Membrane	**LE** – Late Endosome **LY** – Lysosome	**ME** – Melanosome
RE – Recycling Endosome	**SV** – Secretory Vesicle	**TE** – Transcytosing Endosome
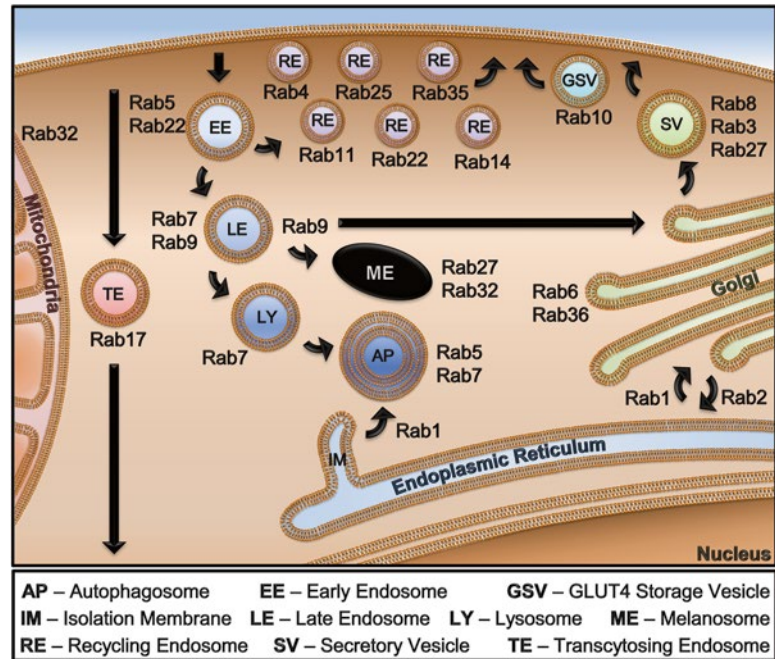
Fig. 2 Rabs throughout the mammalian cell. Rabs are found in virtually every membranous compartment in eukaryotic cells. Above is a schematic representation of intracellular localization of the Rabs from Fig. 1 and discussed in this volume of MiMB

Rab as well as a cognate guanine nucleotide exchange factor (GEF) on the target membrane [8] (Fig. 3). In addition, a GDP displacement factor (GDF) is shown to facilitate Rab membrane targeting to endosomes [9] (Fig. 3). Upon membrane association, the GEF catalyzes nucleotide exchange of GDP with GTP on the Rab [10, 11], and the activated GTP-bound Rab then interacts with effectors and is packaged into transport vesicles to mediate the formation and movement of vesicles and their fusion with the target compartment (Fig. 3). The Rab functional cycle is completed by GTP hydrolysis, which is catalyzed by GTPase-activating proteins (GAPs) [12], and recycling back to the donor compartment, which is mediated by the GDP-dissociation inhibitor (GDI) [13–15] (Fig. 3).

2   Regulation of Rab GTPase Cycle

Like other small GTPases in the Ras superfamily, Rabs show high affinity for guanine nucleotides GTP and GDP (Kd in the nanomolar range) but weak intrinsic GTPase activity in GTP hydrolysis. As a result, both the GDP/GTP exchange reaction and the GTP hydrolysis reaction in a Rab GTPase cycle are accelerated by catalyzing protein factors such as GEFs and GAPs in the cell [12] (Fig. 3).
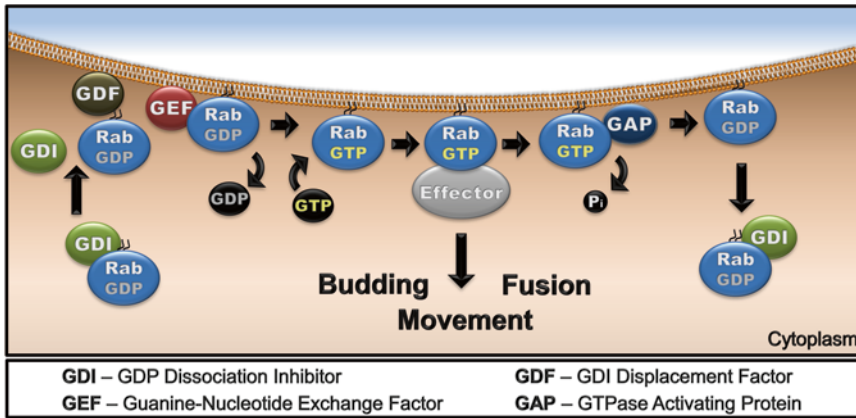
Fig. 3 The Rab GTPase cycle coupled with membrane targeting. Inactive GDP-bound Rabs are found in the cytosol bound to GDI. Upon approaching the target membrane, GDF may interact with the Rab to facilitate GDI dissociation and Rab insertion into the membrane. On the membrane, GEF catalyzes GDP dissociation, allowing for GTP binding and subsequent activation of the Rab, which in turn interacts with multiple effectors to promote vesicle budding, movement, and fusion. Then GTP hydrolysis by the Rab, accelerated by a cognate GAP, converts it to inactive GDP-bound state. The inactive Rab can be removed from the membrane by GDI and recycled back to the donor compartment

Rab GEFs show a general mechanism by displacing the switch I region, disrupting Mg^{2+} coordination, and stabilizing the nucleotide-free form of Rab proteins [12]. As such, the GEFs facilitate GDP dissociation and GTP loading on Rabs in the cell where GTP concentration is two orders of magnitude higher. However, the five families of Rab GEFs identified so far share no sequence and structural homology in the catalytic domain. The Vps9 domain-containing GEFs are specific for the Rab5 subfamily members on early endosomes [16] while the SAND1/Mon1-Ccz1 complex is a specific GEF for Rab7/Ypt7 on late endosomes [17, 18]. These endosomal GEFs promote endocytosis by activation of Rab5 and Rab7. For exocytosis, there are TRAPP complexes [19, 20] and Sec2/Rabin8 proteins [21] that are GEFs for Rab1/Ypt1 and Rab8/Sec4 to promote ER to Golgi transport and post-Golgi transport to the plasma membrane, respectively. In addition, the Ric1/Rgp1 complex is a GEF for Ypt6/Rab6 in the Golgi complex [22]. Finally, the DENN (differentially expressed normal vs. neoplastic) domain-containing GEFs [23] are specific for various Rabs that have no close yeast homologs, such as Rab3, Rab9, Rab10, Rab12, Rab27, Rab28, Rab35, and Rab39.

Rab GAPs, in contrast, contain a TBC (Tre-2/Bud2/Cdc16) domain for catalysis of GTP hydrolysis [12]. The TBC domain contains conserved catalytic motifs IxxDxxR and YxQ from which the Arg and Gln side chains insert into the GTP-binding site on the Rab to stabilize the transition state for GTP hydrolysis in a so-called dual finger mechanism [24].

The GEFs and GAPs are recruited to distinct organelles by proteins and lipids characteristic to each organelle to facilitate the establishment of functional Rab domains on the membrane. In a number of cases, a GEF is recruited to the membrane by an upstream Rab for activation of a downstream Rab, forming a Rab cascade (Fig. 4). For example, Sec2, a GEF for Sec4 in the budding yeast *S. cerevisiae*, is an effector of the upstream Rab Ypt32 and is recruited by Ypt32-GTP to post-Golgi vesicles for activation of Sec4 in exocytosis [25] (Fig. 4). Their mammalian homologs form a similar Rab cascade where Rab11-GTP recruits Rabin8 to secretory vesicles for activation of Rab8 to facilitate cilia biogenesis in mammalian cells [26] (Fig. 4). In addition, the Ric1/Rgp1 complex is recruited by Rab33B to the Golgi membrane to function as a GEF for Rab6 activation [27] (Fig. 4). Along the endocytic pathway, the Sand1/Mon1–Ccz1 complex is a GEF for Rab7 but an effector of the upstream Rab5 [18, 17]. As such, it is recruited by Rab5-GTP to the endosomal membrane for activation of Rab7 (Fig. 4). With the displacement of Rabex5, a Vps9 domain-containing Rab5 GEF, from the membrane, Rab5-GTP undergoes GTP hydrolysis and converts to Rab5-GDP that is removed from the membrane by GDI, leading to the conversion of early endosomes marked by Rab5 to late endosomes marked by Rab7. Interestingly, Rabex-5 itself can be recruited by another upstream Rab, Rab22, to early endosomes to establish a Rab22–Rabex-5–Rab5 cascade within the early endosomal network [28] (Fig. 4). In addition, within a late endosomal/premelanosomal network, there exists a Rab9–BLOC-3–Rab32/Rab38 cascade where Rab9-GTP recruits BLOC-3 to the membrane to function as a GEF for activation of Rab32/Rab38 [29, 30] (Fig. 4).

In contrast to the GEFs recruited by upstream Rabs, a GAP may be recruited by a downstream Rab to the membrane for inactivation of an upstream Rab to establish the boundary between the functional Rab domains. In the budding yeast, it is reported that a Ypt1 GAP, Gyp1, is recruited by a downstream Rab, Ypt32, to the membrane to inactivate and clear Ypt1 from the Ypt32 membrane domain [31]. In mammalian cells, Rab9 is shown to recruit the GAPs (RUTBC1 and RUTBC2) to late endosomes for inactivation of Rab32 and Rab36 on the membrane [32, 33].

The combination of a GEF and a GAP recruited in such a fashion by upstream and downstream Rabs can effectively sharpen the boundary of Rab membrane domains and facilitate the transition from early to late compartments during intracellular transport [34]. It may also generate ultrasensitity and "all-or-none" switch-like behavior in the Rab activity [35, 36]. In addition to the Rabs, other protein and lipid factors in the membrane are also known to regulate the recruitment and activity of Rab GEFs, which is exemplified by the regulation of Sec2/Rabin8 by phosphatidylinositol-4-phosphate (PI4P) [37] and phosphorylation [38].
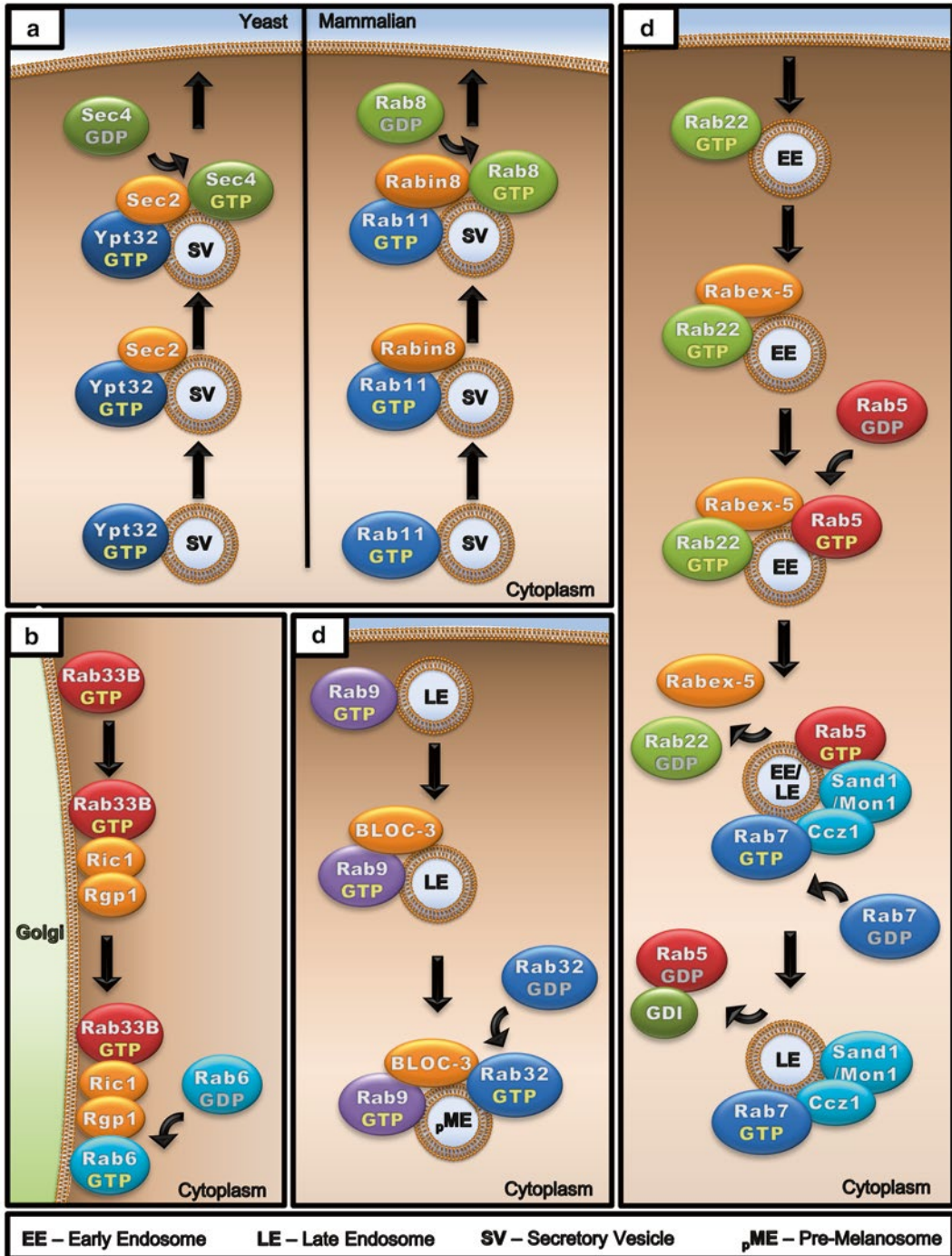
Fig. 4 Rab activation cascades. The GTP loading and activation of a Rab can be regulated as part of an activation cascade from an upstream Rab. (**a**) Rab activation cascades are evolutionarily conserved from yeast to mammals. During polarized exocytosis in *S. cerevisiae*, activated Ypt32 recruits Sec2, a Sec4 GEF, to the membrane of secretory vesicles destined for exocytosis. Sec2 in turn leads to the recruitment and activation of Sec4. The same cascade is seen in mammalian cells with Rab11, Rabin8 (Rab8 GEF), and Rab8. (**b**) On the Golgi membrane, active Rab33B recruits the Ric1–Rgp1 complex (Rab6 GEF), which activates Rab6.

3 Rab Functions in Vesicular Transport

Once activated and GTP bound, Rabs can temporally and spatially interact with multiple effectors to facilitate the selection of cargoes into vesicles, vesicle movement on actin and microtubule cables, and tethering of vesicles to target compartment for membrane fusion.

Rabs can interact with the cytoplasmic domains of transmembrane proteins/receptors to facilitate their packaging into transport vesicles. Rab5 and Rab21 on the early endocytic pathway directly bind to the α subunit of β1 integrins and promote their endocytosis and recycling to remodel the cell surface for migration and cytokinesis [39, 40]. In addition, Rab5 also directly interacts with angiotensin II Type 1A receptor ($AT_{1A}R$) to facilitate its endocytic trafficking [41]. On the exocytic pathway, Rab3b is shown to bind directly to polymeric IgA receptor (pIgR) to modulate its transcytosis in polarized epithelial cells [42]. Furthermore, some Rabs are involved in packaging of cargo proteins into transport vesicles through interactions with adaptor proteins. In this regard, Rab5 is shown to concentrate transferrin receptor into coated pits for endocytosis [43], while Rab9 facilitates the recruitment of the cargo protein (mannose-6-phosphate receptor) into late-endosome derived transport vesicles via its effector TIP47 [44].

Rabs are also known to interact with actin and microtubule motor proteins such as myosins, kinesins, and dyneins to facilitate the movement of transport vesicles on the actin and microtubule cytoskeleton. Class V myosins are actin motors that consist of an N-terminal actin-binding motor domain and a C-terminal cargo-binding globular tail domain (GTD), which can bind to a number of Rabs on post-Golgi secretory vesicles or recycling endosomes and get recruited to these exocytic compartments [45]. These exocytic and recycling Rabs are more closely related in evolution and belong to groups I, IV, and V, including Rab3, Rab6, Rab8/Sec4, Rab10, Rab11, Rab14, Rab25, and Rab39 [1, 46, 2, 45]. In addition, Rab27 indirectly recruits myosin V to melanosomes via a linker protein Slac2/melanophilin [47, 48]. The Rab-myosin V interaction links transport vesicles to actin and facilitate their movement toward the cell surface. These Rabs are also known for recruitment of microtubule-based kinesin and dynein motors, especially Rab6 that directly binds to both kinesin (KIF20A) and

Fig. 4 (continued) (**c**) On late endosomes, Rab9 recruits Bloc-3 (Rab32/33 GEF) to the membrane and activates Rab32 as they move toward lysosomes or melanosomes. (**d**) Active Rab22 binds and recruits Rabex-5 (Rab5 GEF) and activates Rab5 on early endosomes. Active Rab5 in turn binds Sand1 (Mon1 in Yeast) –Ccz1 complex (Rab7 GEF), which recruits and activates Rab7 to facilitate transition to late endosomes. Upon dissociation of Rab22 and Rabex-5, Rab5 is inactivated by GTP hydrolysis and converted to GDP bound state, which is then removed from the membrane by GDI

dynein (DYNLRB1 and dynactin) [49–51]. Rab14 also directly binds to a kinesin, kinesin-3 (KIF16B) [52]. Some of the Rabs interact with kinesins and dyneins indirectly via linker proteins, e.g., Rab11 proteins can recruit kinesin-1, kinesin-2, dynein LIC1, and dynein LIC2 via Rab11 effectors FIP3 and FIP5 [53–56]. Another interesting example is the endocytic Rab5 that binds and activates one of its effectors hVps34, a PI 3 kinase, and its product PI3P on the membrane in turn recruits the kinesin KIF16B [57]. This plus-end microtubule motor may play a role in the peripheral distribution of Rab5-positive early endosomes, suggesting the necessity of Rab5 removal for transition to late endosomes and movement toward perinuclear region.

Another important Rab function in vesicular transport is to tether transport vesicles to target compartments for membrane fusion. In this regard, Rab5/Vps21 is shown to tether vesicles directly via Rab–Rab interaction *in trans* [58]. However, the tethering function is more commonly performed by Rab effectors including long coiled-coil homodimers and large multi-subunit complexes. The former may be exemplified by the Rab5 effectors EEA1/Vac1 and Rabenosyn-5 [59–61] and the Rab1/Ypt1 effectors p115/Uso1 [62, 63], while the latter include the Sec4/Rab8 effector exocyst [64, 65], the Rab5/Vps21 effector CORVET (class C core vacuole/endosome tethering) complex [66], the Rab7/Ypt7 effector HOPS (homotypic fusion and vacuole protein sorting) complex [67], and the Rab1/Ypt1 effectors TRAPPI and TRAPPII complexes [68, 69]. These tethering factors are recruited by the Rabs to mediate vesicle docking and often interact with the SM (Sec1–Munc18) proteins to facilitate the assembly of SNARE complexes for membrane fusion. For example, Rabenosyn-5 contains an N-terminal FYVE domain for binding to PI3P on endosomes and a C-terminal Rab5-binding domain for tethering Rab5-positive vesicles. Furthermore, Rabenosyn-5 interacts with hVps45, a SM protein, to facilitate SNARE-mediated membrane fusion [59].

4 Other Rab Functions

The large number of effectors for each Rab, e.g., more than 20 for Rab5 [70], suggests that Rabs may have additional functions beyond intracellular membrane trafficking. Indeed, Rabs play important roles in signal transduction and autophagy. Some of the Rab5 effectors are signaling molecules such as APPL1 and APPL2, which are recruited to early endosomes by Rab5 [71, 72] and in turn recruit Akt and modulate its phosphorylation specificity for GSK-3β rather than TSC2 [73]. This Rab5-mediated APPL signaling on endosomes is essential for cell survival and development in zebrafish [73]. Another Rab5 effector is Vps34 [74], a class III PI

3-kinase that produces PI3P on early endosomes and promotes autophagosome formation during autophagy [75–77]. Vps34 is also an effector for the late endosome-associated Rab7 [78] and may play a similar role in autophagy on late endosomes. In addition, the exocytic Rab1/Ypt1 is also known for its essential role in the formation of preautophagosomal structure (PAS) via TRAPPIII complex during the initiation of autophagy [79–81].

5   Rabs and Disease

The fundamental function of Rabs and membrane trafficking in cell physiology is reflected by various diseases due to mutations or altered expression of Rab genes. Mutations in five of the 66 human Rab genes (Rab7, Rab23, Rab27, Rab38, and Rab39b) are known to cause genetic disorders. Among them, Rab7 is ubiquitously expressed in all tissues while the other four Rabs are expressed only in certain cell types and tissues. Importantly, they are also different in the nature of mutations.

Four gain-of-function mutations in Rab7 are linked to Charcot–Marie–Tooth Type 2B (CMT2B) disease [82–84], which is a form of hereditary motor and sensory neuropathy with symptoms of distal sensory loss and muscle weakness, leading to toe ulcers, infections, and ultimately amputation [85]. These gain-of-function mutations enhance Rab7 activity by increasing the nucleotide exchange reaction independent of GEFs [86, 87]. It is worth noting that enhanced Rab7 activity affects mainly peripheral neurons and CMT2B is a neurological disease, despite the ubiquitous expression of Rab7 in all tissues.

Mutations in the other four Rabs that lead to autosomal recessive disorders are all loss-of-function mutations. Mutations in Rab23 are linked to Carpenter syndrome [88], which is a neurological disorder of craniosynostosis and limb malformation. Rab23 is highly expressed in the brain and neurons [89] and is localized on the plasma membrane and early endosomes [90] involved in sorting and function of signaling molecules in Sonic Hedgehog signal transduction [91]. The *open brain* (*opb*) gene that inhibits the Sonic Hedgehog signaling in mice is mapped to Rab23 and the *opb* mouse model recapitulates some of the neurological defects of Carpenter syndrome [91]. Mutations in Rab27 are linked to Griscelli syndrome, which is an immunological disorder with excessive T lymphocyte and macrophage activation called hemophagocytic syndrome as well as defects in skin pigmentation [92, 93]. Rab27 is expressed in highly secretory cells such as cytotoxic T lymphocytes (CTL) [94] and melanocytes [95, 96] and localized to secretory granules and melanosomes in these cell types. Inactivation of Rab27 by the mutations blocks the transport and function of the secretory granules and melanosomes and contributes

to the hemophagocytic syndrome and partial albinism in Griscelli patients [93]. This phenotype can be recapitulated by a Rab27 mutation in *ashen* mice [97]. Rab38 is one of multiple genes linked to Hermansky–Pudlak syndrome caused by defective melanocytes and platelets [98]. *Chocolate* mice [99] and *Fawn-hooded and Tester-Moriyama* rats [100] are animal models for Hermansky–Pudlak syndrome and they contain inactivating mutations in the Rab38 gene. A cell biology study suggests that Rab38 is essential for the biogenesis of melanosomes [101]. Finally, Rab39b is specifically expressed in the brain and neurons and mutations in Rab39b are associated with one form of X-linked mental retardation (XLMR) [102].

In addition to mutations, many Rabs show altered expression level or activity in such diseases as cancer, Alzheimer's disease, and diabetes. It appears a common theme that a Rab may be up-regulated in certain types of cancers but down-regulated in other types of cancers [4]. For example, Rab25 is known to promote α5β1 integrin recycling in epithelial cells [103] and overexpression of Rab25 is associated with aggressiveness of ovarian and breast cancers [104], suggesting a role for Rab25 in cancer cell invasion and metastasis. However, Rab25 is down-regulated in colon cancer with poor patient prognosis [105], suggesting a tumor suppressor function. Indeed, Rab25 deficiency in mouse models of colon cancer promotes colonic tumor growth [105]. The reconciliation of this apparent conflict over Rab25 function in promoting or blocking tumor growth in different cancers may involve the CLIC3 protein, which is necessary for Rab25-mediated integrin recycling [106]. It is suggested that Rab25 may sort integrins to lysosomes for degradation in cell types that don't express CLIC3, acting like a tumor suppressor [106]. The opposite may be true in cell types with high levels of CLIC3 where Rab25 can promote integrin recycling and cell migration and invasion [106]. Another example is Rab31, which is overexpressed in breast cancer, brain cancer, skin cancer, and several other types of cancers but is down-regulated in leukemia, lung cancer, and colon cancer [4].

Endocytic Rabs such as Rab5 and Rab7 are overexpressed in hippocampal neurons of Alzheimer's patients [107] and the enhanced endocytic activity is suggested to promote the proteolytic processing of amyloid precursor protein (APP) in endosomes [108], which may lead to increased production and accumulation of amyloid-β peptide (Aβ) in the brain, a hallmark of Alzheimer's disease. Recycling Rabs such as Rab10 and Rab14 are activated by insulin signal transduction to promote the translocation of glucose transporter 4 (GLUT4) from intracellular vesicles to the plasma membrane of adipocytes for glucose uptake and metabolism [109]. Rab10 and Rab14 are kept in the inactive GDP-bound state by AS160, a GAP for both Rabs [110]. Upon insulin stimulation, AS160 is inactivated by phosphorylation [111, 112] and

consequently Rab10 and Rab14 can be activated by GTP loading to promote docking and fusion of GLUT4-containing vesicles with the plasma membrane [109]. Malfunction of the Rab10- and Rab14-mediated GLUT4 translocation processes is implicated in type II diabetes.

Acknowledgement

References

1. Diekmann Y, Seixas E, Gouw M et al (2011) Thousands of rab GTPases for the cell biologist. PLoS Comput Biol 7:e1002217

2. Klopper TH, Kienle N, Fasshauer D et al (2012) Untangling the evolution of Rab G proteins: implications of a comprehensive genomic analysis. BMC Biol 10:71

3. Li G, Segev N (2012) Ypt/Rab GTPases and Intracellular Membrane Trafficking: an Overview. In: Li G, Segev N (eds) Rab GTPases and Membrane Trafficking. Bentham Science Publishers, Sharjah, pp 3–17

4. Rodrigues ML, Pereira-Leal JB (2012) Novel Rab GTPases. In: Li G, Segev N (eds) Rab GTPases and Membrane Trafficking. Bentham Science Publishers, Sharjah, pp 155–168

5. Hutagalung AH, Novick PJ (2011) Role of Rab GTPases in membrane traffic and cell physiology. Physiol Rev 91:119–149

6. Pfeffer SR (2013) Rab GTPase regulation of membrane identity. Curr Opin Cell Biol 25:414–419

7. Chavrier P, Parton RG, Hauri HP et al (1990) Localization of low molecular weight GTP binding proteins to exocytic and endocytic compartments. Cell 62:317–329

8. Blumer J, Rey J, Dehmelt L et al (2013) RabGEFs are a major determinant for specific Rab membrane targeting. J Cell Biol 200:287–300

9. Sivars U, Aivazian D, Pfeffer SR (2003) Yip3 catalyses the dissociation of endosomal Rab-GDI complexes. Nature 425:856–859

10. Soldati T, Shapiro AD, Svejstrup AB et al (1994) Membrane targeting of the small GTPase Rab9 is accompanied by nucleotide exchange. Nature 369:76–78

11. Ullrich O, Horiuchi H, Bucci C et al (1994) Membrane association of Rab5 mediated by GDP-dissociation inhibitor and accompanied by GDP/GTP exchange. Nature 368:157–160

12. Barr F, Lambright DG (2010) Rab GEFs and GAPs. Curr Opin Cell Biol 22:461–470

13. Soldati T, Riederer MA, Pfeffer SR (1993) Rab GDI: a solubilizing and recycling factor for rab9 protein. Mol Biol Cell 4:425–434

14. Garrett MD, Kabcenell AK, Zahner JE et al (1993) Interaction of Sec4 with GDI proteins from bovine brain, Drosophila melanogaster and Saccharomyces cerevisiae. Conservation of GDI membrane dissociation activity. FEBS Lett 331:233–238

15. Ullrich O, Stenmark H, Alexandrov K et al (1993) Rab GDP dissociation inhibitor as a general regulator for the membrane association of rab proteins. J Biol Chem 268:18143–18150

16. Carney DS, Davies BA, Horazdovsky BF (2006) Vps9 domain-containing proteins: activators of Rab5 GTPases from yeast to neurons. Trends Cell Biol 16:27–35

17. Nordmann M, Cabrera M, Perz A et al (2010) The Mon1-Ccz1 complex is the GEF of the late endosomal Rab7 homolog Ypt7. Curr Biol 20:1654–1659

18. Poteryaev D, Datta S, Ackema K et al (2010) Identification of the switch in early-to-late endosome transition. Cell 141:497–508

19. Jones S, Newman C, Liu F et al (2000) The TRAPP complex is a nucleotide exchanger for Ypt1 and Ypt31/32. Mol Biol Cell 11:4403–4411

20. Wang W, Sacher M, Ferro-Novick S (2000) TRAPP stimulates guanine nucleotide exchange on Ypt1p. J Cell Biol 151:289–296

21. Hattula K, Furuhjelm J, Arffman A et al (2002) A Rab8-specific GDP/GTP exchange factor is involved in actin remodeling and

polarized membrane transport. Mol Biol Cell 13:3268–3280

22. Siniossoglou S, Peak-Chew SY, Pelham HR (2000) Ric1p and Rgp1p form a complex that catalyses nucleotide exchange on Ypt6p. EMBO J 19:4885–4894

23. Marat AL, Dokainish H, McPherson PS (2011) DENN domain proteins: regulators of Rab GTPases. J Biol Chem 286:13791–13800

24. Pan X, Eathiraj S, Munson M et al (2006) TBC-domain GAPs for Rab GTPases accelerate GTP hydrolysis by a dual-finger mechanism. Nature 442:303–306

25. Ortiz D, Medkova M, Walch-Solimena C et al (2002) Ypt32 recruits the Sec4p guanine nucleotide exchange factor, Sec2p, to secretory vesicles; evidence for a Rab cascade in yeast. J Cell Biol 157:1005–1015

26. Knodler A, Feng S, Zhang J et al (2010) Coordination of Rab8 and Rab11 in primary ciliogenesis. Proc Natl Acad Sci U S A 107: 6346–6351

27. Pusapati GV, Luchetti G, Pfeffer SR (2012) Ric1-Rgp1 complex is a guanine nucleotide exchange factor for the late Golgi Rab6A GTPase and an effector of the medial Golgi Rab33B GTPase. J Biol Chem 287:42129–42137

28. Zhu H, Liang Z, Li G (2009) Rabex-5 is a Rab22 effector and mediates a Rab22-Rab5 signaling cascade in endocytosis. Mol Biol Cell 20:4720–4729

29. Gerondopoulos A, Langemeyer L, Liang JR et al (2012) BLOC-3 mutated in Hermansky-Pudlak syndrome is a Rab32/38 guanine nucleotide exchange factor. Curr Biol 22: 2135–2139

30. Kloer DP, Rojas R, Ivan V et al (2010) Assembly of the biogenesis of lysosome-related organelles complex-3 (BLOC-3) and its interaction with Rab9. J Biol Chem 285: 7794–7804

31. Rivera-Molina FE, Novick PJ (2009) A Rab GAP cascade defines the boundary between two Rab GTPases on the secretory pathway. Proc Natl Acad Sci U S A 106:14408–14413

32. Nottingham RM, Pusapati GV, Ganley IG et al (2012) RUTBC2 protein, a Rab9A effector and GTPase-activating protein for Rab36. J Biol Chem 287:22740–22748

33. Nottingham RM, Ganley IG, Barr FA et al (2011) RUTBC1 protein, a Rab9A effector that activates GTP hydrolysis by Rab32 and Rab33B proteins. J Biol Chem 286: 33213–33222

34. Nottingham RM, Pfeffer SR (2009) Defining the boundaries: Rab GEFs and GAPs. Proc Natl Acad Sci U S A 106:14185–14186

35. Li G, Qian H (2003) Sensitivity and specificity amplification in signal transduction. Cell Biochem Biophys 39:45–59

36. Barr FA (2013) Review series: Rab GTPases and membrane identity: causal or inconsequential? J Cell Biol 202:191–199

37. Mizuno-Yamasaki E, Medkova M, Coleman J et al (2010) Phosphatidylinositol 4-phosphate controls both membrane recruitment and a regulatory switch of the Rab GEF Sec2p. Dev Cell 18:828–840

38. Stalder D, Mizuno-Yamasaki E, Ghassemian M et al (2013) Phosphorylation of the Rab exchange factor Sec2p directs a switch in regulatory binding partners. Proc Natl Acad Sci U S A 110:19995–20002

39. Pellinen T, Arjonen A, Vuoriluoto K et al (2006) Small GTPase Rab21 regulates cell adhesion and controls endosomal traffic of beta1-integrins. J Cell Biol 173:767–780

40. Pellinen T, Tuomi S, Arjonen A et al (2008) Integrin trafficking regulated by Rab21 is necessary for cytokinesis. Dev Cell 15:371–385

41. Seachrist JL, Laporte SA, Dale LB et al (2002) Rab5 association with the angiotensin II type 1A receptor promotes Rab5 GTP binding and vesicular fusion. J Biol Chem 277:679–685

42. Van IJzendoorn SC, Tuvim MJ, Weimbs T et al (2002) Direct interaction between Rab3b and the polymeric immunoglobulin receptor controls ligand-stimulated transcytosis in epithelial cells. Dev Cell 2:219–228

43. McLauchlan H, Newell J, Morrice N et al (1998) A novel role for Rab5-GDI in ligand sequestration into clathrin-coated pits. Curr Biol 8:34–45

44. Carroll KS, Hanna J, Simon I et al (2001) Role of Rab9 GTPase in facilitating receptor recruitment by TIP47. Science 292:1373–1376

45. Lindsay AJ, Jollivet F, Horgan CP et al (2013) Identification and characterization of multiple novel Rab-myosin Va interactions. Mol Biol Cell 24:3420–3434

46. Govindan B, Bowser R, Novick P (1995) The role of Myo2, a yeast class V myosin, in vesicular transport. J Cell Biol 128:1055–1068

47. Fukuda M, Kuroda TS, Mikoshiba K (2002) Slac2-a/melanophilin, the missing link between Rab27 and myosin Va: implications of a tripartite protein complex for melanosome transport. J Biol Chem 277: 12432–12436

48. Wu X, Wang F, Rao K et al (2002) Rab27a is an essential component of melanosome receptor for myosin Va. Mol Biol Cell 13:1735–1749

49. Short B, Preisinger C, Schaletzky J et al (2002) The Rab6 GTPase regulates recruitment

of the dynactin complex to Golgi membranes. Curr Biol 12:1792–1795

50. Wanschers B, van de Vorstenbosch R, Wijers M et al (2008) Rab6 family proteins interact with the dynein light chain protein DYNLRB1. Cell Motil Cytoskeleton 65:183–196

51. Echard A, Jollivet F, Martinez O et al (1998) Interaction of a Golgi-associated kinesin-like protein with Rab6. Science 279:580–585

52. Ueno H, Huang X, Tanaka Y et al (2011) KIF16B/Rab14 molecular motor complex is critical for early embryonic development by transporting FGF receptor. Dev Cell 20:60–71

53. Horgan CP, Hanscom SR, Jolly RS et al (2010) Rab11-FIP3 binds dynein light intermediate chain 2 and its overexpression fragments the Golgi complex. Biochem Biophys Res Commun 394:387–392

54. Horgan CP, Hanscom SR, Jolly RS et al (2010) Rab11-FIP3 links the Rab11 GTPase and cytoplasmic dynein to mediate transport to the endosomal-recycling compartment. J Cell Sci 123:181–191

55. Schonteich E, Wilson GM, Burden J et al (2008) The Rip11/Rab11-FIP5 and kinesin II complex regulates endocytic protein recycling. J Cell Sci 121:3824–3833

56. Simon GC, Prekeris R (2008) Mechanisms regulating targeting of recycling endosomes to the cleavage furrow during cytokinesis. Biochem Soc Trans 36:391–394

57. Hoepfner S, Severin F, Cabezas A et al (2005) Modulation of receptor recycling and degradation by the endosomal kinesin KIF16B. Cell 121:437–450

58. Lo SY, Brett CL, Plemel RL et al (2012) Intrinsic tethering activity of endosomal Rab proteins. Nat Struct Mol Biol 19:40–47

59. Ohya T, Miaczynska M, Coskun U et al (2009) Reconstitution of Rab- and SNARE-dependent membrane fusion by synthetic endosomes. Nature 459:1091–1097

60. Simonsen A, Lippe R, Christoforidis S et al (1998) EEA1 links PI(3)K function to Rab5 regulation of endosome fusion. Nature 394:494–498

61. Tall GG, Hama H, DeWald DB et al (1999) The phosphatidylinositol 3-phosphate binding protein Vac1p interacts with a Rab GTPase and a Sec1p homologue to facilitate vesicle-mediated vacuolar protein sorting. Mol Biol Cell 10:1873–1889

62. Sapperstein SK, Walter DM, Grosvenor AR et al (1995) p115 is a general vesicular transport factor related to the yeast endoplasmic reticulum to Golgi transport factor Uso1p. Proc Natl Acad Sci U S A 92:522–526

63. Barroso M, Nelson DS, Sztul E (1995) Transcytosis-associated protein (TAP)/p115 is a general fusion factor required for binding of vesicles to acceptor membranes. Proc Natl Acad Sci U S A 92:527–531

64. TerBush DR, Maurice T, Roth D et al (1996) The Exocyst is a multiprotein complex required for exocytosis in Saccharomyces cerevisiae. EMBO J 15:6483–6494

65. Guo W, Roth D, Walch-Solimena C et al (1999) The exocyst is an effector for Sec4p, targeting secretory vesicles to sites of exocytosis. EMBO J 18:1071–1080

66. Balderhaar HJ, Lachmann J, Yavavli E et al (2013) The CORVET complex promotes tethering and fusion of Rab5/Vps21-positive membranes. Proc Natl Acad Sci U S A 110:3823–3828

67. Hickey CM, Wickner W (2010) HOPS initiates vacuole docking by tethering membranes before trans-SNARE complex assembly. Mol Biol Cell 21:2297–2305

68. Barrowman J, Bhandari D, Reinisch K et al (2010) TRAPP complexes in membrane traffic: convergence through a common Rab. Nat Rev Mol Cell Biol 11:759–763

69. Sacher M, Kim YG, Lavie A et al (2008) The TRAPP complex: insights into its architecture and function. Traffic 9:2032–2042

70. Christoforidis S, McBride HM, Burgoyne RD et al (1999) The Rab5 effector EEA1 is a core component of endosome docking. Nature 397:621–625

71. Miaczynska M, Christoforidis S, Giner A et al (2004) APPL proteins link Rab5 to nuclear signal transduction via an endosomal compartment. Cell 116:445–456

72. Zhu G, Chen J, Liu J et al (2007) Structure of the APPL1 BAR-PH domain and characterization of its interaction with Rab5. EMBO J 26:3484–3493

73. Schenck A, Goto-Silva L, Collinet C et al (2008) The endosomal protein Appl1 mediates Akt substrate specificity and cell survival in vertebrate development. Cell 133:486–497

74. Christoforidis S, Miaczynska M, Ashman K et al (1999) Phosphatidylinositol-3-OH kinases are Rab5 effectors. Nat Cell Biol 1:249–252

75. Jaber N, Dou Z, Chen JS et al (2012) Class III PI3K Vps34 plays an essential role in autophagy and in heart and liver function. Proc Natl Acad Sci U S A 109:2003–2008

76. Simonsen A, Tooze SA (2009) Coordination of membrane events during autophagy by

multiple class III PI3-kinase complexes. J Cell Biol 186:773–782

77. Vergne I, Roberts E, Elmaoued RA et al (2009) Control of autophagy initiation by phosphoinositide 3-phosphatase Jumpy. EMBO J 28:2244–2258

78. Stein MP, Feng Y, Cooper KL et al (2003) Human VPS34 and p150 are Rab7 interacting partners. Traffic 4:754–771

79. Lipatova Z, Segev N (2012) A Ypt/Rab GTPase module makes a PAS. Autophagy 8:1271–1272

80. Lynch-Day MA, Bhandari D, Menon S et al (2010) Trs85 directs a Ypt1 GEF, TRAPPIII, to the phagophore to promote autophagy. Proc Natl Acad Sci U S A 107:7811–7816

81. Wang J, Menon S, Yamasaki A et al (2013) Ypt1 recruits the Atg1 kinase to the preautophagosomal structure. Proc Natl Acad Sci U S A 110:9800–9805

82. Verhoeven K, De Jonghe P, Coen K et al (2003) Mutations in the small GTP-ase late endosomal protein RAB7 cause Charcot-Marie-Tooth type 2B neuropathy. Am J Hum Genet 72:722–727

83. Houlden H, King RH, Muddle JR et al (2004) A novel RAB7 mutation associated with ulcero-mutilating neuropathy. Ann Neurol 56:586–590

84. Meggouh F, Bienfait HM, Weterman MA et al (2006) Charcot-Marie-Tooth disease due to a de novo mutation of the RAB7 gene. Neurology 67:1476–1478

85. Zuchner S, Vance JM (2006) Molecular genetics of autosomal-dominant axonal Charcot-Marie-Tooth disease. Neuromol Med 8:63–74

86. Spinosa MR, Progida C, De Luca A et al (2008) Functional characterization of Rab7 mutant proteins associated with Charcot-Marie-Tooth type 2B disease. J Neurosci 28:1640–1648

87. McCray BA, Skordalakes E, Taylor JP (2010) Disease mutations in Rab7 result in unregulated nucleotide exchange and inappropriate activation. Hum Mol Genet 19:1033–1047

88. Jenkins D, Seelow D, Jehee FS et al (2007) RAB23 mutations in Carpenter syndrome imply an unexpected role for hedgehog signaling in cranial-suture development and obesity. Am J Hum Genet 80:1162–1170

89. Olkkonen VM, Peterson JR, Dupree P et al (1994) Isolation of a mouse cDNA encoding Rab23, a small novel GTPase expressed predominantly in the brain. Gene 138:207–211

90. Evans TM, Ferguson C, Wainwright BJ et al (2003) Rab23, a negative regulator of hedgehog signaling, localizes to the plasma membrane and the endocytic pathway. Traffic 4:869–884

91. Eggenschwiler JT, Espinoza E, Anderson KV (2001) Rab23 is an essential negative regulator of the mouse Sonic hedgehog signalling pathway. Nature 412:194–198

92. Griscelli C, Durandy A, Guy-Grand D et al (1978) A syndrome associating partial albinism and immunodeficiency. Am J Med 65:691–702

93. Menasche G, Pastural E, Feldmann J et al (2000) Mutations in RAB27A cause Griscelli syndrome associated with haemophagocytic syndrome. Nat Genet 25:173–176

94. Stinchcombe JC, Barral DC, Mules EH et al (2001) Rab27a is required for regulated secretion in cytotoxic T lymphocytes. J Cell Biol 152:825–834

95. Hume AN, Collinson LM, Rapak A et al (2001) Rab27a regulates the peripheral distribution of melanosomes in melanocytes. J Cell Biol 152:795–808

96. Wu X, Rao K, Bowers MB et al (2001) Rab27a enables myosin Va-dependent melanosome capture by recruiting the myosin to the organelle. J Cell Sci 114:1091–1100

97. Wilson SM, Yip R, Swing DA et al (2000) A mutation in Rab27a causes the vesicle transport defects observed in ashen mice. Proc Natl Acad Sci U S A 97:7933–7938

98. Di Pietro SM, Dell'Angelica EC (2005) The cell biology of Hermansky-Pudlak syndrome: recent advances. Traffic 6:525–533

99. Loftus SK, Larson DM, Baxter LL et al (2002) Mutation of melanosome protein RAB38 in chocolate mice. Proc Natl Acad Sci U S A 99:4471–4476

100. Oiso N, Riddle SR, Serikawa T et al (2004) The rat Ruby (R) locus is Rab38: identical mutations in Fawn-hooded and Tester-Moriyama rats derived from an ancestral Long Evans rat sub-strain. Mamm Genome 15:307–314

101. Wasmeier C, Romao M, Plowright L et al (2006) Rab38 and Rab32 control post-Golgi trafficking of melanogenic enzymes. J Cell Biol 175:271–281

102. Giannandrea M, Bianchi V, Mignogna ML et al (2010) Mutations in the small GTPase gene RAB39B are responsible for X-linked mental retardation associated with autism, epilepsy, and macrocephaly. Am J Hum Genet 86:185–195

103. Caswell PT, Spence HJ, Parsons M et al (2007) Rab25 associates with alpha5beta1 integrin to promote invasive migration in 3D microenvironments. Dev Cell 13:496–510

104. Cheng KW, Lahad JP, Kuo WL et al (2004) The RAB25 small GTPase determines aggressiveness of ovarian and breast cancers. Nat Med 10:1251–1256

105. Nam KT, Lee HJ, Smith JJ et al (2010) Loss of Rab25 promotes the development of intestinal neoplasia in mice and is associated with human colorectal adenocarcinomas. J Clin Invest 120:840–849

106. Dozynkiewicz MA, Jamieson NB, Macpherson I et al (2012) Rab25 and CLIC3 collaborate to promote integrin recycling from late endosomes/lysosomes and drive cancer progression. Dev Cell 22:131–145

107. Ginsberg SD, Alldred MJ, Counts SE et al (2010) Microarray analysis of hippocampal CA1 neurons implicates early endosomal dysfunction during Alzheimer's disease progression. Biol Psychiatry 68:885–893

108. Cataldo AM, Peterhoff CM, Troncoso JC et al (2000) Endocytic pathway abnormalities precede amyloid beta deposition in sporadic Alzheimer's disease and Down syndrome: differential effects of APOE genotype and presenilin mutations. Am J Pathol 157:277–286

109. Chen Y, Wang Y, Zhang J et al (2012) Rab10 and myosin-Va mediate insulin-stimulated GLUT4 storage vesicle translocation in adipocytes. J Cell Biol 198:545–560

110. Miinea CP, Sano H, Kane S et al (2005) AS160, the Akt substrate regulating GLUT4 translocation, has a functional Rab GTPase-activating protein domain. Biochem J 391:87–93

111. Zeigerer A, McBrayer MK, McGraw TE (2004) Insulin stimulation of GLUT4 exocytosis, but not its inhibition of endocytosis, is dependent on RabGAP AS160. Mol Biol Cell 15:4406–4415

112. Sano H, Kane S, Sano E et al (2003) Insulin-stimulated phosphorylation of a Rab GTPase-activating protein regulates GLUT4 translocation. J Biol Chem 278:14599–14602

Bioinformatic Approaches to Identifying and Classifying Rab Proteins

Yoan Diekmann and José B. Pereira-Leal

Abstract

The bioinformatic annotation of Rab GTPases is important, for example, to understand the evolution of the endomembrane system. However, Rabs are particularly challenging for standard annotation pipelines because they are similar to other small GTPases and form a large family with many paralogous subfamilies. Here, we describe a bioinformatic annotation pipeline specifically tailored to Rab GTPases. It proceeds in two steps: first, Rabs are distinguished from other proteins based on GTPase-specific motifs, overall sequence similarity to other Rabs, and the occurrence of Rab-specific motifs. Second, Rabs are classified taking either a more accurate but slower phylogenetic approach or a slightly less accurate but much faster bioinformatic approach. All necessary steps can either be performed locally or using the referenced online tools. An implementation of a slightly more involved version of the pipeline presented here is available at RabDB.org.

Key words Bioinformatics, RabF motifs, RabSF regions, Subfamily classification, RabDB.org, Evolution

1 Introduction

Rab GTPases are a large family of proteins that function as critical regulators of intracellular trafficking. Their specific localization to membrane domains of various organelles and pathways make them ideal markers, like, for example, Rab5 and Rab7 that identify early and late endosomes, respectively. In an evolutionary context, this property can be exploited to study the evolutionary history of specific trafficking pathways and the endomembrane system in general. For example, Rabs are present in all eukaryotes and different studies have predicted independently that the Last Eukaryotic Common Ancestor (LECA) already had a large Rab repertoire [1–3]. This suggests that the LECA already had a sophisticated endomembrane system. Furthermore, as Rabs are not detected in bacteria, that the origins of eukaryotes was associated with the emergence and diversification of Rab proteins. While some Rabs

perform housekeeping functions and are strictly conserved throughout evolution, the family as a whole is extremely dynamic. One finds taxon-specific innovation and loss of subfamilies, and frequent duplications that expand conserved subfamilies independently, e.g., from one ancestral Rab5 to several isoforms in mammals and fungi [4]. The rapid pace of full genome sequencing gives us the unprecedented possibility to understand the evolution of the endomembrane system; however, it raises the challenge of identifying and classifying the members of dynamic protein families like, for example, Rabs. Here, we describe the bioinformatic pipeline addressing the annotation problem for Rabs.

Rabs are relatively short proteins of length around 220 amino acids. Yet, in rare cases they can be fused with other domains appearing thus as large proteins, as for example Rab45 which contains an N-terminal EF-hand domain [5]. The Rab domain can be partitioned roughly into two divergent "hypervariable" termini that flank a central conserved region. The latter contains various GTPase and Rab-specific motifs described below. Rabs are the largest family of the Ras superfamily, also referred to as small GTPases. The Ras superfamily has a canonical P-loop NTPase fold, one of the chain folds found in proteins that bind and hydrolyze nucleoside triphosphates including ATP and GTP, and one of the most abundant folds. GTPases are a monophyletic superclass within P-loop NTPases and can be further divided into two large classes one of which (TRAFAC, for translation factor related) includes the extended Ras-like superfamily [6]. This hierarchical classification scheme is based on structural and sequence motifs that determine the membership of a sequence to these nested classes. Two motifs define P-loop NTPases: the N-terminal Walker A (GxxxGK[ST]) motif or P-loop that binds phosphate and the distal Walker B motif (DxxG) that binds a Mg ion. The distinctive features of GTPases are a specific form of the Walker B motif, and an additional distal [NT]KxD motif conferring specificity to GTP and thus not found in other P-loop NTPases. Besides of a common structural organization consisting of six β-sheets and five α-helices, small GTPases in particular share four further motifs, two single conserved [FY] and T residues and two conserved strips with consensus DTAGQ and SAK, respectively, which participate in the interactions with guanine, phosphate, and Mg [6]. Finally, within small GTPases, bioinformatic analysis determined five Rab family (RabF) motifs distinguishing them from other families of the Ras superfamily [7]. However, unlike the strictly conserved motifs described so far, RabF motifs are variable to a certain extent, both among Rab subfamilies and possibly across major eukaryotic taxa. Furthermore, some Rabs may have lost specific RabF motifs and therefore not have the entire complement of five motifs. Figure 1 summarizes the different Rabs motifs discussed in this section, including further motifs found in Rab sequences (RabSF and prenylation motifs) that are less relevant in the context of identification and classification of Rabs.
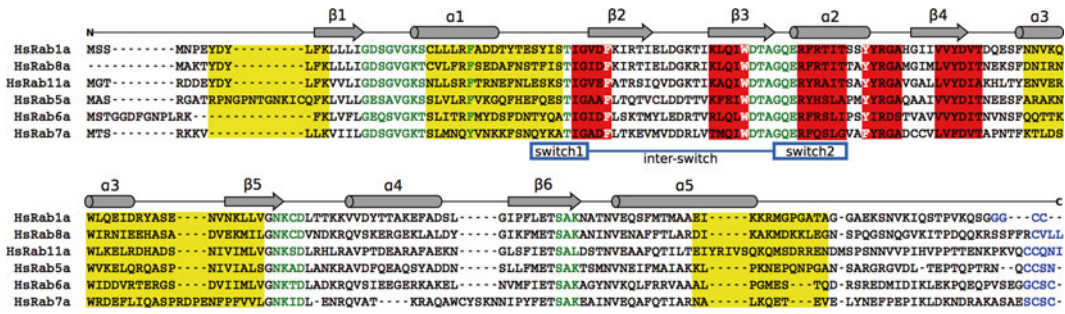
Fig. 1 *Sequence motifs defining Rab small GTPases*—Multiple sequence alignment (generated with Prank [13]) of some human Rabs (Uniprot accessions P62820, P61006, P62491, P20339, P20340, P51149), representing ancestral subfamilies found in most eukaryotes. The *coloured residues* and regions correspond to motifs required for different aspects of Rab function that define the identity of the sequence as a Rab (see main text). Shown are the catalytic triad (*white residues*), i.e., three amino acids shared by certain hydrolase and transferase enzymes; motifs required for the enzymatic function which are referred to as G1–G3 (regions interacting with guanine) and PM1–PM3 (regions interacting with phospate or Mg) (*green residues*) and occurring in the order PM1 (corresponding to the P-loop), G1, PM2 (the Walker B motif), PM3, G2 (the GTP-specificity motif), G3; the RabF1–5 (Rab family) motifs [7] (*red areas*); and the RabSF1–4 (Rab subfamily) motifs [7, 29] (*yellow areas*) which have been proposed to confer specificity to the distinct sets of effectors of Rab subfamilies (reviewed in refs. [30, 31]) but tend to be poorly conserved; the variable prenylation motifs (common are XXXCC, XXCCX, XCCXX, CCXXX, or XXCXC [7]) at the C-terminus that are frequent but not always present (*blue residues*). Moreover, the secondary structure elements are indicated above the sequence, and the switch region is shown which is the site of conformational change upon nucleotide binding (*blue*)

2 Materials

In this chapter, we propose two different approaches to annotate Rab sequences. First, a browser-based solution that is less powerful but can be performed on any computer with internet access. The links to the corresponding websites are given in Subheading 3. Second, a more powerful command-line version, however, that does require the installation of several tools. This is easiest on a computer running an operating system from the UNIX family, i.e., OSX or some flavor of LINUX. If you are using a Windows machine, you can still install and use all required tools within the cygwin[1] environment. The requirements are the SUPERFAMILY [8] annotation pipeline[2] (which needs HMMER[3] and Perl[4]), BLAST [9], MAST [10] (from the MEME suite [11], requires cygwin under windows), MAFFT [12] or Prank [13] and FastTree [14] or PhyML [15] for many or few sequences to be annotated, respectively.

---

[1] https://www.cygwin.com/
[2] http://supfam.org/SUPERFAMILY/downloads.html
[3] hmmer.org
[4] http://www.perl.org/get.html

3 Methods

The bioinformatic annotation of Rab small GTPases in sequence data can conceptually be divided in two steps. First, Rabs have to be identified, i.e., distinguished from other proteins, in particular from other small GTPases like, for example, Rans. In other words, the first question is if a given protein sequence is a Rab or not. The answer is ideally based on three different bioinformatic approaches assessing different aspects of the Rab sequence which we detail below (Subheading 3.1, **steps 2–4**). Once a list of candidate sequences has been cleared of sequences that are not Rabs, the sequence can be classified in a second step, i.e., assigned to a certain subfamily like, for example, Rab1. In other words, the second question is which subfamily (if any) a given Rab belongs to. Two alternative approaches can be followed that differ in speed and potentially accuracy that we discuss in the second subsection (Subheading 3.2, **step 2**(**a** or **b**). In the following, we refer to annotating a Rab sequence with a subfamily simply as Rab classification.

Note that we assume throughout this chapter that sequences to be classified correspond to genes, i.e., are the output of an appropriate gene-finding procedure rather than unprocessed sequences coming directly from genome sequencing projects. Moreover, we only consider translated amino acid sequences. All parameters left unspecified in the following remain at their default values.

An overview of the pipeline detailed in the following is given in Fig. 2.

3.1 Identifying Rabs

1. Prepare input file: generate a file in FASTA format that contains the candidate sequences to be annotated.

2. Annotate at superclass or superfamily level: align sequences against profile Hidden Markov Models (pHMMs). This is done either online by pasting the sequences into the SUPERFAMILY[5] [8] or PFAM[6] [16] sequence searches, or locally running the SUPERFAMILY annotation pipeline (a description how to run the models can be found online[7]). Only sequences annotated as 'G proteins' (SCOP [17] identifier 52592[8]) in SUPERFAMILY or 'Ras' (PFAM family identifier PF00071.17[9]) in PFAM pass on to the next step, all others are not Rabs (*see* **Note 1**).

---

[5] http://supfam.org/SUPERFAMILY/hmm.html
[6] http://pfam.xfam.org/
[7] http://supfam.org/SUPERFAMILY/howto_use_models.html
[8] http://supfam.org/SUPERFAMILY/cgi-bin/scop.cgi?sunid = 52592
[9] http://pfam.xfam.org/family/PF00071.17
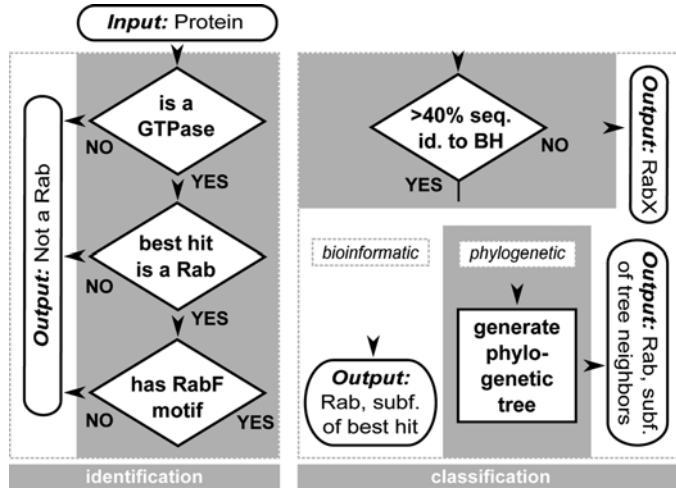
Fig. 2 *The Rab annotation pipeline*—Rabs are annotated in two steps. Given a protein sequence, it is first determined if it is a Rab or not (identification). If affirmative, the sequence can be annotated at the subfamily level in a second step (classification). If it is not similar enough (more than 40 % sequence identity) to a manually annotated Rab in a reference set used for the annotation, the Rab is attributed to the unspecific subfamily 'RabX.' Otherwise, one of two approaches (bioinformatic or phylogenetic) can be chosen to classify the Rab, i.e., generate an annotation at subfamily level. *See* Subheadings 3 and 4 for the details on the procedure. Abbreviations: Rab family (RabF) motif, identity (id.), best hit (BH), subfamily (subf.)

3. Find best local pairwise alignment hit: BLAST [9] the remaining candidate sequences against a manually curated set of Rab and non-Rab sequences, for example those provided on our Rab website.[10] This can be done either using the online version of the NCBI protein BLAST[11] (choosing the 'Align two or more sequences' option) or with a locally installed version of BLAST. Only those sequences that align better (i.e., at a lower *e*-value) to a Rab than to a non-Rab and with an *e*-value lower than 10^{-10} are considered Rabs and pass on to the next step (*see* **Note 2**). In anticipation of **step 1** of classifying Rabs phase, keep track of the sequence identity of each candidate sequence to its best hit and of the Rab subfamily of the best hit.

---

4. Detect RabF motifs: the remaining sequences are scanned for the presence of at least one RabF motif. This is done either with the online[12] or local version of MAST [10] using an *e*-value threshold of 0.0001. The necessary motif file can be obtained on our website.[13] Sequences with no detectable RabF motif are discarded (*see* **Note 3**).

3.2 Classifying Rabs

1. Ensure minimal sequence identity: all sequences that aligned at sequence identity lower than 40 % to their respective best hit in the reference set of Rabs (*see* **step 3**) are annotated as 'RabX,' corresponding to no annotation at subfamily level. The remaining sequences can be classified using either approach A or B (*see* **Note 4**).

2. Classify subfamily:

   (a) Phylogenetic approach: Generate a FASTA file with the sequences to be classified, plus the full set of human Rabs (can be extracted from the Rab file provided above) and optionally an additional Rab complement from an organism that is taxonomically close (if known) to the sequences to be classified. Multiply align the sequences, for a few sequences using Prank [13] either online (webPrank[14] [18]) or locally, for many sequences using MAFFT [12] online[15] or locally. Next, generate a phylogenetic tree from the multiple sequence alignment (MSA), for a few sequences either using PhyML [15] online[16] or locally, and for many sequences using FastTree [14] locally (no online version available). PhyML requires to convert the MSA to Phylip format, which can for example be done programmatically with the common bioinformatics toolboxes Biopython [19] or Bioperl [20], or online using some format conversion tool like, for example, the one hosted at NIH.[17] The phylogenetic trees can be visualized, for example, with FigTree.[18] The annotation for the candidate sequences is derived from the tree by transferring the subfamily from the neighboring sequences in the tree (*see* **Note 5**).

   (b) Bioinformatic approach: Transfer the annotation from the best BLAST hit obtained in **step 3** (*see* **Note 6**).

---

[12] http://meme.nbcr.net/meme/cgi-bin/mast.cgi
[13] http://www.rabdb.org/about/RabF_motifs.meme
[14] http://www.ebi.ac.uk/goldman-srv/webprank/
[15] http://mafft.cbrc.jp/alignment/server/
[16] http://atgc.lirmm.fr/phyml/
[17] http://genome.nci.nih.gov/tools/reformat.html
[18] http://tree.bio.ed.ac.uk/software/figtree/

4   Notes

1. This step can be seen as an initial filter and does not directly decide if a sequence is a Rab. Therefore, it is not strictly necessary, but it is a safe way to reduce the complexity of large annotation efforts, e.g., of protein complements from entire genomes.

   The presence of well-conserved sequence motifs and the signature from the overall protein structure of a family is most proficiently assessed by aligning a sequence against so-called profile Hidden Markov Models (pHMM). pHMMs are probabilistic models derived from Multiple Sequence Alignments (MSA) that represent the position-specific information contained in MSAs. A pHMM preserves the information on variability of residues at certain positions in a family of proteins and is therefore well suited to represent families of related proteins [21].

   For Rabs, at least two precomputed pHMMs are available from Superfamily [22] and PFAM [16] built on GTPases[19] and small GTPases,[20] respectively. For a small number of sequences, uploading the sequences and using the online utilities has the advantage to avoid the overhead of downloading and installing the databases' annotation pipelines. This becomes necessary if one wants to keep the sequence in case the (small) GTPase pHMM provides the best fit among all other alternative models, rather than aligning a sequence solely against the (small) GTPase pHMM and defining success by an arbitrary e-value cutoff.

   Classification of (small) GTPases via pHHMs works very well, i.e., makes virtually no errors and is a useful way to reduce the size of the candidate list proceeding through the next steps. The only disadvantage is that aligning sequences to pHMMs may be computationally costly, although newer versions of HMMER are now closing the speed gap to conceptually simpler tools like BLAST [9].

   In summary, although it is not strictly necessary to perform a pHMM analysis to decide if a sequence is a Rab, it is a safe way to reduce the complexity of large annotation efforts.

2. The core of most annotations is the assessment of pairwise sequence similarity and the transfer of annotations from the closest match. In the context of identifying Rabs, the underlying reasoning is that if a sequence most resembles a Rab, it is most likely a Rab itself. This represents the strongest piece of evidence for the bioinformatic identification of Rabs.

---

[19] http://supfam.org/SUPERFAMILY/cgi-bin/scop.cgi?sunid=52592
[20] http://pfam.xfam.org/family/PF00071.17

The most common tool to measure pairwise sequence similarity is BLAST [9]. BLAST is a local pairwise alignment tool, which means that two sequences are aligned only in regions where similarity is high enough and not necessarily over the entire length of the sequence. This is important to take into consideration, for example, in the case of multidomain proteins, where individual domains can align to other proteins independently of the rest of the protein.

Most Rabs consist only of a single domain, and the local alignment approach can therefore be used without additional care. However, in cases where other domains are fused to Rabs, for example in Rab44 or Rab45, one has to make sure that it is the Rab domain that aligns. The critical issue when using BLAST for identification of Rabs is the database of sequences against which candidate sequences are aligned. Most commonly, especially when using the online BLAST resource hosted at NCBI,[21] this is the NCBI nonredundant database (nr, which consists of all nonredundant GenBank [23] CDS translations merged with PDB [24], SwissProt [25], PIR [26], and PRF[22] entries excluding environmental samples from whole genome shotgun projects). A first problem with this choice is that nr contains many sequences that have been annotated purely in an automated manner without manual curation. This frequently results in annotations like "putative Rab" or "Rab-like," or even less informative annotations that cannot be transferred. Other problems arise, for example, from sequence fragments or misassembled chimeric sequences in the database. The solution is to use a manually curated set of Rabs against which candidate sequences can be BLASTed and the annotation from the closest hit transferred. We provide such a reference set of annotated Rab sequences on our website;[23] however, especially in the case of divergence taxa it may be expanded with additional manually curated sequences of taxa close to the one of interest. A second type of problem is that sequences that are not Rabs, but are closely related like, for example, Rans or most problematically Rab-like proteins just by chance may have a best BLAST hit that is a Rab and would therefore be annotated as being Rabs. This problem can be solved by using a second database of sequences that should explicitly be excluded, including overall very close sequences like RabL3, RabL5, or Rans. Whenever a candidate aligns better to a sequence from that second negative reference set, it

---

[21] http://blast.ncbi.nlm.nih.gov/Blast.cgi?PROGRAM = blastp& PAGE_TYPE = BlastSearch&LINK_LOC = blasthome
[22] http://www.prf.or.jp/index-e.html
[23] http://www.rabdb.org/about/rabs.fasta

can be excluded as not a Rab. We provide such a set of sequences at the same site given earlier.[24]

We previously benchmarked the ability to identify Rabs by pairwise sequence alignments using BLAST against the curated databases of Rabs and non-Rabs provided earlier, and compared it to using the nr database. While BLAST against the reference databases correctly identified 100 % of 25 Rabs from *Monosiga brevicollis*, transferring the annotation from the best BLAST hit in the nr database missed 8 Rabs, corresponding to 68 % correct identifications [1]. Note that the list of candidates was obtained by filtering the entire genome using pHMMs as described earlier.

Hence, pairwise alignments using BLAST represent the core strategy for the identification of Rabs. Especially when hand-curated databases of Rabs and non-Rabs are used, the error rate can be expected to be very low, resulting in a simple and efficient strategy for Rab identification.

3. Although the previous steps are expected to result in very few errors, a third strategy can be applied to filter out potentially remaining sequences that strongly resemble Rabs overall, but lack the canonical RabF motifs shown, for example, in Fig. 1. If a sequence lacks any detectable RabF motif, it can be safely concluded that it is not a Rab. This third step is thus a safety measure to augment the confidence that the sequences that pass this last step indeed are Rabs.

Sets of motifs that cooccur and are positionally conserved can be well represented by pHMMs. However, when motif's relative position and even present can vary, it is desirable to search for them individually and pHMMs are not the approach of choice. Rather, dedicated motif search tools like, for example, programs found in the MEME suite [11] are able to find occurrences for every motif independently and statistically score each match.

RabF motifs are a set of motifs which are best searched for individually. This is because some Rabs may not have a full set of five RabF motifs. Alternatively, the actual motifs could have diverged from the canonical sequence in mammals and therefore appear to have been lost. In any case, we provide a representation of the motifs[25] and their variability in amino acid sequence generated with MEME [27]. This was build based on a large Rab MSA mentioned earlier. It can be used as input to MAST [10], which allows to find occurrences of the motifs in the input sequences. If no motif is found, the sequence can safely be discarded as not a Rab.

---

[24] http://www.rabdb.org/media/files/on_rabs.fasta
[25] http://www.rabdb.org/media/files/rabF_motifs.meme

In a previous large-scale annotation of Rabs in 247 full genomes covering the whole eukaryotic tree of life, the previous two steps yielded 7865 candidate sequences, which were reduced to 7742 by applying the filter based on RabF motif detection. This corresponds to a reduction by 1.6 %, implying that roughly one in 50 sequences annotated purely by BLAST is not Rabs. Note that this step also tends to eliminate Rab sequence fragments, as they may perfectly align to reference Rab sequences, but should not be considered Rabs as they do not correspond to a biochemically functional protein.

In summary, detecting and requiring at least one RabF motif is a minor last filter to make sure no sequences have falsely been annotated as Rabs.

4. One should avoid transferring subfamily annotations among sequences that share less than 40 % sequence identity. The use of this threshold has been validated, for example, in the Supplementary Fig. 1 from ref. [1]. If the sequence is not at least 40 % identical to any sequence in the reference set of Rab sequences, an unspecific classification as RabX is a saver option.

5. Molecular phylogenies are hypotheses about the evolutionary histories of proteins, mostly taking the form of phylogenetic trees. They are now commonly based on probabilistic models of the evolutionary process by which protein sequences diverge. Given a set of annotated sequences and a moderate proportion of sequences to be classified, the annotation of the latter is obtained from a phylogenetic tree by annotation transfer from the neighboring leaves. In the ideal case, the unknown sequences are found in clear clusters or clades that are formed by sequences with coherent annotation, which can then be transferred with great confidence.

The Rab family, similar to other small GTPases, evolves by divergent evolution [28], i.e., sequence divergence is greater after duplications than after speciations resulting in clades of paralogs (defined as genes related by a duplication rather than a speciation event) in phylogenetic trees. For example, in a tree of human, mouse, and fly Rab1 and Rab5, the Rab1s and the Rab5s are going to cluster together, and not the human, mouse, and fly sequences, respectively. This is the basis for the proposed annotation strategy: an unknown Rab is going to cluster together with other members of its subfamily in the tree, and the subfamily can therefore be transferred.

A phylogenetic approach is expected to be more accurate than bioinformatic ones that are mostly based on pairwise sequence similarities. However, the conceptual superiority comes at a cost: trees with hundreds of sequences are computationally demanding to generate and cumbersome to analyze by hand or in an automated manner. Therefore, this option is only feasible for relatively few sequences at a time.

In summary, phylogenetic approaches are powerful, accurate but computationally expensive. They have been used successfully on Rabs (*see,* e.g., [3]), but in simple cases like, for example, Opisthokont Rabs a less involved bioinformatic approach described below may be sufficient.

6. The entire bioinformatic pipeline described in this chapter including a few improvements has been implemented in a tool coined the "Rabifier" which is available online at www.RabDB. org [1]. Alternatively, an approach entirely based on pHMMs of Rab subfamilies is described in ref. [2] and available at http://bioinformatics.mpibpc.mpg.de/rab/.

Acknowledgements

References

1. Diekmann Y, Seixas E, Gouw M et al (2011) Thousands of Rab GTPases for the cell biologist. PLoS Comput Biol 7:e1002217. doi:10.1371/journal.pcbi.1002217

2. Kloepper TH, Kienle N, Fasshauer D, Munro S (2012) Untangling the evolution of Rab G proteins: implications of a comprehensive genomic analysis. BMC Biol 10:71. doi:10.1186/1741-7007-10-71

3. Eliáš M, Brighouse A, Gabernet-Castello C et al (2012) Sculpting the endomembrane system in deep time: high resolution phylogenetics of Rab GTPases. J Cell Sci 125:2500–2508. doi:10.1242/jcs.101378

4. Pereira-Leal JB (2008) The Ypt/Rab family and the evolution of trafficking in fungi. Traffic 9:27–38. doi:10.1111/j.1600-0854.2007.00667.x

5. Shintani M, Tada M, Kobayashi T et al (2007) Characterization of Rab45/RASEF containing EF-hand domain and a coiled-coil motif as a self-associating GTPase. Biochem Biophys Res Commun 357:661–667. doi:10.1016/j.bbrc.2007.03.206

6. Leipe DD, Wolf YI, Koonin EV, Aravind L (2002) Classification and evolution of P-loop GTPases and related ATPases. J Mol Biol 317:41–72. doi:10.1006/jmbi.2001.5378

7. Pereira-Leal JB, Seabra MC (2000) The mammalian Rab family of small GTPases: definition of family and subfamily sequence motifs suggests a mechanism for functional specificity in the Ras superfamily. J Mol Biol 301:1077–1087. doi:10.1006/jmbi.2000.4010

8. de Lima Morais DA, Fang H, Rackham OJL et al (2011) SUPERFAMILY 1.75 including a domain-centric gene ontology method. Nucleic Acids Res 39:D427–D434. doi:10.1093/nar/gkq1130

9. Camacho C, Coulouris G, Avagyan V et al (2009) BLAST+: architecture and applications. BMC Bioinformatics 10:421. doi:10.1186/1471-2105-10-421

10. Bailey TL, Gribskov M (1998) Combining evidence using p-values: application to sequence homology searches. Bioinformatics 14:48–54. doi:10.1093/bioinformatics/14.1.48

11. Bailey TL, Bodén M, Buske FA et al (2009) MEME SUITE: tools for motif discovery and searching. Nucleic Acids Res 37:W202–W208. doi:10.1093/nar/gkp335

12. Katoh K, Standley DM (2013) MAFFT multiple sequence alignment software version 7: improvements in performance and usability. Mol Biol Evol 30:772–780. doi:10.1093/molbev/mst010

13. Löytynoja A, Goldman N (2005) An algorithm for progressive multiple alignment of sequences with insertions. PNAS 102:10557–10562. doi:10.1073/pnas.0409137102

14. Price MN, Dehal PS, Arkin AP (2010) FastTree 2—approximately maximum-likelihood trees for large alignments. PLoS One 5:e9490. doi:10.1371/journal.pone.0009490

15. Guindon S, Dufayard J-F, Lefort V et al (2010) New algorithms and methods to estimate maximum-likelihood phylogenies: assessing the performance of PhyML 3.0. Syst Biol 59:307–321. doi:10.1093/sysbio/syq010

16. Finn RD, Bateman A, Clements J et al (2014) Pfam: the protein families database. Nucleic Acids Res 42:D222–D230. doi:10.1093/nar/gkt1223

17. Andreeva A, Howorth D, Chandonia J-M et al (2008) Data growth and its impact on the SCOP database: new developments. Nucleic Acids Res 36:D419–D425. doi:10.1093/nar/gkm993

18. Löytynoja A, Goldman N (2010) webprank: a phylogeny-aware multiple sequence aligner with interactive alignment browser. BMC Bioinformatics11:579.doi:10.1186/1471-2105-11-579

19. Cock PJA, Antao T, Chang JT et al (2009) Biopython: freely available Python tools for computational molecular biology and bioinformatics. Bioinformatics 25:1422–1423. doi:10.1093/bioinformatics/btp163

20. Stajich JE, Block D, Boulez K et al (2002) The Bioperl toolkit: Perl modules for the life sciences. Genome Res 12:1611–1618. doi:10.1101/gr.361602

21. Eddy SR (1998) Profile hidden Markov models. Bioinformatics 14:755–763. doi:10.1093/bioinformatics/14.9.755

22. Gough J, Chothia C (2002) SUPERFAMILY: HMMs representing all proteins of known structure. SCOP sequence searches, alignments and genome assignments. Nucleic Acids Res 30:268–272. doi:10.1093/nar/30.1.268

23. Benson DA, Clark K, Karsch-Mizrachi I et al (2014) GenBank. Nucleic Acids Res 42:D32–D37. doi:10.1093/nar/gkt1030

24. Berman HM, Westbrook J, Feng Z et al (2000) The protein data bank. Nucleic Acids Res 28:235–242. doi:10.1093/nar/28.1.235

25. UniProt Consortium (2014) Activities at the universal protein resource (UniProt). Nucleic Acids Res 42:D191–D198. doi:10.1093/nar/gkt1140

26. Wu CH, Yeh L-SL, Huang H et al (2003) The protein information resource. Nucleic Acids Res 31:345–347. doi:10.1093/nar/gkg040

27. Bailey TL, Elkan C (1994) Fitting a mixture model by expectation maximization to discover motifs in biopolymers. Proc Int Conf Intell Syst Mol Biol 2:28–36

28. Nei M, Rooney AP (2005) Concerted and birth-and-death evolution of multigene families. Annu Rev Genet 39:121–152. doi:10.1146/annurev.genet.39.073003.112240

29. Moore I, Schell J, Palme K (1995) Subclass-specific sequence motifs identified in Rab GTPases. Trends Biochem Sci 20:10–12

30. Pfeffer SR (2005) Structural clues to Rab GTPase functional diversity. J Biol Chem 280:15485–15488. doi:10.1074/jbc.R500003200

31. Khan AR, Ménétrey J (2013) Structural biology of Arf and Rab GTPases' effector recruitment and specificity. Structure 21:1284–1297. doi:10.1016/j.str.2013.06.016

Chapter 3

Rab-NANOPS: FRET Biosensors for Rab Membrane Nanoclustering and Prenylation Detection in Mammalian Cells

Arafath Kaja Najumudeen, Camilo Guzmán, Itziar M.D. Posada, and Daniel Abankwa

Abstract

Rab proteins constitute the largest subfamily of Ras-like small GTPases. They are central to vesicular transport and organelle definition in eukaryotic cells. Unlike their Ras counterparts, they are not a hallmark of cancer. However, a number of diseases, including cancer, show a misregulation of Rab protein activity. As for all membrane-anchored signaling proteins, correct membrane organization is critical for Rabs to operate. In this chapter, we provide a detailed protocol for the use of a flow cytometry-based Fluorescence Resonance Energy Transfer (FRET)-biosensors assay, which allows to detect changes in membrane anchorage, subcellular distribution, and of the nanoscale organization of Rab-GTPases in mammalian cell lines. This assay is high-throughput amenable and can therefore be utilized in chemical-genomic and drug discovery efforts.

Key words Rab, GTPase, Geranylgeranylation, FRET, Flow cytometry, Nanocluster, Trafficking, Membrane, Drug discovery

1 Introduction

1.1 The Emergence of Signaling Protein Nanocluster

The Singer–Nicolson fluid mosaic model of cellular membranes integrated membrane proteins into a functional two-dimensional lipid matrix [1]. They already acknowledged that clustering of proteins by antibodies could induce biological functions. Another step in the conceptualization of the membrane organization emerged in the mid-1990s with the lipid-raft model. Simons et al. proposed dynamic cholesterol- and sphingolipid-rich lipid platforms that organize signaling proteins [2, 3]. This represented a new perspective, as it associated special signaling units with specific submicroscopic lipid domains. Literally the invisibility of these submicroscopic domains as well as ambiguities and inappropriateness of standard biochemical approaches that were used in this context rendered this model very contentious [4]. Only with the application of sophisticated fluorescence microscopic techniques was it recently possible

to demonstrate that specific lipids experience transient trapping when diffusing in the membrane; an observation, which was however not explained with stable lipid domains [5, 6].

Already earlier in the wake of the lipid-raft model, submicroscopic clusters of proteins were found. The group of Jitu Mayor described nanoscale clusters of GPI-anchored proteins [7–9], while Hancock and Parton demonstrated the existence of similarly dimensioned Ras signaling packages in the plasma membrane, which they called nanocluster [10–12]. In the following years, their work showed that the activity of the small GTPase Ras is not only regulated by GTP loading, but in addition requires its up-concentration into 6–8 protein-containing membrane nanodomains that depend partially on the integrity of the actin cytoskeleton and a specific lipid content [13–15]. Most importantly, nanoclusters of activated Ras are the only effective sites of Ras-binding protein recruitment [15–18]. Thus, Ras nanocluster represents the true gate keepers in Ras-signaling propagation, as downstream effectors typically require binding to membrane anchored (nanoclustered) Ras for their activation. These signaling protein packages can be regulated by nanocluster scaffolding proteins, such as galectin-1 or -3, which increase the stability of H- and K-ras nanocluster, respectively [18–22]. Surprisingly, also inhibitors of the Ras effector Raf have been found to specifically increase K- and N-ras nanoclustering; a finding which provides an explanation for the paradoxical up-regulation of the MAPK pathway in Ras-transformed cells [23]. Instructed by their very C-terminal membrane anchoring part, nanoclusters of H- and K-ras are laterally segregated [13, 19, 24]. Interestingly, it is this C-terminal hypervariable region, which differs most between Ras paralogs, suggesting the exciting possibility that biological and functional specialization may be intimately linked to distinct types of nanoclusters.

These features and the general importance of Ras nanoclustering advocate that targeting Ras nanoclustering with innovative drugs could provide an unprecedented avenue to attenuate, even paralog-specifically, oncogenic Ras signaling. Indeed, recent reports suggest that compounds can be discovered, which modulate Ras nanoclustering and signaling in a paralog-specific fashion [25–28].

1.2 Rab Protein Membrane Anchorage and Nanoclustering

In principle, many fundamental observations made around Ras nanoclustering should also apply to other signaling proteins, as the further up-concentration of the proteins in nanoclusters would in general increase the rate of successful protein (from the cytosol)-to-protein (in the membrane) collisions. However, signaling protein nanoclustering remains underexplored, with only very few research groups working in the field. We postulate that this signaling architecture may be more common, or even the default situation for membrane proteins, as suggested by the evidence for other signaling nanoclusters of Rho proteins, heterotrimeric G proteins

[29, 30] and Src-kinases [29, 31], as well as Rab small GTPases [25]. Interestingly, the nanoclusters of Rab8a and Rab23 that were demonstrated to exist in the plasma membrane using electron microscopic- and FRET-analysis, had a similar size yet a distinct co-clustering behavior in the membrane [25].

In order to be anchored to the membrane, Rab proteins require the prenylation of one or two C-terminal cysteines [32, 33]. As compared to other small GTPases, Rab proteins require complexation with REP (Rab escort protein), which recognizes the full-length Rab and presents it to RabGGT (Rab geranylgeranyl transferase) for prenylation [34]. Correct subcellular distribution of Rabs seems to be a complex process, which is not only determined by the specific C-terminus but requires the interplay with regulators of Rabs [35].

Functional impairment of several Rab proteins and their prenylation apparatus have been associated with cancer promotion and other diseases [36, 37]. However, only few moderately potent inhibitors of RabGGT exist [38–42] and nothing is known about the regulators of Rab nanoclustering.

1.3 Functioning and Design of Rab-NANOclustering and Prenylation Sensors (NANOPS)

Nanoclusters have dimensions below the resolution limit of classical light microscopes and can therefore only be detected by advanced microscopic techniques, including electron microscopy and superresolution microscopic methods [18, 43]. Also Förster (or fluorescence) resonance energy transfer (FRET) can report on nanoclustering, as FRET can increase in a two-dimensional surface system such a biological membrane, due to protein clustering [44–46]. In order to study FRET in membranes, biomolecules such as proteins are labeled with donor and acceptor fluorophores and the dependence of FRET on the donor–acceptor ratio, as well as on the acceptor surface density is determined [29, 45]. FRET is then a measure not for specific protein binding, but for the nanoscale packing of the labeled proteins in the membrane.

We have implemented this approach in a flow cytometric analysis procedure, which offers the advantage of analyzing thousands of cells within seconds on one continuous fluorescence intensity scale that covers the biologically accessible expression levels. To this end, we adapted a sensitized acceptor emission FRET approach, where three fluorescence channels for donor, acceptor, and FRET signal are set up [47]. Crosstalk between these channels is determined, using cells that express either of the FRET fluorophores. We use monomeric derivatives of EGFP fluorescent proteins [48, 49], the cyan mCFP as donor and the yellow mCit as acceptor. The latter is yet a derivative of citrine, an improved version of EYFP [50]. Normalization for the acceptor expression level is performed with fluorescent beads of fixed intensity, while calibration for the donor–acceptor ratio, as well as for the FRET efficiency is conducted with cells expressing a mCFP–mCit fusion protein.

Using this approach, we recently designed Rab-NANOPS (NANOclustering and Prenylation Sensors) that report on the functional membrane anchorage of Rab proteins [25]. As compared to related FRET biosensors that we have developed, the Rab biosensor requires the full-length protein as a fusion partner of the fluorescent proteins, due to the demands of the prenylation machinery. In the course of establishing the biosensor, we could show that the nanoclustering-associated FRET value, E_{max}, may be specific for the Rab protein that was genetically fused to the C-terminus of fluorescent proteins mCFP or mCit. We selected the Rab5aQ79L mutant as a prototypic sensor, as it exhibits a comparatively good dynamic FRET range. As membrane nanoclustering-associated FRET of Rab proteins certainly depends on Rabs being membrane anchored, this assay is suitable to detect inhibitors of Rab membrane anchorage and distribution. Thus, inhibitors of the prenyl-biosynthesis pathway, such as statins, as well as specific inhibitors of RabGGT can be discovered with this method.

In summary, inhibiting, e.g., Rab prenylation lowers the membrane-bound fraction of the Rab-NANOPS, thus leading to a lower FRET signal in mammalian cells. Therefore, Rab-NANOPS represents a unique tool to screen in cells not only for chemical, but also genetic modulators of Rab subcellular distribution, membrane anchorage, and nanoclustering.

Here we describe in detail the flow cytometric FRET analysis of the cellular activity of a RabGGT inhibitor on Rab-NANOPS.

2   Materials

2.1   Cell Culture

1. Human Embryonic Kidney (HEK) EBNA cells (ATCC® CRL-1573™) and Baby Hamster Kidney (BHK) cells (ATTC® CCL-10™). Other cell lines can also be used; however, the transfection efficiency and overexpression potential of the cells should be determined or considered before use (*see* **Note 1**).

2. Cell culture dishes (100 mm), sterile glass pipettes, autoclaved pipette tips, cell counting chamber (hemocytometer), and light microscope.

3. Dulbecco's Modified Eagle's Medium (DMEM) supplemented with 10 % FBS, L-glutamine, penicillin (100 U/ml), and streptomycin (100 μl/ml): Medium used for cell culture.

4. Trypsin–EDTA, Phosphate Buffer Saline (PBS): Other solutions needed to culture BHK cells.

5. 6-Well and 96-well cell culture plates: other plates needed for preparing samples.

6. jetPRIME transfection reagent (Polyplus-transfection SA): Reagent used for plasmid transfection. If desired another transfection reagent can be used (*see* **Note 1**).

7. pmCFP-C1, pmCit-C1, pmCFP-Cit-N1: Plasmids encoding the monomeric cyan (mCFP), monomeric citrine (an enhanced and halogen insensitive YFP derivative [50]) fluorescent proteins, and a genetic fusion construct of mCFP–mCit that is used as FRET positive control and for calibration purposes.

8. pmCFP-C1-Rab5aQ79L, pmCit-C1-Rab5aQ79L, pmCFP-C1-Rab8a, pmCit-C1-Rab8a: Plasmids encoding the constitutively active Rab5a and wild-type Rab8a, N-terminally labeled with either mCFP or mCit fluorescent proteins.

9. The chemical compound NE-10790 (3-PEHPC, 2-hydroxy-2-phosphono-3-pyridin-3-yl-propionic acid) was a generous gift from Dr. Katarzyna Błażewska, Institute of Organic Chemistry, Łódź University of Technology, Poland and was described in [51]. NE-10790 is first dissolved in PBS and adjusted to pH 7.0. This stock solution was then further diluted with culture medium to the desired concentration for testing.

10. 5 mM EDTA in PBS and 4 % paraformaldehyde (PFA) in PBS: solutions for detaching and fixing cells, respectively.

2.2 Flow Cytometer Settings and Sensitized Acceptor Emission FRET Channel Setup

The flow cytometer should be equipped with a high-throughput sampler (HTS) unit for analyzing samples from 96-well plates. Moreover, it should allow for the setup of three channels for measuring FRET using the sensitized acceptor emission FRET method.

The following settings and filters are appropriate for measuring FRET between ECFP and EYFP derivatives on a LSRII flow cytometer (BD Biosciences).

1. Two lasers were used on the BD LSRII: (1) a Coherent Vioflame™ 20 mW solid-state GaN laser equipped with violet optics was used for direct excitation of mCFP; (2) a Coherent Sapphire™ 25 mW solid-state Argon-ion laser was used for mCit excitation.

2. mCFP fluorescence was detected using a 440/40 nm Band-Pass (BP) filter. A 505 Long-Pass (LP) dichroic was used for separating mCFP fluorescence and FRET emission. FRET signal was detected using a 585/42 nm BP filter. The mCit fluorescence was detected using a 530/30 nm BP filter (Table 1).

Table 1
Filter setup for FRET measurements on LSRII flow cytometer

Laser name	Excitation (nm)	Emission filters (nm)	Detection channel
Violet	405	440/40 BP	Donor
	405	585/42 BP	FRET
Blue	488	530/30 BP	Acceptor

3. Fluorescein isothiocyanate (FITC) beads (Bangs Laboratories) with a mean diameter 7.30 μm and Molecular Equivalent of Soluble Fluorophore (MESF) value of 1,445,293 were used to calibrate normalized acceptor levels.

2.3 Data Evaluation and Analysis Software

To perform the FRET analysis of flow cytometer data, we use a custom-written procedure in Igor Pro (WaveMetrics) that is available upon request.

3 Methods

The following protocol describes the experimental steps to record in duplicate nine-point dose–response curves of NE-10790 with Rab5-NANOPS and Rab8-NANOPS; note however, the latter is a monoprenylated Rab, which is not inhibited by that compound [38]. The protocol can be adjusted depending on the investigator's needs.

3.1 Preparation of Cells

1. Preheat the cell culture medium and PBS to 37 °C for 30 min in a water bath. Bring the trypsin–EDTA to room temperature before use.

2. Cell culture should be done in the aseptic environment of a laminar flow cabinet using sterile cell culture dishes, glass pipettes, and autoclaved pipette tips.

3. Grow cells to a maximal confluency of 80 % in 100 mm cell culture dishes. Once the cells reach confluency, remove the medium from the culture dish and gently wash the cells with 10 ml of sterile PBS. Remove PBS and detach the cells with 1 ml of 0.25 % trypsin–EDTA. Put the plate back into the incubator for 1–5 min.

4. As soon as cells detach add 10 ml of culture medium and suspend the cells by pipetting using a glass pipette.

5. To count the number of cells in the suspension, put a cover glass on the hemocytometer and pipette 10 μl of cell suspension to one of the counting areas. Count the cells using the light microscope.

6. To each well of a sterile six-well cell culture plate, add 2×10^5 cells from the cell suspension and fresh culture medium to a final volume of 2,000 μl (*see* Fig. 1 *for details*).

7. After 24 h, do the transfections following the instructions from the manufacturer of the transfection reagent used. Here, transfections with jetPrime are described. Prepare a transfection mix with 200 μl of jetPrime buffer and 4 μl of jetPrime transfection reagent for each transfection. Prepare the following set of samples using the amount of DNA specified for each plasmid (*see* Fig. 1 *for details and refer to* **Note 2**).
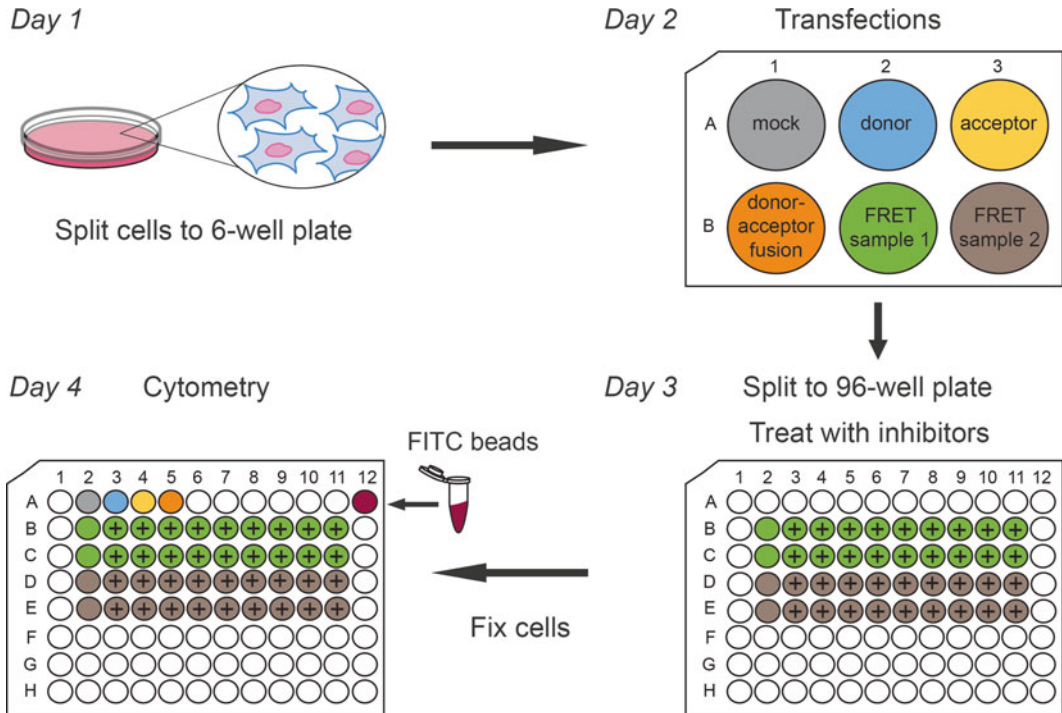
Fig. 1 Schematic representation of sample workflow for flow cytometric FRET analysis of cells expressing Rab-NANOPS. BHK cells are split into a 6-well plate (Day 1) and transfected 24 h later with plasmids as indicated in color-coded wells (Day 2). 24 h after transfection, the FRET samples are split into 96-well plates for compound treatment (denoted with "+") (Day 3). After treatment, the cells are detached with 5 mM EDTA in PBS and fixed with 4 % PFA in PBS. Then fixed control cells including mock/untransfected, donor, acceptor, and FRET-positive control cells are added to the plate. The plate with these cell samples along with FITC beads is then analyzed using a fluorescence flow cytometer (Day 4)

FRET calibration control samples

(a) Mock transfected (e.g., with pcDNA3) or untransfected cells

(b) 2.0 μg of pmCFP-C1

(c) 2.0 μg of pmCit-C1

(d) 2.0 μg of pmCFP-Cit-N1

FRET samples

(a) 1.0 μg of pmCFP-C1-Rab5aQ79L+1.0 μg pmCit-C1-Rab5aQ79L

(b) 1.0 μg of pmCFP-C1-Rab8a+1.0 μg pmCit-C1-Rab8a

     Vortex the transfection mix and incubate for 10 min at room temperature. Add the transfection mix to the wells drop wise, gently rock the plate and place it back in the incubator.

8. Sixteen hours after transfection remove the medium from the FRET samples and add 200 μl of 5 mM EDTA in PBS and incubate the plate at 37 °C for 2–5 min to detach the cells. After the cells detach, add 800 μl of fresh medium and suspend the cells. Harvest the cells by centrifugation for 3 min at 200 RCF (relative centrifugal force), discard the supernatant medium and resuspend the cell pellet in 500 μl of fresh medium. Count the cells as mentioned in **step 5** of Subheading 3.1.

9. To a 96-well multiwell culture plate, add 50,000 cells in 200 μl fresh culture medium per well to 20 wells (1 untreated + 9 treated conditions = 10 together × 2). Return the plate to the incubator (*see* **Note 3**).

10. After the cells have attached to the bottom of the 96-well plate (usually after 5–7 h), remove the medium and treat the cells with fresh medium containing inhibitors (in this case, NE-10790) at the desired final concentrations (*see* **Note 4**).

11. Twenty-four hours after treatment remove the medium and add 75 μl of 5 mM EDTA in PBS to each well of the 96-well plate. Incubate the plate for 2–5 min; after the cells detach, add 75 μl of 4 % PFA to fix the cells for 15 min at room temperature.

12. Store the samples at 4 °C until cytometric analysis.

3.2 Sample Preparation Before Flow Cytometry

1. Resuspend the cells in PBS or better run the individual samples through a cell strainer cap tube to make single-cell suspensions.

2. Prepare for cytometer FRET calibration using the mock control (mock or untransfected cells), pmCFP-C1, pmCit-C1 and pmCFP-Cit-N1 transfected samples.

3. Before cytometry make sure the control samples and FRET samples are in the same 96-well plate in approximately equal volume of 150 μl (*see* Subheading 3.3, **step 6**).

3.3 Flow Cytometry and Data Acquisition

Cells were analyzed here on a LSR II flow cytometer, while comparable instruments can be used. To perform the following procedure, it is necessary to have at least basic knowledge of flow cytometry and usage of the particular cytometer. The following measurements have to be performed without any fluorescence compensation enabled on the cytometer (*see* **Note 5**).

1. Start with the pmCFP-Cit-N1 transfected sample as the control that gives signal in all channels.

2. Set the forward-scatter area (FSC-A) and side-scatter area (SSC-A) in linear mode to see the population on the scatter plot

   (a) Create a polygonal gate 1 (Intact cells) around the major, intact cell population (*see* Fig. 2a *for details*).
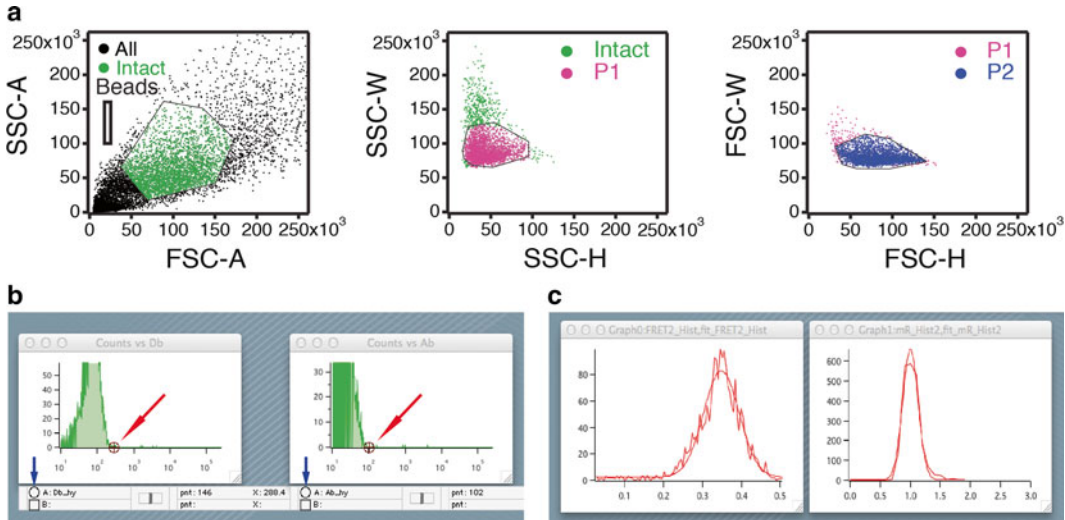
Fig. 2 Flow cytometer doublet discrimination and analysis steps of FRET data using "FACS-FRET.pxp" in Igor Pro. (**a**) Intact cells *(green)* were identified by their forward-scatter area (FSC-A) and side-scatter area (SSC-A) profile. The cells in the intact gate (*green*) are plotted in SSC-W/SSC-H to discriminate doublet cells by their side-scatter signal (P1-*pink*). The cells from P1 are plotted in FSC-W/FSC-H to discriminate doublet cells further by forward scatter (P2-*blue*). Only cells from P2 are used for data analysis. The small rectangular gate on the left in the FSC-A/SSC-A plot marks the beads. (**b**) Example of windows "Counts vs. Db" and "Counts vs. Ab" illustrating where to position the cursor A for selection of background thresholds. *Blue arrows point* to the location of cursor A from where it is dragged and dropped to the position of the *red arrows*. (**c**) *Left*: Example of plot "FRET2_Hist" showing a Gaussian distribution of the positive control sample with a centre close to 0.35 after calibration of the G-factor. *Right*: Example of plot "mR_Hist2" showing Gaussian distribution of the same sample with the centre on 1 after calibration for the donor–acceptor ratio correction factor

     (b) Create a SSC-W/SSC-H plot so that only cells from gate 1 are displayed.

     (c) Create population-1 (P1) as shown to discriminate doublet cells by their side-scatter signal.

     (d) Create an FSC-W/FSC-H plot to display only cells from population-1 and create population-2 (P2) to discriminate forward-scatter doublet cells.

     (e) Only singlet cells from this population-2 (P2) are used in this analysis.

3. Next create the following plots of the fluorescence channels in logarithmic scale.

     (a) Three histogram plots for monitoring fluorescence intensities of the donor, acceptor, and FRET detection channels. With these histograms the amplification voltage of the channels is set such that all events fall within the detection range. Nonexpressing cells can typically be recognized as a large low-intensity peak to the left.

     (b) Three dot plots for correlation of signals for the channel pairs of donor/acceptor, donor/FRET, and FRET/acceptor.

(c) One histogram plot for monitoring FITC beads in the acceptor channel.

4. Set the cytometer to acquire a total of 10,000 events. Set the gated populations to display 5,000 events.

5. Run the FITC beads sample and create a rectangular gate to mark the beads in the FSC-A/SSC-A plot (*see* Fig. 2a *for details*) and store these beads events in the *beads gate* (*see* **Note 6**).

6. Run the following samples in a 96-well plate as illustrated in Fig. 1.

   (a) Mock or untransfected (colored in gray in Fig. 1, *see* **Note 7**)

   (b) Donor (pmCFP-C1) (blue)

   (c) Acceptor (pmCit-C1) (yellow)

   (d) Donor–acceptor fusion (pmCFP-Cit-N1) (orange)

   (e) FRET sample 1 (Rab5a-NANOPS) (green)

   (f) FRET sample 1 (Rab5a-NANOPS treated with concentration series of NE-10790) (green with '+')

   (g) FRET sample 2 (Rab8a-NANOPS) (brown)

   (h) FRET sample 2 (Rab8a-NANOPS treated with concentration series of NE-10790) (brown with '+')

7. After acquisition, export the data from 5. Only from that beads gate and from 6. Only from the gated population 2 (P2) in both cases saving them as FCS 3.0 format files with extension ".fcs".

3.4 Flow Cytometer FRET Data Analysis   The analysis described here corresponds to the steps performed in our custom-written Igor Pro procedure that can be obtained upon request (*see* **Note 8**). Expert performance of this analysis requires a thorough understanding of FRET in a two-dimensional (membrane) system, e.g., as described in Berney et al. [45]. Our procedure converts the three detection channel flow cytometric data into FRET data that can be compared across independent experiments. In brief, it normalizes the acceptor concentration for each experiment to that of the fluorescent beads and calibrates the FRET efficiency and donor–acceptor ratio. All of these parameters are calculated per cell/event using an adapted sensitized acceptor emission method [47]. For each sample, the cellular FRET levels are plotted in dependence of the acceptor expression levels, at constant donor–acceptor ratio. A typical plot shows an increase of FRET with increasing acceptor levels following approximately a saturation curve (Fig. 3). This data trend is then fitted with an exponential curve function that yields the maximum FRET efficiency, E_{max}, as the parameter characteristic of the nanoclustering-associated FRET in the sample. E_{max} is determined as the FRET efficiency at high acceptor expression levels [24, 29].
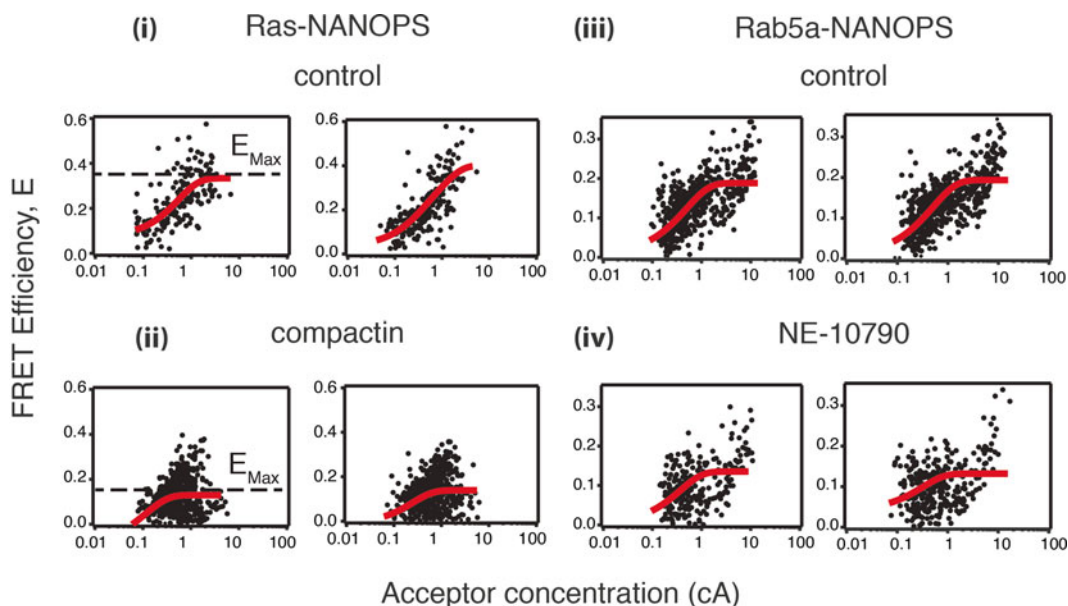
Fig. 3 Examples of nanoclustering FRET plots from NANOPS samples. Representative plots of processed cytometer FRET data of Ras- and Rab-NANOPS that will individually also be stored in the folder containing the FRET samples. Examples of analyzed cells, expressing (i) Ras-NANOPS, as compound solvent-treated control; (ii) Ras-NANOPS treated with 5 μM compactin; (iii) Rab5a-NANOPS, as compound solvent-treated control; (iv) Rab5a-NANOPS treated with 500 μM NE-10790. The plots show the dependence of the FRET efficiency, E, on the acceptor concentration (cA) at a constant donor–acceptor ratio of ~1:1. The characteristic E_{max} value (*dotted line*) was determined by exponential fitting (*red curve*) of single cell data (*black dots*)

In this section, we present the main steps that need to be executed within this Igor Pro procedure, together with a brief description of the analysis and calibration performed by those steps.

1. Using Igor Pro open the file "FACS-FRET.pxp."

2. On the menu bar tab "FRET-FACS" go to "1. Input Control Data." This will create a new button menu. Click on "Load Donor" to import the ".fcs" file from the donor-only sample (pmCFP-C1 transfected cells).

3. Make sure that the donor-only data are correct by visually inspecting the different plots that will appear. These plots should correspond to the plots that you have set up during data acquisition on the flow cytometer. Close all the plots by clicking on "Close Donor Graphs."

4. Click on "Load Acceptor" to import the ".fcs" file from the acceptor-only sample (pmCit-C1 transfected cells).

5. Make sure that the acceptor-only data are correct by visually inspecting the different plots in analogy to what is described under 3. Close all the plots by clicking on "Close Acceptor Graphs."

6. On the menu tab "FRET-FACS" go to "2. Cross Talk Factors." This will create a second button menu. Click on "Calculate Factors" to calculate crosstalk factors (R), which are needed to correct the signals in the donor-, acceptor-, and FRET-detection channels for the true signals that emerge only from the donor, etc. The plots display the R-factors calculated for each individual cell on the y-axes vs. the donor (Dd) or acceptor (Aa) signal of the cell on the x-axes. At low signal, the error on the signals is too high (strong deviation from otherwise constant R-factor), which requires us to discard these data points by thresholding.

7. Click on "Threshold" and enter into the popup window the approximate signal levels from the x-axis above which the R-factors do not deviate anymore (*see* **Note 9**).

8. Click on "Average" to calculate the final crosstalk factors by averaging over all the thresholded data points. This will also close all the R-factor graphs.

9. On the menu tab "FRET-FACS" go to "3. Beads and Untransfected Cells." This will create a third button menu. Click on "Load Beads" to import the ".fcs" file from the fluorescein isothiocynate (FITC) beads, which are used for cell size and acceptor signal normalization.

10. Make sure that the beads data is correct by visually inspecting the different plots, which are again re-created from the cytometer acquisition layout. Size and intensity parameters from the beads are obtained by clicking on "Mark Beads." This will also close all corresponding plots.

11. Click on "Load Untransfected Cells" to import the ".fcs" file from the mock or untransfected sample.

12. Make sure that the data from this sample is correct by visually inspecting the different plots that will appear. These plots correspond to the same plots you had during data acquisition on the flow cytometer.

13. On the window "Counts vs. Db" mark the point where the histogram of the donor channel signal has dropped close to zero. This marks the background level below which nontransfected cells are detected in that channel. To do this simply drag the A cursor (circle on the bottom left of the panel below the plot) to the right side of the histogram. Repeat the same procedure in the "Counts vs. Ab" window (*see* Fig. 2b).

14. Click on "Mark Background" and confirm in the popup menu that the background was marked, by selecting "Done" twice. Then click continue (*see* **Note 10**). After this, all plots will be closed.

15. On the menu tab "FRET-FACS" go to "4. Input FRET Positive Control." This will create a fourth button menu. Click on "Load FRET Positive" to import the ".fcs" file from the FRET-positive control sample (pmCFP-Cit-N1).

16. Make sure that the FRET positive control data is correct by visually inspecting the different plots that will appear. Again these plots should correspond to the same plots you had during data acquisition on the flow cytometer. Click on "Threshold" to apply the background threshold that was set in **step 13**. This will also close all the plots and display FRET data plots (*see* **Note 11**). In particular, the plot "FRET2 vs. Ab" should show all data points at approximately the same FRET2 value, except for those at low Ab values, which is due to noise in the biological system (*see* **Note 12**).

17. Click on "Calculate G" to calibrate for the correct value of G (*see* **Note 13**). This factor is essential to convert the FRET2 value to the correct FRET efficiency (relative to the fusion protein). A popup window will appear that allows the user to input an estimated starting value, typically ranging from 0.5 to 4. New plots will appear that allow the user to control if the G value has been calibrated correctly. Visually inspect the plot containing "FRET2_Hist" in its title bar and verify that the centre of the Gaussian fit is very close to 0.35 on the *x*-axis (*see* Fig. 2c and **Note 13**). Moreover, the centre of the Gaussian fit in the plot containing "mR_Hist2" in its title bar should be on 1. If either of this is not the case, repeat the procedure using a different starting value for G, which differs, e.g., by 0.5 from the one chosen before. Once you are satisfied with the results click "G is good," this will close all the plots and store the final G value.

18. On the menu tab "FRET-FACS" go to "5. Batch Analysis" the final step, where you will calculate the calibrated FRET analysis parameters of your NANOPS FRET samples. Click on "Analyse Batch" on the new button menu and choose the folder with your NANOPS FRET samples. This folder should contain the ".fcs" files corresponding samples saved during the data acquisition. Results will be displayed in a table with the name of each ".fcs" file, the corresponding maximum FRET efficiency E_{max} and other parameters which can be disregarded at this step (*see* **Note 14**). Examples of processed FRET efficiency plots are presented in Fig. 3.

4 Notes

1. BHK21 cells are well tested and give the required high protein expression and transfection efficiency. However, other cell lines like HEK 293 and HEK 293 EBNA cells have also been

used successfully for this FRET analysis [24, 25, 31]. For all of these cell lines, jetPrime or Fugene6 have been the transfection reagents of choice, due to their consistency in yielding high protein expression levels. This is needed in order to determine the maximal FRET efficiency at high acceptor expression levels. However, the investigator should establish the desired transfection efficiency and high protein expression levels of the cell line of choice before starting with drug treatment experiments. Cell culture and growth requirements of different cell lines should be monitored as they can significantly affect the transfection efficiency.

2. For FRET measurements at 1:1 donor–acceptor protein ratio, a DNA ratio of 1:1 of donor and acceptor DNA plasmids is recommended to begin with. It may however be important that the investigator empirically determines the DNA ratio for each pair of FRET plasmids, which yields approximately a 1:1 protein ratio. This can be followed in the saved results files "[sample name]_oligo.jpg," which plot the FRET efficiency vs. the molar fraction of the donor. A molar fraction of 0.5 corresponds to 1:1 donor–acceptor ratio. It is advisable to prepare the control samples in 6-well plates as it gives more sample volume for both instrument calibration and final acquisition.

3. The FRET samples in the 96-well plate can be used to test different inhibitors or different concentrations of the same inhibitor.

4. Whenever possible, take efforts to keep the final concentration of DMSO at less than 1 % of the final volume of the medium on cells.

5. The LSRII flow cytometer used here is equipped with a 405 nm laser that is used for mCFP excitation. Other models of flow cytometers can be used provided a separate laser tuned to ≤440 nm is available for mCFP excitation. In some cytometers, one might have to change filters for proper detection and acquisition of the fluorescence signals. Technical expert advice by the flow cytometer manufacturer is recommended.

6. It is important to save the beads in a separate gate to remove the defective or doublet beads from the analysis. It is not possible to do such gating in the Igor Pro procedure.

7. Mock cells (transfected with empty plasmid vector) or untransfected cells (no transfection) can be used. However, it is advisable to prepare both samples whenever a new transfection reagent is tested. For example, we have observed that using Lipofectamine can affect the scattering pattern of mock cells and subsequent nanoclustering-FRET readouts.

8. A license for Igor Pro by WaveMetrics is required if the reader intends to use the FRET analysis routine that we describe in this book chapter.

9. If the user is not satisfied with the chosen threshold value, there is the possibility to revert this threshold, using the button "Unthreshold" in the "Cross Talk Factors" button menu.

10. In this particular popup window, if you choose the option "Not Yet" or click on "Cancel," the window will be closed and nothing will happen, until you actually mark the background threshold and choose "Done."

11. The plots are: FRET2 vs. mR, FRET2 vs. Ab, Aba vs. Ab, and Aba vs. Dbd. These variables are basically as described in [47]. Specifically, FRET2 is the uncalibrated, but fully crosstalk corrected FRET efficiency; Ab is the signal of the FRET sample in the acceptor channel; Aba is the corrected signal of only the acceptor in the acceptor channel in the FRET sample; Dbd is the corrected signal of only the donor in the donor channel in the FRET sample; mR is linked to the calibration factor for the donor–acceptor ratio, R: $mR = Dbd/(Aba*R)$, therefore mR corresponds to [donor]/[acceptor].

12. These plots are made using a calibration factor $G = 1$. This G value is not necessarily the correct one and on further steps it will be fitted to its correct value using the known FRET efficiency of our fusion protein (FRET-positive control).

13. In the case of our FRET-positive control sample (pmCFP-Cit-N1), FRET has been determined to have an $E_{max} = 0.35 \pm 0.03$ [29]. This value is therefore used to calibrate for the correct value of G that was assigned arbitrarily in step 16 of this analysis. This value remains constant for each experimental run, where the gain settings on the detection channels of the cytometer are not altered.

14. On the folder that contains all your study samples and that you selected for analysis, several plots containing the detailed results are automatically stored as ".jpg" files. In particular, you will have a plot named "[sample name].jpg" displaying the FRET efficiency vs. normalized acceptor surface concentration and also containing the fitted curve that yields the maximum FRET efficiency (E_{max}).

References

1. Singer SJ, Nicolson GL (1972) The fluid mosaic model of the structure of cell membranes. Science 175:720–731

2. Simons K, van Meer G (1988) Lipid sorting in epithelial cells. Biochemistry 27:6197–6202

3. Simons K, Ikonen E (1997) Functional rafts in cell membranes. Nature 387:569–572. doi:10.1038/42408

4. Hancock JF (2006) Lipid rafts: contentious only from simplistic standpoints. Nat Rev Mol Cell Biol 7:456–462. doi:10.1038/nrm1925

5. Eggeling C, Ringemann C, Medda R et al (2009) Direct observation of the nanoscale dynamics of membrane lipids in a living cell. Nature 457:1159–1162. doi:10.1038/nature07596

6. Mueller V, Ringemann C, Honigmann A et al (2011) STED Nanoscopy Reveals Molecular Details of Cholesterol- and Cytoskeleton-Modulated Lipid Interactions in Living Cells. Biophys J 101:1651–1660. doi:10.1016/j.bpj.2011.09.006

7. Varma R, Mayor S (1998) GPI-anchored proteins are organized in submicron domains at the cell surface. Nature 394:798–801. doi:10.1038/29563

8. Sharma P, Varma R, Sarasij RC et al (2004) Nanoscale organization of multiple GPI-anchored proteins in living cell membranes. Cell 116:577–589

9. Goswami D, Gowrishankar K, Bilgrami S et al (2008) Nanoclusters of GPI-anchored proteins are formed by cortical actin-driven activity. Cell 135:1085–1097. doi:10.1016/j.cell.2008.11.032

10. Prior IA, Harding A, Yan J et al (2001) GTP-dependent segregation of H-ras from lipid rafts is required for biological activity. Nat Cell Biol 3:368–375. doi:10.1038/35070050

11. Parton RG, Hancock JF (2004) Lipid rafts and plasma membrane microorganization: insights from Ras. Trends Cell Biol 14:141–147. doi:10.1016/j.tcb.2004.02.001

12. Abankwa D, Gorfe AA, Hancock JF (2007) Ras nanoclusters: molecular structure and assembly. Semin Cell Dev Biol 18:599–607. doi:10.1016/j.semcdb.2007.08.003

13. Plowman SJ, Muncke C, Parton RG, Hancock JF (2005) H-ras, K-ras, and inner plasma membrane raft proteins operate in nanoclusters with differential dependence on the actin cytoskeleton. Proc Natl Acad Sci U S A 102:15500–15505. doi:10.1073/pnas.0504114102

14. Zhou Y, Liang H, Rodkey T et al (2014) Signal Integration by Lipid-Mediated Spatial Cross Talk between Ras Nanoclusters. Mol Cell Biol 34:862–876. doi:10.1128/MCB.01227-13

15. Tian T, Harding A, Inder K et al (2007) Plasma membrane nanoswitches generate high-fidelity Ras signal transduction. Nat Cell Biol 9:905–914. doi:10.1038/ncb1615

16. Murakoshi H, Iino R, Kobayashi T et al (2004) Single-molecule imaging analysis of Ras activation in living cells. Proc Natl Acad Sci U S A 101:7317–7322. doi:10.1073/pnas.0401354101

17. Hibino K, Watanabe TM, Kozuka J et al (2003) Single- and Multiple-Molecule Dynamics of the Signaling from H-Ras to cRaf-1 Visualized on the Plasma Membrane of Living Cells. ChemPhysChem 4:748–753. doi:10.1002/cphc.200300731

18. Guzmán C, Šolman M, Ligabue A et al (2014) The efficacy of Raf kinase recruitment to the GTPase H-ras depends on H-ras membrane conformer specific nanoclustering. J Biol Chem. doi:10.1074/jbc.M113.537001

19. Prior IA, Muncke C, Parton RG, Hancock JF (2003) Direct visualization of Ras proteins in spatially distinct cell surface microdomains. J Cell Biol 160:165–170. doi:10.1083/jcb.200209091

20. Rotblat B, Belanis L, Liang H et al (2010) H-Ras nanocluster stability regulates the magnitude of MAPK signal output. PLoS One 5:e11991. doi:10.1371/journal.pone.0011991

21. Belanis L, Plowman SJ, Rotblat B et al (2008) Galectin-1 is a novel structural component and a major regulator of H-Ras nanoclusters. Mol Biol Cell 19:1404–1414. doi:10.1091/mbc.E07-10-1053

22. Shalom-Feuerstein R, Plowman SJ, Rotblat B et al (2008) K-ras nanoclustering is subverted by overexpression of the scaffold protein galectin-3. Cancer Res 68:6608–6616. doi:10.1158/0008-5472.CAN-08-1117

23. Cho K-J, Kasai RS, Park J-H et al (2012) Raf inhibitors target ras spatiotemporal dynamics. Curr Biol 22:945–955. doi:10.1016/j.cub.2012.03.067

24. Abankwa D, Hanzal-Bayer M, Ariotti N et al (2008) A novel switch region regulates H-ras membrane orientation and signal output. EMBO J 27:727–735. doi:10.1038/emboj.2008.10

25. Köhnke M, Schmitt S, Ariotti N et al (2012) Design and Application of In Vivo FRET Biosensors to Identify Protein Prenylation and Nanoclustering Inhibitors. Chem Biol 19:866–874. doi:10.1016/j.chembiol.2012.05.019

26. Cho K-J, Park J-H, Piggott AM et al (2012) Staurosporines disrupt phosphatidylserine trafficking and mislocalize Ras proteins. J Biol Chem 287:43573–43584. doi:10.1074/jbc.M112.424457

27. Zhou Y, Plowman SJ, Lichtenberger LM, Hancock JF (2010) The Anti-inflammatory Drug Indomethacin Alters Nanoclustering in Synthetic and Cell Plasma Membranes. J Biol Chem 285:35188–35195. doi:10.1074/jbc.M110.141200

28. Zhou Y, Cho K-J, Plowman SJ, Hancock JF (2012) Nonsteroidal anti-inflammatory drugs alter the spatiotemporal organization of Ras proteins on the plasma membrane. J Biol Chem 287:16586–16595. doi:10.1074/jbc.M112.348490

29. Abankwa D, Vogel H (2007) A FRET map of membrane anchors suggests distinct microdomains of heterotrimeric G proteins. J Cell Sci 120:2953–2962. doi:10.1242/jcs.001404

30. Crouthamel M, Abankwa D, Zhang L et al (2010) An N-terminal polybasic motif of Gαq is required for signaling and influences membrane nanodomain distribution. Mol Pharmacol 78:767–777. doi:10.1124/mol.110.066340

31. Najumudeen AK, Köhnke M, Šolman M et al (2013) Cellular FRET-Biosensors to Detect Membrane Targeting Inhibitors of N-Myristoylated Proteins. PLoS One 8:e66425. doi:10.1371/journal.pone.0066425.s007

32. Goody RS, Rak A, Alexandrov K (2005) The structural and mechanistic basis for recycling of Rab proteins between membrane compartments. Cell Mol Life Sci 62:1657–1670. doi:10.1007/s00018-005-4486-8

33. Nguyen UT, Goodall A, Alexandrov K, Abankwa D (2010) Isoprenoid Modifications. In: Vidal CJ (ed) Post-Translational Modifications in Health and Disease, 1st edn. Springer, New York, p 486

34. Alexandrov K, Horiuchi H, Steele-Mortimer O et al (1994) Rab escort protein-1 is a multifunctional protein that accompanies newly prenylated rab proteins to their target membranes. EMBO J 13:5262–5273

35. Li F, Yi L, Zhao L et al (2014) The role of the hypervariable C-terminal domain in Rab GTPases membrane targeting. Proc Natl Acad Sci U S A 111:2572–2577. doi:10.1073/pnas.1313655111

36. Seabra MC, Mules EH, Hume AN (2002) Rab GTPases, intracellular traffic and disease. Trends Mol Med 8:23–30

37. Recchi C, Seabra MC (2012) Novel functions for Rab GTPases in multiple aspects of tumour progression. Biochem Soc Trans 40:1398–1403. doi:10.1016/S1471-4914(01)02227-4

38. Baron RA, Tavaré R, Figueiredo AC et al (2009) Phosphonocarboxylates inhibit the second geranylgeranyl addition by Rab geranylgeranyl transferase. J Biol Chem 284:6861–6868. doi:10.1074/jbc.M806952200

39. Lackner MR, Kindt RM, Carroll PM et al (2005) Chemical genetics identifies Rab geranylgeranyl transferase as an apoptotic target of farnesyl transferase inhibitors. Cancer Cell 7:325–336. doi:10.1016/j.ccr.2005.03.024

40. Coxon FP, Ebetino FH, Mules EH et al (2005) Phosphonocarboxylate inhibitors of Rab geranylgeranyl transferase disrupt the prenylation and membrane localization of Rab proteins in osteoclasts in vitro and in vivo. Bone 37:349–358. doi:10.1016/j.bone.2005.04.021

41. Bon RS, Guo Z, Stigter EA et al (2011) Structure-Guided Development of Selective RabGGTase Inhibitors. Angew Chem Int Ed 50:4957–4961. doi:10.1002/anie.201101210

42. Watanabe M, Fiji HDG, Guo L et al (2008) Inhibitors of protein geranylgeranyltransferase I and Rab geranylgeranyltransferase identified from a library of allenoate-derived compounds. J Biol Chem 283:9571–9579. doi:10.1074/jbc.M706229200

43. Prior IA, Parton RG, Hancock JF (2003) Observing cell surface signaling domains using electron microscopy. Sci STKE 2003:PL9

44. Zimet DB, Thevenin BJ, Verkman AS et al (1995) Calculation of resonance energy transfer in crowded biological membranes. Biophys J 68:1592–1603. doi:10.1016/S0006-3495(95)80332-2

45. Berney C, Danuser G (2003) FRET or no FRET: A quantitative comparison. Biophys J 84:3992–4010

46. Wolber PK, Hudson BS (1979) An analytic solution to the Förster energy transfer problem in two dimensions. Biophys J 28:197–210

47. Gordon GW, Berry G, Liang XH et al (1998) Quantitative fluorescence resonance energy transfer measurements using fluorescence microscopy. Biophys J 74:2702

48. Zacharias DA, Violin JD, Newton AC, Tsien RY (2002) Partitioning of lipid-modified monomeric GFPs into membrane microdomains of live cells. Science 296:913–916

49. Zhang J, Campbell RE, Ting AY, Tsien RY (2002) Creating new fluorescent probes for cell biology. Nat Rev Mol Cell Biol 3:906–918. doi:10.1038/nrm976

50. Griesbeck O, Baird GS, Campbell RE et al (2001) Reducing the environmental sensitivity of yellow fluorescent protein. Mechanism and applications. J Biol Chem 276:29188–29194. doi:10.1074/jbc.M102815200

51. Coxon FP, Helfrich MH, Larijani B et al (2001) Identification of a novel phosphonocarboxylate inhibitor of Rab geranylgeranyl transferase that specifically prevents Rab prenylation in osteoclasts and macrophages. J Biol Chem 276:48213–48222. doi:10.1074/jbc.M106473200

Chapter 4

High-Throughput Assay for Profiling the Substrate Specificity of Rab GTPase-Activating Proteins

Ashwini K. Mishra and David G. Lambright

Abstract

Measurement of intrinsic as well as GTPase-Activating Protein (GAP)-catalyzed GTP hydrolysis is central to understanding the molecular mechanism and function of GTPases in diverse cellular processes. For the Rab GTPase family, which comprises at least 60 distinct proteins in humans, putative GAPs have been identified from both eukaryotic organisms and pathogenic bacteria. A major obstacle has involved identification of target substrates and determination of the specificity for the Rab family. Here, we describe a sensitive, high-throughput method to quantitatively profile GAP activity for Rab GTPases in microplate format based on detection of inorganic phosphate released after GTP hydrolysis. The method takes advantage of a well-characterized fluorescent phosphate sensor, requires relatively low protein concentrations, and can in principle be applied to any GAP-GTPase system.

Key words GTPase, Rab GTPase, Phosphate-binding protein, Phosphate, PBP-MDCC, GTP hydrolysis, GAP reaction, High throughput, GAP assay

1 Introduction

Spatiotemporal regulation of the GTP hydrolytic activity of guanine nucleotide-binding proteins (commonly referred to as GTPases) is critical for termination of diverse processes including signal transduction, protein synthesis, cytoskeletal dynamics, and membrane trafficking [1]. Slow intrinsic rates of GTP hydrolysis are generally accelerated by GTPase-activating proteins (GAPs) [2]. Impairment of intrinsic or GAP-catalyzed GTPase activity has been implicated in a number of diseases including cancer and diabetes [3, 4]. Numerous putative GAPs for Rab GTPases have been identified by bioinformatic, proteomic, and genetic approaches but in many cases the target Rab substrates and specificity profiles for the Rab family are either unknown or poorly characterized [5]. Thus, efficient, scalable, and generally applicable methods for quantifying GTP hydrolysis reactions are essential for profiling the catalytic activity of GAPs with respect to candidate GTPase

substrates and can also be used for mechanistic studies of GTP hydrolytic activity in normal and pathogenic contexts, or to support development of mechanism-based therapeutic interventions.

Although GAPs in general stimulate intrinsic GTP hydrolysis by several orders of magnitude or more, the extent of stimulation depends on the kinetic details of the enzyme–substrate combination, including the turnover number k_{cat} and the Michaelis constant K_M. Since many GAP reactions occur on cellular membranes, K_M is often in the mid micromolar to low millimolar range. For the corresponding in vitro reactions in solution, it is generally feasible to measure the catalytic efficiency (k_{cat}/K_M) rather than the individual kinetic constants. Beyond practical considerations per se, k_{cat}/K_M is a salient kinetic property of any enzyme-catalyzed reaction. Indeed, as the concentration-independent rate constant for an enzyme-catalyzed reaction under conditions where the active sites are not saturated by substrate ([GTPase] << K_M), k_{cat}/K_M is directly comparable between different GAPs and GTPases, making it a logical metric for kinetic profiles. The ratio of k_{cat}/K_M to the intrinsic rate constant (analogous to fold activation) can also be used; however, it is evidently sensitive to differences in intrinsic rate constants as well as GAP activities.

A variety of readouts have been used to detect GTP hydrolysis [6–8]. Biophysical methods such as infrared (IR) or nuclear magnetic resonance (NMR) spectroscopies that directly monitor hydrolysis are particularly informative with respect to the structural details of the chemical steps [9, 10]. Other methods indirectly monitor hydrolysis by detecting differences in effector-binding affinity or spectroscopic properties (e.g., intrinsic tryptophan or extrinsic fluorophore-labeled nucleotide fluorescence) between the GTP- and GDP-bound conformations [6, 11] or by monitoring the release of inorganic phosphate (P_i), which can be quantified, for example, by radiolabel detection, enzyme-coupled reactions, or binding to phosphate-binding proteins [12–14]. Despite strengths for particular applications, most readouts for hydrolysis are either inefficient, insensitive, poorly scalable, not generally applicable, reagent consumptive, or measure end points rather than real-time kinetics.

In this chapter, we describe a quantitative, high-throughput method for profiling Rab GAP catalytic efficiency in which release of inorganic phosphate (P_i) following GTP hydrolysis is continuously monitored using a rapid, fluorescence-based "phosphate sensor" consisting of a engineered cysteine variant of the *E. coli* phosphate-binding protein labeled with 7-Diethylamino-3-[*N*-(2-maleimidoethyl) carbamoyl]coumarin (PBP-MDCC) [12, 15]. Due to high binding affinity and rapid association kinetics, the well-characterized PBP-MDCC sensor can detect nanomolar changes in [P_i] on the timescale of a few milliseconds and is suitable for both microplate and stopped flow kinetic measurements [12]. The method described here, along with a related first-generation variation using a less sensitive absorbance-based readout involving

the purine nucleoside phosphorylase-coupled reaction of P_i with 7-methyl-thioguanosine substrate (MESG) [13], has been used to identify Rab substrates for GAPs from eukaryotic organisms as well as prokaryotic pathogens [16–26]. Since the readout is sensitive and does not depend on the details of the particular GAP-GTPase pair, the basic method could easily be adapted to other GTPase families or used for applications requiring large-scale analyses of GAP activity.

2 Materials

2.1 Reagents and Chemicals

1. Tris(hydroxymethyl)aminomethane   hydrochloride   (Tris–HCl), BioUltra grade (Sigma-Aldrich).
2. Sodium Chloride (NaCl), BioXtra grade (Sigma-Aldrich).
3. Ethylenediaminetetraacetic acid (EDTA), trace metal base (Sigma-Aldrich).
4. β-Mercaptoethanol, (BME), BioUltra grade (Sigma-Aldrich).
5. Magnesium chloride hexahydrate ($MgCl_2 \cdot 6H_2O$), BioUltra grade (Sigma-Aldrich).
6. Glycerol, spectrophotometric grade (Sigma-Aldrich).
7. Dimethyl Sulfoxide (DMSO, Sigma).
8. 7-Diethylamino-3-((((2-Maleimidyl)ethyl)amino)carbonyl) coumarin (MDCC, Life Technologies).
9. Guanosine 5′-triphosphate sodium salt hydrate (GTP, Sigma-Aldrich).
10. Dithiothreitol (DTT, Sigma-Aldrich).

2.2 Supplies

1. 2 ml deep well blocks (Corning).
2. Half area 96-well UV transparent microplates (Corning).
3. Black microfuge tubes (Fisher).
4. Multichannel pipettes, 200 μl, 50 μl (Rainin).
5. 25 ml plastic reservoirs (Corning).

2.3 Proteins

1. *Rab GTPases*: Full-length Rab proteins or the isolated GTPase domains can be expressed as GST or His_6 fusions in *E. coli* and purified to >95 % homogeneity by affinity chromatography, ion exchange, and gel filtration as described [26–28].
2. *GAP proteins*: Full-length GAPs including TBC domain proteins or the catalytic domains can be expressed as 6xHis or 6xHis-SUMO fusions in *E. coli* and purified by affinity chromatography, ion exchange, and gel filtration as described [16, 22, 26].
3. *Phosphate sensor*: A His_6 fusion of the *E. coli* phosphate-binding protein (PBP, A197C mutant) can be expressed, purified, and

labeled with MDCC as described [12, 15, 22]. It is important to calibrate the PBP-MDCC sensor using various concentrations of an inorganic phosphate standard. The observed signal to background will depend on the excitation and emission wavelengths/bandwidths and may vary between sensor preparations and concentrations, due in part to differences in labeling efficiency and ambient levels of P_i. Thus, calibration should be performed on the same batch/concentration of sensor and same fluorescence reader or spectrometer used for GAP assays. With our instrumentation and monochromator settings (Tecan Safire reader, 12 nm bandwidth, 425/457 nm excitation/emission wavelengths), a three- to fourfold maximum change in fluorescence is typically observed in phosphate standard assays using 2.5 µM sensor.

Proteins can be dispensed into aliquots and stored as 10 % glycerol stocks at –80 °C.

2.4 Buffers

Solutions should be prepared in ultrapure sterile water (Mill-Q 18 MΩ water, 0.2 µm filtered) using analytical/ultrapure grade reagents. Unless indicated otherwise, store all reagents and solutions at room temperature.

1. Loading buffer: 20 mM Tris–HCl, pH 8.0, 150 mM NaCl, 5 mM EDTA, 1 mM DTT.
2. Column buffer: 20 mM Tris–HCl, pH 8.0, 150 mM NaCl.
3. Assay buffer: 20 mM Tris–HCl, pH 8.0, 150 mM NaCl, 10 mM $MgCl_2$.

2.5 Chromatographic Columns

The following columns can be used to remove excess nucleotides following GTP loading. GTP-loaded Rabs can be eluted from 10 ml desalting columns into deep well blocks in 1 ml fractions using a total of 8 ml of Column buffer. GTP-bound Rab proteins generally elute in fractions 4–5 while excess GTP elutes in later fractions. Desalting columns should be inspected for packing defects or separation between the column bead and frits before use and repacked if necessary. Analytical Superdex 75/200 columns can be used to achieve better separation (e.g., for secondary GAP assays on a smaller number of Rab substrates).

1. Pierce Dextran D-salt columns (Thermo Scientific).
2. Superdex 75/200 columns (GE Healthcare).

2.6 Instruments

The instruments listed below are used in our laboratory. Other equivalent instruments can be substituted with minor changes to the protocols described below as required.

1. Microcentrifuge (Eppendorf).
2. Fluorescence/Absorbance, top/bottom, plate reader with emission/excitation monochromators (Tecan Safire).

3. UV/VIS Spectrophotometer (HP 8453).

4. ÄKTA FPLC (GE Healthcare).

2.7 Software

1. Xflour4 (TECAN Safire detection suite); Excel-based data acquisition.

2. DELA (Data Evaluation and Likelihood Analysis); Intel Mac OSX application for efficient data plotting, processing, and analysis; available on request.

3. GraphPad Prism or other graphical analysis software; alternative to DELA.

3   Methods

The steps involved in a typical GAP assay are summarized in Fig. 1 and described in detail in the following sections. GAP reactions for as many as 8 Rab GTPases can be analyzed in parallel in a single 96-well plate and it is convenient to process up to three plates per day.

3.1 GTP Loading and Preparation of 2× Solutions

Rab GTPases are typically loaded with guanine nucleotides in a buffer containing EDTA and a 25-fold molar excess of the replacing nucleotide. EDTA reduces free Mg^{2+} to submicromolar levels, which substantially increases the off-rate for nucleotide binding and consequently the rate of nucleotide exchange. Adequate GTP loading is critical for monitoring GTP hydrolysis reactions. Loading should be >50 % in order to achieve reasonable estimates of kinetic parameters such as catalytic efficiency (*see* **Note 1**).

1. From a concentrated (>10 mg/ml) Rab GTPase stock solution, dispense a volume equivalent to 1 mg for GST fusions or 0.5 mg for His_6 fusions into 0.5 ml of loading buffer supplemented with 5 μl from a 100 mM GTP stock solution. The final Rab and GTP concentrations after mixing should be approximately 0.04 and 1.0 mM, respectively (*see* **Note 2**).

2. Incubate the reaction mixture for 3 h at room temperature.

3. Equilibrate a 10 ml D-Salt column with 50 ml of Mg^{2+} free Column buffer (*see* **Note 3**).

4. Load the reaction mixture onto the D-salt column. Elute into a deep well block with 1 ml aliquots of column buffer per well (*see* **Note 4**).

5. Using a multichannel pipette, transfer 167 μl of the eluted fractions into a UV transparent microplate for analysis of the A_{280}/A_{260} chromatogram and estimation of the GTP-bound Rab protein concentration.

6. Pool the peak Rab-GTP fractions (typically fractions 4–5 or even the single fraction with the highest A_{280}/A_{260} ratio) and determine the concentration (*see* **Notes 5** and **6**).

Load with GTP
Mix RabGTPase with 25 fold molar excess of GTP in buffer containing EDTA and incubate for 3 hrs at room temperature.

Remove excess GTP
Load reaction mixture onto a D-salt column and elute fractions into a deep well block with buffer lacking Mg^{2+}.

Estimate protein concentration
Using a multichannel pipette transfer a volume equivalent to a 1 cm path length from the deep well block to a UV transparent microplate and read A_{280} and A_{260} in a microplate reader to determine the protein concentration and A_{280}/A_{260} ratio. Pool peak fractions with $A_{280} > A_{260}$.

Measure intrinsic and GAP-catalyzed kinetics
Prepare 2X Rab GTP-Sensor solutions in buffer without Mg^{2+} and 2X GAP concentrations in buffer with 2X Mg^{2+}. Initiate reactions by mixing equal volumes of Rab GTP-Sensor and GAP-Mg^{2+} solutions in microplate wells using a multichanel pipette. Continuously monitor emission intensity in a microplate reader.

Analyze data
Analyze data using intial velocity and exponential fit approches to determine catalytic efficiency.

Fig. 1 Flow chart summarizing the overall approach for quantitative high-throughput profiling of the catalytic efficiency and Rab substrate specificity of candidate Rab GAPs

7. Prepare a 2× Rab-GTP/sensor solution by diluting appropriate volumes of the pooled Rab-GTP fractions and sensor stock with Column buffer to final concentrations of 4 and 5 μM, respectively.

8. Prepare 2× GAP solutions of varying concentration (e.g., 0, 0.0625, 0.25, 1, and 4 μM) by diluting the GAP stock with Assay buffer (*see* **Note 7**).

3.2 GAP Assay and Measurement

The GAP assays are initiated by mixing equal volumes of each solution in microplate wells. Prior to mixing, the microplate reader should be equilibrated to the desired temperature (e.g., 30 °C) and prepared with the appropriate data acquisition parameters including the excitation and emission wavelengths, the number of read cycles (i.e., data points), and the time interval between read cycles. The release of inorganic phosphate is monitored continuously at excitation and emission wavelengths of 425 and 457 nm, respectively. A typical GAP screen for 4–8 Rab-GTPases in duplicate at five different GAP concentrations requires ~1.5–3.0 ml of 2× Rab GTPase/sensor solution per Rab and ~0.35–0.7 ml of the 2× GAP solution. A possible format for the microplate is illustrated in Fig. 2.

1. Equilibrate the microplate reader and assay solutions to the desired temperature (e.g., 30 °C). Set the relevant parameters for real-time monitoring of the GTP hydrolysis reaction. For example, excitation wavelength = 425 nm; emission wavelength = 457 nm; bandwidth = 12 nm; integration time = 40 μs; dead time 100 ms; gain = same value used for calibration with the phosphate standard; number of read cycles = 140 (*see* **Note 8**).

2. Using a multichannel pipette, transfer 50 μl of each 2× GAP solution at different concentrations into the microplate wells.
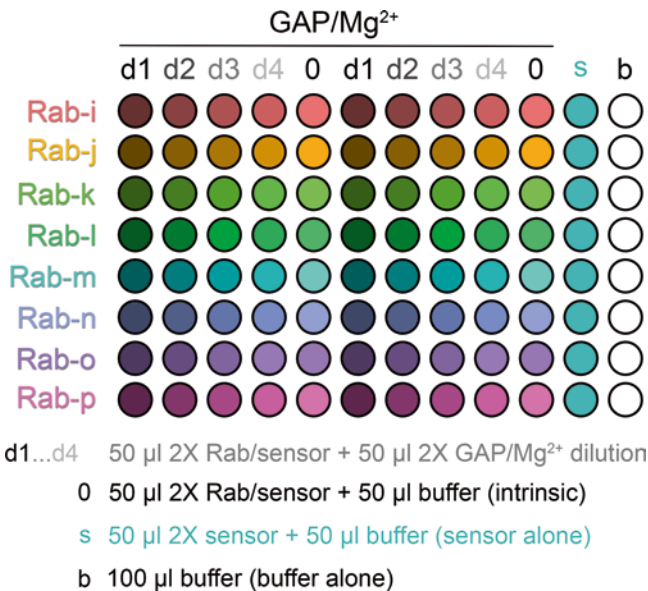
Fig. 2 Example 96-well plate format for high-throughput profile of eight Rab GTPases at four GAP concentrations with two replicate measurements. Also included are two replicates of each Rab GTPase alone and eight replicates each of the phosphate sensor and buffer alone
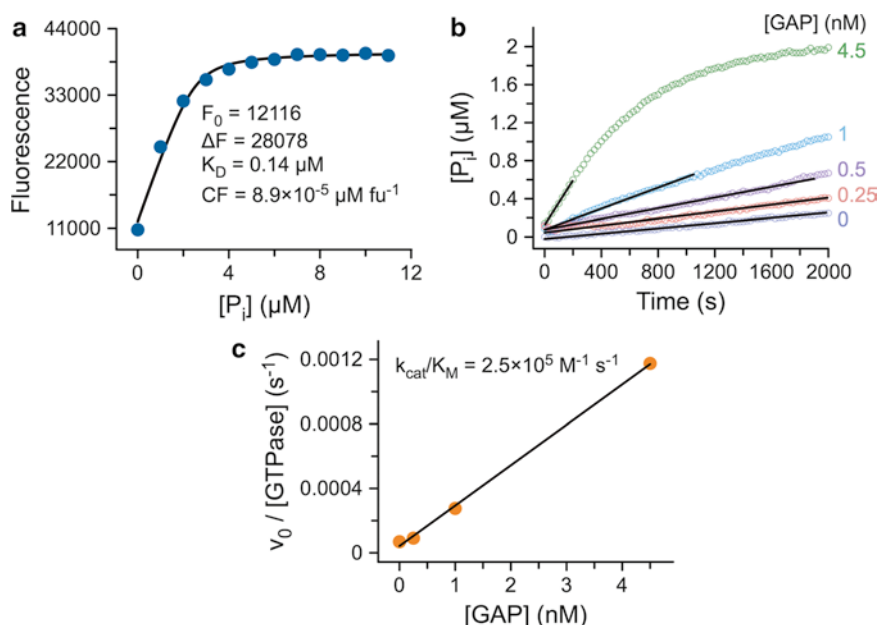
Fig. 3 Initial velocity method for determining the catalytic efficiency of Rab GAPs. (**a**) Calibration of the phosphate sensor using an inorganic phosphate standard as described in Subheading 2.2. The fluorescence intensity as a function of $[P_i]$ was analyzed by fitting with a quadratic binding model and the conversion factor calculated as described in **Note 13**. (**b**) Example time courses with the linear region fit by linear regression. (**c**) Plot of the initial velocity (v_0)/[Rab GTPase] as a function of [GAP], where [Rab GTPase] was expressed in the same concentrations units as the conversion factor in (**a**). The slope of a linear fit (*solid line*) yields k_{cat}/K_M

3. Equilibrate the microplate reader, Rab-GTP/sensor solution, and GAP solution for at least 20 min at the assay temperature (*see* **Note 9**).

4. Transfer each Rab-GTP/sensor solution to a separate reagent reservoir and carefully pipette 50 μl using a multichannel pipette and mix with the GAP solutions (*see* **Note 10**). Typical final concentrations of the individual components are: 2 μM Rab-GTP; 2.5 μM sensor; 2.0, 0.5, 0.125, 0.03125, and 0 μM GAP; and 5 mM Mg^{2+}. A lower concentration range may be required for GAPs with high catalytic efficiencies (*see*, for example, Figs. 3 and 4). The experiments should also include wells with 100 μl buffer and wells with 50 μl sensor + 50 μl buffer for calculation of the conversion factor (*see* **Note 13**).

Data collection should be initiated as soon as reasonably possible after mixing (*see* **Note 11**).

3.3   Kinetic Data Analysis

Analysis of the time courses from the GAP assays is an important step in obtaining estimates of the kinetic constants of interest, in particular, the catalytic efficiencies. Two approaches can in principle be used to analyze the GAP-catalyzed kinetics. In both cases,
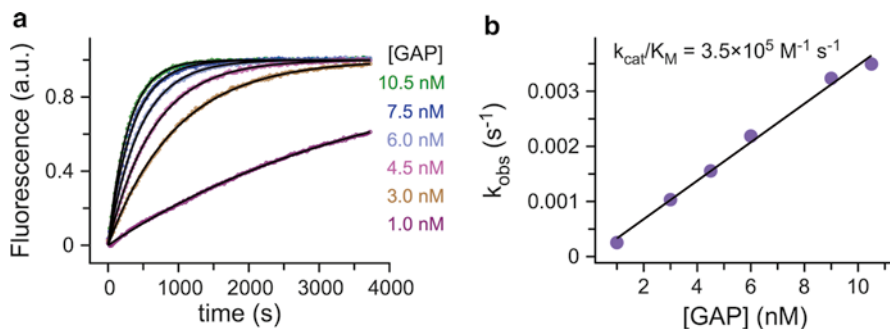
Fig. 4 Determination of the catalytic efficiency of Rab GAPs by exponential fitting. (**a**) Example of experimental fluorescence time courses (symbols) fit with an exponential model function (*solid lines*) as described in Subheading 3.3.2. (**b**) Determination of k_{cat}/K_M from the slope of a linear fit (*solid line*). Note that this method for determining k_{cat}/K_M is independent of [Rab GTPase] and, consequently, is not effected by underloading with GTP

the data are first plotted as fluorescence intensity (in fluorescence units, f.u.) versus time (in seconds, s), inspected for quality, and appropriate regions identified for further analysis. The most general approach, which can be used even in cases where the time courses do not proceed to completion (expected for weak or non-substrates and low GAP concentrations), involves determining the initial velocity (v_0) from the slope of a linear least squares fit to the initial linear phase of each time course. The resulting initial velocities can be converted from f.u. s^{-1} to M s^{-1} (or µM s^{-1}, etc.) by multiplying by a conversion factor derived from the P_i standard calibration curve described in Subheading 2.3 and then dividing by the GTPase concentration to obtain v_0/[Rab GTPase], with common concentration units used for the sensor and Rab GTPase. Alternatively, the conversion factor can be applied to the time course data rather than the initial velocities. In either case, the catalytic efficiency (k_{cat}/K_M) is subsequently obtained from the slope of a linear fit to the data in a plot of v_0/[Rab GTPase] versus [GAP]. A more accurate though less general approach involves fitting complete time courses measured under pseudo-first order conditions ([GTPase] $<< K_M$) to an exponential model to directly obtain an observed rate constant (k_{obs}, s^{-1}), which is then plotted against the GAP concentration and fit with an linear model, the slope of which yields k_{cat}/K_M. Both approaches are easily performed in DELA and the entire analysis can be completed in less than half an hour. Similar analyses can be performed with standard graphical analysis software including Prism. The initial velocity approach is appropriate for a profile of GAP activity whereas exponential fitting is preferred for secondary validation of the "hits" (i.e., best substrates) using an optimized concentration range (e.g., 10–100-fold range in twofold increments). In some cases, it may be possible to obtain separate values for k_{cat} and K_M by fitting to the hyperbolic model $k_{intr} + (k_{cat} - k_{intr})\ [GAP]/(K_M + [GAP])$, where k_{intr} is the

intrinsic hydrolytic rate in absence of a GAP. Here it is worth noting that the actual kinetic mechanisms for GAP reactions involve more steps than used in text book Michaelis–Menten (3 state, rapid equilibrium) or Briggs–Haldane (3 state, steady state) treatments of classical enzyme-catalyzed reactions. Nevertheless, GAP reactions involve an initial bimolecular binding step and exhibit saturation kinetics. Thus, the observed K_M and k_{cat} can be regarded as phenomenological constants related to the steady-state occupation and turnover of active sites as a function of GAP or GTPase concentration. Since phosphate release is detected and may be rate limiting, k_{cat} is likely lower than the rate constants for the chemical steps in the hydrolytic reaction and may even be lower than the rate constant for GAP-GTPase dissociation.

3.3.1 Initial Velocity Approach

1. Import the kinetic data from the Excel spreadsheet generated by Xfluor (or an equivalent data file for other microplate readers) into the preferred graphical analysis software package (*see* **Note 12**).

2. Generate individual plots containing the kinetic time courses for each Rab GTPase at the various GAP concentrations. Repetitions should also be plotted separately.

3. Subtract the initial value (i.e., at $t = 0$ s) for the intrinsic reaction and multiply by the conversion factor derived from the P_i calibration standard (*see* **Note 13**).

4. Limit the data to the initial velocity region by masking any nonlinear regions (*see* **Note 14**).

5. Fit the data with a linear model and divide the slope by the total Rab GTPase concentration (in the same concentration units used for the conversion factor) to obtain $v_0/$[Rab GTPase] (*see* **Note 13**).

6. Plot $v_0/$[Rab GTPase] versus [GAP] and fit the data with a linear model, the slope of which is k_{cat}/K_M in reciprocal GAP concentration units per second (e.g., μM^{-1} s^{-1} if [GAP] was expressed in units of μM). It may be necessary to exclude high concentrations if the time course is too fast for accurate determination of the initial velocity.

An example of the main steps involved in the velocity approach is illustrated in Fig. 3.

3.3.2 Exponential Fit Approach

1. Follow **steps 1** and **2** in Subheading 3.3.1. The data can be multiplied by the phosphate standard conversion factor if desired (*see* **Note 13**); however, conversion to concentration units is not necessary and will have no impact on the determination of k_{cat}/K_M.

2. Fit the time course data to the exponential model function

$$F_t = F_0 + \left(F_\infty - F_0\right)\left(1 - e^{-k_{obs} t}\right)$$

to directly obtain the observed rate constant k_{obs} (*see* **Note 15**).

3. Plot k_{obs} versus [GAP] and fit with a linear model to obtain k_{cat}/K_M from the slope.

An example of the main steps involved in the exponential fit approach is illustrated in Fig. 4.

4 Notes

1. Since the rate of nucleotide release differs between Rab-GTPases, the loading reaction should be incubated for at least 3 h at room temperature to ensure >50 % GTP loading [28].

2. Some Rab GTPases may precipitate in the loading buffer at concentrations in excess of 2 mg/ml. This problem may be more acute for His$_6$ fusions. Precipitation can be minimized by adding the GTPase last or by mixing 2× solutions to achieve the desired final concentrations. The pH and ionic strength can also be adjusted if necessary.

3. GTPase reactions are initiated by mixing GAPs in a buffer containing Mg^{2+}. It is therefore important to exclude Mg^{2+} from the Column buffer.

4. Elution of GTP-bound Rab proteins from 10 ml D-salt columns into deep well blocks can be done in parallel, with staggered starts to avoid conflicts between columns.

5. Avoid pooling protein fractions ($A_{280} > A_{260}$) with fractions containing excess nucleotides ($A_{260} > A_{280}$), which may contain free P_i, resulting in higher background fluorescence and/or multiple turnover kinetics typically manifesting as a linearly increasing fluorescence following the initial exponential phase.

6. The protein concentration can be estimated as $c = A_{280}/(\varepsilon b)$ where b is the path length (=1 cm for 167 µl in Corning Half Area microplates) and ε is the extinction coefficient including the Rab construct, tag, and nucleotide. The Protein Calculator server or equivalent software can be used to calculate the protein contribution to the extinction coefficient. The nucleotide contribution is approximately 8,000 M^{-1} cm^{-1} at 280 nm.

7. As GTP hydrolysis reactions are initiated by adding buffer solutions containing Mg^{2+}, with or without the GAP, it is important to make GAP dilutions in a buffer containing 10 mM $MgCl_2$.

8. To follow the progress of the GTP hydrolysis reactions, it is important to set the measurement parameters to appropriate values. The values provided here were optimized for acquisition

of high signal-to-noise/background kinetic data using a Tecan Safire microplate reader. However, changes may be required if other instruments are used. In particular, the gain should be empirically adjusted to adequately fill but not overflow the digitizer. As a general rule of thumb, the gain can be adjusted such that the initial fluorescence signal is approximately 10–30 % of the maximum signal that can be digitized, assuming a three- to fourfold increase in fluorescence over the time course.

9. Preequilibration is important for avoiding temperature-related artifacts since both fluorescence and reaction rates are temperature dependent.

10. A total reaction volume of 100 μl is reasonable for bottom reads of the fluorescence in microplate wells and for reducing meniscus-related artifacts in fluorescence intensity.

11. Delay in measurement after mixing will result in truncation of initial data points for faster reactions. However, complete mixing without bubbles is more important than speed. For example, a delay of 30–120 s is not unreasonable for GAP reactions monitored for 30–120 min. Indeed, similar delays are common for automated liquid handling devices, which can be used in place of multichannel pipettes.

12. Data can be imported by cut/paste or from files exported from Excel as tab delimited text.

13. The conversion factor from f.u. to concentration units can be determined by fitting the data for the calibration curve to the quadratic binding model:

$$F = F_0 + \Delta F \left\{ \mathrm{b} - \left(\mathrm{b}^2 - 4\,\mathrm{ac} \right)^{-1/2} \right) / 2 \right\}$$

$$\mathrm{b} = 1 + \left[\mathrm{P_i} \right] / \left[\mathrm{PBP\text{-}MDCC} \right] + K_\mathrm{D} / \left[\mathrm{PBP\text{-}MDCC} \right]$$

$$\mathrm{ac} = \left[\mathrm{P_i} \right] / \left[\mathrm{PBP\text{-}MDCC} \right]$$

and dividing the [PBP-MDCC] by the amplitude ΔF:

$$\text{conversion factor} = \left(\left[\mathrm{PBP - MDCC} \right] / \Delta F \right)$$
$$\left(F_\mathrm{sensor} - F_\mathrm{buffer} \right) / \left(F_\mathrm{sensor}^\mathrm{assay} - F_\mathrm{buffer}^\mathrm{assay} \right)$$

where $F_\mathrm{sensor}^\mathrm{assay}$ and $F_\mathrm{buffer}^\mathrm{assay}$ are the fluorescence intensities of the sensor and buffer alone for the GAP assay and F_sensor and F_buffer are the fluorescence intensities of the sensor and buffer alone for the phosphate standard calibration experiment. Note that the concentrations above represent total rather than free concentrations. The quadratic form of the binding isotherm is necessary in this case since $\left[\mathrm{PBP\text{-}MDCC} \right] \sim 2.5\,\mu\mathrm{M} \gg K_\mathrm{D} \sim 100\,\mathrm{nM}$.

It is important to use the same experimental parameters/conditions for both the calibration curve and GAP assays, including wavelengths, bandwidths, gain setting, read mode, well volume, sensor concentration, buffer, and temperature.

14. For initial velocity measurements, only the initial linear portion of the progress curve should be fit (e.g., <30 % of the expected maximum phosphate production, which for 2 μM GTPase would be <0.6 μM). In addition to nonlinear regions at longer times, it may also be necessary in some cases to mask nonlinear regions at short times, possibly due to mixing and/or temperature equilibration artifacts. Data sets containing more serious artifacts (e.g., due to inevitable but hopefully infrequent bubbles or meniscus issues) should be excluded from analysis, as should data sets for which the kinetics are too fast.

15. As a general rule of thumb, progress curves with five $1/e$ times are optimal for exponential fitting. Fitting progress curves with less than one $1/e$ time will yield results with large systematic errors, unless the signal-to-noise is very high or the amplitude $(F_\infty - F_0)$ can be set to a known fixed value. A more sophisticated approach that can be used with data from concentration optimized secondary experiments involves global fitting of the rate constants, which can be done in DELA or other programs with global fitting capabilities.

Acknowledgements

References

1. Bourne HR, Sanders DA, McCormick F (1990) The GTPase superfamily: a conserved switch for diverse cell functions. Nature 348(6297):125–132. doi:10.1038/348125a0

2. Bos JL, Rehmann H, Wittinghofer A (2007) GEFs and GAPs: critical elements in the control of small G proteins. Cell 129(5):865–877

3. Bernards A, Settleman J (2004) GAP control: regulating the regulators of small GTPases. Trends Cell Biol 14(7):377–385. doi:10.1016/j.tcb.2004.05.003

4. Ligeti E, Welti S, Scheffzek K (2012) Inhibition and termination of physiological responses by GTPase activating proteins. Physiol Rev 92(1):237–272. doi:10.1152/physrev.00045.2010

5. Barr F, Lambright DG (2010) Rab GEFs and GAPs. Curr Opin Cell Biol 22:461–470

6. Eberth A, Dvorsky R, Becker CF, Beste A, Goody RS, Ahmadian MR (2005) Monitoring the real-time kinetics of the hydrolysis reaction of guanine nucleotide-binding proteins. Biol Chem 386(11):1105–1114. doi:10.1515/BC.2005.127

7. Scheffzek K, Ahmadian MR, Wittinghofer A (1998) GTPase-activating proteins: helping hands to complement an active site. Trends Biochem Sci 23(7):257–262

8. Gideon P, John J, Frech M, Lautwein A, Clark R, Scheffler JE, Wittinghofer A (1992) Mutational and kinetic analyses of the GTPase-activating protein (GAP)-p21 interaction: the C-terminal domain of GAP is not sufficient for full activity. Mol Cell Biol 12(5):2050–2056

9. Marshall CB, Meiri D, Smith MJ, Mazhab-Jafari MT, Gasmi-Seabrook GM, Rottapel R, Stambolic

V, Ikura M (2012) Probing the GTPase cycle with real-time NMR: GAP and GEF activities in cell extracts. Methods 57(4):473–485. doi:10.1016/j.ymeth.2012.06.014

10. Mazhab-Jafari MT, Marshall CB, Smith M, Gasmi-Seabrook GM, Stambolic V, Rottapel R, Neel BG, Ikura M (2010) Real-time NMR study of three small GTPases reveals that fluorescent 2′(3′)-O-(N-methylanthraniloyl)-tagged nucleotides alter hydrolysis and exchange kinetics. J Biol Chem 285(8):5132–5136. doi:10.1074/jbc.C109.064766

11. Nixon AE, Brune M, Lowe PN, Webb MR (1995) Kinetics of inorganic phosphate release during the interaction of p21ras with the GTPase-activating proteins, p120-GAP and neurofibromin. Biochemistry 34(47):15592–15598

12. Brune M, Hunter JL, Corrie JE, Webb MR (1994) Direct, real-time measurement of rapid inorganic phosphate release using a novel fluorescent probe and its application to actomyosin subfragment 1 ATPase. Biochemistry 33(27):8262–8271

13. Webb MR (1992) A continuous spectrophotometric assay for inorganic phosphate and for measuring phosphate release kinetics in biological systems. Proc Natl Acad Sci U S A 89(11):4884–4887

14. Self AJ, Hall A (1995) Measurement of intrinsic nucleotide exchange and GTP hydrolysis rates. Methods Enzymol 256:67–76

15. Shutes A, Der CJ (2005) Real-time in vitro measurement of GTP hydrolysis. Methods 37(2):183–189. doi:10.1016/j.ymeth.2005.05.019

16. Mishra AK, Del Campo CM, Collins RE, Roy CR, Lambright DG (2013) The Legionella pneumophila GTPase activating protein LepB accelerates Rab1 deactivation by a non-canonical hydrolytic mechanism. J Biol Chem 288(33):24000–24011. doi:10.1074/jbc.M113.470625

17. Yu Q, Hu L, Yao Q, Zhu Y, Dong N, Wang DC, Shao F (2013) Structural analyses of Legionella LepB reveal a new GAP fold that catalytically mimics eukaryotic RasGAP. Cell Res 23(6):775–787. doi:10.1038/cr.2013.54

18. Nottingham RM, Pusapati GV, Ganley IG, Barr FA, Lambright DG, Pfeffer SR (2012) RUTBC2 protein, a Rab9A effector and GTPase-activating protein for Rab36. J Biol Chem 287(27):22740–22748. doi:10.1074/jbc.M112.362558

19. Dong N, Zhu Y, Lu Q, Hu L, Zheng Y, Shao F (2012) Structurally distinct bacterial TBC-like GAPs link Arf GTPase to Rab1 inactivation to counteract host defenses. Cell 150(5):1029–1041. doi:10.1016/j.cell.2012.06.050

20. Davey JR, Humphrey SJ, Junutula JR, Mishra AK, Lambright DG, James DE, Stockli J (2012) TBC1D13 is a RAB35 specific GAP that plays an important role in GLUT4 trafficking in adipocytes. Traffic 13(10):1429–1441. doi:10.1111/j.1600-0854.2012.01397.x

21. Nottingham RM, Ganley IG, Barr FA, Lambright DG, Pfeffer SR (2011) RUTBC1 protein, a Rab9A effector that activates GTP hydrolysis by Rab32 and Rab33B proteins. J Biol Chem 286(38):33213–33222. doi:10.1074/jbc.M111.261115

22. Chotard L, Mishra AK, Sylvain MA, Tuck S, Lambright DG, Rocheleau CE (2010) TBC-2 regulates RAB-5/RAB-7-mediated endosomal trafficking in Caenorhabditis elegans. Mol Biol Cell 21(13):2285–2296. doi:10.1091/mbc.E09-11-0947

23. Ingmundson A, Delprato A, Lambright DG, Roy CR (2007) Legionella pneumophila proteins that regulate Rab1 membrane cycling. Nature 450(7168):365–369. doi:10.1038/nature06336

24. Sklan EH, Serrano RL, Einav S, Pfeffer SR, Lambright DG, Glenn JS (2007) TBC1D20 is a Rab1 GTPase-activating protein that mediates hepatitis C virus replication. J Biol Chem 282(50):36354–36361

25. Mukhopadhyay A, Pan X, Lambright DG, Tissenbaum HA (2007) An endocytic pathway as a target of tubby for regulation of fat storage. EMBO Rep 8(10):931–938

26. Pan X, Eathiraj S, Munson M, Lambright DG (2006) TBC-domain GAPs for Rab GTPases accelerate GTP hydrolysis by a dual-finger mechanism. Nature 442(7100):303–306. doi:10.1038/nature04847

27. Eathiraj S, Pan X, Ritacco C, Lambright DG (2005) Structural basis of family-wide Rab GTPase recognition by rabenosyn-5. Nature 436(7049):415–419. doi:10.1038/nature03798

28. Mishra A, Eathiraj S, Corvera S, Lambright DG (2010) Structural basis for Rab GTPase recognition and endosome tethering by the C2H2 zinc finger of Early Endosomal Autoantigen 1 (EEA1). Proc Natl Acad Sci U S A 107(24):10866–10871. doi:10.1073/pnas.1000843107

Chapter 5

Measuring Rab GTPase-Activating Protein (GAP) Activity in Live Cells and Extracts

Ryan M. Nottingham and Suzanne R. Pfeffer

Abstract

Mammalian cells encode a diverse set of Rab GTPases and their corresponding regulators. In vitro biochemical screening has proven invaluable in assigning particular Rabs as substrates for their cognate GTPase-activating proteins. However, in vitro activity does not always reflect substrate specificity in cells. This method describes a functional test of GAP activity in cells or extracts that takes into account the presence of other factors or conditions that might change observed in vitro specificity.

Key words GTPase-activating protein, Rab GTPase, Effector protein

1   Introduction

Rab GTPases are small Ras-like GTPases that function as master regulators of membrane trafficking [1]. In cells, they act as molecular switches, changing conformations between an active GTP-bound state and an inactive GDP-bound state. In their active form, Rab proteins bind so-called effector molecules that function in all steps of membrane trafficking. Against this background of the nucleotide cycle, there is also a membrane association cycle with almost all Rab-GDP found in the cytosol complexed with a protein named GDI, and Rab-GTP located exclusively on distinct membrane surfaces in organized units called microdomains [2]. Effector binding and Rab localization are thus dependent on the ability of Rab proteins to exchange and hydrolyze guanine nucleotides.

As the intrinsic rates of nucleotide exchange and hydrolysis are quite slow, cells have evolved opposing enzymatic activities to regulate the identity of the bound nucleotide. Guanine nucleotide exchange factors (GEFs) remodel the nucleotide-binding site of a Rab, which accelerates the off-rate of bound GDP [3]. GTPase-activating proteins (GAPs) accelerate GTP hydrolysis by a "dual-finger" mechanism whereby a catalytic arginine and glutamine are

supplied in *trans* by the GAP to properly orient a water molecule for nucleophilic attack on the gamma phosphate group of GTP [4]. Both sets of enzymatic activities seem to be encoded in conserved domains: many RabGEF proteins include a DENN domain that is sufficient for GEF activity [5], while all but one known RabGAP protein possess a Tre2/Bub2/Cdc16 (TBC) domain sufficient to stimulate GTP hydrolysis in vitro [4].

A great deal of recent work has been undertaken to assign the various Rab and GAP proteins into linked pathways called Rab cascades [6]. In this model, Rabs help to recruit GEFs and GAPs for the Rab proteins that function before and after themselves in a particular trafficking pathway like secretion [6] or endocytosis [7]. This model predicts that GEFs and GAPs are likely to be Rab effectors themselves, and the coordinated recruitment of these regulators to membranes ensures directionality to a trafficking pathway by ordering adjacent Rab-organized microdomains according to their stepwise functions.

The human genome encodes approximately 70 Rab proteins and approximately 40 TBC domain-containing proteins. Assigning Rab/GAP substrate pairs can be undertaken through high-throughput biochemical screening [4]. However, activity seen in vitro is not always recapitulated in living cells [8, 9]. In this chapter, we detail methods used to determine the specificity of RabGAP proteins in cells by using a purified, immobilized effector "Rab-binding domain" as an affinity column to report on the amount of active Rab GTPase present in cells under different conditions. Cells are transfected with wild-type RabGAP proteins or GAP-deficient point mutants and the amount of active, GTP-bound Rab present is determined by incubating lysates with the Rab effector column. GAP overexpression in cells should lead to a decrease in the amount of Rab protein retained by the column when compared to a negative control or in the presence of the GAP-deficient mutant. Alternatively, recombinant GAP protein can be added directly to semi-intact cells to overcome low expression of the GAP or a high abundance of effectors. These methods have been applied to other Rab/GAP systems [10] where effectors have been identified.

2   Materials

2.1   Mammalian Expression Plasmids

1. GFP-Rab33: human Rab33b coding sequence was cloned into pEGFP-C1 yielding an N-terminal GFP-tagged protein.

2. Myc-Rab32: human Rab32 coding sequence was cloned into a modified pCDNA3.1(+) vector containing a single N-terminal Myc epitope tag.

3. 3xMyc-RUTBC1: human RUTBC1 (isoform 2) was cloned into a modified pCDNA3.1(+) vector containing an N-terminal

triple Myc epitope tag. 3xMyc-RUTBC1 R803A was generated by site-directed mutagenesis.

4. 3xMyc-RUTBC2: human RUTBC2 (isoform 4) was cloned into a modified pCDNA3.1(+) vector containing an N-terminal triple Myc epitope tag. 3xMyc-RUTBC2 R829A was generated by site-directed mutagenesis.

2.2 Bacterial Expression Plasmids

1. Rab-Binding Domain (RBD) expression plasmids:

   (a) GST-Atg16L1: human Atg16L1 coding sequence (isoform 1, aa. 80–265) was ligated into pGEX 4T-1 resulting in a GST-tagged fusion protein.

   (b) GST-Varp: human Varp coding sequence (aa. 451–730) was also ligated into pGEX 4T-1 resulting in a GST-tagged fusion protein.

2. RUTBC1-C: human RUTBC1 coding sequence (aa. 533–1,066) containing the TBC domain was ligated into pET28a resulting in a 6x-hisitidine-tagged protein (6xHis-RUTBC1-C). 6xHis-RUTBC1-C R803A was generated by site-directed mutagenesis.

2.3 Protein Purification

All protein expression plasmids were transformed into Rosetta2 (DE3) cells for purification.

1. Luria broth (LB): 10 g/L bacto-tryptone, 5 g/L yeast extract, 10 g/L NaCl.

2. Ampicillin or carbenicillin (2,000×): 100 mg/mL in water; stored at –20 °C.

3. Kanamycin (1,000×): 50 mg/mL in water; stored at –20 °C.

4. Chloramphenicol (1,000×): 34 mg/mL in 100 % ethanol; stored at –20 °C.

5. 1 M isopropyl beta-D-thiogalactopyranoside (IPTG); stored at –20 °C.

6. Phosphate-buffered saline (PBS): 137 mM NaCl, 2.7 mM KCl, 8.03 mM Na_2HPO_4, 1.47 mM KH_2PO_4, pH 7.4.

7. PMSF: 100 mM in 100 % ethanol; stored at –20 °C.

8. Protease inhibitors (100×): 100 μg/mL each aprotinin, leupeptin, and pepstatin A; stored at –20 °C.

9. RBD Lysis Buffer: 25 mM HEPES–NaOH, pH 7.4, 150 mM NaCl, 1 mM DTT.

10. RBD Elution Buffer: 25 mM HEPES–NaOH, pH 7.4, 150 mM NaCl, 1 mM DTT, 20 mM reduced glutathione; stored at 4 °C.

11. GAP Lysis Buffer: 25 mM HEPES–NaOH, pH 7.4, 300 mM NaCl, 50 mM imidazole.

12. GAP Elution Buffer: 25 mM HEPES–NaOH, pH 7.4, 300 mM NaCl, 250 mM imidazole.

13. Glutathione-agarose (RBDs) and Ni-NTA agarose (GAPs).

2.4 GAP Assays in Cells and Extracts

1. HEK293T cells (ATCC CRL-3216).

2. Cell transfection reagents.

3. Cell Lysis Buffer: 50 mM HEPES–NaOH, pH 7.4, 150 mM NaCl, 1 mM $MgCl_2$, 1 % Triton X-100.

4. Binding Buffer: 50 mM HEPES–NaOH, pH. 7.4, 150 mM NaCl, 1 mM $MgCl_2$, 0.2 % Triton X-100.

5. Swelling Buffer: 10 mM HEPES–NaOH, pH 7.4, 15 mM NaCl.

6. Scraping Buffer: 10 mM triethanolamine, 10 mM acetic acid, pH 7.4, 1 mM EDTA, 250 mM sucrose, 1 mM ATP, 15 mM creatine phosphate, 21 U/mL creatine phosphokinase, 200 μM PMSF, 2 μg/mL pepstatin A, 1× Roche Complete EDTA-free protease inhibitor cocktail.

7. 10× Reaction Buffer: 500 mM HEPES–NaOH, pH 7.4, 1.5 M NaCl, 20 mM $MgCl_2$.

8. Antibodies for immunoblotting: mouse anti-Myc (9E10) culture supernatant, rabbit anti-GFP.

3 Methods

3.1 Expression and Purification of GST-RBDs

1. A 50 mL overnight culture of each GST-RBD (LB supplemented with 50 μg/mL carbenicillin and 34 μg/mL chloramphenicol) is used to inoculate a 1 L culture of LB/antibiotics.

2. The culture is grown at 37 °C until it reaches an OD_{600} of ~0.6. The cultures are then transferred to 22 °C and induced by bringing them to a final concentration of 0.1 mM IPTG. Cultures are incubated at 22 °C for an additional 4 h and collected by centrifugation ($4,000 \times g$, 10 min, 4 °C). The pellet is resuspended in PBS and then repelleted. The pellets can be snap frozen in liquid nitrogen and stored at –20 °C for later processing, if desired. All buffers used below should be chilled to 4 °C.

3. The washed pellet is then resuspended in 25 mL RBD Lysis Buffer supplemented with 1 mM PMSF and 1× protease inhibitors. The cells are broken by passing twice through an EmulsiFlex-C5 apparatus at 20,000 psi (Avestin) (*see* **Note 1**).

4. The homogenate is diluted to 50 mL with RBD Lysis Buffer and transferred to chilled centrifuge tubes. The diluted homogenate is spun at $30,000 \times g$ for 30 min at 4 °C.

5. Transfer the clarified supernatant to fresh 50 mL conical tubes and incubate them with glutathione-agarose beads (equilibrated in RBD Lysis Buffer) for 2 h at 4 °C with rotation (*see* **Note 2**).

6. Pour supernatant/bead solution into an empty column and wash the beads with 50 column volumes of RBD Lysis Buffer (*see* **Note 3**).

7. GST-RBDs are eluted by incubating the beads with 2 column volumes of RBD Elution Buffer for 10 min at 4 °C. This step is repeated another four times. Eluates are analyzed by SDS-PAGE and fractions containing GST-RBDs are then pooled and dialyzed overnight against RBD Lysis Buffer. The pool is brought to 10 % (v/v) glycerol and yield is determined by Bradford assay (*see* **Note 4**). The pool is then aliquoted, snap frozen in liquid nitrogen, and stored at –80 °C.

3.2 Expression and Purification of 6x-His-RUTBC1-C and 6xHis-RUTBC1-C R803A

1. A 100 mL overnight culture of either the wild-type or mutant construct (LB supplemented with 50 μg/mL kanamycin and 34 μg/mL chloramphenicol) is used to inoculate 3×2 L cultures of LB/antibiotics.

2. The culture is grown at 37 °C until it reaches an OD_{600} of ~0.5. Transfer the cultures to 22 °C and induce expression by bringing them to a final concentration of 0.4 mM IPTG. Cultures are incubated at 22 °C for an additional 4 h and collected by centrifugation at 4 °C ($4,000 \times g$, 10 min, Beckman SX4750A rotor). The pellets are resuspended in PBS and then repelleted as earlier. At this point the pellets can be snap frozen in liquid nitrogen and stored at –20 °C. All buffers used below should be chilled to 4 °C.

3. The washed pellet is resuspended in 100 mL GAP Lysis Buffer supplemented with 1 mM PMSF. The cells are broken by passing twice through an EmulsiFlex-C5 apparatus at 20,000 psi.

4. The homogenate is diluted to 200 mL with GAP Lysis Buffer and transferred to chilled centrifuge tubes and the homogenate is spun at $30,000 \times g$ for 45 min at 4 °C.

5. Transfer the clarified supernatants to fresh 50 mL conical tube and incubate them with 3.0 mL Ni-NTA agarose (equilibrated in GAP Lysis Buffer) for 1 h at 4 °C with end-over-end rotation.

6. Pour supernatant/bead solution into a column and wash the beads with 2×25 column volumes (2×75 mL) of cold GAP Lysis Buffer.

7. Elute the column with 5×1 column volumes (3.0 mL) cold GAP Elution Buffer. Eluates are analyzed by SDS-PAGE and fractions containing 6xHis-RUTBC1-C are then pooled and dialyzed overnight against GAP Storage Buffer to remove

imidazole. The pool is brought to 10 % (v/v) glycerol and yield is determined by Bradford assay. The pool is then aliquoted, snap frozen in liquid nitrogen, and stored at –80 °C.

3.3 GAP Assay in Cells

1. Seed 100 mm dishes of HEK293T (*see* **Note 5**) cells at approximately 40 % confluencey.

2. On the next day, cotransfect the cells with GFP-Rab33b or Myc-Rab32 and either 3xMyc-RUTBC1 or 3xMyc-RUTBC1 R803A (*see* **Note 6**).

3. At approximately 22 h posttransfection, immobilize GST-RBDs by incubating them with glutathione-Sepharose for at least 2 h at 4 °C with end-over-end rotation. At the end of the incubation, pellet the glutathione-Sepharose (1,000 rpm, 1 min, 4 °C, microcentrifuge) and remove the supernatant. Add Binding Buffer to obtain a 50 % slurry and keep the immobilized RBDs on ice.

4. After 1 h of the above RBD incubation, transfer dishes to a chilled steel plate on ice. Wash the cells twice with 5 mL PBS by aspiration and drain the dishes of excess PBS by holding the dish nearly vertical for 10 s.

5. Add 0.5 mL of Cell Lysis Buffer supplemented with protease inhibitor cocktail and incubate on ice for 10 min. Scrape the cells using a rubber policeman and transfer lysates to fresh 1.5 mL tubes.

6. Clarify the lysates by spinning at $16,000 \times g$ in a microcentrifuge for 15 min at 4 °C. Clarified supernatants were then diluted at least five-fold with Binding Buffer to decrease detergent concentration and ensure all supernatants had equal protein concentrations.

7. Aliquot the diluted supernatants to fresh tubes and add 20 μL of 50 % RBD bead slurry (10 μL bed volume) and incubate for 2 h at 4 °C with end-over-end rotation.

8. Pellet the beads as above and remove the supernatant completely (*see* **Note 7**). Wash the beads (in batch) four times with 1.0 mL cold Binding Buffer and elute the bound material in 30 μL 2× SDS-PAGE sample buffer.

9. Analyze the amount of GFP- or 3xMyc-tagged Rab bound in the presence or absence of wild-type RUTBC1 and RUTBC1 R803A by immunoblot (Fig. 1) (*see* **Note 8**).

3.4 Biochemical GAP Assay in Cell Extracts

1. HEK293T cells are transfected and GST-RBDs are immobilized as above.

2. 24 h post-transfection, the cells are transferred to a chilled steel plate on ice and are washed once with PBS and once with Swelling Buffer and then incubated in Swelling Buffer for
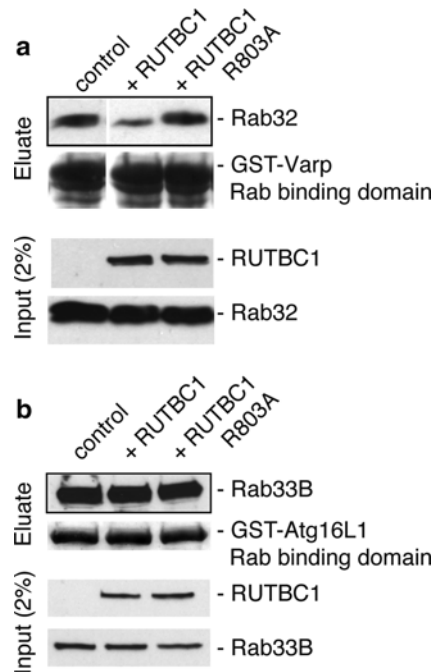
Fig. 1 RUTBC1 can act as a Rab32 GAP in cells. (**a**) Lysates of HEK293T cells transfected with Myc-Rab32 alone or Myc-Rab32 with either 3xMyc-RUTBC1 wildtype or R803A for 24 h were incubated with GST-Varp Rab binding domain. Shown are 2 % input (below) and 100 % of the affinity column eluate (above). (**b**) Lysates of HEK293T cells transfected with GFP-Rab33B alone or GFP-Rab33B with either 3xMyc-RUTBC1 wild type or R803A for 24 h were incubated with GST-Atg16L1 Rab-binding domain. Shown are 2 % input (below) and 100 % of the affinity column eluate (above). Rab32 and RUTBC1 were detected with anti-Myc antibody; Rab33B was detected with anti-GFP antibody. GST-Rab-binding domains were detected by Ponceau S staining. This research was originally published in Journal of Biological Chemistry. Nottingham, R.M. et al. RUTBC1 protein, a Rab9A effector that activates GTP hydrolysis by Rab32 and Rab33B proteins. *J. Biol. Chem.* 2010. 286, 33213–33222. © the American Society for Biochemistry and Molecular Biology

5 min (*see* **Note 9**). Swelling can be confirmed by observing the cells using an inverted light microscope.

3. Aspirate the Swelling Buffer from cells and drain dishes vertically for 10 s.

4. Add 500 μL of 1× SEAT buffer supplemented with ATP-regenerating system and protease inhibitors to each 100 mm dish. Scrape the cells with a trimmed rubber policeman, pipette the cell suspension three times with a 1 mL micropipette, and transfer suspension to a chilled 1.5 mL microcentrifuge tube.

5. Pass the cells through a 25G needle ten times using a 1 mL syringe. Confirm cell breakage by microscopy. Aliquot the cell suspension into three equal volumes of 150 μL.

6. Assemble the GAP reactions as follows: 150 μL lysate, 20 μL 10× Reaction Buffer, the volume required for the desired final concentration of purified GAP or equivalent volume of 1× Reaction Buffer and ddH$_2$O up to 200 μL. Incubate the reactions at 37 °C for 5 min.

7. Stop the reactions by transferring them to ice and fully solubilize cells by adding 10 μL 20 % Triton X-100. Pipette to mix and incubate on ice for 10 min. Spin the lysates for 15 min at 16,000×g in a microcentrifuge at 4 °C.

8. Dilute the clarified supernatants five-fold with Binding Buffer and store on ice until GST-RBD immobilization is complete.

9. Clarify the lysates by spinning at 16,000×g in a microcentrifuge for 15 min at 4 °C. Clarified supernatants are then diluted at least five-fold with Binding Buffer to decrease detergent concentration and ensure all supernatants had equal protein concentrations.

10. Aliquot the diluted supernatants to fresh tubes and add 20 μL of 50 % RBD bead slurry (10 μL bed volume, ~10 μg GST-RBD) and incubate for 2 h at 4 °C with end-over-end rotation.

11. Pellet the beads as above and remove the supernatant completely. Wash the beads (in batch) four times with 1.0 mL cold Binding Buffer and elute the bound material in 30 μL 2× SDS-PAGE sample buffer.

12. Analyze the amount of GFP- or 3xMyc-tagged Rab bound in the presence or absence of wild-type RUTBC1 and RUTBC1 R803A by immunoblot (Fig. 2).

4   Notes

1. Alternatively, the cells can be broken by use of a French pressure cell or the lysozyme/sonication method. We have found the EmulsiFlex-C5 to yield comparable breakage to the French press with good temperature control and without an inherent volume limitation.

2. We routinely use glutathione-Sepharose 4 FF (GE Healthcare). Due to differences in protein expression, GST-Atg16L1 required 3.0 mL bed volume per liter of culture while GST-Varp required 1.0 mL bed volume.

3. The beads can also be washed in batch using centrifugation (1,000×g, 5 min, 4 °C).
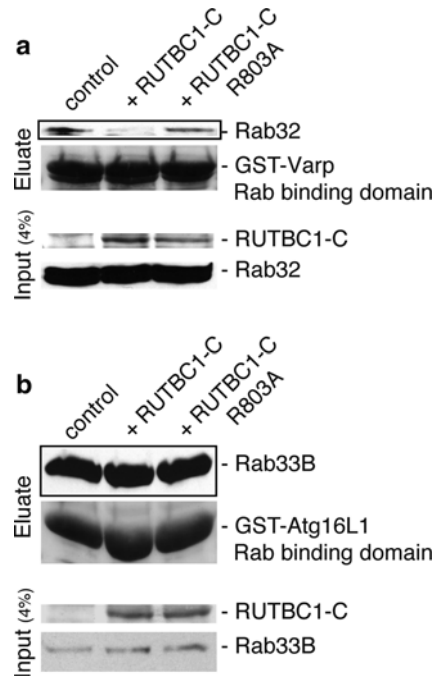
Fig. 2 RUTBC1 GAP activity in crude extracts. (**a**) HEK293T cell extracts from cells transfected with Myc-Rab32 were incubated with purified His-RUTBC1-C and then incubated with GST-Varp Rab-binding domain. Shown are 4 % input (below) and 100 % affinity column eluate (above). (**b**) HEK293T extracts from cells transfected with GFP-Rab33B were incubated with purified His-RUTBC1-C and then incubated with GST-Atg16L1 Rab binding domain. Shown are 4 % input (below) and 100 % affinity column eluate (above). Rab32 was detected with anti-Myc antibody; Rab33B was detected anti-GFP antibody. GST-tagged Rab-binding domains and His-RUTBC1-C were detected by Ponceau S staining. This research was originally published in Journal of Biological Chemistry. Nottingham, R.M et al. RUTBC1 protein, a Rab9A effector that activates GTP hydrolysis by Rab32 and Rab33B proteins. *J. Biol. Chem.* 2010. 286, 33213–33222. © the American Society for Biochemistry and Molecular Biology

4. If desired, the protein pool can be concentrated using Amicon spin concentrators with the appropriate molecular weight cut-off. As the GST-RBDs are later immobilized on a resin, it is likely not necessary for those constructs.

5. Any cell line that is easily transfectable could be used—we had good experience with HEK293T cells but one could also use HeLa, Vero, or COS-7.

6. Our lab routinely uses polyethyleneimine (PEI) to transfect HEK293T cells as it yields high transfection efficiency at low cost. It should be prepared in 1 mg/mL stock concentration (pH 7.4) and stored at –20 °C. Thawed aliquots can be stored

at 4 °C for up to 2 weeks. For a 100 mm dish, 6 μg total DNA is mixed in 970 μL of opti-MEM and then 30 μL PEI stock solution is added to the DNA/medium mixture and incubated at room temperature for 15 min. The transfection mix was added drop-wise to the cells. We have also routinely tested other reagents including cationic lipid-based reagents and found them suitable.

7. The use of a Hamilton syringe (point style 3, 22S needle) is very helpful in removing virtually all supernatant above the bead bed in a microcentrifuge tube.

8. As a reference, so-called dominant negative mutants of Rab GTPases (GDP-preferring mutants, G1 motif S/T to N) can be used as a negative control to give an idea of background binding in the experiment. Additionally, so-called constitutively active mutants (G3 motif Q to L/A) could be used as a positive control. However, be aware that these mutants do not function identically for all Rabs [11] and that TBC domain proteins have been shown to be able to inactivate constitutively active Rabs in vitro [4, 8].

9. Various cell types will respond differently to the hypo-osmotic swelling. COS-7 cells, for example, stay attached to the tissue culture dish for longer time periods (10–15 min) while HEK293T cells start to become unattached from the dish with incubations longer than 5 min.

Acknowledgement

References

1. Stenmark H (2009) Rab GTPases as coordinators of vesicle traffic. Nat Rev Mol Cell Biol 10:513–525

2. Pfeffer SR (2012) Rab GTPase localization and Rab cascades in Golgi transport. Biochem Soc Trans 40:1373–1377

3. Barr F, Lambright DG (2010) Rab GEFs and GAPs. Curr Opin Cell Biol 22:461–470

4. Pan X, Eathiraj S, Munson M, Lambright DG (2006) TBC-domain GAPs for Rab GTPases accelerate GTP hydrolysis by a dual-finger mechanism. Nature 442:303–306

5. Yoshimura S-I, Gerondopoulos A, Linford A, Rigden DJ, Barr FA (2010) Family-wide characterization of the DENN domain Rab GDP-GTP exchange factors. J Cell Biol 191:367–381

6. Rivera-Molina FE, Novick PJ (2009) A Rab GAP cascade defines the boundary between two Rab GTPases on the secretory pathway. Proc Natl Acad Sci U S A 106:14408–14413

7. Rink J, Ghigo E, Kalaidzidis Y, Zerial M (2005) Rab coversion as a mechanism of progression from early to late endosomes. Cell 122:735–749

8. Nottingham RM, Ganley IG, Barr FA, Lambright DG, Pfeffer SR (2010) RUTBC1 protein, a Rab9A effector that activates GTP hydrolysis by Rab32 and Rab33B proteins. J Biol Chem 286:33213–33222

9. Itoh T, Satoh M, Kanno E, Fukuda M (2006) Screening for target Rabs of TBC (Tre-2/Bub2/Cdc16) domain-containing proteins based on their Rab-binding activity. Genes Cells 11:1023–1037

10. Itoh T, Kanno E, Uemura T, Waguri S, Fukuda M (2011) OATL1, a novel autophagosome-resident Rab33B-GAP, regulates autophagosomal maturation. J Cell Biol 192:839–853

11. Langemeyer L, Nunes Bastos R, Cai Y, Itzen A, Reinisch KM, Barr FA (2014) Diversity and plasticity in Rab GTPase nucleotide release mechanism has consequences for Rab activation and inactivation. eLife 3:e01623

Chapter 6

Analysis of the Interactions Between Rab GTPases and Class V Myosins

Andrew J. Lindsay, Stéphanie Miserey-Lenkei, and Bruno Goud

Abstract

Myosins are actin-based motor proteins that are involved in a wide variety of cellular processes such as membrane transport, muscle contraction, and cell division. Humans have over 40 myosins that can be placed into 18 classes, the malfunctioning of a number of which can lead to disease. There are three members of the human class V myosin family, myosins Va, Vb, and Vc. People lacking functional myosin Va suffer from a rare autosomal recessive disease called Griscelli's Syndrome type I (GS1) that is characterized by severe neurological defects and partial albinism. Mutations in the myosin Vb gene lead to an epithelial disorder called microvillus inclusion disease (MVID) that is often fatal in infants. The class V myosins have been implicated in the transport of diverse cargoes such as melanosomes in pigment cells, synaptic vesicles in neurons, RNA transcripts in a variety of cell types, and organelles such as the endoplasmic reticulum. The Rab GTPases play a critical role in recruiting class V myosins to their cargo. We recently published a study in which we used the yeast two-hybrid system to systematically test myosin Va for its ability to interact with each member of the human Rab GTPase family. We present here a detailed description of this yeast two-hybrid "living chip" assay. Furthermore, we present a protocol for validating positive interactions obtained from this screen by coimmunoprecipitation.

Key words Myosin V, Rab GTPases, Protein–protein interactions, Yeast two-hybrid, Coimmunoprecipitation

1 Introduction

The class V family of unconventional myosins is conserved from yeast to humans. The human myosin V family is comprised of three closely related members [1]. Myosin Va is widely expressed, but is enriched in the brain, testes, and melanocytes. Loss of myosin Va causes Griscelli's syndrome type 1 (GS1), an autosomal recessive disorder characterized by severe central nervous system dysfunction and hypopigmentation [2]. Myosin Vb is ubiquitously expressed, and mutations in the *MYO5B* gene cause microvillus inclusion disease (MVID), a predominantly fatal bowel disease that afflicts new born infants [3]. Myosin Vb is also targeted by a number of viruses, such as HIV and RSV (respiratory syncytial virus),

during their replication cycles. Myosin Vc expression is restricted to glandular and epithelial cells and is relatively uncharacterized. Class V myosins play roles in many diverse cellular processes including secretory vesicle transport, cell division, organelle inheritance, and mRNA transport [4, 5]. Given these diverse roles it is evident that their precise regulation is critical to the proper functioning of eukaryotic cells, and any disruption of their regulatory systems can have severe consequences.

Molecules that regulate class V myosins include kinases, phosphatases, Ca^{2+}, and ATP, but key among these are members of the Rab family of small GTPases. The Rab GTPases make up the largest family of the Ras superfamily of GTPases, with over sixty members in humans [6]. Rabs function as molecular switches which control all aspects of membrane transport including vesicle budding, uncoating, transport, tethering, and fusion. They cycle between a GTP-bound active conformation during which they recruit a large number of "effector" proteins that mediate the transport functions of the Rab and a GDP-bound inactive conformation which is mostly cytosolic [7].

Class V myosins are highly processive motors that take large 36 nm steps along actin filaments. They form large homodimers that can be subdivided into several domains. The amino-terminal motor domain binds to the actin filaments. This is followed by a lever arm with six IQ motifs that bind to various accessory factors including calmodulin. Next is a long coiled-coil domain that mediates dimerization and finally there is a carboxy-terminal globular tail domain (GTD) that is involved in cargo selection. An unstructured region in the coiled-coil domain of myosin Va contains six exons (exons A–F) that undergo tissue-specific alternate splicing. A melanocyte-specific isoform possesses exon F but not exon D, whereas an epithelial-specific isoform has exon D but not exon F [8].

Among the first indications that the class V myosins interact with Rab GTPases came from an elegant series of experiments that demonstrated that the melanocyte isoform of myosin Va interacts, via a linker protein called melanophilin, with Rab27A and that this interaction is involved in the transport of pigment-containing melanosomes to the cell periphery where they can then be transferred to keratinocytes [9–12]. Since then a number of publications have reported direct interactions between class V myosins and several Rab GTPases, including Rab3A [13], Rab8A [14], Rab10 [15], and Rab11A [16]. However, to our knowledge, no myosin had been systematically tested for interactions with the entire Rab GTPase family. To that end, we developed a novel yeast two-hybrid assay in which a protein of interest can be systematically tested for interactions with the wild-type, dominant-negative (DN), and dominant-active (DA) mutants of each human Rab GTPase. We used this assay to screen myosin Va and identified several previously unreported Rab interacting partners including Rab6, Rab14, and

Rab39B [17]. We present here a detailed description of this yeast two-hybrid "living chip" assay, plus a protocol to further test positive interactions by coimmunoprecipitation.

2   Materials

2.1   Buffers and Media

1. YPD: 20 g/L peptone, 20 g/L glucose, 10 g/L yeast extract.

2. DO W⁻L⁻: 27 g/L Drop-out base, 0.64 g/L CSM-Leu-Trp (plus 20 g/L agar for plates).

3. DO W⁻L⁻H⁻: 27 g/L Drop-out base, 0.62 g/L CSM-Leu-Trp-His (plus 20 g/L agar for plates).

4. TE/Lithium acetate: 0.1 M lithium acetate, 1 mM EDTA, 10 mM Tris, pH 8.0.

5. 50 % PEG/TE/LiAc: 50 % polyethylene glycol (3350) in TE/LiAc.

6. Z buffer: 60 mM Na_2HPO_4, 40 mM NaH_2PO_4 (anhydrous), 10 mM KCl, 1 mM $MgSO_4$, pH 7.0.

7. NP-40 Lysis Buffer: 50 mM KCl, 0.5 % NP-40, 20 mM Tris, pH 7.4 plus protease inhibitors (*see* **Note 1**).

8. 3× Sample Buffer: 3 % SDS, 30 % glycerol, 0.01 % bromophenol blue, 15 % 2-mercaptoethanol, 188 mM Tris, pH 6.8.

2.2   Preparation of Yeast Lysates

A colony of transformed yeast is cultured overnight in a shaking incubator at 30 °C in 3 ml of appropriate selection medium. A total of 500 μl of the culture is then added into 30 ml of selection medium and incubated overnight at 30 °C, until the OD_{600} reaches a value of ~2.5. Yeast cells are then centrifuged at $3,000 \times g$ for 15 min, resuspended in 100 μl of sterile water, and an equal volume of 0.5 M NaOH is added and incubated at room temperature for 5 min. A total of 100 μl of 3× SDS-PAGE sample buffer is added and samples are boiled for 5 min and immediately placed on ice. The yeast lysates are now ready to be loaded on a SDS-PAGE gel.

2.3   Yeast Transformation: Lithium Acetate Method

A total of 5 ml of YPD medium is inoculated with a single colony of *S. cerevisiae* L40 and incubated overnight at 30 °C. The overnight culture is added to 50 ml fresh YPD (in a 250 ml glass conical flask) and incubated at 30 °C until the absorbance $OD_{600} \geq 0.3$. The yeast are then transferred to a 50 ml tube, centrifuged at $500 \times g$ for 5 min, resuspended in 20 ml of sterile deionized water, centrifuged at $500 \times g$ for 5 min, resuspended in 10 ml of TE/LiAc solution, centrifuged at $500 \times g$ for 5 min, resuspended in 1 ml of TE/LiAc solution, and incubated at 30 °C for 1 h.

During the 1 h incubation, 1.5 ml microcentrifuge tubes are prepared containing 2 μg of plasmid (1 μg of bait and 1 μg of prey plasmids) plus 40 μg of denatured salmon sperm DNA and kept on

ice. A total of 100 μl of yeast in TE/LiAc is added to each tube and incubated at 30 °C for 10 min. A total of 500 μl 50 % PEG/LiAc is added, the tubes are mixed by inversion, and incubated for a further 60 min at 30 °C. The yeast are then heat shocked at 42 °C for 25 min. The tubes are spun at top speed in a bench-top centrifuge for ~10 s and the supernatant containing the PEG is aspirated off. The pellet is washed twice with 1 ml sterile dH$_2$O to remove of all traces of polyethylene glycol, which will inhibit yeast growth. After the final wash the cells are pelleted, resuspended in 100 μl dH$_2$O, and plated on selection medium (DO W⁻L⁻). Colonies should be visible after 3 days at 30 °C.

2.4 Yeast Transformation Protocol: Mating

The library of pLexA-Rab constructs in the yeast Y187 strain is replica plated from the DO W⁻ selection plate onto a YPD plate and colonies are allowed to grow overnight at 30 °C. The prey construct in the pGADGH plasmid is transformed into the L40 strain and selected on DO L⁻ media. A colony is picked from the plate selection grown overnight in DO L⁻ liquid media. A total of 10 μl of this L40 liquid culture is "dropped" onto each colony of the Y187 transformants and incubated for a further 24 h. The colonies on the YPD are then replica plated onto DO W⁻L⁻ plates to select for diploids.

2.5 Replica Plating

Use a sterile yellow tip, or toothpick, to pick individual colonies from the transformation plates and streak the colony in a small patch on a fresh DO W⁻L⁻ plate. It is possible to fit up to four patches in a row and six rows on a single 100 mm petri dish. We therefore usually patch four separate colonies from each transformation plate. After 1–2 days at 30 °C the patches should be ready for replica plating.

For each "master plate" you will need one fresh DO W⁻L⁻H⁻ plate, one DO W⁻L⁻ plate with an ashless filter on the surface, and another DO W⁻L⁻ plate. Place a piece of sterile velvet on a replica plating block (a circular block over which a 100 mm petri dish can be fit snugly), invert the "master plate" with the patches, and press it down evenly on the sterile velvet. Remove the "master plate" and press the DO W⁻L⁻ plate with the filter on the velvet to create an imprint of the yeast patches. Repeat with the DO W⁻L⁻H⁻ plate and finally the DO W⁻L⁻ plate. This last plate is a positive control for the transfer of the yeast.

Incubate the plates at 30 °C for 2–3 days.

For the "living chip" assay, colonies are arrayed in a 96-well type format, i.e., 12 columns × 8 rows. Yeast colonies expressing wild-type, dominant-active, and dominant-negative Rabs are arrayed on separate plates. A 96-well replica-plater (Sigma) is used to transfer colonies between plates (Fig. 1). The prongs of the replica-plater are pressed onto the colonies of the parental plate with a gentle force and replicates are transferred to fresh plates with equally gentle force.
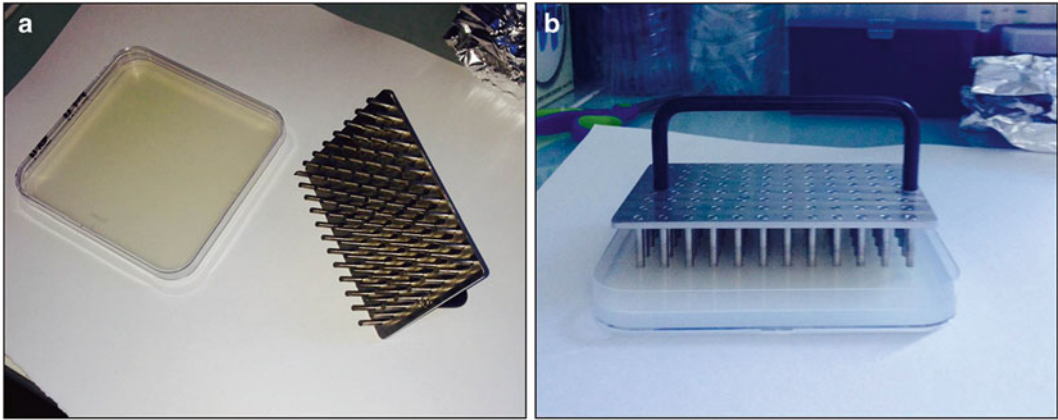
Fig. 1 Replica plating the yeast two-hybrid "living chip" assay. (**a**) Photograph of a 96-well replica-plater and fresh plate containing selection medium. (**b**) Yeast colonies transferred to a fresh selection plate using the 96-well replica-plater

2.6 β-Galactosidase Assay

Once the yeast patches have grown sufficiently on the filter paper (they must be clearly visible) remove the filter and immerse it immediately in liquid nitrogen for >1 min. Remove and allow to thaw at room temperature.

Meanwhile for every filter, prepare 3 ml Z buffer and add 20 µl 2 % (v/v) X-gal solution (dissolved in DMF) plus 8 µl 2-mercaptoethanol. Use this to soak two filter circles and place the yeast filter on top, making sure there are no bubbles between the filters. Leave in a fume hood overnight to allow the color to develop.

Make sure to include positive and negative controls on the filter.

2.7 Cell Culture and Transfection

HeLa cells are cultured in DMEM supplemented with 10 % fetal bovine serum, 100 U/ml penicillin/streptomycin, and 2 mM glutamine in a humidified 95 % air, 5 % CO_2 incubator at 37 °C. One day prior to transfection HeLa cells are detached with trypsin and counted using a hemocytometer. A total of 60,000 cells per well are seeded in each well of a six-well plate. The following day the cells are transfected with 1.5 µg GFP-Rab plasmid using a suitable transfection reagent, according to the manufacturer's instructions. The plate is returned to the incubator for a further 24 h to allow expression of the exogenous protein.

2.8 Coimmunop-recipitations

A total of 1 µg of mouse anti-GFP antibody is bound to 10 µl pre-equilibrated sheep anti-mouse IgG conjugated magnetic beads per CoIP (i.e., if six CoIPs are being performed then 6 µg of anti-GFP and 60 µl of beads are required), in 1 ml NP-40 Lysis Buffer and rotated at 4 °C for at least 1 h.

Twenty-four hours posttransfection the cells are washed twice with 1 ml cold PBS. A total of 500 µl NP-40 Lysis Buffer is added to each well and the plate is rocked in the cold room for approximately 30 min. Lysates are transferred to chilled microcentrifuge tubes and centrifuged at $10,000 \times g$ at 4 °C to remove insoluble debris. The supernatant is used as the starting material for the coimmunoprecipitation and 50 µl is retained at this stage. The antibody-beads complex is isolated with a magnet and resuspended in 50 µl NP-40 Lysis Buffer and added to the starting material. The tubes are then rotated in the cold room for ~4 h. Complexes are isolated with a magnetic strip and washed three times with 250 µl NP-40 Lysis Buffer. After the final wash proteins are eluted from the beads by addition of 50 µl 2× SDS-PAGE sample buffer and heated at 95 °C for 5 min, then placed immediately on ice.

We usually separate 20 µl of the CoIP and 20 µl of the saved starting material by SDS-PAGE and transfer to nitrocellulose. Endogenous myosin Va is detected with a rabbit anti-myosin Va antibody and the GFP-Rabs are detected with a rabbit anti-GFP antibody.

3 Methods

3.1 The Yeast Two-Hybrid System

The yeast two-hybrid system has a number of advantages over other systems for studying protein–protein interactions. One of the major benefits being the speed and ease with which a protein of interest can be tested for interactions with thousands of candidate proteins. Furthermore, in comparison to classical biochemical techniques which may require large amounts of purified proteins or good quality antibodies, the yeast two-hybrid system only requires the cDNA of the protein/s of interest. It is also a eukaryotic system, therefore interactions that require posttranslational modifications of one or both proteins are more likely to be detected in the yeast two-hybrid system than in systems based on a bacterial host. Weak or transient interactions may be more readily detected as the reporter gene response often leads to significant amplification, and finally the strength of interactions can be measured semi-quantitatively.

3.2 Generation of Prey Construct

The first step of this assay is to create an appropriate prey vector and to test it in yeast for expression and potential autoactivation. This may involve the cloning of a full-length protein of interest downstream of a transcription factor activation domain (usually the GAL4 AD), or in the case of larger proteins a truncated version of the protein of interest. As mentioned earlier, the class V myosins form large homodimers and undergo significant conformational changes (from a "closed" inactive conformation to an "open" active conformation) in vivo. Therefore, to create a suitable myosin Va prey vector, the carboxy-terminal 753 amino acids (residues

1,100–1,853) were subcloned into the pGADGH vector. This region of myosin Va contains the previously reported Rab-binding domains, but lacks the motor domain and lever arm and is thus unable to adopt the closed conformation.

In order to test for expression in yeast and to determine if there is any autoactivation, the prey construct is cotransformed into yeast strain L40 (MATa, ura3-52, his3-200, ade2-101, trp1-901, leu2-3, gal4Δ, gal80Δ, URA3::opLEXA-LacZ, LYS2:opLEXA-HIS3) with empty pLexA (bait construct) and grown for 3 days at 30 °C on plates containing synthetic medium lacking tryptophan and leucine (DO W⁻L⁻). Individual colonies are picked and patched, in quadruplicate, onto fresh DO W⁻L⁻ plates. Next day the patches are replica plated onto one DO W⁻L⁻ plate, one DO W⁻L⁻ plate with a circular ashless filter paper placed on the surface, and one DO W⁻L⁻H⁻ plate. The plates were returned to 30 °C for a further 2–3 days. Once patches become visible the filter paper is removed and a β-galactosidase assay is performed. No growth on DO W⁻L⁻H⁻ plates and no blue color in the β-galactosidase assay indicates that the prey construct does not autoactivate the reporter genes (*see* **Notes 2** and **3**).

In order to confirm that the prey fusion protein is expressed, a colony from the transformation plates is cultured in liquid selection medium. Once the yeast reach an $OD_{600} \sim 2.5$ the cells are pelleted and lysed. Lysates (containing the prey vector and lysates from the negative control transformation) are separated by SDS-PAGE, transferred to nitrocellulose and probed with an antibody to the GAL4 activation domain, or to the protein of interest. A band corresponding to the combined size of the protein of interest and the activation domain should be observed in the lysate containing the prey construct but not in the negative control lysate.

3.3   Yeast Two-Hybrid "Living Chip" Assay

Once the prey vector has been validated it is possible to proceed to the "living chip" assay. The yeast strain Y187 (MATα, ura3-52, his3-200, ade2-101, trp1-901, leu2-3, gal4Δ, gal8Δ, met-, URA3::GAL1UAS-GAL1TATAlacZ MEL1) is transformed with the pLexA-Rab constructs (wild-type, DA, and DN mutants for each Rab). Transformants were selected on synthetic medium lacking tryptophan. Yeast stocks in glycerol were distributed on 96-well plates and kept at –80 °C. Before experiments, plates were replica plated onto YPD-rich medium in 120 mm × 120 mm square petri dishes and then onto selective medium.

The pGADGH-myosin Va constructs are transformed into the yeast strain L40ΔGal4 (MATa, ura3-52, his3-200, ade2-101, trp1-901, leu2-3, gal4Δ, gal80Δ, URA3::opLexA-LacZ, LYS2 :opLEXA-HIS3) and selected on synthetic medium lacking leucine. After an overnight incubation on rich medium at 30 °C, Y187 and L40 strains form diploids. Diploid cells containing the pLEX and pGADGH plasmids were selected on synthetic medium lacking leucine and tryptophan, and then replica plated onto synthetic medium also lacking histidine and incubated for a further 3–6 days.
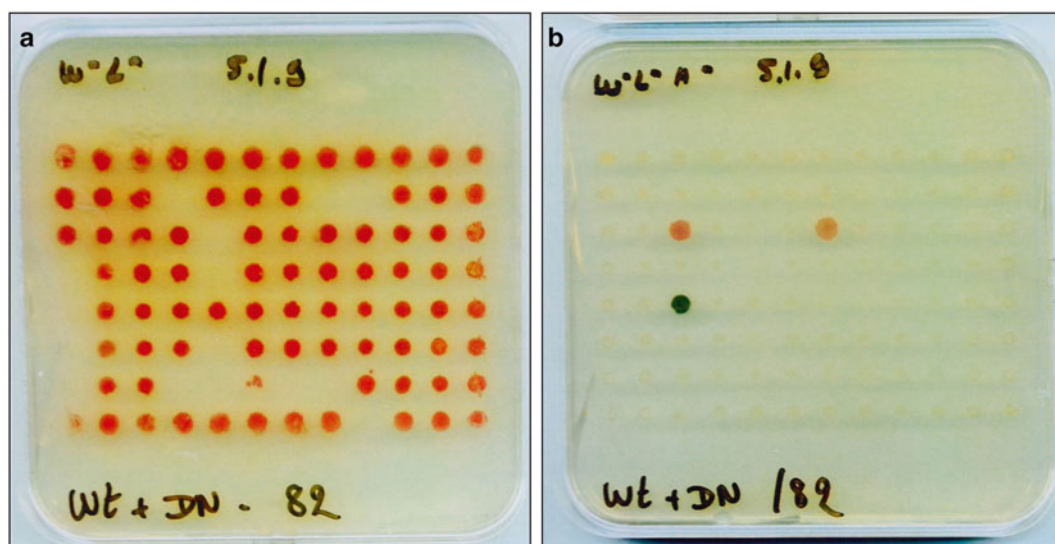
Fig. 2 Yeast two-hybrid "living chip" assay. (**a**) An array of yeast colonies growing on media lacking tryptophan and leucine which selects for transformants containing both the bait and prey plasmids. (**b**) The array in (**a**) was replica plated onto medium lacking tryptophan, leucine, and histidine and containing X-gal. Three colonies grow on medium lacking histidine, one of which also expresses the β-galactosidase gene (as indicated by the *blue* color)

His + colonies were patched on selective plates and assayed for β-galactosidase activity. This technique has been successfully validated for several Rab6 effectors, as well as other proteins such as molecular motors (Fig. 2).

Each positive interaction should be retested individually by cotransforming the pLexA-Rab constructs with the pGADGH prey construct into the L40 yeast strain [18].

3.4 GFP-Rab Coimmunoprecipitations

One of the major disadvantages of the yeast two-hybrid system is the relatively high rate of false-positives. Therefore, the yeast two-hybrid system alone is usually not sufficient to convince reviewers that a protein–protein interaction is physiologically relevant and further proof is typically required.

In this section, we describe a method for analyzing the interaction of a protein of interest, myosin Va, with the DA- and DN-mutants of the Rab GTPases that were positive in the "living chip" assay. The advantage of this method over GST pulldowns is that it does not require the purification of each Rab from bacteria. This can save a lot of time, especially if the living chip assay produced several "hits." Also, some Rabs (e.g., Rab8 and Rab10) can be extremely difficult to purify in sufficient quantities from *E. coli*. It also eliminates the need for a nucleotide exchange step. The inclusion of the dominant-negative mutant of each Rab provides the most appropriate negative control for each interaction.

HeLa cells are seeded in six-well plates at a density such that they are 70–80 % confluent the next day (*see* **Note 4**). The cells are

transfected with equal amounts of GFP-fused DA- and DN-Rab plasmids using an appropriate transfection reagent (*see* **Notes 5** and **6**). It is important to use a quantity of plasmid and transfection reagent that achieve a high enough transfection efficiency without causing significant cell death (*see* **Note 7**). Twenty-four hours post-transfection the cells are washed twice with cold PBS and lysed in 500 μl NP-40 Lysis Buffer with appropriate protease inhibitors. We use a mouse monoclonal anti-GFP antibody bound to anti-mouse IgG-conjugated magnetic beads to immunoprecipitate the GFP-fusion Rabs. Magnetic beads allow for the rapid isolation of antibody–antigen complexes and are gentler than standard Sepharose-bead techniques as they eliminate the centrifugation steps. After extensive washing the bound proteins are eluted in SDS-PAGE sample buffer and boiled. Eluates are separated by SDS-PAGE, transferred to nitrocellulose, and probed with the appropriate antibodies. In our case, we use a rabbit anti-myosin Va antibody to detect endogenous myosin Va in the immunoprecipitates. Since the GFP-Rabs have a molecular weight of ~50 kDa, close to the MW of the mouse heavy chain, we use a rabbit anti-GFP antibody to detect the overexpressed Rabs by Western blot. We typically observe a strong myosin Va band in the Rab-DA CoIP lane and a fainter band in the –DN lane (Fig. 3).
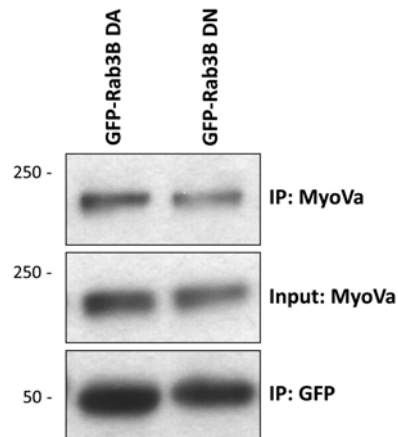
Fig. 3 GFP-Rab Coimmunoprecipitation. Lysates generated from HeLa cells transfected with GFP-Rab3B DA or GFP-Rab3B DN were subjected to immunoprecipitation with a mouse anti-GFP antibody. Samples of the starting material (input) and proteins eluted from the magnetic beads after the coimmunoprecipitation (IP) were separated by SDS-PAGE, transferred to nitrocellulose, and probed with antibodies to myosin Va and GFP. Note the roughly equivalent amounts of endogenous myosin Va in the input lanes, but the stronger band for myosin Va in the GFP-Rab3B DA IP lane (quantification indicates that the myosin Va band displays ~50 % greater intensity in the Rab3B DA lane). Similar amounts of GFP-Rab3B DA and GFP-Rab3B DN fusion proteins have been immunoprecipitated with the anti-GFP antibody. The location of molecular weight markers is indicated to the left of each Western blot

4   Notes

1. When examining class V myosin interactions it is advisable not to include EDTA or EGTA in the NP-40 Lysis Buffer as this will chelate the calcium, thus providing favorable conditions for the myosin to adopt the closed conformation which may mask the Rab-binding domains.

2. It is important to include appropriate positive and negative controls. A widely used positive control is the interaction between Ras and Raf, and yeast cotransformed with the empty pGADGH and pLexA vectors can be used as negative controls.

3. The *LacZ* gene is much less prone to autoactivation than the *HIS3* gene. If autoactivation does occur it may be possible to reduce it by including 3-amino-triazole (3-AT), an inhibitor of the *HIS3* gene product, in the media. Too little 3-AT will lead to false-positives whereas too much may lead to loss of weak interactions. Therefore, the optimal concentration of 3-AT should be determined prior to the living chip assay by testing cotransformants for *HIS3* expression at a range of 3-AT concentrations (from 0 to 50 mM).

4. Other cell lines that can be transfected with high efficiency, such as HEK293 and COS-1, may be used instead of HeLa cells.

5. It is important that the plasmids are sufficiently pure to achieve high levels of transfection efficiency. Most commercial midi- or maxi-rep kits produce plasmids of sufficient purity ($A260/A280 \geq 1.8$).

6. We have successfully used several transfection reagents including XtremeGene9 (Roche Applied Science), Lipofectamine 2000 (Life Technologies), and TurboFect (Fermentas). The calcium phosphate technique can also be used.

7. In general, GFP-fused Rabs are expressed with high efficiency in HeLa cells and show little toxicity. Rabs that are difficult to express in bacterial expression systems (e.g., Rab8 and Rab10) are readily expressed in mammalian cells.

Acknowledgements

References

1. Sellers JR (2000) Myosins: a diverse superfamily. Biochim Biophys Acta 1496(1):3–22

2. Rudolf R, Bittins CM, Gerdes HH (2011) The role of myosin V in exocytosis and synaptic plasticity. J Neurochem 116(2):177–191. doi:10.1111/j.1471-4159.2010.07110.x

3. Muller T, Hess MW, Schiefermeier N, Pfaller K, Ebner HL, Heinz-Erian P, Ponstingl H, Partsch J, Rollinghoff B, Kohler H, Berger T, Lenhartz H, Schlenck B, Houwen RJ, Taylor CJ, Zoller H, Lechner S, Goulet O, Utermann G, Ruemmele FM, Huber LA, Janecke AR (2008) MYO5B mutations cause microvillus inclusion disease and disrupt epithelial cell polarity. Nat Genet 40(10):1163–1165

4. McCaffrey MW, Lindsay AJ (2012) Roles for myosin Va in RNA transport and turnover. Biochem Soc Trans 40(6):1416–1420

5. Hammer JA 3rd, Sellers JR (2011) Walking to work: roles for class V myosins as cargo transporters. Nat Rev Mol Cell Biol 13(1):13–26

6. Kelly EE, Horgan CP, Goud B, McCaffrey MW (2012) The Rab family of proteins: 25 years on. Biochem Soc Trans 40(6):1337–1347

7. Stenmark H (2009) Rab GTPases as coordinators of vesicle traffic. Nat Rev Mol Cell Biol 10(8):513–525

8. Trybus KM (2008) Myosin V from head to tail. Cell Mol Life Sci 65(9):1378–1389

9. Fukuda M, Kuroda TS, Mikoshiba K (2002) Slac2-a/Melanophilin, the Missing Link between Rab27 and Myosin Va: implications of a tripartite protein complex for melanosome transport. J Biol Chem 277(14):12432–12436

10. Wu X, Wang F, Rao K, Sellers JR, Hammer JA 3rd (2002) Rab27a is an essential component of melanosome receptor for myosin Va. Mol Biol Cell 13(5):1735–1749

11. Wu XS, Rao K, Zhang H, Wang F, Sellers JR, Matesic LE, Copeland NG, Jenkins NA, Hammer JA 3rd (2002) Identification of an organelle receptor for myosin-Va. Nat Cell Biol 4(4):271–278

12. Hume AN, Collinson LM, Hopkins CR, Strom M, Barral DC, Bossi G, Griffiths GM, Seabra MC (2002) The leaden gene product is required with Rab27a to recruit myosin Va to melanosomes in melanocytes. Traffic 3(3):193–202

13. Wollert T, Patel A, Lee YL, Provance DW Jr, Vought VE, Cosgrove MS, Mercer JA, Langford GM (2011) Myosin5a tail associates directly with Rab3A-containing compartments in neurons. J Biol Chem 286(16): 14352–14361

14. Roland JT, Kenworthy AK, Peranen J, Caplan S, Goldenring JR (2007) Myosin Vb interacts with Rab8a on a tubular network containing EHD1 and EHD3. Mol Biol Cell 18(8):2828–2837

15. Roland JT, Lapierre LA, Goldenring JR (2009) Alternative splicing in class v myosins determines association with rab10. J Biol Chem 284(2):1213–1223

16. Lapierre LA, Kumar R, Hales CM, Navarre J, Bhartur SG, Burnette JO, Provance DW Jr, Mercer JA, Bahler M, Goldenring JR (2001) Myosin vb is associated with plasma membrane recycling systems. Mol Biol Cell 12(6):1843–1857

17. Lindsay AJ, Jollivet F, Horgan CP, Khan AR, Raposo G, McCaffrey MW, Goud B (2013) Identification and characterization of multiple novel Rab-myosin Va interactions. Mol Biol Cell 24(21):3420–3434. doi:10.1091/mbc.E13-05-0236

18. Janoueix-Lerosey I, Jollivet F, Camonis J, Marche PN, Goud B (1995) Two-hybrid system screen with the small GTP-binding protein Rab6. Identification of a novel mouse GDP dissociation inhibitor isoform and two other potential partners of Rab6. J Biol Chem 270(24):14801–14808

Chapter 7

Assaying the Interaction of the Rab Guanine Nucleotide Exchange Protein Sec2 with the Upstream Rab, a Downstream Effector, and a Phosphoinositide

Danièle Stalder and Peter J. Novick

Abstract

Rabs are activated by guanine nucleotide exchange proteins, which are in turn controlled by complex regulatory mechanisms. Here we describe several different assays that have been used to delineate the mechanisms by which Sec2p, the exchange factor for the Rab Sec4p, is regulated. These assays assess the interaction of Sec2p with the upstream Rab, Ypt32p, a downstream Sec4p effector, Sec15p, and the lipid, phosphatidylinositol-4-phosphate.

Key words Sec2p, Sec4p, Sec15p, Ypt32p, Phosphatidylinositol-4-phosphate, Guanine nucleotide exchange factor, Effector

1 Introduction

GTPases of the Rab family act as molecular switches that control specific stages of membrane traffic by recruiting or activating distinct sets of effectors [1]. Sec4p is the Rab controlling the final stage of the yeast exocytic pathway [2], while Sec2p is the guanine nucleotide exchange protein (GEF) that specifically activates Sec4p on the surface of secretory vesicles [3, 4]. Sec2p is recruited to the vesicle membrane by binding to the activated form of Ypt32p [5], a Rab that acts just upstream of Sec4p on the exocytic pathway [6, 7]. This constitutes a regulatory circuit we have termed as Rab GEF cascade [8]. Sec2p recruitment also requires an interaction with phosphatidylinositol-4-phosphate (PI(4)P) and Sec2p acts as a coincidence detector, binding specifically to membranes containing both Ypt32-GTP and PI(4)P [9]. Sec2p also binds to Sec15p, a direct effector of Sec4p and a component of the vesicle tethering complex termed the exocyst [10]. The interaction of a GEF with one of the effectors of the Rab that it activates could generate a positive feedback loop that leads to the formation of a membrane

domain marked by highly activated Rab protein and highly concentrated effectors [8]. Competition binding studies indicate that Ypt32p and Sec15p compete for the same site on Sec2p [10], implying that Sec2p can be involved in either a GEF cascade or a GEF-effector positive feedback loop, but not both at the same time. We have used several different assays to explore how this choice in the binding partner of Sec2p is directed. Here we describe assays for the interaction of Sec2p with Ypt32p, Sec15p, and PI(4)P. Our studies have indicated a role for both PI(4)P and phosphorylation of Sec2p in this regulatory choice [9, 11].

2   Materials

2.1 Expression and Purification of GST-Sec2p and GST Alone

1. 1× PBS: 137 mM NaCl, 10 mM Na_2HPO_4, 1.8 mM KH_2PO_4, 2.7 mM KCl, adjust pH to 7.2.

2. Lysis buffer: 1× PBS pH 7.2, 5 mM $MgCl_2$, 1 mM phenylmethylsulfonyl fluoride (PMSF), 1× protease inhibitors (complete EDTA-free proteases inhibitor mixture tablets from Roche), 1 mM dithiothreitol (DTT).

3. Wash buffer: 1× PBS pH 7.2, 1 mM $MgCl_2$, 1 mM DTT, 0.1 % Triton X-100.

4. Elution buffer: 100 mM Tris pH 8, 300 mM NaCl, 20 mM glutathione.

5. Freeze buffer: 20 mM Tris pH 7.2, 100 mM NaCl, 1 mM $MgCl_2$, 10 % glycerol (vol/vol), 1 mM DTT.

2.2 Expression and Purification of HIS$_6$-Ypt32p

1. 1× PBS: 137 mM NaCl, 10 mM Na_2HPO_4, 1.8 mM KH_2PO_4, 2.7 mM KCl, adjust pH to 7.2.

2. Lysis buffer: 1× PBS pH 7.2, 160 mM NaCl, 1 mM $MgCl_2$, 1 mM phenylmethylsulfonyl fluoride (PMSF), 1× protease inhibitors (complete EDTA-free proteases inhibitor mixture tablets from Roche), 15 mM Imidazole pH 8.

3. Wash buffer: 1× PBS pH 7.2, 160 mM NaCl, 1 mM $MgCl_2$, 0.1 % Triton X-100, 25 mM Imidazole pH 8.

4. Elution buffer: 1× PBS pH 7.2, 160 mM NaCl, 1 mM $MgCl_2$, 300 mM Imidazole pH 8.

5. Freeze buffer: 20 mM Tris pH 7.2, 100 mM NaCl, 1 mM $MgCl_2$, 10 % glycerol (vol/vol), 1 mM DTT.

2.3 Expression and Purification of HIS$_6$-Sec15p

1. Terrific Broth (TB) media:
   - YPG base: 12 g bacto-tryptone, 24 g bacto-yeast extract, 4 mL glycerol, adjust to 900 mL with H_2O.
   - Potassium phosphate solution: 2.31 g KH_2PO_4, 12.54 g K_2HPO_4, adjust to 100 mL with H_2O.

Autoclave separately, add potassium phosphate solution to YPG base after cool down.

2. Lysis buffer: 1× PBS pH 7.2, 160 mM NaCl, 1 mM $MgCl_2$, 1 mM phenylmethylsulfonyl fluoride (PMSF), 1× protease inhibitors (complete EDTA-free proteases inhibitor mixture tablets from Roche), 15 mM Imidazole pH 8.

3. Wash buffer: 1× PBS pH 7.2, 160 mM NaCl, 1 mM $MgCl_2$, 0.1 % Triton X-100, 25 mM Imidazole pH 8.

4. Elution buffer: 1× PBS pH 7.2, 160 mM NaCl, 1 mM $MgCl_2$, 300 mM Imidazole pH 8.

5. Freeze buffer: 20 mM Tris pH 7.2, 100 mM NaCl, 1 mM $MgCl_2$, 10 % glycerol (vol/vol), 1 mM DTT.

2.4 Expression and Purification of Lyticase

1. Sodium citrate buffer: 6.4 g citric acid, 48.8 g sodium citrate, adjust to 4 L with H_2O, adjust the pH to 5.8.

2.5 In Vitro Binding Assay

– GST-Sec2p/HIS$_6$-Ypt32p interaction.

1. Nucleotide exchange buffer: 1× PBS pH 7.2, 1 mM GTPγS (Roche), 1 mg/mL BSA, 1 mM EDTA, 1 mM DTT.

2. Binding buffer: 1× PBS pH 7.2, 0.5 mg/mL BSA, 0.025 % Triton X-100, 0.5 mM $MgCl_2$, 0.5 mM DTT, 0.1 mM GTPγS.

3. Wash buffer: 1× PBS pH 7.2, 0.05 % Triton X-100, 5 mM $MgCl_2$, 1 mM DTT, 10 µM GTPγS.

– GST-Sec2p/HIS$_6$-Sec15p interaction.

1. Binding buffer: 1× PBS pH 7.2, 0.5 mg/mL BSA, 0.5 mM $MgCl_2$, 0.5 mM DTT.

2. Wash buffer: 1× PBS pH 7.2, 0.05 % TX-100, 5 mM $MgCl_2$, 1 mM DTT.

2.6 Immunoprecipitation Assay

1. YPD media:
   – YP media: 10 g yeast extract, 20 g peptone, adjust to 950 mL with H_2O.
   – 40 % glucose solution: 40 g glucose, adjust to 100 mL with H_2O.
   – Autoclave separately, cool down, and add 50 mL of the 40 % glucose solution to the YP media (2 % glucose).

2. Spheroplasting media: 50 mM KPO_4 pH 7.5, 1.2 M sorbitol, 1 mM $MgCl_2$, 24 µg/mL lyticase.

3. Lysis buffer: 10 mM triethanolamine-AcOH pH 7.2, 0.4 M sorbitol, 1 mM EDTA, 5 mM PMSF, 1× protease inhibitors (complete EDTA-free proteases inhibitor mixture tablets from Roche).

2.7 Liposomes Preparation and Sedimentation Experiment	1. HEPES–sucrose buffer: 50 mM HEPES pH 7.2, 210 mM sucrose.

2.7 Liposomes Preparation and Sedimentation Experiment

1. HEPES–sucrose buffer: 50 mM HEPES pH 7.2, 210 mM sucrose.

2. HK buffer: 50 mM HEPES pH 7.2, 120 mM potassium acetate.

3. Sedimentation buffer: 50 mM HEPES pH 7.2, 120 mM potassium acetate, 1 mM $MgCl_2$, 1 mM DTT.

3 Methods

3.1 Expression and Purification of GST-Sec2p and GST Alone

1. *E. coli* Bl21 cells were transformed with the empty plasmid, pGEX4T1 (for expression of GST alone) or pGEX4T1-Sec2p WT (NRB1152 constructed as described in [5]). The GST tag is fused to the N-terminus of Sec2p.

2. Several transformants were screened by small-scale induction. One transformant with a high level of expression was stored at –80 °C in 15 % glycerol.

3. Inoculate one colony in 3 mL Luri-Bertani (LB) medium containing 0.05 mg/mL ampicillin. Grow overnight at 37 °C.

4. The next day, inoculate 2.5 mL of the overnight culture into 250 mL LB containing 0.05 mg/mL ampicillin. Grow at 37 °C to an OD_{600} of 0.6.

5. Add isopropyl-β-D-thiogalactopyranoside (IPTG) to 0.1 mM and grow overnight at 16 °C.

6. Harvest the cells by centrifugation at 5,000 rpm for 15 min at 4 °C using a JA-10 rotor from Beckman Coulter (~2,800 × g).

7. Wash the pellet with 50 mL ice-cold 1× PBS.

8. Harvest the cells by centrifugation at 3,500 rpm for 20 min at 4 °C with a GH-3.8 rotor from Beckman Coulter (~1,400 × g). The pellet can be stored at –80 °C.

9. Resuspend the pellet with 25 mL of ice-cold Lysis buffer.

10. Sonicate on ice for 2 min by alternating 10 s burst/10 s break using a Fisher Scientific sonic dismembrator model 500 set at 50 % amplitude.

11. Add 1 % Triton X-100 (2.5 mL of 10 % Triton X-100 into 25 mL lysate) and incubate at 4 °C for 15 min on a nutator.

12. Clear the suspension by centrifugation at 15,000 rpm for 30 min at 4 °C with a JA-20 rotor from Beckman Coulter (~18,000 × g)

13. Add to the supernatant 250 µL of glutathione-Sepharose beads prewashed with Lysis buffer. Incubate for 60 min at 4 °C on a nutator.

14. Pellet the beads by centrifugation at 1,500 rpm for 5 min at 4 °C using a GH-3.8 rotor from Beckman Coulter (~250 × g).

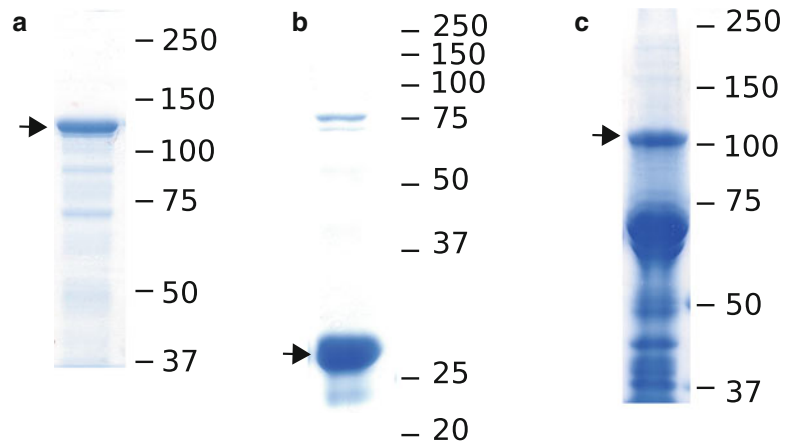15. Wash the beads twice with 10 mL ice-cold Wash buffer.

Fig. 1 (**a**) Bacterially expressed GST-Sec2p was purified on glutathione-Sepharose beads (5 μL of a 50 % beads slurry) then electrophoresed on a 8 % SDS-PAGE gel and visualized by Coomassie Brilliant Blue staining. (**b**, **c**) Bacterially expressed HIS_6-Ypt32p (**b**) and HIS_6-Sec15p (**c**) were purified on Ni^{2+}-NTA resin (5 μL of eluted protein) and then electrophoresed on a SDS-PAGE gel (13.5 and 8 %, respectively) and visualized by Coomassie Brilliant Blue staining. *Arrows* indicate the protein of interest

16. Stop at this step for in vitro binding assays (*see* **Note 1** and Fig. 1a).

17. Transfer the beads to a Poly-Prep Chromatography Column (Bio-Rad). Work in the cold room.

18. Wash with 1 mL of Wash buffer (fraction 1). Elute with 100 μL Elution buffer about ten times. Check the amount of protein in each fraction with a SDS-PAGE gel 8 % (load 5 μL, GST-Sec2p migrates at approximately 130 kDa). Pool the fractions containing the highest amount of GST-Sec2p (usually fractions 3–7).

19. Load the protein sample into a Slide-A-Lyzer dialysis cassette 3.5 K. Dialyze overnight at 4 °C against 2 L ice-cold Freeze buffer.

20. Store the proteins directly at –80 °C after freezing in liquid nitrogen.

3.2 Expression and Purification of HIS₆-Ypt32p

The plasmid pET-15b Ypt32p (NRB845) was expressed in *E. coli* Rosetta 2 cells (*see* **Note 2**). The hexahistidine tag (HIS_6) is attached to the N-terminus of Ypt32p. The protein migrates at approximately 25 kDa (*see* Fig. 1b).

Follow the same protocol as for GST-Sec2p except use the buffers of the composition indicated earlier and use Ni^{2+}-NTA resin instead of glutathione-Sepharose beads. After elution and dialysis of HIS_6-Ypt32p, the protein can be stored at –80 °C for months and can be used directly for in vitro binding assays.

3.3 Expression and Purification of HIS$_6$-Sec15p

The expression and purification of recombinant, full-length Sec15p protein has proven to be quite difficult. It is a large protein, of a bit more than 100 kDa, that is highly insoluble when expressed in bacteria and easily degraded during purification (*see* Fig. 1c). The protocol presented here allows us to partially purify full-length Sec15p protein, albeit in small amounts, but still sufficient to be able to perform in vitro binding assays.

1. The plasmid pET-46 Sec15p (NRB1426) was expressed in *E. coli* Rosetta 2 cells (*see* **Note 3**). The hexahistidine tag (HIS$_6$) is fused to the N-terminus of Sec15p. Several transformants were screened by small-scale induction. The transformant with the highest level of expression was stored at –80 °C in 15 % glycerol.

2. Inoculate one colony in 10 mL TB media containing 0.05 mg/mL ampicillin and 0.034 mg/mL chloramphenicol. Grow overnight at 37 °C.

3. The following day, inoculate 10 mL of the overnight culture into 1 L TB media containing 0.05 mg/mL ampicillin and 0.034 mg/mL chloramphenicol. Grow at 37 °C to an OD$_{600}$ of 1 (*see* **Note 4**).

4. Chill the cells on ice for 30 min.

5. Add 0.1 mM IPTG and grow overnight at 16 °C.

6. Harvest the cells by centrifugation at 5,000 rpm for 15 min at 4 °C with a JA-10 rotor from Beckman Coulter (~2,800 × g).

7. Wash the pellet with 50 mL ice-cold 1× PBS.

8. Harvest the cells by centrifugation at 3,500 rpm for 20 min at 4 °C with a GH-3.8 rotor from Beckman Coulter (~1,400 × g) (*see* **Note 5**).

9. Resuspend the pellet in 25 mL of ice-cold Lysis buffer.

10. Sonicate on ice three times for 1 min by alternating 10 s burst/10 s break with a Fisher Scientific sonic dismembrator model 500 set at 50 % amplitude. Allow the suspension to cool down for 5 min between each sonication round.

11. Add 1 % Triton X-100 (2.5 mL of 10 % TX-100 into 25 mL lysate) and incubate at 4 °C for 15 min on a nutator.

12. Clear the suspension by centrifugation at 15,000 rpm for 30 min at 4 °C using a JA-20 rotor from Beckman Coulter (~18,000 × g).

13. Add to the supernatant 1 mL of Ni^{2+}-NTA resin prewashed with Lysis buffer. Incubate for 60 min at 4 °C on a nutator.

14. Pellet the beads by centrifugation at 1,500 rpm for 5 min at 4 °C with a GH-3.8 rotor from Beckman Coulter (~250 × g).

15. Wash the resin twice with 10 mL ice-cold Wash buffer.

16. Transfer the resin to a Poly-Prep Chromatography Column (Bio-Rad). Work in the cold room.

17. Wash the resin with 1 mL of Wash buffer (fraction 1). Elute with 100 µL Elution buffer about 15 times. Check the amount of protein in each fraction with a SDS-PAGE gel 8 % (load 5 µL). Pool the fractions containing the highest amount of full-length HIS_6-Sec15p.

18. Load the protein sample into a Slide-A-Lyzer dialysis cassette 3.5 K. Dialyze overnight at 4 °C against 2 L ice-cold Freeze buffer.

19. Store the proteins directly at –80 °C after freezing in liquid nitrogen.

3.4 Expression and Purification of Lyticase

The purification of lyticase was performed in a similar manner as described in [12].

1. The plasmid NRB1202 (from J. Weissman laboratory) was expressed in *E. coli* Rosetta 2 cells.

2. Inoculate one colony into 50 mL LB media containing 0.05 mg/mL ampicillin and 0.034 mg/mL chloramphenicol. Grow overnight at 37 °C.

3. The following morning, transfer 20 mL of the culture into 1 L LB media containing 0.05 mg/mL ampicillin and 0.034 mg/mL chloramphenicol. Grow at 37 °C.

4. When OD_{600} reaches 0.7, add 0.5 mM IPTG.

5. After 3 h at 37 °C, harvest the cells by centrifugation at 5,000 rpm for 30 min at 25 °C with a JA-10 rotor from Beckman Coulter (~2,800 × g).

6. Resuspend the cells in 20 mL of 25 mM Tris, pH 7.4, and incubate at room temperature with gentle agitation for 30 min.

7. Centrifuge at 7,500 rpm for 10 min at 4 °C with a JA-10 rotor from Beckman Coulter (~6,200 × g).

8. Resuspend the pellet in 20 mL of 5 mM $MgCl_2$, incubate on ice for 30 min.

9. Spin at 15,000 rpm for 30 min at 4 °C with a JA-20 rotor from Beckman Coulter (~18,000 × g).

10. Load the supernatant in a spectra/por membrane tubing MWCO 6000-8000 32 mm (hydrate the membrane before use with H_2O for 30 min minimum and wash several times).

11. Dialyze against 4 L of sodium citrate buffer overnight at 4 °C.

12. Concentrate from 20 to around 1 mL with a Amicon ultra centrifugal filter (Millipore, UFC900324).

13. Measure protein concentration using the Bradford assay (it is usually between 0.5 and 1 mg/mL). Use at 24 µg/mL for spheroplasting.

14. Store directly at –80 °C.

3.5 In Vitro Binding Assay (See Note 1)

– GST-Sec2p/HIS$_6$-Ypt32p GTPγS interaction.

Preloading of HIS$_6$-Ypt32p with GTPγS

1. Incubate 5 μM of eluted HIS$_6$-Ypt32p protein in 200 μL Nucleotide exchange buffer for 1 h at room temperature on a nutator.

2. Stop the reaction by addition of 5 mM MgCl$_2$.

3. Incubate for 30 min more.

4. Put on ice until use.

Binding Assay

1. Mix 0.6 μM of GTPγS loaded HIS$_6$-Ypt32p protein with 2.5 μg of freshly purified GST (as a negative control) or GST-Sec2p protein immobilized on glutathione-Sepharose beads into 200 μL Binding buffer. Add to the reaction 10 μL of empty glutathione-Sepharose beads prewashed with PBS 1× buffer (*see* **Note 6**).

2. Save 10 μL of one reaction tube for the input.

3. Incubate for 1 h at 4 °C on a tube rotator.

4. Pellet the beads by centrifugation at 3,500 rpm for 1 min at 4 °C with a Swing-bucket rotor A-8-11 from Eppendorf (~1,300 × g).

5. Wash the beads three times with 0.5 mL Wash buffer for 3 min at 4 °C on a nutator.

6. Add 30 μL of 2× Sample buffer on the beads.

7. Boil the samples for 10 min.

8. 15 and 5 μL of the samples were separated on a 13.5 % SDS/PAGE gel and analyzed by western blotting, respectively, with an anti-Ypt32p antibody (1:6,000 dilution, a gift from the Ferro-Novick laboratory, University of California, San Diego, La Jolla, CA) (*see* **Note 7**) and with an anti-GST antibody (1:1,000 dilution; sc-459; Santa Cruz Biotechnology; to verify the amount of GST-Sec2p) as primary antibodies. HRP-conjugated goat anti-rabbit IgG (1:10,000 dilution) was used as the secondary antibody and was detected with Pierce ECL Western Blotting Substrate (Thermo Scientific) (*see* Fig. 2a).

– GST-Sec2p/HIS$_6$-Sec15p interaction.

The binding of HIS$_6$-Sec15p to GST alone or GST-Sec2p immobilized on glutathione-Sepharose beads was conducted in a manner similar to that described earlier except that only 0.5 μg HIS$_6$-Sec15p was used, the Binding buffer was free of both GTPγS and Triton X-100 and the Wash buffer was GTPγS free (*see* **Note 8**). The samples were separated on an 8 % SDS/PAGE gel. Bound HIS$_6$-Sec15p protein was analyzed by western blotting with an anti-Sec15p antibody (1:2,000 dilution) as the primary antibody (*see* Fig. 2b).
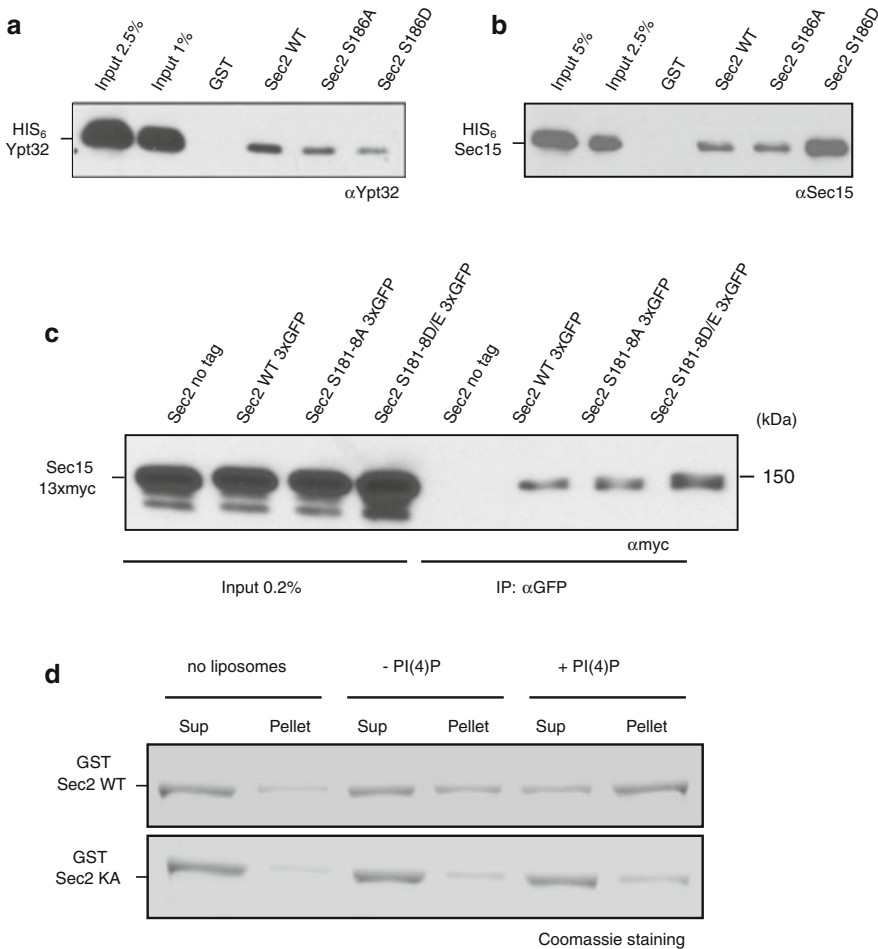
Fig. 2 (**a**, **b**) GST, GST-Sec2p, HIS_6-Ypt32p, and HIS_6-Sec15p were purified from bacteria. Eluted HIS_6-Ypt32p, preloaded with GTPγS (**a**) and eluted full-length HIS_6-Sec15p (**b**) were incubated with GST or GST-Sec2p immobilized on glutathione-Sepharose beads. Bound proteins were subjected to western blot analysis using anti-Ypt32p antibody or anti-Sec15p antibody. To verify that an equal amount of GST-Sec2p was present in each reaction, an anti-GST antibody was used (data not shown). By this approach, we showed that a phosphomimetic mutant of GST-Sec2p, GST-Sec2p S186D, exhibits in vitro a decrease in binding to HIS_6-Ypt32p and a correlated increase in binding to HIS_6-Sec15p [11]. (**c**) Sec2p tagged with 3xGFP was immunoprecipitated with an anti-GFP antibody from a yeast lysate coexpressing Sec15p tagged with 13xmyc. As a negative control, a yeast lysate expressing untagged Sec2p was used. The amount of Sec15p-13xmyc in the immunoprecipitates and in 0.2 % of the lysates was detected by western blot using an anti-myc antibody. To verify that an equal amount of Sec2p-3xGFP was present in each lysate, an anti-GFP antibody was used (data not shown). By this approach, we showed that, in vivo, a phosphomimetic allele of Sec2p, Sec2p S181-8D/E, exhibits increased binding to Sec15p-13xmyc [11]. (**d**) Bacterial purified and eluted GST-Sec2p was incubated with liposomes containing or not the phosphoinositide PI(4)P (45 or 50 mol % DPPC, 20 mol % DPPE, 30 mol % POPS, with or without 5 mol % PI(4)P). Liposomes were pelleted and GST-Sec2p in the supernatant (Sup) and in the pellet were visualized by Coomassie Brilliant Blue staining after SDS-PAGE gel. By this approach, we showed that mutations within three positively charged patches prevent GST-Sec2p (GST-Sec2p KA) from binding to PI(4)P [9, 11]

3.6 Immunoprecipitation Assay

1. Yeast cells expressing under endogenous promoters Sec2p tagged with 3xGFP and Sec15p tagged with 13xmyc are inoculated into 100 mL YPD media and grown overnight at 25 °C to midlog phase (OD_{600} between 0.5 and 1). As a control, we use yeast cells expressing Sec15p tagged with 13xmyc and untagged Sec2p.

2. A total of 75 OD_{600} units of cells are harvested by centrifugation at 3,000 rpm for 10 min at 4 °C with a GH-3.8 rotor from Beckman Coulter ($\sim 1,000 \times g$).

3. Wash the cells with 1 mL 1.2 M sorbitol and 10 mM NaN_3.

4. Harvest the cells by centrifugation at 3,000 rpm for 5 min at 4 °C with a GH-3.8 rotor from Beckman Coulter ($\sim 1,000 \times g$).

5. Resuspend the cells with 1 mL 50 mM Tris–HCl pH 8.0 and 1 % 2-mercaptoethanol.

6. Incubate for 10 min at 30 °C with gentle shaking.

7. Harvest the cells by centrifugation at 3,000 rpm for 5 min at 4 °C with a GH-3.8 rotor from Beckman Coulter ($\sim 1,000 \times g$).

8. Resuspend the cells with 1 mL Spheroplasting media (*see* **Note 9**).

9. Incubate for 60 min at 30 °C with gentle shaking.

10. Harvest the cells by centrifugation at $\sim 2,115$ rpm for 5 min at 4 °C with a GH-3.8 rotor from Beckman Coulter ($500 \times g$).

11. Wash the cells with 1 mL ice-cold 1.2 M sorbitol and harvest the cells by centrifugation at $\sim 2,115$ rpm for 5 min at 4 °C with a GH-3.8 rotor from Beckman Coulter ($500 \times g$).

12. Repeat **step 11**.

13. Resuspend the cells in 1.2 mL of ice-cold lysis buffer.

14. Homogenize on ice 50 times in a small clearance 2 mL glass Teflon homogenizer.

15. Add 1 % Triton X-100 to the lysate and incubate at 4 °C for 15 min on a nutator.

16. Clear the suspension by centrifugation at 13,200 rpm for 20 min at 4 °C with a fixed-angle rotor 45-30-11 from Eppendorf ($\sim 18,000 \times g$).

17. Measure the total protein concentration in the supernatant using the Bradford protein assay (Bio-Rad laboratories). The amount of protein is usually between 5 and 10 mg. Adjust to the same amount for each condition with Lysis buffer (between 1 and 1.3 mL final volume).

18. Save 50 μL of each sample to check the amount of Sec15p-13xmyc in the lysates.

19. Add 10 μL of protein A/G beads (Thermo Scientific) and incubate for 60 min at 4 °C on a tube rotator.

20. Pellet the beads by centrifugation at 3,500 rpm for 1 min at 4 °C with a Swing-bucket rotor A-8-11 from Eppendorf (~1,300×*g*).

21. Transfer the supernatant to a new tube and add 2 μL of purified anti-GFP polyclonal antibody (a gift from the Ferro-Novick laboratory).

22. Incubate overnight at 4 °C on a tube rotator (*see* **Note 10**).

23. The next morning, add 10 μL of protein A/G beads (Thermo Scientific) and incubate for 2 more hours at 4 °C on a tube rotator.

24. Pellet the beads by centrifugation at 3,500 rpm for 1 min at 4 °C with a Swing-bucket rotor A-8-11 from Eppendorf (~1,300×*g*).

25. Wash the beads four times with 1 mL 1× PBS for 3 min at 4 °C on a tube rotator.

26. Add 30 μL of 2× Sample buffer on the beads and boil the samples for 10 min.

27. A total of 15 and 5 μL of the samples were separated on a 8 % SDS/PAGE gel and analyzed by western blotting, respectively, with an anti-myc antibody (1:1,000 dilution; 9B11 mouse; Cell Signalling Technology) and anti-GFP antibody (1:1,000 dilution; sc-8334; Santa Cruz Biotechnology) as primary antibodies. A total of 0.2 % of the lysates was also loaded in order to verify the amount of Sec15p-13xmyc. HRP-conjugated goat anti-mouse or anti-rabbit IgG (1:10,000 dilution) was used as the secondary antibody and was detected with Super Signal West Femto Maximum Sensitivity Substrate (Thermo Scientific) (*see* Fig. 2c).

3.7 Liposomes Preparation and Sedimentation Experiment

– Liposome preparation.

Lipids were from Avanti Polar Lipids. We generally use 1-Palmitoyl-2-Oleoyl-sn-Glycero-3-Phospho-L-serine (POPS), 1,2-Dipalmitoyl-sn-Glycero-3-Phosphoethanolamine (DPPE), 1,2-Dipalmitoyl-sn-Glycero-3-Phosphocholine (DPPC), and brain-L-a-Phosphatidylinositol-4-Phosphate (PI(4)P). To work with Sec2p, we prepared liposomes containing 20 mol % DPPE, 30 mol % POPS, with or without 5 mol % PI(4)P. The remaining lipid was DPPC [11]. The protocol presented here is very similar to the one described in [13].

1. Store the lipids in chloroform at –20 °C in 2 mL glass vials (Wheaton) under argon and with the cap tightly sealed with tape to prevent oxidation. Use glass syringes (Hamilton) to pipette the lipids and work under the hood.

2. Mix the lipids at the desired molar ratio in a pear-shaped glass. Add to the mix 1 mL extra chloroform.

3. Attach the glass container to a rotary evaporator. Immerse it in a water bath at 33 °C and rotate it at 500 rpm for 5 min without vacuum (*see* **Note 11**).

4. Turn on the vacuum and the lipid film is then produced by rapid evaporation of chloroform. After all the chloroform has evaporated, maintain the film under vacuum for 30 additional min to ensure that the film is completely dry.

5. Resuspend by vortexing the lipid film in HEPES–sucrose buffer at a final concentration of 1–4 mM. This step results in a suspension of multilamellar lipid vesicles.

6. Freeze the suspension in liquid nitrogen and thaw it in a water bath at 37 °C.

7. Repeat the **step 6** four times. The lipids can be stored for months at –20 °C.

8. Extrude the suspension with a mini-extruder (Avanti Polar lipids) through a polycarbonate filter (Millipore) with a pore of defined size (0.1 μm in our case). Pass the suspension 21 times (*see* **Note 12**).

9. The extruded suspension can be stored at room temperature for 3 days maximum.

– Sedimentation Experiment

1. Dilute the liposomes five times in HK buffer and spin at 100,000 rpm at 20 °C for 20 min in a TLA 120.2 rotor (~356,000 × g) (*see* **Note 13**).

2. Resuspend the liposome pellet in HK buffer (the same volume as before dilution to maintain the same concentration).

3. Just before the sedimentation experiment, clear any aggregates by centrifugation of the GST-Sec2p protein at 55,000 rpm for 15 min at 4 °C in a TLA 120.2 rotor (~108,000 × g) (*see* **Note 14**).

4. Incubate 0.4 μM GST-Sec2p protein with 0.4 mM extruded, sucrose-loaded, liposomes in a final volume of 70 μL Sedimentation buffer. Mix directly in polycarbonate centrifuge tubes (1 mL, 11 × 34 mm, Beckman).

5. Incubate for 15 min at room temperature.

6. Centrifuge the suspension at 55,000 rpm for 15 min at 25 °C in a TLA 120.2 rotor (~108,000 × g).

7. Transfer the supernatant (70 μL) into 25 μL of 4× Sample buffer.

8. Add 25 μL of 4× Sample buffer to the liposome pellet, vortex 20 s, add 70 μL of Sedimentation buffer, vortex again 20 s.

9. Boil the samples for 10 min.

10. Separate 25 μL of supernatant and pellet samples on a 8 % SDS/PAGE gel and visualize by Coomassie Brilliant Blue staining (*see* Fig. 2d).

11. Analyze the intensity of the bands with ImageJ.

4   Notes

1. For in vitro binding assays, we find that it is best to work with freshly purified GST-Sec2p proteins each time. Keep the beads in 250 μL Wash buffer at 4 °C until use. Do not store the proteins on glutathione-Sepharose beads at –80 °C.

2. Expression and purification of HIS$_6$-Ypt32p from *E. coli* Rosetta 2 cells instead of from *E. coli* Bl21 cells increases the purity of the protein.

3. We observed that using *E. coli* Rosetta 2 cells instead of *E. coli* Bl21 cells increases the expression of HIS$_6$-Sec15p.

4. We observed that the use of a 4 L flask improves the expression.

5. We find that is best to perform the purification on a fresh pellet, i.e., not one previously stored at –80 °C.

6. The empty glutathione-Sepharose beads are helpful during the washing steps to make the bead pellet visible.

7. We observed that the use of an anti-His primary antibody to detect HIS$_6$-Ypt32p doesn't lead to an adequate signal by the following protocol.

8. We observed that the HIS$_6$-Sec15p/GST-Sec2p binding is highly sensitive to the pH. A higher pH correlates with a weaker observed interaction.

9. We observed that spheroplasting the yeast cells with commercial zymolase leads to extensive degradation of Sec2p-3xGFP protein. Using lyticase instead avoids that degradation.

10. A 2 h incubation with anti-GFP antibody at 4 °C is sufficient. In our case, reducing the incubation time, as well as the addition of phosphatase inhibitors (PhosSTOP from Roche) into the lysis buffer, was important to preserve Sec2p phosphorylation (our unpublished data).

11. This step improves phosphoinositides homogenization with other lipids [14].

12. The extrusion step leads to the fragmentation of the multilamellar lipid vesicles into smaller and unilamellar liposomes of defined diameter [15].

13. This step allows removal of the external sucrose from the sucrose-loaded liposomes solution.

14. We observed that GST-Sec2p protein tends to aggregate. To limit that, we prepare freshly purified GST-Sec2p protein for each experiment and clear the preparation by centrifugation before performing the sedimentation experiment. For some large proteins, this is not sufficient to prevent aggregation and thus, the inverse method, a flotation assay, is more appropriate [13].

Acknowledgements

References

1. Grosshans BL, Ortiz D, Novick P (2006) Rabs and their effectors: achieving specificity in membrane traffic. Proc Natl Acad Sci U S A 103(32):11821–11827. doi:10.1073/pnas.0601617103

2. Salminen A, Novick PJ (1987) A ras-like protein is required for a post-Golgi event in yeast secretion. Cell 49(4):527–538

3. Elkind NB, Walch-Solimena C, Novick PJ (2000) The role of the COOH terminus of Sec2p in the transport of post-Golgi vesicles. J Cell Biol 149(1):95–110

4. Walch-Solimena C, Collins RN, Novick PJ (1997) Sec2p mediates nucleotide exchange on Sec4p and is involved in polarized delivery of post-Golgi vesicles. J Cell Biol 137(7): 1495–1509

5. Ortiz D, Medkova M, Walch-Solimena C, Novick P (2002) Ypt32 recruits the Sec4p guanine nucleotide exchange factor, Sec2p, to secretory vesicles; evidence for a Rab cascade in yeast. J Cell Biol 157(6):1005–1015. doi:10.1083/jcb.200201003

6. Benli M, Doring F, Robinson DG, Yang X, Gallwitz D (1996) Two GTPase isoforms, Ypt31p and Ypt32p, are essential for Golgi function in yeast. EMBO J 15(23):6460–6475

7. Jedd G, Mulholland J, Segev N (1997) Two new Ypt GTPases are required for exit from the yeast trans-Golgi compartment. J Cell Biol 137(3):563–580

8. Mizuno-Yamasaki E, Rivera-Molina F, Novick P (2012) GTPase networks in membrane traffic. Annu Rev Biochem. doi:10.1146/annurev-biochem-052810-093700

9. Mizuno-Yamasaki E, Medkova M, Coleman J, Novick P (2010) Phosphatidylinositol 4-phosphate controls both membrane recruitment and a regulatory switch of the Rab GEF Sec2p. Dev Cell 18(5):828–840. doi:10.1016/j.devcel.2010.03.016

10. Medkova M, France YE, Coleman J, Novick P (2006) The rab exchange factor Sec2p reversibly associates with the exocyst. Mol Biol Cell17(6):2757–2769.doi:10.1091/mbc.E05-10-0917

11. Stalder D, Mizuno-Yamasaki E, Ghassemian M, Novick PJ (2013) Phosphorylation of the Rab exchange factor Sec2p directs a switch in regulatory binding partners. Proc Natl Acad Sci U S A 110(50):19995–20002. doi:10.1073/pnas.1320029110

12. Tanaka M, Weissman JS (2006) An efficient protein transformation protocol for introducing prions into yeast. Methods Enzymol 412:185–200. doi:10.1016/S0076-6879(06)12012-1

13. Manneville JB, Leduc C, Sorre B, Drin G (2012) Studying in vitro membrane curvature recognition by proteins and its role in vesicular trafficking. Methods Cell Biol 108:47–71. doi:10.1016/B978-0-12-386487-1.00003-1

14. Wang J, Gambhir A, Hangyas-Mihalyne G, Murray D, Golebiewska U, McLaughlin S (2002) Lateral sequestration of phosphatidylinositol 4,5-bisphosphate by the basic effector domain of myristoylated alanine-rich C kinase substrate is due to nonspecific electrostatic interactions. J Biol Chem 277(37):34401–34412. doi:10.1074/jbc.M203954200

15. MacDonald RC, MacDonald RI, Menco BP, Takeshita K, Subbarao NK, Hu LR (1991) Small-volume extrusion apparatus for preparation of large, unilamellar vesicles. Biochim Biophys Acta 1061(2):297–303

Chapter 8

Kinetic Activation of Rab8 Guanine Nucleotide Exchange Factor Rabin8 by Rab11

Shanshan Feng, Bin Wu, Johan Peränen, and Wei Guo

Abstract

The Rab family of small GTPases acts as molecular switches that control various stages of vesicular transport. Rab8 functions in exocytic trafficking from the *trans*-Golgi network (TGN) and recycling endosomes to the plasma membrane. Rabin8 is a major guanine nucleotide exchange factor (GEF) for Rab8. It activates Rab8 by catalyzing its GDP release for subsequent GTP loading. However, how Rabin8 itself is activated in cells is unclear. Recently, it was found that Rabin8 is a downstream effector of Rab11, which controls vesicle exit from the recycling endosomes. Rab11, in its GTP-bound form, stimulates the GEF activity of Rabin8. The Rab11–Rabin8–Rab8 interactions thus couple vesicle generation from the donor compartment to its delivery to plasma membrane. Here we describe the methods we used to express and purify several Rab proteins, and to assay for the effect of Rab11 in the kinetic activation of Rabin8 GEF activity.

Key words GTPase, Guanine nucleotide exchange, Rab11, Rabin8, Rab8

1 Introduction

The Rab family of small GTP-binding proteins are important regulators of membrane trafficking in eukaryotic cells [1]. Rab proteins cycle between their active GTP-bound and inactive GDP-bound states. The guanine nucleotide exchange factors (GEFs) promote GDP dissociation from the Rab proteins to allow subsequent GTP loading. On the other hand, the GTPase-activating proteins (GAPs) stimulate the GTPase activity of the Rabs, therefore placing them in the GDP-bound inactive state.

Recently, a recurring theme in the field is that Rab proteins functioning at different stages of trafficking coordinate with each other in their activation [2]. For exocytic trafficking in budding yeast *S. Cerevisiae*, Ypt32p, which mediates vesicle generation from the TGN, interacts with Sec2p, the GEF for Sec4p, a key regulator of exocytosis [3]. This interaction participates in the recruitment of Sec2p to the secretory vesicles for the subsequent activation of Sec4p. It was thus speculated that this Rab cascade coordinates

vesicular trafficking between individual transport steps to ensure proper transition along the exocytic pathway [3]. In mammalian cells, a similar type of coordination has been observed for Rab11 (the Ypt32p homolog), which mediates the generation of vesicles from the TGN and recycling endosomes, and Rabin8 (the Sec2p homolog), the GEF for Rab8 (Sec4p homolog) implicated in vesicle trafficking to the plasma membrane. Rab11, in its GTP-bound form, directly interacts with Rabin8. The binding sequence in Rabin8 was mapped to a region adjacent to the GEF domain [4–6]. While it is possible that Rab11 mediates the recruitment of Rabin8 to the donor membrane, we found that Rab11, in its activated form, stimulates the GEF activity of Rabin8 toward Rab8. The stimulatory effect on Rabin8 was specific to Rab11 because neither Rab5a (involved in early endosomal trafficking) nor Rab3a (involved in regulated exocytosis) had any effect on Rabin8-mediated guanine nucleotide exchange toward Rab8 [5]. This Rab cascade may couple cargo transport from the TGN/recycling endosomes involving Rab11 to later activation of vesicle docking and fusion at the plasma membrane mediated by Rab8. This basic mechanism has been found to operate in a number of physiological processes such as primary ciliogenesis and epithelial cell cystogenesis [4–8].

In this chapter, we describe the in vitro biochemistry assays we have used to study the regulation of Rabin8 GEF activity by Rab11.

2 Materials

2.1 Protein Purification Reagents

1. DNA constructs: Nus-His-Rab8a was constructed by cloning the open reading frame of canine Rab8a cDNA in pET43a. Rab11a[Q70L], Rab5a[Q79L], or Rab3a[Q81L] was cloned into pET32a(+) to generate Trx-Hisx6-S tagged Rabs. GST-Rabin8 was constructed by cloning human Rabin8 (a.k.a. RAB3IP) into pGEX4T-1.

2. 2×YT medium broth: To ~900 ml of distilled H_2O, add 16 g Bacto Tryptone, 10 g Bacto Yeast Extract, 5 g NaCl. Adjust pH to 7.0, adjust to 1 L with distilled water, and then sterilize by autoclaving.

3. Ampicillin (sodium salt): 50 mg/ml in deionized water. Filter-sterilize and store at –20 °C. Use at 50 μg/ml.

4. Carbenicillin (disodium salt): 50 mg/ml in deionized water. Filter-sterilize and store at –20 °C. Use at 50 μg/ml.

5. Rab buffer: 50 mM phosphate buffer, pH 7.0, 300 mM NaCl, 5 mM $MgCl_2$, 200 mM GDP, 5 mM β-mercaptoethanol, 0.5 % Triton X-100, 10 % glycerol, 1 mM PMSF.

6. Thrombin cleavage buffer: 50 mM Tris–HCl, pH 7.5, 150 mM NaCl, 5 mM $MgCl_2$, 2.5 mM $CaCl_2$.

7. GEF buffer: 20 mM Tris–HCl, pH 7.5, 150 mM NaCl, 1 % Triton X-100, 0.4 mM PMSF.

8. Talon Metal Affinity Resin.

9. Glutathione agarose beads.

10. Thrombin protease.

2.2 GEF Activity Assay Reagents

1. Preloading buffer: 20 mM Hepes, pH 7.2, 1 mM EDTA, 1 mM DTT, 10 mM $MgCl_2$.

2. Binding buffer: 20 mM Hepes, pH 7.2, 1 mM DTT, 10 mM $MgCl_2$.

3. "GDP-saturation" buffer: 20 mM Hepes, pH 7.2, 2 mM GDP, 1 mM DTT, 10 mM $MgCl_2$.

4. Reaction buffer: 20 mM Hepes, pH 7.2, 1 mM DTT, 2 mM GDP, 1 mM EDTA, 10 mM $MgCl_2$.

5. Washing buffer: 20 mM Tris–HCl, pH 8.0, 20 mM NaCl, 1 mM DTT, 10 mM $MgCl_2$.

2.3 Antibodies

The anti-Rab8 polyclonal antibody and affinity-purified anti-Rabin8 antibody was generated as previously described [9].

3 Methods

3.1 Expression and Purification of Rab8a

1. Nus-His-Rab8a in pET43 vector was transformed into BL-21 (DE3) *E. coli* cell strain and selected with Carbenicillin resistant LB plate (*see* **Note 1**).

2. A single colony was used to inoculate 3 ml of LB medium with ampicillin overnight at 37 °C.

3. The cells were transferred to 500 ml 2×YT medium and incubated at 37 °C until the OD_{600} reached 0.6–0.8. Then IPTG was added to the medium with a final concentration of 0.1 mM and the cells were incubated at 37 °C for 3 more hours.

4. Cells were collected by centrifugation at $3,750 \times g$ for 10 min at 4 °C, and the pellet was washed with PBS twice.

5. The pellet was resuspended in 30 ml Rab buffer and cells were lysed using a sonicator.

6. The cell lysate was then incubated on a rotator at 4 °C for 1 h, followed by centrifugation for 30 min at $21,600 \times g$ at 4 °C.

7. The supernatant containing soluble Nus-His-Rab8a was incubated with Talon metal affinity resin at 4 °C for 4 h or overnight on a rotator (*see* **Note 2**).

8. The beads were washed with prechilled Rab buffer without PMSF four times (each for 10 min) and three times in thrombin buffer.

9. The beads were resuspended in 500 μl Thrombin buffer and then incubated with 20 μl thrombin at 4 °C on a rotator overnight (*see* **Note 3**).

10. The beads were centrifuged at $800 \times g$ for 5 min at 4 °C and the supernatant containing Rab8a was collected and concentrated with a 10-kDa centrifugal filter.

3.2 Expression and Purification of the Constitutively Activated Rab11a, Rab5a, and Rab3a Mutants

1. Rab11a[Q70L], Rab5a[Q79L], and Rab3a[Q81L] were expressed in the pET32a(+) vector at 37 °C for 3 h with 0.5 mM IPTG.

2. Cells from a 200 ml culture were pelleted and resuspended in Rab buffer.

3. Cells were lysed using a sonicator.

4. The cell lysate was then incubated on a rotator at 4 °C for 1 h, followed by centrifugation for 30 min at $21,600 \times g$ at 4 °C.

5. The supernatant fraction was incubated with Talon metal affinity resin at 4 °C for 4 h or overnight and then washed three times during 30 min with lysis buffer.

6. The beads were incubated with 500 µl elution buffer containing 10 mM imidazole for 20 min.

7. Centrifuge the beads for 5 min at $800 \times g$ at 4 °C and discard the supernatant.

8. Elute the beads with 500 µl elution buffer containing 200 mM imidazole for 20 min for four times at 4 °C (*see* **Note 4**).

9. Collect all the eluents and the purified proteins were dialyzed overnight with 20 mM Tris–HCl (pH 7.4), 100 mM NaCl, and 1 mM DTT.

10. The dialyzed solutions containing these Rab proteins were collected and concentrated with a 10-kDa centrifugal filter.

3.3 Expression and Purification of Rabin8

1. The pGEX4T-1-Rabin8 plasmid was transformed into BL21(DE3) cells.

2. The induction of GST-Rabin8 was performed using 0.5 mM IPTG at 18 °C overnight. The low induction temperature helps to minimize GST-Rabin8 inclusion body formation.

3. Cells from a 500 ml culture were then pelleted and resuspended in ice-cold GEF buffer.

4. Cells were lysed using a sonicator.

5. The cell lysate was then centrifuged for 30 min at $21,600 \times g$ at 4 °C.

6. The supernatant fraction containing soluble GST-Rabin8 was incubated with glutathione agarose beads at 4 °C for 4 h or overnight and then washed three times during 30 min with GEF buffer without PMSF (*see* **Note 5**).

7. Rabin8 is cleaved from the GST tag using thrombin.

8. The beads were centrifuged at $800 \times g$ for 5 min at 4 °C and the supernatant containing Rabin8 was collected and concentrated with a 10-kDa centrifugal filter.
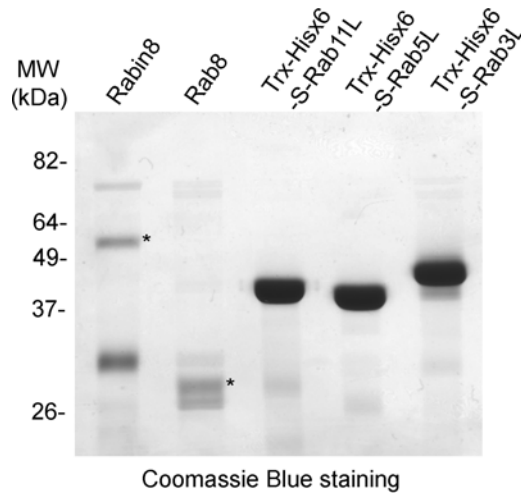
Fig. 1 Coomassie Blue-stained SDS-PAGE showing purified Rabin8, Rab8a, and Trx-Hisx6-S-tagged Rab11a[Q70L], Rab5a[Q79L], Rab3a[Q81L]. Molecular weight (MW) is indicated to the *left*. The *asterisks* indicate the positions of Rabin8 cleaved from the GST tag and Rab8a cleaved from the NusA-Hisx6 tag, respectively. The additional bands present in the purification are most likely the degradation products of Rabin8 or Rab8a based on the fact that they can be recognized by the anti-Rabin8 or Rab8a antibodies. Trx-Hisx6-S-tagged Rab11a[Q70L], Rab5a[Q79L], Rab3a[Q81L] have the predicted molecular weights as they are fusions of the Rab proteins with the 18 kDa Trx-Hisx6-S tag

The expression patterns of all the above proteins are shown in Fig. 1 [5].

3.4 Assay for the Activation of Rabin8 GEF Activity by Rab11

1. A total of 15 pmol of purified Rab8a was first labeled with 100 pmol [³H]GDP (14.2 Ci/mmol) in a preloading buffer for 30 min at 30 °C with a total volume of 20 μl.

2. A total of 5 pmol of Rabin8 was incubated with 0.5 nmol of Rab11a[Q70L], Rab5a[Q79L], or Rab3a[Q81L] in the binding buffer with a total volume of 8 μl for 40 min followed by additional 8 μl "GDP-saturation" buffer (*see* **Note 6**).

3. The protein mixtures were then added with 13 μl reaction buffer and 1 μl water.

4. Rabin8 and different Rab proteins were then mixed with 20 μl [³H]GDP-labeled Rab8a on ice in a total volume of 50 μl and the release of [³H]GDP was measured immediately by placing the mixtures at 25 °C.

5. A total of 10 μl samples were taken at various time points (0, 5, 10, and 20 min) and immediately diluted into 1.5 ml ice-cold washing buffer.

6. The samples were then applied to wet nitrocellulose filters mounted on a vacuum manifold and washed 4 times with 3 ml ice-cold washing buffer.
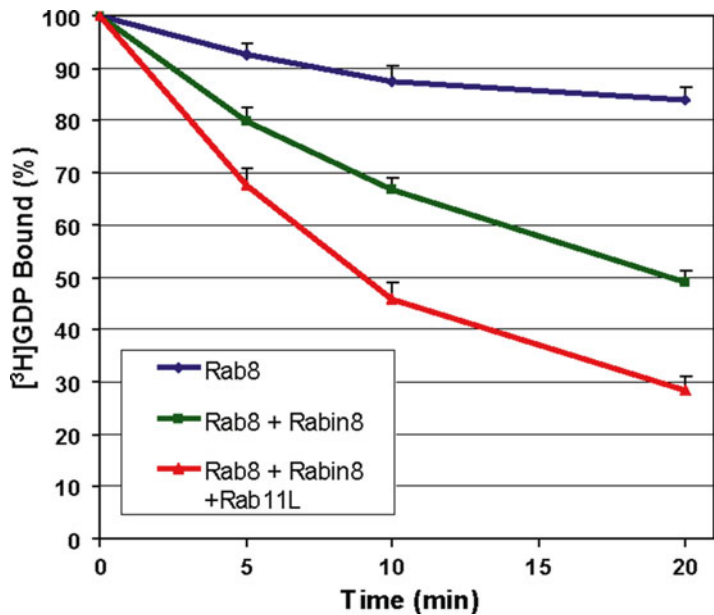
Fig. 2 The release of [³H]GDP from Rab8a catalyzed by Rabin8 in the presence or absence of Rab11a[Q70L] was analyzed as described. Rab11a[Q70L] stimulated the release of [³H]GDP from Rab8a in the presence of Rabin8 (*red*). Rab11a[Q70L] significantly enhanced the GEF activity of Rabin8 toward Rab8a ($p < 0.01$, $n = 3$)
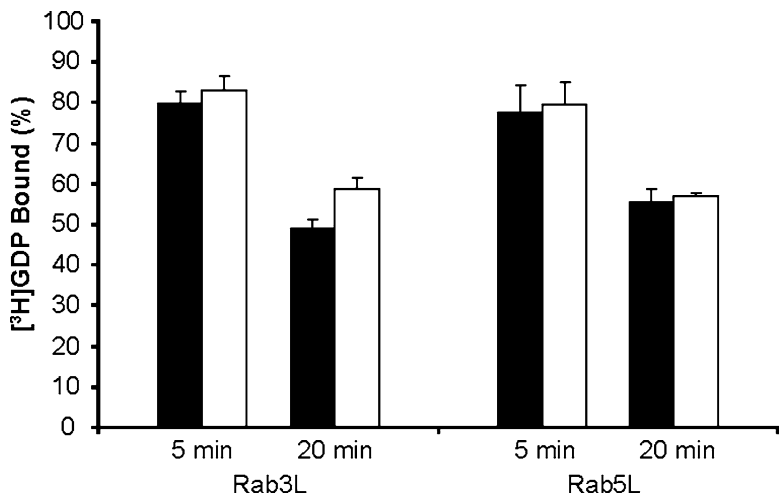
Fig. 3 Rabin8-mediated [³H]GDP release from Rab8a was tested in the absence (*black bars*) and presence (*white bars*) of Rab5a[Q79L] or Rab3a[Q81L] at 5 min and 20 min ($n = 3$). Rab5a[Q79L] or Rab3a[Q81L] did not stimulate Rabin8-mediated release of [³H]GDP from Rab8a

7. After drying, 4 ml scintillation fluid was added and the amounts of [³H]GDP remaining on the filter were measured in a scintillation counter (*see* Figs. 2 and 3) [5].

4 Notes

1. There are two major paralogs of Rab8: Rab8a and Rab8b. We used Rab8a in our in vitro assays. It may take up to 24 h or longer for sufficient pET43-Rab8a colony growth. To avoid satellite colony formation, use carbenicillin, instead of ampicillin, for the selection of vectors encoding ampicillin resistance.

2. A fraction of NusA-Rab8a was not bound to the Talon column; the Hisx6 tag was probably masked.

3. Much of the cleaved Rab8a was retained on the beads and cannot be eluted by thrombin buffer. It is possible that some fraction of Rab8a is incorrectly folded.

4. The Rab proteins were purified from bacteria as Trx-Hisx6-S-tagged (18 kDa added to the molecular weight) fusion proteins.

5. GST-Rabin8 beads were very sticky and easy to attach to the centrifuge tubes. Addition of Triton X-100 to the wash buffer helps to alleviate this problem.

6. The use of excess unlabeled GDP in this step minimizes the binding of Rab11a[Q70L], Rab5a[Q79L], or Rab3a[Q81L] to [^{3}H]GDP in later steps.

Acknowledgments

References

1. Zerial M, McBride H (2001) Rab proteins as membrane organizers. Nat Rev Mol Cell Biol 2:107–117

2. Mizuno-Yamasaki E, Rivera-Molina F, Novick P (2012) GTPase networks in membrane traffic. Annu Rev Biochem 81:637–659

3. Ortiz D, Medkova M, Walch-Solimena C, Novick P (2002) Ypt32 recruits the Sec4p guanine nucleotide exchange factor, Sec2p, to secretory vesicles; evidence for a Rab cascade in yeast. J Cell Biol 157:1005–1015

4. Westlake CJ, Baye LM, Nachury MV, Wright KJ, Ervin KE, Phu L, Chalouni C, Beck JS, Kirkpatrick DS, Slusarski DC, Sheffield VC, Scheller RH, Jackson PK (2011) Primary cilia membrane assembly is initiated by Rab11 and transport protein particle II (TRAPPII) complex-dependent trafficking of Rabin8 to the centrosome. Proc Natl Acad Sci U S A 108:2759–2764

5. Knodler A, Feng S, Zhang J, Zhang X, Das A, Peranen J, Guo W (2010) Coordination of Rab8 and Rab11 in primary ciliogenesis. Proc Natl Acad Sci U S A 107:6346–6351

6. Feng S, Knödler A, Ren J, Zhang J, Zhang X, Hong Y, Huang S, Peränen J, Guo W (2012) A Rab8 guanine nucleotide exchange factor-effector interaction network regulates primary ciliogenesis. J Biol Chem 287:15602–15609

7. Bryant DM, Datta A, Rodríguez-Fraticelli AE, Peränen J, Martín-Belmonte F, Mostov KE (2010) A molecular network for de novo gen-

eration of the apical surface and lumen. Nat Cell Biol 12:1035–1045

8. Das A, Guo W (2011) Rabs and the exocyst in ciliogenesis, tubulogenesis and beyond. Trends Cell Biol 21:383–386

9. Hattula K, Furuhjelm J, Arffman A, Peränen J (2002) A Rab8-specific GDP/GTP exchange factor is involved in actin remodeling and polarized membrane transport. Mol Biol Cell 13: 3268–3280

Chapter 9

Ypt1 and TRAPP Interactions: Optimization of Multicolor Bimolecular Fluorescence Complementation in Yeast

Zhanna Lipatova*, Jane J. Kim*, and Nava Segev

Abstract

Ypt/Rab GTPases are conserved molecular switches that regulate the multiple vesicular transport steps of all intracellular trafficking pathways. They are stimulated by guanine-nucleotide exchange factors (GEFs). In yeast, Ypt1 regulates transport from the endoplasmic reticulum (ER) to two alternative pathways: secretion and autophagy. Ypt1 is activated by TRAPP, a modular multi-subunit GEF. Whereas TRAPP I activates Ypt1 to mediate transport through the Golgi, TRAPP III, which contains all the subunits of TRAPP I plus Trs85, activates Ypt1-mediated transport to autophagosomes. The functional pair Ypt31/32 regulates traffic in and out of the trans-Golgi and is activated by TRAPP II, which consists of TRAPP I plus two specific subunits, Trs120 and Trs130. To study the interaction of Ypts with specific TRAPP subunits and interactions between the different subunits of TRAPP, including the cellular sites of these interactions, we have employed a number of approaches. One approach that we have recently optimized for the use in yeast is multicolor bimolecular fluorescence complementation (BiFC). BiFC, which employs split fluorescent tags, has emerged as a powerful approach for determining protein interaction in vivo. Because proteins work in complexes, the ability to determine more than one interaction at a time using multicolor BiFC is even more powerful. Defining the sites of protein interaction is possible by co-localization of the BiFC puncta with compartmental markers. Here, we describe a set of plasmids for multicolor BiFC optimized for use in yeast. We combined their use with a set of available yeast strains that express red fluorescence compartmental markers. We have recently used these constructs to determine Ypt1 and TRAPP interactions in two different processes: intracellular trafficking and autophagy.

Key words BiFC, Multicolor BiFC, In vivo interaction, Ypt/Rab GTPase, TRAPP, Trs85, Atg11, Trs20, Trs120, Ypt1

1 Introduction

In the last two decades it became apparent that proteins that mediate and regulate intracellular trafficking function in large complexes that can be thought of as "molecular machines." For example, each Ypt/Rab GTPase interacts with upstream regulators, e.g., GEFs, and multiple downstream effectors to regulate and coordinate vesicular trafficking [1, 2]. In many cases, both the

---

Ypt/Rab GEFs and their effectors are multiple-protein complexes. These complexes are conserved both among organisms and between the different steps of the intracellular pathways.

In yeast, the Ypt1 GTPase regulates two alternative intracellular trafficking pathways: in the exocytic pathway it is required for endoplasmic reticulum (ER)-to-Golgi transport, whereas in the autophagic pathway it is required for formation of autophagosomes (APs) [3, 4]. The modular complex TRAPP acts as the Ypt1 GEF in both pathways, but in different configurations. The multi-subunit TRAPP I activates Ypt1 in the exocytic pathway and TRAPP III, which in addition to the TRAPP I contains Trs85, activates Ypt1 in autophagy [4–6]. In autophagy, activated Ypt1 interacts with its effector Atg11 to form the multi-protein complex pre-autophagosomal structure (PAS) [4]. A third TRAPP complex, TRAPP II, activates Ypt31 at the trans-Golgi [6]. All these players and their functions are conserved from yeast to humans [7–9].

While in vitro analyses are important for defining protein interactions and complex composition, in vivo studies are crucial for providing the physiological relevance of such analyses and for determining the intracellular sites where these interactions occur. One such approach is live-cell microscopy. We have used co-localization analyses of fluorescently tagged Ypts, TRAPP subunits, and Ypt effectors to address multiple questions about Ypts and their accessory factors. This approach is even more effective when combined with mutations. For example, using a combination of in vitro and co-localization analyses in wild-type and mutant cells, we have recently shown that the TRAPP III-specific subunit Trs85 is required for recruitment of TRAPP I to PAS via the interaction of Trs85 with the TRAPP subunit Trs20 [10].

Bimolecular fluorescence complementation (BiFC) has emerged as a powerful approach for determining interaction between two proteins in vivo [11]. We have used this approach in combination with in vitro studies to determine interactions between two TRAPP subunits, Trs20 and the TRAPP II-specific subunit Trs120 [12]. Multicolor BiFC allows to determine interactions of one protein with two other proteins [13]. We have used this approach in combination with in vitro studies to determine interactions of Ypt1 with the TRAPP III-specific subunit Trs85 and with its autophagy-specific effector Atg11 [4]. In both cases, the effect of mutations on BiFC and co-localization of the BiFC puncta with compartmental markers were used to support the BiFC results. To do this, we constructed a set of plasmids optimized for the use of multicolor BiFC in yeast [4]. These plasmids were used in combination with an available set of yeast strains that express RFP-tagged compartmental markers [14]. Here, we describe the sets of plasmids and strains optimized for using multicolor BiFC interactions and their intracellular localization in yeast, recount examples of their use for determining Ypt1 and TRAPP interactions, and discuss important controls and limitations of this approach.

2 Materials

We designed six plasmids that can be used for tagging your proteins of interest for multicolor BiFC analysis in a versatile manner (Table 1). Some of these plasmids were previously used for cloning Ypt1, Atg11, and TRAPP subunits [4, 12]. All plasmids are CEN (low copy number), and the tagged proteins are expressed from the constitutive *ADH1* promoter and have the *CYC1* terminator. The two split fluorophores that we chose are yeast codon-optimized enhanced Venus, yEVenus, because it is the fastest maturing yellow fluorescent protein (YFP) and is yeast codon-optimized [15], and Cerulean, because it is the "bluest" cyan fluorescent protein (CFP) and, importantly, its fluorescence can be separated easily from that of Venus [16]. Typically, 6–11 amino acids linkers were designed between the fluorophore fragment and the protein.

The first two plasmids, pNS1499 and pNS1500, are for tagging proteins at their N terminus with YFP-N: The N terminus of yEVenus, amino acids 1–172, is followed by a multiple cloning site (MCS). These plasmids contain the *URA3* and *HIS3* selectable markers, respectively. To generate pNS1499, the VF1 fragment in p416-VF1 [17] was replaced by the fragment encoding amino acids 1–172 of yEVenus, which was amplified from pKT103 [15], using the SpeI/XbaI and BspEI restriction sites. To construct pNS1500, the piece containing the *ADH1* promoter, amino acids 1–172 of yEVenus, and the *CYC1* terminator from pNS1499 was sub-cloned into pRS413 using the PvuII sites.

The next two plasmids, pNS1501 and pNS1502, are for tagging proteins at their C terminus with the N terminus (amino acids 1–172) of Cerulean or yEVenus, respectively. In both plasmids, the MCS is at the N terminus of the fluorophore fragment, and the protein should be cloned without its stop codon. The selectable marker for both plasmids is *LEU2*. To construct pNS1501 and pNS1502, the VF2 fragment of p415-VF2 [17] was replaced by

Table 1
A list of plasmids constructed for the use of multicolor BiFC analysis in yeast

Plasmid	Alias	Used for	Genotype	Source
pNS1499	p416-YFP-N for N	Tag N terminus with YFP-N	*CEN*, *URA3*, Amp[r]	This study
pNS1500	p413-YFP-N for N	Tag N terminus with YFP-N	*CEN*, *HIS3*, Amp[r]	This study
pNS1501	p415-CFP-N for C	Tag C terminus with CFP-N	*CEN*, *LEU2*, Amp[r]	This study
pNS1502	p415-YFP-N for C	Tag C terminus with YFP-N	*CEN*, *LEU2*, Amp[r]	This study
pNS1503	p416-Y/CFP-C for N	Tag N terminus with Y/CFP-C	*CEN*, *URA3*, Amp[r]	This study
pNS1504	p413-Y/CFP-C for N	Tag N terminus with Y/CFP-C	*CEN*, *HIS3*, Amp[r]	This study

amino acids 1–172 of Cerulean [16] or yEVenus, respectively, using the BspEI and XhoI sites.

The last two plasmids, pNS1503 and pNS1504, are for tagging proteins at their N terminus with the C terminus of yECFP, amino acids 155–238. Because this fragment does not affect the BiFC color it is termed Y/CFP-C, and it is followed by a MCS. The selectable markers are *URA3* and *HIS3*, respectively. To construct pNS1503, the VF1 fragment in p416-VF1 [17] was replaced by amino acids 155–238 of yECFP, amplified from pKT102 [15], using the SpeI/XbaI and BspEI sites. To generate pNS1504, the piece containing the *ADH1* promoter, amino acids 155–238 of yECFP, and the *CYC1* terminator from pNS1503 was sub-cloned into pRS413 using the PvuII sites.

3   Methods

We have successfully employed BiFC and multicolor BiFC to determine interactions between TRAPP II subunits and of Ypt1 GTPase with its autophagy-specific GEF and effector, including determination of the sites of these interactions. To achieve that, we constructed a set of plasmids (*see* Subheading 2) and used yeast strains, which were previously employed for GFP-tagged protein localization, for BiFC localization. Both plasmids and strains should be useful for determining other interactions in yeast. The multicolor BiFC principle, rationale of plasmid optimization, BiFC localization, and examples and important controls are described below. Please, *see* **Notes 1–3** for BiFC limitations.

3.1   Multicolor BiFC Principle

BiFC is a protein fragment complementation assay (PCA). In PCA, two proteins are tagged with two fragments of a reporter, an enzyme or a fluorophore, and the reporter can assemble only if the two proteins interact. The readout of the interaction depends on the nature of the reporter [18]. For BiFC analyses, a fluorophore, YFP or CFP, is split into its N and C terminal fragments and each fragment is fused to two different proteins of interest. The two tagged proteins are co-expressed in the same cell. The two fragments can reconstruct the fluorophore only if the two proteins are adjacent and the readout is fluorescence (Fig. 1a). Because the C terminal fragment of the YFP and CFP proteins are identical, the N terminal fragment determines the excitation/emission range or color of the fluorophore. The C terminal Y/CFP fragment will fluoresce when adjacent to either the N terminal YFP or CFP fragment (Fig. 1b). Exploiting this property, interactions of one protein with two other proteins can be visualized using multicolor BiFC.

3.2   Optimized Plasmids for Use in Yeast

The optimization was done for three purposes. First, the set of plasmids described here was designed for allowing the use of multicolor BiFC in yeast while improving available split YFP BiFC.
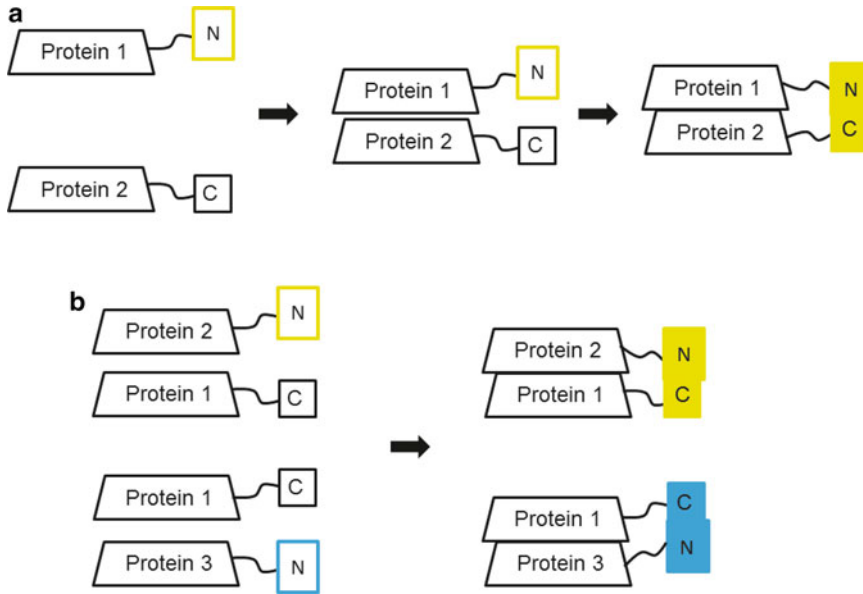
Fig. 1 The principles of BiFC and multicolor BiFC. (**a**) BiFC analysis between two proteins. Protein 1 and Protein 2 are tagged with the N and C fragments of YFP, respectively. The YFP fluorophore can assemble and fluoresce only if Proteins 1 and 2 come in close proximity. (**b**) Multicolor BiFC analysis of three proteins. Protein 1 is tagged with the C terminal fragment of a fluorophore, which can assemble with the N terminus of either YFP or CFP. Proteins 2 and 3 are tagged with the N terminal fragment of YFP and CFP, respectively. When Protein 1 interacts with Protein 2, the assembled fluorophore fluoresces in the YFP channel. When Protein 1 interacts with Protein 3, the assembled fluorophore fluoresces in the CFP channel. The proteins can be tagged with the fluorophore fragment at either terminus (see text)

In addition to construction of plasmids for tagging proteins with split CFP, the following changes were made to the previously reported split yEVenus [17]: The length of the split Venus fragments, VF1 and VF2, was changed to allow better assembly of the fluorophore [11]. In addition, the C terminal fragment of the fluorophore was cloned from the version of yEVenus that contains the A206K alteration [15]. This mutation results in a monomeric fluorescent protein, which should prevent fluorophore aggregation [19].

The second goal was to design plasmids that would allow versatility of tagging proteins at their N or C termini because some proteins can be tagged successfully only at one end; e.g., Ypts can only be tagged at their N terminus because the C terminus is required for their prenylation and membrane attachment. The third goal was to allow transformation of the same yeast cells with three different plasmids. We used plasmids with three different selectable auxotrophic markers, *URA3* (pRS416), *LEU2* (pRS415), and *HIS3* (pRS413) [20, 21]; therefore, the yeast strains have to carry the appropriate mutations, *ura3*, *leu2*, and *his3*.

When designing multicolor BIFC in yeast, we have two recommendations. It has been our experience that for some protein pairs both the position of the tag and the fluorophore fragment

(N or C) can affect the BiFC result: the configuration can affect either the reconstruction of the fluorophore or its localization. Therefore, we suggest trying different configurations. In addition, we find it important for expression of tagged proteins to use yeast codon-optimized tags, especially when tagging proteins at their N terminus. Because the YFP-N and Y/CFP-C fragments in our plasmids are yeast codon-optimized, but not the CFP-N, we constructed vectors for tagging proteins at their N or C terminus with YFP, but only at the C terminus with CFP.

3.3 BiFC Localization in Red Strains

One extension of the BiFC analysis is determination of the intracellular site where the two proteins interact. At the same time, such co-localization also helps ruling out false positive BiFC interaction due to aggregation in the cytoplasm. Because the BiFC fluorophores fluoresce in the YFP and CFP channels, we used red fluorescence to visualize the compartments. Yeast strains expressing RFP-tagged compartmental markers were previously constructed and are available from the Yeast Resource Center [14]. The BiFC plasmids described above have the right auxotrophic markers to be used in this background and can be transformed directly to these strains. When necessary, we tagged a desired cellular site with a red marker. For example, we used mCherry-Atg8 expressed from a plasmid or Atg9-mCherry expressed from the chromosome to visualize autophagosomes [4].

3.4 Examples of Using BiFC for Studying Ypt1, TRAPP II, and Beyond

We have reported BiFC interactions in two publications. In the first project, BiFC was used to determine interaction between two TRAPP II subunits, Trs20 and Trs120. This interaction occurs mostly on the trans-Golgi, based on the co-localization of the BiFC puncta with the trans-Golgi marker Chc1-RFP [12]. In the second project, multicolor BiFC was used to determine the co-localization of Ypt1 interactions with its autophagy-specific GEF and effector, Trs85 and Atg11, respectively. Whereas only a single Ypt1-Atg11 BiFC punctum per cell was observed, there were multiple Ypt1-Trs85 BiFC puncta. Importantly, in each cell, one of the Ypt1-Trs85 punctum co-localized with the Ypt1-Atg11 punctum (Fig. 2). In this case, the BiFC interactions were localized to autophagosomes, based on the co-localization of the Ypt1-Atg11 BiFC punctum and one of the Ypt1-Trs85 BiFC puncta with the autophagosomal marker mCherry-Atg8. The rest of the Ypt1-Trs85 BiFC puncta co-localized with Atg9-mCherry, but not with any other markers of secretory compartments [4].

Using our constructs, Lee et al. determined a BiFC interaction between the MAPK Hog1 and the glycerol channel Fps1, which was induced by an hyper-osmotic shock [22].

3.5 Important Controls and Parameters

When employing BiFC, it is important to use appropriate controls. Negative controls should be used to support the idea that the observed BiFC puncta represent bona fide interactions.
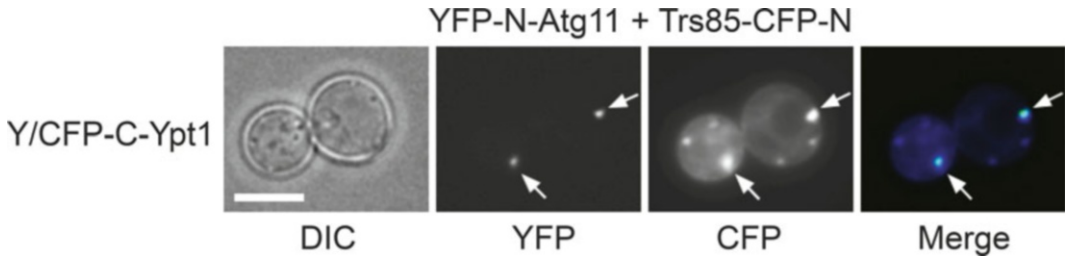
YFP-N-Atg11 + Trs85-CFP-N

Y/CFP-C-Ypt1

DIC   YFP   CFP   Merge

Fig. 2 Co-localization of interactions Ypt1 with its autophagy-specific GEF (Trs85) and effector (Atg11) using multicolor BiFC. Yeast cells were transformed with three plasmids expressing: (1) Y/CFP-C-Ypt1, Ypt1 was tagged at its N terminus with the C terminal fragment of Y/CFP; (2) YFP-N-Atg11, Atg11 tagged at its N terminus with the N terminal fragment of YFP; and (3) Trs85-CFP-N, Trs85 tagged at its C terminus with the N terminal fragment of CFP. Every cell shows multiple puncta in the CFP channel representing the Ypt1-Trs85 interaction. One of these puncta (*arrows*) co-localizes with the single punctum in the YFP channel representing the Ypt1-Atg11 interaction (*merge*). Size bar, 5 μm. See details in Lipatova et al. [4]

One possibility is to use the empty vector control as was done previously by Paquin et al. for the Yck1 and Kdh1 interaction [17]. If the interaction between two proteins is dependent on growth conditions, growing the cells under conditions that do not support the interaction can be used as a negative control, as was done for the Hog1-Fps1 BiFC interaction [22]. Alternatively, the BiFC interaction could be studied in mutant cells that do not support the specific interaction. Below, we recount several controls and parameters used in our BiFC studies.

a. *Interaction mutants.* One of the most convincing controls for an interaction is the use of mutations known to abrogate this interaction. It is expected that BiFC interaction would occur with the wild type and not with interaction-defective mutant proteins. For negative BiFC controls, it is important to show that the tagged proteins are expressed, and if possible, that they can interact with other proteins in the BiFC assay.

For the Trs20–Trs120 interaction, we used the *trs20*-D46Y mutation, which inhibits the Trs20–Trs120 interaction in other assays: yeast two-hybrid and co-precipitation of recombinant proteins. We showed that the tagged mutant Trs20-D46Y protein was expressed (using immunoblot analysis) and interacted in the BiFC assay with another TRAPP subunit, Bet3, but not with Trs120 [12].

For the Ypt1 interaction with Trs85 and Atg11 we used two Ypt1 mutations, one that locks the Ypt in its GTP-bound form, "Ypt1-GTP," and the other in the effector-binding domain, Ypt1-1. GTPase effectors, but not GEFs, should interact with the GTP-bound form of the GTPase. Conversely, the effector domain mutation should affect the interaction of the Ypt with its effectors, but not with its GEF. As expected for bona fide interactions, Ypt1-Trs85 BiFC was abolished when Ypt1-GTP

was used, but remained when Ypt1-1 was used. Conversely, the Ypt1-Atg11 interaction was abolished when Ypt1-1 was used and remained when the Ypt1-GTP was used [4]. To show the specificity of the Ypt1-Atg11 interaction, we used Atg1, a known Atg11 interactor [23]. While Atg1 could form one BiFC punctum per cell when tested with Atg11 (representing the autophagosome), it did not show interaction with Ypt1. We also used Atg11 interaction mutants deleted for the coil-coiled domains CC2 and CC3, which were independently shown to be important for the Ypt1-Atg11 interaction. The relevance of these Atg11 mutants was supported by the fact that they did show BiFC interaction with another Atg11 interactor, Atg19, but not with Ypt1.

b. *Co-localization with compartmental markers.* One of the limitations of BiFC is the irreversibility of fluorophore assembly. Once the YFP or CFP fluorophore reconstructs, the proteins that are linked are also held together. This can lead to protein aggregation and signal amplification. To ensure that the signal from the BiFC tagged proteins is pertinent to the protein's native localization, the BiFC puncta should be localized to compartmental markers. We would like to emphasize that it is important to establish that the marker is relevant for the BiFC interaction by showing the co-localization of each tagged protein with the same compartment.

As explained above, we co-localized each BiFC interaction with a compartmental marker or another relevant protein, and supported the BiFC puncta localization by co-localization of each individual protein. For the Trs20–Trs120 BiFC, which co-localizes mostly with the late Golgi marker Chc1, the co-localization of Trs120-GFP predominantly with this marker was shown independently [12]. Trs20-GFP was previously localized to this compartment [14]. For the Ypt1-Trs85 BiFC interaction, while the co-localization with the autophagosomal marker, Atg8, was expected, the co-localization with Atg9, but not with any other secretory compartment, was new. Therefore, the co-localization of Trs85-GFP with Atg9 was confirmed independently [4].

c. *Quantification.* When drawing conclusions about BiFC experiments, quantification should be performed. For example, when comparing the Trs20–Trs120 BiFC with the wild-type Trs20 and the interaction-defective Trs20-D46Y mutant, the portion of cells with BiFC puncta in each case was determined and the number of cells visualized was stated. The same quantification was done also for the Trs20-Bet3 BiFC, which served as a positive control for the Trs20 mutant defective in the interaction with Trs120, but not with Bet3 [12]. Another possibility is to determine the increase in the intensity of the signal, as was done for the Fps1-Hog1 BiFC interaction in different growth

conditions [22]. As a rule, we always perform at least two independent experiments (using two independent transformants) for each experiment. Co-localization of the BiFC puncta with compartmental markers should also be quantified as done for any localization analysis.

d. *Support of interaction by other methods.* It is possible to get a positive BiFC interaction between two proteins if they are the same complex, even if they do not interact directly. To support a conclusion about direct interaction between proteins, other methods such as co-precipitation of recombinant proteins or yeast two-hybrid should be used. For example, to support direct interaction between Trs20 and Trs120, and the effect of the Trs20-D46Y mutation on the interaction with Trs120 and not with Bet3, co-precipitation of bacterially expressed proteins and the yeast two-hybrid assay were used [12]. Similarly, identification of the Atg11 domain CC2-CC3 as the Ypt1-interaction domain was shown by co-precipitation of recombinant proteins and yeast two-hybrid assay, in addition to BiFC [4].

4   Notes

1. While extremely informative as in vivo evidence for an interaction and its intracellular localization, it is important to support BiFC results with independent approaches.

2. In principle, BiFC can be observed between two subunits in a complex even if they do not interact directly. Therefore, to determine a direct interaction, the analysis should be supported by other approaches, e.g., interaction of bacterially expressed proteins, as was done for the interactions described here [4, 12].

3. Because the fluorophore reconstruction is irreversible [11], BiFC cannot be used to follow dynamics of interactions.

Acknowledgments

References

1. Segev N (2001) Ypt and Rab GTPases: insight into functions through novel interactions. Curr Opin Cell Biol 13:500–511

2. Segev N (2011) Coordination of intracellular transport steps by GTPases. Semin Cell Dev Biol 22:33–38

3. Jedd G, Richardson C, Litt R, Segev N (1995) The Ypt1 GTPase is essential for the first two steps of the yeast secretory pathway. J Cell Biol 131:583–590

4. Lipatova Z, Belogortseva N, Zhang XQ, Kim J, Taussig D, Segev N (2012) Regulation of

selective autophagy onset by a Ypt/Rab GTPase module. Proc Natl Acad Sci U S A 109:6981–6986

5. Jones S, Newman C, Liu F, Segev N (2000) The TRAPP complex is a nucleotide exchanger for Ypt1 and Ypt31/32. Mol Biol Cell 11:4403–4411

6. Morozova N, Liang Y, Tokarev AA, Chen SH, Cox R, Andrejic J, Lipatova Z, Sciorra VA, Emr SD, Segev N (2006) TRAPPII subunits are required for the specificity switch of a Ypt-Rab GEF. Nat Cell Biol 8:1263–1269

7. Ohsumi Y (2014) Historical landmarks of autophagy research. Cell Res 24:9–23

8. Sacher M, Kim YG, Lavie A, Oh BH, Segev N (2008) The TRAPP complex: insight into its architecture and function. Traffic 9: 2032–2042

9. Segev N (2001) Ypt/Rab GTPases: regulators of protein trafficking. Sci STKE 2001:re11

10. Taussig D, Lipatova Z, Segev N (2014) Trs20 is required for TRAPPIII complex assembly at the PAS and its function in autophagy. Traffic 15:327–337

11. Kerppola TK (2008) Biomolecular fluorescence complementation (BiFC) analysis as a probe of protein interactions in living cells. Annu Rev Biophys 37:465–487

12. Taussig D, Lipatova Z, Kim JJ, Zhang X, Segev N (2013) Trs20 is required for TRAPPII assembly. Traffic 14:678–690

13. Hu CD, Kerppola TK (2003) Simultaneous visualization of multiple protein interactions in living cells using multicolor fluorescence complementation analysis. Nat Biotechnol 21:539–545

14. Huh WK, Falvo JV, Gerke LC, Carroll AS, Howson RW, Weissman JS, O'Shea EK (2003) Global analysis of protein localization in budding yeast. Nature 425:686–691

15. Sheff MA, Thorn KS (2004) Optimized cassettes for fluorescent protein tagging in Saccharomyces cerevisiae. Yeast 21:661–670

16. Rizzo MA, Springer GH, Granada B, Piston DW (2004) An improved cyan fluorescent protein variant useful for FRET. Nat Biotechnol 22:445–449

17. Paquin N, Menade M, Poirier G, Donato D, Drouet E, Chartrand P (2007) Local activation of yeast ASH1 mRNA translation through phosphorylation of Khd1p by the casein kinase Yck1p. Mol Cell 26:795–809

18. Michnick SW (2001) Exploring protein interactions by interaction-induced folding of proteins from complementary peptide fragments. Curr Opin Struct Biol 11:472–477

19. Zacharias DA, Violin JD, Newton AC, Tsien RY (2002) Partitioning of lipid-modified monomeric GFPs into membrane microdomains of live cells. Science 296:913–916

20. Christianson TW, Sikorski RS, Dante M, Shero JH, Hieter P (1992) Multifunctional yeast high-copy-number shuttle vectors. Gene 110: 119–122

21. Sikorski RS, Hieter P (1989) A system of shuttle vectors and yeast host strains designed for efficient manipulation of DNA in Saccharomyces cerevisiae. Genetics 122:19–27

22. Lee J, Reiter W, Dohnal I, Gregori C, Beese-Sims S, Kuchler K, Ammerer G, Levin DE (2013) MAPK Hog1 closes the S. cerevisiae glycerol channel Fps1 by phosphorylating and displacing its positive regulators. Genes Dev 27:2590–2601

23. Kim J, Kamada Y, Stromhaug PE, Guan J, Hefner-Gravink A, Baba M, Scott SV, Ohsumi Y, Dunn WA Jr, Klionsky DJ (2001) Cvt9/Gsa9 functions in sequestering selective cytosolic cargo destined for the vacuole. J Cell Biol 153:381–396

Chapter 10

Identifying a Rab Effector on the Macroautophagy Pathway

Juan Wang, Serena Cervantes, Saralin Davis, and Susan Ferro-Novick

Abstract

Rab GTPases are key regulators of membrane traffic. The Rab GTPase Ypt1 is essential for endoplasmic reticulum (ER)-Golgi traffic, intra-Golgi traffic, and the macroautophagy pathway. To identify effectors on the macroautophagy pathway, known autophagy-related genes (Atg genes) required for macroautophagy were tagged with GFP and screened for mislocalization in the *ypt1-2* mutant. At the pre-autophagosomal structure (PAS), the localization of the serine/threonine kinase Atg1 was affected in the *ypt1-2* mutant. We then used an in vitro binding assay to determine if Atg1 and Ypt1 physically interact with each other and co-immunoprecipitation experiments were performed to address if Atg1 preferentially interacts with the GTP-bound form of Ypt1.

Key words Ypt1, Rab GTPase, Effector, Atg1, Macroautophagy

1 Introduction

Membrane traffic between intracellular organelles is a highly dynamic and organized network. While different membranous organelles communicate through the continuous flow of membrane and protein, each organelle must maintain its unique structure and function. Every step of membrane traffic including vesicle budding, tethering, and fusion needs to be precisely regulated to ensure that cargoes are delivered to their correct destination. This regulation is coordinated largely by Rab proteins, which are guanosine triphosphatases (GTPases) of the Ras GTPase superfamily [1, 2]. There are 11 Rabs in yeast and more than 60 Rabs in mammalian cells [3]. Rabs localize to distinct intracellular membranes to precisely regulate each step of membrane traffic [4].

Rab GTPases act as molecular switches that cycle between an inactive (GDP-bound) and active form (GTP-bound) (Fig. 1). Guanine nucleotide exchange factors (GEFs) control this switch by stimulating the release of GDP from the Rab and accelerating the uptake of GTP. Conversely, GTPase-activating proteins (GAPs) inactivate GTPases by accelerating GTP hydrolysis. This nucleotide cycle is coupled with the insertion and release of the Rab from membranes.
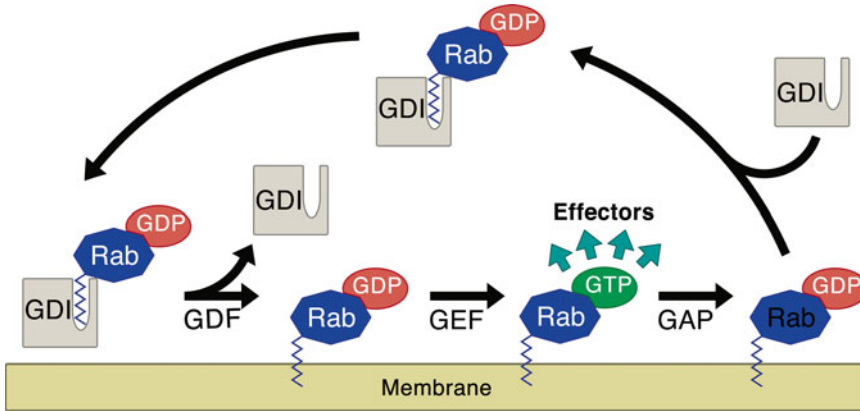
Fig. 1 The life cycle of a Rab. Rab proteins cycle between an active (GTP-bound) membrane bound form and inactive (GDP-bound) cytosolic form. When bound to a guanine nucleotide dissociation inhibitor (GDI), the inactive GDP-bound Rab remains in the cytosol. A GDI dissociation factor (GDF) mediates the release of GDI, which allows the Rab to insert into the target membrane. The Rab is activated when GDP is exchanged for GTP by a guanine nucleotide exchange factor (GEF). The active GTP-bound form of the Rab then interacts with its effector proteins. A GTPase activating protein (GAP) catalyzes hydrolysis of GTP on the Rab and the Rab becomes inactive. The Rab is then excised from the membrane by GDI to complete the Rab cycle

In order for Rabs to insert into membranes, a pair of C-terminal cysteines is modified with prenyl moieties (geranylgeranyl). GDI (GDP dissociation inhibitor) extracts the GDP-bound form of the Rab from membranes and conceals its isoprenyl group, allowing the Rab to be released into the cytosol. In the cytosol, the Rab remains in a complex with GDI. A GDI displacement factor (GDF) then dissociates GDI from the Rab, which allows the Rab to attach to a specific membrane where it is activated by its GEF. Once the Rab is membrane-bound and active, it can interact with specific effectors. The Rab is then inactivated by a specific GAP before it is extracted by GDI and released into the cytosol [2, 4–7].

The Rab GTPase Ypt1 is recruited to the macroautophagy pathway by the transport protein particle (TRAPP) III complex, a nucleotide exchange factor (GEF) for Ypt1 [8]. Macroautophagy is a highly conserved and specialized membrane trafficking pathway that controls protein and organelle degradation under starvation conditions [9, 10]. The morphological hallmark of autophagy is the formation of double-membrane vesicles called autophagosomes, which sequester its contents from the cytosol and transport them to the lysosome or vacuole for degradation. More than 30 *ATG* (autophagy-related) genes have been identified in the yeast *Saccharomyces cerevisiae* [11] that assemble in a hierarchical manner and colocalize at the preautophagosomal structure (PAS), a perivacuolar compartment responsible for autophagosome formation [12].

To address if a known Atg protein functions as a downstream effector of Ypt1, we fused all Atg proteins that are required for macroautophagy to GFP and screened for defects in PAS localization in the *ypt1-2* mutant by fluorescence microscopy. Atg1, a

serine/threonine kinase essential for the induction of autophagy, was found to mislocalize in the *ypt1-2* mutant under starvation conditions. To begin to address if Atg1 is an effector of Ypt1 on the macroautophagy pathway, we determined if Atg1 directly binds to Ypt1 in a nucleotide-dependent fashion. As we have found glutathione-S-transferase (GST)-Ypt1 preloaded with GDP or GTP is not fully functional, we performed in vitro binding studies with Ypt1-His$_6$. When we purified Ypt1-His$_6$ Q67L (GTP-bound form) and S22N (GDP-bound form), however, Ypt1-His$_6$ S22N was partially denatured and showed nonspecific binding. This lead us to demonstrate a direct interaction between Atg1 and Ypt1 by performing in vitro binding studies between GST-tagged Atg1 and wild-type Ypt1-His$_6$. After determining that Atg1 and Ypt1 directly bind to each other, we performed co-immunoprecipitation experiments to show that Atg1 preferentially interacts with the GTP-bound form of Ypt1 in vivo. Here we present the methods used in Wang et al. [13], which collectively show that activated Ypt1 recruits its downstream effector, the serine/threonine Atg1 kinase.

2 Materials

2.1 Culture Media

1. Growth medium (YPD): 1 % yeast extract, 2 % peptone, and 2 % dextrose or synthetic minimal media (SMD): 0.67 % yeast nitrogen base, 2 % dextrose, and auxotrophic amino acids as needed. For solid media, agar was added to a final concentration of 2 %. Autoclaved media are stable at room temperature for months.

2. Starvation medium (synthetic minimal medium lacking nitrogen (SD-N)): 0.17 % yeast nitrogen base without amino acids or ammonium sulfate, and 2 % dextrose. Autoclaved media are stable at room temperature for months.

3. LB medium: 10 g tryptone, 5 g yeast extract, 5 g NaCl into 1 l of water. Autoclaved media are stable at room temperature for months. The drugs 30 μg/ml kanamycin or 100 μg/ml ampicillin were added before use.

2.2 Solutions

1. DNA transformation buffer: 100 mM lithium acetate, 10 mM Tris–HCl, 1 mM EDTA, pH 7.5, sterilized by filtration.

2. Other transformation reagents: 50 % PEG: 50 % polyethylene glycol 3350 in water. Autoclave to sterilize these reagents.

3. Bacterial lysis buffer 1: 20 mM Tris pH 8, 150 mM NaCl, 1 mM DTT, 1 mM PMSF, 15 mM Imidazole.

4. Bacterial lysis buffer 2: 1× PBS, 1 mM PMSF and 1 mM DTT.

5. Elution buffer: 20 mM Tris pH 8, 150 mM NaCl, 1 mM DTT, 1 mM PMSF, 250 mM Imidazole.

6. Binding buffer: 50 mM HEPES pH 7.2, 150 mM NaCl, 1 mM DTT, 1 mM EDTA, 2 % Triton X100, 5X PIC.

7. SDS sample buffer: 50 mM Tris–HCl pH 6.8, 2 % SDS, 10 % glycerol, 1 % β-mercaptoethanol, 12.5 mM EDTA, 0.02 % bromophenol blue.

8. Yeast lysis buffer: 1× PBS, 200 mM sorbitol, 1 mM MgCl$_2$, 0.1 % Tween 20, 1× protease inhibitor cocktail.

9. Transfer buffer: 25 mM Tris, 192 mM glycine, 20 % methanol.

10. TBST buffer: 50 mM Tris pH 7.5, 150 mM NaCl, 0.05 % Tween 20.

11. Blocking and antibody-binding buffer: 10 % milk, 50 mM Tris pH 7.5, 150 mM NaCl, 0.05 % Tween 20.

2.3 Plasmids

1. pFA6a-GFP(S65T)-His3MX6 [14].

2. pRS315-Ape1-RFP (*CEN LEU2*). A 2.9 kb insert of APE1 (379 bp of the 5′ UTR, APE1 coding region without the stop codon)-RFP-ADH terminator was cloned into the SalI and NotI sites of pRS315.

2.4 Reagents

1. Ni-NTA Agarose.

2. Glutathione-sepharose beads.

3. Spin column containing a cut-off filter of 10 kDa.

4. Nitrocellulose membranes.

5. Anti-His antibody.

6. Anti-HA antibody.

7. Anti-Ypt1 serum.

8. Anti-rabbit IgG.

9. Anti-mouse IgG.

10. HA affinity matrix.

11. Enhanced chemiluminescence (ECL) detection kit.

12. Zymolyase 100 T.

13. Rapamycin: 1 mg/ml in DMSO.

3   Methods

3.1 Determination of the PAS Localization of Atg Proteins in the ypt1-2 Mutant by Fluorescence Microscopy to Identify a Candidate Ypt1 Effector on the Macroautophagy Pathway

1. Wild type and *ypt1-2* cells expressing GFP-tagged Atg proteins and Ape1-RFP were cultured in SMD selective medium at 25 °C to log phase (*see* **Note 1**). For the nitrogen starvation experiments, cells were washed twice in SD-N medium and shifted to SD-N medium for 4 h.

2. Cells were centrifuged at $1,500 \times g$ for 2 min and approximately 2 μl of the cell pellet was examined on a slide (*see* **Note 2**).

3. Image acquisition of GFP-tagged Atg proteins and the PAS marker Ape1-RFP was performed on an Axio Imager Z1 fluorescence microscope using a 100× oil-immersion objective. More than 150 cells from three different experiments were

examined. The PAS targeting index (PTI) was calculated by multiplying the percent of cells that contain colocalized GFP-tagged Atg proteins and Ape1–RFP to the total GFP signal that resides at the PAS. Atg1-GFP displayed a defect in PAS localization in the *ypt1-2* mutant. Atg1 was further analyzed as a candidate Ypt1 effector on the macroautophagy pathway.

3.2   In Vitro Binding Assay of Ypt1 and Atg1 to Determine If Atg1 and Ypt1 Physically Interact with Each Other

3.2.1   Purification of Ypt1-His$_6$

1. Ypt1 was cloned into the pET-29a plasmid and transformed into BL21(DE3) *E. coli* cells to express Ypt1-His$_6$.

2. A single colony was inoculated in 50 ml LB medium with 30 μg/ml kanamycin overnight at 37 °C.

3. Overnight culture was inoculated into 1 l LB medium containing 30 μg/ml kanamycin at 37 °C with a starting OD600 of approximately 0.1. When the OD600 reached 0.6, filter sterilized IPTG was added to a final concentration of 0.5 mM. Ypt1-His$_6$ expression was induced overnight at 20 °C.

4. Cells were centrifuged at $6,000 \times g$ for 5 min and resuspended in 20 ml of bacterial lysis buffer 1.

5. The cells were sonicated for 15 s on and off at 50 % amplitude for a total of 2 min.

6. The sample was centrifuged at $12,000 \times g$ for 15 min at 4 °C.

7. The cleared lysate was transfered into a fresh 50 ml tube. Prewashed 2 ml Ni-NTA agarose beads were added and incubated at 4 °C with rotation (20 rpm) for 30 min (*see* **Note 3**).

8. The slurry of Ni-NTA beads and lysate was loaded onto a 0.8×12 cm polypropylene column and washed with 20 ml of bacterial lysis buffer 1.

9. The bound protein was eluted with 8 ml of elution buffer.

10. A spin column containing a cut-off filter of 10 kDa was used to concentrate the eluate to approximately 0.5 ml.

11. Purified Ypt1-His$_6$ was analyzed on a 13 % SDS-PAGE gel and stained with Coomassie Brilliant Blue. The protein concentration of Ypt1-His$_6$ was measured using BSA as a standard and analyzed using Alphaview software.

3.2.2   Purification of Glutathione-Sepharose Beads Containing GST-Atg1 (1–500aa, 501–897aa) and GST

1. Atg1 (1–1500 bp and 1501–2694 bp) was cloned into plasmid pGEX-4 T-2 and transfected into BL21(DE3) *E. coli* cells to express GST-Atg1 truncations.

2. A single colony was inoculated in 50 ml of LB medium with 100 μg/ml ampicillin overnight at 37 °C.

3. An overnight culture was inoculated into 1 l of LB medium with 100 μg/ml ampicillin at 37 °C with a starting OD600 of approximately 0.1. When the OD600 reached 0.6, IPTG was added to a final concentration of 0.5 mM and the expression of GST and GST-Atg1 was induced overnight at 20 °C.

4. Cells were centrifuged at $6,000 \times g$ for 10 min and resuspended in 20 ml of bacterial lysis buffer 2.

5. The suspension was sonicated for 15 s on and off at 50 % amplitude for a total of 2 min.

6. Triton X-100 was added to the sample to a final concentration of 1 %.

7. The sample was centrifuged at $12,000 \times g$ for 15 min.

8. The cleared lysates were transferred into a fresh 50 ml tube. Prewashed glutathione-sepharose beads (1 ml) were added and incubated at 4 °C with rotation (20 rpm) for 30 min (*see* **Note 4**).

9. The beads were centrifuged at $500 \times g$ for 2 min and washed three times with 10 ml of PBS.

10. SDS-PAGE sample buffer (50 μl) was added to the glutathione-sepharose beads containing GST fusion proteins. The bound proteins were analyzed on an 8 % SDS-PAGE gel and stained with Coomassie Brilliant Blue. The protein concentration of GST and GST-Atg1 truncations were measured using BSA as a standard and analyzed using Alphaview software.

3.2.3   In Vitro Binding Assay with GST-Atg1 Constructs (1–500aa, 501–897aa) and Ypt1-His$_6$

1. Varying concentrations of Ypt1–His$_6$ (250nM, 500nM, 1000nM) were incubated with equimolar amounts (0.1 μM) of immobilized GST or GST-Atg1 truncations in a total volume of 500 μl of binding buffer for 3 h at 4 °C with rotation (20 rpm) (*see* **Notes 5** and **6**).

2. The beads were washed three times with 1 ml of binding buffer without protease inhibitors.

3. The beads were resuspended in 50 μl of SDS-PAGE sample buffer and heated at 100 °C for 5 min.

4. The eluate was fractionated on a 13 % SDS-PAGE gel and transferred onto nitrocellulose membranes in transfer buffer.

5. The membranes were blocked with blocking solution for 1 h.

6. Anti-His antibody was added to the membranes and incubated at 4 °C overnight.

7. The membranes were washed with 10 ml of the TBST buffer three times.

8. Anti-mouse IgG (1:10,000 dilution) was added and incubated for 1 h.

9. The membranes were washed with 10 ml of the TBST buffer three times and then analyzed using the ECL method.

3.3 Coimmunopre-cipitation of Atg1-3HA and Ypt1 Demonstrated That Atg1 Preferentially Interacts with the GTP-Bound form of Ypt1 In Vivo

1. Yeast strains expressing Atg1-3HA were constructed using an integration vector pRS305 [15]. The Atg1 C-terminus lacking its stop codon (2041 bp–2091 bp)-3HA-ADH terminator was cloned into the SalI and NotI sites of pRS305. The linearized plasmid was transformed into *S. cerevisiae* cells using the lithium acetate procedure [16].

2. Ypt1 with its own promoter and terminator was cloned into pRS315. pRS315-YPT1 with the S22N and Q67L mutations were constructed by site-directed mutagenesis [17].

3. Exponentially growing yeast cells expressing Ypt1 Q67L or S22N or Atg1-3HA were grown in SC-Leu medium and treated with zymolyase 100 T at 37 °C for 30 min to generate spheroplasts.

4. The resulting spheroplasts were divided into two aliquots and treated with or without 0.2 μg/ml rapamycin for 30 min at 25 °C.

5. The spheroplasts were lysed with ice-cold yeast lysis buffer in a pre-chilled dounce homogenizer.

6. The lysed samples were centrifuged at $15,000 \times g$ for 15 min and the supernatants were collected into fresh 15 ml tubes.

7. The cell lysates were incubated with 15 μl HA affinity matrix for 4 h at 4 °C (*see* **Note 7**).

8. The HA affinity matrix was washed with 1 ml of yeast lysis buffer three times at 4 °C.

9. SDS sample buffer was used to elute protein from the HA affinity matrix. The eluate was fractionated on a 13 % SDS-PAGE gel and transferred onto a nitrocellulose membrane in transfer buffer.

10. The membranes were blocked with blocking solution for 1 h.

11. To detect Ypt1 and Atg1-HA, anti-Ypt1 serum and anti-HA antibody were added respectively to the membranes and incubated at 4 °C overnight.

12. The membranes were washed with 10 ml of the TBST buffer three times.

13. To detect Ypt1, anti-rabbit IgG (1:10,000 dilution) was added and incubated for 1 h. To detect Atg1-3HA, anti-mouse IgG (1:10,000 dilution) was added and incubated for 1 h.

14. The membranes were washed with 10 ml of the TBST buffer three times and analyzed using the ECL method.

4   Notes

1. The *ypt1-2* mutant was used because it does not disrupt the secretory pathway in vivo [18].

2. Press the coverslip gently to create a monolayer of cells.

3. Prewash Ni-NTA agarose beads with 10 ml of bacterial lysis buffer 1 three times before use.

4. Prewash glutathione-sepharose beads with 10 ml of bacterial lysis buffer 2 three times before use.

5. Use blank beads to ensure each binding reaction has the same amount of beads. To make blank beads, glutathione-sepharose beads were treated with 1 mg/ml BSA for 30 min and washed with 10 ml of PBS three times.

6. Use varying concentrations of Ypt1–His$_6$ to find the best binding conditions and show the binding is concentration dependent.

7. Incubation times can vary from 2 h to overnight.

Acknowledgements

References

1. Stenmark H (2009) Rab GTPases as coordinators of vesicle traffic. Nat Rev Mol Cell Biol 10(8):513–525

2. Mizuno-Yamasaki E, Rivera-Molina F, Novick P (2012) GTPase networks in membrane traffic. Annu Rev Biochem 81:637–659

3. Pereira-Leal JB, Seabra MC (2001) Evolution of the Rab family of small GTP-binding proteins. J Mol Biol 313(4):889–901

4. Grosshans BL, Ortiz D, Novick P (2006) Rabs and their effectors: achieving specificity in membrane traffic. Proc Natl Acad Sci U S A 103(32):11821–11827

5. Pfeffer SR (2001) Rab GTPases: specifying and deciphering organelle identity and function. Trends Cell Biol 11(12):487–491

6. Pfeffer S, Aivazian D (2004) Targeting Rab GTPases to distinct membrane compartments. Nat Rev Mol Cell Biol 5(11):886–896

7. Goody RS, Rak A, Alexandrov K (2005) The structural and mechanistic basis for recycling of Rab proteins between membrane compartments. Cell Mol Life Sci 62(15):1657–1670

8. Lynch-Day MA, Bhandari D, Menon S, Huang J, Cai H, Bartholomew CR, Brumell JH, Ferro-Novick S, Klionsky DJ (2010) Trs85 directs a Ypt1 GEF, TRAPPIII, to the phagophore to promote autophagy. Proc Natl Acad Sci U S A 107(17):7811–7816

9. Klionsky DJ (2007) Autophagy: from phenomenology to molecular understanding in less than a decade. Nat Rev Mol Cell Biol 8(11):931–937

10. Mizushima N (2007) Autophagy: process and function. Genes Dev 21(22):2861–2873

11. Nakatogawa H, Suzuki K, Kamada Y, Ohsumi Y (2009) Dynamics and diversity in autophagy mechanisms: lessons from yeast. Nat Rev Mol Cell Biol 10(7):458–467

12. Suzuki K, Kubota Y, Sekito T, Ohsumi Y (2007) Hierarchy of Atg proteins in pre-autophagosomal structure organization. Genes Cells 12(2):209–218

13. Wang J, Menon S, Yamasaki A, Chou HT, Walz T, Jiang Y, Ferro-Novick S (2013) Ypt1 recruits the Atg1 kinase to the preautophagosomal structure. Proc Natl Acad Sci U S A 110(24):9800–9805

14. Longtine MS, McKenzie A 3rd, Demarini DJ, Shah NG, Wach A, Brachat A, Philippsen P, Pringle JR (1998) Additional modules for versatile and economical PCR-based gene deletion and modification in Saccharomyces cerevisiae. Yeast 14(10):953–961

15. Sikorski RS, Hieter P (1989) A system of shuttle vectors and yeast host strains designed for efficient manipulation of DNA in Saccharomyces cerevisiae. Genetics 122(1):19–27

16. Gietz D, St Jean A, Woods RA, Schiestl RH (1992) Improved method for high efficiency transformation of intact yeast cells. Nucleic Acids Res 20(6):1425

17. Fisher CL, Pei GK (1997) Modification of a PCR-based site-directed mutagenesis method. Biotechniques 23 (4):570–571, 574

18. Bacon RA, Salminen A, Ruohola H, Novick P, Ferro-Novick S (1989) The GTP-binding protein Ypt1 is required for transport in vitro: the Golgi apparatus is defective in ypt1 mutants. J Cell Biol 109(3):1015–1022

Chapter 11

Functional Analysis of Rab27A and Its Effector Slp2-a in Renal Epithelial Cells

Takao Yasuda, Paulina S. Mrozowska, and Mitsunori Fukuda

Abstract

Polarized epithelial cells have two distinct plasma membrane domains, i.e., an apical membrane domain and a basolateral membrane domain, that are the result of polarized trafficking of proteins and lipids. Several members of the Rab-type small GTPases, which are general regulators of membrane trafficking, have been reported to be involved in the regulation of polarized trafficking in epithelial cells, but their precise role in polarized trafficking is poorly understood. In a recent study we used Madin-Darby canine kidney (MDCK) II cells as a model of polarized cells and concluded from the results that Rab27A and its effector synaptotagmin-like protein 2-a (Slp2-a) regulate apical transport of Rab27-bearing vesicles in polarized epithelial cells. Both Rab27A and Slp2-a are uniformly localized at the plasma membrane in subconfluent, non-polarized MDCK II cells, but their expression increases as the cells become polarized, and they are specifically localized at the apical membrane in polarized MDCK II cells (i.e., two-dimensional cell culture). Slp2-a is also localized at the apical membrane of tubular MDCK II cysts (i.e., three-dimensional cell culture) and promotes the formation of a single apical domain in the cysts by regulating polarized trafficking of Rab27-bearing vesicles. In this chapter we describe the assay procedures for analyzing the expression and localization of Rab27A and Slp2-a in non-polarized and polarized renal epithelial cells.

Key words Rab27A, Slp2-a, MDCK II cells, Renal proximal tubules

1 Introduction

Cell polarity is a characteristic property of well-differentiated eukaryotic cells, e.g., epithelial cells and neurons. Polarized epithelial cells have two morphologically and functionally distinct membrane domains, an apical membrane domain (simply referred to as the "apical membrane" below) that faces the lumen and a basolateral membrane domain (simply referred to as the "basolateral membrane" below) that faces the extracellular matrix and neighboring cells, which are separated by tight junctions, thereby defining and maintaining their unique identities and functions. Since polarized trafficking of proteins and lipids to each of these membranes is a process that is crucial to maintaining cell polarity,

considerable attention has been directed to identifying the molecular mechanism of the polarized trafficking in epithelial cells [1, 2]. Polarized trafficking is a special type of membrane trafficking that is also thought to be regulated by Rab-type small GTPases, which are general regulators of membrane trafficking [3–5]. Several Rab isoforms, e.g., Rab8, Rab11, and Rab27A, have recently been reported to be involved in the regulation of polarized trafficking in epithelial cells [1, 2].

We recently found that Rab27A and its effector synaptotagmin-like protein 2-a (Slp2-a) are expressed in Madin-Darby canine kidney (MDCK) II cells, a model of polarized cells (Fig. 1a), and in mouse kidney, and that they control apical transport of a signaling molecule, podocalyxin, in polarized MDCK II cells [6, 7]. Slp2-a is a member of the synaptotagmin-like protein (Slp) family, whose members consist of an N-terminal Slp homology domain (SHD) and C-terminal tandem C2 domains (named the C2A domain and C2B domain) [8, 9]. Slp2-a was originally characterized as an effector molecule for the small GTPase Rab27 [10], and it has been shown to promote certain Rab27A-dependent membrane trafficking events, especially during the docking of Rab27A-containing vesicles/organelles to the plasma membrane [11, 12]. For example, Slp2-a has been shown to promote melanosome anchoring to the plasma membrane through interaction with Rab27A on the melanosome via the SHD and with phospholipids in the plasma membrane via the C2A domain [13, 14]. Similarly, Slp2-a has been shown to promote docking of secretory vesicles to the plasma membrane in certain types of secretory cells [15–18]. Intriguingly, Slp2-a is also expressed in non-polarized and polarized MDCK II cells, and its expression and localization have been shown to undergo dramatic changes during polarization (Fig. 1a), i.e., an increase in Slp2-a expression level and change in its distribution from the plasma membrane to the apical membrane [6]. In earlier studies conducted on polarized MDCK II cells we discovered that Slp2-a is involved in the regulation of cell signaling and tubulogenesis by promoting docking of Rab27A-bearing podocalyxin-containing vesicles to the apical membrane [6, 7], and more recently, we found that Slp2-a has an additional role in controlling the cell size of MDCK II cells independently of Rab27A [19]. In this chapter we describe the assay procedures for analyzing the expression and localization of Rab27A and Slp2-a in renal epithelial cells in different cell cultures, including single cell cultures (non-polarized cell cultures), polarized cultures (two-dimensional cell cultures), and tubular cyst cultures (three-dimensional cell cultures). Other assay procedures for analyzing the function of Rab27A and its effectors in melanosome transport and secretory vesicle exocytosis have been described elsewhere [20, 21].
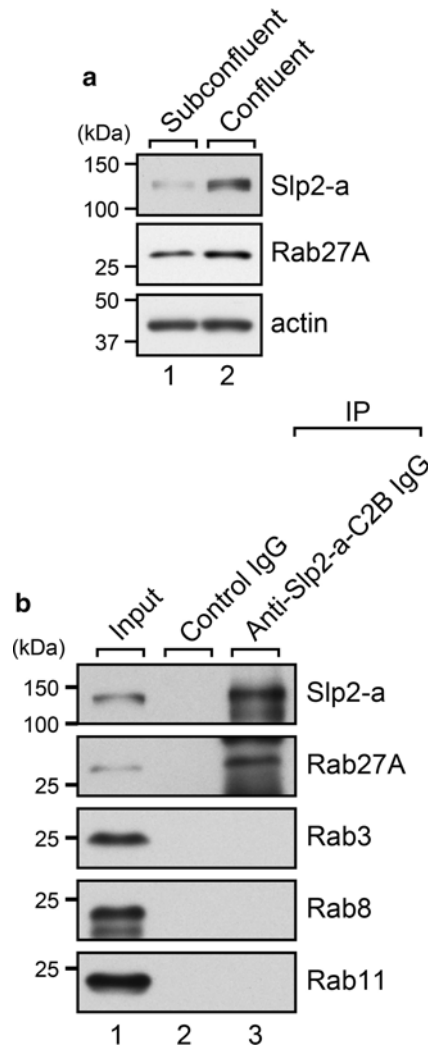
Fig. 1 Expression of Rab27A and Slp2-a and their specific interaction in MDCK II cells. (**a**) Up-regulation of Slp2-a protein in polarized MDCK II cells. Total cell lysates of subconfluent MDCK II cells (i.e., non-polarized cells) and confluent MDCK II cells (i.e., polarized cells) were subjected to immunoblot analysis with anti-Slp2-a-SHD rabbit polyclonal antibody (1 μg/mL; *top panel*), anti-Rab27A rabbit polyclonal antibody (1.5 μg/mL; *middle panel*), and anti-β-actin mouse monoclonal antibody (1/10,000 dilution; *bottom panel*). (**b**) Endogenous interaction between Rab27A and Slp2-a in MDCK II cells. Endogenous Slp2-a protein was immunoprecipitated with anti-Slp2-a-C2B rabbit polyclonal antibody (*lane 3*) or control rabbit IgG (*lane 2*) from total cell lysates (input; *lane 1*) of confluent MDCK II cells. The immunoprecipitated samples were subjected to 10 % SDS-PAGE followed by immunoblotting with the antibodies indicated on the *right*. Slp2-a specifically interacted with Rab27A, but did not interact with any of the other Rabs tested. The positions of the molecular mass markers (in kDa) are shown on the *left*

2   Materials

Prepare all solutions by using ultrapure water (Milli-Q Advantage A10 Ultrapure Water Purification System) and analytical grade reagents commercially available (unless otherwise specified). The solutions prepared are stored at 4 °C until used (unless otherwise specified).

2.1 Immunopre-cipitation

1. MDCK II cells (*see* **Note 1**).

2. MDCK II cell culture medium: Dulbecco's Modified Eagle Medium (DMEM) supplemented with 10 % fetal bovine serum, 100 U/mL penicillin G, and 100 μg/mL streptomycin.

3. 0.25 % trypsin-EDTA (*see* **Note 2**).

4. 100-mm cell culture dishes.

5. Bio-Rad Protein Assay Kit.

6. Antibodies: anti-Slp2-a-SHD rabbit polyclonal antibody [22], anti-Slp2-a-C2B rabbit polyclonal antibody [10], anti-Rab3 mouse monoclonal antibody, anti-Rab8 mouse monoclonal antibody, anti-Rab11 mouse monoclonal antibody, anti-Rab27A rabbit polyclonal antibody [15], and normal rabbit IgG.

7. Dulbecco's phosphate-buffered saline (PBS) stored at room temperature.

8. Cell lysis buffer: 50 mM HEPES-KOH, pH 7.2, 150 mM NaCl, 1 mM MgCl$_2$, and 1 % Triton X-100 supplemented with complete EDTA-free protease inhibitor cocktail.

9. Washing buffer: 50 mM HEPES-KOH, pH 7.2, 150 mM NaCl, 1 mM MgCl$_2$, and 0.2 % Triton X-100.

10. Protein A-Sepharose beads (*see* **Note 3**).

11. HRP (horseradish peroxidase)-conjugated secondary antibodies.

12. ECL Western Blotting Detection System.

2.2 Immunocyto-chemical Analysis of MDCK II Cells

1. MDCK II cells.

2. 60-mm cell culture dishes.

3. 35-mm glass-bottom dishes.

4. 12-well cell culture plate.

5. 12-mm diameter round microscope coverglass.

6. BD Matrigel™ Basement Membrane Matrix Growth Factor Reduced (*see* **Note 4**).

7. 1 μg/μL pEGFP-C1 vector harboring mouse Slp2-a cDNA (pEGFP-C1-Slp2-a) [13] in ultrapure water purified with the QIAGEN Plasmid Midi kit.

8. Lipofectamine® 2000.

9. 4 % paraformaldehyde (PFA) in 0.1 M sodium phosphate buffer: 0.084 M Na$_2$HPO$_4$, 0.016 M NaH$_2$PO$_4$, pH 7.4.

10. 100 % (w/v) Trichloroacetic acid solution (TCA).

11. PBS.

12. Blocking buffer: 1 % BSA and 0.1 % Triton X-100 in PBS.

13. Anti-Slp2-a-SHD rabbit polyclonal antibody [22], anti-Rab27A mouse monoclonal antibody, and anti-Rab27A rabbit polyclonal antibody [15].

14. Alexa Fluor® 488-conjugated anti-rabbit antibody, Alexa Fluor® 594-conjugated anti-mouse antibody, Texas-Red®-X-conjugated phalloidin, and DAPI dihydrochloride.

15. Can Get Signal® Immunoreaction Enhancer Solution.

16. Microscope slides.

17. Fluoromount/Plus™.

18. Confocal fluorescence microscope (Olympus Fluoview 1000).

2.3 Immunohisto-
chemical Analysis
of Mouse Kidney

1. Specific-pathogen-free (SPF) male mice (e.g., DBA/2JJcl).

2. 4 % PFA.

3. PBS.

4. 10 % sucrose solution and 20 % sucrose solution in PBS.

5. Tissue-Tek O.C.T. compound.

6. Cryostat.

7. Microscope slides and coverglasses.

8. Fluoromount/Plus™.

9. Blocking buffer: 10 % fetal bovine serum in PBS.

10. Anti-Slp2-a-SHD rabbit polyclonal antibody [22], and anti-Rab27A mouse monoclonal antibody.

11. Alexa Fluor® 488-conjugated anti-rabbit antibody and Alexa Fluor® 594-conjugated anti-mouse antibody.

12. Confocal fluorescence microscope (Olympus Fluoview 1000).

3 Methods

3.1 Immunopre-
cipitation Analysis
of Endogenous
Interaction Between
Slp2-a and Rab27A
in MDCK II cells

1. Seed MDCK II cells in two 100-mm dishes (2×10^6 cells in 10 mL of MDCK II culture medium per dish), and incubate them at 37 °C under 5 % CO_2.

2. 48 h after seeding, wash the MDCK II cells once with 5 mL of ice-cold PBS, add 1 mL of cell lysis buffer to the MDCK II cells, and use a scraper to transfer the cells from the two dishes into each of two 1.5-mL microtubes.

3. Rotate at 4 °C for 30 min.

4. Centrifuge at $15,000 \times g$ at 4 °C for 20 min, and collect the supernatant from the two microtubes into a 15-mL Falcon tube.

5. Measure the protein concentration of the supernatant by using a Bio-Rad Protein Assay Kit according to the manufacturer's instructions.

6. Dispense 1 mg of the cell lysate into two new microtubes (approximately 800 µL per tube).

7. Add 1 µg of anti-Slp2-a-C2B rabbit polyclonal antibody and 1 µg of normal rabbit IgG to each microtube.

8. Rotate overnight at 4 °C.

9. Add 15 µL of protein A-Sepharose beads to each microtube.

10. Rotate at 4 °C for 2 h.

11. Centrifuge at $500 \times g$ at 4 °C for 1 min, and discard the supernatant.

12. Wash the beads three times with 1 mL of washing buffer each time.

13. Analyze proteins bound to the beads by performing 10 % SDS polyacrylamide gel electrophoresis (PAGE) followed by conventional immunoblotting with the primary antibodies at the following concentrations: anti-Slp2-a-SHD rabbit polyclonal antibody, 1 µg/mL; anti-Rab27A rabbit polyclonal antibody, 1.5 µg/mL; anti-Rab3 mouse monoclonal antibody, 1/500 dilution; anti-Rab8 mouse monoclonal antibody, 1/4,000 dilution; and anti-Rab11 mouse monoclonal antibody, 1/4,000 dilution.

14. Detect the immunoreactive bands by using the ECL Western Blotting Detection System according to the manufacturer's instructions (representative results are shown in Fig. 1b).

3.2 Immunocytochemical Analysis of Slp2-a and Rab27A in MDCK II Cells

3.2.1 Localization of Slp2-a and Rab27A in a Single MDCK II Cell

1. Seed MDCK II cells in a 60-mm dish (2×10^5 cells in 5 mL of MDCK II culture medium per dish) and incubate them overnight at 37 °C under 5 % CO_2.

2. Transfect the MDCK II cells with 1 µg of pEGFP-C1-Slp2-a by using 2 µL of Lipofectamine® 2000 according to the manufacturer's instructions (*see* **Note 5**).

3. 24 h after transfection, replate 1/20 volume of the transfected cells (1×10^4 cells) in 2 mL of MDCK II culture medium in a 35-mm glass-bottom dish, and incubate the cells at 37 °C under 5 % CO_2 (*see* **Note 6**).

4. 24 h after replating, fix the MDCK II cells with 150 µL of 4 % PFA for 10 min at room temperature (*see* **Note 7**). Perform all of the following steps at room temperature.

5. Wash the MDCK II cells three times with 1 mL of PBS each time.

6. Permeabilize the MDCK II cells with 150 µL of 0.3 % Triton X-100 in PBS for 2 min.

7. Wash the MDCK II cells three times with 1 mL of PBS each time.

8. Block with 150 μL of blocking buffer for 30 min.

9. Incubate the MDCK II cells for 3 h in 150 μL of Can Get Signal® Immunoreaction Enhancer Solution containing anti-Rab27A rabbit polyclonal antibody (6 μg/mL).

10. Wash the MDCK II cells three times with 1 mL of PBS each time.

11. Incubate the MDCK II cells for 2 h in 150 μL of Can Get Signal® Immunoreaction Enhancer Solution containing the secondary antibody (Alexa Fluor® 594-conjugated anti-rabbit antibody, 1/5,000 dilution) under light-protected conditions. Perform all of the following steps under light-protected conditions.

12. Wash the MDCK II cells three times with 1 mL of PBS each time.

13. Incubate the MDCK II cells for 20 min in 150 μL of PBS containing 0.25 mg of DAPI.

14. Wash the MDCK II cells three times with 1 mL of PBS each time.

15. Capture fluorescence images of EGFP-Slp2-a and endogenous Rab27A in the MDCK II cells under a confocal fluorescence microscope (representative images are shown in Fig. 2a).

3.2.2 Localization of Slp2-a and Rab27A in Polarized MDCK II Cells

1. Seed 5×10^5 MDCK II cells in 2 mL of MDCK II culture medium in a 35-mm glass-bottom dish, and incubate the cells at 37 °C under 5 % CO_2.

2. 72 h after seeding, fix the cells with 150 μL of 4 % PFA for 10 min at room temperature (*see* **Note 7**). Perform all of the following steps at room temperature.

3. Follow **steps 5–8** in Subheading 3.2.1.

4. Incubate the MDCK II cells for 3 h in 150 μL of Can Get Signal® Immunoreaction Enhancer Solution containing anti-Slp2-a-SHD rabbit polyclonal antibody (8 μg/mL) and anti-Rab27A mouse monoclonal antibody (1/100 dilution).

5. Follow **steps 10–14** in Subheading 3.2.1.

6. Capture fluorescence images of endogenous Slp2-a and Rab27A in the MDCK II cells under a confocal fluorescence microscope (representative images are shown in Fig. 2b).

3.2.3 Localization of Slp2-a and Rab27A in MDCK II Cysts

1. One day before the experiment, seed 2×10^5 MDCK II cells in 10 mL of MDCK II culture medium in a 100-mm dish, and incubate them overnight at 37 °C under 5 % CO_2 (*see* **Note 8**).
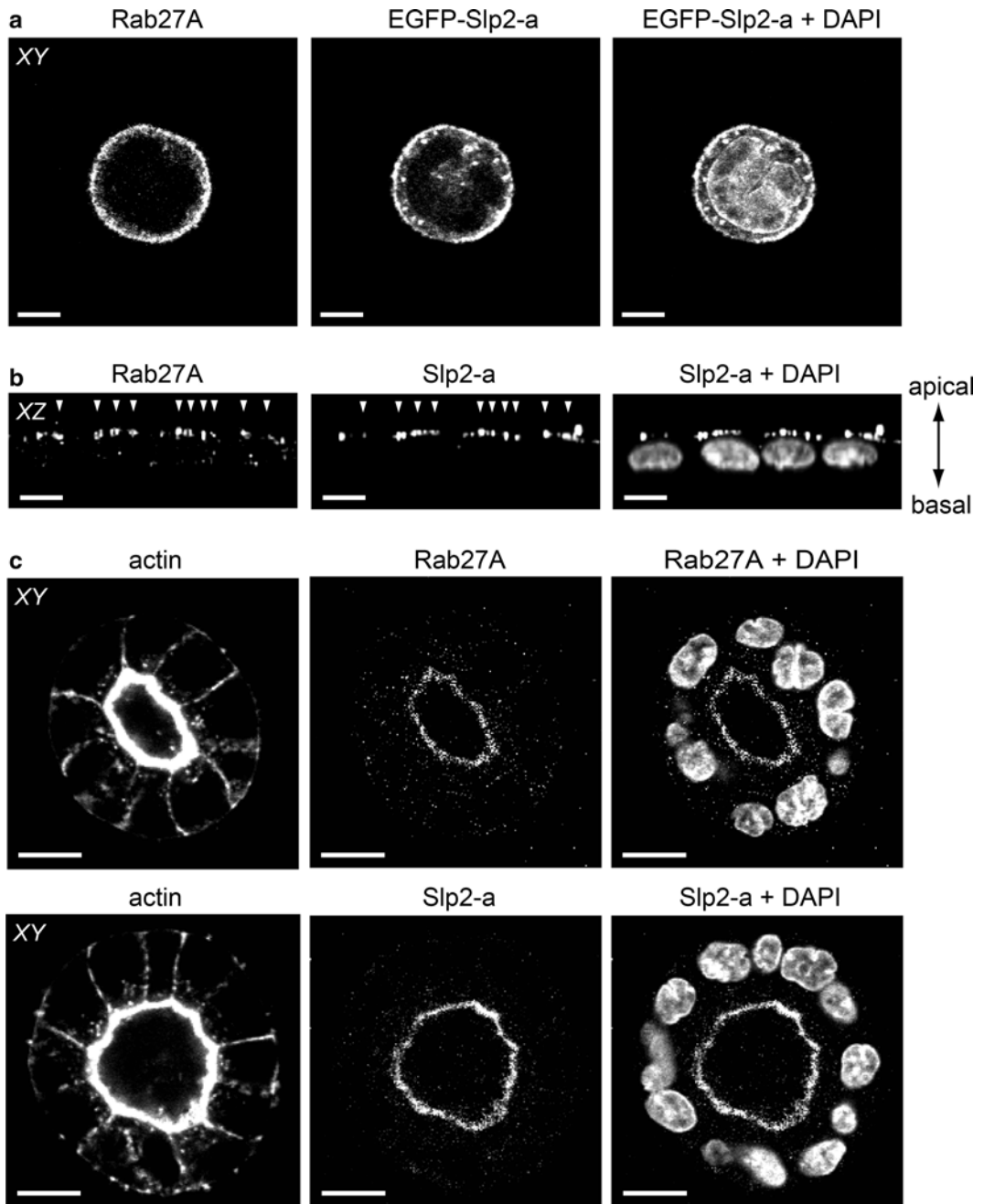
Fig. 2 Localization of Rab27A and Slp2-a in MDCK II cells. (**a**) Colocalization of Rab27A and Slp2-a at the plasma membrane in non-polarized MDCK II cells (single cell culture). MDCK II cells transiently expressing EGFP-Slp2-a (*middle panel*) were stained with anti-Rab27A antibody (*left panel*). Nuclei were stained with DAPI (*right panel*, merged image with EGFP-Slp2-a). Confocal xy sections are shown. (**b**) Colocalization of Rab27A and Slp2-a at the apical membrane in polarized MDCK II cells (two-dimensional cell culture). Confluent MDCK II cells were co-stained with anti-Rab27A antibody (*left panel*) and anti-Slp2-a antibody (*middle panel*). Nuclei were stained with DAPI (*right panel*, merged image with Slp2-a). Confocal xz sections are shown. The *arrowheads* indicate the sites of colocalization between Rab27A and Slp2-a at the apical membrane of polarized MDCK II cells. (**c**) Localization of Rab27A and Slp2-a at the apical membrane in MDCK II cysts. MDCK II cysts were stained with anti-Rab27A antibody (*upper panels*), anti-Slp2-a antibody (*lower panels*), and Texas Red®-X-conjugated phalloidin (*left panels*). Nuclei were stained with DAPI (*right panels*, merged image with Rab27A or Slp2-a). Confocal xy sections of lumens are shown. *Scale bars*, 10 μm

2. One day before the experiment, thaw a BD Matrigel matrix aliquot overnight at 4 °C (*see* **Note 4**) and keep it on ice until used.

3. Set autoclaved 12-mm diameter round microscope cover-glasses in a 12-well cell culture plate, and keep the plate on ice. Place 50 μL of the BD Matrigel matrix on each coverglass with wide bore cell-saver tips, and spread to cover the entire surface of the coverglass. Allow the plate to stand at 37 °C for 30 min (*see* **Note 9**).

4. Prepare an MDCK II cell suspension by trypsinizing the cells and resuspending them in MDCK II culture medium at 0.4×10^4 cells/mL with 20 μL of the BD Matrigel matrix for each mL of the cell suspension (final 2 % BD Matrigel matrix) (*see* **Note 8**).

5. Add 1 mL of the cell suspension (0.4×10^4 cells of MDCK II cells) to each well and incubate the cells at 37 °C under 5 % CO_2.

6. 60 h after plating, fix the MDCK II cysts with 500 μL of 4 % PFA for 30 min at room temperature. Gently change the buffer with pipettes and perform all of the following steps at room temperature.

7. Wash the MDCK II cysts three times with 1 mL of PBS each time.

8. Permeabilize the MDCK II cysts with 500 μL of 0.3 % Triton X-100 in PBS for 30 min.

9. Wash the MDCK II cysts three times with 1 mL of PBS each time.

10. Block with 500 μL of blocking buffer for 30 min.

11. Incubate the MDCK II cysts overnight at 4 °C in 500 μL of Can Get Signal® Immunoreaction Enhancer Solution containing anti-Slp2-a-SHD rabbit polyclonal antibody (20 μg/mL) or anti-Rab27A rabbit polyclonal antibody (30 μg/mL).

12. Wash the MDCK II cysts three times with 1 mL of PBS each time.

13. Incubate the MDCK II cysts for 2 h in 500 μL of Can Get Signal® Immunoreaction Enhancer Solution containing Alexa Fluor® 488-conjugated anti-rabbit antibody (1/5,000 dilution) under light-protected conditions. Perform all of the following steps under light-protected conditions.

14. Wash the MDCK II cysts three times with 1 mL of PBS each time.

15. Incubate the MDCK II cysts for 2 h in 500 μL of PBS containing Texas Red®-X-conjugated phalloidin (1/100 dilution) (*see* **Note 10**).

16. Wash the MDCK II cysts three times with 1 mL of PBS each time.

17. Incubate the MDCK II cysts for 30 min in 500 μL of PBS containing 0.25 mg of DAPI.

18. Wash the MDCK II cysts three times with 1 mL of PBS each time.

19. Turn the MDCK II cysts on the microscope coverglass upside down, and mount them on a microscope slide with Fluoromount/Plus™.

20. Capture fluorescence images of endogenous Slp2-a and endogenous Rab27A in the MDCK II cysts under a confocal fluorescence microscope (representative images are shown in Fig. 2c).

3.3 Immunohisto-chemical Analysis of Slp2-a and Rab27A in Mouse Kidney

1. Sacrifice a male mouse and remove the kidneys at room temperature.

2. Wash the kidneys once with 50 mL of PBS in a 100-mL beaker.

3. Fix the kidneys with 50 mL of 4 % PFA in a 100-mL beaker for 16 h at room temperature.

4. Wash the kidneys three times with 50 mL of PBS in a 100-mL beaker each time.

5. Equilibrate the kidneys in 50 mL of pre-cooled 10 % sucrose solution in a 100-mL beaker at 4 °C for 8 h, and then in 50 mL of pre-cooled 20 % sucrose solution in a 100-mL beaker overnight at 4 °C (*see* **Note 11**).

6. Embed the kidneys in Tissue-Tek O.C.T. compound for 1 h, freeze with liquid nitrogen, and store at –80 °C until used.

7. Cut the frozen kidneys into 10-μm sections with a cryostat and transfer them to microscope slides (*see* **Note 12**).

8. Permeabilize the sections with 100 mL of 0.3 % Triton X-100 in a glass container for 1 h at room temperature (*see* **Note 13**).

9. Wash the sections three times with 100 mL of PBS in a glass container each time.

10. Block with 150 μL of blocking buffer for 1 h at room temperature in a humid chamber.

11. Incubate the sections overnight at 4 °C in 150 μL of blocking buffer containing anti-Slp2-a-SHD rabbit polyclonal antibody (8 μg/mL) and anti-Rab27A mouse monoclonal antibody (1/100 dilution) in a humid chamber.

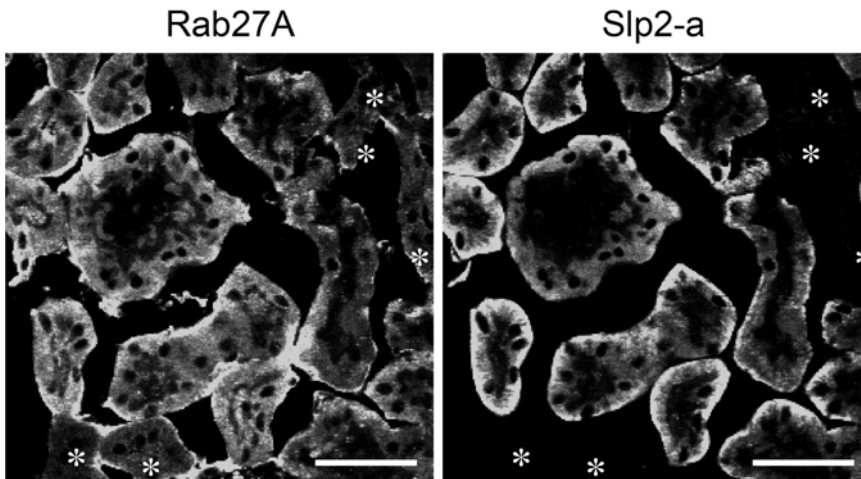12. Wash the sections three times with 100 mL of PBS in a glass container each time.

Fig. 3 Expression of Rab27A and Slp2-a in mouse kidney. The kidneys of DBA/2JJcl male mice were stained with anti-Rab27A antibody (*left panel*) and anti-Slp2-a antibody (*right panel*). Rab27A was expressed in all segments of the renal tubules and in the glomeruli, whereas Slp2-a was expressed in the renal proximal tubules and in the glomeruli alone. The *asterisks* indicate the sites that are Rab27A-positive but Slp2-a-negative. *Scale bars*, 50 μm

13. Incubate the sections for 2 h at room temperature in blocking buffer containing secondary antibodies (Alexa Fluor® 488-conjugated anti-rabbit antibody, 1/5,000 dilution, and Alexa Fluor® 594-conjugated anti-mouse antibody, 1/5,000 dilution) in a humid chamber under light-protected conditions. Perform all of the following steps under light-protected conditions.

14. Wash the sections three times with 100 mL of PBS in a glass container each time.

15. Mount a microscope coverglass on the sections with Fluoromount/Plus™.

16. Capture fluorescence images of endogenous Slp2-a and Rab27A in the kidneys under a confocal fluorescence microscope (representative images are shown in Fig. 3).

4   Notes

1. Many MDCK strains have been reported in the literature [23]. We recommend using an MDCK II strain for the assays described here, because the MDCK II cell line is the most commonly used strain, and the cells are larger and taller than MDCK I cells, making it easier to observe the subcellular localization of specific proteins in polarized cells.

2. To subculture MDCK II cells, the cells are treated with 0.125 % trypsin-EDTA in PBS (a higher trypsin concentration is required than to subculture most cell types) at 37 °C for 10 min. Once MDCK II cells have become confluent, it is difficult to dissociate them from the culture dish under the above conditions, and the MDCK II cells are instead incubated with 0.125 % trypsin-EDTA for a longer period (~15 min) to completely detach them from the culture dish.

3. The beads are handled with wide bore cell-saver tips to avoid damaging them.

4. BD Matrigel matrix should be reconstituted, aliquoted, and stored at –20 °C beforehand. Avoid multiple freeze-thaws. Use pre-cooled pipettes, tips, and tubes when preparing BD Matrigel matrix on coverglasses.

5. Because the level of endogenous Slp2-a expression in subconfluent, non-polarized MDCK II cells (Fig. 1a) is too low to detect with our anti-Slp2-a antibody, exogenous expression of EGFP-tagged Slp2-a is required to observe the localization of Slp2-a in a single MDCK II cell.

6. Because MDCK II cells tend to attach to each other, small numbers of MDCK II cells must be seeded in order to be able to observe the cells at the single cell level.

7. If specific immunoreactive signals are not obtained by the 4 % PFA fixation method, 10 % TCA in ultrapure water may be used to fix the cells.

8. Since cell density affects single lumen formation, MDCK II cells should be plated at a low density [24].

9. BD Matrigel matrix will gel rapidly at 22–35 °C.

10. TCA fixation should be avoided if phalloidin staining is going to be performed.

11. The kidneys float on the sucrose solution at first, and then gradually sink to the bottom of the solution.

12. Sections can be stored at –80 °C for several weeks.

13. Do not shake the microscope slides, because shaking them may cause the sections to detach from the microscope slides.

Acknowledgments

References

1. Rodriguez-Boulan E, Kreitzer G, Müsch A (2005) Organization of vesicular trafficking in epithelia. Nat Rev Mol Cell Biol 6:233–247

2. Rodríguez-Fraticelli AE, Gálvez-Santisteban M, Martín-Belmonte F (2011) Divide and polarize: recent advances in the molecular mechanism regulating epithelial tubulogenesis. Curr Opin Cell Biol 23:638–646

3. Fukuda M (2008) Regulation of secretory vesicle traffic by Rab small GTPases. Cell Mol Life Sci 65:2801–2813

4. Hutagalung AH, Novick PJ (2011) Role of Rab GTPases in membrane traffic and cell physiology. Physiol Rev 91:119–149

5. Stenmark H (2009) Rab GTPases as coordinators of vesicle traffic. Nat Rev Mol Cell Biol 10:513–525

6. Yasuda T, Saegusa C, Kamakura S, Sumimoto H, Fukuda M (2012) Rab27 effector Slp2-a transports the apical signaling molecule podocalyxin to the apical surface of MDCK II cells and regulates claudin-2 expression. Mol Biol Cell 23:3229–3239

7. Gálvez-Santisteban M, Rodriguez-Fraticelli AE, Bryant DM, Vergarajauregui S, Yasuda T, Bañón-Rodríguez I, Bernascone I, Datta A, Spivak N, Young K, Slim CL, Brakeman PR, Fukuda M, Mostov KE, Martín-Belmonte F (2012) Synaptotagmin-like proteins control the formation of a single apical membrane domain in epithelial cells. Nat Cell Biol 14:838–849

8. Fukuda M, Mikoshiba K (2001) Synaptotagmin-like protein 1–3: a novel family of C-terminal-type tandem C2 proteins. Biochem Biophys Res Commun 281:1226–1233

9. Fukuda M, Saegusa C, Mikoshiba K (2001) Novel splicing isoforms of synaptotagmin-like proteins 2 and 3: identification of the Slp homology domain. Biochem Biophys Res Commun 283:513–519

10. Kuroda TS, Fukuda M, Ariga H, Mikoshiba K (2002) The Slp homology domain of synaptotagmin-like proteins 1–4 and Slac2 functions as a novel Rab27A binding domain. J Biol Chem 277:9212–9218

11. Fukuda M (2006) Rab27 and its effectors in secretory granule exocytosis: a novel docking machinery composed of a Rab27·effector complex. Biochem Soc Trans 34:691–695

12. Fukuda M (2013) Rab27 effectors, pleiotropic regulators in secretory pathways. Traffic 14:949–963

13. Kuroda TS, Fukuda M (2004) Rab27A-binding protein Slp2-a is required for periph-eral melanosome distribution and elongated cell shape in melanocytes. Nat Cell Biol 6:1195–1203

14. Fukuda M (2005) Versatile role of Rab27 in membrane trafficking: focus on the Rab27 effector families. J Biochem 137:9–16

15. Saegusa C, Tanaka T, Tani S, Itohara S, Mikoshiba K, Fukuda M (2006) Decreased basal mucus secretion by Slp2-a-deficient gastric surface mucous cells. Genes Cells 11:623–631

16. Yu M, Kasai K, Nagashima K, Torii S, Yokota-Hashimoto H, Okamoto K, Takeuchi T, Gomi H, Izumi T (2007) Exophilin4/Slp2-a targets glucagon granules to the plasma membrane through unique Ca^{2+}-inhibitory phospholipid-binding activity of the C2A domain. Mol Biol Cell 18:688–696

17. Holt O, Kanno E, Bossi G, Booth S, Daniele T, Santoro A, Arico M, Saegusa C, Fukuda M, Griffiths GM (2008) Slp1 and Slp2-a localize to the plasma membrane of CTL and contribute to secretion from the immunological synapse. Traffic 9:446–457

18. Ménasché G, Ménager MM, Lefebvre JM, Deutsch E, Athman R, Lambert N, Mahlaoui N, Court M, Garin J, Fischer A, de Saint Basile G (2008) A newly identified isoform of Slp2a associates with Rab27a in cytotoxic T cells and participates to cytotoxic granule secretion. Blood 112:5052–5062

19. Yasuda T, Fukuda M (2014) Slp2-a controls renal epithelial cell size through regulation of Rap—ezrin signaling independently of Rab27. J Cell Sci 127:557–570

20. Kuroda TS, Itoh T, Fukuda M (2005) Functional analysis of Slac2-a/melaonophilin as a linker protein between Rab27A and myosin Va in melanosome transport. Methods Enzymol 403:419–431

21. Fukuda M, Kanno E (2005) Analysis of the role of Rab27 effector Slp4-a/granuphilin-a in dense-core vesicle exocytosis. Methods Enzymol 403:445–457

22. Imai A, Yoshie S, Nashida T, Shimomura H, Fukuda M (2004) The small GTPase Rab27B regulates amylase release from rat parotid acinar cells. J Cell Sci 117:1945–1953

23. Dukes JD, Whitley P, Chalmers AD (2011) The MDCK variety pack: choosing the right strain. BMC Cell Biol 12:1–4

24. Martín-Belmonte F, Yu W, Rodríguez-Fraticelli AE, Ewald A, Werb Z, Alonso MA, Mostov K (2008) Cell-polarity dynamics controls the mechanism of lumen formation in epithelial morphogenesis. Curr Biol 18:507–513

Chapter 12

Small GTPases in Acrosomal Exocytosis

Matias A. Bustos, Ornella Lucchesi, Maria C. Ruete, Luis S. Mayorga, and Claudia N. Tomes

Abstract

Regulated exocytosis employs a conserved molecular machinery in all secretory cells. Soluble *N*-ethylmaleimide-sensitive factor attachment protein receptor (SNARE) and Rab superfamilies are members of this machinery. Rab proteins are small GTPases that organize membrane microdomains on organelles by recruiting specific effectors that strongly influence the movement, fusion and fission dynamics of intracellular compartments. Rab3 and Rab27 are the prevalent exocytotic isoforms. Many events occur in mammalian spermatozoa before they can fertilize the egg, one of them is the acrosome reaction (AR), a type of regulated exocytosis. The AR relies on the same fusion machinery as all other cell types, which includes members of the exocytotic SNARE and Rab superfamilies. Here, we describe in depth two protocols designed to determine the activation status of small G proteins. One of them also serves to determine the subcellular localization of active Rabs, something not achievable with other methods. By means of these techniques, we have reported that Rab27 and Rab3 act sequentially and are organized in a RabGEF cascade during the AR. Although we developed them to scrutinize the exocytosis of the acrosome in human sperm, the protocols can potentially be extended to study other Ras-related proteins in virtually any cellular model.

Key words Acrosome reaction, Exocytosis, Rab27, Rab3, Sperm

1 Introduction

Secretion of vesicles is orchestrated by a complex molecular machinery conserved among all cells and organisms [1, 2]. The proteinaceous machinery involved in this process includes members of SNARE and Rab superfamilies and their interacting and regulatory proteins [2–5]. During regulated exocytosis, secretory Rabs play an essential role recruiting tethering and docking factors required for membrane recognition and fusion [6]. These small GTPases act as molecular "on/off" switches cycling between inactive (GDP-bound) and active (GTP-bound) states [3, 6]. Two kinds of proteins regulate the GDP-GTP cycling, guanine nucleotide exchange factors (GEFs), and GTPase-activating proteins (GAPs). These proteins control not only the activity of small GTPases but also their association/dissociation to/from membranes, both critical

for the proper functioning of Rab proteins. GEF stimulates the exchange of GDP for GTP, generating the activated form of Rab. Rab-GTP interacts with effector proteins responsible for tethering/docking of compartments that are going to fuse [3, 7]. Once Rab has exerted its function, GAP enhances the hydrolysis of the bound GTP to GDP, inactivating Rab. Subsequently, Rab-GDP dissociates from membranes and remains in a cytosolic pool complexed with a GDP dissociation inhibitor (GDI [3, 8]).

Regulated exocytosis consists of multiple steps that lead to the fusion of secretory vesicles with the plasma membrane in response to stimuli. The AR is a calcium-triggered exocytotic process fundamental for fertilization. In this event, sperm's single secretory granule or acrosome fuses with the plasma membrane and releases its contents to the extracellular medium. Release takes place after a complex signaling pathway, invoked by an increase in intracellular calcium, activates the fusion machinery [9–18]. The AR constitutes a straightforward model for regulated exocytosis because there are no interferences due to endocytosis or other types of intracellular transport. Sperm neither transcribe nor translate, so overexpression and silencing RNA technologies to study the role of proteins in exocytosis are not applicable to these cells. To overcome these limitations, we have set up two strategies: (1) a controlled plasma membrane permeabilization protocol with streptolysin O (SLO) or perfringolysin O (PFO) and (2) the delivery of permeable proteins into living cells [19–21].

Rab3A/B/C/D, Rab27A/B, Rab26, and Rab37 are present in a variety of secretory vesicles and modulate their release [8]. We focus here on the roles of Rab3 and Rab27 in the AR. We describe an assay that pulls down active Rabs from whole cell detergent extracts based on their interaction with immobilized protein cassettes (activity probes) that bind specifically Rabs-GTP. Thanks to this assay, we learnt that Rabs are activated in human sperm in response to exocytosis stimuli [22–24, 26]. This assay provides information about the activation state, but tells nothing about the subcellular localization or the number of cells with active Rabs. To address these issues, we developed a technique based on protein–protein interaction and indirect immunofluorescence principles (referred to as far-immunofluorescence [23]). The method consists of overlying sperm smeared on coverslips with the same GST-tagged activity probes used in pull-down assays and later visualizing the binding sites with an anti-GST antibody. The protocol is applicable to permeabilized [23, 25] and non-permeabilized [24] sperm and allowed us to determine that Rabs were activated in the acrosomal region of subpopulations of sperm challenged to undergo the AR. Thanks to this protocol, we also made the unexpected observation that introduction of recombinant Rab27A-GTP into sperm was sufficient to activate endogenous Rab3. We will devote the last part of this chapter to describe a protocol that allowed us to explain these findings and demonstrate that Rab3 and Rab27 act

through a RabGEF cascade during the AR, in which active Rab27A recruits, directly or indirectly, a Rab3A GEF activity [23].

The protocols that we describe here were applied to study Rabs in human sperm exocytosis but they could be extended to scrutinize different biological phenomena in other sperm species or cells types. Moreover, they can be used to analyze other Ras-related proteins. For instance, we applied pull-down [22] and far-immunofluorescence [25] to study the role of Rap during human sperm AR.

2 Materials

2.1 Reagents

Use ultrapure (electrical resistivity 18 MΩ cm at 25 °C) water to dilute all reagents. Utilize analytical grade reagents and follow all of your Institution's disposal regulations when discarding waste materials.

2.1.1 SLO Stock Solutions (See Note 1)

1. Resuspend lyophilized SLO in 20 mM HEPES/K, pH 7, 20 % glycerol, and 0.01 % bovine serum albumin (BSA) to 25,000 UI/ml, aliquot and store at –80 °C. Avoid repeated freezing/thawing.

2. Prepare an SLO 300 UI/ml stock solution (*see* **Note 2**) by diluting 6 μl of 25,000 UI/ml SLO in 500 μl phosphate buffer saline (PBS, 2.5.3) containing 20 % glycerol and 0.01 % BSA. Aliquot and store at –20 °C if you will use it within a month; otherwise store at –80 °C.

2.2 Plasmids

1. *His$_6$-Rab3A*. The cDNA encoding a membrane-permeant version of human Rab3A bearing a Q81L point mutation and subcloned into pQE80L plasmid [20] was generously provided by C. López (University of Cuyo, Mendoza, Argentina).

2. *His$_6$-Rab27A*. The cDNA encoding human Rab27A was subcloned into pET28 plasmid by GenScript Inc. (Piscataway, NJ, USA).

3. *GST-Rab27A*. The cDNA encoding human Rab27A in pGEX-6p was a kind gift from D. Munafó (Scripps Research Institute, La Jolla, CA, USA).

4. *GST-RIM-RBD*. The cDNA encoding the Rab3-binding domain of rat RIM 1α (amino acids 11–398; RIM-RBD) [27] in pGEX-KG was generously provided by R. Regazzi (University of Lausanne, Lausanne, Switzerland).

5. *GST-Slac2-b-SHD*. The cDNA encoding the Rab27-GTP-binding domain of Slac2-b (Synaptotagmin-like protein homology lacking C2 domains-b; amino acids 1–79) [28] in pGEX-2T was a kind gift from R. Shirakawa (Kyoto University, Kyoto, Japan).

6. *GST*. The cDNA encoding GST was from an empty pGEX-2T vector.

2.3 Recombinant Proteins

2.3.1 Expression and Purification of GST-Fused Proteins

1. Competent *E. coli* BL21 were transformed with plasmids carrying the cDNAs encoding GST or GST-fused proteins following standard procedures.

2. Induce expression of GST and GST-Slac2-b-SHD with 0.5 mM isopropyl-β-D-thio-galactoside (IPTG) for 3 h at 37 °C; GST-RIM-RBD with 0.5 mM IPTG, overnight at 22 °C; and GST-Rab27A with 1 mM IPTG, 3 h at 37 °C.

3. Purify GST-fused proteins under native conditions on glutathione-Sepharose beads following standard procedures. The purification buffers contain 100 mM Tris–HCl, pH 7.4, 120 mM NaCl (lysis and washing buffer) and 100 mM Tris–HCl, pH 7.4, 120 mM NaCl, 20 mM reduced glutathione (elution buffer). For pull-down assays, bacterial lysates (containing 5–10 μg/ml GST-Slac2-b-SHD or GST-RIM-RBD) are frozen at –80 °C until use.

2.3.2 Expression and Purification of His_6-Tagged Proteins

1. Transform the cDNAs encoding His_6-Rab27A and His_6-Rab3A into *E. coli* BLR(DE3) made chemically competent.

2. Induce expression with 0.5 mM IPTG for 3 h at 37 °C for His_6-Rab27A and overnight at 22 °C for His_6-Rab3A.

3. Purify His_6-tagged proteins under native conditions on Ni^{2+}-NTA-agarose beads following standard protocols. The purification buffers contain 20 mM Tris–HCl, pH 7.4, 300 mM NaCl, 8–10 mM imidazole (lysis buffer), 20 mM imidazole (washing buffer), and 250 mM imidazole (elution buffer).

2.4 Antibodies

1. Rabbit polyclonal anti-Rab27 and anti-α-tubulin (affinity purified with the immunogens) antibodies and mouse monoclonal anti-Rab3A (clone 42.2, IgG affinity-purified on protein A-Sepharose, subtype IgG2b) were from Synaptic Systems (Goettingen, Germany).

2. Rabbit polyclonal anti-GST antibody (purified IgG) was from EMD Millipore (Billerica, MA, USA).

3. HRP-conjugated goat anti-rabbit and Cy™3-conjugated donkey anti-rabbit IgGs (H+L) were from Jackson ImmunoResearch (West Grove, PA, USA).

4. HRP-conjugated goat anti-mouse IgG (H+L) was from Kirkegaard & Perry Laboratories Inc. (Gaithersburg, MD, USA).

2.5 Buffers

1. *Human Tubal Fluid medium (HTF)*. Dissolve reagents (97.8 mM NaCl, 4.69 mM KCl, 0.20 mM $MgSO_4$, 0.37 mM KH_2PO_4, 2.04 mM $CaCl_2$, 25 mM $NaHCO_3$, 2.7 mM D-glucose, 0.33 mM Na pyruvate, 21.4 mM Na lactate, 0.06 g/l penicillin, 0.05 g/l streptomycin, and 0.01 g/l phenol red) in water at room temperature with constant stirring and bring to final volume (*see* **Note 3**). Before using, place an aliquot in a CO_2 incubator overnight to buffer; the media will turn

reddish-orange (*see* **Note 4**). HTF medium is also commercially available.

2. *HTF/BSA medium.* Supplement HTF medium, previously buffered overnight in 5 % CO_2/95 % air incubator, with 0.5 mg/ml BSA.

3. *Phosphate buffer saline* (*PBS*). Dissolve reagents (137 mM NaCl, 2.7 mM KCl, 10 mM Na_2HPO_4 and 1.8 mM KH_2PO_4) in water at room temperature with constant stirring. Adjust pH to 7.4 with 1 N NaOH and bring to final volume. Filter-sterilize and store at 4 °C. PBS is commercially available in a variety of presentations.

4. *HB-EGTA* (*permeabilization buffer*). Dissolve reagents (20 mM HEPES free acid, 250 mM sucrose, and 0.5 mM EGTA) in water at room temperature with constant stirring. Adjust pH to 7 with 1 N KOH and bring to final volume. Filter-sterilize and store at 4 °C for up to a month.

5. *Pull-down buffer.* Dilute reagents (50 mM Tris–HCl, pH 7.4, 200 mM NaCl, 2.5 mM $MgCl_2$, 1 % (v/v) Igepal, 10 % (v/v) glycerol) in water from stock solutions by vortexing vigorously at room temperature. Adjust pH to 7.4, bring to final volume, and store at 4 °C. Add protease inhibitors (2 mM AEBSF, 0.3 μM aprotinin, 116 μM bestatin, 14 μM E-64, 1 μM leupeptin, 1 mM EDTA, and 1 mM PMSF) right before using.

6. *Binding buffer.* Dilute reagents (20 mM HEPES/K, pH 7.4, 150 mM K acetate 15 mM $MgCl_2$, 0.05 % (v/v) Tween 20, 5 μM GTP) in water from stock solutions at room temperature by vortexing. Adjust pH to 7.4, bring to final volume, and store at 4 °C until used. Add protease inhibitors (2 mM AEBSF, 0.3 μM aprotinin, 116 μM bestatin, 14 μM E-64, 1 μM leupeptin, 1 mM EDTA, and 1 mM PMSF) right before using.

7. *Lysis buffer.* Dilute reagents (50 mM Tris–HCl, pH 7.4, 150 mM NaCl, 5 mM $MgCl_2$, 1 % (v/v) Triton X-100 (TX-100), 10 % (v/v) glycerol) in water from stock solutions at room temperature by vortexing. Adjust pH to 7.4, bring to final volume, and store at 4 °C until used. Add protease inhibitors (2 mM AEBSF, 0.3 μM aprotinin, 116 μM bestatin, 14 μM E-64, 1 μM leupeptin, 1 mM EDTA, and 1 mM PMSF) right before using.

3   Methods

3.1   Human Sperm Samples

3.1.1   Sample Collection

1. Volunteer healthy donors, with at least 48 h of abstinence, should collect semen samples in containers (*see* **Note 5**).

2. Place the specimen container at 37 °C in an incubator until the semen liquefies (30 min to 1 h).

3. Assess semen quality after liquefaction (*see* **Note 6**).

3.1.2 Swim-Up
(See Note 7*)*
and Capacitation
(See Note 8*)*

1. Place 800 μl of HTF/BSA medium in 5 ml polypropylene tubes (12×75 mm).

2. Layer carefully 300 μl of liquefied semen under the medium at the bottom of the tube (*see* **Note 9**).

3. Place tubes at a 45° angle, in order to increase the area of the semen-medium interface and incubate for 1 h at 37 °C in a 5 % CO_2/95 % air incubator.

4. Return the tubes gently to the upright position and carefully remove the uppermost 600–700 μl of medium without disturbing the interface. This fraction is enriched in highly motile sperm.

5. Mix well and assess sperm concentration in a Makler Counting Chamber (SEFI Medical Instruments LTD. Distributed by Irvine Scientific, CA, USA; *see* **Note 10**).

6. Dilute sperm to $10×10^6$ cells/ml in HTF/BSA medium.

7. Incubate the sperm suspensions in HTF/BSA medium for at least 3 h at 37 °C in a 5 % CO_2/95 % air incubator to promote capacitation.

3.1.3 SLO-Permeabilization

1. Wash capacitated sperm twice with one volume each of ice-cold PBS.

2. Resuspend the pellet in one volume of ice-cold PBS by pipetting gently.

3. Count and adjust sperm concentration to $7–10×10^6$/ml.

4. Add SLO (0.4 to 4 U/ml) and incubate for 15 min at 4 °C (s*ee* **Note 11**).

5. Wash once with one volume of ice-cold PBS to remove unbound toxin.

6. Resuspend the pellet in one volume of ice-cold HB-EGTA containing 2 mM dithiotreitol (DTT, *see* **Note 12**) by pipetting gently.

3.2   In Vitro Solid Phase Isoprenylation and Activation of Rab Proteins

Native Rab proteins are geranylgeranylated, presumably to localize to membranes where they participate in signal transduction networks. These proteins bind magnesium ions and guanine nucleotides (GDP in their inactive state or GTP in their active state) to execute their functions. Because bacteria do not isoprenylate, we geranylgeranylate Rabs expressed in *E. coli* and load them with guanine nucleotides in vitro to make them functional.

3.2.1 Geranylgeranylation Mixture

To prepare 2× isoprenylation mixture (*see* **Note 13**):

1. Dilute reagents (40 mM HEPES/K, pH 7.5, 2 μg/μl mouse brain cytosol, 160 μM geranylgeranyl pyrophosphate (GGPP), 400 μM GDP, 2 mM DTT, 2 mg/ml BSA, 6 mM $MgCl_2$, 4 mM AEBSF, 0.6 μM aprotinin, 260 mM bestatin, 232 μM

bestatin, 28 μM E-64, 2 μM leupeptin and 2 mM EDTA) in water from stock solutions.

2. Keep mixture on ice until use.

3.2.2 Immobilization of Recombinant Rabs

1. Incubate 1 ml bacterial lysates (containing GST/His$_6$-Rab proteins) with 100 μl of glutathione-Sepharose beads (GST) or 100 μl Ni^{2+}-NTA-agarose beads (His$_6$) for 1 h a 4 °C.

2. Wash the beads three times (1 ml each) with GST/His$_6$-washing buffer.

3. Quantify Rabs bound to beads and estimate their purity by boiling a small aliquot of the immobilized material in sample buffer and analyzing by SDS-PAGE.

4. Stain gels with Coommassie brilliant blue R-250 following standard procedures.

3.2.3 Solid Phase Isoprenylation Protocol

1. Incubate 100 μl of 10–20 μM immobilized Rab (as described under Immobilization of Recombinant Rabs) with 100 μl of 2× geranylgeranylation mixture for 2 h at 37 °C with constant rocking.

2. Add four volumes of GST/His$_6$-washing buffer and incubate during 30 min at 4 °C with constant rocking (*see* **Note 14**).

3. Wash the beads three times (1 ml each) with GST/His$_6$-washing buffer.

4. Elute geranylgeranylated Rabs with 50 μl GST/His$_6$-elution buffer.

3.2.4 Loading Rabs with Guanine Nucleotides

To prepare 50 μl of loaded-Rabs (10 μM final concentration):

1. Incubate 10 μM purified geranylgeranylated Rab (as described under Solid Phase Isoprenylation Protocol) with 5 μl activation buffer (50 mM HEPES/K, pH 7.2, 5 mM MgCl$_2$, 0.03 % Igepal or Nonidet-P40, 1 mM DTT and 25 mM EDTA) and 125 μM guanosine 5′-(β-thio)-diphosphate (GDP-β-S), guanosine 5′-(γ-thio) triphosphate (GTP-γ-S) or GDP in a final volume of 50 μl for 1 h at 37 °C (*see* **Note 15**).

2. Prepare a Sephadex G25 (pre-hydrated in PBS) column in a 200 μl tip.

3. Wash the mini column three times (one volume each) with 0.1 % BSA in PBS by centrifugation at 1,100×*g* for 2 min at room temperature.

4. Run 50 μl of nucleotide-bound Rab through the Sephadex G25 column (*see* **Note 16**).

5. Recover the protein in the void volume by centrifugation at 1,100×*g* for 2 min at room temperature.

6. Add MgCl$_2$ to 1 mM final concentration (*see* **Note 17**).

7. Aliquot and store at –20 °C for up to a month (*see* **Note 18**).

3.3 Far-Immunofluorescence: Description of a New Method to Detect the Localization of Active Rabs

Cells subjected to different experimental conditions are smeared on coverslips, fixed, permeabilized, and overlaid with activity probes. These are protein cassettes derived from effectors that contain their cognate Rab-GTP binding domains (e.g. GST-RIM-RBD). Because cassettes are GST-tagged (GST) their binding to endogenous targets (e.g. Rab3) is revealed by conventional indirect immunofluorescence with anti-GST (anti-GST) antibodies followed by fluorescently labeled secondary antibodies (anti-rabbit-Cy3; Fig. 1).

3.3.1 Far-Immunofluorescence Protocol

1. Wash 12 mm round coverslips with 96 % ethanol.

2. Flame coverslips and place them on a piece of parafilm, secured in the lid of a 24-well plate.

3. Add 80 μl of poly-L-lysine (dilute 1 μl of stock solution 0.1 % w/v in 20 μl of water) to each coverslip and incubate for 30 min at room temperature in a moisturized chamber (*see* **Note 19**).

4. Attach cell suspensions (treated as detailed in Subheading 3.3.2–3.3.4, *see below*) to poly-L-lysine coated coverslips for 30 min at room temperature in a moisturized chamber (Fig. 1).

5. Store cells in 100 mM glycine in PBS overnight at 4 °C in a moisturized chamber (*see* **Note 20**).

6. Permeabilize the plasma membrane with 0.1 % Triton X-100 (TX-100) for 10 min at room temperature.

7. Wash cells three times, 6 min each at room temperature, with 1 ml of PBS-0.1 % polyvinylpyrrolidone (PBS-PVP; average MW = 40,000).

8. Block non-specific reactivity with 50 μl of 5 % BSA in PBS-PVP for 1 h at 37 °C.

9. Overlay with 50 μl of 140 nM affinity-purified GST, GST-RIM-RBD, or GST-Slac2-b-SHD in 5 % BSA in PBS-PVP and incubate for 1 h at 37 °C (Fig. 1).

10. Wash cells three times, 6 min each at room temperature, with 1 ml PBS-PVP.

11. Add 25 μl of 210 nM (31.5 μg/ml) anti-GST in 3 % BSA in PBS-PVP and incubate for 1 h at 37 °C (Fig. 1).

12. Wash cells twice, 10 min each at room temperature, with 1 ml PBS-PVP.

13. Add 50 μl of 11 nM (1.67 μg/ml) Cy3-conjugated goat anti-rabbit IgG in 1 % BSA in PBS-PVP and incubate for 1 h at room temperature protected from light (Fig. 1).

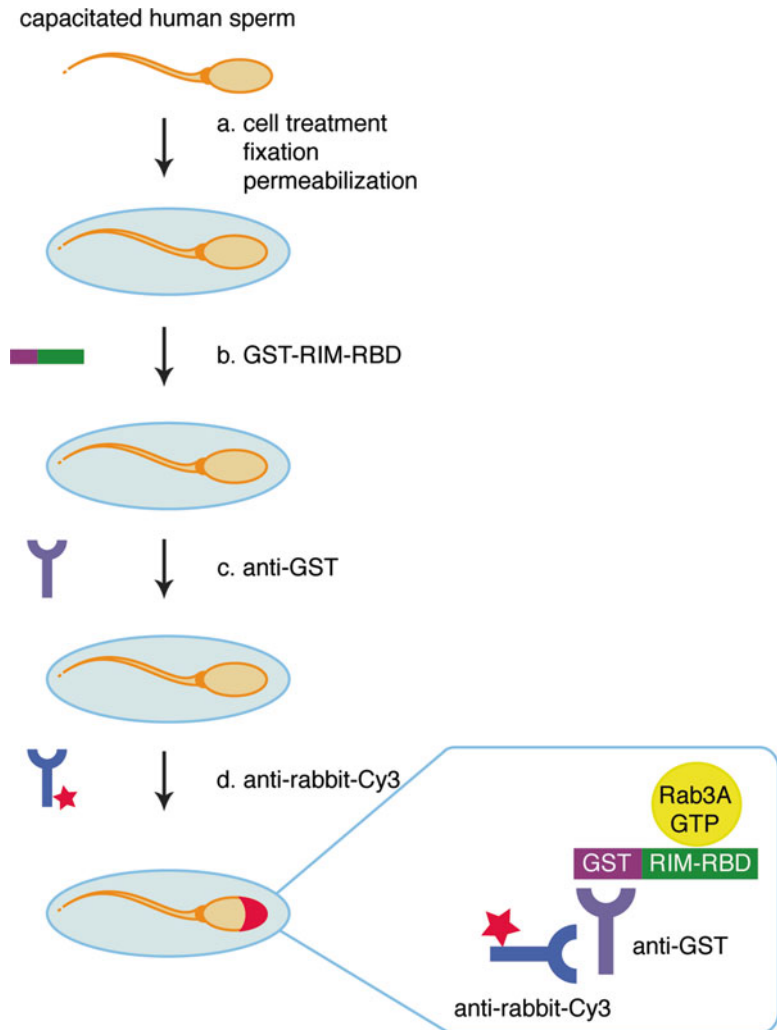14. Wash cells six times, 6 min each at room temperature, with 1 ml PBS-PVP.

Fig. 1 Schematic representation of the far-immunofluorescence protocol developed to detect GTP-bound Rab proteins. Cells are fixed, immobilized on poly-L-lysine coated coverslips and sperm membranes are permeabilized with TX-100 (**A**). Attached sperm are overlaid with protein domains that bind Rab proteins in their GTP state (shown here is GST-RIM-RBD cassette that interacts with Rab3-GTP, **B**). Sperm are incubated with an anti-GST antibody to detect the cassette bound to endogenous Rab3-GTP (**C**). Slides are exposed to a secondary Cy3-conjugated antibody (**D**) to detect anti-GST in the anti-GST/GST-RIM-RBD/Rab3-GTP complex (*inset*). Finally, cells are mounted and the percentage of sperm with acrosomal Rab3-GTP is scored by fluorescence microscopy. *Inset*: GST-RIM-RBD domain (*green/purple*) bound to Rab3-GTP (*yellow*) is recognized by the primary anti-GST antibody (*violet*), which is detected by a secondary Cy3-conjugated (*red star*) anti-rabbit antibody (*blue*)

15. Treat cells with ice-cold methanol for 20 s to permeabilize the acrosomal membrane.

16. Add 80 μl of 25 μg/ml fluorescein-isothiocyanate-coupled *Pisum sativum* agglutinin (FITC-PSA, *see* **Note 21**) to each coverslip and incubate for 40 min in the dark.

17. Wash cells three times, 6 min each at room temperature, with 1 ml PBS-PVP.

18. Mount the coverslips (with the cells attached) in a drop of 5 μl of 1 % propyl-gallate/50 % glycerol in PBS containing 2 μM Hoechst 33342 (*see* **Note 22**) placed on a slide.

19. Seal the edge of coverslips with clear nail polish and allow to dry.

20. Store at –20 °C in the dark until examination (*see* **Note 23**).

3.3.2 Sperm Treatment 1 for Standardization of Activity Probes Binding to Endogenous Active Rabs in Permeabilized Cells (Fig. 2a–d)

1. Add 50 μl (350,000–500,000 cells) of capacitated, SLO-permeabilized sperm in HB-EGTA to each tube.

2. Incubate with 100 μM 2-aminoethoxydiphenylborate (2-APB, *see* **Note 24**) and 5 mM EDTA/1 mM MgCl$_2$ (*see* **Note 25**) for 10 min at 37 °C.

3. Load cells with 40 μM GDP-β-S or GTP-γ-S during 10 min at 37 °C (Fig. 2a–d).

4. Incubate with 15 mM MgCl$_2$ during 5 min at 37 °C (*see* **Note 17**).

5. Incubate with 50 μl of 4 % paraformaldehyde during 15 min at room temperature to fix cell suspensions.

6. Wash fixed cells by centrifugation at $12,600 \times g$ for 2 min at room temperature.

7. Resuspend the pellet in 100 μl 100 mM glycine in PBS by gentle mixing and continue as described under Far-Immunofluorescence Protocol.

Fig. 2 (continued) but in only 6 % of sperm treated with GDP-β-S (**d**). Scale bars: 5 μm. (**e**) SLO-permeabilized human sperm treated as described under Far-Immunofluorescence Protocol (3.3.3) are overlaid with GST-Slac2-b-SHD to detect active Rab27 (**e**, *gray bars*) or GST-RIM-RBD to detect active Rab3 (**e**, *black bars*) and counted to score the percentage of cells immunodecorated in the acrosomal region by the anti-GST antibodies. The population of active Rabs increases upon incubation with GTP plus CaCl$_2$ compared with controls incubated with GDP (***$P < 0.001$). Note that by itself, GTP is unable to increase the number of cells depicting active Rabs compared with those treated with GDP (ns, non-statistically significant). Recombinant Rab27A augments the number of cells depicting endogenous Rab3A-GTP in the acrosomal region (ns, with respect to GTP/CaCl$_2$; ***$P < 0.001$, compared with GDP). The converse is not true; recombinant Rab3A does not influence the number of cells with active Rab27 in the head (ns compared with controls loaded with GDP). The Tukey–Kramer post hoc test was used for pairwise comparisons. The data represent mean $\pm$ SEM of at least three independent experiments [23]
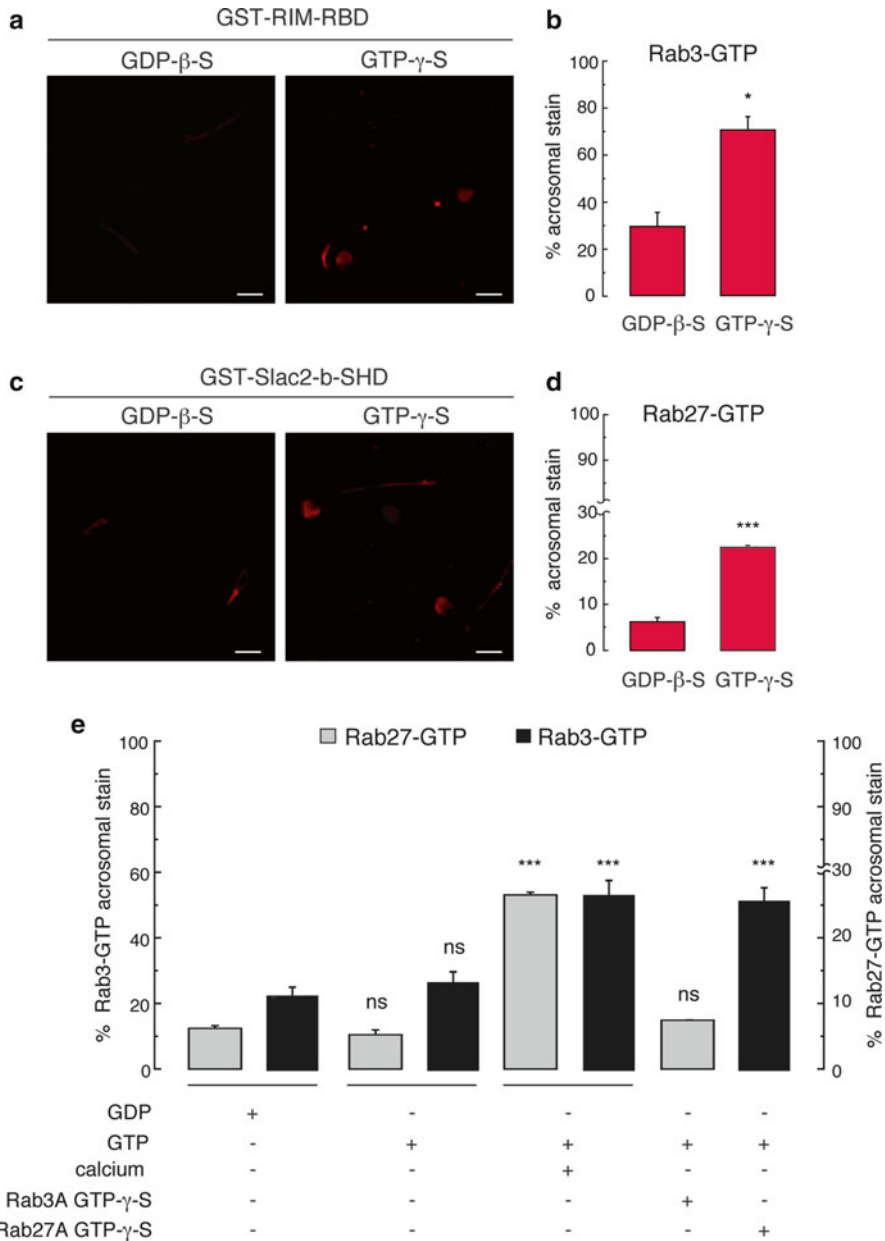
Fig. 2 Detection of nucleotide-binding status of endogenous Rab3 and Rab27. Capacitated, SLO-permeabilized sperm are treated as described under Far-immunofluorescence protocol. Cells are stained with an anti-GST antibody as readout for the activity probes that detect active Rab3 (**a**) and Rab27 (**c**). Quantifications (mean ± SEM of at least three independent experiments) of cells immunostained in the acrosomal region by the anti-GST antibodies are shown to the *right* (**b**, **d**). The activity probe GST-RIM-RBD binds to endogenous Rab3 in 70 % of the cells loaded with GTP-γ-S, whereas only 29 % of sperm treated with GDP-β-S give a detectable signal (**b**). Slac2-b-SHD binds the acrosomal region in 23 % of sperm treated with GTP-γ-S,

3.3.3   Sperm Treatment 2
for Analysis of Rab
Activation in Response
to Exogenous Stimuli
(Fig. 2e)

1. Add 50 μl (350,000–500,000 cells) of capacitated, SLO-permeabilized sperm in HB-EGTA to each tube.

2. Incubate with 100 μM 2-APB (*see* **Note 24**) and 5 mM EDTA/1 mM MgCl$_2$ (*see* **Note 25**) for 10 min at 37 °C.

3. Load cells with 40 μM GDP during 10 min at 37 °C (*see* **Note 26**).

4. Incubate with 15 mM MgCl$_2$ during 5 min at 37 °C (*see* **Note 17**).

5. Incubate the cells with: (1) 200 μM GTP, (2) 200 μM GTP plus 0.5 mM CaCl$_2$ (10 μM free calcium, *see* **Note 27**), (3) 200 μM GTP plus 300 nM geranylgeranylated His$_6$-Rab3A loaded with GTP-γ-S or (4) 200 μM GTP plus 300 nM geranylgeranylated His$_6$-Rab27A loaded with GTP-γ-S, for 15 min at 37 °C (Fig. 2e).

6. Continue as described in Subheading 3.3.2 (**steps 5–7**).

3.3.4   Sperm Treatment 3
for Analysis of Rab3-GTP
Levels After A23187
Treatment in Non-
permeabilized Cells [24]

1. Add 50 μl (350,000–500,000 cells) of capacitated sperm in HTF to each tube.

2. Incubate with 100 μM 2-APB (*see* **Note 24**) for 10 min at 37 °C.

3. Initiate the AR with 10 μM A23187 (*see* **Note 28**) incubating for 15 min at 37 °C.

4. Continue as described in Subheading 3.3.2 (**steps 5–7**).

3.4   Pull-Down
Assays for Active
Rab27 and Rab3

Immobilization of the activity probes

1. Wash glutathione-Sepharose beads twice with one volume each of pull-down buffer and recover by centrifugation at 1,100×*g* for 2 min at 4 °C.

2. Incubate 60–90 μl washed beads with 1 ml of bacterial lysates containing GST-Slac2-b-SHD or GST-RIM-RBD for 1 h at 4 °C under constant rocking.

3. Wash the beads twice with one volume each of ice-cold PBS and once with one volume of ice-cold pull-down buffer by centrifugation at 1,100×*g* for 2 min at 4 °C.

4. Recover the GST-Slac2-b-SHD or GST-RIM-RBD bound-beads by centrifugation at 1,100×*g* for 2 min 4 °C and continue immediately (as described under Subheading 3.4.2, *see below*).

3.4.1   Preparation
of Human Sperm Lysates

1. Wash 5 ml of capacitated sperm (50×10^6 cells) twice with ice-cold PBS by centrifugation at 6,200×*g* for 2 min at room temperature.

2. Resuspend the pellet in 1 ml HTF medium and incubate with 100 μM 2-APB (*see* **Note 24**) for 10 min at 37 °C.

3. Challenge cells with 10 μM A23187 (*see* **Note 28**) for 15 min at 37 °C.

4. Spin down cells by centrifugation at $12,600 \times g$ for 5 min at 4 °C.

5. Resuspend the pellet in 1 ml ice-cold pull-down buffer.

6. Lyse the cells by sonication at 40 Hz twice for 15 s each, with a 10 s interval, keeping them on ice at all times.

7. Extract proteins by incubation for 15 min at 4 °C.

8. Clarify the whole cell detergent extracts by centrifugation at $14,000 \times g$ for 5 min at 4 °C and use immediately (continue as described under Subheading 3.4.2).

3.4.2 Pull-Down Assay

1. Add 20–30 μl of glutathione-Sepharose containing 5–10 μg GST-Slac2-b-SHD or GST-RIM-RBD to 1 ml ($20–50 \times 10^6$ cell) whole cell extracts prepared from sperm treated or not with A23187.

2. Incubate the mixtures for 30 min at 4 °C under constant rocking.

3. Wash the beads three times with one volume each of ice-cold pull-down buffer at $1,100 \times g$ for 2 min at 4 °C.

4. Dissolve resin-bound proteins by boiling in 60 μl of sample buffer for 3 min at 95 °C.

5. Analyze Rab27-GTP and Rab3A-GTP levels by Western blot using anti-Rab27 and anti-Rab3 antibodies as probes.

3.5 Recruitment of a Human Sperm Rab3A GEF Activity by Immobilized Rab27A

Rab27-GTP (indirectly) activates sperm Rab3 (Fig. 2e and [23]). The following section summarizes the method we designed to unveil the mechanism behind the (indirect) activation of Rab3 by Rab27. The assay consists of two consecutive pull down assays: one to retain a GEF from human sperm extracts on a Rab27A-column and the other to test its activity by measuring the conversion of Rab3A-GDP into Rab3A-GTP (Fig. 3).

3.5.1 Preparation of Human Sperm Extracts

1. Wash 5 ml of capacitated sperm suspensions (50×10^6 cells) twice with a volume of ice-cold PBS by centrifugation at $6,200 \times g$ for 2 min at room temperature.

2. Resuspend sperm pellet in 0.5 ml of lysis buffer.

3. Extract proteins by sonication at 40 Hz on ice three times for 15 s each, with a 10 s interval.

4. Incubate cell lysates for 45 min at 4 °C under constant rocking.

5. Clarify whole cell detergent extracts by centrifugation at $14,000 \times g$ for 20 min at 4 °C.

6. Recover whole cell extracts (supernatant) and use immediately or store at –20 °C.
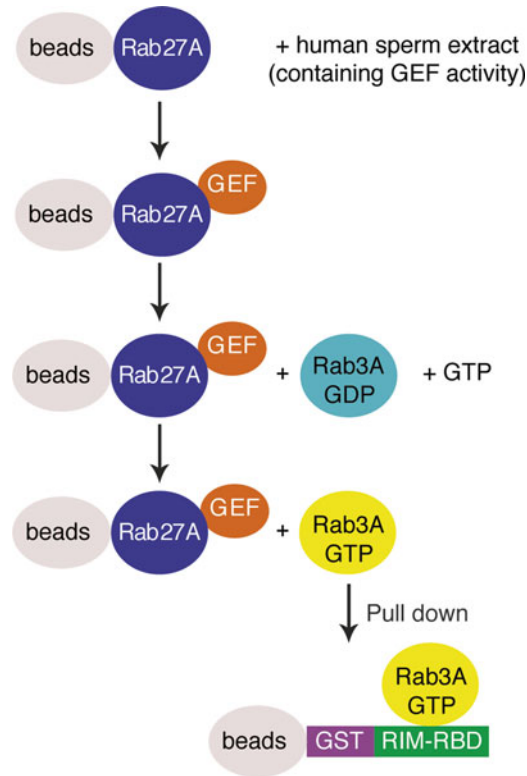
Fig. 3 Schematic representation of the protocol to recruit a Rab3A GEF activity. Geranylgeranylated GST-Rab27A-GTP-γ-S (*violet*) immobilized on glutathione-Sepharose beads (*gray*), are incubated with a human sperm extract with the goal of recruiting a Rab3A GEF protein (*orange*) if present in the lysate. Beads containing sperm proteins that interact with active Rab27A are used as source of Rab3A GEF activity using recombinant His$_6$-Rab3A-GDP (*blue*) and GTP as substrates. After centrifugation, the reaction product His$_6$-Rab3A-GTP (*yellow*) is pulled down with the GST-RIM-RBD cassette (*purple-green*), immobilized on fresh glutathione-Sepharose (*gray*)

3.5.2 Immobilization of Rab27A and Pull-Down of a Rab3A GEF Activity

1. Wash glutathione-Sepharose beads twice with one volume each of 20 mM HEPES/K, pH 7.4 and recover by centrifugation at $1,100 \times g$ for 2 min at 4 °C.

2. Block non-specific binding sites on glutathione-Sepharose by incubating three times with two volumes each of 0.1 % BSA in 20 mM HEPES/K pH 7.4.

3. Incubate 2.5 μg of purified GST (negative control) or GST-Rab27A (geranylgeranylated and loaded with GTP-γ-S) with 20 μl of glutathione-Sepharose beads in binding buffer (200 μl final volume) for 1 h at 4 °C under constant rocking.

4. Wash beads containing immobilized recombinant proteins three times with 200 µl binding buffer by centrifugation at $1,100 \times g$ for 2 min at room temperature.

5. Incubate immobilized recombinant proteins with 0.5 ml of human sperm extract (as described under Subheading 3.5.1) for 30 min at 4 °C under constant rocking.

6. Recover the beads by centrifugation at $2,600 \times g$ for 2 min at 4 °C. Precipitate unbound sperm fractions with CCl_3H–CH_3OH–H_2O (*see below*) and analyze by Western blot with anti-α-tubulin as loading control.

7. Wash the beads three times with 0.5 ml ice-cold binding buffer by centrifugation at $1,100 \times g$ for 2 min at room temperature.

8. Incubate the beads (containing a Rab3A GEF activity from human sperm retained on immobilized, active Rab27A) with 8 nM geranylgeranylated His_6-Rab3A-GDP (Fig. 3, *see* **Note 29**) in 0.5 ml binding buffer for 10 min at 37 °C under constant rocking.

9. Recover the beads by centrifugation at $3,000 \times g$ for 2 min at 4 °C. Dissolve resin-bound proteins by boiling in 60 µl of sample buffer for 3 min at 95 °C and analyze by Western blot with anti-GST antibodies as loading control.

10. Analyze the supernatants from **step 8** by pull-down with the GST-RIM-RBD cassette (*see below* and Fig. 3).

3.5.3 Protein Precipitation

1. Precipitate protein and remove detergent with CCl_3H–CH_3OH–H_2O [29].

2. Dissolve precipitated proteins in 60 µl of sample buffer by heating once for 10 min at 60 °C and once for 3 min at 95 °C.

3.5.4 Analysis of His_6-Rab3A-GTP Levels

1. Add 20 µl of glutathione-Sepharose containing 5–10 µg of GST-RIM-RBD to 0.5 ml supernatants from **step 10** under Subheading 3.5.2.

2. Incubate the mixture for 30 min at 4 °C under constant rocking.

3. Wash the beads three times with one volume each of ice-cold binding buffer by centrifugation at $1,100 \times g$ for 2 min at 4 °C.

4. Dissolve resin-bound proteins by boiling in 60 µl of sample buffer for 3 min at 95 °C.

5. Quantify the His_6-Rab3A-GTP levels by Western blot using the anti-Rab3A antibody as probe.

4 Notes

1. To permeabilize sperm we use recombinant SLO, an exotoxin that belongs to the homologous group of thiol-activated toxins that are synthesized by various Gram-positive bacteria. Monomeric toxin binds to cholesterol present in the plasma membranes and oligomerizes into ring-shaped structures, estimated to contain 50–80 subunits, which surround pores of approximately 30 nm diameter [30–33]. The only SLO we could work with reliably was the recombinant protein expressed and sold by the University of Mainz, Mainz, Germany.

2. The units of SLO are calculated for each batch.

3. Use a glass beaker and add the reagents one at the time to water at room temperature while stirring with a magnetic bar. Make sure that each reagent is completely dissolved before adding the next one and bring to final volume. HTF must be filter-sterilized using aseptic processing techniques. Once prepared, you can store aliquots (30 ml) at 2–8 °C until used. Do not freeze or expose to temperatures above 39 °C.

4. The HTF medium we use is buffered with $CO_2/NaHCO_3$. Tubes containing HTF medium should be placed loosely capped into a 5 % CO_2/95 % air incubator overnight to allow for the exchange of gas and pH equilibration. Check pH range (should be from 7.4 to 7.6) before using.

5. The sample should be obtained by masturbation and ejaculated into a sterile, wide-mouthed container made out of glass or plastic, from a batch that has been confirmed to be non-toxic for spermatozoa. Specimen containers should be labeled with an identification number, the date and time of collection.

6. Detailed protocols to assess semen quality are described in WHO laboratory manual for the examination and processing of human semen [34].

7. The direct swim-up technique is the choice for normal semen samples. Sperm are selected by their ability to swim out of semen placed at the bottom of the tube and up into the culture medium phase. Therefore highly motile sperm are obtained free from contaminants such as leukocytes, germ cells, dead or immotile spermatozoa, and seminal plasma.

8. After leaving the testis, mammalian spermatozoa are morphologically differentiated but are immotile and unable to fertilize. Progressive motility is acquired during epididymal transit. However, freshly ejaculated mammalian sperm are not immediately capable of undergoing the AR and fertilizing an egg. They require a period of several hours in the female reproductive tract or in an appropriate medium in vitro to acquire this

ability; this maturation process is termed capacitation [13, 16]. For all the assays present in this chapter, spermatozoa were capacitated in vitro by incubating in HTF/BSA medium for at least 3 h in a 5 % CO_2/95 % air incubator.

9. Alternatively, you can layer 300 μl of semen at the bottom of the tubes and then pipette carefully HTF/BSA medium over the semen.

10. Makler counting chamber is only 10 μm deep (1/10 of the depth of ordinary hemocytometers), making it the shallowest of known chambers. Constructed from two pieces of optically flat glass, the upper one serves as cover glass, with a 1 mm² fine grid in the center subdivided into 100 squares of 0.1×0.1 mm each. Spacing is firmly secured by four quartz pins [35].

11. The incubation performed in this step allows SLO binding to cholesterol molecules present in the plasma membrane of sperm.

12. DTT reduces and reversibly activates SLO.

13. Reagents should be mixed in the following order: HEPES/K, pH 7.5, DTT, BSA, $MgCl_2$, GDP, and protease inhibitors (AEBSF, aprotinin, bestatin, E-64, leupeptin, and EDTA). Then add Rab immobilized on beads and finally mouse brain cytosol and GGPP.

14. This step favors the recapture of isoprenylated Rabs dissociated from the resin.

15. The nucleotide must be ten times more concentrated than the protein.

16. Small molecules such as nucleotides will be retained in the column whereas large molecules, such as proteins will come out of the column after centrifugation.

17. Magnesium ions help to stabilize the nucleotide bound to the protein.

18. Recombinant protein concentrations are determined by the Bradford method (Bio-Rad) using BSA as a standard in 96-well microplates and quantified on a BioRad 3550 Microplate Reader or from the intensities of the bands in Coomassie Blue-stained SDS-PAGE gels using ImageJ program.

19. From this step on, every time you are going to add something or wash, first remove all excess liquid on the coverslips with lint-free tissue paper.

20. You can continue the protocol on the same day.

21. PSA lectin has specificity toward α-D-mannosyl-containing oligosaccharides present in the acrosome granule. PSA is coupled to FITC, if the acrosome is present then FITC-PSA binds the mannose residues and the structure shows fluorescent green staining [36]. On the contrary, if the acrosome is lost there is no staining.

22. We use Hoechst 33342, a cell-permeant nuclear dye that emits blue fluorescence when bound to dsDNA, to stain the nuclei and detect all cells.

23. We use an Eclipse TE2000 Nikon microscope equipped with a Plan Apo 40×/1.40 oil objective and a Hamamatsu digital C4742-95 camera operated with MetaMorph 6.1 software (Universal Imaging Corp., USA). We score the presence of red and/or green staining in the acrosomal region by manually counting between 100 and 200 cells either directly at the fluorescence microscope or in digital images from at least ten fields.

24. An IP_3-sensitive calcium channel inhibitor, which blocks calcium mobilization from the acrosome and hence avoids losing membranes by AR.

25. EDTA increases the off rate of nucleotides bound to endogenous Rabs present in sperm because it chelates magnesium ions [37].

26. We have stimulated SLO-permeabilized cells without loading endogenous Rabs with guanine nucleotides and the method also works [25].

27. This dilution renders 10 μM free calcium estimated by MAXCHELATOR, a series of programs to determine the free metal concentration in the presence of chelators available on the World Wide Web at http://maxchelator.stanford.edu.

28. A calcium-ionophore that induces the AR in non-permeabilized cells.

29. To measure Rab3A GEF activity retained in the Rab27A-column, we assayed the exchange of GDP for GTP on His_6-Rab3A by pull-down (3.4.2).

Acknowledgments

References

1. Sudhof TC, Rothman JE (2009) Membrane fusion: grappling with SNARE and SM proteins. Science 323:474–477

2. Rizo J, Sudhof TC (2012) The membrane fusion enigma: SNAREs, Sec1/Munc18 proteins, and their accomplices-guilty as charged? Annu Rev Cell Dev Biol 28:279–308

3. Cherfils J, Zeghouf M (2013) Regulation of small GTPases by GEFs, GAPs, and GDIs. Physiol Rev 93:269–309

4. Wickner W (2010) Membrane fusion: five lipids, four SNAREs, three chaperones, two nucleotides, and a Rab, all dancing in a ring on yeast vacuoles. Annu Rev Cell Dev Biol 26:115–136

5. Barr FA (2013) Review series: Rab GTPases and membrane identity: causal or inconsequential? J Cell Biol 202:191–199

6. Stenmark H (2009) Rab GTPases as coordinators of vesicle traffic. Nat Rev Mol Cell Biol 10:513–525

7. Nottingham RM, Pfeffer SR (2009) Defining the boundaries: Rab GEFs and GAPs. Proc Natl Acad Sci U S A 106:14185–14186

8. Fukuda M (2008) Regulation of secretory vesicle traffic by Rab small GTPases. Cell Mol Life Sci 65:2801–2813

9. Yanagimachi R (2011) Mammalian sperm acrosome reaction: where does it begin before fertilization? Biol Reprod 85:4–5

10. Tomes CN (2007) Molecular mechanisms of exocytosis. In: Regazzi R (ed) Molecular mechanisms of membrane fusion during acrosomal exocytosis, 65th edn. Landes Biosciences and Springer Science + Bussiness Media LLC, New York, pp 275–291

11. Mayorga LS, Tomes CN, Belmonte SA (2007) Acrosomal exocytosis, a special type of regulated secretion. IUBMB Life 59:286–292

12. Florman HM, Jungnickel MK, Sutton KA (2008) Regulating the acrosome reaction. Int J Dev Biol 52:503–510

13. Visconti PE, Krapf D, de la Vega-Beltran JL et al (2011) Ion channels, phosphorylation and mammalian sperm capacitation. Asian J Androl 13:395–405

14. Costello S, Michelangeli F, Nash K et al (2009) Ca^{2+}-stores in sperm: their identities and functions. Reproduction 138:425–437

15. Gadella BM, Luna C (2014) Cell biology and functional dynamics of the mammalian sperm surface. Theriogenology 81:74–84

16. Buffone MG, Ijiri TW, Cao W et al (2012) Heads or tails? Structural events and molecular mechanisms that promote mammalian sperm acrosomal exocytosis and motility. Mol Reprod Dev 79:4–18

17. Aitken RJ, Nixon B (2013) Sperm capacitation: a distant landscape glimpsed but unexplored. Mol Hum Reprod 19:785–793

18. Buffone MG, Hirohashi N, Gerton GL (2014) Unresolved questions concerning mammalian sperm acrosomal exocytosis. Biol Reprod 90:112

19. Pocognoni CA, De Blas GA, Heuck AP et al (2013) Perfringolysin O as a useful tool to study human sperm physiology. Fertil Steril 99:99–106

20. Lopez CI, Belmonte SA, De Blas GA et al (2007) Membrane-permeant Rab3A triggers acrosomal exocytosis in living human sperm. FASEB J 21:4121–4130

21. Yunes R, Tomes C, Michaut M et al (2002) Rab3A and calmodulin regulate acrosomal exocytosis by mechanisms that do not require a direct interaction. FEBS Lett 525:126–130

22. Branham MT, Bustos MA, De Blas GA et al (2009) Epac activates the small G proteins Rap1 and Rab3A to achieve exocytosis. J Biol Chem 284:24825–24839

23. Bustos MA, Lucchesi O, Ruete MC et al (2012) Rab27 and Rab3 sequentially regulate human sperm dense-core granule exocytosis. Proc Natl Acad Sci U S A 109:E2057–E2066

24. Bustos MA, Roggero CM, De la Iglesia PX et al (2014) GTP-bound Rab3A exhibits consecutive positive and negative roles during human sperm dense-core granule exocytosis. J Mol Cell Biol 6:286–298

25. Ruete MC, Lucchesi O, Bustos MA et al (2014) Epac, Rap and Rab3 act in concert to mobilize calcium from sperm's acrosome during exocytosis. Cell Commun Signal 12:43

26. Lopez CI, Pelletan LE, Suhaiman L et al (2012) Diacylglycerol stimulates acrosomal exocytosis by feeding into a PKC- and PLD1-dependent positive loop that continuously supplies phosphatidylinositol 4,5-bisphosphate. Biochim Biophys Acta 1821: 1186–1199

27. Coppola T, Perret-Menoud V, Luthi S et al (1999) Disruption of Rab3-calmodulin interaction, but not other effector interactions, prevents Rab3 inhibition of exocytosis. EMBO J 18:5885–5891

28. Kondo H, Shirakawa R, Higashi T et al (2006) Constitutive GDP/GTP exchange and secretion-dependent GTP hydrolysis activity for Rab27 in platelets. J Biol Chem 281:28657–28665

29. Wessel D, Flugge UI (1984) A method for the quantitative recovery of protein in dilute solution in the presence of detergents and lipids. Anal Biochem 138:141–143

30. Sekiya K, Satoh R, Danbara H et al (1993) A ring-shaped structure with a crown formed by streptolysin O on the erythrocyte membrane. J Bacteriol 175:5953–5961

31. Sekiya K, Danbara H, Futaesaku Y (1993) Mechanism of pore formation on erythrocyte membrane by streptolysin-O. Kansenshogaku Zasshi 67:736–740

32. Sekiya K (1995) Electron-microscopic observation of pore formation in the erythrocyte membrane by streptolysin O. Nihon Saikingaku Zasshi 50:509–517

33. Bhakdi S, Tranum-Jensen J, Sziegoleit A (1985) Mechanism of membrane damage by streptolysin-O. Infect Immun 47:52–60

34. World Health Organization Department of Reproductive Health and Research (2010) WHO laboratory manual for the examination and processing of human semen. WHO Press, Geneva

35. Makler A (1980) The improved ten-micrometer chamber for rapid sperm count and motility evaluation. Fertil Steril 33:337–338

36. Mendoza C, Carreras A, Moos J et al (1992) Distinction between true acrosome reaction and degenerative acrosome loss by a one-step staining method using *Pisum sativum* agglutinin. J Reprod Fertil 95:755–763

37. Burstein ES, Macara IG (1992) Interactions of the ras-like protein p25rab3A with Mg^{2+} and guanine nucleotides. Biochem J 282:387–392

Chapter 13

Rab Antibody Characterization: Comparison of Rab14 Antibodies

Andrew J. Lindsay and Mary W. McCaffrey

Abstract

Rab14 functions in the endocytic recycling pathway, having been implicated in the trafficking of the ADAM10 protease, GLUT4, and components of cell–cell junctions to the plasma membrane. It localizes predominantly to endocytic membranes with a pool also found on *trans*-Golgi network (TGN) membranes, and is most closely related to the Rab11 subfamily of GTPases. Certain intracellular bacteria such as *Legionella pneumophila*, *Chlamydia trachomatis*, and *Salmonella enterica* utilize Rab14 to promote their maturation and replication. Furthermore, the HIV envelope glycoprotein complex subverts the function of Rab14, and its effector the Rab Coupling Protein (RCP), in order to direct its transport to the plasma membrane. Since the use of antibodies is critical for the functional characterization of cellular proteins and their specificity and sensitivity is crucial in drawing reliable conclusions, it is important to rigorously characterize antibodies prior to their use in cell biology or biochemistry experiments. This is all the more critical in the case of antibodies raised to a protein which belongs to a protein family. In this chapter, we present our evaluation of the specificity and sensitivity of a number of commercially available Rab14 antibodies. We hope that this analysis provides guidance for researchers for antibody characterization prior to its use in cellular biology or biochemistry.

Key words Rab14, Antibody characterization, Immunofluorescence, Intracellular transport, Effector

1 Introduction

Rab family GTPases are tightly regulated molecular switches that control all aspects of intracellular transport including vesicle budding, uncoating, transport, tethering, and fusion [1]. Humans express over 60 Rab proteins, with some expressed ubiquitously and others expressed in a tissue-specific manner [2]. Rabs cycle between a GTP-bound active conformation during which they recruit a diverse range of 'effector' proteins. It is through these effector proteins that Rabs mediate their vesicular transport functions. When in their GDP-bound inactive conformation Rab GTPases are cytosolic and therefore unavailable to actively participate in membrane transport [3]. Each membrane-bound compartment in the cell is

typically associated with one or more Rabs. Rab14 is expressed in most cell types [4], and localizes primarily to endosomes with a sub-population found at the TGN [5, 6]. A recent phylogenomic analysis of the Rab family categorized Rab14 as a Group IV Rab, a group that also contains Rab2, Rab4, Rab11, and Rab39 [2]. Rab4 and Rab11 both function in the recycling of cargo to the plasma membrane and there is emerging evidence that Rab14 serves a similar role [7–10]. Indeed, it is likely that Rab14 functions coordinately with Rabs 4 and 11 in overlapping transport pathways as it shares effector proteins with these two Rabs [11–14].

Rab14 is also targeted by a number of intracellular pathogens including *Toxoplasma gondii* [15], *Legionella pneumophila* [16], *Chlamydia trachomatis* [17], and *Salmonella enterica* [12]. It seems that these pathogens appropriate Rab14 function in order to divert lipids and nutrients to specialist vacuoles in which the pathogens mature and replicate. Furthermore, the HIV-1 retrovirus appears to require Rab14 and its effector, RCP, to mediate delivery of the viral envelope glycoprotein to the plasma membrane where it is incorporated into developing HIV-1 particles [18].

Antibodies are important tools for studying the function of Rab GTPases, and it is probably no coincidence that the best characterized Rabs are the ones for which good antibodies are available. A good Rab antibody should be specific to that Rab and should not cross-react with its close relatives, or other proteins. It should also be sensitive enough to detect the endogenous protein, preferably by both immunofluorescence and immunoblotting (Western blotting). Despite its obvious importance, Rab14 is currently a relatively understudied Rab with the majority of Rab14 publications being less than 5 years old. We have previously reported on Rab14 localization and its ability to interact with members of the Rab11-FIP effector protein family [13]. In that paper, we presented the standard and widely accepted methods of antibody characterization (*see* Supplementary Fig. 1 in Ref. [13]).

One of the challenges facing researchers working on protein families whose members share a high degree of homology, is the identification of antibodies which are specific for their protein of interest. This challenge is particularly relevant in the case of the Rab family of small GTPases, which has over 60 different members in humans with sequence identities between them ranging from 30 to 80 %. Rab14 has a number of close relatives in the Rab family [19], including Rab4A and Rab11A (Fig. 1). Rab14 shares 61 % identity with Rab4A and 53 % identity with Rab11A. The carboxy-terminal tail, referred to as the Rab hypervariable region, is as its name implies the most divergent region of the Rab GTPases and thus sequences from this region are typically used to design peptides for antibody generation. The objective here being a greater likelihood of generating a Rab specific antibody. One of
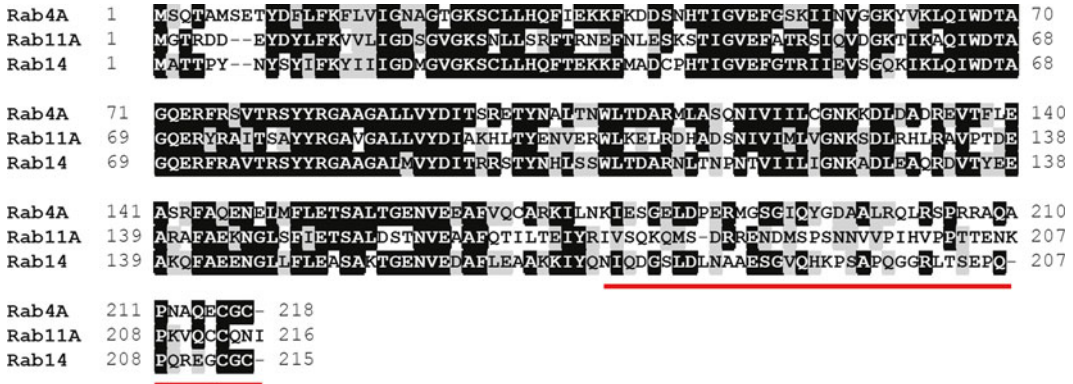
```
Rab4A    1    MSQTAMSETYDELFKFLVIGNAGTGKSCLLHQFIEKKFKDDSNHTIGVEFGSKIINVGGKYVKLQIWDTA  70
Rab11A   1    MGTRDD--EYDYLFKVVLIGDSGVGKSNLLSRFTRNEFNLESKSTIGVEFATRSIQVDGKTIKAQIWDTA  68
Rab14    1    MATTPY--NYSYIFKYIIGDMGVGKSCLLHQFTEKKFMADCPHTIGVEFGTRIIEVSGQKIKLQIWDTA  68

Rab4A    71   GQERFRSVTRSYYRGAAGALLVYDITSRETYNALTNWLTDARMLASCNIVIILCGNKKDLDADREVTFLE  140
Rab11A   69   GQERYRAITSAYYRGAVGALLVYDIAKHLTYENVERWLKELRDHADSNIVIMLVGNKSDLRHLRAVPTDE  138
Rab14    69   GQERFRAVTRSYYRGAAGAIMVYDITRRSTYNHLSSWLTDARNLTNPNTVIILIGNKADLEAQRDVTYEE  138

Rab4A    141  ASRFAQENELMFLETSALTGENVEEAFVQCARKILNKIESGELDPERMGSGIQYGDAALRQLRSPRRAQA  210
Rab11A   139  ARAFAEKNGLSFIETSALDSTNVEAAFQTILTEIYRIVSQKQMS-DRRENDMSPSNNVVPIHVPPTTENK  207
Rab14    139  AKQFAEENGLLFLEASAKTGENVEDAFLEAAKKIYQNIQDGSLDLNAAESGVQHKPSAPQGGRLTSEPQ-  207

Rab4A    211  PNAQECGC-  218
Rab11A   208  PKVQCCQNI  216
Rab14    208  PQREGCGC-  215
```

Fig. 1 ClustalW alignment of the amino acid sequences of Rab14 and its two close homologues Rab4A and Rab11A. The hypervariable domain is underlined in *red*

the first tests to validate any potential Rab14 antibody should be an evaluation of its specificity. Cross-reactivity with another Rab, or indeed with any other protein, will give misleading results and may lead to the drawing of incorrect conclusions. We describe here an evaluation of three commercially available Rab14 antibodies that are frequently used in the literature [Abcam (Cat. No. ab40938); Aviva Systems Biology (Cat. No. AVARP13107); and Sigma (Cat. No. R0656); *see* **Notes 1**, **2** and **3**, respectively]. Each antibody has been raised in rabbits against synthetic peptides corresponding to regions in the hypervariable C-terminal tail of Rab14 (*see* **Notes 1–3**).

To test the specificity of each of the antibodies, we expressed GFP-fusions of Rab14 and its two closest homologues Rab4A and Rab11A in HeLa cells. GFP-Rab7A was also included as an additional control. Twenty-four hours post-transfection the cells were fixed, quenched, permeabilized, and labeled with each Rab14 antibody. All three antibodies displayed immuno-reactivity with GFP-Rab14 at 1:1,000 dilution (Fig. 2a), and no cross-reactivity with the other Rabs. We therefore conclude that in mammalian cells, the three tested antibodies detect Rab14 and do not display any cross-reactivity with these closely related Rab GTPases.

We next compared the sensitivity of the antibodies by probing Western blots loaded with increasing amounts of GST-Rab14 (from 1 to 100 ng). At the antibody concentrations used, the Sigma and Abcam antibodies detected as little as 5 ng of the purified protein while the Aviva Systems Biology antibody detected 10 ng of GST-Rab14 by Western blot (Fig. 2b).

In order to check for antibody specificity by another approach, we analyzed a 100-fold excess of the minimum detectable amount of the Rab14 protein, i.e., 500 ng by Western blot. This amount of
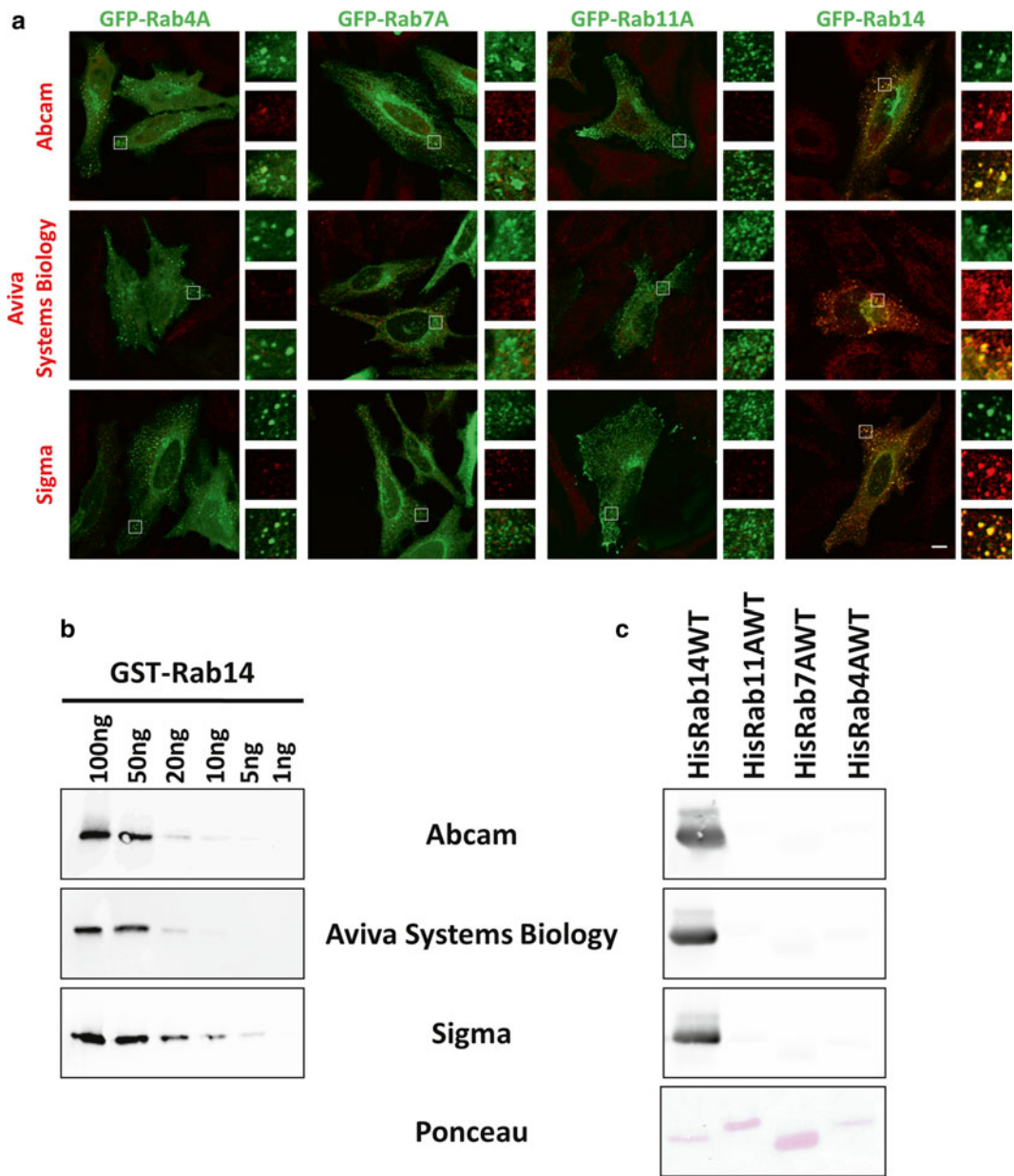
Fig. 2 Evaluation of antibody specificity. (**a**) Single confocal sections of HeLa cells expressing GFP-fusions of Rab4A, Rab7A, Rab11A, and Rab14 were fixed, permeabilized, and labeled with the indicated anti-Rab14 primary antibodies at 1:1,000 dilution (which equates to 0.6 μg/ml for the Abcam antibody, and 1 μg/ml for the Aviva Systems Biology and Sigma antibodies), followed by Cy3-conjugated donkey anti-rabbit secondary antibody. The *boxed regions* were magnified and shown on the *right* of each image. Bar, 10 μm. (**b**) 0.5 μg of purified His- Rab4A, Rab7A, Rab11A, and Rab14 proteins were separated by SDS-PAGE, transferred to nitrocellulose, and probed with each antibody at 1:1,000 dilution (which equates to final antibody concentrations of 0.6 μg/ml for the Abcam antibody, and 1 μg/ml for the Aviva Systems Biology and Sigma antibodies). Westerns were scanned on an Odyssey Infrared Imager. Ponceau S staining shows loading of the purified proteins. (**c**) Increasing amounts of GST-Rab14 were separated by SDS-PAGE, transferred to nitrocellulose, and probed with the indicated antibodies

purified His-tagged Rab4A, Rab7, Rab11A, and Rab14 proteins were separated by SDS-PAGE, transferred to nitrocellulose, and probed with each antibody at a 1:1,000 dilution. After probing with an appropriate secondary antibody the blots were scanned on an Odyssey Infrared Imager. Again, each antibody was specific for Rab14 and displayed no cross-reactivity with the other Rabs (Fig. 2c). Rab protein loading was monitored by Ponceau Red staining. Taken together, we conclude that the three antibodies tested are specific for Rab14 and do not detect the other closely related Rabs used in the test, either in their native conformation in cells or when denatured on nitrocellulose membranes.

We have reported previously characterization of the Abcam antibody [13], and here wished to compare the ability of these two additional antibodies to detect endogenous Rab14 by both immunofluorescence and Western blot. HeLa cells grown on glass coverslips for at least 48 h were fixed, quenched, permeabilized and labeled with each antibody at a 1:1,000 dilution. Single 0.4 μm thick sections were recorded by laser scanning confocal microscopy. All the antibodies predominantly labeled large endosomal structures resembling early/sorting endosomes (Fig. 3a). The Aviva Systems Biology antibody, and to a lesser extent the Sigma antibody, also displayed some localization at Golgi-like structures. This is similar to the previously reported localization patterns for Rab14 [5, 6, 13], and also the localization of GFP-Rab14 in HeLa cells (Fig. 2a).

The ability to detect an endogenous Rab protein by Western blot is important for a wide range of applications, from determining the efficiency of siRNA-mediated protein knockdown and subcellular fractionation to immunoprecipitations and protein quantitation. To investigate the usefulness of the Rab14 antibodies as a means of detecting the endogenous protein by Western blot, lysates from HeLa cells that had been transfected with control siRNA or two different siRNAs targeting Rab14 were separated by SDS-PAGE, transferred to nitrocellulose and probed with each antibody. The membranes were subsequently probed with an antibody to α-tubulin as a loading control. Each antibody detected an approximately 25 kDa band in the control lysate, and the intensity of this band was reduced in lysates from the cells transfected with the Rab14 siRNA, indicating that this band is Rab14. All the antibodies also detected non-specific bands but in each case the band corresponding to Rab14 was the most prominent. The Aviva Systems Biology antibody detected two bands of ~60 and ~75 kDa, while the Sigma antibody detected an ~30 kDa non-specific band.

Taking the various characterization assays together to judge on the specificity and sensitivity of the three Rab14 antibodies we found that all specifically detect the Rab14 protein and not its closest relatives. Each antibody can also detect endogenous Rab14, by both immunofluorescence and Western blot.
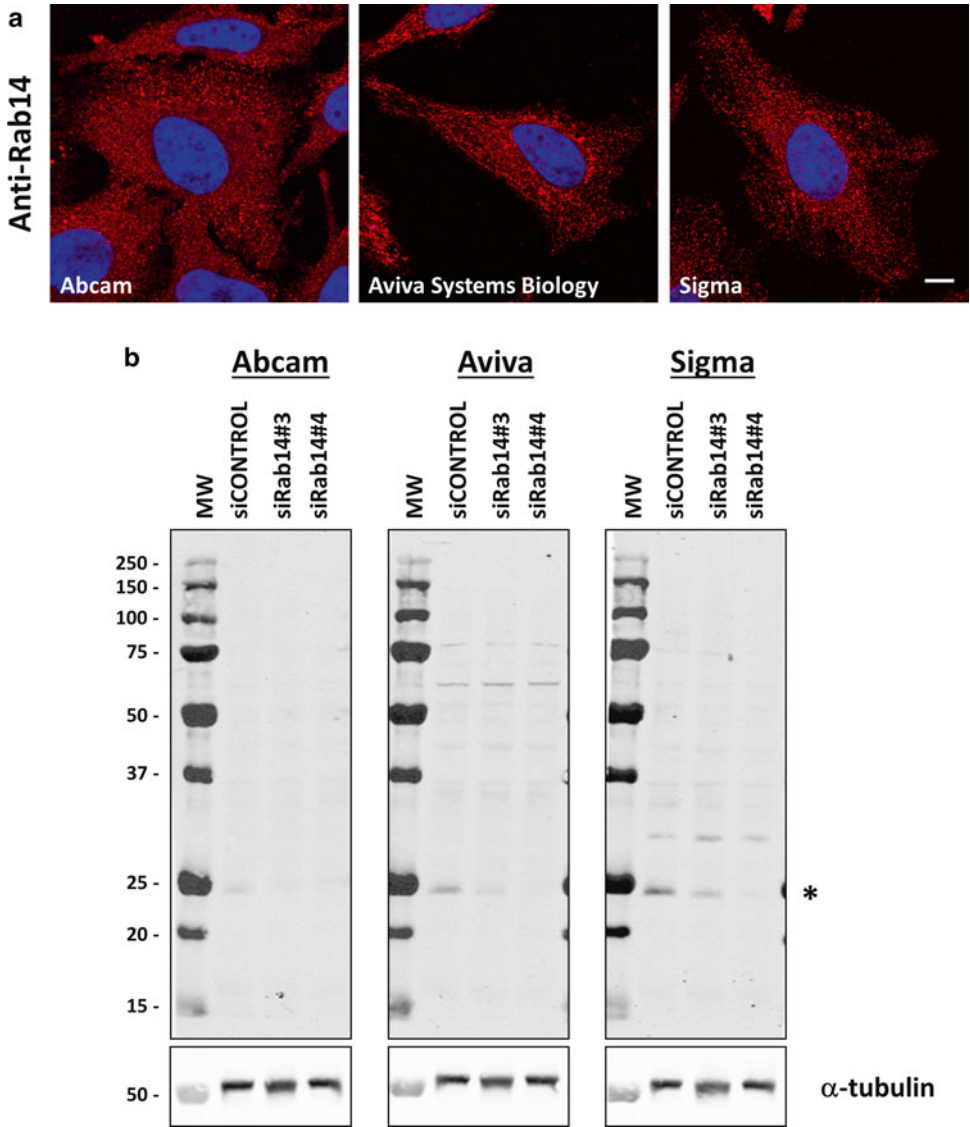
Fig. 3 The antibodies detect endogenous Rab14. (**a**) HeLa cells were fixed, permeabilized, and labeled with each antibody at 1:1,000 dilution (which equates to final antibody concentrations of 0.6 μg/ml for the Abcam antibody, and 1 μg/ml for the Aviva Systems Biology and Sigma antibodies). Bar, 10 μm. (**b**) Lysates from HeLa cells transfected with the indicated siRNA duplexes for 72 h were separated by SDS-PAGE, transferred to nitrocellulose, and probed with the indicated antibody at 1:1,000 dilution (which equates to final antibody concentrations of 0.6 μg/ml for the Abcam antibody, and 1 μg/ml for the Aviva Systems Biology and Sigma antibodies). Blots were scanned with an Odyssey Infrared Imager. The blots were re-probed with an antibody to α-tubulin to show equal loading. *Asterisk* indicates the ~25 kDa Rab14 band

2 Materials

2.1 Bacterial Strains

The *Escherichia coli* strains XL-1 and BL21 (DE3-RIL) were used for subcloning and protein purification, respectively. Both strains were cultured in Luria-Bertani broth with the appropriate antibiotics.

2.2 Cell Lines

HeLa cells were obtained from the European Collection of Cell Cultures and cultured in DMEM supplemented with 10 % (v/v) fetal calf serum (FCS), 2 mM L-glutamine, 100 units/μl penicillin and 0.1 % (w/v) streptomycin. Cells were maintained in a humidified 5 % CO_2 atmosphere at 37 °C.

2.3 Chemicals and Reagents

1. Isopropyl-β-D-thiogalactopyranoside (IPTG).
2. TurboFect Plasmid Transfection Reagent (Thermo Scientific).
3. Lipofectamine RNAiMax Transfection Reagent (Life Technologies).
4. Antibiotics: ampicillin (50 μg/ml), chloramphenicol (34 μg/ml).
5. Secondary antibodies: Cy3-conjugated donkey anti-rabbit (Jackson ImmunoResearch), IRDye800CW goat anti-rabbit (LI-COR).
6. Protease inhibitors: Complete protease inhibitor cocktail (Roche), AEBSF (Sigma).

2.4 Buffers and Solutions

1. PBS: 137 mM NaCl, 2.7 mM KCl, 10 mM Na_2HPO_4, KH_2PO_4.
2. Quench buffer: 50 mM NH_4Cl/PBS.
3. Blocking buffer: 0.05 % saponin/0.2 % BSA/PBS.
4. Lysis buffer: 50 mM Tris–HCl, pH 8.5; 150 mM NaCl; 1 mM DTT.
5. Mowiol mounting medium: 2.4 g Mowiol (Calbiochem), 6 g glycerol, 6 ml dH_2O, 12 ml 0.2 M Tris–HCl (pH 8.5).
6. RIPA buffer: 150 mM NaCl, 1.0 % NP-40, 0.5 % sodium deoxycholate, 0.1 % SDS, and 50 mM Tris–HCl, pH 8.0
7. Tris buffered saline-Tween 20 (TBS-T): 20 mM Tris–HCl (pH 7.5), 150 mM NaCl, 0.1 % Tween-20.
8. 3× sample buffer: 2.4 ml 1 M Tris–HCl (pH 6.8), 3 ml 20 % SDS, 3 ml glycerol, 0.006 g bromophenol blue, 1.6 ml dH_2O.
9. Ponceau Red: 0.2 % (w/v) Ponceau S, 5 % trichloroacetic acid.

3 Methods

3.1 Plasmids

pEGFP-Rab14 was a kind gift from Jacques Neefjes (Cell Biology II, The Netherlands Cancer Institute, Amsterdam, The Netherlands). pEGFP-Rab7A and pET16b-Rab7A were kind gifts from Cecilia Bucci (Department of Biological and Environmental Sciences and Technologies, University of Salento, Lecce, Italy), and pEGFP-C3-Rab11A has been described elsewhere [13]. pTrcHisB-Rab14 was created by subcloning the ~650 bp *Bgl*II/*Kpn*I fragment from pEGFP-Rab14 and ligating it into the *Bgl*II/*Kpn*I sites of pTrcHisB (Invitrogen). pEGFP-C1-Rab4A and pTrcHisA-Rab4A were generated by inserting the 780 bp *Bam*HI fragment from pVJL10-Rab4A into the *Bam*HI site of pEGFP-C1 (Clontech) and pTrcHisA (Invitrogen), respectively.

3.2 Transfections

For transient plasmid transfections, HeLa cells were seeded in 24-well plates such that they were approximately 70 % confluent on the day of transfection. 0.25 μg of each plasmid was diluted in 100 μl DMEM and 0.5 μl of TurboFect transfection reagent was added, the solution was vortexed, incubated at room temperature for 15 min, and then added drop-wise to the cells. The cells were returned to 37 °C for 24 h. For RNAi experiments, HeLa cells were seeded such that they were approximately 50 % confluent by the next day. 10 pmol of each siRNA duplex was diluted in 100 μl DMEM and 1 μl of Lipofectamine RNAiMax was added, the solution was vortexed, incubated at room temperature for 10–15 min, and then added drop-wise to the cells. The cells were returned to 37 °C for a further 72 h (*see* **Notes 4** and **5**).

3.3 Indirect Immunofluorescence

HeLa cells seeded on 10 mm glass coverslips and transfected with plasmid approximately 24 h previously were fixed with 4 % paraformaldehyde at room temperature for 15 min followed by quenching with 50 mM NH$_4$Cl/PBS for 15 min. Cells were permeabilized and blocked in Blocking buffer for a minimum of 20 min at room temperature. Coverslips were then transferred to a humid chamber (a box with wet Whatman filter paper on the bottom and partially covered with Parafilm) with the cell side facing up. Each primary Rab14 antibody was diluted to 1:1,000 in blocking buffer and 50 μl of this solution was added on top of the cells and incubated in the dark at room temperature for 1 h. The coverslips were washed twice with PBS followed by incubation with Cy3-conjugated donkey anti-rabbit secondary antibody at a dilution of 1:400 in blocking buffer for 1 h at room temperature. The coverslips were washed twice with PBS, mounted cell side down in 8 μl drops of Mowiol mounting medium on clean microscope slides, and allowed to dry overnight at room temperature in the dark (*see* **Note 6**). Images were recorded with a Zeiss LSM510 META confocal microscope fitted with a 63×/1.4 plan apochromat lens.

**3.4 Protein
Purification
and Western Blotting**

All His-fused Rab GTPases used were purified as follows: *E. coli*
BL21 (DE3-RIL) cells transformed with the relevant plasmid were
grown in Luria-Bertani broth, supplemented with 34 μg/ml chlor-
amphenicol and 50 μg/ml ampicillin, to an OD_{600} of approximately
0.6 and induced to express the recombinant protein with 0.5 mM
IPTG for 5 h at 37 °C (*see* **Note** 7). Bacteria were pelleted by cen-
trifugation at $5,000 \times g$ for 20 min and resuspended in Lysis Buffer
plus 0.5 mM AEBSF. The cells were lysed by sonication on ice
using a probe sonicator (2×30 s, 50 % cycle, power 6) and insoluble
proteins were removed by centrifugation for 30 min at $10,000 \times g$
at 4 °C. The supernatant containing the soluble proteins was trans-
ferred to a fresh tube and recombinant proteins were then affinity-
purified using Ni-NTA agarose (Qiagen) and rotated in the cold
room for approximately 1 h. The beads were washed three times
with 10 bead volumes of ice-cold Lysis buffer supplemented with
20 mM imidazole, and bound recombinant proteins were eluted
from the beads by incubating in an equal volume of Lysis buffer
supplemented with 200 mM imidazole for 5 min rotating at room
temperature. The elution step was repeated twice more and the
fractions were pooled. Protein concentration was determined by
the Bradford method using a standard curve comprised of increas-
ing concentrations of γ-globulin (from 0 to 100 μg/ml).

To generate HeLa cell lysates, cells transfected with siRNA
duplexes approximately 72 h previously were washed twice with
ice-cold PBS and lysed in 100 μl cold RIPA buffer supplemented
with 1× protease inhibitor cocktail and 0.5 mM AEBSF. The
24-well plate was incubated in the cold room on a rocking plat-
form for 30 min. 50 μl of 3× sample buffer was added to each well
and the lysates were transferred to a clean microcentrifuge tube
and heat denatured for 5 min at 95 °C on a heating block. Tubes
were immediately placed on ice.

For immunoblotting, proteins were resolved by SDS-PAGE
and transferred onto nitrocellulose. Membranes were then blocked
for 1 h with 5 % BSA in TBS-T. The Rab14 primary antibodies
were diluted in 5 % BSA/TBS-T at 1:1,000 dilution and incubated
with the membrane for at least 1 h, followed by three 5 min washes
in TBS-T. Membranes were subsequently probed with
IRDye800CW goat anti-rabbit (1:10,000) followed by three 5 min
washes in TBS-T and a final 5 min wash with TBS. Blots were
imaged on an Odyssey Infrared Scanning system (LI-COR).

4 Notes

1. Abcam; Rabbit anti-Rab14; Cat. No. 40938; Lot No. 50564;
   Immunogenic peptide sequence: GRLTSEPQPQREGCGC;
   Antibody concentration 0.61 mg/ml.

2. Aviva Systems Biology; Rabbit anti-Rab14; Cat. No. AVARP13107; Lot No. QC7005; The sequence of the immunogenic peptide corresponds to a region in the C-terminus of Rab14; Antibody reconstituted to 1 mg/ml.

3. Sigma; Rabbit anti-Rab14; Cat No. R0656; Lot No. 108K4768; Immunogenic peptide sequence: SAPQGGRLTSEPQPQR EG; Antibody concentration 1 mg/ml.

4. Transfection reagents can be quite toxic to HeLa cells so as a general rule we use half the amount of plasmid and transfection reagent recommended by the manufacturer.

5. We have successfully used many different transfection reagents with HeLa cells, including Effectene (Qiagen), XtremeGene9 (Roche Applied Science), Lipofectamine 2000 (Life Technologies), and HiPerFect (Qiagen).

6. The drying process can be speeded up by placing the slides at 37 °C. For long-term storage slides can be placed in the dark at 4 or –20 °C.

7. Rab-fusion proteins are generally very soluble; however, if difficulties with solubility are encountered fusion proteins should be induced overnight at 25 °C with a lower concentration of IPTG.

Acknowledgements

References

1. Kelly EE, Horgan CP, Goud B, McCaffrey MW (2012) The Rab family of proteins: 25 years on. Biochem Soc Trans 40(6):1337–1347

2. Klopper TH, Kienle N, Fasshauer D, Munro S (2012) Untangling the evolution of Rab G proteins: implications of a comprehensive genomic analysis. BMC Biol 10:71. doi:10.1186/1741-7007-10-71

3. Stenmark H (2009) Rab GTPases as coordinators of vesicle traffic. Nat Rev Mol Cell Biol 10(8):513–525

4. Elferink LA, Anzai K, Scheller RH (1992) rab15, a novel low molecular weight GTP-binding protein specifically expressed in rat brain. J Biol Chem 267(9):5768–5775

5. Junutula JR, De Maziere AM, Peden AA, Ervin KE, Advani RJ, van Dijk SM, Klumperman J, Scheller RH (2004) Rab14 is involved in membrane trafficking between the Golgi complex and endosomes. Mol Biol Cell 15(5): 2218–2229

6. Proikas-Cezanne T, Gaugel A, Frickey T, Nordheim A (2006) Rab14 is part of the early endosomal clathrin-coated TGN microdomain. FEBS Lett 580(22):5241–5246

7. Lu R, Johnson DL, Stewart L, Waite K, Elliott D, Wilson JM (2014) Rab14 regulation of claudin-2 trafficking modulates epithelial permeability and lumen morphogenesis. Mol Biol Cell 25(11):1744–1754. doi:10.1091/mbc.E13-12-0724

8. Sadacca LA, Bruno J, Wen J, Xiong W, McGraw TE (2013) Specialized sorting of GLUT4 and its recruitment to the cell surface are independently

regulated by distinct Rabs. Mol Biol Cell 24(16):2544–2557. doi:10.1091/mbc.E13-02-0103

9. Reed SE, Hodgson LR, Song S, May MT, Kelly EE, McCaffrey MW, Mastick CC, Verkade P, Tavare JM (2013) A role for Rab14 in the endocytic trafficking of GLUT4 in 3T3-L1 adipocytes. J Cell Sci 126(Pt 9):1931–1941. doi:10.1242/jcs.104307

10. Linford A, Yoshimura S, Nunes Bastos R, Langemeyer L, Gerondopoulos A, Rigden DJ, Barr FA (2012) Rab14 and its exchange factor FAM116 link endocytic recycling and adherens junction stability in migrating cells. Dev Cell 22(5):952–966

11. Yamamoto H, Koga H, Katoh Y, Takahashi S, Nakayama K, Shin HW (2010) Functional cross-talk between Rab14 and Rab4 through a dual effector, RUFY1/Rabip4. Mol Biol Cell 21(15):2746–2755

12. Kuijl C, Pilli M, Alahari SK, Janssen H, Khoo PS, Ervin KE, Calero M, Jonnalagadda S, Scheller RH, Neefjes J, Junutula JR (2013) Rac and Rab GTPases dual effector Nischarin regulates vesicle maturation to facilitate survival of intracellular bacteria. EMBO J 32(5):713–727. doi:10.1038/emboj.2013.10

13. Kelly EE, Horgan CP, Adams C, Patzer TM, Ni Shuilleabhain DM, Norman JC, McCaffrey MW (2009) Class I Rab11-family interacting proteins are binding targets for the Rab14 GTPase. Biol Cell 102(1):51–62

14. Lindsay AJ, Jollivet F, Horgan CP, Khan AR, Raposo G, McCaffrey MW, Goud B (2013) Identification and characterization of multiple novel Rab-myosin Va interactions. Mol Biol Cell 24(21):3420–3434. doi:10.1091/mbc.E13-05-0236

15. Romano JD, Sonda S, Bergbower E, Smith ME, Coppens I (2013) Toxoplasma gondii salvages sphingolipids from the host Golgi through the rerouting of selected Rab vesicles to the parasitophorous vacuole. Mol Biol Cell 24(12):1974–1995. doi:10.1091/mbc.E12-11-0827

16. Hoffmann C, Finsel I, Otto A, Pfaffinger G, Rothmeier E, Hecker M, Becher D, Hilbi H (2014) Functional analysis of novel Rab GTPases identified in the proteome of purified Legionella-containing vacuoles from macrophages. Cell Microbiol 16(7):1034–1052. doi:10.1111/cmi.12256

17. Capmany A, Damiani MT (2010) Chlamydia trachomatis intercepts Golgi-derived sphingolipids through a Rab14-mediated transport required for bacterial development and replication. PLoS One 5(11):e14084. doi:10.1371/journal.pone.0014084

18. Qi M, Williams JA, Chu H, Chen X, Wang JJ, Ding L, Akhirome E, Wen X, Lapierre LA, Goldenring JR, Spearman P (2013) Rab11-FIP1C and Rab14 direct plasma membrane sorting and particle incorporation of the HIV-1 envelope glycoprotein complex. PLoS Pathog 9(4):e1003278. doi:10.1371/journal.ppat.1003278

19. Pereira-Leal JB, Seabra MC (2001) Evolution of the Rab family of small GTP-binding proteins. J Mol Biol 313(4):889–901

Chapter 14

Selective Visualization of GLUT4 Storage Vesicles and Associated Rab Proteins Using IRAP-pHluorin

Yu Chen and Jennifer Lippincott-Schwartz

Abstract

Fluorescence microscopy and fluorescent protein (FP)-tagged GLUT4 molecule have been great tools to characterize GLUT4 localization and dynamics inside the cell. However, it was difficult to distinguish GLUT4 storage vesicles (GSVs) from other intracellular compartments containing GLUT4 in live cells. Here, we describe the use of IRAP-pHluorin and total internal reflection fluorescence (TIRF) microscopy to selectively visualize GSVs and Rab proteins that associate with GSVs. This assay is also valuable to further defining GSV identity by unraveling other GSV-associated proteins.

Key words GLUT4, IRAP, Rab10, AS160, TIRF, Adipocytes

1 Introduction

Insulin stimulates glucose uptake into adipocytes and muscle tissues by recruiting GLUT4 to the plasma membrane (PM) [1–3]. The exocytosis of GLUT4 in response to insulin is achieved through physical trafficking of storage vesicles enriched in GLUT4 called GLUT4 storage vesicles (GSVs) from intracellular sites to the PM. A signaling cascade involving PI3K, AKT/PKB, AS160, and Rab proteins regulates such trafficking. In this cascade, PI3K and AKT/PKB are activated in response to insulin, causing phosphorylation of the RabGAP protein AS160 by AKT. AS160 phosphorylation inactivates its GAP activity [4, 5], allowing the cognate Rab proteins to become active and mediate GLUT4 translocation to the PM [6–8].

After being delivered to the PM during insulin stimulation, GLUT4 is endocytosed into the endosomal system and recycles through early endosomes, recycling endosomes, and the trans-Golgi network before being reloaded into GSVs [9, 10]. This complex intracellular trafficking itinerary results in GLUT4 having a broad distribution pattern, with steady-state localization in many intracellular compartments [2]. Here, we describe a method to distinguish GSVs from other intracellular compartments containing GLUT4.

This method combines IRAP-pHluorin and total internal reflection fluorescence (TIRF) microscopy to visualize GLUT4-containing vesicles that fuse at the cell membrane after insulin stimulation. Given the most robust insulin responsiveness of GSVs among all intracellular compartments containing GLUT4, they are therefore preferentially observed by this method. In order to highlight GLUT4-containing vesicle fusion at the PM, we used insulin-responsive aminopeptidase (IRAP) tagged with pH-sensitive fluorescent protein pHluorin. IRAP shares identical localization with GLUT4 and has simpler topology (single-pass type II transmembrane). Fusing pHluorin to the C-terminus of IRAP (IRAP-pHluorin) places pHluorin into the vesicular lumen of GLUT4-containing vesicles. pHluorin is a pH-sensitive probe that only fluoresces when exposed to a nonacidic environment. Because the pH inside GLUT4-containing vesicles is acidic and that outside of cells is neutral, IRAP-pHluorin fluoresces brightly when GLUT4-containing vesicles fuse at the PM exposing pHluorin extracellularly. TIRF microscopy restrains illumination to ~150 nm above the coverslip and thus provides great signal-to-noise ratio to observe vesicles fusion-indicating bright flashes appearing at the PM.

Having observed numerous IRAP-pHluorin vesicle fusion events after insulin stimulation, we characterized the identities of these insulin-responsive IRAP-pHluorin vesicles by examining the presence of GLUT4 and transferrin receptor (TfR) on them. In order to do so, IRAP-pHluorin was cotransfected with GLUT4 or TfR tagged with red fluorescent protein into adipocytes and the presence of GLUT4 or TfR on IRAP-pHluorin fusing vesicles was analyzed (Fig. 1).
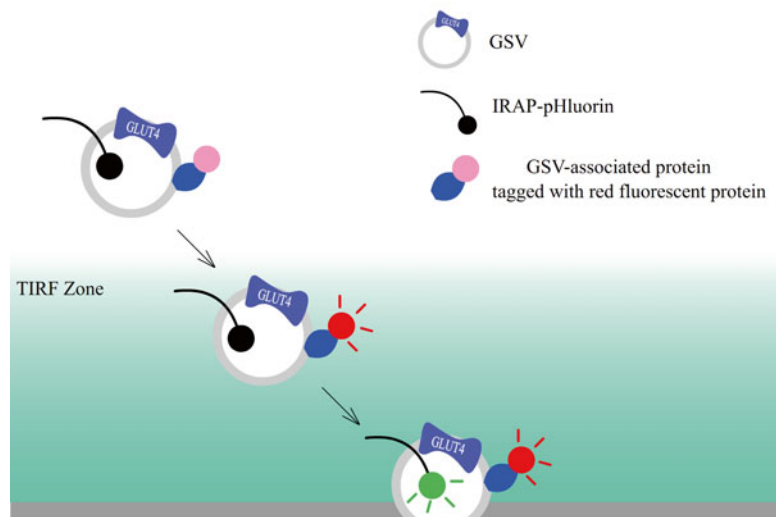
Fig. 1 Illustration of the experimental scheme. GLUT4 storage vesicles (GSVs) are labeled with IRAP-pHluorin, which highlights GSV fusion at the cell surface. Proteins of interest, including various Rab proteins, that potentially associates with GSVs are tagged with red fluorescence protein and their presence on the fusing GSVs is examined using TIRF microscopy

The majority of insulin-responsive IRAP-pHluorin vesicles contained GLUT4 but not TfR. This indicates most of these insulin-responsive IRAP-pHluorin vesicles were bona fide GSVs rather than endosomal compartments, as the latter are known to contain TfR whereas GSVs do not. With IRAP-pHluorin being established as a reliable tool to selectively visualize GSVs, we determined the association of candidate Rab proteins with GSVs. Among Rab proteins tested, only Rab10 was observed to specifically associate with GSVs. Therefore, we have identified Rab10 as the key Rab protein mediating insulin-stimulated GSV delivery to the PM in adipocytes.

2 Materials

2.1 Coverglass Cleaning

1. Hellmanex® III (Hellma Analytics). Working concentration: 2 % in MilliQ water.
2. #1.5 Glass Coverslip 25 mm round (Warner Instrument).
3. 35 mm cell culture dishes.
4. Coverslip Mini-Rack (Life Technology).
5. Glass jar.
6. 200 Proof Ethyl Alcohol.
7. Water bath sonicator.

2.2 Cell Culture and Transfection

1. High-glucose DME.
2. Newborn calf serum.
3. Fetal bovine serum.
4. Rosiglitazone (Cayman Chemical).
5. Bovine insulin.
6. 3-Isobutyl-1-methylxanthine.
7. Dexamethasone.
8. 0.25 % trypsin–EDTA.
9. Phosphate-Buffered Saline.
10. Amaxa® Cell Line Nucleofector® Kit L.

2.3 TIRF Imaging

1. Attofluor® Cell Chamber.
2. NIKON Eclipse Ti Microscope System equipped with an environmental chamber, in which temperature is controlled at 37 °C and CO_2 is at 5 %, a high-speed EM charge-coupled device camera (iXon DU897 from Andor), Apo TIRF 100× objective (N.A. 1.49), and NIS-Elements Ar Microscope Imaging Software.

3 Methods

3.1 Coverglass Cleaning

1. Mount individual coverslips into Coverslip Mini-Rack and place several racks in a glass jar.

2. Fill the glass jar with 2 % Hellmanex® III in MilliQ water and incubate overnight.

3. Sonicate the glass jar in a water bath sonicator for 30 min. Heating may improve cleaning.

4. Rinse the glass jar >9 times with MilliQ water to completely remove Hellmanex® III.

5. Fill the glass jar with 200 Proof Ethyl Alcohol and incubate for several hours. Individual coverslips are then flamed and wrapped with aluminum foil in individual 35 mm cell culture dishes.

3.2 Cell Culture

3T3-L1 fibroblast cells are grown in high-glucose DME supplemented with 10 % newborn calf serum at 37 °C and 5 % CO_2. Two days after reaching confluence, the fibroblast cells are incubated with the differentiation medium containing 10 % FBS, 1 mM Rosiglitazone, 1 mM bovine insulin, 0.5 mM 3-isobutyl-1-methylxanthine, and 0.25 mM dexamethasone for 3 days. Then the medium is changed to high-glucose DME containing 10 % FBS and 1 mM bovine insulin for 2 days. Afterward, cells are maintained in DME with 10 % FBS. Adipocytes typically become apparent beginning on the fourth day after addition of differentiation medium and are ready for transfection 8–10 days after differentiation.

3.3 Transfection

1. Coat cleaned coverslips with 0.01 % Poly-L-lysine solution for 5 min, rinse with MilliQ water, and let them air dry.

2. Wash well-differentiated 3T3-L1 adipocytes (8–10 days after differentiation) in a T-25 cell culture flask twice with PBS. Use at least same volume of PBS as culture media in each wash.

3. Harvest the cells by incubating them with 5 ml 0.25 % trypsin–EDTA for 10 min at 37 °C.

4. Neutralize trypsinization reaction with as much complete medium as trypsin–EDTA used at last step.

5. Centrifuge the cells at $50 \times g$ for 3 min at room temperature in a 15 ml Falcon tube.

6. Remove supernatant completely and resuspend the cell pellet carefully in 100 µl room-temperature Cell Line Nucleofector Solution L.

7. Combine 100 μl of cell suspension with DNA and/or siRNA. Use 4 μg plasmid for each gene to transfect and 1 nmol siRNA for each gene to knock down.

8. Transfer cell/DNA suspension into a cuvette and close the cuvette with the cap.

9. Select the appropriate Nucleofector® Program 2.11 A-033 (A-33 for Nucleofector® I Device).

10. Insert the cuvette with cell/DNA suspension into the Nucleofector® Cuvette Holder and apply the selected program by pressing the X-button.

11. Take the cuvette out of the holder once the program is finished and immediately add 500 μl of the preequilibrated differentiation medium III to the cuvette.

12. Resuspend the cells and transfer them to the cell culture dish containing the coated coverslip. Adipocytes from a T-25 cell culture flask can be split onto 2–4 coverslips to obtain appropriate cell density on coverslips.

13. Put the cell culture dish in cell culture incubator. Adipocytes usually take several hours to attach to the coverslip. Growth medium can be replaced 24 h after transfection.

3.4 TIRF Imaging   Forty-eight hours after transfection the coverslip with adipocytes seeded on is mounted in Attofluor Cell Chamber and imaged in Phenol Red-free DMEM. A total of 100 nM insulin is applied to the cells to stimulate GSV fusion at the PM. High-frequency image acquisition usually starts 3 min after insulin stimulation. Dual-color imaging was achieved using Triggered Acquisition mode, in which only excitation lasers are switched between different imaging channels. Therefore, images from green and red channels were aligned automatically.

3.5 Image Analysis   To identify vesicle fusion sites, a subtraction image stack of the IRAP-pHluorin images is generated with an interval of 1 frame. Individual fusion events appear as bright spots in the maximum projection of the subtraction image stack. With the guidance of located fusion sites, IRAP-pHluorin fusion events indicated by bright flashes at the PM are spotted by eye. In an image sequence of 200 frames acquired at 4 frames/per second, usually 30–50 fusion events are readily identified. For each fusion event detected, the fusion site is examined in the red channel to determine the presence of protein of interest on the fusing vesicle (Fig. 2).
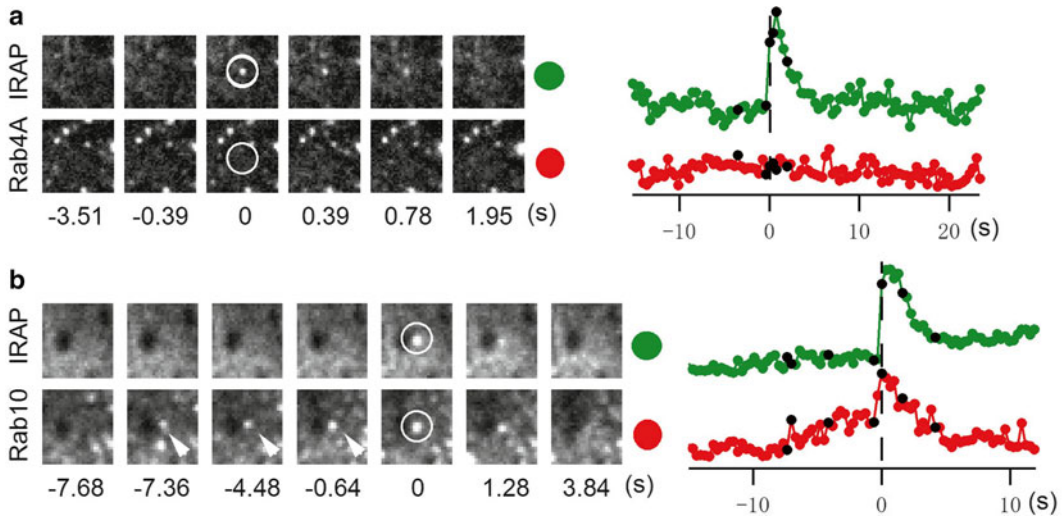
Fig. 2 Adipocytes are cotransfected with IRAP-pHluorin and TagRFP-Rab4A (**a**) or -Rab10 (**b**). Three minutes after insulin stimulation IRAP-pHluorin vesicle fusion at the cell membrane is recorded and the presence of Rab protein on IRAP-PHluorin fusing vesicle is examined

4   Notes

Adipocytes to image need be chosen carefully. Electroporation usually impairs most of the cells and only several cells are left in good condition on each coverslip. Cell morphology is the key criterion to select insulin-responsive cells. Particularly, cells that would respond to insulin stimulation well usually don't have many IRAP-pHluorin fusion events at the PM before insulin stimulation.

Acknowledgement

References

1. Bogan JS (2012) Regulation of glucose transporter translocation in health and diabetes. Annu Rev Biochem 81:507–532

2. Bryant NJ, Govers R, James DE (2002) Regulated transport of the glucose transporter GLUT4. Nat Rev Mol Cell Biol 3:267–277

3. Leto D, Saltiel AR (2012) Regulation of glucose transport by insulin: traffic control of GLUT4. Nat Rev Mol Cell Biol 13:383–396

4. Sano H, Kane S, Sano E, Miinea CP, Asara JM, Lane WS, Garner CW, Lienhard GE (2003) Insulin-stimulated phosphorylation of a Rab GTPase activating protein regulates GLUT4 translocation. J Biol Chem 278:14599–14602

5. Kane S, Sano H, Liu SC, Asara JM, Lane WS, Garner CC, Lienhard GE (2002) A method to identify serine kinase substrates. Akt phosphorylates a novel adipocyte protein with a Rab GTPase-activating protein (GAP) domain. J Biol Chem 277:22115–22118

6. Chen Y, Wang Y, Zhang J, Deng Y, Jiang L, Song E, Wu XS, Hammer JA, Xu T, Lippincott-

Schwartz J (2012) Rab10 and myosin-Va mediate insulin-stimulated GLUT4 storage vesicle translocation in adipocytes. J Cell Biol 198:545–560

7. Chen Y, Lippincott-Schwartz J (2013) Rab10 delivers GLUT4 storage vesicles to the plasma membrane. Commun Integr Biol 6:e23779

8. Sano H, Eguez L, Teruel MN, Fukuda M, Chuang TD, Chavez JA, Lienhard GE, McGraw TE (2007) Rab10, a target of the AS160 Rab GAP, is required for insulin-stimulated translocation of GLUT4 to the adipocyte plasma membrane. Cell Metab 5: 293–303

9. Foley K, Boguslavsky S, Klip A (2011) Endocytosis, recycling, and regulated exocytosis of glucose transporter 4. Biochemistry 50:3048–3061

10. Maxfield FR, McGraw TE (2004) Endocytic recycling. Nat Rev Mol Cell Biol 5:121–132

3D Time-Lapse Analysis of Rab11/FIP5 Complex: Spatiotemporal Dynamics During Apical Lumen Formation

Anthony Mangan and Rytis Prekeris

Abstract

Fluorescent imaging of fixed cells grown in two-dimensional (2D) cultures is one of the most widely used techniques for observing protein localization and distribution within cells. Although this technique can also be applied to polarized epithelial cells that form three-dimensional (3D) cysts when grown in a Matrigel matrix suspension, there are still significant limitations in imaging cells fixed at a particular point in time. Here, we describe the use of 3D time-lapse imaging of live cells to observe the dynamics of apical membrane initiation site (AMIS) formation and lumen expansion in polarized epithelial cells.

Key words Apical lumen, Time-lapse microscopy, Matrigel, 3D tissue culture, Epithelial cell polarity

1   Introduction

Epithelial cells are highly specialized cells that line many tissue cavities and often function as barriers within many organs. Epithelial cells are structurally and functionally polarized to form an apical domain that faces the intertissue cavity, or lumen, and a basolateral domain that mediates the anchoring of epithelial cells to each other and to the extracellular matrix [1, 2]. Additionally, epithelial cells also form highly polarized multicellular structures, the process that is a key step during tissue morphogenesis and function. The coordinated polarization of multiple epithelial cells and the process of lumen formation during tissue morphogenesis remain to be fully understood and have been the focus of research in many laboratories. There are many pathways of apical lumen formation, which include wrapping, budding, and lumen formation *de novo* from nonpolarized progenitor cells [1, 2]. It is now well established that *de novo* lumen formation and epithelial polarization begin at the first cell division and that polarized endocytic transport of apical cargo is crucial to lumen initiation and formation [3]. The budding and transport of these apical vesicles is mediated by the interaction of the small monomeric GTPase, Rab11, with its binding partner

FIP5 (Rab11 family interacting protein-5) [4–6]. It was shown that apical lumen formation is initiated at late telophase by targeted transport and fusion of Rab11/FIP5-containing apical endosomes at a specific location between dividing cells, known as the apical membrane initiation site (AMIS), which is marked by many tight junction proteins including ZO1 and Cingulin [3, 7, 8]. The pathways underlying the regulation and dynamics of Rab11/FIP5-endosome transport during epithelial tissue morphogenesis have yet to be determined.

Fluorescent microscopy has proven to be a useful tool in studying the mechanisms and dynamics of lumen formation and many other pathways by allowing visualization of colocalization and distribution of proteins in cells. While imaging of polarized epithelial cells grown on two-dimensional (2D) filters is most widely used, it is not as sufficient for looking at the development of three-dimensional (3D) multicellular structures such as the apical lumen. Instead, epithelial cells can be grown in 3D culture by suspending in Matrigel matrix, which mimics the extracellular matrix and allows formation of 3D cysts with internal apical environments [7, 8]. Although the 3D cysts can be fixed and immunolabeled, this method limits the viewing of cells at a single time point and thus is not adequate for determining the timing and dynamics of apical lumen formation. These limitations can be overcome with the use of live imaging of tagged proteins in live cells, which enables the following of a single cell through all of the stages of division as well as lumen formation and expansion.

We have created a protocol for 3D time-lapse analysis of apical lumen formation using Madin–Darby canine kidney (MDCK) cells [3, 9]. Using this technique we were able to determine that Cingulin is one of the first proteins recruited to the AMIS during late telophase, and that the Rab11/FIP5 endosomes are transported after AMIS formation around the midbody [3]. This 3D time-lapse microscopy approach has greatly expanded our knowledge of the machinery mediating lumen formation by allowing us to elucidate the timing of certain steps in the overall mechanism. Furthermore, this 3D time-lapse imaging method can now also be used to further expand our understanding of many molecular processes governing epithelial tissue morphogenesis.

2   Materials

2.1   3D Tissue Culture

1. Type II Madin–Darby canine kidney (MDCK) cells.

2. MDCK media: Add 50 mL fetal bovine serum (FBS) and 5 mL penicillin–streptomycin (10,000 U/mL) to 500 mL 1× Dulbecco's Modified Eagle Medium (DMEM, 4.5 g/L glucose, L-glutamine) and filter-sterilize.

3. 1× Phosphate buffered saline (PBS).

4. 1× 0.25 % Trypsin–EDTA.

5. Matrigel growth factor reduced basement membrane matrix (Corning Life Sciences).

6. Tissue culture (100 mm) and 5 cm gridded glass-bottom (35 mm) dishes (Ibidi).

2.2 Microscopy

1. Inverted Axiovert 200 M fluorescent microscope (Zeiss) with 63× oil immersion lens and QE charged-couple device camera (Sensicam).

2. Slidebook 5.0 (Intelligent Imaging Innovations) 3D rendering and exploration software.

3 Methods

Carry out **steps 1–8** in a tissue culture hood.

1. Plate MDCK cells on 100 mm tissue culture plate in 10 mL MDCK media and let grow for 24 h at 37 °C (*see* **Note 1**).

2. 1–2 h before plating cells take an aliquot of Matrigel and set in on ice to thaw out. It is very important to keep Matrigel cold even while thawing, since it rapidly solidifies at room temperature.

3. Aspirate media and rinse cells with 10 mL PBS. This is the key step. Leaving some of the serum-supplemented media will inhibit trypsin and will make very difficult to lift individual MDCK cells.

4. Add 2 mL 0.25 % trypsin–EDTA and let sit at 37 °C for 10–15 min. MDCK cells are usually difficult to dislodge. Thus, if needed, they can be incubated for 20–25 min.

5. Dislodge cells by gently tapping at the side of 100 mm dish. Harvest cells by adding 8 mL MDCK media to plate and transferring cells to 15 mL tube. Sediment cells by centrifugation at $128 \times g$ for 3 min.

6. Aspirate media and resuspend cells in 1 mL of MDCK media by pipetting up and down 50–100 times using 1 mL pipette tip (*see* **Note 2**).

7. Count cells to determine number of cells/mL and add 20,000 cells (*see* **Note 3**) to 25 μL MDCK media in 1.5 mL Eppendorf tube (*see* **Note 4**).

8. Make a 75 % Matrigel solution by adding 75 μL Matrigel to the 25 μL cell solution from **step 7** (*see* **Note 4**). Gently mix by pipetting up and down. Immediately place cell/Matrigel mix by placing a drop onto center of 5 cm gridded glass-bottom dish.

This step needs to be done quickly, since Matrigel–cell mixture solidifies readily at room temperature.

9. Put cells in the incubator and let solidify in tissue culture incubator at 37 °C for 30 min.

10. Add 5 mL MDCK media to dish and let cells acclimate for 6–12 h at 37 °C. Typically cells will start dividing within 12 h after embedding. Imaging them within 6–12 h time period will ensure that at least some cells will be undergoing first cell division.

11. Mount dish on fluorescent microscope and use a gridded chart to label the location of several individual cells (*see* **Note 5**), especially those that may be in metaphase (starting division).

12. Adjust focus to set top and bottom of each cell (*see* **Note 6**) and take initial 0.2 μm-step z-stack images.

13. Repeat imaging according to time frame for desired observation. This will result in taking a mini-z-stack for every time point. Generally, avoid taking more than 50 time-lapse z-stacks (*see* **Note 7**). To visualize AMIS formation during cell division, we typically use 10 min time lapse (Fig. 1). To visualize lumen formation and expansion, we use 30 min time lapses (Fig. 2). Finally, if the motility of individual Rab11/FIP5 endosomes needs to be observed, we use 200–500 min time lapse. Use grid etched in glass to locate various cells for imaging at different time points.

14. Taking mini-z-stacks at every time point allows the use of post-acquisition image analysis to generate three-dimensional images of MDCK cells at each time point during lumen formation. Alternatively, individual images that best represent the lumen formation dynamics can be selected and displayed/analyzed for every time point.
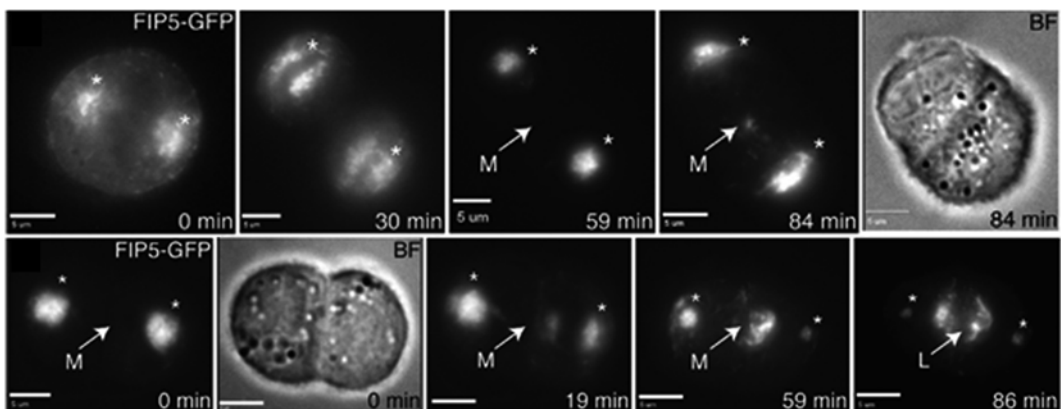
Fig. 1 Live imaging of AMIS formation and lumen expansion in MDCK cells expressing FIP5-GFP. Images were taken every 10 min to follow FIP5 transport from the centrosome to the midbody. Shown are the single images taken from the mini-z-stack at selected time points (reproduced from [3] with permission from EMBO Reports)
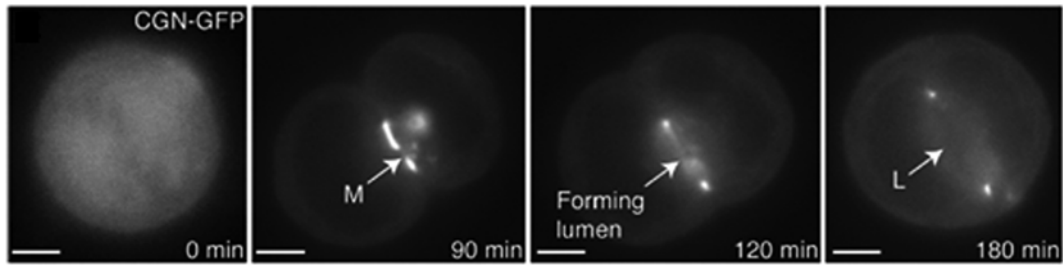
Fig. 2 Live imaging of lumen formation in MDCK cells expressing GFP-Cingulin (CGN). Images were taken every 30 min to follow Cingulin concentration at the midbody and expansion of the lumen during cell division. Shown are the single images taken from the mini-z-stack at selected time points (reproduced from [3] with permission from EMBO Reports)

4   Notes

1. The plated cells should not be fully confluent since cells need to be in growth phase. Typically we want to have cells at 50–70 % confluency after 24 h incubation. Thus, we usually plate cells at 30 % confluency.

2. Pipetting up and down many times helps to separate cells. It is crucial for this assay to embed individual cells in Matrigel. Embedding cell clumps will lead to formation of cell aggregates with multiple lumens. We found that pipetting cells 50 times with a 1 mL pipette usually gives a maximum number of individual cells; however, this number may vary. Thus, it is advisable to initially pipette cells varying number of times, while monitoring the efficiency of cell separation.

3. The optimum number of cells to plate may vary. Plating too many cells may cause clumping of dividing cells and overlap of fluorescence, making it difficult to distinguish single cells and observe them over time. Plating too few cells will make it more difficult to find single cells that are entering metaphase. We recommend testing a range of 10,000–50,000 cells to find the optimum number of cells for each assay.

4. The percentage of Matrigel may also vary between 25 and 80 %. The volume of media to suspend cells in and volume of Matrigel added can be adjusted to determine ideal conditions. In lower concentrations of Matrigel, cells may sink through the Matrigel matrix (during process of solidifying the Matrigel) and stick to the bottom of the plate, counteracting the function of the Matrigel to observe the cells suspended in the matrix. If the Matrigel concentration is too high, the cells might not be able to suspend in the matrix and instead would just sit on top, which is again not ideal for 3D imaging.

5. Isolated cells will be more ideal for imaging. As nearby cells divide and form cysts, the fluorescence can interfere with the cells you are trying to follow.

6. To be sure to include the whole cell in the range of imaging from top to bottom, it is best to set the focus a little beyond the point when the cell first begins to blur.

7. Taking fewer time points or fewer images in each mini-z-stack will decrease photodamage to cells. Excessive imaging can be a problem, since mitotic cells are especially sensitive to photo-damage. Shorter exposures will also reduce photobleaching. On the other hand, using long time lapses increases the risk of missing the critical steps of the observation.

Acknowledgement

References

1. Martin-Belmonte F et al (2008) Cell-polarity dynamics controls the mechanism of lumen formation in epithelial morphogenesis. Curr Biol 18(7):507–513

2. Bryant DM, Mostov KE (2008) From cells to organs: building polarized tissue. Nat Rev Mol Cell Biol 9(11):887–901

3. Li D et al (2014) FIP5 phosphorylation during mitosis regulates apical trafficking and lumenogenesis. EMBO Rep 15(4):428–437

4. Prekeris R, Davies JM, Scheller RH (2001) Identification of a novel Rab11/25 binding domain present in Eferin and Rip proteins. J Biol Chem 276(42):38966–38970

5. Prekeris R, Klumperman J, Scheller RH (2000) A Rab11/Rip11 protein complex regulates apical membrane trafficking via recycling endosomes. Mol Cell 6(6):1437–1448

6. Hales CM et al (2001) Identification and characterization of a family of Rab11-interacting proteins. J Biol Chem 276(42): 39067–39075

7. Bryant DM et al (2010) A molecular network for de novo generation of the apical surface and lumen. Nat Cell Biol 12(11):1035–1045

8. Willenborg C et al (2011) Interaction between FIP5 and SNX18 regulates epithelial lumen formation. J Cell Biol 195(1):71–86

9. Li D, Kuehn EW, Prekeris R (2014) Kinesin-2 mediates apical endosome transport during epithelial lumen formation. Cell Logist 4(1): e28928

Chapter 16

In Vitro and In Vivo Characterization of the Rab11-GAP Activity of *Drosophila* Evi5

Carl Laflamme and Gregory Emery

Abstract

Small GTPases of the Rab family are master regulators of vesicular trafficking. As such, they control the spatial distribution of various proteins, including proteins involved in cell signaling and the regulation of cell polarity. Misregulation of Rab proteins is associated with a large array of diseases. Surprisingly, the target of some key regulators of Rab proteins, including many GTPase-activating protein (GAP) is still unknown. Identifying the target of a specific GAP requires the combination of both in vitro and in vivo experiments to avoid any misinterpretation. Here is described the methodology we used to characterize the Rab11-GAP activity of *Drosophila* Evi5. We first focus on the in vitro Rab11 effector pull-down assay we developed and then we detail the in vivo characterization of Rab11 activity during *Drosophila* border cell migration.

Key words GTPase-activating protein, Rab, Evi5, Rab11

1 Introduction

Small GTPases of the Rab family promote vesicle trafficking through their interaction with molecular motors and the initiation of the assembly of SNARE complexes. As every small GTPase, Rabs cycle between an active GTP-bound state and an inactive GDP-bound state. The transition between these states requires the interaction with helper proteins: GTPase-activating proteins (GAPs) and GDP–GTP exchange factors (GEF). Whereas the GEF proteins activate small GTPases, GAPs accelerate the GTPase activity of Rabs, resulting in their inactivation (Fig. 1). Here, we detail the methodology we used to characterize the Rab11-GAP activity of *Drosophila* Evi5, both in vitro and in vivo [1].

In vitro, the activity of a small GTPase can be determined by different methods. Among these, the direct measure of the amount of phosphate cleaved by the couple Rab/GAP to be tested is the most quantitative [2]. However, it requires purifying full-length Rab and GAP proteins, or the TBC domain (catalytic GAP domain)
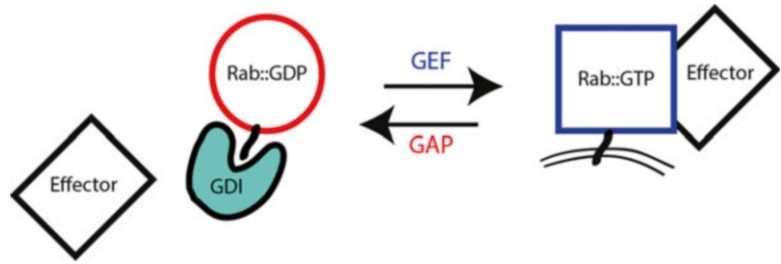
Fig. 1 Scheme of the Rab regulatory cycle. Inactive Rabs bind GDP and their geranylgeranyl groups at their C-terminus are masked through their interaction with GDI (GDP dissociation inhibitor). GEF proteins catalyze the release of GDP from the Rabs, thereby promoting the binding to GTP. Active GTP-bound Rabs are recruited to the surface of endomembranes where they interact with their specific effectors. GAP proteins accelerate the GTPase activity of the Rabs, promoting their inactivation

of the latter. Frequently GAPs are large proteins that become insoluble during the purification process. Since *Drosophila* Evi5 is precisely insoluble, we developed an effector pull-down assay that is described here. This method does not require protein purification and is based on the interaction between the small GTPase studied and an effector. Effectors bind to specific Rabs in their active confirmation. Effector pull-down assays are commonly performed for different GTPases (Rho and Arf GTPases), but have not been used systematically for Rab proteins. Here we measure the amount of Rip11, a member of the Rab11 family interacting protein (Rab11-FIP) [3], bound to Rab11 [1]. The expression of a GAP protein in cells should promote the GTPase activity, and hence the inactivation, of its target Rab. As a consequence, the GAP activity of Evi5 should decrease the quantity of Rip11 recovered after pull down of Rab11. Quantifying the amount of bound Rip11 in control condition or after the expression of Evi5 gives a valuable semiquantitative indication of Rab11 activity. A catalytic dead form of the GAP protein is a powerful control to demonstrate that the effect of a particular GAP is indeed due to its ability to induce the GTPase activity of its target [4].

Next we describe how to monitor Rab11 activity in vivo. Evaluating the GAP activity of a Rab-GAP in a physiological context using both gain- and loss-of-function increases significantly the confidence that a certain GAP indeed acts on a particular Rab. In our case, we used both phenotypical analysis of *Drosophila* border cell migration (not shown) and quantification of the distribution of the Rab11 effector Sec15 to demonstrate unambiguously that Evi5 acts as a Rab11-GAP during this particular migration. Briefly, we used the well-characterized UAS/Gal4 system to express a GFP fusion of the Rab11 effector Sec15 specifically in the border cell cluster [5]. Sec15 is a member of the exocyst complex [6] and is

distributed in small punctae in a wild-type situation. This distribution changes dramatically upon modulation of Rab11 activity. Indeed, expressing a GTP-locked (Rab11^{CA}) or a GDP-locked (Rab11^{DN}) form of Rab11 leads to larger or smaller GFP-Sec15 vesicles, respectively. Hence, the measure of the Sec15 vesicles can be used as an in vivo reporter for Rab11 activity [1]. Accordingly, depleting the Rab11-GAP should increase the size of GFP-Sec15 vesicles through the accumulation of GTP-bound Rab11. Conversely, overexpressing a Rab11-GAP should decrease the size of vesicles by promoting GTP hydrolysis. Since varying the expression level of Evi5 in border cells followed these predictions we concluded that indeed Evi5 acts as a Rab11-GAP. To describe very precisely the size of vesicles, we combined confocal analysis with a segmentation analysis software [1]. We think that similar approaches could be used to define other potential Rab/GAP pairs.

2 Materials

2.1 Effector Pull Down Using Copper-Inducible Stable Cell Lines Components

1. *Drosophila* S2 cells. Schneider's medium (Invitrogen) supplemented with 10 % FBS and 1 % Penicillin–Streptomycin.

2. Copper solution: 10 ml of a 0.5 M of $CuSO_4$. Weight 1.25 g of $CuSO_4$ in 10 ml of water. Sterilize by filtration.

3. Nonidet P-40 lysis buffer: 20 mM Tris, pH 8.0, 137 mM NaCl, 1 % Nonidet P-40, 10 % glycerol, and 1 mM EDTA, pH 8.0 with protease inhibitors. Prepare 1 l of a 1 M Tris pH 8 stock solution by adding 500 ml of H_2O in a 1 l glass beaker. Weigh 181.7 g Tris and transfer to the beaker. Mix and adjust pH with HCl. Pour solution in a 1 l cylinder and complete to 1 l with water. Store at 4 °C. Prepare 1 l of a 0.5 M EDTA pH 8 stock solution. Weigh 186.12 g of EDTA.$Na_2\cdot2H_2O$ and transfer it to 800 ml of H_2O in a 1 l glass beaker. Adjust pH using NaOH pellets or 10 N NaOH. Complete the volume of the solution to 1 l with H_2O.

2.2 In Vivo Rab11-GAP Assay Component

1. Fly stocks used. For expression of different transgenes specifically in border cells, the slbo-Gal4 driver was used, whereas c306-Gal4 was used to express Evi5 RNAi.: Slbo-Gal4/CyO; UAS-GFP-Sec15/TM3, c306-Gal4/FM7; UAS-GFP-Sec15/TM3, UAS- Evi5-Cherry/TM3, UAS-Evi5(RNAi)/TM3, UAS-Rab11(CA)/TM3, UAS-Rab11(DN)/CyO, UAS-Rab4(DN)/TM3

2. Fixing solution: PBS, 4 % PFA.

3. Permeabilization buffer: PBS, 0.3 % Triton

4. Alexa Fluor 555-labelled phalloidin to visualize F-actin.

5. DAPI to stain nuclei.

3 Methods

3.1 Characterization of Evi5 GAP Activity Toward Rab11 In Vitro

3.1.1 Generation of GST-Rab11-Inducible Stable Cell Lines

1. Culture S2 cells in Schneider's medium (Invitrogen) supplemented with 10 % FBS and 1 % Penicillin–Streptomycin. Plate three 10 cm cell culture dishes with 10×10^6 S2 cells in 10 ml of medium. The next day, transfect cells with one individual DNA construct: (a) GST-Rab11^{WT}, (b) GST-Rab11^{CA}, (c) a negative control plasmid (*see* **Note 1**). Two days posttransfection, add blasticidin to a final concentration of 20 μg/ml in each of the cell culture dishes to induce selection. Keep adding blasticidin while passing cells.

2. Optimize the concentration of copper ($CuSO_4$) to be used which leads to strong and even GST-Rab11 protein expression between your cell populations. Plate each well of a six well-plate for both GST-Rab11^{WT} and GST-Rab11^{CA} stable cell lines. Treat cells with (a) 0.05 mM, (b) 0.1 mM, (c) 0.3 mM, (d) 0.5 mM, (e) 0.8 mM, and (f) 1.0 mM for 24 h. Lyse your cells and perform a Western blot to observe which copper treatment induced the desired protein expression (*see* **Note 2**).

3.1.2 Effector Pull-Down Assay

1. Plate three 10 cm cell culture dishes of (a) GST-Rab11^{WT} cells and (b) GST-Rab11^{CA} with 16×10^6 cells per dish. The next day (Day 1), transfect both cell lines with (a) control plasmid, (b) HA-Evi5^{WT}, (c) HA-Evi5^{RA}, and, in all cases, with GFP-Rip11 (*see* **Note 3**).

2. One day posttransfection (Day 2), incubate cells with 0.8 mM of $CuSO_4$ for 24 h.

3. The next day (Day 3), detach cells by pipetting medium up and down. Transfer medium to 15 ml canonical tubes on ice. Centrifuge tubes at $400 \times g$ for 5 min. Remove the medium carefully and add 1 ml of Nonidet P-40 lysis buffer to the cell pellet. Transfer to 1.5 ml tubes with repetitive pipetting up and down. Incubate on ice for 30 min for proper cell lysis.

4. Centrifuge at $18,000 \times g$ for 10 min at 4 °C to get rid of cell debris. Transfer supernatant to fresh 1.5 ml tubes. Conserve 50 μl of supernatant for later use (lysate control).

5. Add 50 μl of 50 % slurry of glutathione-Sepharose beads equilibrated in lysis buffer to protein lysates and rock for 4 h at 4 °C. Centrifuge beads at $5,200 \times g$ for 30 s at room temperature. Wash beads with 1 ml of lysis buffer and incubate on ice for 1 min. Repeat the wash steps four times. Remove the last wash and add 4× loading buffer to the beads and to the lysate samples.

6. Run total protein lysates or eluted proteins on an 8–10 % SDS-PAGE; transfer proteins to nitrocellulose membranes; and detect Rab11, Evi5, and Rip11 using specific GFP, GST, and HA antibodies (Fig. 2).
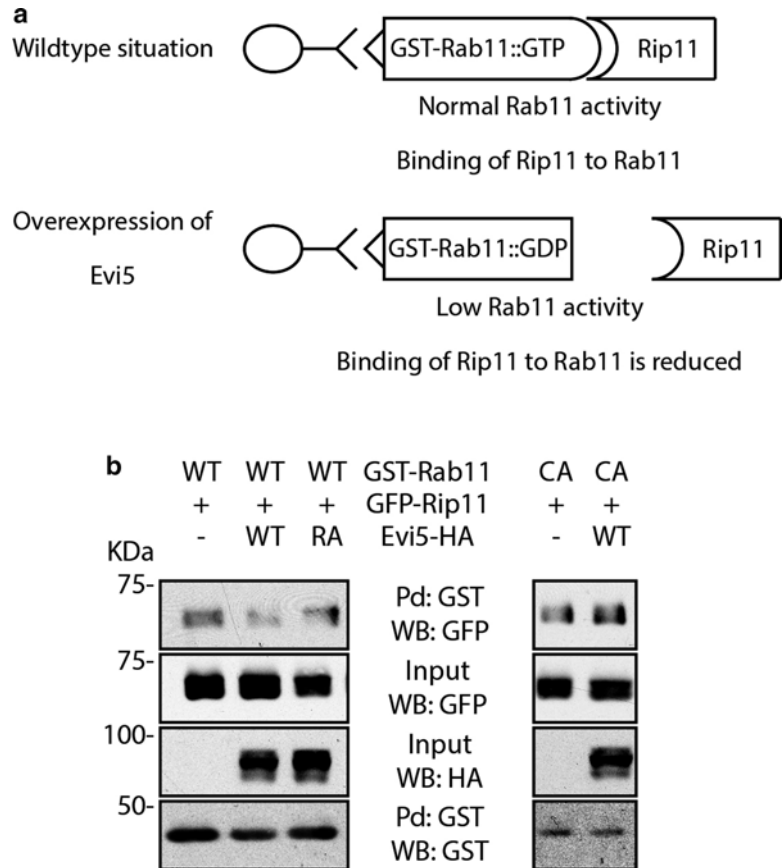
Fig. 2 (**a**) Schematic representation of the effector pull-down assay. Overexpression of Evi5 promotes the inactivation of Rab11, leading to the dissociation of Rip11 from Rab11. As a consequence, the amount of Rip11 recovered after Rab11 pull down is reduced. (**b**) Typical effector pull-down assay. S2 cells are cotransfected with GST-Rab11^{wt} (*left*) or GST-Rab11^{CA} (*right*) together with GFP-Rip11 with or without Evi5. Pull downs of Rab11 are performed and bound Rip11 is analyzed by western blotting. Reduction of Rip11 recovered after GST-Rab11^{WT} pull down when Evi5^{wt} is expressed (*lane 2*), but not when Evi5^{RA} is expressed (*lane 3*) as compared to a control situation (*lane 1*) indicates that Evi5 has a Rab11-GAP activity. Pull down of Rab11^{CA} (*lane 4* and *5*) is used to control that the decrease of Rip11 binding to Rab11^{wt} in the presence of Evi5^{wt} is not caused by a steric effect. Indeed, expressing Evi5 does not cause a decrease in Rip11 binding to Rab11^{ca}

3.2 Characterization of Evi5 GAP Activity for Rab11 In Vivo

3.2.1 Preparation of Drosophila Ovaries to Monitor Rab11 Activity

1. Cross slbo-Gal4/CyO, UAS-GFP-Sec15/TM3 females with males of different genotypes (a) w1118 (control), (b) UAS-Rab11DN, (c) UAS-Rab11^{CA}, (d) UAS-Rab4^{DN} (negative control), (e) UAS-mCherry:Evi5 and c306-Gal4; UAS-GFP-Sec15 females with (a) UAS-Evi5(RNAi) or (b) UAS-Cherry(RNAi) (control RNAi) males.

2. Keep female progeny of the proper genotype for later dissection. Put eight to ten females of 2–3 days old in fresh vials with dry

yeast at the bottom. Store vials at 29 °C. Repeat this procedure for one more day.

3. Dissect female ovaries [7]. Using sharp dissecting forceps, grab a female and hold it under PBS (in a small dissection pad). Pull off the tip of the abdomen and transfer the ovaries to a 200 µl tube containing PBS. Transfer up to ten pairs of ovaries in the same tubes.

4. Remove PBS from the tube and add 200 µl of fixing solution. Incubate for 20 min at room temperature. Wash three times with PBS. Incubate ovaries with permeabilization buffer for 30 min.

5. Stain ovaries with DAPI (10 µg/ml) and Alexa Fluor 555-labelled phalloidin (500×) for 1 h under rotation. Protect tubes from light. Wash ovaries three times with permeabilization buffer and incubate the last wash for 30 min under rotation. Do a final wash with PBS only to remove Triton.

6. Transfer ovaries to a microscopic slide. Gently tease apart the ovaries using forceps and make sure to spread as much as possible the ovarioles (*see* **Note 4**). Remove all the PBS and add a 50 µl drop of mounting media on the ovarioles. Carefully add the coverslip on the top of the mounting media. Seal with nail polish as needed.

3.2.2 Imaging Stage 9 Egg Chamber and Vesicle Analysis

1. With a 60× objective, search for stage 9 egg chambers where border cells have just detached from the epithelium. Select the proper orientation, crop up to three times on the cluster, and adjust the different parameters for optimal confocal images. Image all the different markers using adequate wavelengths and filter sets. Scan the entire border cell cluster by using 0.5 µm z-section. Image at least ten clusters for proper statistical measure (Fig. 3).

2. Perform analysis of GFP-Sec15 vesicles volume using your favorite segmentation algorithm. Determine the number and the volume (or the surface) of the vesicles. Represent the distribution of the number of vesicles by their size or, alternatively, the mean volume size. Perform adequate statistical analyses.

4 Notes

1. Rab11^{wt} was first subcloned in pGEX-6P1 to introduce a GST tag in N-terminus. GST-Rab11^{wt} was then cloned in the pMet-picoblast plasmid. The pMet promoter is active in presence of copper, which allows inducible GST-Rab11 expression. The gene picoblast encodes for resistance to blasticidin. We next introduce mutation to create S25N (DN) and the Q90L (CA)
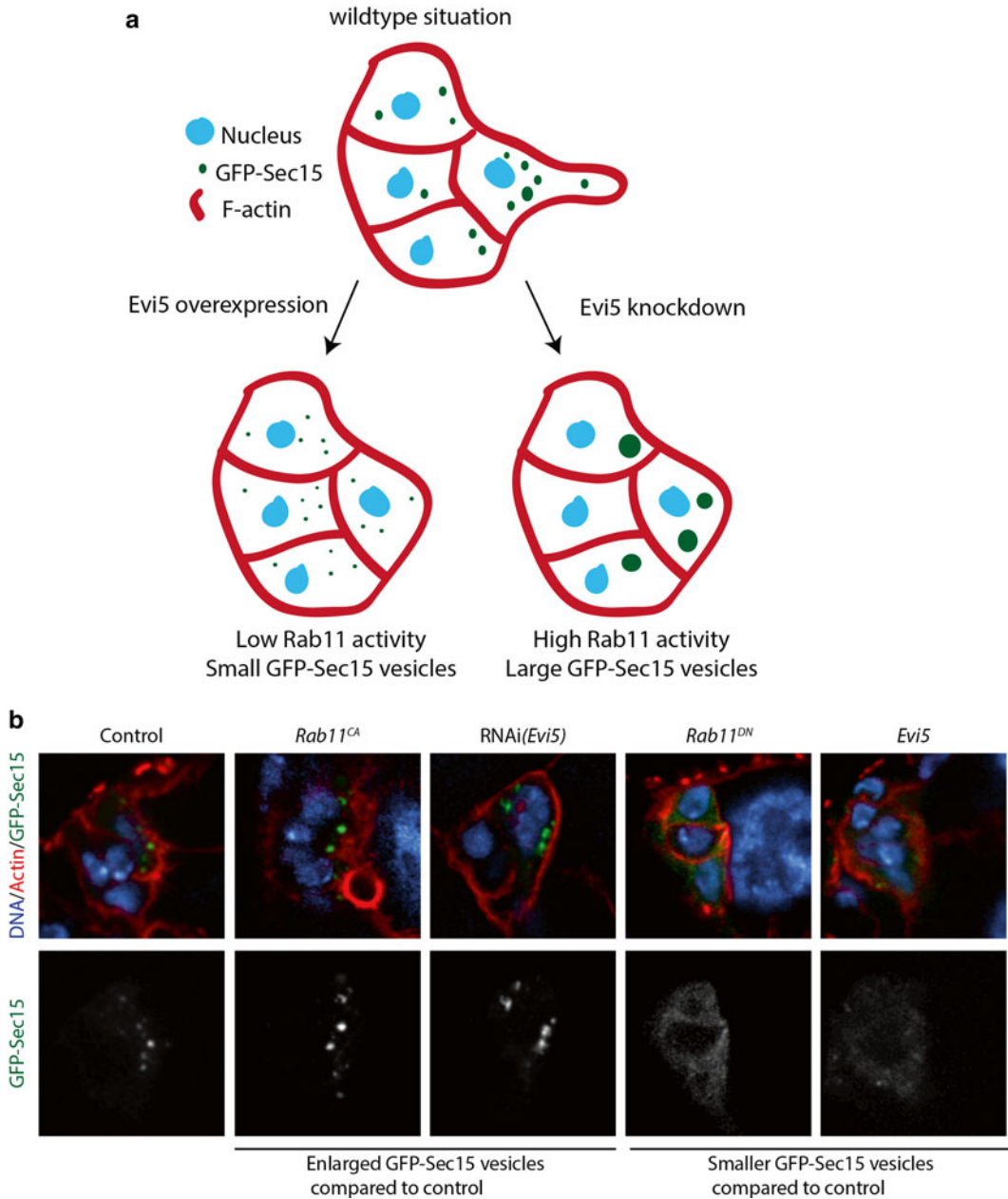
Fig. 3 (**a**) Schematic representation of the in vivo assay to determine Rab11 activity. Overexpression of Evi5 or Rab11^{DN} leads to the inactivation of Rab11, decreasing the volume of GFP-Sec15 vesicles. Conversely, knocking down Evi5 or expressing Rab11^{CA} leads to an increase in GFP-Sec15 vesicles volume. (**b**) Representative images showing GFP-Sec15 distribution in border cells in different conditions at the onset of migration

in Rab11 using the Quickchange site-directed mutagenesis technology (Agilent).

2. You may have to use different copper concentrations in your different cell lines to obtain even protein expression. In our

hand, optimal copper concentration was 0.8 mM for 24 h for each of our GST-Rab11 cell lines.

3. Evi5 was first subcloned in pDonor221 and transferred in pUASt-Dest29 using the Gateway system (Invitrogen). pUASt-Dest29 has a UAS promoter which requires GAL4 to be expressed. It is fused to GFP at its N-terminus. Evi5 Arg160 to Ala (Evi5^RA) catalytic dead mutant was generated by site-directed mutagenesis as before. Rip11 was cloned in the pAGW plasmid to express an N-terminal tagged version of Rip11 under the control of the actin promoter.

4. The ovarioles needs to be properly separated to take proper images of isolated egg chambers.

Acknowledgements

References

1. Laflamme C, Assaker G, Ramel D, Dorn JF, She D, Maddox PS, Emery G (2012) Evi5 promotes collective cell migration through its Rab-GAP activity. J Cell Biol 198(1):57–67. doi:10.1083/jcb.201112114

2. Yoshimura S, Haas AK, Barr FA (2008) Analysis of Rab GTPase and GTPase-activating protein function at primary cilia. Methods Enzymol 439:353–364. doi:10.1016/S0076-6879(07)00426-0

3. Prekeris R, Klumperman J, Scheller RH (2000) A Rab11/Rip11 protein complex regulates apical membrane trafficking via recycling endosomes. Mol Cell 6(6):1437–1448

4. Pan X, Eathiraj S, Munson M, Lambright DG (2006) TBC-domain GAPs for Rab GTPases accelerate GTP hydrolysis by a dual-finger mechanism. Nature 442(7100):303–306. doi:10.1038/nature04847

5. Assaker G, Ramel D, Wculek SK, Gonzalez-Gaitan M, Emery G (2010) Spatial restriction of receptor tyrosine kinase activity through a polarized endocytic cycle controls border cell migration. Proc Natl Acad Sci U S A 107(52):22558–22563. doi:10.1073/pnas.1010795108

6. Zhang XM, Ellis S, Sriratana A, Mitchell CA, Rowe T (2004) Sec15 is an effector for the Rab11 GTPase in mammalian cells. J Biol Chem 279(41):43027–43034. doi:10.1074/jbc.M402264200

7. Wong LC, Schedl P (2006) Dissection of Drosophila ovaries. J Vis Exp 1:52. doi:10.3791/52

Chapter 17

Characterization of the Role Rab25 in Energy Metabolism and Cancer Using Extracellular Flux Analysis and Material Balance

Shreya Mitra, Jennifer Molina, Gordon B. Mills, and Jennifer B. Dennison

Abstract

Rab25, by altering trafficking of critical cellular resources, influences cell metabolism and survival during stress conditions. Overall, perturbations in the vesicular trafficking machinery change cellular bioenergetics that can be directly measured in real time as Oxygen Consumption Rate, OCR (mitochondrial respiration) and Extracellular Acidification Rate, ECAR (glycolysis) by an extracellular flux analyzer (XF96, Seahorse Biosciences, MA). Additionally, overall turnover of glucose, lactate, as well as glutamine and glutamate can be measured biochemically using the YSI2900 Biochemistry Analyzer (YSI Incorporated, Life Sciences, OH). A combination of these two methods allows a precise and quantitative approach to interrogate the role of Rab25 as well as other Rab GTPases in central carbon energy metabolism.

Key words Extracellular flux, Glycolytic index, Rab25, XF 96 extracellular flux analyzer, YSI biochemistry analyzer, Glucose, Lactate, Glutamine, Breast cancer

1 Introduction

Cellular energy is generated from both mitochondrial and nonmitochondrial compartments with the relative contribution of each having prognostic value in cancer progression [1–5]. Upstream control of oxidative phosphorylation as well as glycolysis involves regulation of growth factor and nutrient receptors by trafficking molecules [6–9]. In cancer, derailed endocytosis [10, 11] is an emerging trait with Rab25-mediated trafficking of receptors and transporters likely to contribute toward bioenergetic fitness of cancer cells in response to nutrient and other stresses [9, 12–14].

Membrane-associated Rab25 forms an integrated system with its GAPs, GEFs, effectors, as well as actin–myosin motors proteins [15–17]. Experimental conditions must be simultaneously stringent and benign to maintain the specific organic interactions that allow evaluation of contributions of Rab25 and other GTPases toward cellular energetics. Furthermore, the complex and dynamic nature of a

cancer cell's metabolic profile introduces an added challenge to experimental design. The two complementary methods described here are noninvasive, involve minimal processing of cells, require small amounts of sample, maintain physiologic nutrient conditions, and allow interrogation of multiple parameters at the same time.

The XF Extracellular Flux analyzer provides a comprehensive metabolic image of the cell by simultaneously measuring changes in cellular respiration and glycolysis from extracellular oxygen (measured as the oxygen consumption rate or OCR) and free protons (a readout of extracellular acidification rate or ECAR). The measurements are performed in real time using solid-state sensor probes (an optode composed of an oxygen-sensitive fluorescent metal complex and a pH-sensitive fluorophore, respectively) which plunge 200 μm above the cell monolayer and entrap a transiently isolated microchamber of less than 2 μl of medium within the well of a 96-well plate. Metabolites or drugs can be added successively by an in-built automated delivery system. Because cell viability is maintained during the assay, multiple measurements, including cell count or protein content in each well, can be obtained from the same cell population. However, the most accurate readings for normalization require a separate plate because drug treatment can cause the cells to detach after the Seahorse readings. The indices of mitochondrial function are tested using pharmacological inhibitors of the bioenergetics pathway. Typically, a chemical uncoupler of electron transport and oxidative phosphorylation that depolarizes the inner mitochondrial membrane potential (FCCP) is used along with a mitochondrial inhibitor of complex I (Rotenone) and ATP-synthase/complex V inhibitor (Oligomycin A) (Fig. 1).

The O_2 flux is a direct readout for oxidation, both mitochondrial and nonmitochondrial. The major component of ECAR for cancer cells is lactate flux, a measure of glycolysis in the cytoplasm known as the Warburg Effect [18, 19]. Rab25-mediated uptake and recycling of RTKs, glucose transporters, as well as other nutrient molecules alter metabolite turnover within cells, which, in turn, affects cellular energy reserves such as glycogen storage [12]. Complementing the OCAR and ECAR measurements with data assessment of turnover of key metabolite in the system will provide additional mechanistic insights. Concentrations of glucose and lactate (as well as glutamine and glutamate) in the media surrounding the cell can be measured from plates using an enzyme electrode biosensor technology-based Biochemistry Analyzer, namely, the YSI 2900 (Fig. 2).

2   Materials

2.1   Cell Lines and Constructs

Breast and ovarian cancer cell lines, namely, MCF7, T47D, MDA 231, Hey, and A2780 (all from ATCC) were regularly cultured and maintained in DMEM 1× with 4.5 g/l glucose and
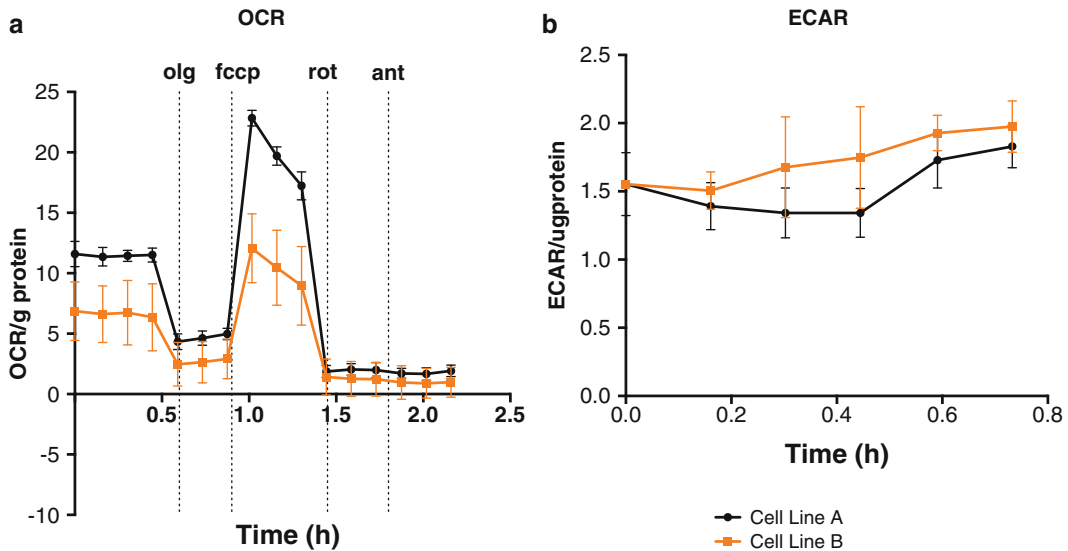
Fig. 1 Example of XF96 analyzer data. A representative example in (**a**) shows the mitochondrial respiration and glycolytic activity derived from a typical experiment using ovarian cancer cells. Measurement of four initial baseline OCR readings are followed by recording the effects of sequential addition of Oligomycin (1 mg/ml), FCCP (1 μM), Rotenone (1 μM), and Antimycin A (1 μM) on OCR in two isogenic lines with variable levels of Rab25. Altering Rab25 significantly changes baseline OCR as well as ATP-dependent respiration (addition of Oligomycin). A striking effect is observed with FCCP suggesting that the cells with altered Rab25, represented in *yellow*, will have reduced respiratory capacity. Addition of Rotenone and Antimycin inhibits complex III and I, respectively, further decreasing OCR. These inhibitors diagnose the nonmitochondrial fraction of respiration. Overall the OCR data suggests that Rab25 levels shifts cell toward a more glycolytic profile. Analysis of baseline ECAR (**b**) shows rapid increase in ECAR in the cells represented by the *yellow line*. This increase in ECAR is due to a shift toward glycolysis and increased lactic acid export from cells leading to acidification of the surrounding media, i.e., the Warburg Effect. The OCR and ECAR data represented here are normalized to total protein in that well

L-GLUTAMINE, without sodium pyruvate (Corning CellGro 10-017CV, VA-20109) with 5 % FBS. Rab25 expression was manipulated in the cell lines using Lenti-viral Rab25 overexpressing vectors (Open Biosystem, GE Dharmacon, CO), as well as short hairpin RNA targeting Rab25 (On-Target Plus Smartpool™ small interfering RNAs toward Rab25 Dharmacon, GE) following manufacturer's instructions. The overexpression and knockdown conditions were optimized and tested for mRNA as well as protein expression before using the lines for the metabolic assays.

2.2   Equipment

1. XF 96 Extracellular Flux Analyzer (Seahorse Bioscience, MA): Quantifies oxygen consumption and extracellular acidification rates.

2. YSI 2900 Biochemistry Analyzer equipped with Glucose/L-LACTATE membranes and Glutamine/Glutamate membrane with YSI Buffer (Life Sciences, Yellow Springs, OH): Quantifies glucose and lactate levels in media.

a   Inputs and Outputs from the Krebs Cycle
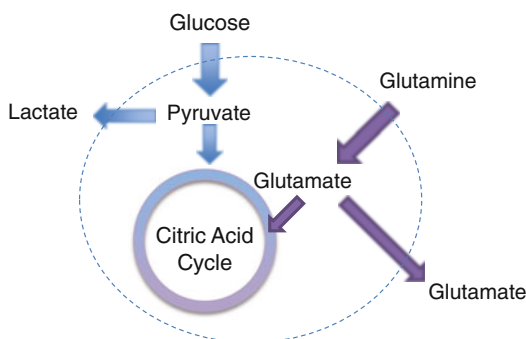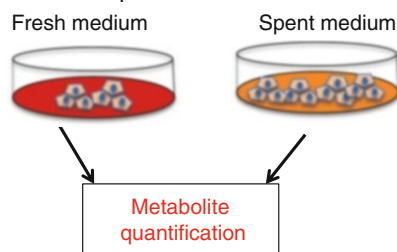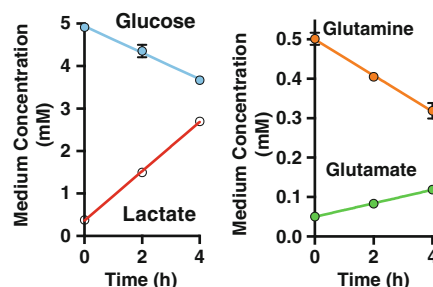
Fig. 2 Material balance for cell lines using YSI bioanalyzer. (**a**) Shows the input and output of key metabolites in the Krebs Cycle that are measured by the YSI bioanalyzer to calculate metabolite flux. (**b**) Represents the experimental design while (**c**) formulates a calculation for net changes in output and input over time. Finally (**d**) is a representative figure showing increased glucose and glutamine uptake from the media and increased lactate and glutamate production

2.3 Materials for XF96 Extracellular Flux Assay (Seahorse)

1. 96-Well PET plates supplied by Seahorse Biosciences.

2. Flux packs (Seahorse)-V-bottom 96-well drug-loading plate (Sensor Cartridge).

3. Multichannel Pipette.

4. Non-CO_2 Incubator.

5. *XF Assay Medium*: Bicarbonate free DMEM (Seahorse Bio, 100965-000), 0.1 N NaOH, Glutamax (Gibco, 35050-061), Sodium Pyruvate (Sigma, P4562), D-Glucose (Sigma), Na-Lactate (Sigma), L-Glutamine (Sigma). Adjust pH to 7.4 at 37 °C.

6. *Calibration Buffer*: Seahorse Calibrant (Seahorse Bio, 100840-000).

7. *Drugs:* Carbonyl cyanide p-trifluoromethoxyphenylhydrazone or FCCP (0.1 μM, 1 μM, 3 μM, 10 μM); Oligomycin (1 mg/ml); Rotenone (1 μM) Antimycin (1 μM).

2.4 Materials for YSI 2900 Biochemistry Analyzer

1. Glucose membrane (Cat # 2365).

2. L-Lactate membrane (Cat # 2329).

3. Glutamine membrane (Cat # 2735).

4. Glutamate membrane (Cat # 2754).

5. YSI Buffer (Cat # 2357).

6. Standard Solutions for standard curves for Glucose (10 mM) and L-Lactate (5 mM).

7. 96 Well plates for YSI reading; 12 or 24 well plates for cell seeding.

8. *YSI Assay Media* (*for physiological conditions*): Glucose free, L-Glutamine free, Na-Pyruvate free DMEM (Cat#17207-CV Corning CellGro) with addition of 5 mmol/l glucose, 0.5 glutamine.

9. PBS (Hyclone, Thermo).

---

3 Methods

3.1 XF 96 Extracellular Flux Analyzer (Seahorse Bioscience)

Cell Plating and Plate Preparation for XF 96 Analyzer

1. Rab25 expression is manipulated stably or transiently in cells using standard transfection or transformation protocols [20, 21]. In case of transient genetic manipulations, cells were harvested and replated for the assays 24 h after transfection or transformation. Alternatively, the assay can be performed after a selection for stable clones has been verified.

2. For adherent cells with 15–18 h duplication time, at least 5 replicate wells are seeded at 8,000–16,000 cells per well in a final volume of 80 μl of regular growth media. Seeding is designed to have approximately 70 % cell confluence at the start of the Seahorse run (*see* **Notes 1** and **3**). The corner wells (*A1, H1, A12, H12*) of the plate should be cell free and loaded with media alone for background correction. To obtain uniform loading, it is recommended to make up appropriate stock solutions and then pipette 80 μl of final cell suspension using a multichannel pipettor. If cells are clumpy, they should be separated either by gentle vortexing or by aspirating through a suitable sized needed to obtain a single-cell suspension for even plating (*see* **Note 6)**. Cells are allowed to attach as a monolayer and grow overnight in the incubator at 37 °C under 5 % CO_2. Cells should be seeded in standard DMEM, 5 % FBS medium.

3. To maximize reproducibility, XF96 Sensor Cartridges should be hydrated overnight in 200 μl of XF Calibrant Buffer at room temperature.

Media Exchange

4. Inspect the cells in the XF96 cell culture plate under microscope to ensure uniform cell seeding.

5. The growth media in the well is exchanged out manually about 1 h prior to the assay and replaced with XF assay medium (serum-free, bicarbonate-free DMEM without phenol red with addition of 5 mmol/l glucose, 0.5 mM glutamine) adjusted pH to 7.4 at 37 °C. The medium provided by the manufacturer contains Glutamax, so it does not require glutamine supplementation. However, Glutamax due to its prolonged stability may mask subtle changes and skew the data. The instrument does not have CO_2 atmosphere control; hence a bicarbonate-free medium is required. Because ECAR readings are dependent on buffer capacity, higher buffer capacity reduces the sensitivity of ECAR measurements. If desired, the net proton production rate can be determined if the buffer capacity is factored into the calculations (*see* **Note 5**).

6. To prevent disruption of the monolayer, 50 μl of original medium is removed and wells washed twice with 200 μl of XF assay medium. After the last wash 130 μl of assay medium is added back resulting in total 160 μl of medium per well. Incubate the XF96 cell culture plate at 37 °C in a non-CO_2 incubator for at least 30 min prior to loading plate in XF96 instrument to allow cells to equilibrate to the new media. Alternatively, all of the medium can be removed by hand pipetting and replaced with XF Assay Medium without washing the wells. Hand pipetting is required because removal of medium by vacuum will dehydrate and lyse the cells.

Loading the Sensor Cartridge

7. The instrument is turned on and the XF software initiated to stabilize the instrument at 37 °C before preparing the Sensor Cartridge.

8. Drugs are typically dissolved in DMSO and need to equilibrate to room temperature.

   For initial experiments, the FCCP response needs to be tested by using serial dilutions of FCCP in DMSO, beginning by diluting the 10 mM stock to 2 mM (*see* **Note 2**).

   Up to four drugs per well may be loaded on the assay cartridge.

9. The assay cartridge is incubated at 37 °C non-CO_2 incubator until ready for use. However, the cartridge can be effectively hydrated at room temperature. Incubation in a 37 °C oven without a water pan will evaporate the calibrant solution in the outer wells, so the plate should not be kept for prolonged periods at 37 °C without wrapping the plate in plastic wrap (*see* **Note 4**).

10. Once the instrument is calibrated, the assay cartridge is carefully placed into the XF Analyzer plate holder aligning with the orientation markers. This is done prior to loading the cell plate to allow automatic calibration of optical sensors. When the

calibration process is complete (screen readout), the cell culture plate is inserted (without the lid) into the instrument, ensuring correct orientation. Prior to calibration, the assay cartridge is equilibrated for at least 10-min in the instrument. This equilibration time is set as a default by the software. More time may be required to increase the temperature of the calibrant solution to 37 °C depending on the length of time to load the drug solutions.

XF Analyzer Readings and Interpretation

11. The software is set up to measure baseline OCR (nmoles/minute) and ECAR (mpH/minute) rates thrice before the preloaded inhibitors, stimulants, substrates, or compounds are pneumatically injected into the media in each well and allowed to mix. However, baseline OCR and ECAR measurement readings can be extended if needed. OCR and ECAR measurements following addition of drugs are measured multiple times. After baseline oxygen consumption is determined, Oligomycin is injected through the ports, followed by FCCP and Rotenone/Antimycin A. The *ATP-dependent* OCR fraction is calculated by subtracting the decrease in OCR post Oligomycin addition. The remaining OCR at this point is *non-ATP proton leak* and the *nonmitochondrial oxygen* consumption. Addition of a correctly titrated amount of FCCP allows determination of the *maximal respiration capacity*. Lastly, the *nonmitochondrial* oxygen consumption is determined when all mitochondrial function is inhibited via electron flux through complex III with injection of Rotenone or Antimycin A.

12. Typically, for each condition, measurements are averaged over 3–4 readings taken at 5-min intervals. For initial set up, the 5-min cycle can be set up as a 2-min mix period, 1-min wait, and a 2-min measuring time. This 5-min cycle should be modified based on the inherent metabolic nature of the cells. For cells with high respiration rate, the measuring time should be lowered and mixing time increased and vice versa for cells with low oxidative potential. A total of about six cycles is recommended for each drug treatment. Longer times may be required for the initial readings, especially if the plate is loaded immediately after medium exchange. A standard assay time is 35–90-min depending on the optimized measuring and mixing cycles set. The cells remain viable during the whole process. With robust cells, the assays can be extended for several hours.

13. Normalization of data can be done via cell number, protein content, or the basal OCR and ECAR rates. At the end of the XF assay, the plate can be examined to evaluate the viability and characteristics of cells since some of the treatments and the plunger action may cause cell detachment or death. The exist-

ing media is carefully aspirated and cells lysed for protein content with a BCA assay. A more reliable approach is to fix the cells with paraformaldehyde and stain with a nuclear dye (DAPI) for automated imaging. Alternatively, nuclear stains such as Hoechst #33342 Fluorescent Stain can be used directly to quantify live or fixed cells.

3.2 Measuring Metabolite Turnover by YSI 2900

1. The YSI2900 is used to measure the total flux of glucose and lactate in cell lines. Typically cells are seeded in triplicate wells in 12- or 24-well plates for overnight in usual growth medium. Seeding is dictated by the duration of the assay. For up to 24-h time points, cells are seeded to reach 70–80 % confluence at the time of the YSI assay. The same time points can be seeded on the same plate if the time periods are relatively short (0, 1, 3, 6 h) so that the cell number does not change significantly.

2. Next day the growth medium is removed, cells are washed twice with medium, and replaced with YSI Assay media that can be either physiological levels of nutrients or other desired amounts (known amounts of glucose, glutamine, and lactate) (*see* **Notes 7** and **8**). The relative number of cells to the volume of media needs to be titrated to achieve robust and measurable levels or analytes at shorter time points. Typically this requires a confluency of at least 50 %. Low volumes of medium (i.e., 300 μl in 12-well plate) and physiological concentrations of glucose (5 mM) and glutamine (0.5 mM) are essential for this assay to work properly because depletion must be detected over a relatively short period of time.

3. About 500 ml of the YSI buffer is prepared following manufacturer's instruction and the respective membranes (Glucose and Lactate, or, Glutamine and Glutamate) are fitted on the instrument.

4. Next the YSI 2900 Instrument is calibrated and standard curves test run before loading the assay samples. One point calibration is typically used for this instrument with an intercept of zero.

5. Glucose and lactate in the extracellular media is measured at 0, 6, 12, and 24 h. At each time point, 250 μl of media from each well of the seeding plate is collected in a 96-well plate and kept at –20 °C till completion of collection for all the time points. The plate should be sealed with parafilm between collection points because the medium can evaporate and alter the reliability of the results. Because the machine uses 10–50 μl per reading and the prescribed volume allows measurement of multiple chemistry from the same plate, and the high volume minimizes any effect of evaporation. The zero hour is calculated at the point when the YSI Assay media is added. Standard solutions

for each of the analytes should be added at the end of each row to allow one-point calibration for each row.

6. At the time of media collection, cell number or protein concentration in the corresponding seeding well should be used to normalize the metabolite concentrations.

7. If the collected media samples were frozen they need to be thawed to room temperature before loading them on the instrument. The medium on the plate has to be well mixed. Because the volume is high (250 μl), a plate shaker is not adequate. Pipetting is required for effective mixing after freeze/thaw.

8. The media used at time "zero" is essential to calculate consumption and production.

9. After completion of instrument calibration, the 96-well plate design is laid out by using the Station tab. The instrument performed the appropriate biochemical analysis on the selected wells (*see* **Note 9**).

10. Output can be represented as changes in Lactate and Glutamate over time.

Output: $d[\text{Lactate}]/dt \; d[\text{Glutamate}]/dt$.

Similarly Input can be represented as: $-d[\text{Glucose}]/dt$ $-d[\text{Glutamine}]/dt$.

4 Notes

1. It is critical to establish an optimal plating density for the XF plates prior to running experiments. Typical seeding densities are 2–16,000 cells/well and these are typically grown over 24-h. We recommend testing the cells on the XF instrument measuring four basal rates followed by injection of 0.5 μM FCCP and measuring an additional four rates. An ideal plating density will give robust basal and FCCP-uncoupled rates. If the cells are too dense, the basal rates might be low and the uncoupled rate will often be unstable. Cell seeding number will depend on cell type and cell growth characteristics.

2. The optimum FCCP concentration is typically between 0.1 and 2 μM. These values are cell line dependent.

3. For suspension cell lines, wells can be pretreated with CellTak™ cell and tissue adhesive (Corning, Cat # 354240) per the manufacturer instructions on the day of the reading. In such cases about 1.6×10^4 cells per well is prepared in the exchange medium and plated on the day of the readings postapplication of CellTak™. OCR and ECAR readings are determined as mentioned earlier.

4. If the cartridge is being stored for more than 24-h, wrap para film around the edges to prevent evaporation.

5. The XF Assay medium is DMEM modified to use low phosphate (1 mM) to accommodate ECAR changes. The manufacturer also provides a low buffer DMEM but many other buffers can be used as long as they are devoid of bicarbonate buffer since the XF Analyzer instrument only maintains temperature and not CO_2 control.

6. Using a 200 μl pipette and dropping the cell suspension with moderate force on the walls toward the bottom of the well allows even cell distribution in 80 μl of media

7. Based on a specific query, the YSI as well as XF-assay media composition can be varied by altering or withdrawing glucose, lactate, or glutamate. Since many biochemical reactions are reversible, removing a key metabolite from the culture medium will allow a more sensitive assay condition.

8. Finally, the main cargo, such as RTKs and or integrins or glucose transporters trafficked by the Rab GTPase can be manipulated to further analyze the role of the Rab protein in cancer cell metabolism.

9. Typically, the most striking conditions from the YSI Assay are further analyzed to interrogate alterations in signaling pathways using a high-throughput proteomic assay, namely, the Reverse Phase Protein Array (RPPA) [22, 23].

Acknowledgements

References

1. Altenberg B, Greulich KO (2004) Genes of glycolysis are ubiquitously overexpressed in 24 cancer classes. Genomics 84(6):1014–1020. doi:10.1016/j.ygeno.2004.08.010

2. Tu SH, Chang CC, Chen CS, Tam KW, Wang YJ, Lee CH, Lin HW, Cheng TC, Huang CS, Chu JS, Shih NY, Chen LC, Leu SJ, Ho YS, Wu CH (2010) Increased expression of enolase alpha in human breast cancer confers tamoxifen resistance in human breast cancer cells. Breast Cancer Res Treat 121(3):539–553. doi:10.1007/s10549-009-0492-0

3. Geiger T, Madden SF, Gallagher WM, Cox J, Mann M (2012) Proteomic portrait of human breast cancer progression identifies novel prognostic markers. Cancer Res 72(9): 2428–2439. doi:10.1158/0008-5472.CAN-11-3711

4. Jerby L, Wolf L, Denkert C, Stein GY, Hilvo M, Oresic M, Geiger T, Ruppin E (2012) Metabolic associations of reduced proliferation and oxidative stress in advanced breast cancer. Cancer Res 72(22):5712–5720. doi:10.1158/0008-5472.CAN-12-2215

5. Dennison JB, Molina JR, Mitra S, Gonzalez-Angulo AM, Balko JM, Kuba MG, Sanders ME, Pinto JA, Gomez HL, Arteaga CL, Brown RE, Mills GB (2013) Lactate dehydrogenase B: a metabolic marker of response to neoadjuvant chemotherapy in breast cancer. Clin Cancer Res 19(13):3703–3713. doi:10.1158/1078-0432. CCR-13-0623

6. Cormont M, Le Marchand-Brustel Y (2001) The role of small G-proteins in the regulation of glucose transport (review). Mol Mem Biol 18(3):213–220

7. Handley MT, Morris-Rosendahl DJ, Brown S, Macdonald F, Hardy C, Bem D, Carpanini SM, Borck G, Martorell L, Izzi C, Faravelli F, Accorsi P, Pinelli L, Basel-Vanagaite L, Peretz G, Abdel-Salam GM, Zaki MS, Jansen A, Mowat D, Glass I, Stewart H, Mancini G, Lederer D, Roscioli T, Giuliano F, Plomp AS, Rolfs A, Graham JM, Seemanova E, Poo P, Garcia-Cazorla A, Edery P, Jackson IJ, Maher ER, Aligianis IA (2013) Mutation spectrum in RAB3GAP1, RAB3GAP2, and RAB18 and genotype-phenotype correlations in warburg micro syndrome and Martsolf syndrome. Hum Mut 34(5):686–696. doi:10.1002/ humu.22296

8. Honscher C, Mari M, Auffarth K, Bohnert M, Griffith J, Geerts W, van der Laan M, Cabrera M, Reggiori F, Ungermann C (2014) Cellular metabolism regulates contact sites between vacuoles and mitochondria. Dev Cell 30(1):86–94. doi:10.1016/j.devcel.2014.06.006

9. Shreya Mitra GBM (2013) Aberrant vesicular trafficking contributes to altered polarity and metabolism in cancer, vol ISBN 978-1-4614-6527, Vesicle trafficking in cancer. Springer, New York, NY

10. Mosesson Y, Mills GB, Yarden Y (2008) Derailed endocytosis: an emerging feature of cancer. Nat Rev Cancer 8(11):835–850. doi:10.1038/nrc2521

11. Mitra S, Cheng KW, Mills GB (2011) Rab GTPases implicated in inherited and acquired disorders. Seminars Cell Dev Biol 22(1):57–68. doi:10.1016/j.semcdb.2010.12.005

12. Cheng KW, Agarwal R, Mitra S, Lee JS, Carey M, Gray JW, Mills GB (2012) Rab25 increases cellular ATP and glycogen stores protecting cancer cells from bioenergetic stress. EMBO Mol Med 4(2):125–141. doi:10.1002/ emmm.201100193

13. Liu Y, Tao X, Jia L, Cheng KW, Lu Y, Yu Y, Feng Y (2012) Knockdown of RAB25 promotes autophagy and inhibits cell growth in ovarian cancer cells. Mol Med Rep 6(5):1006–1012. doi:10.3892/mmr.2012.1052

14. Agarwal R, Jurisica I, Mills GB, Cheng KW (2009) The emerging role of the RAB25 small GTPase in cancer. Traffic 10(11):1561–1568. doi:10.1111/j.1600-0854.2009.00969.x

15. Casanova JE, Wang X, Kumar R, Bhartur SG, Navarre J, Woodrum JE, Altschuler Y, Ray GS, Goldenring JR (1999) Association of Rab25 and Rab11a with the apical recycling system of polarized Madin-Darby canine kidney cells. Mol Biol Cell 10(1):47–61

16. Goldenring JR, Aron LM, Lapierre LA, Navarre J, Casanova JE (2001) Expression and properties of Rab25 in polarized Madin-Darby canine kidney cells. Methods Enzymol 329:225–234

17. Goldenring JR, Shen KR, Vaughan HD, Modlin IM (1993) Identification of a small GTP-binding protein, Rab25, expressed in the gastrointestinal mucosa, kidney, and lung. J Biol Chem 268(25):18419–18422

18. Vander Heiden MG, Cantley LC, Thompson CB (2009) Understanding the Warburg effect: the metabolic requirements of cell proliferation. Science 324(5930):1029–1033. doi:10.1126/science.1160809

19. DeBerardinis RJ, Lum JJ, Hatzivassiliou G, Thompson CB (2008) The biology of cancer: metabolic reprogramming fuels cell growth and proliferation. Cell Metabolism 7(1):11–20. doi:10.1016/j.cmet.2007.10.002

20. Cheng KW, Lahad JP, Kuo WL, Lapuk A, Yamada K, Auersperg N, Liu J, Smith-McCune K, Lu KH, Fishman D, Gray JW, Mills GB (2004) The RAB25 small GTPase determines aggressiveness of ovarian and breast cancers. Nat Med 10(11):1251–1256. doi:10.1038/ nm1125

21. Cheng KW, Lu Y, Mills GB (2005) Assay of Rab25 function in ovarian and breast cancers. Methods Enzymol 403:202–215. doi:10.1016/S0076-6879(05)03017-X

22. Hennessy BT, Lu Y, Gonzalez-Angulo AM, Carey MS, Myhre S, Ju Z, Davies MA, Liu W, Coombes K, Meric-Bernstam F, Bedrosian I, McGahren M, Agarwal R, Zhang F, Overgaard J, Alsner J, Neve RM, Kuo WL, Gray JW, Borresen-Dale AL, Mills GB (2010) A technical assessment of the utility of reverse phase protein arrays for the study of the functional proteome in non-microdissected human breast cancers. Clin Proteomics 6(4):129–151. doi:10.1007/s12014-010-9055-y

23. Carey MS, Agarwal R, Gilks B, Swenerton K, Kalloger S, Santos J, Ju Z, Lu Y, Zhang F, Coombes KR, Miller D, Huntsman D, Mills GB, Hennessy BT (2010) Functional proteomic analysis of advanced serous ovarian cancer using reverse phase protein array: TGF-beta pathway signaling indicates response to primary chemotherapy. Clin Cancer Res 16(10):2852–2860. doi:10.1158/1078-0432.CCR-09-2502

Chapter 18

Measurement of Rab35 Activity with the GTP-Rab35 Trapper RBD35

Hotaka Kobayashi, Kan Etoh, Soujiro Marubashi, Norihiko Ohbayashi, and Mitsunori Fukuda

Abstract

Small GTPase Rab35 functions as a molecular switch for membrane trafficking, specifically for endocytic recycling, by cycling between a GTP-bound active form and a GDP-bound inactive form. Although Rab35 has been shown to regulate various cellular processes, including cytokinesis, cell migration, and neurite outgrowth, its precise roles in these processes are not fully understood. Since a molecular tool that could be used to measure Rab35 activity would be useful for identifying the mechanisms by which Rab35 mediates membrane trafficking, we recently used a RUN domain-containing region of RUSC2 to develop an active Rab35 trapper, and we named it RBD35 (*R*ab-*b*inding *d*omain specific for Rab*35*). Because RBD35 specifically interacts with the GTP-bound active form of Rab35 and does not interact with any of the other 59 Rab proteins identified in humans and mice, RBD35 is a useful tool for measuring the level of active Rab35 by pull-down assays and for inhibiting the function of Rab35 by overexpression. In this chapter, we describe the assay procedures for analyzing Rab35 with RBD35.

Key words Rab35, RBD35, RUSC2, RUN domain, Neurite outgrowth

1 Introduction

Rab family small GTPases are intracellular molecular switches that regulate membrane trafficking. The mammalian Rab family consists of approximately 60 isoforms that localize to various organelles and vesicles [1–3]. Rabs cycle between a GTP-bound active form and a GDP-bound inactive form and active Rabs promote membrane trafficking by recruiting specific effector molecules [4]. Rab35 functions as a molecular switch for endocytic recycling, a process by which molecules that have been internalized are recycled back to the plasma membrane [5, 6]. During neurite outgrowth of PC12 cells, Rab35 has been shown to localize to recycling endosomes and recruit its effector molecules centaurin-β2/ACAP2 and MICAL-L1, both of which subsequently recruit EHD1, a facilitator of endocytic recycling [7–10]. Rab35 also controls various cellular processes,

including cytokinesis and cell migration, likely through regulating endocytic recycling [11–13]. Although considerable attention has recently been directed toward Rab35 because of its significance in endocytic recycling [14], the precise roles of Rab35 in various cellular processes are not fully understood.

In order to be able to measure Rab35 activity at the cellular level, we recently developed a novel molecular tool, i.e., RBD35 (Rab-binding domain specific for Rab35), that specifically traps active Rab35 [15]. RBD35 corresponds to the Rab35-binding region of RUSC2 (RUN and SH3 domain-containing 2; amino acid residues 982–1,199), which contains a RUN domain [16] (Fig. 1a). Since RBD35 specifically interacts with active Rab35 and does not interact with any of the other 59 mammalian Rab proteins tested (Fig. 1b), RBD35 is capable of trapping active Rab35 in cell lysates when a pull-down experiment is performed with RBD35-conjugated beads. Moreover, when RBD35 is overexpressed in cells, it is capable of inhibiting the function of Rab35 presumably by disrupting the interaction between Rab35 and its effector molecule(s). Actually, overexpression of RBD35 in
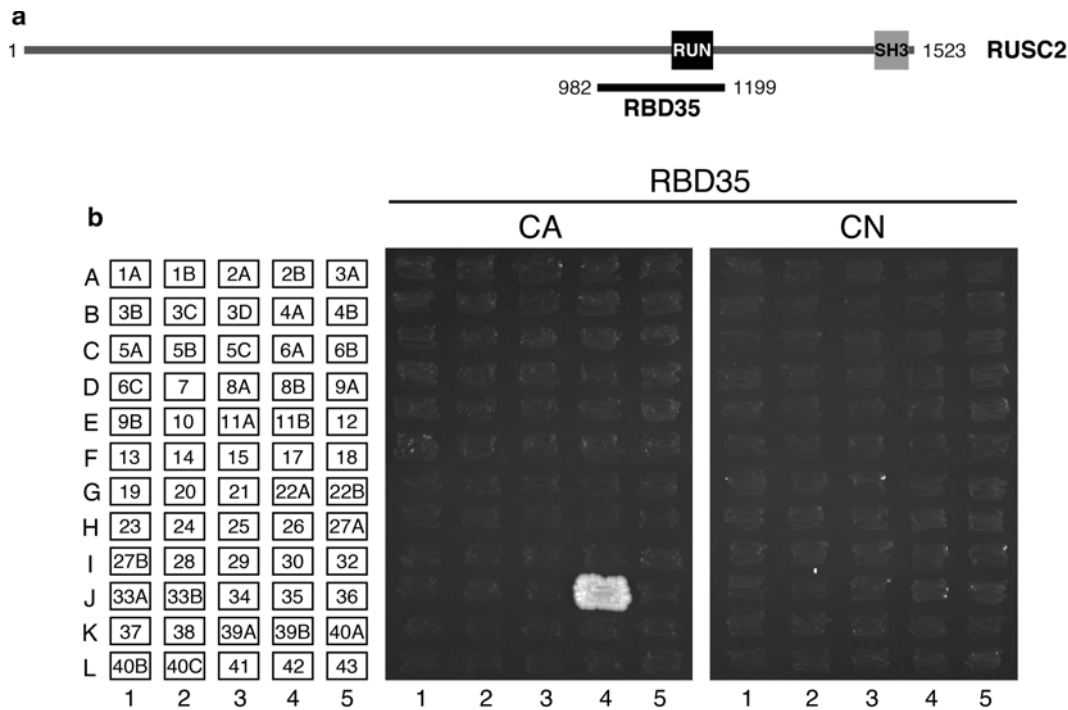
Fig. 1 Specific recognition of the GTP-bound active form of Rab35 by RBD35. (**a**) Domain organization of mouse RUSC2, which contains a RUN domain in the middle region and an SH3 domain at the C terminus. RBD35 is defined as a RUN domain-containing region (amino acid residues 982–1,199) of mouse RUSC2 [15]. (**b**) Rab-binding specificity of RBD35 as revealed by yeast two-hybrid panels. Yeast cells containing pGBD-C1 plasmid expressing constitutive active (CA) or negative (CN) mutants of Rab (positions indicated in the *left panels*) [4, 15] and pGAD-C1 plasmid expressing RBD35 were streaked on SC-AHLW and incubated at 30 °C for 1 week. Note that RBD35 specifically recognized Rab35(CA) and did not recognize Rab35(CN)

PC12 cells (a model system for neuronal differentiation) has been shown to inhibit nerve growth factor (NGF)-induced neurite outgrowth [15]. In this chapter, we describe a brief method of determining the binding specificity of RBD35 for 60 Rab proteins and then describe procedures for measuring the level of GTP-Rab35 with RBD35-conjugated beads and for inhibiting the function of Rab35 in PC12 cells by overexpressing RBD35.

2 Materials

Make up all solutions by using ultrapure water (we prepare ultrapure water by using the Milli-Q Advantage A10 Ultrapure Water Purification System) and analytical grade or the highest grade reagents commercially available (unless otherwise specified).

2.1 Determining the Binding Specificity of RBD35 for 60 Rab Proteins

1. Yeast strain pJ69-4A expressing pGBD-C1-Rab1-43(CN/CA) ΔCys vectors, which express GAL4 DNA-binding domain fusion proteins [17] of constitutive negative (CN, GDP-fixed) or constitutive active (CA, GTP-fixed) mutants of Rab1-43 lacking the C-terminal geranylgeranylation site [4, 15].

2. pGAD-C1 vector harboring RBD35 cDNA [15] (pGAD-C1-RBD35), which expresses a GAL4 activation domain fusion protein of RBD35 [17], and a minimum of 600 μL of pGAD-C1-RBD35 prepared with the Wizard® *Plus* Minipreps DNA Purification System.

3. Synthetic complete (SC) medium lacking tryptophan (SC-W): 0.67 % yeast nitrogen base without amino acids, 2 % glucose, 0.5 % casamino acid, 0.02 % adenine, 0.01 % uracil, and 2 % Bacto agar.

4. SC-LW medium: 0.67 % yeast nitrogen base without amino acids, 2 % glucose, 0.02 % adenine, 0.01 % uracil, 0.01 % histidine, 0.0125 % lysine, 0.01 % methionine, and 2 % Bacto agar.

5. SC-AHLW medium: 0.67 % yeast nitrogen base without amino acids, 2 % glucose, 0.01 % uracil, 0.0125 % lysine, 0.01 % methionine, and 2 % Bacto agar.

6. 0.1 M lithium acetate (LA) in 10 mM Tris–HCl (pH 7.5) and 1 mM EDTA (sterilized in an autoclave).

7. 50 % polyethylene glycol 4,000 (PEG) in water (sterilized in an autoclave).

8. 60 % glycerol in water (filtered through a 0.2-μm filter).

2.2 Measuring Rab35 Activity

1. COS-7 cells.

2. COS-7 cell culture medium: Dulbecco's Modified Eagle Medium (DMEM) supplemented with 10 % fetal bovine serum, 100 U/mL penicillin G, and 100 μg/mL streptomycin.

3. 100-mm cell culture dishes.

4. 1 μg/μL pEF-HA vector [18] harboring mouse Rab35 cDNA (pEF-HA-Rab35) in water purified with the QIAGEN Plasmid Midi kit or with another transfection-grade plasmid purification kit.

5. Lipofectamine® LTX and PLUS™ Reagents.

6. Phosphate-buffered saline (PBS).

7. Cell lysis buffer (filtered through a 0.2-μm filter): 50 mM HEPES–KOH, pH 7.2, 150 mM NaCl, 1 mM MgCl$_2$, and 1 % Triton X-100 supplemented with complete EDTA-free protease inhibitor cocktail.

8. Washing buffer (filtered through a 0.2-μm filter): 50 mM HEPES–KOH, pH 7.2, 150 mM NaCl, 1 mM MgCl$_2$, and 0.2 % Triton X-100.

9. Guanosine diphosphate (GDP) and guanosine 5'-O-(3-thio) triphosphate (GTPγS).

10. Glutathione-Sepharose beads (*see* **Note 1**).

11. GST (glutathione *S*-transferase) and GST-RBD35 protein purified by a standard purification protocol [18] from lysates of *Escherichia coli* BL21(DE3)pLysS transformed with pGEX4T-3 vector harboring nothing and RBD35 cDNA, respectively.

12. HRP (horseradish peroxidase)-conjugated anti-GST antibody and HRP-conjugated anti-HA antibody.

13. ECL Western Blotting Detection System.

2.3 Inhibiting the Function of Rab35

1. PC12 cells (*see* **Note 2**).

2. PC12 cell culture medium: DMEM supplemented with 10 % fetal bovine serum, 10 % horse serum, 100 U/mL penicillin G, and 100 μg/mL streptomycin.

3. 35-mm glass-bottom dishes coated with 100 μg/mL poly-L-lysine in water.

4. 1 μg/μL pmStr (monomeric Strawberry)-C1 vector [8] (used as a cell shape marker) in water purified with the QIAGEN Plasmid Midi kit or with another transfection-grade plasmid purification kit.

5. 1 μg/μL pEGFP (enhanced green fluorescent protein)-C1 vector in water purified with the QIAGEN Plasmid Midi kit.

6. 1 μg/μL pEGFP-C1 vector harboring RBD35 cDNA [15] (pEGFP-C1-RBD35) in water purified with the QIAGEN Plasmid Midi kit.

7. Lipofectamine® 2000.

8. 10 μg/mL NGF in PBS supplemented with 0.1 % bovine serum albumin (BSA).

9. 4 % paraformaldehyde (PFA) in 0.1 M sodium phosphate buffer: 0.084 M Na_2HPO_4 and 0.016 M NaH_2PO_4, pH 7.4.

10. PBS.

11. Fluorescence microscope.

12. MetaMorph software.

3   Methods

3.1   Assay to Determine the Binding Specificity of RBD35 for 60 Rab Proteins

1. Streak the pJ69-4A yeast cells expressing each pGBD-C1-Rab(CA/CN)ΔCys on SC-W medium and incubate them at 30 °C overnight (*see* **Note 3**).

2. Dispense 12 μL of 0.1 M LA into each of 120 sterilized 1.5-mL microtubes (for 60 Rab(CA) and 60 Rab(CN)).

3. Transfer the yeast cells expressing the pGBD-C1-Rab(CA/CN)ΔCys in each of the cultures into a separate microtube containing the LA solution, and suspend by pipetting.

4. Add 5 μL of pGAD-C1-RBD35 to each microtube, and suspend by pipetting.

5. Add 45 μL of 50 % PEG to each microtube, and mix completely with a vortex mixer.

6. Incubate for 30 min at room temperature.

7. Add 6 μL of 60 % glycerol to each microtube.

8. Incubate at 42 °C for 15 min (heat shock).

9. Streak the yeast cells on SC-LW medium and incubate them at 30 °C for 2–3 days.

10. Streak fresh colonies of the yeast cells expressing both pGBD-C1-Rab(CA/CN)ΔCys and pGAD-C1-RBD35 on SC-AHLW medium (selection medium).

11. After incubation at 30 °C for 1 week, check growth of the yeast cells on SC-AHLW medium. Only the yeast cells that express both pGBD-C1-Rab35(CA)ΔCys and pGAD-C1-RBD35 will have grown on SC-AHLW medium (Fig. 1b, CA panel, position 4-J), confirming that RBD35 specifically recognizes only the GTP-bound active form of Rab35 (*see* **Note 4**).

3.2   Assay to Measure Rab35 Activity

1. Seed COS-7 cells in two 100-mm dishes (1×10^6 cells in 10 mL of COS-7 culture medium per dish), and incubate them overnight at 37 °C under 5 % CO_2.

2. Prepare a transfection mix containing 5 μg of pEF-HA-Rab35, 5 μL of PLUS™ Reagents, and 12.5 μL of Lipofectamine®

LTX per dish according to the manufacturer's instructions. Add the transfection mix dropwise to the COS-7 cells, and incubate them at 37 °C under 5 % CO_2 (*see* **Note 5**).

3. 36–48 h after transfection, wash the COS-7 cells once with 10 mL of ice-cold PBS, and transfer the COS-7 cells from the two dishes into one 1.5-mL microtube with a scraper.

4. Centrifuge at $1,000 \times g$ at 4 °C for 3 min, and discard the supernatant (*see* **Note 6**).

5. Add 1 mL of the cell lysis buffer to the COS-7 cell pellet in the microtube, and gently rotate it at 4 °C for 30 min.

6. Centrifuge at $17,400 \times g$ at 4 °C for 10 min, and collect the supernatant into a new 1.5-mL microtube.

7. Add 5 μL of 0.5 M EDTA, and mix thoroughly by tapping (*see* **Note 7**).

8. Incubate on ice for 10 min.

9. Dispense the COS-7 cell lysate into 4 microtubes (250 μL per tube), and add 5 μL of 100 mM GDP to each of two tubes (samples #2 and #4) and 5 μL of 50 mM GTPγS to each of the other two tubes (samples #1 and #3).

10. Incubate on ice for 20 min.

11. Add 5 μL of 1 M $MgCl_2$ to each microtube.

12. Incubate on ice for an additional 10 min.

13. Dilute each COS-7 cell lysate to 600 μL with the cell lysis buffer, and dispense 6 μL of each into a new microtube for input, and 594 μL of each into a new microtube for the pull-down assay.

14. Prepare 2 microtubes each containing 1.25 μg of GST (samples #1 and #2) in 100 μL of the cell lysis buffer and 2 microtubes each containing 1.25 μg of GST-RBD35 (samples #3 and #4) in 100 μL of the cell lysis buffer (*see* **Note 8**), and add 15 μL of glutathione-Sepharose beads (wet volume) to each microtube.

15. Rotate at 4 °C for 1 h.

16. Centrifuge at $1,000 \times g$ for 3 min at 4 °C, and discard the supernatant.

17. Wash the glutathione-Sepharose beads coupled with GST (samples #1 and #2) or GST-RBD35 (samples #3 and #4) three times with 1 mL of the cell lysis buffer each time.

18. Add the COS-7 cell lysates expressing HA-Rab35 (prepared in **step 13**) to the GST- or GST-RBD35-coupled beads.

19. Rotate at 4 °C for 3 h.

20. Centrifuge at $1,000 \times g$ for 3 min at 4 °C, and discard the supernatant.
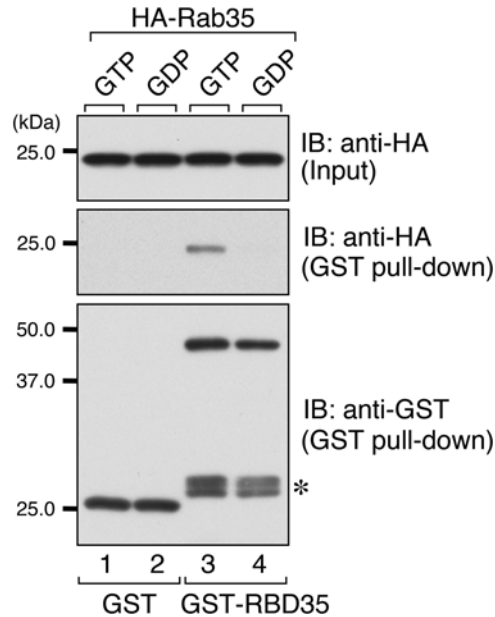
Fig. 2 RBD35 specifically traps active Rab35 in COS-7 cells. Glutathione-Sepharose beads coupled with GST alone (*lanes 1* and *2*) or GST-RBD35 (*lanes 3* and *4*) were incubated with COS-7 cell lysates expressing HA-Rab35 in the presence of 0.5 mM GTPγS (*lanes 1* and *3*) or 1 mM GDP (*lanes 2* and *4*). Proteins bound to the beads were analyzed by 10 % SDS-PAGE followed by immunoblotting with HRP-conjugated anti-HA tag antibody (1/5,000 dilution; *top* and *middle panels*) and with HRP-conjugated anti-GST antibody (1/5,000 dilution; *bottom panel*). The positions of the molecular mass markers (in kDa) are shown at the *left* of each panel. Note that RBD35 specifically trapped GTP-bound active Rab35 and did not trap GDP-bound inactive Rab35 (compare *lanes 3* and *4* in the *middle panel*). The asterisk indicates the GST-RBD35 degradation products

21. Wash the beads three times with 1 mL of the washing buffer each time.

22. Analyze the proteins bound to the beads by performing 10 % SDS polyacrylamide gel electrophoresis (PAGE) followed by conventional immunoblotting with HRP-conjugated anti-GST antibody and HRP-conjugated anti-HA antibody (*see* **Note 9**).

23. Detect the immunoreactive bands by using the ECL Western Blotting Detection System according to the manufacturer's instructions (Fig. 2).

3.3 Assay to Inhibit the Function of Rab35

1. Seed 2×10^5 PC12 cells in 2 mL of PC12 cell medium in each of two glass-bottom dishes, one for transfection of pmStr-C1 and pEGFP-C1, and the other for transfection of pmStr-C1 and pEGFP-C1-RBD35.

2. 24 h after seeding, transfect the PC12 cells with 0.5 μL of pmStr-C1 and pEGFP-C1 each or with 0.5 μL of pmStr-C1
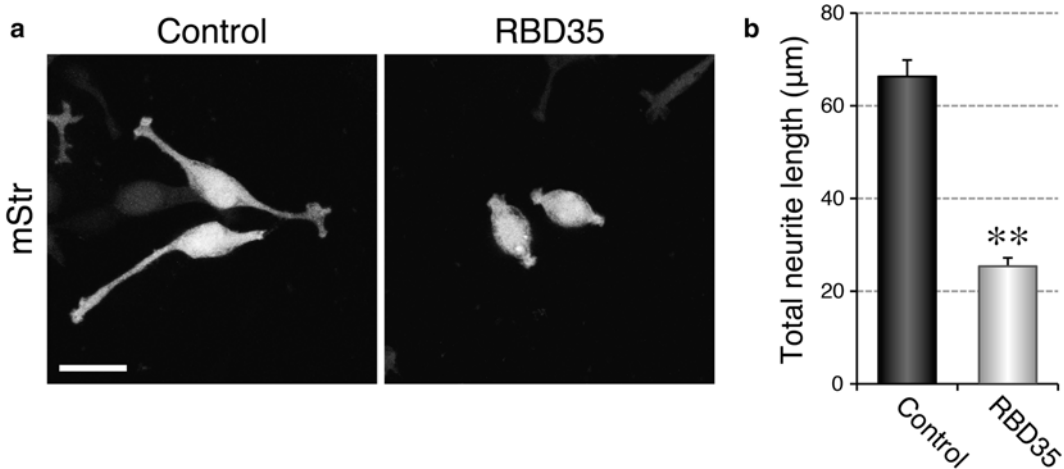
Fig. 3 Overexpression of RBD35 in PC12 cells inhibits NGF-induced neurite outgrowth. (**a**) Typical mStr fluorescence images of control EGFP-expressing and EGFP-RBD35-expressing PC12 cells after NGF stimulation for 36 h. mStr was used as a cell shape marker. Scale bar, 30 μm. (**b**) Total neurite length (mean and standard error) of EGFP-expressing PC12 cells and EGFP-RBD35-expressing PC12 cells ($n > 100$). Student's unpaired t-test was used to test the difference between the results obtained in EGFP-expressing PC12 cells and EGFP-RBD35-expressing PC12 cells for statistical significance. The double asterisk (**) in the bar chart indicates a t-test p value <0.01. Note that the EGFP-RBD35-expressing PC12 cells had significantly shorter neurites than the EGFP-expressing PC12 cells

and pEGFP-C1-RBD35 each, by using 2 μL of Lipofectamine® 2000 according to the manufacturer's instructions.

3. 24 h after transfection, add 20 μL of NGF to the medium (final concentration: 100 ng/mL) and incubate the cells at 37 °C under 5 % CO_2 (*see* **Note 10**).

4. 36 h after NGF stimulation, fix the PC12 cells with 1 mL of 4 % PFA for 20 min at room temperature.
   Perform all of the following steps at room temperature:

5. Wash the PC12 cells three times with 1 mL of PBS each time (*see* **Note 11**).

6. Capture fluorescence images of the PC12 cells expressing mStr and EGFP or mStr and EGFP-RBD35 with a fluorescence microscope ($n > 100$) (*see* **Note 12**) (Fig. 3a).

7. Use MetaMorph software to measure the length of all neurites extended from each cell (total neurite length of the individual cells) based on the mStr-signals.

8. Evaluate the difference between the results obtained in EGFP-expressing PC12 cells and EGFP-RBD35-expressing PC12 cells for statistical significance by Student's unpaired t-test. The difference in the total neurite length reflects the effect of overexpression of RBD35 (i.e., inhibition of Rab35) on NGF-induced neurite outgrowth of PC12 cells (Fig. 3b).

4   Notes

1. Handle the beads with wide-bore cell-saver tips to avoid damaging them.

2. Maintain PC12 cells at less than 100 % confluence, because 100 % confluence often alters the growth rate, morphology, and responsiveness to NGF of PC12 cells.

3. Maintain sterility throughout the procedures in Subheading 3.1.

4. Although RBD35 specifically recognizes active Rab35, the original RUSC2 RUN construct (amino acid residues 982–1,351) also interacts with active Rab1A, Rab1B, and Rab41 [15].

5. Skip **step 2**, i.e., expression of recombinant Rab35, when measuring endogenous Rab35 activity in cell lysates.

6. COS-7 cell pellets immediately frozen with liquid nitrogen can be stored at –80 °C until used.

7. Skip **steps 7–12**, i.e., the GDP/GTP-loading procedure, when measuring Rab35 activity in cell lysates.

8. The concentration of GST-RBD35 must be determined in advance by immunoblotting with GST as a standard because aliquots of purified GST-RBD35 are often contaminated by degradation products (~30 kDa; asterisk in Fig. 2) that presumably are produced by cleavage in the region between GST and RBD35.

9. Use anti-Rab35-specific antibody when measuring the activity of endogenous Rab35 in cell lysates.

10. Add all reagents to the dishes gently, because PC12 cells tend to detach from the bottom of dishes during pipetting.

11. Fixed PC12 cells can be stored at 4 °C for several weeks under light-protected conditions.

12. Select PC12 cells at random to exclude selection bias.

Acknowledgements

References

1. Zerial M, McBride H (2001) Rab proteins as membrane organizers. Nat Rev Mol Cell Biol 2:107–117

2. Fukuda M (2008) Regulation of secretory vesicle traffic by Rab small GTPases. Cell Mol Life Sci 65:2801–2813

3. Stenmark H (2009) Rab GTPases as coordinators of vesicle traffic. Nat Rev Mol Cell Biol 10:513–525

4. Fukuda M, Kanno E, Ishibashi K, Itoh T (2008) Large scale screening for novel Rab effectors reveals unexpected broad Rab binding specificity. Mol Cell Proteomics 7: 1031–1042

5. Kouranti I, Sachse M, Arouche N, Goud B, Echard A (2006) Rab35 regulates an endocytic recycling pathway essential for the terminal steps of cytokinesis. Curr Biol 16:1719–1725

6. Sato M, Sato K, Liou W, Pant S, Harada A, Grant BD (2008) Regulation of endocytic recycling by *C. elegans* Rab35 and its regulator RME-4, a coated-pit protein. EMBO J 27: 1183–1196

7. Kanno E, Ishibashi K, Kobayashi H, Matsui T, Ohbayashi N, Fukuda M (2010) Comprehensive screening for novel Rab-binding proteins by GST pull-down assay using 60 different mammalian Rabs. Traffic 11: 491–507

8. Kobayashi H, Fukuda M (2012) Rab35 regulates Arf6 activity through centaurin-β2 (ACAP2) during neurite outgrowth. J Cell Sci 125:2235–2243

9. Kobayashi H, Fukuda M (2013) Rab35 establishes the EHD1-association site by coordinating two distinct effectors during neurite outgrowth. J Cell Sci 126:2424–2435

10. Kobayashi H, Fukuda M (2013) Arf6, Rab11 and transferrin receptor define distinct populations of recycling endosomes. Commun Integr Biol 6:e25036

11. Chevallier J, Koop C, Srivastava A, Petrie RJ, Lamarche-Vane N, Presley JF (2009) Rab35 regulates neurite outgrowth and cell shape. FEBS Lett 583:1096–1101

12. Chesneau L, Dambournet D, Machicoane M, Kouranti I, Fukuda M, Goud B, Echard A (2012) An ARF6/Rab35 GTPase cascade for endocytic recycling and successful cytokinesis. Curr Biol 22:147–153

13. Allaire PD, Seyed Sadr M, Chaineau M, Seyed Sadr E, Konefal S, Fotouhi M, Maret D, Ritter B, Del Maestro RF, McPherson PS (2013) Interplay between Rab35 and Arf6 controls cargo recycling to coordinate cell adhesion and migration. J Cell Sci 126:722–731

14. Chaineau M, Ioannou MS, McPherson PS (2013) Rab35: GEFs, GAPs and effectors. Traffic 14:1109–1117

15. Fukuda M, Kobayashi H, Ishibashi K, Ohbayashi N (2011) Genome-wide investigation of the Rab binding activity of RUN domains: development of a novel tool that specifically traps GTP-Rab35. Cell Struct Funct 36:155–170

16. Callebaut I, de Gunzburg J, Goud B, Mornon JP (2001) RUN domains: a new family of domains involved in Ras-like GTPase signaling. Trends Biochem Sci 26:79–83

17. James P, Halladay J, Craig EA (1996) Genomic libraries and a host strain designed for highly efficient two-hybrid selection in yeast. Genetics 144:1425–1436

18. Kuroda TS, Fukuda M (2005) Identification and biochemical analysis of Slac2-c/MyRIP as a Rab27A-, myosin Va/VIIa-, and actin-binding protein. Methods Enzymol 403: 431–444

Chapter 19

Analysis of Connecdenn 1–3 (DENN1A-C) GEF Activity for Rab35

Patrick D. Allaire, Peter S. McPherson, and Brigitte Ritter

Abstract

Rabs (Ras-related proteins in brain) form the largest family of small GTPases and control numerous aspects of membrane trafficking at multiple cellular sites. Rab GTPases toggle between an inactive GDP-bound state and an active GTP-bound state. Activation of Rab GTPases requires guanine nucleotide exchange factors (GEFs) that interact with inactive GDP-bound Rabs and catalyze the removal of GDP, allowing GTP to bind. The largest single family of GEFs for Rabs is comprised of proteins bearing a DENN (differentially expressed in normal and neoplastic cells) domain. In this chapter we describe a biochemical method that directly measures the exchange activity of DENN domains by monitoring loading of GTP onto a Rab GTPase. Rabs are first purified from bacterial or mammalian sources and are then loaded with GDP. Purified DENN domains or DENN domain-bearing proteins are added in the presence of $[^{35}S]$ GTPγS and the transfer of $[^{35}S]$GTPγS to the Rab is measured by filtering the reaction over nitrocellulose membranes to trap the Rab and thus the associated $[^{35}S]$GTPγS.

Key words C9ORF72, Connecdenn, DENN domain, DENND, Endocytosis, Endosome, GEF, GTPase, Guanine nucleotide exchange factor, Membrane traffic

1 Introduction

A major challenge faced by eukaryotic cells is to maintain the integrity and protein composition of organelles in the face of an extensive flow of membrane and lipid components between the various cellular compartments. Maintenance of organelle integrity depends on the formation of cargo carriers that selectively incorporate cargos, engage the cytoskeleton for transport, and dock and fuse with appropriate target membranes. Rab GTPases are remarkable in that they control all of these trafficking processes and do so for nearly all trafficking pathways. Thus, in order to understand how intracellular trafficking is controlled, it is critical to determine how Rabs are regulated.

GTPases are enzymes that catalyze the hydrolysis of guanosine triphosphate (GTP) to guanosine diphosphate (GDP). Rab GTPases

typically have low intrinsic GTPase activity, which is greatly enhanced by GTPase activating proteins (GAPs). Hydrolysis of GTP to GDP changes the GTPase into an inactive conformation incapable of binding effector proteins. Reactivation of the Rab requires guanine nucleotide exchange factors (GEFs), which bind specifically to the GDP-bound GTPases and mediate conformational changes in the Rab that lower its affinity for GDP, allowing for GDP dissociation. Either GDP or GTP can then bind the Rab but since GTP is at tenfold higher levels in the cell than GDP, GTP typically occupies the nucleotide-binding site. Upon GTP binding, the Rab changes to an active-state conformation that results in GEF release and the exposure of a binding surface for the recruitment of specific effector molecules. These effector molecules then establish the conditions for cargo transport between membrane bound compartments. Thus, GEFs and GAPs function to switch GTPases on or off, respectively.

While Rab GAP activity, encoded by the Tre-2/Bub2/Cdc16 (TBC) domain has been known since 1995 [1], it was not until recently that a dedicated Rab GEF domain was identified. Early studies in *C. elegans* demonstrated that Rab3GEP and its *C. elegans* homologue AEX-3 are required to activate Rab3 [2–4]. Rab3GEP is also known as differentially expressed in normal and neoplastic cells (DENN) and contains a protein region from residues 19 to 557 that was subsequently recognized in other proteins as a module called the DENN domain [5, 6]. More recently, a genetic screen in *C. elegans* focused on identifying genes involved in receptor-mediated endocytosis (RME) led to the discovery of the DENN domain containing protein RME-4 as a positive regulator of RME-5 (Rab35), and it was proposed that the DENN domain of RME-4 provided Rab35 GEF activity [7]. The mammalian homologue of RME-4 is connecdenn 1/DENND1A, a protein originally identified in a proteomic analysis of clathrin-coated vesicles [8]. Using in vitro GEF assays, it was demonstrated that the DENN domain of connecdenn functions directly as a GEF for Rab35, strongly implicating the DENN domain as a general GEF module for Rabs [9]. In fact, RabGEP/DENN also has GEF activity for Rab27, likely mediated by the DENN domain [10]. Based on standard bioinformatics tools, there are 18 genes in humans that encode DENN domain proteins, and these are grouped into eight families, each of which has GEF activity against a selective Rab [10, 11].

With 18 members, DENN domain proteins are the largest family of Rab GEFs, but excitingly it appears that the family may be much larger. For example, the C-terminal region of the tumor suppressor protein folliculin has only 11 % sequence homology with the DENN domain of DENND1B/connecdenn 2. Yet, the crystal structure of this region of folliculin reveals striking structural similarity with the DENN domain [12, 13]. This suggests

that there may be other DENN domain proteins that are difficult to recognize based on sequence analysis alone. In fact, sensitive structure-based homology searches predict at least seven other DENN domain encoding genes, namely C9ORF72, a gene of unknown function that is a major locus mutated in ALS; LCHN, a protein of unknown function that is up-regulated by transient global ischemia in adult hippocampus [14]; Smith-Magerus syndrome chromosome region candidate gene 8 (SMCR 8) protein; nitrogen permease regulator 2 (NPR 2) and NPR 3; and folliculin interacting protein 1 (FNIP 1) and FNIP 2 [15, 16]. This expands the number of DENN domain proteins in the human genome to potentially 26. It will be interesting to determine if these predicted DENN domain containing protein are indeed Rab GEFs, and thus establishing robust GEF assays is required.

Various in vivo and in vitro methods can test the GEF activity of a candidate protein or domain. In vivo methods include increasing or decreasing of Rab-effector interactions using overexpression or knockdown/knockout of the candidate GEF. However, these approaches do not provide direct evidence of GEF activity and do not allow for any kinetic measurements. In vitro methods using purified proteins include either directly measuring the rate of exchange of GDP to GTP on the Rab itself or measuring the rate of GDP release. In this chapter, we will describe a method to test for GDP/GTP exchange activity by measuring incorporation of radioactive-labeled GTP onto the Rab GTPase.

2 Materials

Prepare all solutions using ultrapure deionized water (18 MΩ at 25 °C). In addition, sterilize all solutions to be used with live cells, e.g., by filtration through 0.22 μm PES membrane filter units. Purified proteins and nucleotide stock solutions should be stored at −70 °C and repeated freeze-thaw cycles should be avoided. The experiments require BSL-2 approval and a radioactivity permit for the use of [35]S. Diligently follow all safety and waste disposal regulations.

2.1 Cloning and DNA Purification

1. pEBG vector: Addgene plasmid ID 22227 for mammalian expression of N-terminally GST-tagged fusion proteins under the EF1α promoter.

2. LB medium. Dissolve 25 g LB medium in 1,000 ml deionized water. Transfer 500 ml each into 2 l Erlenmeyer flasks, autoclave, and store at room temperature.

2.2 Protein Purification

1. PBS: 20 mM NaH_2PO_4, 150 mM NaCl, pH 7.4. Dissolve 2.4 g sodium phosphate monobasic anhydrous (NaH_2PO_4)

and 8.77 g NaCl in 900 ml ultrapure deionized water, adjust pH to 7.4, and top up with ultrapure deionized water to a final volume of 1,000 ml. Solution can be stored at room temperature. For protein purifications, store/pre-cool PBS at 4 °C and keep on ice during the experiment.

2. PBS buffer with protease inhibitors: 20 mM NaH_2PO_4, 150 mM NaCl, pH 7.4, 0.83 mM benzamidine, 0.23 mM phenylmethyl-sulphonyl fluoride (PMSF), 0.5 μg/ml aprotinin, and 0.5 μg/ml leupeptin. To 100 ml pre-cooled PBS, add 1 ml benzamidine, 10 μl aprotinin, 10 μl leupeptin, 200 μl PMSF. Make sure to add PMSF just before cell lysis.

3. 83 mM benzamidine stock. Dissolve 1.45 g benzamidine hydrochloride hydrate in 100 ml ultrapure deionized water. Filter-sterilize and store at 4 °C.

4. 115 mM PMSF stock. Dissolve 2 g in 100 ml 100 % ethanol. Store at room temperature.

5. 5 mg/ml aprotinin stock. Dissolve 10 mg in 2 ml ultrapure deionized water. Aliquot and store at –20 °C.

6. 5 mg/ml leupeptin stock. Dissolve 10 mg in 2 ml ultrapure deionized water. Aliquot and store at –20 °C.

7. 10 % Triton X-100 in PBS. Dissolve 50 g 100 % Triton X-100 in 450 ml PBS to obtain 10 % (w/v) Triton X-100 in PBS. Store at 4 °C.

8. Thrombin cleavage buffer: 50 mM Tris–HCl, pH 8.0, 150 mM NaCl, 5 mM $MgCl_2$, 2.5 mM $CaCl_2$, 1 mM dithiothreitol (DTT). For 10 ml, Add 0.5 ml 1 M Tris, pH 8.0, 375 μl 4 M NaCl, 10 μl 2.5 M $CaCl_2$, and 10 μl 1 M DTT. Adjust to a final volume of 10 ml with ultrapure deionized water and cool down on ice prior to use.

9. 1 M Tris–HCl stock, pH 8.0. Dissolve 121.14 g Tris base in 900 ml ultrapure deionized water, cool solution on ice prior to adjusting the pH to 8.0, and top up with ultrapure deionized water to a final volume of 1,000 ml. After autoclaving, solution can be stored at room temperature or 4 °C; make sure to cool down on ice prior to use.

10. 4 M NaCl. Dissolve 116.88 g NaCl in ultrapure deionized water in a final volume of 500 ml in a 1-l bottle. Autoclave and store at room temperature.

11. 2 M $MgCl_2$. Dissolve 203.3 g magnesium chloride hexahydrate ($MgCl_2 \cdot 6H_2O$) in ultrapure deionized water in a final volume of 500 ml in a 1-l bottle. Autoclave and store at room temperature.

12. 2.5 M $CaCl_2$. Dissolve 183.78 g calcium chloride dihydrate ($CaCl_2 \cdot 2H_2O$) in ultrapure deionized water in a final volume of 500 ml in a 1 l bottle. Autoclave and store at room temperature.

13. 1 M DTT. Dissolve 1.54 g DTT in 10 ml ultrapure deionized water. Aliquot and store at –20 °C.

14. 5× loading sample buffer (LSB): 15 % (w/v) sodium dodecyl sulfate (SDS), 575 mM sucrose, 325 mM Tris, pH 6.8, 5 % β-mercaptoethanol, touch of bromophenol blue. For 100 ml 5× LSB, mix 50 ml 30 % SDS, 28.75 ml 2 M sucrose, 16.25 ml 2 M Tris, pH 6.8, and 5 ml 100 % β-mercaptoethanol. Add a tad of bromophenol blue, enough to yield an obvious blue color to a 1× LSB solution.

15. 30 % (w/v) SDS stock. Dissolve 300 g SDS in ultrapure deionized water in a total volume of 1 l (*see* **Note 1**). Store at room temperature.

16. 2 M sucrose stock. Dissolve 684.6 g sucrose in ultrapure deionized water in a total volume of 1 l. Autoclave and store at room temperature.

17. 2 M Tris–HCl stock, pH 6.8. Dissolve 242.28 g Tris base in 900 ml ultrapure deionized water, adjust the pH to 6.8, and top up with ultrapure deionized water to a final volume of 1,000 ml. Autoclave and store at room temperature.

18. 2× HBS: 280 mM NaCl, 1.5 mM Na_2HPO_4, 50 mM HEPES. Dissolve 32.73 g NaCl, 0.43 g sodium phosphate dibasic anhydrous (Na_2HPO_4), and 23.83 g HEPES in ultrapure deionized water in a final volume of 2 l. While stirring, carefully adjust the pH to 6.98, to avoid overshooting the pH. Set aside 500 ml, remember to label with the pH value. Continue to adjust the pH of the original solution to 7.00, again to avoid overshooting the pH. Set aside another 500 ml aliquot and label with pH. Continue the same way, adjusting the pH to 7.02 before taking the next 500 ml aliquot and adjusting the pH to 7.04 for the last 500 ml aliquot. In a biosafety cabinet (cell culture hood, not fume hood), sterilize solutions by vacuum-filtering through a 0.22 μm PES bottle top filter into sterile bottles (*see* **Note 2**). Store at room temperature or aliquot and store at –20 °C (*see* **Note 3**).

19. 0.1× TE: 1 mM Tris–HCl, pH 8.0, 0.1 mM ethylendiaminetetraacetic acid (EDTA). Dissolve 0.12 g Tris base in 950 ml ultrapure deionized water and add 200 μl 0.5 M EDTA. Adjust pH to 8.0 and top up the solution with ultrapure deionized water to a final volume of 1 l. In a biosafety cabinet (cell culture hood, not fume hood), sterilize solution by vacuum-filtering through a 0.22 μm PES bottle top filter into sterile bottles. Store at room temperature.

20. 0.5 M EDTA stock. Dissolve 93.06 g ethylenediaminetetraacetic acid, disodium salt dihydrate ($Na_2EDTA \cdot 2H_2O$) in ultrapure deionized water by stirring while adjusting the pH to 8.0 using sodium hydroxide (NaOH). Autoclave solution and store at room temperature.

21. 2 M CaCl$_2$. Dissolve 29.4 g calcium chloride dihydrate (CaCl$_2$·2H$_2$O) in a final volume of 100 ml ultrapure deionized water. In a biosafety cabinet (cell culture hood, not fume hood), sterilize solution by vacuum-filtering through a 0.22 μm PES bottle top filter into sterile bottles. Store at room temperature.

22. HEK 293-T cells. Following standard cell culture procedures, HEK-293-T (human embryonic kidney) cells were maintained in DMEM High Glucose containing 10 % iron-supplemented calf serum, 100 U/ml penicillin, and 100 μg/ml streptomycin in a water-saturated atmosphere with 5 % CO$_2$ (*see* **Note 4**).

2.3 GTPase Loading and GEF Assay

1. GEF loading buffer. 20 mM Tris–HCl, pH 7.5, 100 mM NaCl. Dissolve 1.21 g Tris base and 2.92 g NaCl in 450 ml ultrapure deionized water. Adjust pH to 7.5 and top up with ultrapure deionized water to a final volume of 500 ml. Solution can be stored at room temperature.

2. GEF incubation buffer: 20 mM Tris–HCl, pH 7.5, 100 mM NaCl, 5 mM MgCl$_2$. Dissolve 1.21 g Tris base, 2.92 g NaCl, and 0.51 g MgCl$_2$·6H$_2$O in 450 ml ultrapure deionized water. Adjust pH to 7.5 and top up with ultrapure deionized water to a final volume of 500 ml. Solution can be stored at room temperature.

3. Wash buffer: 20 mM Tris–HCl, pH 7.5, 100 mM NaCl, 20 mM MgCl$_2$. Dissolve 1.21 g Tris base, 2.92 g NaCl, and 2.03 g MgCl$_2$·6H$_2$O in 450 ml ultrapure deionized water. Adjust pH to 7.5 and top up with ultrapure deionized water to a final volume of 500 ml. Solution can be stored at room temperature.

4. 40 mM Guanosine 5′-diphosphate (GDP) sodium salt. Dissolve 10 mg GDP in 564 μl ultrapure deionized water. Aliquot in small amounts and store at –70 °C.

5. 10 mM Guanosine 5′-[γ-thio]triphosphate (GTPγS) tetralithium salt. Dissolve 1 mg GTPγS in 177.6 μl ultrapure deionized water. Aliquot in small amounts and store at –70 °C.

3 Methods

3.1 Expression Constructs

3.1.1 Connecdenn DENN Domain

1. The mRNA region of mouse connecdenn encoding the DENN domain (amino acids 1–403) was amplified by PCR.

2. Following restriction digest, the PCR product was cloned into the BamHI and NotI restriction sites in the multiple cloning site of the pEBG plasmid using standard molecular biology techniques.

3.1.2 Rab35	1. The mRNA region encoding full-length human Rab35 was amplified by PCR.
	2. Following restriction digest, the PCR product was cloned into the BamHI and NotI restriction sites in the multiple cloning site of the pEBG plasmid using standard molecular biology techniques.
3.2 DNA Purification	1. Sequence-verified pEBG constructs for the connecdenn DENN domain and Rab35 were transformed into chemically competent DH5α *E. coli*.
	2. 500 ml LB cultures were grown in 2 l Erlenmeyer flasks for about 18 h at 37 °C, shaking at 220 rpm.
	3. The bacteria were harvested by centrifugation for 5 min at $8,300 \times g$ and high quality DNA was purified using a commercial kit according to the manufacturer's instructions.
3.3 Protein Expression and Purification	1. For expression of each construct, between six and twelve 15 cm dishes are seeded with 3×10^6 HEK 293T cells on the day prior to transfection (*see* **Note 5**).
	2. Next day, each plate is transfected with 10 μg DNA using the calcium phosphate method (*see* **Note 6**). Make sure to perform all steps in a biosafety cabinet/cell culture hood. For each plate,

- Prepare tube A with 1.25 ml 2× HBS.
- In tube B, mix 1.1 ml 0.1× TE with 10 μg DNA, then mix in 150 μl 2 M CaCl$_2$.
- While bubbling or vortexing tube A, drop-wise add content of tube B.
- Incubate transfection mix for 20–25 min at room temperature.
- Drop-wise add transfection mix to cells and incubate under standard cell culture conditions.
- The transfection mix preparation can be scaled up. Using 50 ml conical tubes for tube A and B, a mix for up to six 15 cm dishes to be transfected with the same DNA construct can be prepared at a time (*see* **Note 7**).

3. After 8 h, remove the medium containing the transfection mix from all plates and replace it with 25 ml/plate of regular culture medium (*see* **Note 8**).

4. After 48 h, the plates are rinsed 2–3 times with PBS to remove the culture medium and all liquid is removed by aspiration.

5. Keeping the dishes and cells on ice as much as possible, scrape cells off the plates in 1–2 ml/plate of PBS with protease inhibitors using a cell scraper or rubber policeman. Pool solutions from

all plates for each construct and lyse cells by sonication (*see* **Note 9**).

6. Add Triton X-100 to a final concentration of 1 % using a 10 % Triton X-100 in PBS stock. Mix and incubate lysates for 30 min on a nutator at 4 °C.

7. The lysate are spun for 30 min at 205,000 × *g*.

8. In the meantime, pre-wash 200 μl glutathione beads for each fusion protein to remove preservative (ethanol). Cut off approx. 1/8 of an inch of the tip of a 1,000 μl pipet tip to widen the opening and avoid clogging, transfer the beads into a 15 ml conical tube, and mix with 10 ml PBS. Pellet the beads by centrifugation for 5 min at 3,500 × *g* and discard the supernatant. It is sufficient to pour off the liquid (*see* **Note 10**). If using aspiration, be careful not to lose any beads.

9. Transfer the cell lysate supernatants into the tubes containing the pre-washed glutathione beads and allow for GST-protein binding by shaking for 1 h on a nutator at 4 °C.

10. Pellet the beads by centrifugation for 5 min at 3,500 × *g* at 4 °C, discard the supernatant, and resuspend the beads in 10 ml PBS with protease inhibitors (*see* **Note 10**). Repeat 3 times.

11. Pellet the beads by centrifugation for 5 min at 3,500 × *g* at 4 °C, discard the supernatant, and resuspend the beads in 10 ml thrombin cleavage buffer. Repeat once.

12. Resuspend the beads in thrombin cleavage buffer in 500 μl total volume and transfer into 1.5 ml microfuge tubes using tips with widened openings.

13. The purified fusion proteins are cleaved off the GST tag by overnight incubation with 5 U of thrombin at 4 °C in 500 μl total volume.

14. Pellet the glutathione beads by a quick pulse centrifugation in a microfuge and transfer the supernatant to fresh microfuge tubes.

15. Add 50 μl of benzamidine-Sepharose beads using a recessed tip to each supernatant to clear the thrombin. Incubate 1–2 h shaking on a nutator at 4 °C.

16. Pellet the benzamidine-Sepharose beads by a quick pulse centrifugation in a microfuge and transfer the supernatant to a filter-centrifugation/concentration unit. Use a 10 kDa molecular weight cut off filter for the cleaved DENN domain and a 4 kDa molecular weight cut off filter for cleaved Rab35.

17. Add 5 ml GEF loading buffer to the cleaved Rab35 in the sample chamber of the concentrator unit and spin at 3,500 × *g* until the sample volume is reduced back to 500 μl. Discard the flow-through from the collection tube and add another 5 ml

GEF loading buffer to the sample. Spin at $3,500 \times g$ until the sample is reduced to 500 µl or less. Transfer the purified Rab35 to a microfuge tube and keep on ice. For longer storage, aliquot and store at –70 °C.

18. Add 5 ml GEF incubation buffer to the cleaved connecdenn DENN domain in the sample chamber of the concentrator unit and spin at $3,500 \times g$ until the sample volume is reduced back to 500 µl. Discard the flow-through from the collection tube and add another 5 ml GEF incubation buffer to the sample. Spin at $3,500 \times g$ until the sample is reduced to 500 µl or less. Transfer the purified connecdenn DENN domain to a microfuge tube and keep on ice. For longer storage, aliquot and store at –70 °C.

19. Determine protein concentrations by running aliquots of the purified proteins (e.g., 5 and 20 µl) together with a BSA standard curve (1, 2, 5, 10, 20 µg) on an SDS-acrylamide gel, followed by Coomassie staining. To minimize pipetting errors, add each sample to 40 µl PBS, add 10 µl 5× LSB, and load the whole sample onto the acrylamide gel. When comparing the purified proteins to the BSA standard curve, consider both area and staining intensity to estimate sample concentration.

3.4 Rab35 Loading

1. The minimal concentration of Rab35 required is 12.8 ng/µl. Based on the concentration determined by the Coomassie-stained acrylamide gel, calculate the volume needed for 345.4 ng of purified Rab35, which will yield a concentration of 15 µM in a reaction with a final volume of 30 µl.

2. Dilute the 40 mM GDP stock 1:50 with GEF loading buffer to yield a 400 µM working stock. Keep on ice.

3. Dilute the 0.5 M EDTA stock 1:5 with GEF loading buffer to yield a 100 mM working stock.

4. Dilute the 2 M $MgCl_2$ stock 1:10 with GEF loading buffer to yield a 200 mM working stock.

5. Mix Rab35 (amount as calculated above to yield 15 µM in a 30 µl volume), 1.5 µl 400 µM GDP, and 1.5 µl 100 mM EDTA. Top up to a final volume of 30 µl with GEF loading buffer.

6. Incubate for 10 min at 30 °C in a dry bath or water bath to load Rab35 with GDP.

7. Add 1.5 µl 200 mM $MgCl_2$ to stabilize the nucleotide on the GTPase and store sample on ice.

3.5 GEF Assay

1. Based on the concentration determined by the Coomassie-stained acrylamide gel, calculate the volume needed for 461 ng of purified connecdenn DENN domain, which will yield a con-

centration of 100 nM in a reaction with a final volume of 130 μl (*see* **Note 11**).

2. Prepare 2× 8 microfuge tubes with 1 ml ice-cold wash buffer each. Keep on ice in microfuge tube racks or better, spare metal dry bath tube blocks. Label each set of 8 tubes in a different color (or distinguish some other way) with the time-points at which samples will be taken from the enzymatic reactions, e.g., 0, 15, 30, 45, 60, 90, 120, 180 s (*see* **Note 12**).

3. Cut out round pieces of 0.22 μm nitrocellulose filters, one for each sample and large enough to fully cover the support screen of a 25 mm Glass Microanalysis Vacuum Filter Unit. Wet filters in wash buffer.

4. Dilute the 1 M DTT stock 1:20 with GEF incubation buffer to yield a 50 mM working stock.

5. Dilute the 10 mM GTPγS stock 1:200 with GEF incubation buffer to yield a 50 μM working stock. Keep on ice.

6. In a microfuge tube on ice, mix
   - 10.8 μl GDP-loaded Rab35 (1.25 μM final concentration)
   - 461 ng purified connecdenn DENN domain (100 nM final concentration)
   - 6.5 μl 10 mg/ml bovine serum albumin (BSA)
   - 13 μl 50 μM GTPγS
   - 4.33 μCi [^{35}S] GTPγS (*see* **Note 13**)
   - 1.3 μl 50 mM DTT
   - Top up with GEF incubation buffer to a final volume of 130 μl and incubate at room temperature (*see* **Note 11**).
   - Add the GDP-loaded Rab35 last, mix, immediately remove 15 μl from the reaction, and transfer into a microfuge tube containing 1 ml ice-cold wash buffer (0 s time-point), keep on ice.

7. Basal exchange activity of Rab35 is measured in a parallel reaction, in which the DENN domain is replaced with GEF incubation buffer.

8. Remove 15 μl from each reaction at each time-point (15, 30, 45, 60, 90, 120, and 180 s), transfer into a microfuge tube containing 1 ml ice-cold wash buffer and keep on ice.

9. Once all the samples have been collected, insert a nitrocellulose filter into the Glass Microanalysis Vacuum Filter Unit, apply vacuum, and pass sample through. Handle all samples, solutions, and equipment carefully and according to any rules and guidelines applicable to the use of radioactivity.

10. Immediately wash filter by passing through 5 ml wash buffer.

11. Disassemble unit and transfer filter into a 7 ml scintillation vial containing 5 ml of scintillation cocktail.

a	Rab35		Rab35+CD1 DENN	
sec	**cpm**	**pmol**	**cpm**	**pmol**
0	9,987	0.8	2,448	0.2
15	8,781	0.7	104,644	7.9
30	11,672	0.9	162,536	12.3
45	9,069	0.7	198,103	15.0
60	9,083	0.7	203,016	15.4
90	11,894	0.9	232,100	17.6
120	9,470	0.7	245,810	18.6
180	11,402	0.9	240,743	18.2
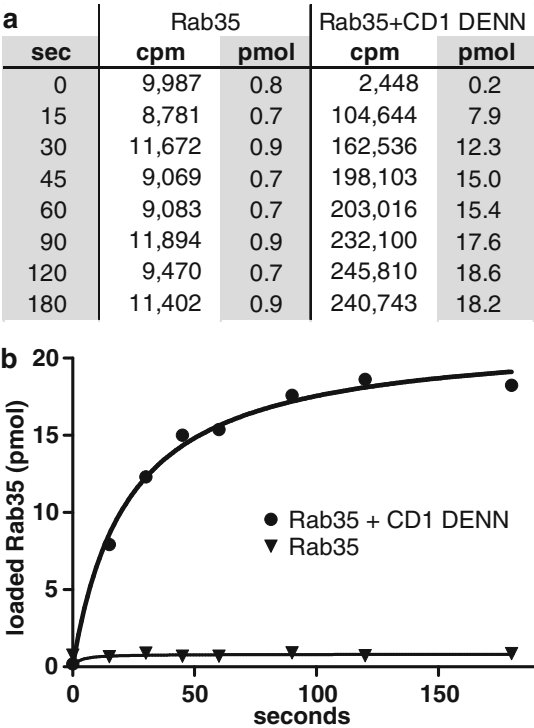
Fig. 1 Example of GEF assay results. The table in (**a**) shows results of an individual experiment testing for Rab35 loading with GTPγS in the absence or presence of the connecdenn1/DENND1A DENN domain (+ CD1 DENN) over time. Cpm was converted into pmol of loaded Rab35 as described in **Note 15**. (**b**) The amount of loaded Rab35 for each condition was plotted over time and the curve was fit by nonlinear regression. The results shown in figure are part of the data published in ref. 9

12. Repeat until each sample has been processed.

13. Measure levels of bound [³⁵S] GTPγS in a liquid scintillation counter (*see* **Note 14**).

14. Repeat experiment 3–4 times, using independent protein preps each time.

15. Data can be analyzed and plotted using common software packages and curves can be fitted using a nonlinear regression one-phase association (Fig. 1) (*see* **Note 15**).

4   Notes

1. The 30 % SDS solution will require extensive stirring, sometimes over night, and often require to heat the solution to ~50 °C until all SDS has dissolved. Keep covered to avoid evaporation. Store at room temperature and if precipitation

occurs, incubate the solution in a ~40 °C water bath until clear again.

2. To ensure high transfection efficiency, test all four solutions/pH values by transfecting HEK 293-T cells with e.g., a mammalian GFP expression construct. Next day, determine which 2× HBS stock yields the highest percentage of GFP-positive cells. Usually, one or two pH values will work well, discard the others. The absolute value of the optimal pH will vary between batches and needs to be empirically determined for each new batch. As pH measurements may vary with the type of electrode used and the frequency of calibration, consider covering a wider pH range for the first time(s) ranging from 6.95 to 7.10. Make sure to calibrate the electrode before preparing the 2× HBS solutions.

3. Though we are not sure why, 2× HBS solutions stored at room temperature will "age" over time and lose transfection efficiency. If transfections will not be done frequently, either set up smaller batches or aliquot, e.g., into sterile 50 ml conical tubes (do not fill higher than 40 ml) and store at –20 °C. We have not noticed a drop in transfection efficiency for solutions stored frozen; however, it is critical to let all solutions reach room temperature before setting up the transfection mix, otherwise the size of the precipitate formed may be too large to allow for high transfection efficiency.

4. The medium for the HEK 293-T cell line can also be supplemented with fetal bovine serum. However, we have not seen any difference in growth or performance using the cheaper iron-supplemented calf serum. We have not tested how normal calf serum (not iron-supplemented) compares.

5. The expression levels for different DENN domains may vary between transfections and different DENN domains. In some cases, the number of plates used for expression may need to be scaled up accordingly and we recommend six 15 cm dishes per construct as a starting point.

6. Some recipes for calcium phosphate transfections call for higher DNA amounts; however, on occasion, we noticed impaired cell proliferation and even cell death following transfection when using higher DNA amounts (up to 25 μg/plate), while negatively impacted protein yield.

7. After the 20–25 min incubation time, the transfection mix should look just a bit less clear due to the precipitate that formed. However, if large cloudy flakes and/or a sediment forms, conditions are not optimal and transfection efficiency will be low. The precipitation can be caused by protein contamination in the DNA prep (we prefer $OD_{260/280} > 1.85$) or the solutions not being at room temperature. Also, make sure

to use ultrapure deionized water because traces of calcium and other bivalent ions will interfere with the precipitation reaction.

8. While not absolutely required, this step improves cell viability. If needed, the incubation time can be cut to 6 h.

9. Do not let the probe touch the container and be sure to keep cells on ice during sonication as samples will heat up. Lyse with three bursts of 5 s at 30–50 % output. Settings will have to be optimized for each sonicator and efficient lysis can be verified by light microscopy.

10. Due to the difference in angle, 15 ml conical tubes retain the bead pellet better than 50 ml conical tubes and should thus be the first choice. When pouring the supernatant off, pour slowly and steadily, do not hesitate or reverse the tube into an upright position in between as this will resuspend some of the beads in the liquid and could cause loss of material. However, once embraced, pouring off is the fastest and safest way of washing beads.

11. Different DENN domains can vary in their enzymatic activity and we have used up to 350 nM purified DENN domain per GEF assay in some cases. The maximum amount of DENN domain that can be used is determined by the concentration of the purified protein and the maximum volume allotted in the reaction mix.

12. Different DENN domains can vary in enzymatic activity and the time course of the assay should be adjusted such that the reaction reaches (close-to) saturation.

13. The volume needed for a constant amount of radioactive [^{35}S] GTPγS will vary depending on the calibration date of the solution and the number of half-life gone by and should be adjusted as needed. The impact of these adjustments on the total amount of cold GTPγS in the reaction can be considered neglectable for the calculations outlined in **Note 15**.

14. The detection efficiency for [^{35}S] GTPγS varies between scintillation counters and when presenting data as molar exchange, instead of counts per minute (cpm), it is best to empirically determine the detection efficiency for the counter used. Simply measure cpm for a known [^{35}S] GTPγS amounts, for which the disintegrations per minute (dpm) can be calculated based on the fact that 1 Ci = 2.2×10^{12} dpm. If the counter has 100 % efficiency, the number of cpm equals the number of dpm. More likely, the cpm detected will be lower and the cpm/dpm ratio can be used to correct the data obtained for the GEF assays. The dpm also allows one to calculate the number of Ci in each sample.

15. The data can be graphed in multiple ways: The raw data can be plotted as cpm (or dpm) over time or GEF concentrations. To determine the molar exchange rate, which will allows one to compare results to other GEFs, the cpm need to be converted into pmol of loaded Rab. If the exchange reaction is set up as described above, each 15 µl sample will contain 0.5 µCi [^{35}S] GTPγS, which equals 0.4 pmol. The reaction also contains 75 pmol cold GTPγS (a 187.5 fold excess). Based on a specific activity of 1,250 Ci/mmol for the [^{35}S] GTPγS stock, the specific activity in each sample is 6.7 Ci/mmol. The cpm detected for each sample can be converted into dpm and Ci as described in **Note 14** above. The number of Ci per sample together with the specific activity of each sample and the dilution factor of hot and cold GTPγS allows one to calculate the molar exchange.

Example: When a sample is measured with 180,000 cpm and the detection efficiency of the counter is 90 %, the sample contains 200,000 dpm. 200,000 dpm equal 90 nCi and based on the specific activity of the sample of 6.7 Ci/mmol, this equals 72 fmol of loaded Rab. Correcting for the dilution factor of hot with cold GTPγS (187.5 fold), the sample contains 13.5 pmol of GTPγS-loaded Rab.

References

1. Richardson PM, Zon LI (1995) Molecular cloning of a cDNA with a novel domain present in the tre-2 oncogene and the yeast cell cycle regulators BUB2 and cdc16. Oncogene 11:1139–1148

2. Fukui K, Sasaki T, Imazumi K et al (1997) Isolation and characterization of a GTPase activating protein specific for the Rab3 subfamily of small G proteins. J Biol Chem 272:4655–4658

3. Wada M, Nakanishi H, Satoh A et al (1997) Isolation and characterization of a GDP/GTP exchange protein specific for the Rab3 subfamily small G proteins. J Biol Chem 272:3875–3878

4. Iwasaki K, Staunton J, Saifee O et al (1997) aex-3 encodes a novel regulator of presynaptic activity in *C. elegans*. Neuron 18:613–622

5. Levivier E, Goud B, Souchet M et al (2001) uDENN, DENN, and dDENN: indissociable domains in Rab and MAP kinases signaling pathways. Biochem Biophys Res Commun 287:688–695

6. Marat AL, Dokainish H, McPherson PS (2011) DENN domain proteins: regulators of Rab GTPases. J Biol Chem 286:13791–13800

7. Sato M, Sato K, Liou W et al (2008) Regulation of endocytic recycling by *C. elegans* Rab35 and its regulator RME-4, a coated-pit protein. EMBO J 27:1183–1196

8. Allaire PD, Ritter B, Thomas S et al (2006) Connecdenn, a novel DENN domain-containing protein of neuronal clathrin-coated vesicles functioning in synaptic vesicle endocytosis. J Neurosci 26:13202–13212

9. Allaire PD, Marat AL, Dall'Armi C et al (2010) The Connecdenn DENN domain: a GEF for Rab35 mediating cargo-specific exit from early endosomes. Mol Cell 37:370–382

10. Yoshimura S, Gerondopoulos A, Linford A et al (2010) Family-wide characterization of the DENN domain Rab GDP-GTP exchange factors. J Cell Biol 191:367–381

11. Marat AL, McPherson PS (2010) The connecdenn family, Rab35 guanine nucleotide exchange factors interfacing with the clathrin machinery. J Biol Chem 285:10627–10637

12. Wu X, Bradley MJ, Cai Y et al (2011) Insights regarding guanine nucleotide exchange from the structure of a DENN-domain protein complexed with its Rab GTPase substrate. Proc Natl Acad Sci U S A 108:18672–18677

13. Nookala RK, Langemeyer L, Pacitto A et al (2012) Crystal structure of folliculin reveals a hidDENN function in genetically inherited renal cancer. Open Biol 2:120071

14. Zhang G, Jung BP, Ho W et al (2007) Isolation and characterization of LCHN: a

novel factor induced by transient global ischemia in the adult rat hippocampus. J Neurochem 101:263–273

15. Levine TP, Daniels RD, Gatta AT et al (2013) The product of C9orf72, a gene strongly implicated in neurodegeneration, is structurally related to DENN Rab-GEFs. Bioinformatics 29:499–503

16. Zhang D, Iyer LM, He F et al (2012) Discovery of Novel DENN proteins: implications for the evolution of eukaryotic intracellular membrane structures and human disease. Front Genet 3:283

Chapter 20

Assay of Rab17 and Its Guanine Nucleotide Exchange Factor Rabex-5 in the Dendrites of Hippocampal Neurons

Yasunori Mori and Mitsunori Fukuda

Abstract

Neurons are functionally and morphologically compartmentalized into axons and dendrites, and the localization of specific proteins within these compartments is critical to the proper formation of neuronal networks, which includes neurite morphogenesis and synapse formation. The small GTPase Rab17 is specifically localized in dendrites and is not found in axons, and it regulates the dendrite morphogenesis and postsynaptic development of mouse hippocampal neurons. However, the spatiotemporal regulation of Rab17 is poorly understood. We recently identified Rabex-5, originally described as a Rab5-guanine nucleotide exchange factor (GEF), as a physiological Rab17-GEF that promotes translocation of Rab17 from the cell body to the dendrites of developing hippocampal neurons. Knockdown of Rab17 in mouse hippocampal neurons resulted in reductions in dendrite growth, branch numbers, filopodium density, and active synapse numbers. Knockdown of Rab17-GEF Rabex-5 in hippocampal neurons resulted in decreased targeting of Rab17 to the dendrites, which led to a reduction in dendrite growth. In this chapter we describe the assay procedures for analyzing Rab17 and Rabex-5 in cultured mouse hippocampal neurons, and we particularly focus on the measurement of total dendrite (or axon) length and total dendrite (or axon) branch numbers, filopodium density, number of active synapses, and dendritic Rab17 signals.

Key words Rab17, Rabex-5, Dendrite, Postsynapse, Hippocampal neuron

1 Introduction

Neurons are highly polarized cells that possess two distinct subcellular compartments: axons and dendrites. Dendrite development, which includes dendritogenesis and postsynaptic maturation, is an important step in the process by which neurons establish proper neuronal networks [1]; however, its precise molecular mechanisms, specifically the mechanisms by which specific proteins and lipids are targeted to dendrites, are poorly understood.

Rab-type small GTPases are conserved membrane trafficking proteins in all eukaryotes, and they mediate a variety of steps in membrane trafficking, including vesicle budding, vesicle movement, vesicle docking to specific membranes, and vesicle fusion [2, 3]. Rabs function as a molecular switch by cycling between two

nucleotide-bound states, a GDP-bound inactive state and a GTP-bound active state, and their activation is generally thought to be achieved by the actions of specific guanine nucleotide exchange factors (GEFs) [4]. As indicated by the origin of the word Rab, i.e., Ras homologues in *ra*t *b*rain [5], most members of the Rab family are abundantly expressed in brain, and several of them have been shown to regulate neuronal functions, including neurite morphogenesis and neurotransmission [2, 6]. Rab17 is the only Rab protein identified in neurons thus far that is exclusively targeted to dendrites with none at all being found in axons, and it has been found to regulates dendrite morphogenesis, i.e., dendrite growth and branching, and postsynaptic development, i.e., active synapse formation, in mouse cultured hippocampal neurons [7]. In an attempt to determine the activation mechanism of Rab17 we recently identified Rabex-5, originally described as a Rab5-GEF [8, 9], as a Rab17-GEF that is required for the translocation of Rab17 from the cell body to the dendrites in mouse hippocampal neurons [10]. Knockdown of either Rab17 or Rabex-5 in hippocampal neurons caused abnormal dendrite morphogenesis, e.g., short dendrites [7, 10]. In this chapter we summarize the methods that we have used to analyze Rab17 and Rabex-5 during dendrite development in cultured mouse hippocampal neurons.

2   Materials

Prepare all solutions by using ultrapure water (we prepare ultrapure water by using the Milli-Q Advantage A10 Ultrapure Water Purification System) and analytical grade or the highest grade reagents commercially available (unless otherwise specified).

2.1   Mouse Hippocampal Neuron Culture and Transfection

1. A specific pathogen-free (SPF) embryonic day 16.5 (E16.5) pregnant ICR mouse.

2. 100-mm cell culture dishes.

3. HEPES/HBSS: Hank's Balanced Salt Solution (HBSS) with calcium and magnesium, no phenol red, supplemented with 15 mM HEPES.

4. Stereoscopic microscope.

5. 2.5 % trypsin (10×, no phenol red).

6. 0.8 % DNase-I in HBSS with calcium and magnesium, no phenol red.

7. MEM (minimum essential medium): 5.4 mM KCl, 116 mM NaCl, 26 mM $NaHCO_3$, 1 mM NaH_2PO_4, 39 mM glucose, 0.8 mM $MgSO_4$, and 1.8 mM $CaCl_2$, pH 7.25.

8. 200× Vitamin Mix solution: Ca-panthothenate 200 mg/L, choline chloride 200 mg/L, folic acid 200 mg/L, i-inositol 360 mg/L, niacinamide 200 mg/L, pyridoxal HCl 200 mg/L, and thiamine HCl 200 mg/L in ultrapure water.

9. Riboflavin 200 mg/L in ultrapure water.

10. MEM plus Vitamin Mix solution: Add 5 mL of 200× Vitamin and 400 μL of riboflavin solution to 1 L of MEM, and filter through a 0.2-μm filter.

11. Stop solution: MEM plus Vitamin Mix solution supplemented with 2 % MEM amino acid solution, 15 mM HEPES, and 10 % fetal bovine serum (FBS).

12. Plating medium: MEM plus Vitamin Mix solution supplemented with 2 % MEM amino acid solution, 15 mM HEPES, 0.5 % FBS, 2 % B27, 0.5 mM glutamine, and penicillin/streptomycin 50 U/L (*see* **Note 1**).

13. Cell strainer 40 μm.

14. Autoclaved 12-mm glass coverslips in a 6-well plate and 35-mm glass-bottom dishes. The glass coverslips and glass-bottom dishes have been coated in advance by immersion in 1 mg/mL poly-L-lysine hydrobromide MW 30,000–70,000 (PLL-HBr) in ultrapure water for 1 day, washed three times with ultrapure water, and immersed in 2 mL of Stop solution.

15. 10 mM cytosine-β-D-arabinofuranoside (Ara-C) in ultrapure water.

16. Plasmid DNAs dissolved in ultrapure water (1 μg/μL) after the DNAs have been purified in advance with the QIAGEN Plasmid Midi kit or with another transfection-grade plasmid purification kit.

17. Lipofectamine® 2000.

2.2 Immunostaining

1. 4 % paraformaldehyde (PFA) solution: 4 % PFA, 4 % sucrose in 0.1 M sodium phosphate buffer: 0.084 M Na_2HPO_4, 0.016 M NaH_2PO_4, pH 7.4.

2. Phosphate buffered saline (PBS).

3. 0.25 % Triton X-100 in PBS.

4. Blocking solution: 10 % FBS in PBS.

5. Primary antibodies (*see* **item 2** in Subheadings 2.3, 2.5, and 2.6 for details).

6. Secondary antibodies (*see* **item 3** in Subheadings 2.3, 2.5, and 2.6 for details).

7. Fluoromount™ Aqueous Mounting Medium.

2.3 Evaluation of Neurite Morphogenesis

1. 1 μg/μL pSilencer-SV40-EGFP-Control and pSilencer-SV40-EGFP-shRab17 [7].

2. Anti-GFP rabbit polyclonal antibody (1/1,000 dilution), anti-neurofilament-H mouse monoclonal antibody (1/500 dilution), and anti-MAP2 chick polyclonal antibody (1/1,000 dilution).

3. Alexa Fluor® 488-conjugated anti-rabbit IgG goat antibody, Alexa Fluor® 594-conjugated anti-mouse IgG goat antibody, and Alexa Fluor® 633-conjugated anti-chick IgG goat antibody.

4. Confocal fluorescence microscope with a 40× oil-immersion objective.

5. NeuronJ (version 1.1.0) [11] plug-in software for the ImageJ software program (version 1.42q).

2.4 Measurement of Filopodium Density

1. 1 μg/μL pCAG-gap-Venus, pSilencer-neo-Control, and pSilencer-neo-shRab17 [7, 10].

2. Confocal fluorescence microscope with a 63× oil-immersion objective.

2.5 Anti-Syt I-N Antibody Uptake Experiment

1. 1 μg/μL pSilence-SV40-EGFP-Control and pSilencer-SV40-EGFP-shRab17 [7].

2. Anti-GFP rabbit polyclonal antibody (1/1,000 dilution), anti-MAP2 chick polyclonal antibody (1/1,000 dilution), and anti-Syt I-N rabbit polyclonal antibody [12].

3. Alexa Fluor® 488-conjugated anti-rabbit IgG goat antibody, Alexa Fluor® 594-conjugated anti-mouse IgG goat antibody, and Alexa Fluor® 633-conjugated anti-chick IgG goat antibody (1/5,000 dilution).

4. Confocal fluorescence microscope with a 63× oil-immersion objective.

2.6 Measurement of Dendritic Rab17 Signals

1. 1 μg/μL pEGFP-C1, pEGFP-C1-Rabex-5-C, pEGFP-C1-Rabex-5-C-D313A, and pmCherry-C1-Rab17 [10].

2. Anti-GFP guinea pig polyclonal antibody (1/1,000 dilution) [7], anti-MAP2 chick polyclonal antibody (1/1,000 dilution), and anti-Rab17 rabbit polyclonal antibody (1/500 dilution) [7].

3. Alexa Fluor® 488-conjugated anti-guinea pig IgG goat antibody, Alexa Fluor® 594-conjugated anti-rabbit IgG goat antibody, and Alexa Fluor® 633-conjugated anti-chick IgG goat antibody (1/5,000 dilution).

4. Confocal fluorescence microscope with a 63× oil-immersion objective.

5. ImageJ (version 1.42q).

3 Methods

3.1 Mouse Hippocampal Neuron Culture and Transfection

1. Sacrifice a pregnant mouse, remove the uterus, and transfer it to a 100-mm dish containing HEPES/HBSS.

2. Remove the embryos from the uterus, and remove their brains.

3. Dissect out of the bilateral hippocampi in a 100-mm dish containing HEPES/HBSS on ice under a stereoscopic microscope.

4. Transfer all of the hippocampi into 4 mL of HEPES/HBSS in a 15-mL conical centrifuge tube, and add 500 μL of 2.5 % trypsin and 500 μL of 0.8 % DNase-I solution.

5. Incubate at 37 °C for 15 min in a water bath, and gently shake every 3 min.

6. Gently remove the solution, add 10 mL of Stop solution, and incubate on ice for 5 min. Perform this step twice.

7. Gently remove the solution, add 900 μL of Stop solution and 100 μL of 0.8 % DNase-I solution, and then gently pipette up and down 10–12 times with a P1000 pipette.

8. Centrifuge $100 \times g$ at room temperature for 5 min.

9. Remove the supernatant, and add 4 mL of Plating medium.

10. Filter the cell suspensions through a cell strainer.

11. Determine cell density by applying a drop of the cell suspension to a hemacytometer.

12. Remove the Stop solution from PLL-HBr-coated dishes, add 2–4 mL of Plating medium, and seed mouse hippocampal neurons in the dishes ($3–6 \times 10^4$ cells).

13. Incubate the cells at 37 °C under 5 % CO_2.

14. At 3–4 DIV, add Ara-C solution to a final concentration of 2.5 μM.

15. At 4 DIV, transfect the neurons with 0.25 μg of plasmid DNAs by using 0.5 μL of Lipofectamine® 2000 according to the manufacturer's instructions (*see* **Note 2**).

16. Incubate the cells at 37 °C under 5 % CO_2 until fixation.

3.2 Immunostaining

1. Fix the mouse hippocampal neurons (from **step 16**, Subheading 3.1) with 2 mL of 4 % PFA solution for 10 min at room temperature.

2. Wash the neurons three times with 1 mL of PBS each time.

3. Permeabilize the neurons with 0.25 % Triton X-100 in PBS for 3 min.

4. Wash the neurons three times with 1 mL of PBS each time.

5. Incubate with Blocking solution for 30 min.

6. Incubate with the appropriate primary antibodies in Blocking solution for 1 h at room temperature.

7. Wash the neurons three times with 1 mL of PBS each time. Incubate with the appropriate secondary antibodies in blocking solution for 30 min at room temperature under light-protected conditions. Perform the following steps under light-protected conditions.

8. Mount coverglasses on a microscope slide with Fluoromount™ Aqueous Mounting Medium.

9. Allow to dry for 1 h to overnight.

3.3 Evaluation of Neurite Morphogenesis

1. Place 12-mm coverglasses in each of 2 wells of a 6-well dish.

2. Seed 3×10^4 neurons (from **step 12**, Subheading 3.1) in 2 mL of Plating medium in each well, one for transfection of pSilencer-SV40-EGFP-Control and the other for transfection of pSilencer-SV40-EGFP-shRab17, and incubate them at 37 °C under 5 % CO_2.

3. At 4 DIV, transfect neurons with 0.25 µg of the above plasmids by using 0.5 µL of Lipofectamine® 2000 according to the manufacturer's instructions.

4. At 11 DIV, fix the neurons and immunostain as described above.

5. Capture fluorescence images of EGFP, neurofilament-H, and MAP2 in EGFP-expressing neurons at random under a confocal fluorescence microscope. All quantitative analyses are carried out based on the immunostaining of the morphometric marker EGFP. Dendrites and axons are identified by the immunostaining of a dendrite-specific marker (MAP2) and an axon-specific marker (neurofilament-H), respectively (*see* **Note 3**).

6. Evaluate the neurite morphology of the neurons by manually measuring the total dendrite length, total dendrite branch tip numbers, total axon length, and total axon branch tip numbers of each neuron with NeuronJ. The length of each neurite is measured from the edge of the cell body (or the branch point of the neurite) to the tip of the neurite. Total dendrite (or axon) length means the sum of the lengths of all of the dendrites (or axons) of a single neuron (representative images and results are shown in Fig. 1a–c).

3.4 Measurement of Filopodium Density

1. Seed 3×10^4 neurons (from **step 12**, Subheading 3.1) in 2 mL of Plating medium in each of two glass-bottom dishes, one for transfection of pCAG-gap-Venus and pSilencer-neo-Control and the other for transfection of pCAG-gap-Venus and pSilencer-neo-shRab17, and incubate them at 37 °C under 5 % CO_2.
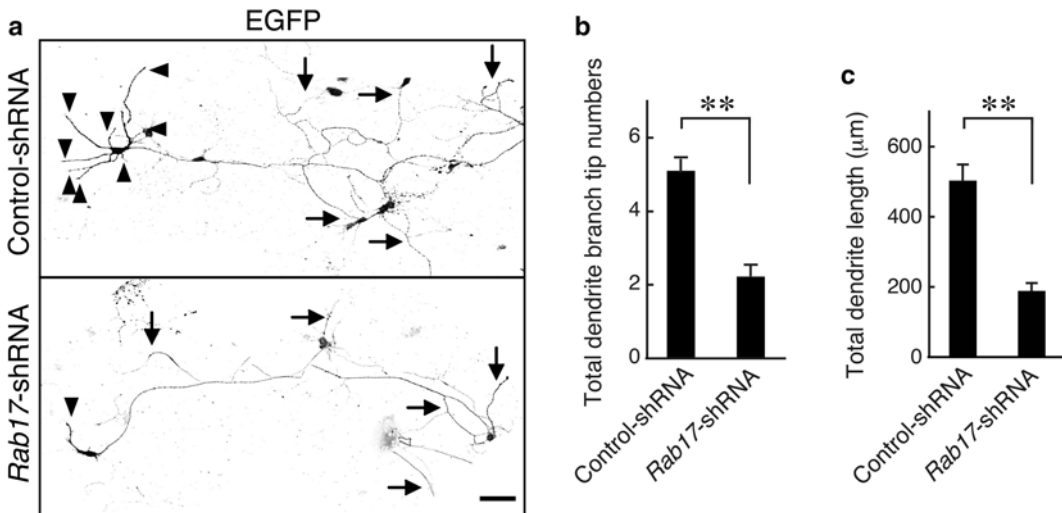
Fig. 1 Rab17 regulates dendritic morphogenesis in mouse hippocampal neurons. (**a–c**) At 4 DIV, hippocampal neurons were transfected with a vector encoding EGFP and control-shRNA (*upper panel* in (**a**)) or *Rab17*-shRNA (*lower panel* in (**a**)), and the neurons were fixed at 11 DIV and immunostained with antibodies against GFP, neurofilament-H, and MAP2. (**a**) Typical EGFP fluorescence image of a Rab17-knockdown neuron. The *arrows* and *arrowheads* point to axons (neurofilament-H-positive) and dendrites (MAP2-positive), respectively. Bar, 50 μm. (**b** and **c**) Quantification of total dendrite branch tip numbers (**b**) and total dendrite length (**c**) of the control neurons and Rab17-knockdown neurons. **$p < 0.0025$. Note that both the total dendrite length and total dendrite branch tip numbers of the Rab17-knockdown neurons were significantly lower than in the control cells. However, neither axonal branching nor axonal outgrowth was affected by the Rab17 knockdown (not shown)

2. At 4 DIV, transfect the neurons with 0.2 μg of pCAG-gap-Venus and 0.05 μg of pSilencer-neo-Control or with 0.2 μg of pCAG-gap-Venus and 0.05 μg of pSilencer-neo-shRab17, by using 0.5 μL of Lipofectamine® 2000 according to the manufacturer's instructions.

3. At 11 DIV, capture live images of gap-Venus-expressing hippocampal neurons under a confocal fluorescence microscope.

4. Manually count the dendritic filopodia, i.e., headless filaments that protrude more than 1.5 μm from the main shaft of dendrites. Filopodium density is expressed as number per 10-μm dendrite length (representative images and results are shown in Fig. 2a, b).

3.5 Anti-Syt I-N Antibody Uptake Experiment

1. Place 12-mm coverglasses in each of 2 wells of 6-well dish.

2. Seed 6×10^4 neurons (from **step 12**, Subheading 3.1) in 4 mL of Plating medium in each of 2 wells, one for transfection of pSilencer-SV40-EGFP-Control and the other for transfection of pSilencer-SV40-EGFP-shRab17, and incubate them at 37 °C under 5 % CO_2.
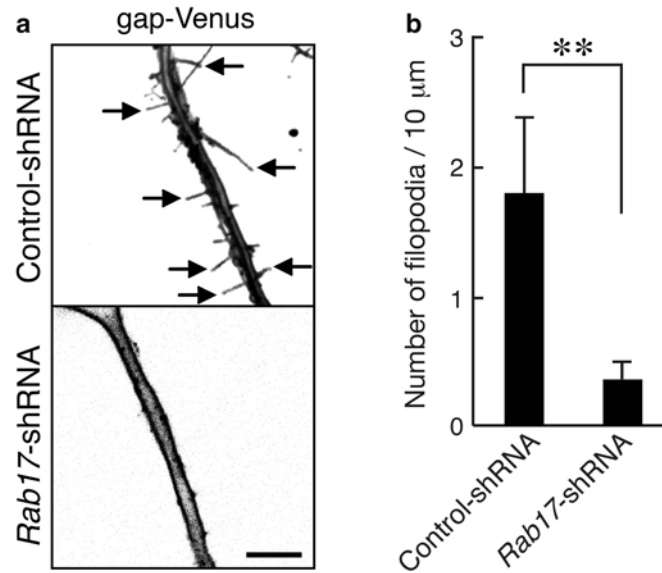
Fig. 2 Rab17 is required for filopodium formation in dendrites. (**a**) Typical image of a Rab17-knockdown neuron with reduced numbers of filopodia. At 4 DIV, hippocampal neurons were transfected with a vector encoding gap-Venus together with control-shRNA (*upper panel*) or *Rab17*-shRNA (*lower panel*), and the neurons were examined at 11 DIV. Bar, 5 μm. (**b**) Quantification of the number of dendritic filopodia in the control neurons and Rab17-knockdown neurons. *******p*<0.0025. Note the presence of a considerable number of filopodia along the dendrites (*arrows*) of the control neurons, but few filopodia in the Rab17-knockdown neurons

3. At 4 DIV, transfect the neurons with 0.25 μg of pSilencer-SV40-EGFP-Control or with 0.25 μg of pSilencer-SV40-EGFP-shRab17, by using 0.5 μL of Lipofectamine® 2000 according to the manufacturer's instructions.

4. At 21 DIV, replace Plating medium with 0.5 mL of MEM medium containing 25 mM KCl and anti-Syt I-N antibody (0.5 μg/mL), and incubate at 37 °C for 10 min.

5. Fix the neurons immediately, and immunostain them as described in Subheadings 2.2 and 3.2 by using the primary antibodies and secondary antibodies.

6. Capture fluorescence images of EGFP, MAP2, and anti-Syt I-N antibody in EGFP-expressing neurons under a confocal fluorescence microscope (*see* **Note 4**).

7. Count the number of Syt I-N positive dots manually, and express the number per 10-μm dendrite length (representative images and results are shown in Fig. 3a, b).
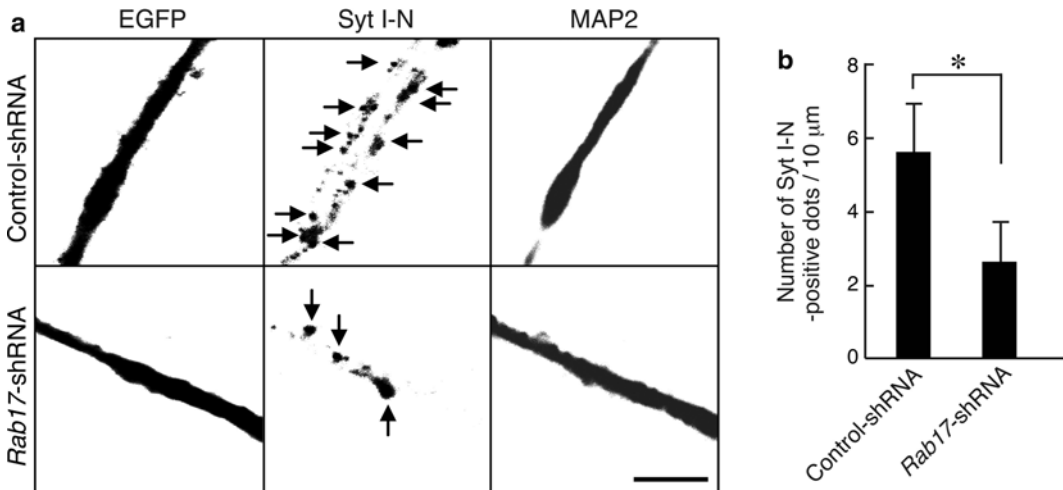
Fig. 3 Rab17 is required for postsynaptic development. (**a**) Typical images of a Rab17-knockdown neuron with reduced numbers of active synapses. At 4 DIV, hippocampal neurons were transfected with a vector encoding EGFP and control-shRNA (*upper panels* in (**a**)) or *Rab17*-shRNA (*lower panels* in (**a**)), and at 21 DIV, they were incubated for 10 min with 25 mM KCl-containing medium in the presence of anti-Syt I-N antibody. The neurons were then fixed and immunostained with antibodies against GFP (*left panels*), rabbit IgG (*middle panels*), and MAP2 (*right panels*). The *arrows* point to anti-Syt I-N antibody that has been incorporated into neurons (*arrows*). Bar, 5 μm. (**b**) Quantification of the number of anti-Syt I-N antibody-positive dots in the control neurons and Rab17-knockdown neurons. *$p < 0.01$. Note that the control neurons took up massive amounts of Syt I N-terminal antibody, whereas the Rab17-knockdown neurons took up far smaller amounts

3.6 Measurement of Dendritic Rab17 Signals in Rabex-5-Expressing Neurons

1. Place 12-mm coverglasses in each of 3 wells of 6-well dish.

2. Seed 3×10^4 neurons (from **step 12**, Subheading 3.1) in 2 mL of Plating medium in each of the 3 wells, one for transfection of pEGFP-C1 and pmCherry-C1-Rab17, another for transfection of pEGFP-Rabex-5-C and pmCherry-C1-Rab17, and the third for transfection of pEGFP-Rabex-5-C-D313A and pmCherry-C1-Rab17, and incubate them at 37 °C under 5 % CO_2.

3. At 4 DIV, transfect the neurons with 0.125 μg of pEGFP-C1 and 0.125 μg of pmCherry-C1-Rab17, with 0.125 μg of pEGFP-C1-Rabex-5-C and 0.125 μg of pmCherry-C1-Rab17, or with 0.125 μg of pEGFP-C1-Rabex-5-C-D313A and 0.125 μg of pmCherry-C1-Rab17, by using 0.5 μL of Lipofectamine® 2000 according to the manufacturer's instructions.

4. At 7 DIV, fix the neurons, and immunostain them as described above.

5. Capture fluorescence images of EGFP, mCherry-Rab17, and MAP2 in neurons expressing EGFP, EGFP-Rabex-5-C, or EGFP-Rabex-5-C-D313A under a confocal fluorescence microscope. Dendrites are identified by positive immunostaining for a dendrite-specific marker (MAP2).

6. To quantify the mCherry-Rab17 signals throughout the entire neuron (cell body, dendrites, and axon) or just the dendrite region, imageJ software is used to set image thresholds to exclude pixels that do not fall over the cell body, the axon, or the dendrites. After subtracting the background intensity values from each image before quantification, the integrated fluorescence intensity of mCherry-Rab17 throughout the entire neuron or in just the dendrite region is calculated.

7. Calculate the amount of mCherry-Rab17 in the dendrites as a proportion of the mCherry-Rab17 in the neuron as a whole by dividing the fluorescence intensity of the dendrite region by the fluorescence intensity of the entire neuron (i.e., total fluorescence intensity) (representative images and results are shown in Fig. 4a, b).
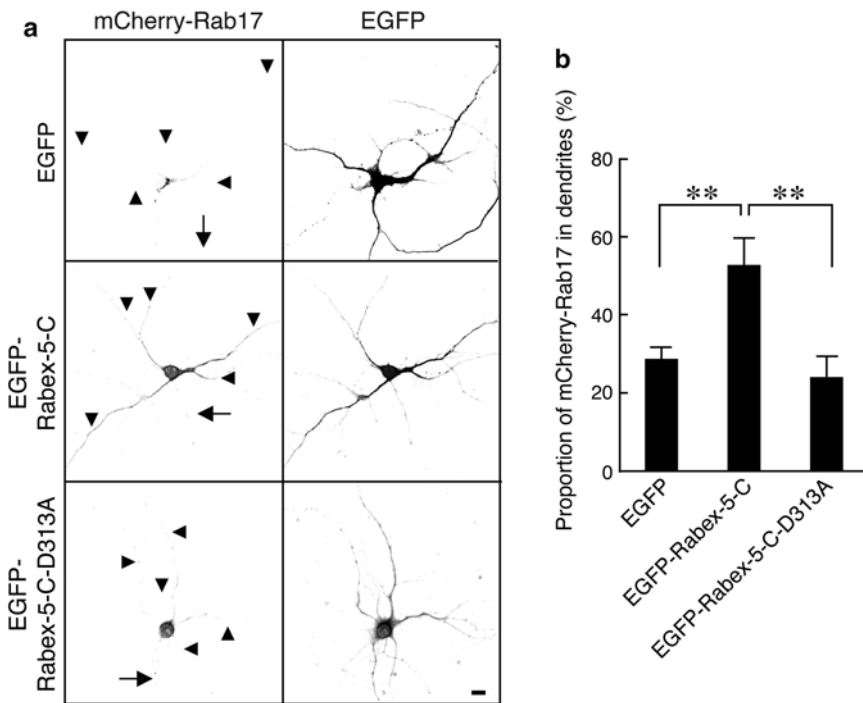
Fig. 4 Rabex-5 promotes translocation of Rab17 to the dendrites of hippocampal neurons. (**a**) Typical images of mCherry-Rab17 in Rabex-5-C-expressing neurons. At 4 DIV, hippocampal neurons were transfected with vectors encoding mCherry-tagged Rab17 and EGFP (*upper panels* in (**a**)), EGFP-Rabex-5-C (*middle panels* in (**a**)), or EGFP-Rabex-5-C-D313A (*bottom panels* in (**a**)), and at 7 DIV, the neurons were fixed and immunostained with antibodies against GFP, Rab17, and MAP2. The *arrows* and *arrowheads* point to axons and dendrites, respectively. Bar, 10 μm. (**b**) Quantification of the proportion of mCherry-Rab17 in the dendrites in the presence of EGFP, EGFP-Rabex-5-C, or EGFP-Rabex-5-C-D313A shown in (**a**). The proportion (%) of dendrite-localized mCherry-Rab17 was calculated by dividing the dendrite-specific mCherry-Rab17 fluorescence intensity by the total mCherry-Rab17 fluorescence intensity. Note that EGFP-Rabex-5-C, but not EGFP-Rabex-5-C-D313A, promoted translocation of mCherry-Rab17 from the cell body to the dendrites. ** $p < 0.0025$

4   Notes

1. The FBS concentration in Plating medium varies from lot to lot of FBS. The optimal FBS concentration should be determined during the initial experiment (usually in the 0.25–5 % range).

2. At 2–6 DIV, neurons that have been prepared by our procedures are capable of being transfected with plasmids.

3. Hippocampal neurons often extend very long axons, and several images must be captured to cover the entire length of their axons.

4. In order to be able to quantify the proportion of Rab17 in the dendrites, avoid saturation by not capturing images that are too bright or too high contrast.

Acknowledgments

References

1. Yoshihara Y, De Roo M, Muller D (2009) Dendritic spine formation and stabilization. Curr Opin Neurobiol 19:146–153

2. Fukuda M (2008) Regulation of secretory vesicle traffic by Rab small GTPases. Cell Mol Life Sci 65:2801–2813

3. Stenmark H (2009) Rab GTPases as coordinators of vesicle traffic. Nat Rev Mol Cell Biol 10:513–525

4. Barr F, Lambright DG (2010) Rab GEFs and GAPs. Curr Opin Cell Biol 22:461–470

5. Touchot N, Chardin P, Tavitian A (1987) Four additional members of the *ras* gene superfamily isolated by an oligonucleotide strategy: molecular cloning of YPT-related cDNAs from a rat brain library. Proc Natl Acad Sci U S A 84:8210–8214

6. Mori Y, Fukuda M (2013) Rabex-5 determines the neurite localization of its downstream Rab proteins in hippocampal neurons. Commun Integr Biol 6:e25433

7. Mori Y, Matsui T, Furutani Y, Yoshihara Y, Fukuda M (2012) Small GTPase Rab17 regulates dendritic morphogenesis and postsynaptic development of hippocampal neurons. J Biol Chem 287:8963–8973

8. Horiuchi H, Lippé R, McBride HM, Rubino M, Woodman P, Stenmark H, Rybin V, Wilm M, Ashman K, Mann M, Zerial M (1997) A novel Rab5 GDP/GTP exchange factor complexed to Rabaptin-5 links nucleotide exchange to effector recruitment and function. Cell 90:1149–1159

9. Yoshimura S, Gerondopoulos A, Linford A, Rigden DJ, Barr FA (2010) Family-wide characterization of the DENN domain Rab GDP-GTP exchange factors. J Cell Biol 191:367–381

10. Mori Y, Matsui T, Fukuda M (2013) Rabex-5 protein regulates dendritic localization of small GTPase Rab17 and neurite morphogenesis in hippocampal neurons. J Biol Chem 288:9835–9847

11. Meijering E, Jacob M, Sarria J-CF, Steiner P, Hirling H, Unser M (2004) Design and validation of a tool for neurite tracing and analysis in fluorescence microscopy images. Cytometry A 58:167–176

12. Fukuda M, Kowalchyk JA, Zhang X, Martin TFJ, Mikoshiba K (2002) Synaptotagmin IX regulates Ca^{2+}-dependent secretion in PC12 cells. J Biol Chem 277:4601–4604

Chapter 21

Methods for Analysis of AP-3/Rabin4′ in Regulation of Lysosome Distribution

Viorica Ivan and Peter van der Sluijs

Abstract

The position of lysosomes in the cytoplasm is important for their ability to fuse with the plasma membrane and release of proteases that are involved in tissue remodeling. Motor-directed bidirectional transport along microtubules is a critical process determining the distribution of lysosomes. How lysosomes are tethered to microtubules is incompletely understood, but a role for small GTPases of rab and arl families has been documented. We recently found that the rab5 and rab4 effector rabip4′ interacts with the adaptor complex AP-3 in a rab4-dependent manner on tubular endosomes. We here describe the assays that led to the identification of AP-3 as a rabip4′ partner and the role of the complex in regulating the spatial distribution of lysosomes.

Key words rabip4/rabip4′, AP-3 complex, Lysosomes, Microtubules

1 Introduction

Lysosomes are membrane-bound organelles with an acidic lumen ($pH < 5$). The limiting membrane is thought to be protected from the acid hydrolase-rich lumen by extensively *N*-glycosylated membrane glycoproteins of the LAMP family. Lysosomes have long been appreciated for their catabolic role in cellular homeostasis. The past decade however witnessed the discovery of many other lysosomal functions including roles as a platform for nutrient signaling, wound healing, and tissue remodeling [1, 2]. Collectively the new information argues for a broader, more dynamic role of lysosomes that transcends well beyond protein and lipid degradation only. Melanocytes and immune cells have lysosome-related organelles that share features with lysosomes, but also have secretory content involved in cell-type specific functions [3]. Lysosomes and lysosome-related organelles undergo motor-directed bidirectional transport along microtubules, the net direction of which is determined by the relative activity of opposing kinesin and cytoplasmic dynein motor proteins [4]. Mechanisms for tethering

lysosomes to microtubule and the recruitment of motor proteins is incompletely understood, but it is clear that small GTPases of rab and arl families play key roles [5].

Previously we identified rabip4′, a long form of the RUN and FYVE domain containing protein RUFY1/rabip4 on endosomes [6, 7]. In search for rabip4′ function, we analyzed the intracellular itineraries of several cargo proteins after rabip4′/rabip4 silencing, and discovered that lysosomal proteins become specifically localized to peripheral protrusions. Preparative pull down for rabip4′ interacting proteins yielded AP-3, an endosomal adaptor complex that defines an exit pathway for tyrosinase to melanosomes and for LAMPs to lysosomes [8, 9]. Loss of AP-3 function amongst others increases LAMP expression on the plasma membrane [10] and microtubule-directed movement of lysosome-related organelles to the immunological synapse and impairs cytotoxicity suggesting a link between AP-3 and microtubule motors [11].

This chapter describes the method we employed to screen for rabip4′ interacting proteins from tissue. It is a simplication of the assay we used before to search for proteins that together with rab4 regulate recycling form the early endosomal system [12, 13]. We here describe this interaction between rabip4′ and AP-3 and the assays to investigate the role of AP-3 and rabip4′ in the intracellular distribution of lysosomes.

2   Materials

2.1   Bacterial Strains

We use *E. coli* strains BL21DE3 and BL21(DE3) Rosetta from Novagen to express recombinant mammalian proteins.

2.2   Mammalian Cell Lines

MNT-1, SKMel28, MelJuSo, B16, HeLa, and HEK293T cells.

2.3   Chemicals

1. siRNA target sequences 5′-GGAGCAUGAAAGAAUU ACUtt-3′ for human RUFY1 encoding rabip4s [14] and 5′-GGUCAUUUGUUGCGUUGAAtt-3′ for human AP3D1 are from Ambion.

2. Lipofectamine RNAiMAX (Invitrogen).

3. Fugene 6 transfection reagent (Roche).

4. Bromo Cresol Green (BCG) protein assay kit (Pierce).

5. Protease inhibitor cocktail tablets (Roche).

6. GSH-Sepharose 4B beads (GE Healthcare Life Sciences).

7. Protein A sepharose CL-4B beads (GE Healthcare Life Sciences).

8. Moviol mounting solution (Hoechst).

9. Prolong Gold anti-fade with DAPI (Invitrogen).

10. Sodium butyrate (Fluka).

11. Isopropyl β-D-1-thiogalactopyranoside.

2.4 Buffers

1. Homogenization buffer 1: PBS containing 10 μg/ml DNase, 10 μg/ml RNase, 5 mM 2-mercaptoethanol, 100 μg/ml lysozyme, 5 μg/ml leupeptin, 10 μg/ml aprotinin, 1 μg/ml pepstatin, 100 μM PMSF.

2. Homogenization buffer 2: PBS containing 5 mM 2-mercaptoethanol, 100 μg/ml lysozyme, 10 μg/ml DNase, 10 μg/ml RNase, 5 μg/ml aprotinin, 5 μg/ml leupeptin, 1 μg/ml pepstatin, 100 μM PMSF.

3. Lysis buffer: 50 mM Na-HEPES pH 7.4, 100 mM NaCl, 1 % Triton X-100, protease inhibitor cocktail (Roche complete).

4. Elution buffer 1: 50 mM Na-HEPES pH 8.0, 25 mM GSH, 2 mM DTT.

5. Elution buffer 2: 20 mM Na-HEPES pH 7.4, 1.5 M NaCl, 1 mM DTT.

6. Cytosol buffer: 20 mM Na-HEPES pH 7.4, 100 mM NaCl, 5 mM $MgCl_2$, 1 mM DTT, 5 μg/ml leupeptin, 10 μg/ml aprotinin, 1 μg/ml pepstatin, 100 μM PMSF.

7. Wash buffer 1: 20 mM Na-HEPES pH 7.4, 100 mM NaCl, 5 mM $MgCl_2$, 1 mM DTT.

8. Wash buffer 2: 20 mM Na-HEPES pH 7.4, 250 mM NaCl, 5 mM $MgCl_2$, 1 mM DTT.

9. Wash buffer 3: 50 mM Na-HEPES pH 7.4, 150 mM NaCl, 0.1 % Triton X-100.

10. Immunoprecipitation buffer: 50 mM Na-HEPES pH 7.4, 100 mM NaCl, 1.5 mM $MgCl_2$, 1 mM EDTA, 1 % Triton X-100, complete protease inhibitor cocktail.

11. Fixing solution: 3 % paraformaldehyde in 100 mM phosphate buffer pH 7.

12. Quench buffer: PBS containing 50 mM NH_4Cl.

13. Blocking buffer: PBS containing 0.5 % BSA and 0.1 % saponin.

2.5 Plasmids

1. pGEX4T3.

2. pGEX4T3-rabip4′(299–708).

3. pGEX4T3-rabip4′(509–708).

4. pCIneo-VSVG-rabip4′.

5. pEGFP-rab4.

6. pEGFP-rab4Q67L.

7. pEYFP-rab4N121I.

2.6   Primary Antibodies

1. Mouse monoclonal antibody against VSVG (Developmental Studies Hybridoma Bank).

2. Mouse monoclonal SA4 against δ-adaptin (Developmental Studies Hybridoma Bank).

3. Mouse monoclonal against β3B-adaptin/β-NAP (BD Biosciences).

4. Mouse monoclonal against μ3A-adaptin/p47A (BD Biosciences).

5. Mouse monoclonal 100/1 against α-adaptin (Sigma).

6. Mouse monoclonal 100/2 against β1,2-adaptin (Sigma).

7. Mouse monoclonal 100/3 against Q1-adaptin (Sigma).

8. Mouse monoclonal antibody against EEA1 (BD Biosciences).

9. Mouse monoclonal 2G11 against CI-MPR (Santa Cruz Biotechnology).

10. Mouse monoclonal H5G11 against LAMP-1 (Santa Cruz Biotechnology)

11. Mouse monoclonal MX-49.129.15 against CD63 (Santa Cruz Biotechnology).

12. Mouse monoclonal H68.4 against human TfR (Santa Cruz Biotechnology).

13. Mouse monoclonal against tubulin (Invitrogen).

14. Mouse monoclonal antibody C4 against actin (ICN Biomedicals).

15. Rabbit antibody against Ti-VAMP (T. Galli, INSERM, Paris).

16. Rabbit antibody against cathepsin D (A. Hasilik, University of Marburg).

17. Rabbit antibody against β3A-adaptin (M.S. Robinson (CMR, Cambridge).

18. Rabbit #444 anti-rabip4/rabip4' (this chapter).

2.7   Labeled Secondary Antibodies

1. Alexa488-phalloidin (Invitrogen).

2. Alexa488-goat anti-mouse IgG (Invitrogen).

3. Alexa488-goat anti-rabbit IgG (Invitrogen).

4. Alexa594-goat anti-mouse IgG (Invitrogen).

5. Alexa594-goat anti-rabbit IgG (Invitrogen).

6. rabbit anti-mouse IgG (Jackson ImmunoResearch).

3   Methods

3.1 Expression and Purification of GST-rabip4′(509–708) for Immunization

1. cDNA encoding a common rabip4 and rabip4′ epitope (aa 509–708) is generated by PCR and subcloned between EcoRI and NotI sites of the bacterial expression plasmid pGEX4T3.

2. The construct is transformed into *E. coli* BL21 (DE3) and grown on LB/agar plates containing 0.1 mg/ml ampicillin. Three colonies are picked and grown at 37 °C in LB containing 0.1 mg/ml ampicillin. After 4–8 h and establishing that the bacteria in suspension have grown, the cultures are pooled, diluted 20 times, and shaken o/n at 30 °C.

3. The next morning the culture is diluted 10–20 times and grown at 30 °C until $OD_{600} \sim 0.6$. IPTG is added to 0.5 mM and the culture is continued at the same temperature.

4. After 5 h, bacteria are harvested by centrifugation in a Sorvall SLA-3000 rotor for 15 min at $4,000 \times g$ and 4 °C. Pellets are washed with PBS, snap-frozen in liquid nitrogen, and stored at –80 °C, or immediately processed.

5. Pellets are resuspended in 60 ml homogenization buffer 1 and bacteria are homogenized on ice in two sonication steps of 45 s each. Extracts are centrifuged for 30 min at 4 °C and $100,000 \times g$ following which the supernatant is retrieved and incubated by end over end rotation with 0.5 ml GSH-Sepharose 4B beads for 2 h at 4 °C. Unbound material is removed by centrifugation, and beads are washed 4 times with 10 ml PBS, 5 mM 2-mercaptoethanol.

6. GST-rabip4′(aa 509–708) is eluted at 4 °C in two steps of 45 min, with each 2.5 ml elution buffer 1 (*see* **Note 1**). The yield of recombinant protein is estimated by running an aliquot on a 10 % SDS-PAA gel stained with Coomassie Brilliant Blue using BSA as a standard. This procedure gives ~4 to 5 mg of GST-rabip4′(509–708) per liter of *E. coli* culture. Rabbits are then immunized with the recombinant protein either by investigators or by commercial parties (*see* **Note 2**).

3.2 Preparation of Cell Lysate for Detection of rabip4′ by Western Blot

1. Confluent HeLa, MNT-1, SKMel28, MelJuSo, B16, and HEK293T cells are grown as in Subheading 3.7. Cells are transfected with control or rabip4/rabip4′ siRNA (Subheading 3.8), washed in PBS and solubilized in 0.2 ml lysis buffer containing protease inhibitor cocktail for 30 min on a rocker, scraped and collected in Eppendorf tubes.

2. After short vortexing, lysates are cleared by centrifugation for 10 min at $16,000 \times g$ in a microfuge. Protein concentration is determined using the BCG method. Twenty microgram of total proteins from each cell lysate are separated on a 10 % SDS-PAA
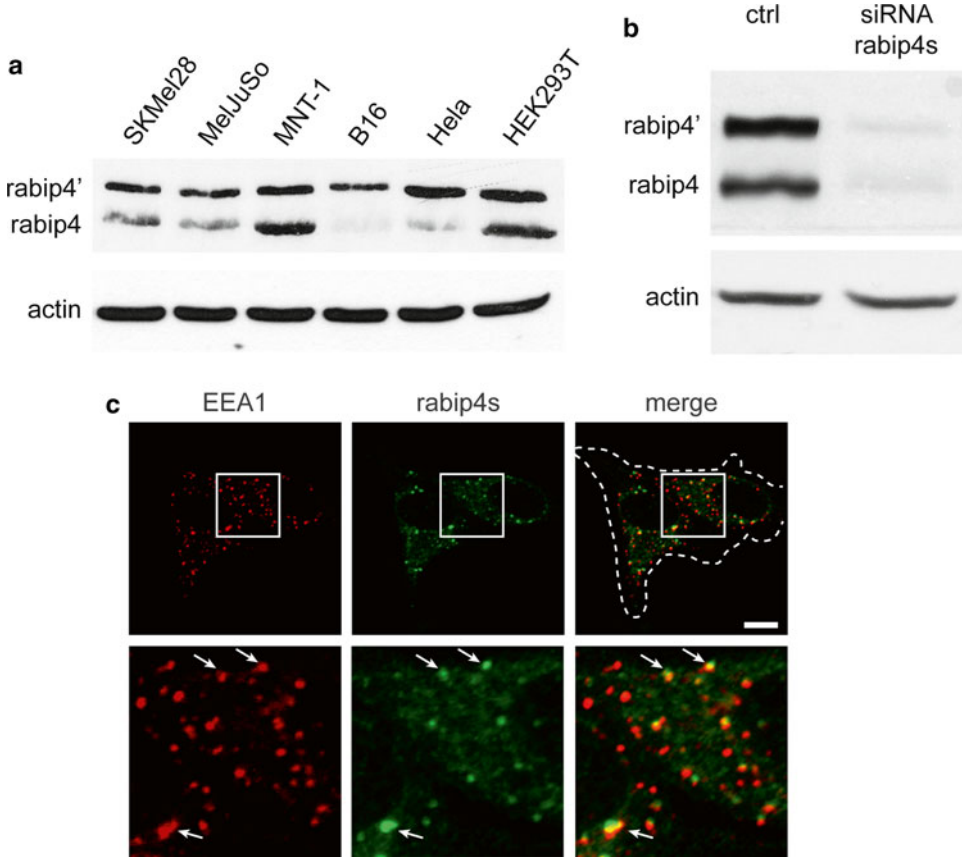
Fig. 1 Antibody detection of rabip4/rabip4′. Expression of rabip4s in different cell lines determined by Western blot (**a**). siRNA-mediated knockdown of rabip4s in HEK293T cells shows >90 % reduction of expression (**b**). HeLa cells labeled for endogenous rabip4s (*green*) and EEA1 (*red*). *Arrows* denote colocalization of the two proteins. The contour of cells is marked by the *dashed line. Bottom row* represents an enlargement of indicated area. Scale bar is 10 μm (**c**). Data taken from Ivan et al. [16]

gel and subjected to Western blot with the #444 antibody against rabip4′ (prepared as described in Subheading 3.1) and actin as a loading control. The #444 antibody detects both rabip4′ and rabip4 isoforms, collectively referred to as rabip4s. As can be seen in Fig. 1a, we detect high levels of the two proteins in HEK293T cells and the MNT-1 melanoma cell line, while rabip4 expression is lower in the other cell lines tested. The signals are specific since the siRNA that targets a common region in rabip4/rabip4′ reduces expression of both proteins to <7 % (Fig. 1b) in HEK293T cells.

3.3 Cell Culture and Assays for Immunofluorescence Localization

Cells are cultured in DMEM, supplemented with 10 % heat-inactivated fetal calf serum, 100 U/ml penicillin, 100 μg/ml streptomycin, and 5 mM L-glutamine. To analyze the localization of endogenous rabip4s, confluent cells are harvested by trypsinization,

diluted 10 times in DMEM, seeded on 10 mm coverslips (day 0), and grown to ~50 % confluency (2 days). Cells are washed once in PBS, incubated for 30 min at room temperature in fixing solution (*see* **Note 3**), washed again in PBS, and incubated for 5 min in quench buffer. After another wash with PBS, fixed cells are incubated in blocking buffer for 1 h, following incubation with first antibody diluted appropriately in blocking buffer for 1 h at room temperature. Excess antibody is removed by three consecutive, 5-min washes with blocking buffer. Incubation with fluorescent dye-labeled secondary antibodies used at appropriate dilution in blocking buffer is done for 30 min at room temperature. Following three consecutive washes in blocking buffer as described above and one wash in PBS, labeled coverslips are gently dipped in distilled water to remove the PBS, mounted in Moviol, and examined with a Zeiss-LSM-710 confocal microscope. Double label confocal fluorescence microscopy (single confocal sections) of endogenous rabip4/rabip4′ shows that their distribution is not restricted to EEA1 structures but clearly resides on a subpopulation of these endosomes (Fig. 1c).

3.4 Purification of GST-rabip4′ (299–708) for Affinity Isolation of Effectors

1. A cDNA encoding aa 299–708 was cloned between the EcoRI and NotI sites of pGEX4T3. The plasmid encoding the fusion protein and as control the pGEX4T3 plasmid are transformed into *E. coli* strain BL21DE3 Rosetta. Growth, induction, and harvesting are as in Subheading 3.1. Bacterial pellets corresponding to 250 ml culture volume are snap-frozen in liquid nitrogen and stored at −80 °C until further use.

2. For purification of GST-rabip4′(299–708) and GST, pellets are thawed on ice and resuspended in ice-cold homogenization buffer 2 (0.05 culture volume). A cleared homogenate is prepared as in Subheading 3.1 and incubated with 0.4 ml (80 % v/v) GSH-Sepharose 4B beads for 2 h in a cold room with rotation (*see* **Note 4**). Unbound proteins are removed by washing the beads for 3 times with 20 volumes of ice-cold PBS containing 5 mM 2-mercaptoethanol. The amount of isolated proteins is estimated by running an aliquot of the beads on a 10 % SDS-PAA gel stained with Coomassie Brilliant Blue using BSA as a standard. Equal amounts of GSH-immobilized GST-rabip4′ (299–708) and GST are further used in binding assays (*see* **Note 5**).

3.5 Preparation of Pig Brain Cytosol

Frozen pig brain is thawed in 1.5 volume ice-cold cytosol buffer and processed in a Waring blender operating in 10 s time intervals and maximum speed (*see* **Note 6**). The suspension is subsequently homogenized in a Kinematica tissue homogenizer operating at 20–30 % of maximum power. The sample is then centrifuged for 40 min at 4 °C and $10,000 \times g$ in a Sorvall SLA 3000 rotor. The supernatant is next centrifuged for 1 h at 4 °C and $100,000 \times g$

in a Ti45 rotor to generate a cytosol fraction. Cytosol is either used immediately or snap-frozen in liquid nitrogen and stored at –80 °C. In the latter case it is recentrifuged for 1 h at 4 °C and $100,000 \times g$ in a Ti45 rotor before use. Protein concentration in the cytosol is determined with the BCG assay and routinely amounts to 25–30 mg/ml.

3.6 Affinity Isolation of Cytosolic Proteins on GST-rabip4′(299–708) Beads

1. Normalized amounts of GST-rabip4′(299–708) or GST beads are incubated with 20 ml cytosol for 2 h in the cold room under rotation. Beads are then washed twice with 2 ml washing buffer 1, followed by two washes with washing buffer 2 and dried with a 30 gauge needle. Bound proteins are eluted in a bead equivalent volume of elution buffer 2 for 30 min on a shaker in the cold room. Eighty microliter eluates are denatured by heating at 95 °C for 5 min in reducing Laemmli sample buffer and resolved on a 7.5 % SDS-PAA gel (16/19 cm) followed by Coomassie Brilliant Blue staining (*see* **Note** 7). The results are shown in Fig. 2a. The specific bands in the GST-rabip4′(299–708) lane are excised and in-gel digested using modified trypsin in 50 mM ammonium bicarbonate. Digests are analyzed by nanoflow liquid chromatography-tandem mass spectrometry (LC-MS/MS), using an electrospray ionization quadrupole time-of-flight mass spectrometer
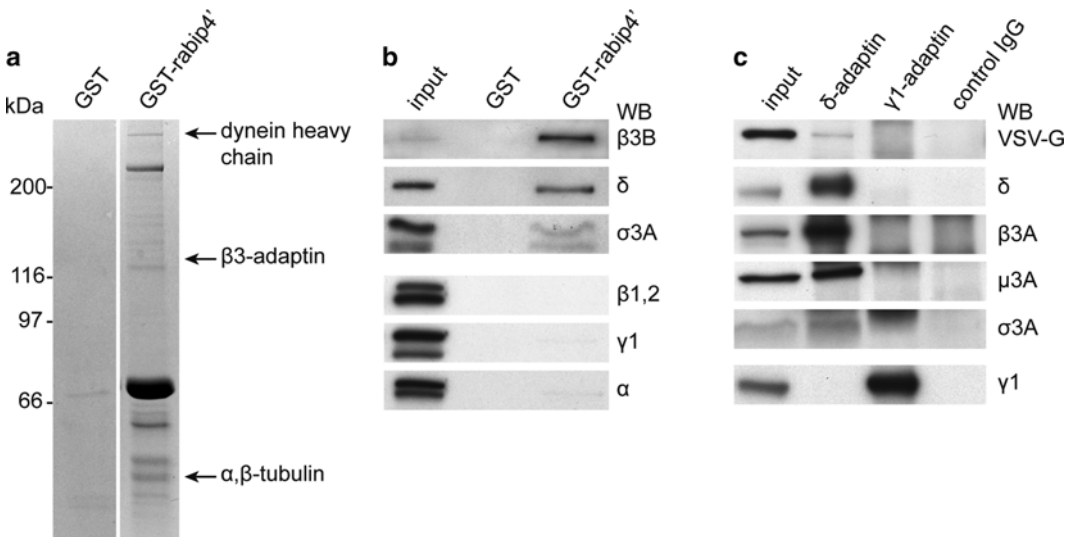
Fig. 2 Rabip4′ interacts specifically with AP-3. Immobilized GST-rabip4′(aa 299–708) is incubated with pig brain cytosol. Bound proteins are resolved by SDS-PAGE and analyzed by tandem mass spectrometry. β3B-adaptin is specifically identified on GST-rabip4′(aa 299–708) column (**a**). Western blot of eluates are probed with antibodies against adaptor complexes AP-3, AP-1, and AP-2. Note the specificity of AP-3 for GST-rabip4′ column (**b**). Lysates from HeLa cells expressing VSVG-rabip4′ are subjected to immunoprecipitation with the indicated antibodies. Western blots of immunoprecipitates reveal binding of rabip4′ to δ-adaptin, but not to δ1-adaptin (**c**). Data taken from Ivan et al. [16]

operating in positive ion mode. A nano liquid chromatography system is coupled to the quadrupole time-of-flight essentially as described previously [15]. Peptide mixtures are delivered to the system at 3 μl/min and trapped on an AquaTM C18RP column of 1 cm × 100 μm (Phenomenex). After flow splitting down to 150–200 nl/min peptides are transferred to an analytical column of 25 cm × 50 μm (PepMap, LC Packings) in a gradient of acetonitrile (1 %/min). Database searches are performed using Mascot software.

2. Conformation of AP-3 as candidate rabip4′ partner can be done by analyzing the eluate of the affinity column by Western blot with antibodies against subunits of adaptor complexes. The results of Fig. 2b show the selective enrichment of AP-3 subunits over the AP-1 and AP-2 adaptor complexes.

3.7 Preparation of Cell Lysates and Co-immunoprecipitation

1. HeLa cells are cultured in DMEM as described in Subheading 3.7. Confluent cells are diluted 5 times and seeded on 10 cm dishes. The next day cells are transfected with 4 μg pCIneo-VSVG-rabip4′ using 8 μl FuGene 6 per dish. Six hours post-transfections cells are treated with 5 mM Na-butyrate (*see* **Note 8**) and grown for another 15–18 h. Non-transfected cells are used as controls. All steps of lysate preparation are performed on ice. Cells are washed in 10 ml PBS and lysed in 1 ml immunoprecipitation buffer for 30 min on a rocker, scraped and spun for 10 min at 16,000 × g in a microfuge to generate a cleared lysate.

2. 50 μl Protein A sepharose CL-4B beads are washed 2 times with 0.5 μl PBS containing 0.1 % BSA. Beads are then incubated with mouse monoclonal antibodies specific to δ-adaptin, γ1-adaptin, or control IgG to which 10 μl affinity purified rabbit anti-mouse IgG bridging antibodies are added in 0.5 ml PBS containing 0.1 % BSA for 1 h in the cold room with rotation. Beads are then washed for 2 times with 0.5 μl immunoprecipitation buffer without protease inhibitors and for another 2 times with 0.5 ml washing buffer 3 and dried with a 30 gauge needle. Bound proteins are eluted in 0.1 ml reducing Laemmli sample buffer, resolved on 7.5 and 10 % SDS-PAA gels and detected by Western blot using specific antibodies for AP-3, AP-1, and the VSV-G tag. The results are shown in Fig. 3c documenting the presence of rabip4′-AP-3 complexes in vivo.

3.8 Localization of rabip4 and AP-3, Transfection and Morphological Assays

1. To determine the localization of endogenous rabip4/rabip4′ with respect to AP-3 we use immunofluorescence microscopy. HeLa cells are processed as in Subheading 3.2 and labeled with the rabbit antibody #444 against rabip4s and the SA4 mouse anti-δ-adaptin antibody as in Subheading 3.2. The two proteins show partial colocalization on endosomes as seen in the single confocal sections (Fig. 3a).
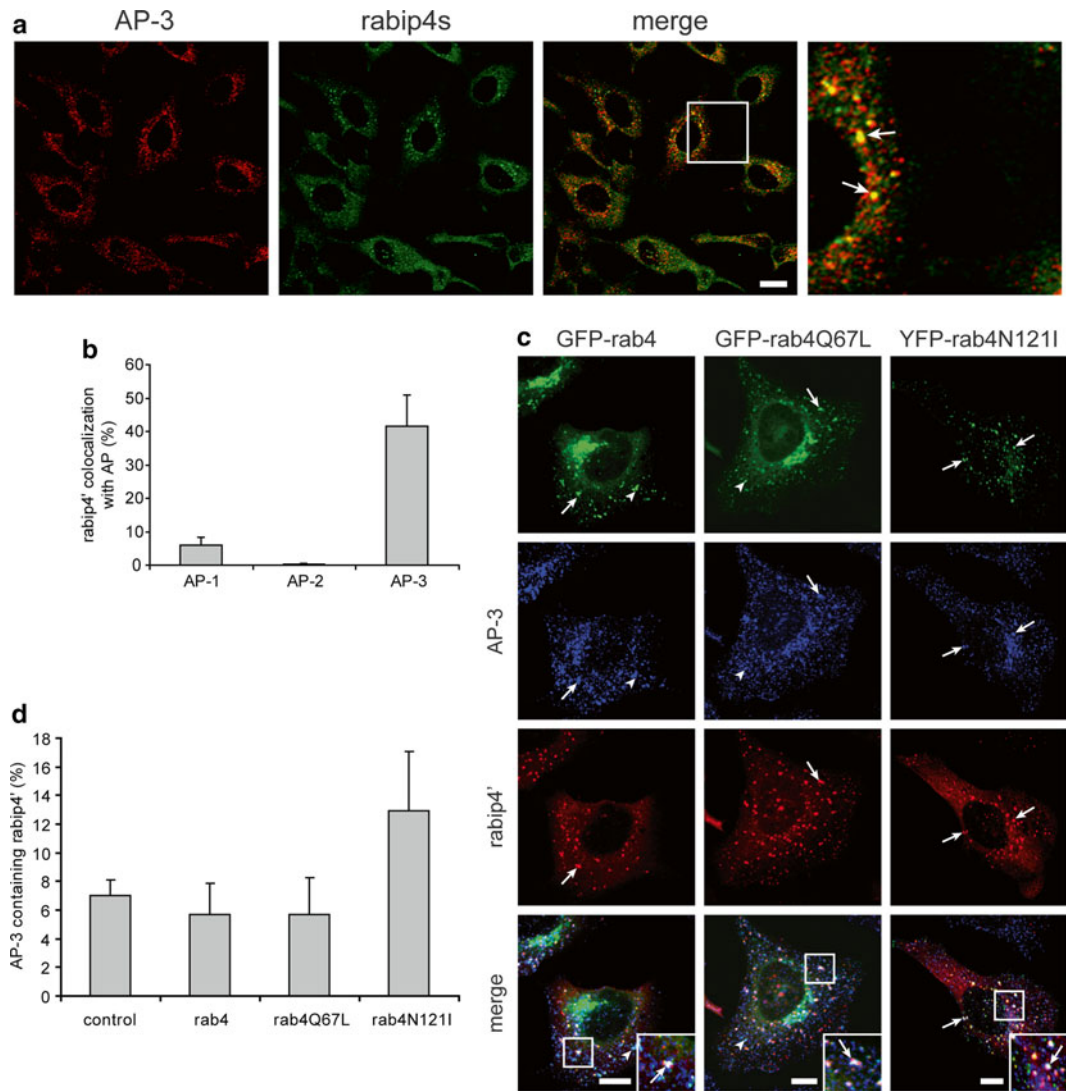
Fig. 3 Rabip4′ and AP-3 colocalize on endosomes. HeLa cells are labeled for endogenous δ-adaptin (*red*) and rabip4s (*green*). Rabip4s and AP-3 partially colocalize (*arrows in insets*). Scale bar is 2.5 μm (**a**). The degree of colocalization between expressed VSVG-rabip4′ and AP-3, AP-1, or AP-2 is quantified (**b**). HeLa cells co-transfected with VSVG-rabip4′ and the indicated GFP/YFP-rab4 constructs are labeled for rabip4′ (*red*) and δ-adaptin (*blue*). Rab4, rabip4′, and AP-3 colocalize in the perinuclear area (*insets*, *arrows*). *Arrowheads* indicate colocalization between rab4 and AP-3. Scale bar is 10 μm (**c**). Quantitation of colocalization between AP-3 and rabip4′ in the absence (control) and in the presence of rab4 variants. Expression of rab4N121I induces a twofold increase in the extent of colocalization between rabip4′ and AP-3 (**d**). Data taken from Ivan et al. [16]

2. To establish the degree of colocalization between rabip4′ and AP-3 relative to AP-1 and AP-2, Hela cells are transfected at day 1 with 1 μg VSVG-rabip4′ using 2.5 μl FuGene 6 per 35 mm dish, fixed as above and co-labeled with a rabbit anti-VSVG antibody and mouse antibodies against δ-adaptin, γ1-adaptin,

and α-adaptin. Quantification of the overlap degree is performed with the MetaMorph software (Universal Imaging, Downingtown, PA). Approximately 40 % of rabip4′ colocalizes with AP-3 (Fig. 3b).

3. To investigate a potential role for rab4 in the interaction between rabip4′ and AP-3, Hela cells co-transfected at day 1 with 1 μg VSVG-rabip4′ and 1 μg of either GFP-rab4, GFP-rab4Q67L or YFP-rab4N121I (using 5 μl FuGene 6 per 35 mm dish) are co-labeled for δ-adaptin (with the mouse SA4 antibody) and VSVG-rabip4′ (with the rabbit anti-VSVG antibody). While GFP-rab4 and GFP-rab4Q67L redistribute and colocalize with AP-3 more peripherally in both single and double transfectants, expression of dominant-negative YFP-rab4N121I mutant does not affect AP-3 distribution but increases the colocalization between rabip4′ and AP-3 by two-fold (Fig. 3c, d).

3.9   Morphological Analysis of AP-3 and rabip4/rabip4′ Function

1. To establish the function of rabip4/rabip4′, we employ the RNAi method to knockdown both isoforms, collectively referred to as rabip4s, in parallel to AP-3 silencing. Immunofluorescence microscopy is then used as a read out for cellular and molecular alterations induced by rabip4s or AP-3 silencing.

2. HEK293T cells are cultured in DMEM, supplemented with 10 % heat-inactivated fetal calf serum and 5 mM L-glutamine (*see* **Note 9**). For RNAi experiments, confluent cells are washed with PBS and trypsinized. Routinely, ~10^6 cells are resuspended in 1 ml growth medium to which the transfection mix is added (siRNA final concentration is 40 nM, *see* below), seeded in a 6-well plate, and allowed to grow for 24 h to ~90–95 % confluency. Cells are then washed with PBS, trypsinized, and resuspended in normal growth medium. Approximately 10^5 cells are seeded on 10 mm coverslips and grown for another 48 h prior to processing for morphological assay. RNAi transfection mix is prepared as follows: 1.6 μl of 50 μM siRNA stock against either δ-adaptin or rabip4s is mixed with 0.5 ml serum-free DMEM in a polycarbonate tube. In a separate tube, 5 μl Lipofectamine RNAiMAX are mixed with 0.5 ml serum-free DMEM and kept at room temperature for 10 min. The content of both tubes is then mixed and kept at room temperature for 30 min before adding to transfecting cells. Indicated mounts of reagents are per 3.5 cm well.

3. Cells are processed for double label fluorescence microscopy as in Subheading 3.3, mounted in Prolong Gold anti-fade with DAPI, and examined with a Zeiss-LSM-710 confocal microscope. Confocal *z*-stacks (20–30 confocal slices of 0.3 μm thickness) are acquired and shown as projections. siRNA

depletion of either rabip4s or AP-3 induces an overgrowth of cellular projections and a selective redistribution of lysosomes (labeled for CD63, LAMP-1, cathepsin D, and Ti-VAMP) to the tips of these protrusions, including within the cortical actin network (Fig. 4). Quantification of RNAi phenotype is done manually by analyzing six random fields from two independent experiments for each condition. The number of cells that show overgrown cellular protrusions and a redistribution of lysosomes from the cell body to these protrusions is expressed as percentage of the total (~100 cells for each condition).
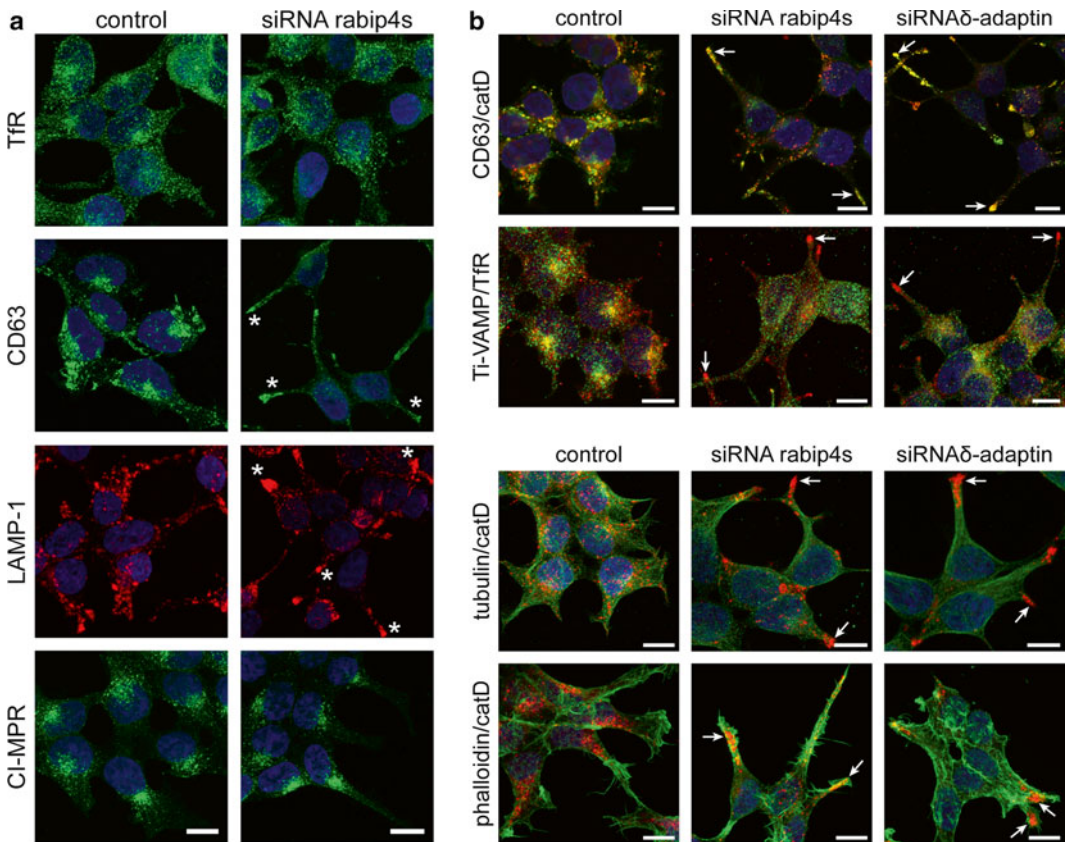
Fig. 4 Rabip4s and AP-3 regulate lysosome positioning. HEK293T cells are labeled for CD63, LAMP-1, CI-MPR, and TfR. LAMP-1 is counterstained with Alexa 594-, and CD63, CI-MPR, and TfR with Alexa 488-labeled secondary antibodies. Nuclei are stained with DAPI. Images represent projections of confocal *Z*-stacks. *Asterisks* denote plasma membrane protrusions, enriched in CD63 and LAMP-1, induced by depletion of rabip4s. Scale bar, 10 μm (**a**). HEK293T control cells or depleted of rabip4s and AP-3 are labeled for CD63 or TfR (*green*) and cathepsin D or Ti-VAMP (*red*), respectively. Nuclei are stained with DAPI (**b**). HEK293T cells are processed as above and labeled for cathepsin D (*red*) and tubulin (*green*) or cathepsin D (*red*) and Alexa-488-conjugated phalloidin for actin staining. Nuclei are stained with DAPI. Images represent projections of confocal *Z*-stacks. Scale bar, 10 μm (**c**). Depletion of rabip4s and AP-3 selectively redistributes lysosomal markers CD63, cathepsin D, and Ti-VAMP to cellular protrusions (*arrows*). Data taken from Ivan et al. [16]

4 Notes

1. Since reduced glutathione is acidic. It is important to verify pH of elution buffer 1 and adjust to pH 8.0 with a NaOH solution or by increasing the concentration of Na-HEPES.

2. In principle antibodies are generated against native proteins in this procedure. If there is a need for antibodies against denatured protein that recognize proteins on glutaraldehyde fixed material for immuno electronmicroscopy, it is advisable to denature fusion protein and immunize rabbits with this material.

3. The 0.1 M sodium phosphate buffer is used to dissolve paraformaldehyde because the fixation reaction generates protons. PBS is less suited because it does not have sufficient buffer capacity.

4. To minimize non specific binding sites, we use 0.1–0.25 ml GSH beads per liter *E. coli* culture, instead of 1 ml as recommended by the manufacturer.

5. We store the GST-rabip4′ affinity beads overnight before using them in the affinity isolation procedure. Longer storage jeopardizes the "quality" of the matrix.

6. Fresh pig brain is obtained from a local slaughter house, transported on ice to the lab, and immediately frozen in liquid N_2. Frozen brain is stored at –80 °C.

7. We found that best results are obtained if freshly eluted binding proteins are immediately resolved by SDS-PAGE. Freezing and thawing reduce yield.

8. Sodium butyrate (1–10 mM) is added overnight to enhance expression from cmv-driven plasmids. Importantly concentrations above 2.5 mM affect integrity of cytoplasmic organelles.

9. HEK293T cells are used because of their high expression of rabip4s and δ-adaptin as determined by Western blot (cf Fig. 1a).

Acknowledgments

References

1. Luzio JP, Pryor PR, Bright NA (2007) Lysosomes: fusion and function. Nat Rev Mol Cell Biol 8:622–632

2. Settembre C, Fraldi A, Medina DL, Ballabio A (2013) Signals from the lysosome: a control centre for cellular clearance and energy metabolism. Nat Rev Mol Cell Biol 14:283–296

3. Marks MS, Heijnen HF, Raposo G (2013) Lysosome-related organelles: unusual compartments become mainstream. Curr Opin Cell Biol 25:495–505

4. Hendricks AG, Perlson E, Ross JL, Schroeder HW, Tokito M, Holzbauer ELF (2010) Motor coordination via a tug of war mechanism drives bidirectional vesicle transport. Curr Biol 20:697–702

5. Rosa-Ferreira C, Munro S (2011) Arl8 and SKIP act together to link lysosomes to kinesin-1. Dev Cell 21:1171–1178

6. Fouraux M, Deneka M, Ivan V, van der Heijden A, Raymackers J, van Suylekom D, van Venrooij WJ, van der Sluijs P, Pruijn GJM (2004) rabip4' is an effector of rab5 and rab4 and regulates transport through early endosomes. Mol Biol Cell 15:611–624

7. Cormont M, Mari M, Galmiche A, Hofman P, Le Marchand-Brustel Y (2001) A FYVE finger-containing protein, rabip4, is a rab4 effector protein involved in early endosomal traffic. Proc Natl Acad Sci U S A 98:1637–1642

8. Theos AC, Tenza D, Martina JA, Hurbain I, Peden AA, Sviderskaya EV, Stewart A, Robinson MS, Bennett DC, Cutler DF et al (2005) Functions of adaptor protein AP-3 and AP-1 in tyrosinase sorting from endosomes to melanosomes. Mol Biol Cell 16:5356–5372

9. Peden AA, Oorschot V, Hesser BA, Austin CD, Scheller RH, Klumperman J (2004) Localization of the AP-3 adaptor complex defines a novel endosomal exit site for lysosomal membrane proteins. J Cell Biol 164:1065–1076

10. Dell'Angelica EC, Shotelersuk V, Aguilar RC, Gahl WA, Bonifacino JS (1999) Altered trafficking of lysosomal proteins in Hermansky-Pudlak syndrome due to mutations in the beta3A subunit of the AP-3 adaptor. Mol Cell 3:11–21

11. Clark RH, Stinchcombe JC, Day A, Blott E, Booth S, Bossi G, Hamblin T, Davies EG, Griffiths GM (2003) Adaptor protein 3-dependent microtubule mediated movement of lytic granules to the immunological synapse. Nat Immunol 4:1111–1120

12. Deneka M, Neeft M, Popa I, van Oort M, Sprong H, Oorschot V, Klumperman J, Schu P, van der Sluijs P (2003) rabaptin-5a/rabaptin-4 serves as a linker between rab4 and γ1-adaptin in membrane recycling from endosomes. EMBO J 22:2645–2657

13. Hoogenraad CC, Popa I, Futai K, Martinez-Sanchez E, Wulf PS, van Vlijmen T, Dortland B, Oorschot V, Govers R, Monti M et al (2010) Neuron specific rab4 effector GRASP-1 coordinates membrane specialization and maturation of recycling endosomes. PLoS Biol 8:e1000283

14. Yang J, Kim O, Qiu Y (2002) Interaction between tyrosine kinase Etk and a RUN domain and FYVE domain containing protein RUFY1. J Biol Chem 277:30219–30226

15. Yatsuda AP, Krijgsveld J, Cornelissen AW, Heck AJ, de Vries E (2003) Comprehensive analysis of the secreted proteins of the parasite *Haemonchus contortus* reveals extensive sequence variation and differential immune recognition. J Biol Chem 278:16941–16951

16. Ivan V, Martinez-Sanchez W, Sima LE, Oorschot V, Klumperman J, Petrescu SM, van der Sluijs P (2012) AP-3 and Rabip4' coordinately regulate spatial distribution of lysosomes. PLoS One 7:e48142

Chapter 22

Determination of Rab5 Activity in the Cell by Effector Pull-Down Assay

Yaoyao Qi, Zhimin Liang, Zonghua Wang, Guodong Lu, and Guangpu Li

Abstract

Rab5 targets to early endosomes and is a master regulator of early endosome fusion and endocytosis in all eukaryotic cells. Like other GTPases, Rab5 functions as a molecular switch by alternating between GTP-bound and GDP-bound forms, with the former being biologically active via interactions with multiple effector proteins. Thus the Rab5-GTP level in the cell reflects Rab5 activity in promoting endosome fusion and endocytosis and is indicative of cellular endocytic activity. In this chapter, we describe a Rab5 activity assay by using GST fusion proteins with the Rab5 effectors such as Rabaptin-5, Rabenosyn-5, and EEA1 that specifically bind to GTP-bound Rab5. We compare the efficiencies of the three GST fusion proteins in the pull-down of mammalian and fungal Rab5 proteins.

Key words Rab5, Rabaptin-5, EEA1, Rabenosyn-5, Endocytosis, Endosome

1 Introduction

Rab5 is localized on early endosomes and plasma membrane, and plays an important role in the formation, movement, and fusion of endocytic vesicles and early endosomes during endocytosis [1, 2]. As a member of the Rab GTPase family, Rab5 alternates between inactive GDP-bound and active GTP-bound conformations, and this GTPase cycle is facilitated by guanine nucleotide exchange factors (GEFs), e.g., Rabex-5 [3] and RIN1 [4], and GTPase-activating proteins (GAPs), e.g., RabGAP5 [5]. In the active GTP-bound conformation, Rab5 interacts with multiple effector proteins to promote the aforementioned early events of endocytosis.

Endocytosis is a fundamental function of all eukaryotic cells for uptake of extracellular nutrients and regulation of cell surface proteins such as receptors, channels, and adhesion proteins. Growth factor receptors control cell growth, differentiation, and migration via various signal transduction pathways, which may affect and/or be affected by Rab5 activity and endosomal sorting by recruitment of Rab5 GEFs or GAPs to the membrane.

As a result, it's necessary to determine Rab5 activity, i.e., Rab5-GTP level, in the cell to gauge endocytic activity and physiological changes during signal transduction processes.

The first method for determining Rab5-GTP levels in the cell involves metabolic labeling with [32P]orthophosphate, followed by immunoprecipitation of cell lysates with a Rab5 antibody and then separation of [32P]-labeled GDP and GTP bound to Rab5 by thin-layer chromatography and detection by autoradiography. This approach, however, is time-consuming and involves the usage of radioactivity. More recently, glutathione S-transferase (GST) pull-down assays [6] have been adopted to determine Rab5 activity in the cell (Fig. 1). In this case, GST fusion proteins with a Rab5 effector, which specifically binds to GTP-bound Rab5, is bound to glutathione-coupled Sepharose beads and used to affinity-purify Rab5-GTP in cell lysates. The captured Rab5-GTP is then detected by immunoblot analysis. We previously used the Rab5-binding domain (R5BD) of the Rab5 effector Rabaptin-5 [7, 8] as a bait in the GST fusion protein to determine Rab5-GTP levels in PC12 cells and showed rapid down-regulation of Rab5 activity by nerve growth factor (NGF) signaling to facilitate cell differentiation [9]. In addition to Rabaptin-5, other Rab5 effectors such as Rabenosyn-5 [10] and EEA1 [11] have also been used as GST fusion proteins in determining Rab5 activity in the cell [12, 13]. Here we compare the efficiencies of these three Rab5 effectors in the detection of Rab5-GTP in the cell in GST pull-down assays. In addition, we characterize two Rab5 homologs (MoRab5A and MoRab5B) from *Magnaporthe oryzae*, a pathogenic fungus that infects plants and causes rice blast disease [14], in the GST pull-down assay and show that they differentially interact with the Rab5 effectors.

2   Materials

Millipore filtered H_2O is used in all experiments.

2.1   Preparation of GST Fusion Proteins

1. Plasmids. pGEX-4 T-2/Rabaptin-5:R5BD, pGEX-4 T-2/EEA1:R5BD, and pGEX-2 T/Rabenosyn-5:R5BD. The pGEX vectors are commercially available from GE Healthcare.

2. Bacterial strains. *E. coli* DH5α and MC1061.

3. Growth media. LB liquid and LB Agar as liquid and solid media, respectively, for bacterial growth.

4. Reduced Glutathione (GSH)-Sepharose 4B resin.

5. Isopropyl-β-D-thiogalactopyranoside (IPTG): 1,000× stock solution (0.5 M in H_2O, aliquoted and stored at –20 °C).
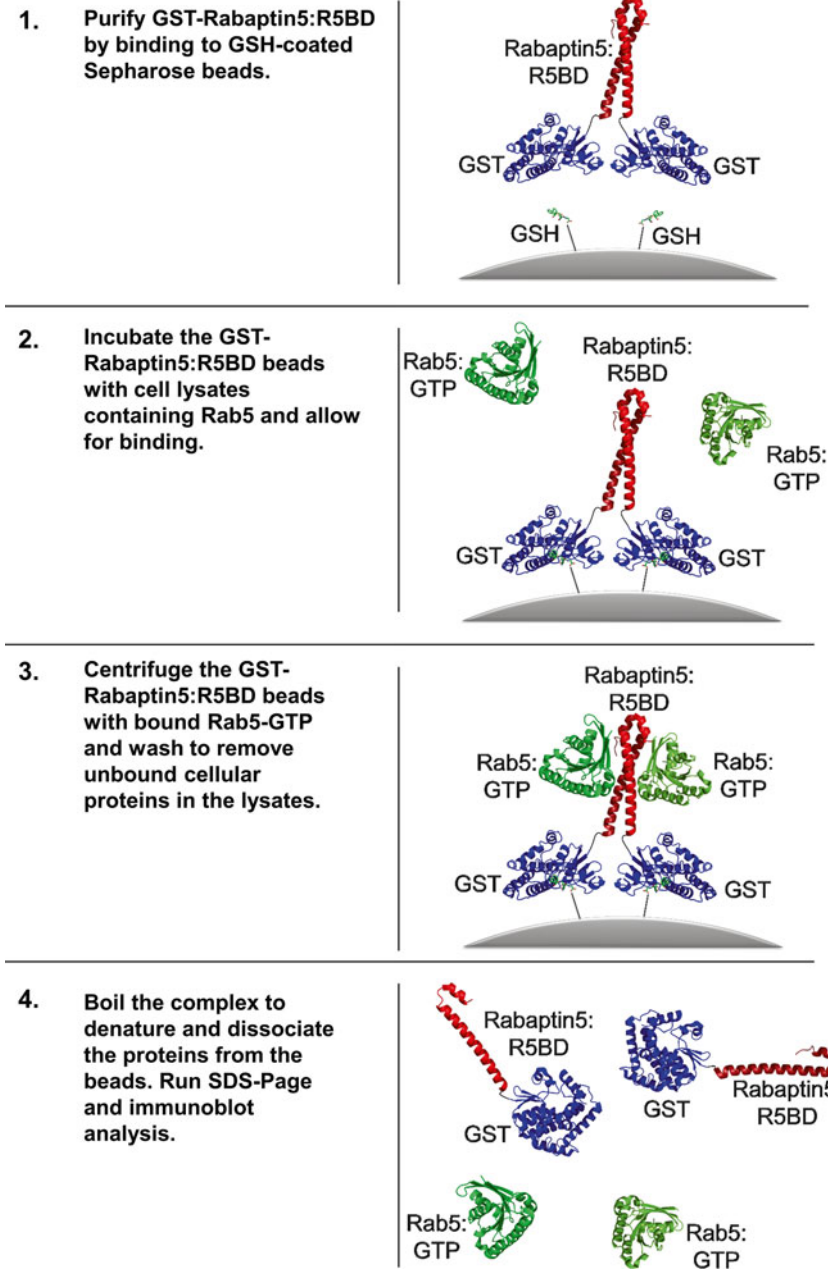
Fig. 1 Schematic illustration of GST:R5BD pull-down assay. Rab5 (*green*) and Rabaptin5:R5BD (*red*) structures are from PDB: 1TU3 [8]. The structure for GST (*blue*) is from PDB: 2GST [17]. GSH-conjugated Sepharose beads are shown in *grey*

6. Ampicillin: 1,000× stock solution (50 mg/ml in H_2O sterilized by filtration, aliquoted and stored at –20 °C).

7. Reagents. Phosphate-buffered saline (PBS), Triton X-100.

2.2 Expression of Rab5, MoRab5A, MoRab5B, and Their Mutants in Tissue Cultures and Preparation of Cell Lysates	1. Plasmids. pBI-Tet-Off, pBI/eGFP, pBI/eGFP/Myc-Rab5, pBI/eGFP/Myc-Rab5:Q79L, pBI/eGFP/Myc-Rab5:S34N, pBI/eGFP/Myc-MoRab5A, pBI/eGFP/Myc-MoRab5A: Q70L, pBI/eGFP/Myc-MoRab5A:S25N, pBI/eGFP/ Myc-MoRab5B, pBI/eGFP/Myc-MoRab5B:Q79L, pBI/ eGFP/Myc-MoRab5B:S33N.

2. Tissue cultures. Baby hamster kidney (BHK) cells (BHK-21 cell line from ATCC).

3. Growth media. α-Minimal Essential Medium (MEM) containing 5 % fetal bovine serum (FBS), glutamine, penicillin/streptomycin.

4. Lipofectamine 2000 transfection reagent (Invitrogen).

5. Lysis buffer: 25 mM HEPES-KOH (pH 7.4), 100 mM NaCl, 5 mM $MgCl_2$, 0.1 % NP40, 10 % Glycerol, 1 mM DTT (add before use), 1:250 protease inhibitor cocktail for mammalian tissue cultures (add before use).

6. Reagents. Phosphate-buffered saline (PBS), Triton X-100.

2.3 SDS-PAGE and Coomassie Blue Staining	1. 3× SDS loading buffer: 150 mM Tris–HCl (pH 6.8), 6 % SDS (W/V), 0.3 % bromophenol blue (W/V), 30 % glycerol (V/V), 300 mM β-mercaptoethanol (add before use).

2. 16 % separation gel for SDS-PAGE.

3. Electrophoresis buffer: For 1 l of 5× running buffer: 15.2 g Tris base, 72 g Glycine, 5 g SDS, add H_2O to 1 l.

4. Staining buffer: 0.6 % Coomassie Brilliant Blue, 50 % Methanol (v/v), 10 % Glacial acetic acid (v/v), add H_2O to 100 %.

5. Destaining buffer: 15 % methanol (v/v), 10 % acetic acid (v/v).

2.4 Immunoblot Assay with Bio-Rad Semi-dry Transfer Apparatus	1. Transfer buffer: For 1 l : 2.9 g Glycine, 5.8 g Tris base, 0.37 g SDS, 200 ml methanol, add H_2O to 1 l.

2. Washing buffer: 1× TBS (Tris-buffered Saline) containing 0.04 % Tween-20. For 1 l of 5× TBS: dissolve 40 g NaCl, 1 g KCl, and 15 g Tris base in 800 ml of H_2O, adjust pH to 7.4 with HCl, and then add H_2O to 1 l.

3. Blocking buffer: 1× TBS containing 8 % non-fat dry milk.

4. Antibodies: anti-Myc monoclonal antibody, IRDye 680CW-conjugated goat anti-mouse or anti-rabbit IgG (LI-COR Biosciences).

5. Immobilon-P PVDF Membrane.

6. Odyssey Infrared Imaging System (LI-COR Biosciences).

3 Methods

3.1 Expression and Purification of GST-R5BD Fusion Proteins

1. R5BD here refers to a Rab5-binding domain from Rabaptin-5 (residues 739–862), EEA1 (residues 1–209), or Rabenosyn-5 (residues 1–40). For Rabaptin-5 and EEA1, the R5BD cDNA fragments are generated by PCR using human Rabaptin-5 and EEA1 cDNA as templates and cloned into the BamHI and EcoRI sites of pGEX-4 T-2, resulting in the expression constructs pGEX-4 T-2/Rabaptin-5:R5BD and pGEX-4 T-2/EEA1:R5BD. For Rabenosyn-5, the expression construct pGEX-2 T/Rabenosyn-5:R5BD contains the N-terminal R5BD domain repeated four times in tandem and cloned in-frame in the pGEX vector, as described previously [12], and was kindly provided by Dr. John Colicelli (Department of Biological Chemistry, UCLA).

2. The GST-R5BD constructs are transformed into bacterial strain DH5α or MC1061, and the transformants are grown on LB/Amp agar plates at 37 °C overnight. Single colonies are picked with toothpicks and grown in 2 ml LB containing 50 μg/ml Amp in a 37 °C incubating shaker at 250 rpm overnight.

3. Take 1 ml of the overnight culture and dilute into 100 ml of fresh LB/Amp growth media. Continue the incubation in the 37 °C shaker for about 4–5 h until the OD_{600} reaches 0.5–0.8 (log phase growth).

4. Add IPTG to a final concentration of 0.5 mM to induce protein expression, and continue the incubation in the 37 °C shaker for 4 h (*see* **Note 1**).

5. Harvest the cells in polypropylene bottles by centrifugation at $8,000 \times g$ in a Beckman Aventi J-20 centrifuge for 10 min. Discard the supernatant (*see* **Note 2**).

6. Resuspend the cell pellet in 850 μl of PBS containing 1 % Triton X-100 by pipetting (*see* **Note 3**).

7. Transfer the suspension to a 1.5 ml Eppendorf tube, and then sonicate 6 times (10 s each time), with 10-s interval on ice to avoid overheating. Incubate the bacterial lysates on ice for 5 min.

8. Centrifuge at $9,300 \times g$ for 30 min in a refrigerated (4 °C) Eppendorf centrifuge and transfer the supernatant to a new tube. Keep it on ice.

9. Take 250 μl of glutathione (GSH) Sepharose 4B beads and rinse three times in a 1.5 ml Eppendorf tube with PBS containing 1 % Triton X-100, by centrifugation at $2,300 \times g$ for 30 s, aspiration of the supernatant, and resuspension of the beads (*see* **Notes 4** and **5**).
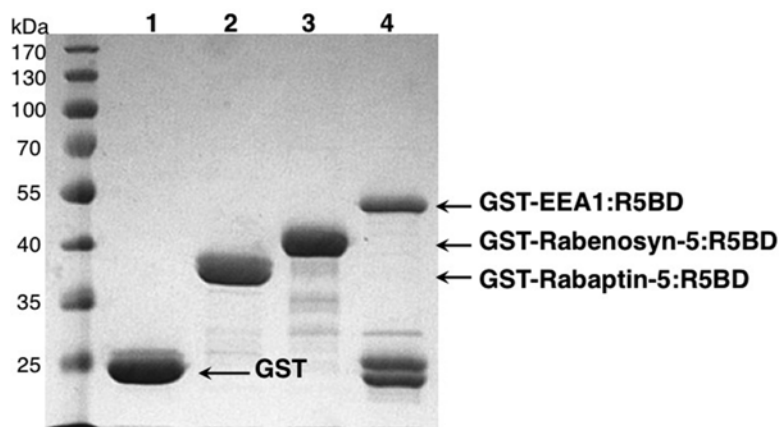
Fig. 2 Affinity-purified GST-R5BD fusion proteins on GSH beads analyzed by SDS-PAGE and Coomassie Blue staining. GST and GST-R5BD fusion proteins, as indicated, were dissociated from the GSH beads in SDS sample buffer and subjected to SDS-PAGE (16 % gel), followed by Coomassie Blue staining (1 h) and destaining (2 h). Approximately 20 μg of each protein were loaded in each lane and represented 2 % of the total purified protein. To some extent, the GST-EEA1:R5BD fusion protein undergoes auto-proteolytic cleavage separating GST and EEA1:R5BD (*see* **Note 6**), but there is enough fusion protein for the pull-down assay

10. After the final wash, aspirate the washing buffer and add 750 μl of the bacterial supernatant prepared above (**step 6**) to the GSH beads. Mix and incubate at room temperature on a rotating mixer for 30 min.

11. Centrifuge at $400 \times g$ for 1-min and aspirate the supernatant.

12. Wash the beads three times with 1 ml of PBS containing 1 % Triton X-100, as described above (**step 7**).

13. Wash the beads once with PBS, and then resuspend the beads in 150 μl PBS. A fraction of the GST-R5BD fusion protein bound to the beads (2 %) is analyzed by SDS-PAGE and visualized by Coomassie Blue staining (Fig. 2). The remainder of GST-R5BD beads is used for the pull-down assay below (*see* **Note 8**).

3.2 Preparation of Mammalian Cell Lysates for the Pull-Down Assay

1. BHK cell monolayers are grown in individual or 6-well 35 mm tissue culture plates in a 37 °C tissue culture incubator with 5 % CO_2, respectively, and transfected with the plasmid constructs listed in Table 1 (3 wells per construct) for expression of human and *Magnaporthe oryzae* Rab5 and mutant proteins via Lipofectamine 2000 (*see* **Note 9**).

2. At 24 h post-transfection, aspirate the growth medium and wash the cell monolayers once with ice-cold PBS (1 ml per wash).

Table 1
List of expression constructs

Plasmid name	Protein expression
pBI/eGFP/MycRab5:WT	Human Rab5 (wild-type), with N-terminal Myc-tag
pBI/eGFP /MycRab5:Q79L	Human Rab5 (Q79L mutant), with N-terminal Myc-tag
pBI/eGFP /MycRab5:S34N	Human Rab5 (S34N mutant), with N-terminal Myc-tag
pBI/eGFP /MycMoRab5A:WT	Magnaporthe oryze Rab5A (wild-type), with N-terminal Myc-tag
pBI/eGFP /MycMoRab5A:Q70L	Magnaporthe oryze Rab5A (Q70L mutant), with N-terminal Myc-tag
pBI/eGFP /MycMoRab5A:S25N	Magnaporthe oryze Rab5A (S25N mutant), with N-terminal Myc-tag
pBI/eGFP /MycMoRab5B:WT	Magnaporthe oryze Rab5B (wild-type), with N-terminal Myc-tag
pBI/eGFP /MycMoRab5B:Q79L	Magnaporthe oryze Rab5B (Q79L mutant), with N-terminal Myc-tag
pBI/eGFP /MycMoRab5B:S33N	Magnaporthe oryze Rab5B (S33N mutant), with N-terminal Myc-tag
pTet-Off	Tet-responsive transcription activator (tTA)

3. Add 300 μl of ice-cold lysis buffer to one of the triplicate wells transfected with each construct and incubate on ice for 5 min, then transfer the lysate to the next two wells sequentially and incubate for 5 min on ice each time.

4. Homogenize the cells by going through a 1 ml syringe with a 25G3/8 needle 10 times, and further incubate the cell lysate on ice for 5 min.

5. Spin down the nuclei and cell debris by a 3-min centrifugation at $9,300 \times g$ in a refrigerated (4 °C) Eppendorf centrifuge.

6. An aliquot of the supernatant (10 μl) is directly subjected to immunoblot analysis to gauge the total amount of Rab5 in the cell lysate (Figs. 3 and 4), and the remainder is used for the pull-down assay as described below (Figs. 3 and 4).

3.3 GST-R5BD Pull-Down Assay

1. Add 150 μl of the pre-cleared cell lysate above to 20 μl of the GSH beads bound with the GST-R5BD fusion protein.

2. Mix and incubate for 30 min at 4 °C on a rotating mixer.

3. Spin down the beads by 1-min centrifugation at $400 \times g$ in a refrigerated Eppendorf centrifuge, and aspirate the supernatant to remove unbound cellular proteins.
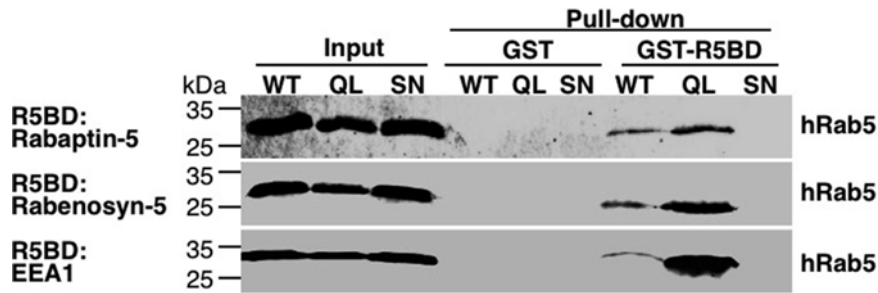
Fig. 3 GST-R5BD fusion proteins specifically pull-down GTP-bound human Rab5 proteins. Shown are immunoblots with the anti-Myc antibody indicating the levels of human Rab5 proteins (Myc-tagged) expressed in BHK cells, including wild-type (WT) and constitutively active and dominant negative mutants (QL and SN), before and after the pull-down assay. The input represents 4 % of the total cell lysates directly subjected to the immunoblot analysis. The rest of the cell lysates are divided equally for pull-down assays by GST (as the negative control) and GST-R5BD beads, respectively, as indicated. Note that the three types of GST-R5BD beads (Rabaptin-5, Rabenosyn-5, and EEA1) show similar pull-down results with strongest binding for the GTP-bound mutant (QL), followed by WT. No binding was observed for the GDP-bound mutant (SN) (*see* **Note 11**)
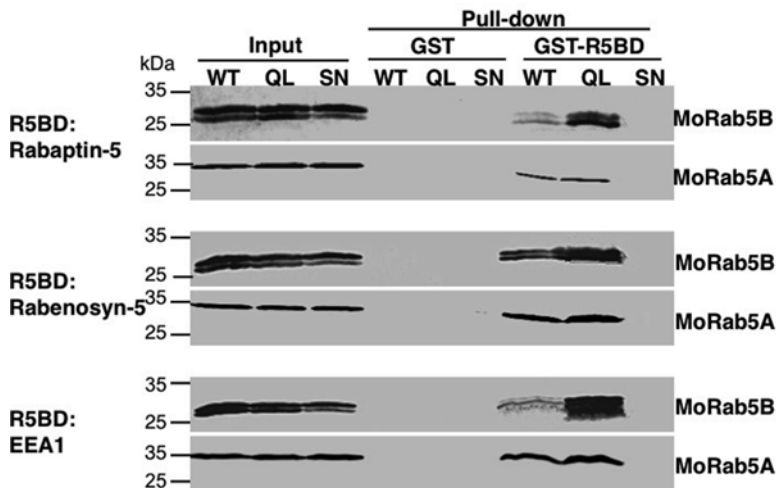
Fig. 4 Distinct binding properties of MoRab5A and MoRab5B in the GST-R5BD pull-down assay. The pull-down procedure is the same as that for Fig. 3 except the cells expressing MoRab5A and MoRab5B, respectively, as indicated. Note that the pull-down profiles of MoRab5B are similar to those of human Rab5 in Fig. 3, i.e., the QL mutant shows the strongest binding signal while the WT signal is much weaker. In contrast, the WT and the QL mutant of MoRab5A show similar binding strength in the pull-down assay (*see* **Note 12**). The MoRab5B doublet is due to post-translational isoprenylation whereas MoRab5A is larger and the two forms are not readily resolved by the SDS-PAGE

4. Wash the beads once by centrifugation and resuspension in 1 ml of ice-cold lysis buffer without detergent.

5. Spin down the beads and aspirate the supernatant.

6. Add 10 μl of 1× SDS loading buffer containing freshly added β-Mercaptoethanol to the beads. Boil the samples for 3 min to denature, reduce, and dissociate the proteins from the beads. Spin down the beads for 30 s at 10,000 rpm ($9,300 \times g$) and subject the supernatant for SDS-PAGE and immunoblot analysis with the anti-Myc antibody as described below (Figs. 3 and 4).

3.4 SDS-PAGE and Immunoblot Analysis

1. Run the 16 % SDS-PAGE at 160 V for about 1 h until the blue dye front reaches the end of the gel.

2. Disassemble the gel apparatus and carefully pry the plates apart with a spatula, then cut off the stacking gel with a clean razor blade and soak the separating gel in transfer buffer for 10 min.

3. Cut PVDF membrane and Whatman filter papers to the gel size, wet the PVDF membrane in methanol for 10 s, and then soak it in the transfer buffer with eight pieces of the Whatman papers.

4. Place four pieces of the wet Whatman papers on the Bio-Rad transfer apparatus, then place the PVDF membrane, the gel, and four Whatman papers in that order (*see* **Note 6**).

5. Connect the electrodes and allow protein transfer from the gel to the PVDF membrane at 25 V for 35 min.

6. Incubate the membrane in blocking buffer for 1 h at room temperature on a shaker.

7. Wash the membrane 3 times in washing buffer on the shaker (5 min per wash).

8. Dilute the primary antibody with washing Buffer (1:10,000 for the anti-Myc antibody) and incubate the membrane in the diluted antibody solution for 1 h at room temperature on the shaker (*see* **Note 10**).

9. Repeat the washing **step 7** to remove unbound primary antibody.

10. Dilute the secondary antibody 1:15,000 with washing buffer and incubate the membrane in the diluted secondary antibody solution in the dark by covering the container with aluminum foil for 1 h at room temperature on the shaker.

11. Repeat the washing **step 7** to remove unbound secondary antibody in the dark.

12. Visualize and quantify the membrane with a LI-COR Odyssey Infrared Imaging System, according to the manufacturer's instructions (*see* **Note 11**).

4   Notes

1. The temperature and incubation time are important factors in bacterial protein expression. Lower temperature (e.g., 30 °C or room temperature) and longer incubation time can increase the yield of soluble GST-R5BD fusion proteins.

2. If desired, the bottles containing the bacterial pellets can be stored at –80 °C for at least a month before use.

3. Avoid formation of bubbles.

4. The amount of GSH beads used depends on the GST fusion protein yield and may be adjusted upward if larger volumes of bacterial cultures are grown and higher protein yields are expected.

5. Use pipette tips with large opening to transfer the GSH beads. Regular tips may be used after cutting the end off with a clean razor blade.

6. Remove air bubbles by rolling a glass pipette or rod on the membrane.

7. Human Rab5 expressed in BHK cells binds to all three effectors (Rabaptin-5, Rabenosyn-5, and EEA1) in the pull-down assay (Fig. 3) [16]. The GTP hydrolysis defective Rab5:Q79L mutant shows the strongest binding signal. Wild-type Rab5 shows much weaker signal indicating that less than 10 % of Rab5 in the cell are in GTP-bound state. The GDP-bound Rab5:S34N mutant shows no binding to the GST-R5BD fusion proteins above the background binding to GST alone. GST is used here as a negative control to gauge nonspecific binding in the pull-down assay.

8. The GST-R5BD beads should be used on the same day to avoid protein degradation. The three GST-R5BD fusion proteins used here exemplify the difference in stability among GST fusion proteins. While GST-Rabaptin-5:R5BD and GST-Rabenosyn-5:R5BD are relatively stable, GST-EEA1:R5BD is less stable and appears to undergo auto-proteolysis separating GST from EEA1:R5BD (Fig. 2). Similar auto-proteolysis was observed in other GST fusion proteins, e.g., the GST-RBD35 in Chapter 18. The mechanism of such auto-proteolysis is unclear at present.

9. Three 35 mm plates of transfected cell monolayers should provide sufficient amount of Rab5 protein for the pull-down assay. For detection of endogenous Rab5 activity, more cells may be necessary depending on Rab5 levels and activation state in a given cell type [15].

10. Make sure that the membrane is immersed in the solution rather than floating on the surface.

11. We use the LI-COR Infra-red Imaging system in immunoblot analysis for quantification and sensitivity of detection, but other detection methods such as chemiluminescence can also be used with similar results.

12. MoRab5B shows the same binding profile as human Rab5, i.e., wild-type and mutant MoRab5B proteins bind to the effectors in the order of MoRab5B:Q79L > MoRab5B:WT > MoRab5B: S33N (Fig. 4) [16]. In contrast, MoRab5A shows distinct effector binding property, with wild-type and GTP hydrolysis-defective mutant (MoRab5A:Q70L) binding the effectors with identical affinity (Fig. 4) [16], suggesting that the wild-type protein is defective in GTP hydrolysis. As expected, the GDP-bound MoRab5A:S25N does not interact with any of the effectors.

Acknowledgments

References

1. Bucci C, Parton RG, Mather IH et al (1992) The small GTPase rab5 functions as a regulatory factor in the early endocytic pathway. Cell 70:715–728

2. Li G (2012) Early endocytosis: Rab5, Rab21 and Rab22. In: Li G, Segev N (eds) Rab GTPases and membrane trafficking. Bentham Science Publishers, Sharjah

3. Horiuchi H, Giner A, Hoflack B et al (1995) A GDP/GTP exchange-stimulatory activity for the Rab5-RabGDI complex on clathrin-coated vesicles from bovine brain. J Biol Chem 270: 11257–11262

4. Tall GG, Barbieri MA, Stahl PD et al (2001) Ras-activated endocytosis is mediated by the Rab5 guanine nucleotide exchange activity of RIN1. Dev Cell 1:73–82

5. Haas AK, Fuchs E, Kopajtich R et al (2005) A GTPase-activating protein controls Rab5 function in endocytic trafficking. Nat Cell Biol 7:887–893

6. Kaelin WG Jr, Pallas DC, DeCaprio JA et al (1991) Identification of cellular proteins that can interact specifically with the T/E1A-binding region of the retinoblastoma gene product. Cell 64:521–532

7. Stenmark H, Vitale G, Ullrich O et al (1995) Rabaptin-5 is a direct effector of the small GTPase Rab5 in endocytic membrane fusion. Cell 83:423–432

8. Zhu G, Zhai P, Liu J et al (2004) Structural basis of Rab5-Rabaptin5 interaction in endocytosis. Nat Struct Mol Biol 11:975–983

9. Liu J, Lamb D, Chou MM et al (2007) Nerve growth factor-mediated neurite outgrowth via regulation of Rab5. Mol Biol Cell 18: 1375–1384

10. Nielsen E, Christoforidis S, Uttenweiler-Joseph S et al (2000) Rabenosyn-5, a novel Rab5 effector, is complexed with hVPS45 and recruited to endosomes through a FYVE finger domain. J Cell Biol 151:601–612

11. Simonsen A, Lippe R, Christoforidis S et al (1998) EEA1 links PI(3)K function to Rab5 regulation of endosome fusion. Nature 394: 494–498

12. Balaji K, Mooser C, Janson CM et al (2012) RIN1 orchestrates the activation of RAB5

GTPases and ABL tyrosine kinases to determine the fate of EGFR. J Cell Sci 125:5887–5896

13. Lodhi IJ, Chiang SH, Chang L et al (2007) Gapex-5, a Rab31 guanine nucleotide exchange factor that regulates Glut4 trafficking in adipocytes. Cell Metab 5:59–72

14. Ebbole DJ (2007) Magnaporthe as a model for understanding host-pathogen interactions. Annu Rev Phytopathol 45:437–456

15. Dou Z, Pan JA, Dbouk HA et al (2013) Class IA PI3K p110beta subunit promotes autophagy through Rab5 small GTPase in response to growth factor limitation. Mol Cell 50:29–42

16. Qi Y, Marlin MC, Liang Z et al (2014) Distinct biochemical and functional properties of Two Rab5 homologs from the rice blast fungus *Magnaporthe oryzae*. J Biol Chem 289: 28299–28309

17. Ji X, Johnson WW, Sesay MA et al (1994) Structure and function of the xenobiotic substrate binding site of a glutathione S-transferase as revealed by X-ray crystallographic analysis of product complexes with the diastereomers of 9-(S-glutathionyl)-10-hydroxy-9,10-dihydrophenanthrene. Biochemistry 33: 1043–1052

Chapter 23

Identification of the Rab5 Binding Site in p110β: Assays for PI3Kβ Binding to Rab5

Rachel S. Salamon, Hashem A. Dbouk, Denise Collado, Jaclyn Lopiccolo, Anne R. Bresnick, and Jonthan M. Backer

Abstract

Isoform-specific signaling by Class IA PI 3-kinases depends in part on the interactions between distinct catalytic subunits and upstream regulatory proteins. From among the class IA catalytic subunits (p110α, p110β, and p110δ), p110β has unique properties. Unlike the other family members, p110β directly binds to Gβγ subunits, downstream from activated G-protein coupled receptors, and to activated Rab5. Furthermore, the Ras-binding domain (RBD) of p110β binds to Rac and Cdc42 but not to Ras. Defining mutations that specifically disrupt these regulatory interactions is critical for defining their role in p110β signaling. This chapter describes the approach that was used to identify the Rab5 binding site in p110β, and discusses methods for the analysis of p110β-Rab5 interactions.

Key words PIK3CB, Class IA PI 3-kinase, p110beta, Rab5, Lipid kinases, Phosphoinositide 3-kinases, Small GTPases

1 Introduction

The Class I Phosphoinositide 3-kinases (PI 3-kinases) are activated by signals from receptor tyrosine kinases and G-protein-coupled receptors, and they produce phosphatidylinositol [3,4,5]-trisphosphate (PIP3) in metazoan cells. Of the four catalytic isoforms of PI 3-kinase, the PIK3CB gene product p110β is unique in that it couples to both RTKs and GPCRs [1, 2], has a so-called Ras-binding domain that instead binds to activated Rac and Cdc42 [3], and binds directly to the endosomal GTPase Rab5 in its activated, GTP-bound state [4].

Rab5 plays crucial roles in the sorting of internalized endocytic vesicles. Through its interactions with its effectors EEA1 and the Class III PI3 Kinase hVps34, Rab5 regulates docking and fusion of early endosomes, as well as their attachment to and movement along microtubules [5]. GTP-bound Rab5 has been shown to interact with a number of proteins involved in endocytic sorting,
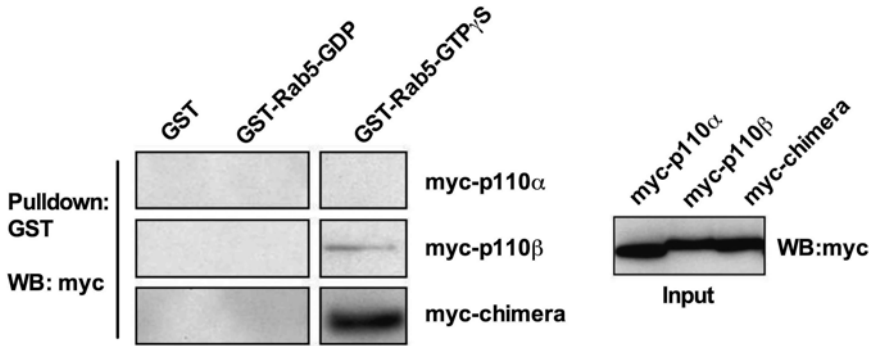
Fig. 1 Binding of p110β/p110β chimera to Rab5^GTP. Chimera of p110α ABD-RBD and p110β C2-helical-kinase domains binds Rab5. HEK293T cells were transfected with HA-p85 and myc-tagged p110α, p110β, or a p110α/p110β chimera. Cleared lysates were subjected to a GST-Rab5 pulldown, and samples were run on a western blot probing for myc

including the Rabaptin-5/Rabex-5 complex [6], the endosomal tethering protein EEA1 [7], and the hVps45-associated Rabenosyn-5 [8], as well as signaling proteins like APPL1/2 [9] and p110β [4].

Previous studies on p110β binding to Rab5 suggested that the binding site lay within residues 136–270, containing portions of the Adaptor-binding domain (ABD) and the Ras-binding domain (RBD), and residues 658–759, containing portions of the helical and kinase domains [10]. We have previously described a fully active p110α/p110β chimera containing the ABD and RBD domains of p110α linked to the C2, helical, and kinase domains of p110β [11]. This chimera showed specific GTP-dependent binding to GTP-Rab5 (Fig. 1). Taken together, these data and the published work suggested that the Rab5 binding site was within the helical and kinase domains of p110β.

In order to identify point mutations that would disrupt p110β binding to Rab5, we mutated candidate residues within the helical and kinase domains based on the following criteria.

1. The residues should be poorly conserved between human p110β and p110δ, which is the isoform most homologous to p110β, but which does not bind to Rab5.

2. We eliminated residues that were predicted to be poorly surface accessible, based on the crystal structure of p110β.

3. We eliminated residues that were poorly conserved in p110β orthologs from other species.

This analysis (*see* **Note 1**) defined 22 residues as potential binding sites for Rab5 (Fig. 2). The binding assay described below was then used to screen for mutants that disrupted p85/p110β binding to GST-Rab5-GTP beads (*see* **Note 2**). Two consecutive residues were found to be required for Rab5 binding: Q596C and I597S (Fig. 3a). Although p85 has been reported to directly bind

```
p110beta    NKKQPYYYPPFDKIIEKAAEIASSDSANVSSRGGKKFLPVLKEILDRDPL
p110delta   VAPHPVYYPALEKILELGR---HSECVHVTEEE----QLQLREILERRGS
            :* ***.::**:*  .         *:..:*:..      *:***:*

p110beta    SQLCENEMDLIWTLRQDCREIFPQSLPKLLLSIKWNKLEDVAQLQALLQI
p110delta   GELYEHEKDLVWKLRHEVQEHFPEALARLLLVTKWNKHEDVAQMLYLLCS
            .:* *:* **:*.**:: :* **::*.:*** **** *****:  **

p110beta    WPKLPPREALELLDFNYPDQYVREYAVGCLRQMSDEELSQYLLQLVQVLK
p110delta   WPELPVL SALELLDFSFPDCHVGSFAIKSLRKLTDDELFQYLLQLVQVLK
            **:**  .*******.:** :* .:*: .**::*:** **********

p110beta    YEPFLDCALSRFLLERALGNRRIGQFLFWHLRSEVHIPAVSVQFGVILEA
p110delta   YESYLDCELTKFLLDRALANRKIGHFLFWHLRSEMHVPSVALRFGLILEA
            **.:*** *:.***.***.**.**:**:*********:*:*:*::**:****
```

```
p110beta    YCRGSVGHMKVLSKQVEALNKLKTLNSLIKLNAVKLNRAKGKEAMHTCLK
p110delta   YCRGSTHHMKVLMKQGEALSKLKALNDFVKLSSQKTPKPQTKELMHLCMR
            *****. ***** ** ***.***:**.::**.: *  :.: ** ** *::

p110beta    QSAYREALSDLQSPLNPCVILSELYVEKCKYMDSKMKPLWLVYNNKVFGE
p110delta   QEAYLEALSHLQSPLDPSTLLAEVCVEQCTFMDSKMKPLWIMYSNEEAGS
            *.** ****.*****:*..:*:*: **:*.:**********::*.*: *.

p110beta    -DSVGVIFKNGDDLRQDMLTLQMLRLMDLLWKEAGLDLRMLPYGCLATGD
p110delta   GGSVGIIFKNGDDLRQDMLTLQMIQLMDVLWKQEGLDLRMTPYGCLPTGD
            .***:*************:***:***: ****** ***** .***

p110beta    RSGLIEVVSTSETIADIQLNSSNVAAAAAFNKDALLNWLKEYNSGDDLDR
p110delta   RTGLIEVVLRSDTIANIQLNKSNMAATAAFNKDALLNWLKSKNPGEALDR
            *:****** *:***:****.**:**:**************. *.*: ***

p110beta    AIEEFTLSCAGYCVASYVLGIGDRHSDNIMVKKTGQLFHIDFGHILGNFK
p110delta   AIEEFTLSCAGYCVATYVLGIGDRHSDNIMIRESGQLFHIDFGHFLGNFK
            ***************:**************.::::*********:*.*****

p110beta    SKFGIKRERVPFILTYDFIHVIQQGKTGNTEKFGRFRQCCEDAYLILRRH
p110delta   TKFGINRERVPFILTYDFVHVIQQGKTNNSEKFERFRGYCERAYTILRRH
            :****:************:**********.*:*** *** ** ** *****

p110beta    GNLFITLFALMLTAGLPELTSVKDIQYLKDSLALGKSEEEALKQFKQKFD
p110delta   GLLFLHLFALMRAAGLPELSCSKDIQYLKDSLALGKTEEEALKHFRVKFN
            * **:. ***** :*****:.  *************:******:*: **:

p110beta    EALRESWTTKVNWMAHTVRKDYRS
p110delta   EALRESWKTKVNWLAHNVSKDNRQ
            *******.*****:**.* ** *.
```

Not exposed
Exposed, not conserved
Conserved and Exposed
Conserved – no structural data

Fig. 2 Sequence analysis of p110β. The helical and kinase domains of p110β and p110δ were aligned using T-Coffee, and surface exposure was analyzed using NACCESS [17]. Residues that were not similar between p110β and p110δ are color coded as follows: *Green*—not surface exposed; *Magenta*—exposed but not conserved in p110β orthologs; *Yellow*—exposed and conserved; *Blue*—conserved but not visible in existing structures
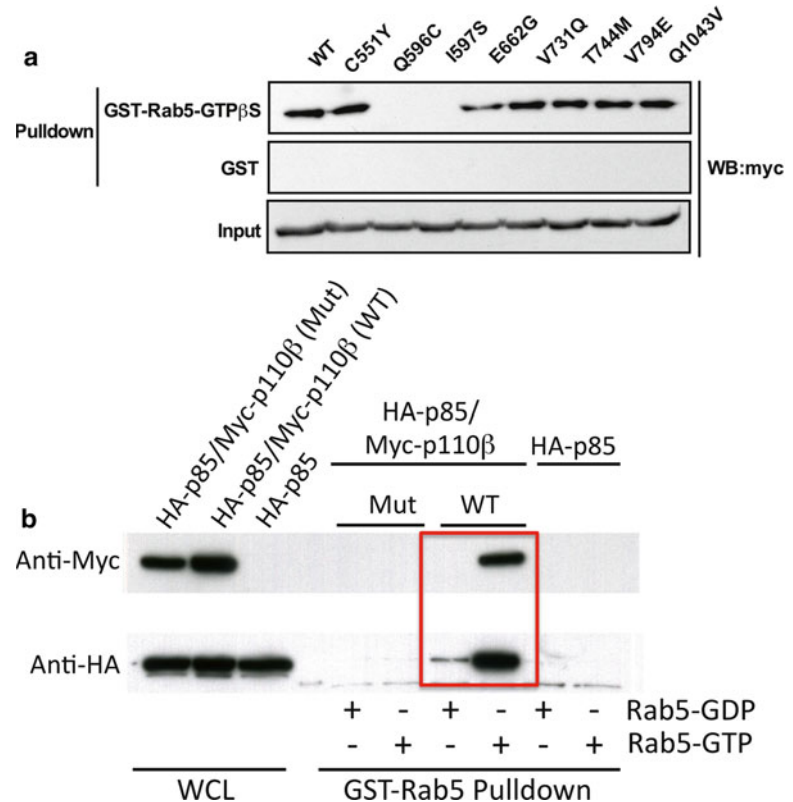
Fig. 3 (**a**) Identification of Rab5-binding deficient p110β mutants. HEK293T cells were transfected with HA-p85 and myc-p110β WT or one of eight p110β point mutants. Cleared lysates were subjected to a GST-Rab5-GTPγS pulldown, and samples analyzed by western blot. (**b**) HEK 293T cells were transfrected with HA-p85, HA-p85 plus wild type myc-p110β, or HA-p85 plus myc-p110β^{I597S} (Mut). Cell lysates were incubated with immobilized GST-Rab loaded with GDP or GTP-γS, and the beads were washed and analyzed by western blot for p110β (myc) or p85 (HA)

to Rab5 [12], we detected no binding to either p85 or dimers of p85 and p110β^{I597S} in this assay (Fig. 3b).

The p110β residues required for Rab5 binding lie immediately behind the Gβγ loop in p110β (Fig. 4). Subsequent analysis showed that these mutants had no effect on in vitro activation of p85/p110β by tyrosine phosphorylated peptides or by recombinant Gβγ (data not shown). The Rab5-uncoupled p110β mutants defined by these methods were subsequently used to implicate Rab5-p110β interactions in macroautophagy [13].

In this chapter, we describe the assay for Rab5-p110β binding that was used to identify the Rab5 binding site in p110β. The protocol has four major parts: purification of GST-Rab5 from bacteria, preparation of recombinant p85/p110β in HEK293T cells, loading of immobilized GST-Rab5 with GDP or GTP-γS, and GST-Rab5 pulldowns of recombinant p85/p110β.
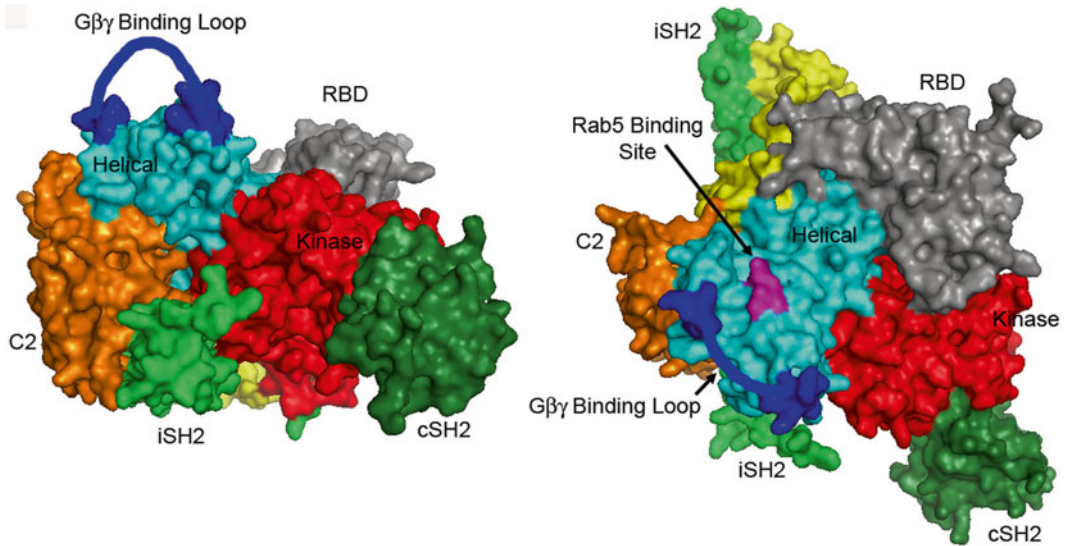
Fig. 4 Location of p110β mutants that disrupt binding to Rab^GTP. The crystal structure of p85(iSH2-cSH2)/ p110β [18] is shown with the C2 and kinase domains of p110β facing frontward (*left panel*), and rotated 90 to show the Rab5 binding site, which lies between the Gβγ binding loop and the RBD (*right panel*)

2   Materials

2.1   Plasmids

1. GST-Rab5A in pGEX-2T or pGEX-6P (GE Healthcare).
2. Human myc-tagged p110β in pSG5 (Stratagene) [2].
3. Human HA-tagged p85α in pSG5 (Stratagene) [2].

2.2   Buffers for Bacterial Expression of GST-Rab5

1. Resuspension Buffer: 50 mM Tris–HCl pH 8.0, 100 mM NaCl, 2 mM EDTA, 2 mM DTT, 10 % glycerol, 1 % CHAPS, Roche Protease Inhibitor tablet (1 tablet per 10 ml buffer), 0.35 mg/ml PMSF (1:100 dilution from freshly made 35 mg/ml PMSF in ethanol) (*see* **Note 3**).
2. Wash Buffer 1: Phosphate buffered saline containing 0.5 % NP-40 and 2 mM DTT.
3. Wash buffer 2: 50 mM Tris–HCl pH 8.0, 100 mM NaCl, 2 mM EDTA, 2 mM DTT, 10 % glycerol, 1 % CHAPS.
4. Elution Buffer: Wash Buffer 2 containing 15 mM reduced glutathione.

2.3   Buffers for Mammalian Expression of p85/ p110β

1. HEK lysis buffer: 20 mM Tris–HCl pH 7.5, 137 mM NaCl, 5 mM MgCl$_2$, 1 mM CaCl$_2$, 2 mM DTT, 10 % glycerol, 1.0 % NP-40, Roche protease inhibitor tablet (1 tablet/10 ml lysis buffer), PSMF (1:100 dilution from freshly made 35 mg/ml PMSF in ethanol), CalBiochem phosphatase inhibitor Cocktail 1 (1:100 dilution), Sigma phosphatase inhibitor Cocktail 2 (1:100 dilution).

2.4 Buffers for Rab5 Nucleotide Loading	1. Nucleotide Loading Buffer: 25 mM Tris–HCl pH 7.5, 50 mM NaCl, 10 mM EDTA, 5 mM $MgCl_2$, 2 mM DTT, 0.06 % CHAPS.
	2. Nucleotide Stabilization Buffer: 25 mM Tris–HCl pH 7.5, 50 mM NaCl, 10 mM $MgCl_2$, 2 mM DTT, 0.06 % CHAPS.

3 Methods

3.1 Production of Recombinant GST-Rab5 in Bacteria

1. Day 1: Transform BL21 bacteria with GST-Rab plasmid and plate onto LB-Agar plates (100 μg/ml ampicillin).

2. Day 2: Take a single colony from the plate and inoculate 5 ml of LB containing 100 μg/ml ampicillin. Shake overnight at 37 °C.

3. Day 3. Empty the 5 ml culture into 500 ml LB-amp and shake in a 2 l flask at 37 °C until the OD_{600} measures 0.6–0.8. Remove 50 μl sample for analysis, boil in Laemmli Sample Buffer, and store at –20 °C for subsequent analysis (*see* **Note 4**).

4. Add IPTG to the bacterial culture, to a final concentration of 0.2 mM. Shake overnight (16–18 h) at 18 °C. Remove 50 μl sample for analysis at the end of the induction, and process and store as above.

3.2 Purification of GST-Rab5 (Adapted from Ref. 14)

1. Centrifuge bacterial culture in refrigerated GSA rotor at $9,000 \times g$ for 10 min. Discard the supernatant. Supernatant should be clear and the pellet tightly packed.

2. Resuspend pellet in Resuspension Buffer (10 ml for a 500 ml culture) and transfer to 50 cc conical tube. Keep on ice at all times.

3. At this point, resuspended pellet can be flash frozen in dry ice/ethanol bath and stored at –80 °C. Allow room in tube for expansion during freezing. To resume the purification, thaw resuspended pellets in ice water. Add fresh PMSF (1:100 dilution of 35 mg/ml in ethanol) once thawed.

4. Lyse the resuspended bacteria by sonicating for 20 s in ice water, followed by 40 s recovery on ice, 4 times (total = 80 s sonication). Typical sonication uses a Branson Sonicator with a microprobe tip at output level 5. Keep sample tubes in a beaker with ice water during sonication.

5. Add Triton X-100 to a final concentration of 1 % v/v. Incubate at 4 °C on rotating wheel in cold room for 20 min.

6. Centrifuge at $15,000 \times g$ in a Sorvall SS-34 or equivalent rotor for 30 min to remove the insoluble material.

7. When spin is finished, filter the supernatant using a 0.45 μm filter. Remove 50 μl sample for analysis, and process and store as above.

8. Prepare a glutathione Sepharose column. For a 0.5 L culture, transfer 4 ml of 50 % GST bead slurry to a plastic column. Let the storage buffer drain out and then wash with 10 bed volumes of Wash Buffer 2.

9. Apply the filtered lysate to the glutathione Sepharose column, adjusting the outlet tube so that sample takes 30–60 min to run through. Save the flow through. Alternatively, incubate beads with filtered lysate in a 15 cc conical tube, rotating slowly at 4 °C for 2 h, then pour into plastic column. Save the flow through. (In either case, remove 50 μl sample of flow through for analysis; process and store as above.)

10. Wash column with 30–50 column volumes of ice cold Wash Buffer 1.

11. Wash column with 10 volumes ice cold Wash Buffer 2.

12. The GST-Rab5 beads can be used in pulldown assays at this point. The beads can be stored by diluting into 10 column volumes of Wash Buffer 2 made up to 50 % glycerol. After mixing on a wheel at 4 °C for 10 min, the beads can be stored for several weeks at –20 °C. Alternatively, GST-Rab5 can be eluted, dialyzed, and stored at –80 °C as described below.

13. To determine the amount of bound GST-Rab5, resuspend the beads 1:1 with Wash Buffer 2. Remove 30 μl of slurry (cut the pipette tip to avoid clogging), and spin the beads briefly at $13,000 \times g$. Remove the supernatant, and add 30 μl of Laemmli Sample Buffer containing 100 mM DTT. Boil for 3 min, spin at $13,000 \times g$ for 2 min, and analyze by reducing SDS-PAGE.

3.3   Elution of GST-Rab5

While Rab5 pulldown experiments can be performed using the beads as described above, eluting and dialyzing the protein have several advantages. First, the protein can be stored at –80 °C, enhancing its stability as compared to storage on beads at –20 °C in glycerol. Second, when comparing GST-Rab5 to other proteins (e.g., other Rabs, or GST as a control), one can easily prepare sets of glutathione beads containing identical amounts of bound GST fusion protein.

1. Elute washed beads (from **step 12**, above) with 20 column volumes Elution Buffer. Collect 1 ml fractions.

2. Measure OD 280 of each fraction, blanked against Elution Buffer. Yield for a 500 ml bacterial prep is approximately 5–10 mg of GST-Rab5.

3. Pool peak fractions, and dialyze 2 times for at least 8 h against Wash Buffer 2, with at least a 1000-fold excess of buffer over sample. Alternatively, dialyze 3 times with a 100-fold excess of buffer over sample.

4. Analyze protein purity by reducing SDS-PAGE.

5. Freeze and store in aliquots at –80 °C.

3.4 Analysis of Protein Concentration	If the eluted GST-Rab5 (or Rab of interest) appears as a single band on SDS-PAGE, then conventional protein assays (such as Biorad DC) can be used to determine protein concentration. If contaminating proteins are present in the preparation, or for analysis of GST-Rab5 bound to glutathione beads, then protein concentration of the Rab5 can be estimated by comparison to a Coomassie stained standard curve. Varying amounts of eluted protein or bead-bound protein (e.g., 10–40 μl of protein or 1:1 bead slurry) are analyzed by reducing SDS-PAGE in parallel with a standard curve of a known protein (BSA, or ideally a recombinant purified Rab). After fixing and Coomassie staining, the bands can be quantitated using a LI-COR Odyssey scanner, reading at 700 nm. The slope of the standard curve and the sample curve are determined, and the estimated protein concentration is:

$$1 / \text{Slope of standard curve}\,(\mu g\,/\,A700) \times \text{slope of the sample curve}\,(A700\,/\,\mu l)$$
$$= \text{concentration of sample}\,(\mu g\,/\,\mu l).$$

3.5 Preparation of Recombinant p85/p110β	Recombinant p85/p110β can be readily prepared in HEK293T cells as epitope tagged proteins. Class IA PI 3-kinase catalytic subunits are unstable as monomers and must be co-expressed with p85 regulatory subunits [15]. For HEK293T cells, we obtain high level expression using the pSG5 vector from Stratagene. We typically use myc-p110β and HA-p85.

1. Plate HEK293T cells on 10 cm tissue cultures dishes in DMEM/10 % fetal bovine serum. One dish yields enough protein for three pulldown assays.

2. When cells reach 70 % confluence, transfect with 3 μg each of plasmids coding for human p85α and p110β. While we have used Fugene HD, any commercial transfection reagent will work.

3. 2 days after transfection, lyse the cells in 1 ml/dish HEK Lysis Buffer. Pool the samples, rotate for 15 min at 4 °C, and then spin at $13,000 \times g$ for 5 min. The supernatant can be used directly for analysis of p110β-Rab5 binding (Subheading 4 below).

3.6 Nucleotide Loading of GST-Rab5A (Adapted from Ref. 14)	This section assumes the use of eluted and dialyzed GST-Rab5, which is then bound to glutathione sepharose beads. If using GST-Rab5 beads stored in 50 % glycerol, proceed as indicated but start at **step 2**. Use enough beads to provide 30 μg of GST-Rab5. Use at least 15 μl of beads per assay so the pellet will be visible during the washes.

1. Incubate glutathione beads with GST-Rab5 for 2 h in Wash Buffer 2 at 4 °C on a rotating wheel. Use 30 μg GST-Rab5 per 15 μl of packed beads. To achieve effective mixing during rota-

tion, the total volume of Wash Buffer should be at least 500 μl per 1.5 ml tube.

2. Wash beads four times with Wash Buffer.

3. Wash beads 2 times with Nucleotide Loading Buffer.

4. Add GDP or GTP-γS to a final concentration of 1 mM. Mix and incubate at 30 °C for 15 min.

5. Add MgCl$_2$ to a final concentration of 20 mM.

6. Mix and incubate at 30 °C for 3 min.

7. Hold on ice.

3.7 Analysis of Rab5-p85/p110β Binding

All samples are kept on ice. Use of a refrigerated centrifuge is recommended.

1. Pool lysates from transfected HEK293T, then dilute and divide into the number of aliquots needed. We typically use the lysate from one 10 cm dish for three GST-Rab5 pulldowns, and dilute so as to have 0.5 ml of lysate per pulldown. Remove 50 μl for analysis of total protein expression by western blot.

2. Add GDP or GTP-γS (10 μM final) to each tube.

3. Add 15 μl of GDP or GTP-γS-loaded GST-Rab beads per tube.

4. Incubate at 4 °C for 2 h on wheel.

5. Spin down samples for 10 s at 13,000 × g.

6. Wash the pellets three times in Nucleotide Stabilization Buffer. For each wash, resuspend the pellet in buffer, invert several times to mix, and then centrifuge (*see* **Note 5**).

7. Remove final wash, and remove last residues of wash buffer with 25G insulin syringe.

8. Add 40 μl Laemmli Sample Buffer containing 100 mM DTT.

9. Boil samples for 3 min.

10. Separate proteins by reducing SDS-PAGE (7.5 % resolving).

11. Analyze Rab5 pulldown by western blot (anti-myc for p110β, anti-HA for p85), using standard methods.

4 Notes

1. The combination of structural analysis (to define surface residues) and sequence analysis (to define residues conserved in orthologs) can provide a powerful approach for identifying putative binding sites that mediate protein–protein interactions. In the case of PI 3-kinase, this approach identified mutations that specifically disrupted p110β binding to Gβγ and Rab5, and p110γ binding to Gβγ. Since mutations can have conformational effects that act at a distance, this analysis should

be verified using an empirical approach such as deuterium exchange/mass spectrometry [2, 16].

2. The pulldown experiment can be readily adapted for testing small molecule inhibitors or Rab5-p110β binding by including the inhibitors in the binding and wash steps.

3. The use of CHAPS in the GST-Rab5 preparation is critical to maintain solubility of the enzyme. Preparations without CHAPS precipitate during dialysis.

4. The samples taken for analysis at various stages (before and after induction, after lysis and clearing by centrifugation, etc.) are needed for trouble shooting in case of a poor yield. Similarly, the whole cell lysate sample from the HEK293T cells is required to insure that the substrate for the binding assay (p85/p110β) was successfully produced, and to determine whether the mutants being analyzed show altered expression.

5. Use of GTP-γS in the GST-Rab5 pulldown prevents hydrolysis of GTP by the intrinsic GTPase activity of Rab5. Nonetheless, the assay should be performed quickly, so that the entire washing procedure takes approximately 15 min.

References

1. Maier U, Babich A, Nürnberg B (1999) Roles of non-catalytic subunits in Gβγ-induced activation of class I phosphoinositide 3-kinase isoforms beta and gamma. J Biol Chem 274(41):29311–29317

2. Dbouk HA, Vadas O, Shymanets A, Burke JE, Salamon RS, Khalil BD, Barrett MO, Waldo GL, Surve C, Hsueh C, Perisic O, Harteneck C, Shepherd PR, Harden TK, Smrcka AV, Taussig R, Bresnick AR, Nurnberg B, Williams RL, Backer JM (2012) G protein-coupled receptor-mediated activation of p110beta by Gbetagamma is required for cellular transformation and invasiveness. Sci Signal 5(253):ra89. doi:10.1126/scisignal.2003264

3. Fritsch R, de Krijger I, Fritsch K, George R, Reason B, Kumar MS, Diefenbacher M, Stamp G, Downward J (2013) RAS and RHO families of GTPases directly regulate distinct phosphoinositide 3-kinase isoforms. Cell 153(5):1050–1063. doi:10.1016/j.cell.2013.04.031

4. Christoforidis S, Miaczynska M, Ashman K, Wilm M, Zhao L, Yip SC, Waterfield MD, Backer JM, Zerial M (1999) Phosphatidylinositol-3-OH kinases are Rab5 effectors. Nat Cell Biol 1(4):249–252. doi:10.1038/12075

5. Zerial M, McBride H (2001) Rab proteins as membrane organizers. Nat Rev Mol Cell Biol 2(2):107–117

6. Horiuchi H, Lippe R, McBride HM, Rubino M, Woodman P, Stenmark H, Rybin V, Wilm M, Ashman K, Mann M, Zerial M (1997) A novel Rab5 GDP/GTP exchange factor complexed to Rabaptin-5 links nucleotide exchange to effector recruitment and function. Cell 90(6):1149–1159

7. Simonsen A, Lippe R, Christoforidis S, Gaullier JM, Brech A, Callaghan J, Toh BH, Murphy C, Zerial M, Stenmark H (1998) EEA1 links PI(3)K function to Rab5 regulation of endosome fusion. Nature 394(6692):494–498. doi:10.1038/28879

8. Nielsen E, Christoforidis S, Uttenweiler-Joseph S, Miaczynska M, Dewitte F, Wilm M, Hoflack B, Zerial M (2000) Rabenosyn-5, a novel Rab5 effector, is complexed with hVPS45 and recruited to endosomes through a FYVE finger domain. J Cell Biol 151(3):601–612

9. Miaczynska M, Christoforidis S, Giner A, Shevchenko A, Uttenweiler-Joseph S, Habermann B, Wilm M, Parton RG, Zerial M (2004) APPL proteins link Rab5 to nuclear signal transduction via an endosomal compartment. Cell 116(3):445–456

10. Kurosu H, Katada T (2001) Association of phosphatidylinositol 3-kinase composed of p110β-catalytic and p85-regulatory subunits with the small GTPase Rab5. J Biochem 130(1):73–78

11. Dbouk HA, Pang H, Fiser A, Backer JM (2010) A biochemical mechanism for the oncogenic potential of the p110beta catalytic subunit of phosphoinositide 3-kinase. Proc Natl Acad Sci U S A 107(46):19897–19902. doi:10.1073/pnas.1008739107

12. Chamberlain MD, Anderson DH (2005) Measurement of the interaction of the p85alpha subunit of phosphatidylinositol 3-kinase with Rab5. Methods Enzymol 403:541–552. doi:10.1016/S0076-6879(05)03047-8

13. Dou Z, Pan JA, Dbouk HA, Ballou LM, DeLeon JL, Fan Y, Chen JS, Liang Z, Li G, Backer JM, Lin RZ, Zong WX (2013) Class IA PI3K p110beta subunit promotes autophagy through Rab5 small GTPase in response to growth factor limitation. Mol Cell 50(1):29–42. doi:10.1016/j.molcel.2013.01.022

14. Hadano S, Ikeda JE (2005) Purification and functional analyses of ALS2 and its homologue. Methods Enzymol 403:310–321. doi:10.1016/S0076-6879(05)03026-0

15. Yu J, Zhang Y, McIlroy J, Rordorf-Nikolic T, Orr GA, Backer JM (1998) Regulation of the p85/p110 phosphatidylinositol 3'-kinase: stabilization and inhibition of the p110-alpha catalytic subunit by the p85 regulatory subunit. Mol Cell Biol 18:1379–1387

16. Vadas O, Dbouk HA, Shymanets A, Perisic O, Burke JE, Abi Saab WF, Khalil BD, Harteneck C, Bresnick AR, Nurnberg B, Backer JM, Williams RL (2013) Molecular determinants of PI3Kgamma-mediated activation downstream of G-protein-coupled receptors (GPCRs). Proc Natl Acad Sci U S A 110(47):18862–18867. doi:10.1073/pnas.1304801110

17. Hubbard SJ, Thornton JM (1993) NACCESS. Dept. of Biochemistry and Molecular Biology, University College London, London

18. Zhang X, Vadas O, Perisic O, Anderson KE, Clark J, Hawkins PT, Stephens LR, Williams RL (2011) Structure of lipid kinase p110 beta/p85beta elucidates an unusual SH2-domain-mediated inhibitory mechanism. Mol Cell 41(5):567–578. doi:10.1016/j.molcel.2011.01.026

Chapter 24

Role of the Rab5 Guanine Nucleotide Exchange Factor, Rme-6, in the Regulation of Clathrin-Coated Vesicle Uncoating

Elizabeth Smythe

Abstract

Clathrin-coated pits are major ports of entry into eukaryotic cells. Following scission of clathrin-coated pits to form coated vesicles, the peripheral membrane proteins that form the coat need to be removed. Here we describe an assay that provides a measure of the extent of clathrin coat uncoating in intact cells. This assay has been used to investigate rab5-dependent modulation of uncoating. Specifically, it has been used to identify functional differences between rab5 guanine nucleotide exchange factors.

Key words Endocytosis, rab5, Guanine nucleotide exchange factors, Rme-6, AP2, Clathrin, Coated vesicles, Uncoating

1   Introduction

Endocytosis is responsible for the cellular uptake of a variety of biologically important macromolecules, including nutrients, hormones, and signaling receptors. Clathrin-mediated endocytosis is one well-defined uptake pathway. Cargo that is internalized via this route is captured at specialized areas of the plasma membrane, termed clathrin-coated pits. These form by the directed assembly of the protein clathrin from the cytoplasm onto the plasma membrane. Clathrin-coated pits become increasingly invaginated before pinching off to form coated vesicles. Clathrin does not directly bind to the membrane, rather it is linked by means of adaptor proteins that recognize internalization motifs in the cytoplasmic domains of transmembrane proteins, allowing them to be internalized. In addition to adaptor proteins that recognize cargo, there are many other accessory proteins within the clathrin lattice, which act as structural and regulatory components. These components interact with each other through a myriad of low affinity interactions, thus creating high avidity [1, 2].

Following clathrin-coated vesicle scission, the coat needs to be removed from the endocytic vesicle to facilitate its fusion with endosomal compartments so that it can deliver its cargo. Clathrin uncoating is effected by the action of the heat shock protein, hsc70, and its co-factor, auxilin in neuronal cells and GAK in non-neuronal cells [3]. A classical view of the mechanism of uncoating is that removal of clathrin is sufficient to cause dissociation of the inner shell of adaptor and accessory proteins. However this view was challenged by our results demonstrating that AP2 uncoating is specifically regulated by the small GTPase, rab5. Rab5 is a major regulator of the early endocytic pathway, controlling early endosomal fusion, endosome motility, cargo recruitment and signaling as well as uncoating. It regulates these specific functions by acting as a classical molecular switch, recruiting different complements of effector molecules when in its active GTP conformation [4]. Guanine nucleotide exchange factors, GEFs, exchange GDP for GTP on rab5 thus activating it. In mammals there are several rab5 GEFs, all of which are characterized by the presence of a VPS9 domain responsible for GEF activity [5]. We have demonstrated that one particular GEF, Rme-6, is responsible for rab5-dependent regulation of AP2 uncoating. By contrast rabex5, the canonical rab5GEF which functions at the early endosome [6], does not appear to participate in uncoating. Moreover we have demonstrated that Rme-6 is targeted to clathrin-coated vesicles via interactions with the AP2 adaptor complex, thus providing spatial control of the activation of a subset of rab5 effectors important in uncoating of this adaptor complex [7] (Fig. 1).

This chapter describes an assay that estimates the extent of clathrin-coated vesicle uncoating in intact cells. It is based on the premise that, at steady state, there will be a constant number of clathrin-coated vesicles in the cell which can be identified by co-localization with cargoes such as transferrin which is a well-established marker of clathrin-coated pits [8–10]. Transferrin is internalized for a short time (~5 min) which is sufficient to label clathrin-coated pits and coated vesicles. The surface transferrin is then removed by acid stripping and the extent of co-localization with coat proteins measured. Under conditions where uncoating is perturbed, it is to be expected that there will be changes in the association of coat proteins with cargo-filled vesicles. Thus a delay in uncoating should result in enhanced association of coat proteins with cargo while an increase in the rate of uncoating should result in a decrease in the extent of co-localization of coat proteins with cargo. Using this approach it is possible to explore whether uncoating is affected by perturbation of cellular function by, for example, knockdown of proteins using siRNA or overexpression of wild-type or mutant endocytic proteins (*see* **Note 1**).

In the example described below, we examine the effects of siRNA-mediated knockdown of rab5GEFs on the regulation of uncoating.
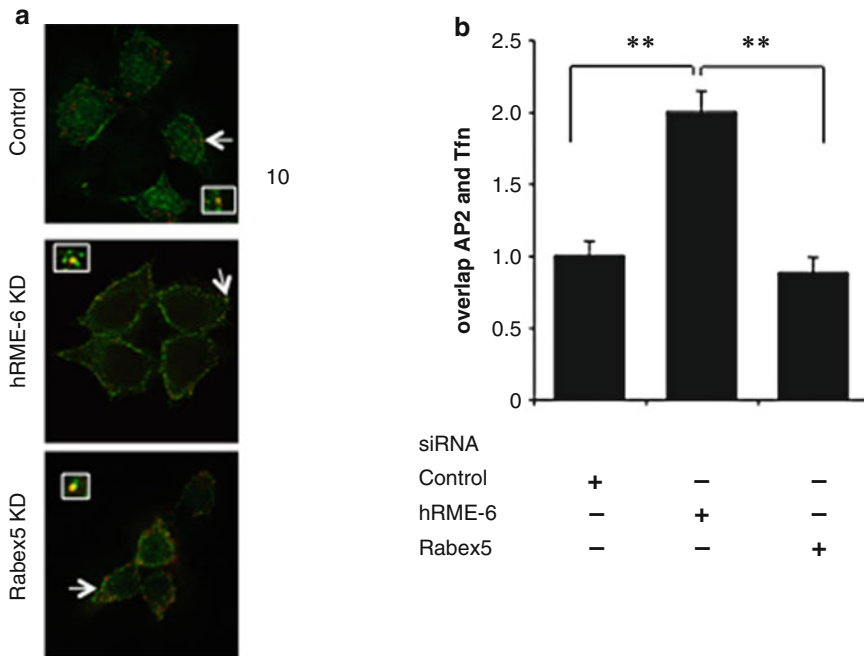
Fig. 1 Rme-6 acts as a rab5GEF for AP2 uncoating from clathrin-coated vesicles. (**a**) Representative images of siRNA-treated cells incubated with Texas Red transferrin and, after acid stripping, stained for AP2 (*green*) using AP.6 monoclonal antibody. The *white arrowheads* indicate an area of overlap which is enlarged in the inset. (**b**) Quantitation of the degree of overlap between AP2 and Texas Red (*see* **Note 23**) transferrin in cells treated with control siRNA, and siRNA targeting Rme-6 and rabex-5. The degree of overlap was set at 1 in control cells. Results are expressed as the fold change in overlap compared with control cells ±SEM and are the results of three experiments where at least 25 cells were analyzed. Values are significant at $P < 0.01$ (**) for control versus Rme-6 knockdown and rabex-5 versus Rme-6 knockdown. Note that the number of overlapping spots per cell is small because most of the AP.6 positive spots represent clathrin-coated pits versus coated vesicles. In addition the differences caused by modulation of rab5 by knockdown of Rme-6 are not obvious in images from single planes and require quantitation of the extent of overlap over the whole cell. Figure originally published in J Cell Biol 183: 499–511. doi: 10.1083/jcb.200806016

The steps that will be described in the protocol include tissue culture, transfection of cells with siRNA, immunofluorescence protocol for measurement of uncoating, collection of images and data analysis.

2   Materials

2.1   Solutions and Reagents

1. All solutions should be prepared using milliQ water.

2. Dulbecco's modified Phosphate buffered saline (PBS): 8 mM sodium phosphate, 2 mM potassium phosphate, 0.14 M NaCl 10 mM KCl, pH 7.4.

3. Tris buffered saline (TBS): 50 mM Tris–HCl, pH 7.5, 150 mM NaCl.

4. Dulbecco's Modified Eagle's Medium: commercially available.

5. Roswell Park Memorial Institute Medium 1640 (RPMI): commercially available.

6. Fetal calf serum.

7. L-Glutamine, supplied commercially as 200 mM (100× stock).

8. Penicillin/streptomycin, supplied commercially as 10,000 units/ml and 10 mg/ml respectively (100× stock).

9. 4 % formaldehyde (PFA): For 50 ml, add 2 g of paraformaldehyde to 25 ml dH$_2$O at 60 °C, add 1–2 drops 1 M NaOH to depolymerise the PFA. Incubate at 60 °C until the PFA is dissolved. Make up the volume to 50 ml. Check the pH to confirm it is between 7.0 and 7.5. Filter sterilize and either use fresh or aliquot and store at –20 °C. Once thawed do not refreeze.

10. Triton X-100 (TX-100).

11. Ammonium chloride (NH$_4$Cl).

12. Fish-skin gelatin: Prepare 20 % (v/v) stock solution.

13. Serum free medium (SFM): 0.2 % (w/v) Bovine serum albumin in DMEM.

14. Stripping buffer: 50 mM glycine–HCl, pH3.0, containing 2 M urea and 100 mM NaCl.

15. Antibodies: Anti-clathrin and anti-AP2 antibodies can be produced in conditioned medium from X22 and AP.6 cells respectively. Cells may be purchased from the American Tissue Culture Collection (http://www.lgcstandards-atcc.org). Culture X22 cells in DMEM containing 15 % FBS and supplemented with 2 mM glutamine, 100 μg/ml streptomycin and 100 units/ml penicillin at 37 °C with 10 % CO$_2$. Maintain cells in suspension at a density of between 1×10^5 and 1×10^6 cells per ml. Harvest conditioned medium from the cells when they have been growing for 1–2 weeks by centrifugation at $1000 \times g$ for 5 min. Remove up to half of the cell supernatant and maintain under sterile conditions at 4 °C for use in immunofluorescence. Resuspend the cell pellet in the remaining supernatant supplemented with fresh medium. Collect conditioned medium at regular intervals while the cells are growing well. The optimal dilution at which to use the conditioned media needs to be determined empirically. Culture AP.6 cells in RPMI 1640 containing 15 % FBS and supplemented with 2 mM glutamine, 100 μg/ml streptomycin, and 100 units/ml penicillin at 37 °C with 5 % CO$_2$. Maintain cells in suspension at a density of between 1×10^5 and 1×10^6 cells per ml. Harvest conditioned medium from the cells when they have been growing for

1–2 weeks by centrifugation at $1000 \times g$ for 5 min. Remove up to half of the cell supernatant and maintain under sterile conditions at 4 °C for use in immunofluorescence. Resuspend the cell pellet in the remaining supernatant supplemented with fresh medium. Collect conditioned medium at regular intervals while the cells are growing well. The optimal dilution at which to use the conditioned media needs to be determined empirically.

16. Alexa 568 transferrin: available commercially.

17. Alexa 488 anti mouse antibodies: commercially available.

18. Poly-L-lysine: available commercially as a stock of 0.1 %. Dilute 1:10 to use.

19. Mounting medium containing anti-fade: commercially available.

20. 4′,6-diamidino-2-phenylindole (DAPI). Make 5 mg/ml stock solution. Aliquot and store at –20 °C.

21. Reagents for siRNA transfection: Oligofectamine and Opti-MEM I Reduced Serum Medium (Invitrogen).

22. siRNAs against target proteins and scrambled siRNAs as controls: These can be designed and purchased commercially.

23. Microscope slides and coverslips.

24. Parafilm.

2.2 Equipment

1. Tissue culture hoods and incubators.

2. Wide-field or confocal microscope with 63× objective.

3. Software data analysis package: FIJI (Open Source) or Volocity (Closed source).

3 Methods

3.1 Culturing HEK293 Cells (See Note 2)

1. Grow cells in tissue culture flasks or plates in DMEM containing 10 % serum, 2 mM glutamine, 100 μg/ml streptomycin, and 100 units/ml penicillin at 37 °C with 5 % CO_2.

2. Passage cells every 2–3 days by first washing two times with warmed PBS (*see* **Note 3**).

3. For a 10 cm plate add 1 ml of trypsin.

4. Check cells under the microscope and when the cells begin to round up, gently slap the side of the dish to dislodge cells.

5. Quench with 9ml of DMEM containing 10 % serum, 2 mM glutamine, 100 μg/ml streptomycin, and 100 units/ml penicillin.

6. Dilute as needed into appropriately sized dishes (*see* **Note 4**). Dilutions should be in the range of 1:10–1:2.

3.2 Setting Up Coverslips for an Experiment

1. Coat coverslips with poly-L-lysine to improve adherence of the cells to the glass under sterile conditions in a tissue culture hood (*see* **Note 5**).

2. Incubate glass coverslips in poly-L-lysine (0.01 % v/v) diluted in PBS for 30 min at room temperature.

3. Wash extensively to remove the poly-L-lysine (*see* **Note 6**). Coated coverslips are stable for at least a week as long as they are maintained under sterile conditions.

3.3 Transfection of Cells with siRNA

siRNA depletion of target proteins is carried out as described [11] (*see* **Note 7**).

1. Day 0: Plate HEK293 cells overnight in DMEM containing 10 % FBS and 2 mM glutamine but no penicillin/streptomycin so that they reach 30 % confluency on the day of transfection.

2. Day1: Add relevant siRNA against Rme-5, rabex5, or luciferase as a control (*see* **Note 8**) at a concentration of 0.2 μM using a suitable transfection agent, e.g., Oligofectamine, according to the manufacturer's instructions.

3. Day 2: Split cells in DMEM containing 10 % FBS and 2 mM glutamine but no penicillin/streptomycin to achieve 30 % confluency on Day 3.

4. Day 3: Add another batch of siRNA using Oligofectamine to the cells at the same concentration as on Day 1.

5. Day 4: Split cells onto poly-L-lysine coated coverslips in DMEM containing 10 % serum, 2 mM glutamine, 100 μg/ml streptomycin, and 100 units/ml penicillin in either 35 mm plates or 6-well tissue culture dishes to achieve 80 % confluency on Day 5.

6. Day 5: Carry out uncoating assay as outlined below.

3.4 Assay for Uncoating

1. Pre-incubate cells in pre-warmed SFM for 30 min (*see* **Note 9**).

2. Wash cells once with warmed PBS.

3. Incubate with Alexa 568 transferrin (5 μg/ml) diluted in SFM for 5 min at 37 °C.

4. Remove from incubator and place on ice.

5. Aspirate media and replace with ice cold PBS.

6. Wash 2× with ice-cold PBS.

7. To remove surface bound Alexa 568 transferrin, add 1 ml of acid stripping buffer for 5 min.

8. Rinse with ice-cold PBS.

9. Repeat **steps 7** and **8** two more times (*see* **Note 10**).

10. Fix cells in 4 % PFA for 20 min at room temperature.

11. Quench the PFA with PBS containing 50 mM NH_4Cl (*see* **Note 11**).

12. Permeabilize with TBS (*see* **Note 12**) containing 0.1 %TX-100 for 5 min at room temperature.

13. Block with TBS containing 0.2 % fish skin gelatin (*see* **Note 13**) for 5 min.

14. Incubate with primary antibody diluted in TBS/0.2 % gelatin (*see* **Note 14**) for 20 min at room temperature in a humidified chamber (*see* **Note 15**).

15. Return the coverslips to the 6-well dish and wash 3× with 2 ml of TBS or PBS (*see* **Note 16**).

16. Incubate with an appropriate fluorescently labeled secondary antibody that recognizes the species subtype of the primary antibody for 20 min at room temperature. Dilute antibodies in TBS/0.2 % fish skin gelatin.

17. Wash 3× with TBS as per **step 15**.

18. Incubate with DAPI (300 nM final concentration) in TBS for 1 min (*see* **Note 17**).

19. Wash 3× with TBS as per **steps 15** and **17**.

20. Place one drop of mounting medium on a microscope slide.

21. Lift each coverslip with a tweezer and immerse sequentially in three beakers of distilled water (*see* **Note 18**).

22. Blot excess water from the coverslips by holding paper towel at one edge. Place the coverslip cell side down on the mounting medium. This step should be done at a slight angle to avoid trapping air bubbles.

23. Leave the coverslips to prove overnight at room temperature in the dark (*see* **Note 19**).

3.5 Imaging

1. Capture images using a DeltaVision-Real Time (RT) Deconvolution Microscope (Applied Precision) with Linux-based softWoRx version 3.5.1 (Applied Precision) and 60× or 100× objectives (*see* **Note 20**). Collect stacks of images at room temperature with 0.2-µm z-step from the bottom to the top of the cells.

2. Deconvolve images using softWoRx with a conservative ratio, medium noise filtering and 15 cycles.

3.6 Image Processing

To quantitate fluorescence and extent of overlap between cargo and coat proteins, use FIJI or Volocity software or equivalent to calculate the Manders co-localization coefficient [12].

1. Set background for each channel per experiment. Set the lower limit of fluorescence intensity based on values taken for at least five different pixels in an area of the cell with background staining. Set the high limit of fluorescence intensity at virtual infinity. Measure fluorescence from 20 to 30 cells (*see* **Note 21**).

2. Calculate Manders co-localization coefficient [12] (*see* **Note 22**).

3. Use GraphPadPrism or equivalent to calculate the mean co-localization coefficient per condition.

4. Calculate differences between the means using one-way ANOVA followed by Tukey's multiple comparison test.

5. Set the degree of co-localization between coat proteins (clathrin or AP2) in mock-treated cells as 1. Figure 1 shows an example of how knockdown of the rab5GEF, Rme-6, but not rabex5, delays the extent of uncoating of AP2 from clathrin-coated vesicles in intact cells by increasing the degree of co-localization.

4   Notes

1. When using this assay to estimate the extent of uncoating, it is important to consider that cellular perturbations might have indirect effects on uncoating. For example, rab5 carries out many different roles on the endocytic pathway and hence observed effects on uncoating might result from indirect effects on cargo recruitment and/or recycling of components required for coated pit invagination or scission rather than direct effects on uncoating. This could give rise to changes in the association of transferrin with coat proteins. In the case of overexpression of dominant negative rab5 which showed a delay in uncoating of AP2, it was possible that rab5 negatively regulated transferrin recruitment into clathrin-coated pits and hence expression of rab5^{S34N} might result in an apparent increase in the extent of co-localization of AP2 with transferrin. We were able to eliminate this possibility by demonstrating that the amount of transferrin recruitment into clathrin-coated pits was independent of overexpression of rab5 wild-type or mutants [7].

2. The details of the assay described in this chapter refer specifically to HEK293 cells but the assay is applicable to any adherent cell type.

3. HEK293 cells are easily dislodged from the plastic tissue culture dish. It is important to perform the washes with care by adding PBS slowly at the side of the dish.

4. HEK293 cells divide approximately every 24 h. Cells for an experiment should be plated at least 1, and ideally 2, days in advance so that they are 80 % confluent on the day of the experiment.

5. HEK293 cells are easily dislodged from the coverslip and hence plating on poly-L-lysine is necessary to avoid losing many cells during the course of an uncoating assay. For cells

that adhere more strongly to glass (e.g., HeLa or A431 cells), this step can be omitted.

6. Poly-L-lysine is toxic to many cells; so it is key that this step is thorough to remove unreacted poly-L-lysine.

7. Endocytic proteins in general are relatively long-lived with half-times in the region of 24–48 h. In order to achieve a significant knockdown in protein levels using siRNA, it is often necessary to perform a double transfection as detailed in the protocol. It is useful to carry out pilot studies using different amounts of siRNA and single and double transfections to optimize the level of knockdown of the target protein.

8. siRNA against Luciferase is used as a control to eliminate off-target effects of siRNA transfection.

9. There is a high concentration of bovine transferrin in serum which needs to be removed in order to maximize binding of human transferrin to the transferrin receptor in HEK293 cells. Transferrin bound to its receptor recycles from early endosomes and 30 min is sufficient for internalized transferrin to recycle to the cell surface for release into the medium.

10. It is essential that the acid stripping step is effective. The efficacy of the procedure can be tested by pre-incubating two sets of cells on coverslips at 4 °C for 30 min with 5 μg/ml Alexa 568 transferrin. This will allow surface binding but will prevent internalization. One set of cells should be processed as per **steps 7–9** above before fixation with PFA while the other set should be fixed immediately. The fluorescence intensity of both sets should be captured on a wide-field microscope using identical settings. Acid stripping should result in at least 90 % reduction in fluorescence intensity.

11. Some antibodies may be sensitive to the kind of fixation being used. It is also possible to use methanol fixation as follows:

    (a) Add slides to methanol at –20 °C for 5 min.

    (b) Incubate slides in acetone (–20 °C) for 30 s. (Note: incubations at –20 °C should be carried out in a spark-proof freezer).

    (c) Wash 6× with PBS to remove acetone. Continue with blocking as per **step 11** above.

12. Following quenching with NH_4Cl, it is possible to use either TBS or PBS. PBS should be avoided if using phospho-specific antibodies.

13. Fish skin gelatin is a blocking agent of choice as it tends to give reduced background. For some antibodies, blocking agents such as bovine serum albumin (0.1–0.2 % w/v) can also be used. The optimal blocking agent should be determined empirically.

14. The optimal dilution of the primary antibody should be determined prior to the start of the experiment by carrying out a range of dilutions and determining which antibody concentration gives the best signal-to-noise ratio, i.e., a strong signal and little background fluorescence, as this will facilitate subsequent image analysis.

15. To reduce the amount of antibody required for this step, apply 40 μl of diluted antibody onto a strip of parafilm. Sprinkle a few drops of water on the bench to increase the adherence of the parafilm to the surface. The coverslip is then inverted gently and slowly onto the drop, taking care to minimize trapping air bubbles. The coverslips can then be covered and protected from light by using a humidified chamber. This can be prepared simply by attaching damp paper towels to the inside of a polystyrene box which can then be inverted over the coverslips. The humidified atmosphere will prevent drying at the edges of the coverslip.

16. It is important during the washes that the cells do not dry out. The easiest way to avoid this is by aspirating off the buffer with a pump-driven aspirator and quickly adding the next wash with a glass pipette using a pipette boy.

17. DAPI is a nuclear stain. Staining the nuclei with DAPI makes it easier to locate cells under the microscope. However avoid using DAPI if using an Alexa 350 labeled secondary antibody.

18. Rinsing the coverslip with water is important to remove salts that may interfere with the quality of the images subsequently captured on the microscope.

19. After this step slides can be stored in a slide holder at –20 °C until you are ready to image them. Current fluorophores are very stable and so the fluorescence will be maintained under these conditions for several weeks.

20. Images can be captured on a wide-field microscope and the images deconvolved. Deconvolution allows removal of out-of-focus fluorescence post acquisition, thus improving quantitation [13].

21. It is important to collect data from a statistically significant number of cells (approximately 20–30) and from several experiments (usually 3).

22. Manders co-localization coefficient is used in preference to other measures of co-localization as the coefficient is not sensitive to differences in signal intensity that were often observed between fluorophores.

23. In the example shown, TexasRed transferrin was used but newer Alexa dyes tend to have a higher quantum yield.

Acknowledgments

References

1. McMahon HT, Boucrot E (2011) Molecular mechanism and physiological functions of clathrin-mediated endocytosis. Nat Rev Mol Cell Biol 12:517–533

2. Traub LM, Bonifacino JS (2013) Cargo recognition in clathrin-mediated endocytosis. Cold Spring Harb Perspect Biol 5(11):a016790

3. Eisenberg E, Greene LE (2007) Multiple roles of auxilin and hsc70 in clathrin-mediated endocytosis. Traffic 8:640–646

4. Stenmark H (2009) Rab GTPases as coordinators of vesicle traffic. Nat Rev Mol Cell Biol 10:513–525

5. Carney DS, Davies BA, Horazdovsky BF (2006) Vps9 domain-containing proteins: activators of Rab5 GTPases from yeast to neurons. Trends Cell Biol 16:27–35

6. Horiuchi H, Lippe R, McBride HM, Rubino M, Woodman P, Stenmark H, Rybin V, Wilm M, Ashman K, Mann M, Zerial M (1997) A novel Rab5 GDP/GTP exchange factor complexed to Rabaptin-5 links nucleotide exchange to effector recruitment and function. Cell 90:1149–1159

7. Semerdjieva S, Shortt B, Maxwell E, Singh S, Fonarev P, Hansen J, Schiavo G, Grant BD, Smythe E (2008) Co-ordinated regulation of AP2 uncoating from clathrin coated vesicles by rab5 and hRME-6. J Cell Biol 183:499–511

8. Hopkins CR, Trowbridge IS (1983) Internalization and processing of transferrin and the transferrin receptor in human carcinoma A431-cells. J Cell Biol 97:508–521

9. Smythe E, Pypaert M, Lucocq J, Warren G (1989) Formation of coated vesicles from coated pits in broken A431 cells. J Cell Biol 108:843–853

10. Schmid SL, Smythe E (1991) Stage-specific assays for coated pit formation and coated vesicle budding in vitro. J Cell Biol 114:869–880

11. Motley A, Bright NA, Seaman MN, Robinson MS (2003) Clathrin-mediated endocytosis in AP-2-depleted cells. J Cell Biol 162:909–918

12. Manders EM, Stap J, Brakenhoff GJ, van Driel R, Aten JA (1992) Dynamics of three-dimensional replication patterns during the S-phase, analysed by double labelling of DNA and confocal microscopy. J Cell Sci 103:857–862

13. Wallace W, Schaefer LH, Swedlow JR (2001) A workingperson's guide to deconvolution in light microscopy. Biotechniques 31:1076–1097

Chapter 25

Differential Effects of Overexpression of Rab5 and Rab22 on Autophagy in PC12 Cells with or without NGF

M. Caleb Marlin and Guangpu Li

Abstract

Macroautophagy selectively recycles damaged or unneeded proteins and organelles by degradation via targeting to the autophagosome. The following method seeks to identify candidate Rab GTPases that likely modulate autophagy in PC12 cells during nerve growth factor (NGF) starvation. This microscopy-based assay is a single cell-based quantification of the presence of autophagosomes by fluorescently labeled markers in response to the overexpression of Rabs and mutants in the presence or absence of NGF.

Key words Autophagy, LC3B, Rab, GTPase, GTP-binding protein, NGF, PC12 cells

1 Introduction

Macroautophagy is a bulk degradation/recycling stress response in eukaryotes. This complex system works to degrade intracellular components by targeting damaged, aggregated, or nonessential proteins and organelles to the autophagosome [1]. Though autophagy is continually active at basal levels, autophagy progression above basal level is highly regulated by growth factor stimulation or nutrient loss, particularly in neurons [2]. This work is aimed to provide useful tools for furthering our understanding of key regulators of autophagy.

The prototypical neurotrophin, nerve growth factor (NGF), binds to TrkA, its high affinity receptor, in mammalian neurons and stimulates survival and differentiation [3]. Phosphorylated TrkA dimers are internalized and trafficked from early, to late endosomes, and subsequently degraded at the lysosome. However, other pathways exist which divert TrkA from canonical endocytic trafficking and alter both the temporal and spatial regulation of TrkA. One such example is the signaling endosome, which is a particularly important subset of vesicles to TrkA signaling, neuron survival, and differentiation, though their biogenesis and function is not completely understood. As our understanding of the

complex trafficking of TrkA increases, so does our appreciation for the endocytic and recycling machinery in the life of growth factor signaling.

TrkA enlists a plethora of prosurvival signaling cascades leading to a complex network of survival and differentiation signals that are necessary to the life of neurons. PI3K is one such effector that promotes the activation of AKT and mTORC1 in response to NGF. mTORC1 inhibits autophagy by phosphorylation of the ATG1/ULK1 complex, an important component of the preautophagic complex and a critical step for initiation of autophagy [4]. Therefore, NGF/TrkA signaling leads to a decrease in autophagy and autophagosome production.

The endocytic trafficking of TrkA-positive vesicles is pivotal for the signaling and trafficking of NGF/TrkA in the neuron. Mechanisms governing the endocytosis, sorting, and trafficking of TrkA will have a profound impact on the life and health of the cell. The Rab family of small GTPases facilitate the fusion, sorting, and trafficking of all intracellular membrane compartments; endosomes and autophagosomes are no exceptions [5]. In particular, Rab5 and its subfamily member, Rab22, regulate the formation of NGF/TrkA-containing early and signaling endosomes [6]. Since endocytic trafficking is a major component of the TrkA signaling cascade, modulation of Rab5 and Rab22 will alter the physiologic outcomes of TrkA signaling, including prevention of autophagy. The current method aims to study the effects candidate Rabs may have upon the antiautophagic signaling of NGF in PC12 cells.

A reporter cassette based on the dsRed:LC3B:eGFP reporter [7] was modified by the replacement of dsRed with the more bright tandem dual tomato (tdTom) and inserted into pBI-Tet that contains a bidirectional promoter. The pBI-Tet vector allows for coexpression of both the new tdTom:LC3B:eGFP reporter and a candidate Rab (Fig. 1a). The tdTom:LC3B:eGFP reporter is expected to be processed by ATG4 at a glycine near the C-terminus in LC3B to cleave tdTom:LC3B from GFP to produce two separate cytosolic fractions under normal conditions. During autophagy LC3B-I is lipidated, forming LC3B-II, and causes a gel mobility shift downward during SDS-PAGE (Fig. 1b).

Transfection of PC12 cells with our modified constructs results in the overexpression of tdTom:LC3B:eGFP and the Rabs. Western blotting for LC3B, GFP, Myc-Rab5, Rab22, and actin confirms their expression in the cell (Fig. 2). Meanwhile, transfection of these cells under serum starvation allows for visualization of tdTom-LC3B-II-labeled autophagosome production via fluorescence microscopy (Fig. 3a).

Autophagy with this reporter is calculated by the percent cells that demonstrate a loss of GFP fluorescence and the production of ten or more tdTom-positive punctate autophagosomes,
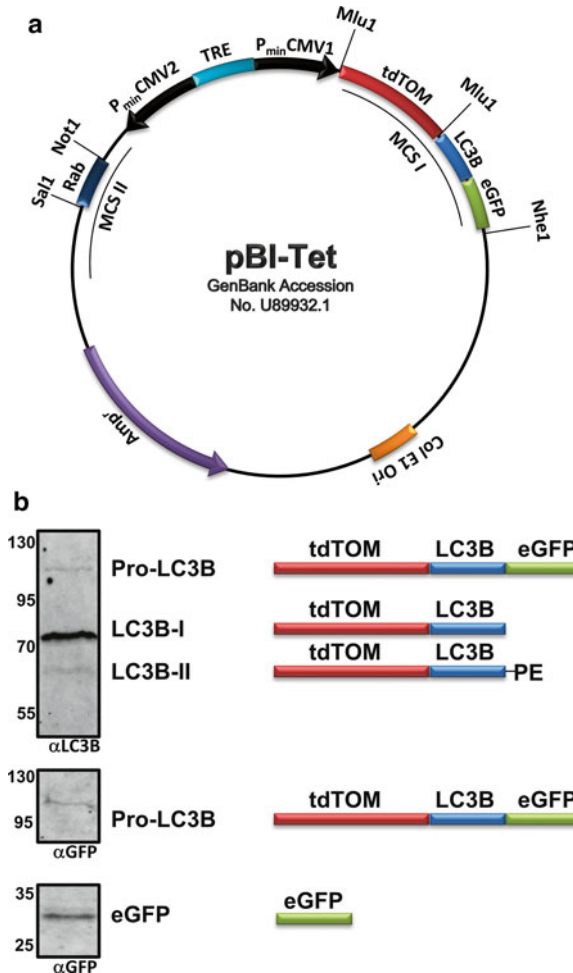
Fig. 1 pBI/LC3B/Rab constructs and protein expression. (**a**) Schematic illustration of the plasmid constructs. The tdTom:LC3B:eGFP cassette was inserted into the MCSI in the pBI-Tet plasmid. Each of the Rab cDNAs was cloned into the MCSII allowing for coexpression of the tdTom:LC3B:eGFP fusion protein and the Rab GTPase. (**b**) Western blot analysis of protein expression. The full-length tdTom:LC3B:eGFP is the pro-LC3B analog. Once cleaved by ATG4 at a Gly residue close to the C-terminus it becomes LC3B-I. Upon addition of Phosphatidylethanolamine (PE) by the ubiquitin-like ATG3-ATG14-ATG8 cascade, LC3B-I is converted to LC3B-II, which exhibits faster mobility during SDS-PAGE and is seen as a distinct lower band. eGFP is detected as the cleavage product and as a part of the pro-LC3B band

compared to total transfected cells. By using multiple conditions (e.g., serum free media with or without NGF) and overexpression of wild-type (WT) or a dominant-negative (SN) Rab mutant, one can quantify the effects of Rab overexpression on autophagy progression (Fig. 3b).
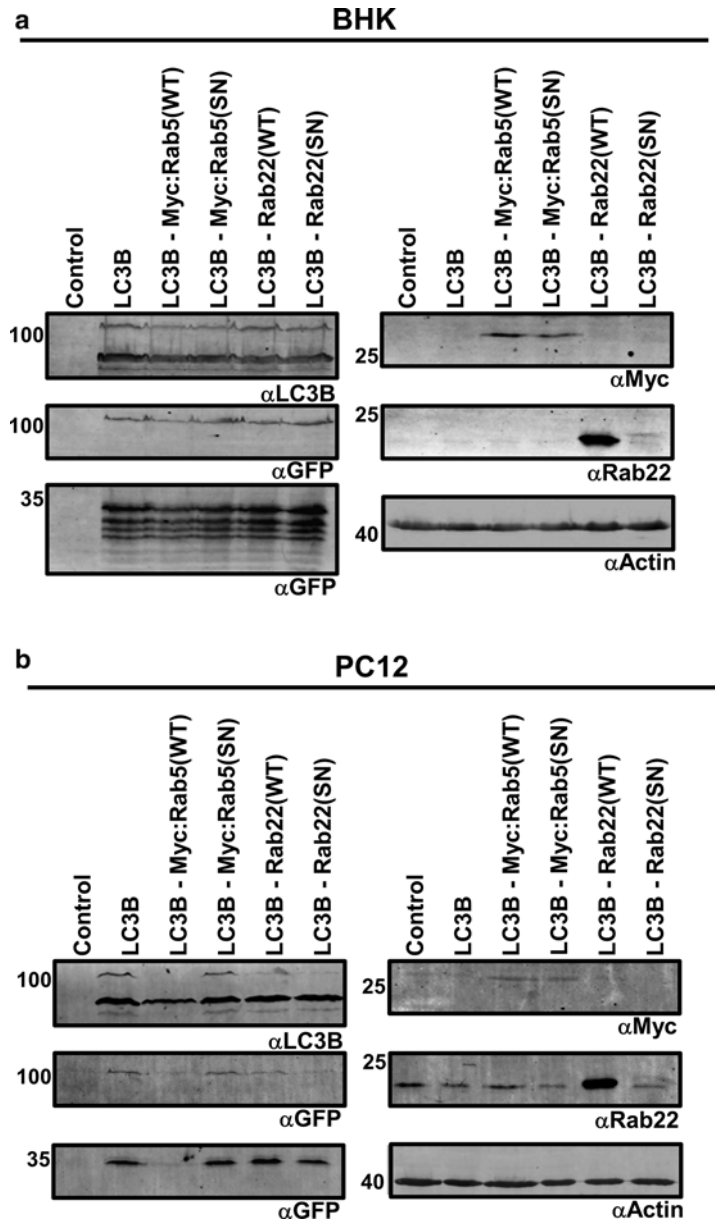
Fig. 2 Overexpression in BHK and PC12 cells. All tdTOM:LC3B:eGFP constructs, as indicated, were transfected into BHK cells (**a**) and PC12 cells (**b**) for 24 h, and the cells were recovered in full growth media for an additional 24 h (PC12 cells only) before harvesting for SDS-PAGE and Western Blot. Samples were probed with antibodies for LC3B, eGFP, Myc, Rab22, and Actin as indicated. Note that the expression level of Rab22(SN) mutant is significantly lower than that of Rab22(WT)
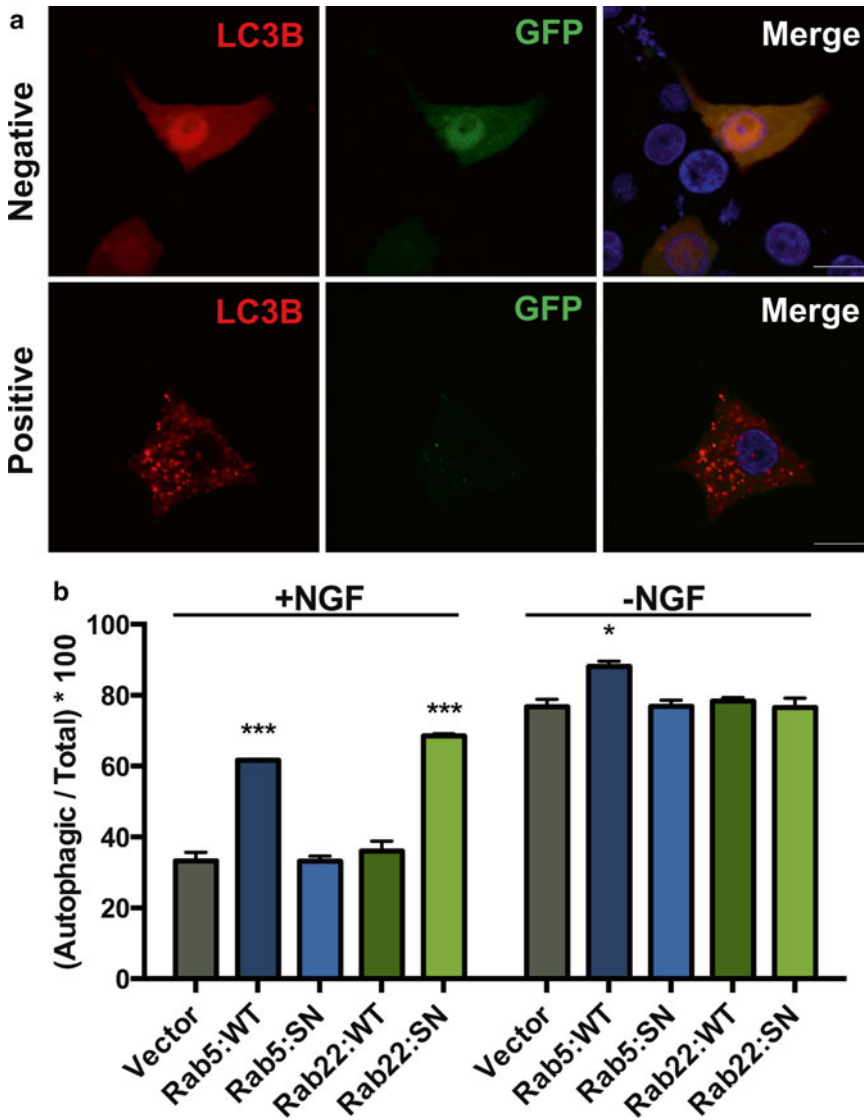
Fig. 3 Fluorescence microscopy and the autophagy assay in PC12 cells overexpressing Rab5 and Rab22 with or without NGF. PC12 cells on coverslips were transfected for 24 h in 24-well plates and recovered in complete DMEM for an additional 24 h. Cells were then treated with serum-free DMEM supplemented with or without NGF for 24 h, followed by fixation and visualization by fluorescence microscopy (**a**). The number of autophagic cells was counted and expressed as the percentage of total transfected cells. Autophagic cells are defined as cells containing greater than ten red fluorescent punctate autophagosomes along with the loss of green fluorescence. Greater than 100 cells were counted per condition (**b**)

2   Materials

2.1   Cell Culture/Transfection

1. Tet-Off PC12 cells and BHK-21 cells.
2. Complete-DMEM: Dulbecco's Modified Eagle's Medium, 10 % horse serum, 5 % FBS, glutamine, and penicillin/streptomycin.
3. Lipofectamine-2000 (Invitrogen).
4. Poly-L-Lysine.
5. NGF.
6. 6-well and 24-well Plates.

2.2   Expression Plasmids

1. pBI-Tet/tdTOM:LC3:eGFP.
2. pBI-Tet/tdTOM:LC3:eGFP/Rab5(WT).
3. pBI-Tet/tdTOM:LC3:eGFP/Rab5(S34N).
4. pBI-Tet/tdTOM:LC3:eGFP/Rab22(WT).
5. pBI-Tet/tdTOM:LC3:eGFP/Rab22(S19N).

2.3   Antibodies

1. Rabbit anti-LC3B antibody.
2. Rabbit anti-GFP antibody.
3. Mouse anti-Myc monoclonal antibody.
4. Rabbit anti-Rab22 antibody.
5. Mouse anti-actin monoclonal antibody.
6. IRDye 800CW Goat anti-Mouse, LI-COR (#926-32210).
7. IRDye 680RD Goat anti-Rabbit, LI-COR (#926-68071).

2.4   Staining Material

1. Mount: ProLong Gold Antifade Reagent with DAPI (Invitrogen).
2. Glass slides: VWR Micro Slides, 25 × 75 mm 1.0 mm thick.
3. Coverslips: 12 Circular −1 (Fisher Scientific).
4. 16 % PFA: paraformaldehyde, 16 % Solution (Electron Microscope Sciences).
5. Fluorescence Microscope: Olympus, IX51 Inverted Microscope.

3   Methods

3.1   Plasmid Construction

1. MluI/NheI–LC3:eGFP and MluI/MluI–tdTOM cDNA fragments were inserted sequentially into Site I of the pBI vector and in the same reading frame.
2. NotI/SalI–Rab cDNAs were each inserted into Site II of a separate pBI vector.

3. A partial digestion product of tdTOM:LC3B:eGFP with MluI/NheI was transferred to the Site I of each pBI/Rab construct (*see* **Note 1**).

4. The resulting constructs have the tdTOM:LC3B:eGFP cassette in Site I and each candidate Rab cDNA in Site II of the pBI vector.

3.2 Cell Culture and Transfection

1. Maintain PC12 cell cultures in a 37 °C incubator with 10 % CO_2.

2. Place the desired number of coverslips in a 24-well dish. Add 500 μl of poly-L-lysine to coat the coverslips for >1 h at 37 °C (*see* **Note 2**).

3. Aspirate the poly-L-lysine solution and wash with sterile H_2O. Let dry for approximately 15 min (*see* **Note 3**).

4. Plate cells at approximately 70–80 % confluence in 400 μl of complete DMEM. Allow cells to adhere to the coverslips overnight.

5. In separate tubes, add 0.8 μg of DNA and 2 μl of Lipofectamine-2000 to 50 μl of room temperature serum-free DMEM, respectively, for every coverslip and incubate for 5 min (*see* **Note 4**).

6. Add the full 50 μl of lipofectamine-2000/DMEM mix dropwise into the 50 μl of DNA/DMEM solution. Let stand for 20 min (*see* **Note 5**).

7. Add the full 100 μl DNA/Lipofectamine/DMEM solution dropwise into the 24-well dish with cells on coverslips. Gently swirl the media. Incubate for 24 h.

8. Check for expression under a fluorescent microscope. Replace the media with complete-DMEM for 24 h for recovery (*see* **Note 6**).

9. Aspirate the complete-DMEM recovery media and add serum-free DMEM supplemented with or without 100 ng/ml NGF for 24 h.

3.3 Fixing/ Mounting Cells

1. In the 24-well plate, aspirate the media and wash coverslips with 1 ml of 37 °C PBS.

2. Fix cells on coverslips in fresh 4 % PFA at 37 °C for 15 min (400 μl per coverslip).

3. Aspirate and wash in room temperature with PBS three times (*see* **Note 7**).

4. Remove coverslips and lay *cell-up* on a kimwipe, dabbing excess liquid. Place 15 μl of Prolong-gold with DAPI onto the cells and place the coverslip cell-down onto the slide (*see* **Note 8**).

5. Let set overnight at room temperature in the dark. Image the next day.

3.4 Autophagy Assay	1. Transfect cells on coverslips in triplicate in a 24-well dish as outlined earlier (*see* **Note 9**).
	2. Upon fixing and mounting, label slides in order to image cells in a blind manner (*see* **Note 10**).
	3. Using a fluorescent microscope, count greater than 100 cells per condition (*see* **Note 11**).
	4. The percent of autophagic cells per total fluorescent cells observed will be reported (*see* **Note 12**).
3.5 Western Blot for Protein Expression	1. Transfect PC12 cells at 80 % confluence in 6-well dishes in a similar manner found in Subheading 3.2 (*see* **Note 13**).
	2. Lyse and collect 2 wells of each condition in 150 μl SDS-PAGE loading buffer.
	3. Run samples on a 12 % acrylamide gel.
	4. Stain for LC3B, GFP, Rab22, Myc, and Actin with specific antibodies.

4   Notes

1. *Partial digest*: The tdTomato sequence is flanked by MluI sites while the LC3B:eGFP construct is flanked by MluI and NheI in the pBI vector. There is a SalI site within the linker region between LC3B and eGFP, therefore the NotI/SalI Rab fragment must be cloned into Site II first. In order to digest and purify the tdTOM:LC3B:eGFP cassette, it is partially digested by MluI and NheI. A short digest of 5–15 min at 37 °C should yield bands that include the fully digested tdTOM and LC3B:eGFP as well as the partially digested large full-length band consisting of tdTOM:LC3B:eGFP (~2 kb). Excise the full-length band and purify it.

2. *Reusing poly-L-lysine*: The Ploy-L-Lysine solution used in coating the coverslips may be reused as long as care is taken to insure sterility. Maintain a working stock at 4 °C in the dark.

3. *Keeping coverslips down*: The coverslips often float in the Poly-L-Lysine solution during the coating process. It has been an advantage to add the solution with the plate at a 45° angle to the bench, and slowly dispense the liquid at the bottommost point, where the coverslip and well wall meet. Once all wells have liquid added in them, then you can lay the plate flat and the solution will cover the coverslip and the coverslip should remain in the liquid.

4. *Mixing lipofectamine-2000*: It is advantageous to calculate and prepare a master mix of the lipofectamine/DMEM mix to add to all of the DNA/DMEM solutions. For example, if you are

making ten coverslips, add the DNA to DMEM into ten separate tubes. Multiply both the lipofectamine and the DMEM by ten and make a large mix. From this master mix, after the 5 min incubation, you can add 50 μl of the Lipofectamine-2000/DMEM mix to each DNA/DMEM mix in a dropwise manner.

5. *Dropwise addition of DMEM-lipofectamine*: Per the manufacture's suggestion, add the lipofectamine/DMEM mix in a dropwise manner into the DNA/DMEM mixture (not vice versa). This facilitates the formation of the liposome/micelle complexes containing the DNA.

6. *Recovering the cells*: Lipofectamine-2000 has cytotoxic effect on PC12 cells and increases basal autophagy in our system based upon preliminary experiments. Recovering the cells for 24 h in complete DMEM decreases the effect of Lipofectamin-2000 toxicity.

7. *Washing off PFA*: PFA can quench fluorescence if left on the sample for too long. Our suggestion is three washes in PBS, which should adequately remove PFA. Also, samples can be left at 4 °C in PBS at this point and is a good stopping point if needed.

8. *Placing coverslips on slides*: Add the Prolong-Gold along one end of the coverslip. Lower a slide to meet the solution of the coverslip and allow the Prolong-Gold mounting solution to cover the entirety of the coverslip as the slide lowers. Using the forceps, push out any bubbles in between the coverslip and slide and remove excess mounting solution around the edge of the coverslip by vacuum.

9. *Triplicate experiments*: Triplicate samples increase the ability to get meaningful statistics. All three of the coverslips for one condition can fit onto the same slide. As in **Note 8**, lay out all three coverslips, add prolong-gold, and mount all three onto one slide.

10. *Labeling cells*: Making a random name for each sample is important for counting cells in an unbiased way. By using a lab mate, make a key that designates each sample with an unspecified name in a random order and relabel each slide accordingly. For example, the slide containing the controls is renamed *1D* and the slide containing Rab5:WT overexpression samples is labeled *3F*. After counting, the lab mate can disclose the key.

11. *Counting cells*: Autophagic cells will exhibit a decrease in cytosolic GFP fluorescence and present ten or more red punctate, or autophagosomes labeled by tdTomato-LC3B-II. While counting, you will switch between the green and red channels in order to visualize the extent of autophagy. Autophagic cells must meet both conditions, loss of green and red punctate.

If only one condition is met, it is not considered autophagic. Also, occasionally green fluorescence is observed within the red, LC3B positive, punctate autophagosomes. This is acceptable, as long as overall cytosolic green fluorescence is greatly reduced.

12. *Graphing the autophagy assay*: For triplicate experiments, the average of each condition and the standard error of the mean are reported. For Fig. 3 graph, we used Prism 7 and included the average, standard error of the mean, and the number of samples per condition. With the data, Student's *t*-test calculated the statistical difference of each condition compared to control.

13. *Transfecting BHK*: PC12 cells have a low transfection efficiency, therefore it is advantageous to use a more easily transfected cell line to validate overexpression. To that end, we transected BHK cells in a similar manner to that performed in PC12 cells, with only minor modification. Only 1 well of a 6-well plate was used and only half the amount of lipofectamine-2000 was needed (1 μl instead of 2 μl). Also, because this cell line is not tetracycline regulatable, we cotransfected with the regulatory pTet-Off vector (0.4 ng of DNA for pTet-Off and 0.4 ng of DNA for the pBI constructs).

Acknowledgment

References

1. Mizushima N (2007) Autophagy: process and function. Genes Dev 21:2861–2873

2. Lee J-A (2012) Neuronal autophagy: a housekeeper or a fighter in neuronal cell survival? Exp Neurobiol 21:1–8

3. Huang EJ, Reichardt LF (2003) Trk receptors: roles in neuronal signal transduction. Annu Rev Biochem 72:609–642

4. Hosokawa N, Hara T, Kaizuka T, Kishi C, Takamura A, Miura Y, Iemura S, Natsume T, Takehana K, Yamada N, Guan JL, Oshiro N, Mizushima N (2009) Nutrient-dependent mTORC1 association with the ULK1-Atg13-FIP200 complex required for autophagy. Mol Biol Cell 20:1981–1991

5. Chua C, Gan B, Tang B (2011) Involvement of members of the Rab family and related small GTPases in autophagosome formation and maturation. Cell Mol Life Sci 68:3349–3358

6. Wang L, Liang Z, Li G (2011) Rab22 controls NGF signaling and neurite outgrowth in PC12 cells. Mol Biol Cell 22:3853–3860

7. Sheen JH, Zoncu R, Kim D, Sabatini DM (2011) Defective regulation of autophagy upon leucine deprivation reveals a targetable liability of human melanoma cells. Cancer Cell 19:613–628

Chapter 26

Determining the Role of Rab7 in Constitutive and Ligand-Mediated Epidermal Growth Factor Receptor Endocytic Trafficking Using Single Cell Assays

Brian P. Ceresa

Abstract

RAB proteins are essential for the proper membrane trafficking of a number of proteins. Each of the 60+ RABs that have been identified has a discrete role in coordinating the movement from one subcellular compartment to another. Early attempts at deciphering the roles of individual RAB proteins relied heavily on the use of activating and/or dominant negative mutants (Ceresa, Histol Histopathol 21:987–993, 2006). However, overexpression of mutant proteins can lead to misleading information; high levels of expression can drive low affinity (and possibly, nonphysiological) interactions as well as cause mislocalization. The use of RNAi for transient protein knock down will reveal which membrane trafficking steps absolutely require the attenuated RAB. When determining the role of RAB protein in epidermal growth factor receptor (EGFR) membrane trafficking, there are special considerations. The EGFR undergoes constitutive and ligand-mediated endocytic trafficking. Both affect receptor signaling, but via different mechanisms. Here, we discuss how to experimentally dissect those two processes.

Key words siRNA, EGFR, Immunofluorescence, Membrane trafficking, RAB7

1 Introduction

The use of RNA interference (RNAi) has been of tremendous value for understanding the contribution of individual RAB proteins in EGFR membrane trafficking [1–3]. By targeting a specific RAB in an experiment, the exact endocytic stages that the RAB regulates can be identified. This method is more advantageous than previous techniques that relied on overexpression of constitutively active or dominant negative RAB mutants, as high levels of these mutants could have off-target effects.

Although many proteins traffic via the same endocytic pathway, receptor tyrosine kinases, like the EGFR, are unique in that their kinetics of trafficking changes in the presence of ligand. There is a slow, but constant, rate of internalization of the unliganded receptor via clathrin-coated pits that subsequently traffic to the

early endosome. The receptors are sorted into recycling endosomes and delivered back to the cell surface [4]. Thus, in the absence of ligand, the steady-state distribution of the EGFR is primarily at the plasma membrane.

In the presence of a ligand, such as the epidermal growth factor (EGF), the ligand:receptor complex internalizes much more quickly and recycling to the plasma membrane is dramatically reduced [5]. As a result, the EGF:EGFR complexes progress from the early endosomes to late endosomes/multivesicular bodies (LE/MVB) during endosome maturation. Subsequently, receptors move from the limiting membrane of the endosome into the intraluminal vesicles. LE/MVBs fuse with lysosomes to transfer the contents where the ligand and receptor are degraded. Under conditions of ligand stimulation, there is a detectable loss of receptors from the plasma membrane and the concomitant appearance of those receptors at some point in the endocytic pathway at early time points, and receptor degradation with longer time points. With these thoughts in mind, to fully understand the role of a RAB protein in EGFR trafficking, or any receptor whose kinetics of trafficking is altered in the presence of ligand, one must study both constitutive and ligand-dependent endocytic trafficking.

2   Materials

2.1   Cells and Cell Culture Reagents

1. HeLa cells are human cervical adenocarcinoma cells (American Type Culture Collection).
2. Dulbecco's Minimal Essential media (DMEM).
3. Growth media: Dulbecco's Minimal Essential media (DMEM) supplemented with 5 % Fetal Bovine Serum, 100 units/ml penicillin, 100 units/ml streptomycin, and 2 mM glutamine.

2.2   RNAi

1. A previously validated pool of four siRNAs that targets RAB7 (Dharmacon) was used for these experiments. Control siRNA ("siCon") was used to ensure any differences seen are not "off target" effects or a consequence of the transfection procedure. Validated control siRNA duplexes are commercially available (Integrated DNA Technology, DS Scrambled Negative). siRNA is reconstituted at 20 mM stocks and stored as 5 µl aliquots at –80 °C. Once an aliquot is thawed, any remaining siRNA is discarded.

2.3   Transfection Reagent

1. Transient, liposome-based transfection reagent is an inexpensive, efficient, and reliable means of transfecting cells with siRNA. Pulsin® (Polyplus) is commercially available from a number of distributors. Using HeLa cells and RAB7 siRNA, transfection efficiency is greater than 95 %.

2.4   Antibodies

1. Validation of RAB7 knock down can be done easily with immunoblots. The RAB7 antibody from Sigma generates clear blots, with no nonspecific bands. The extent of RAB7 knock down can be calculated as a function of RAB7 expression in control (siCon transfected) versus RAB7 siRNA-transfected HeLa cells.

2. Ab-1 (Calbiochem) is a mouse monoclonal antibody that specifically targets the extracellular domain of the EGFR. Ab-1 binds the ligand-binding domain of the EGFR, but does not stimulate kinase activity, making it an excellent reagent for studying the trafficking of the unliganded receptor [6] (*see* **Note 1**).

3. Antibodies that target endocytic compartments are critical for identifying the subcellular localization of the EGFR following constitutive and ligand-mediated endocytosis. Early Endosome Autoantigen 1 (EEA1) characterizes the early endosome and there are excellent mono- and polyclonal antibodies commercially available (Cell Signaling, BD Biosciences). The late endosome can be identified by the presence of Lysosomal-Associated Membrane Proteins 1 and 2 (LAMP1 and LAMP2), which, despite its name, shuttles between late endosomes and lysosomes. LAMP1 and LAMP2 mono- and polyclonal antibodies can be purchased through a variety of sources (Cell Signaling, BD Biosciences, and The University of Iowa Hybridoma Bank).

NaOH-Washed Coverslips

1. Plating cells on coverslips facilitates fluorescence analysis and testing multiple conditions and time points. Pretreatment of the coverslips with NaOH helps the cells adhere to the coverslips through multiple washing steps. To NaOH-treat coverslips, soak 12 mm thickness #1 coverslips (Bellco Glass) in 50 ml of 2 M NaOH in a 100 ml beaker for 30 min, stirring occasionally with a glass, stirring rod. Transfer coverslips to a 100 ml beaker with 50 ml ddH$_2$O, and rinse three times with ddH$_2$O. Place monolayers of coverslips in a glass petri dish using 3MM chromatography paper (Whatman) to separate layers. Autoclave the coverslips for 25 min. Standard glass microscope slides are used to mount coverslips.

2.5   Monitoring Ligand-Mediated Receptor Trafficking

1. Alexa 488 EGF (Invitrogen): store as a 50 μg/ml stock in DMEM, use at 4 ng/ml (dilute immediately before using).

2. PBS pH 7.4. PBS^{++++}: 0.5 mM MgCl$_2$, 0.5 mM CaCl$_2$, 0.2 % BSA, 5 mM glucose, PBS pH 7.4.

3. PBS^{++}: 0.5 mM MgCl$_2$, 0.5 mM CaCl$_2$, PBS pH 7.4.

4. Citrate Buffer: 25.5 mM Citric Acid, 24.5 mM Sodium Citrate, 280 mM Sucrose, pH 4.6. Make immediately before using.

5. 4 % paraformaldehyde, diluted from 16 % stock immediately before using.

6. 1 % saponin (10 mg/ml) made fresh daily.

7. Blocking buffer: 5 % Fetal bovine serum, 0.01 % saponin, 0.5 mM $MgCl_2$, 0.5 mM $CaCl_2$/PBS pH 7.4 made fresh daily.

8. Slidewarmer that warms to 37 °C.

9. Mounting media (i.e., Prolong® with or without Dapi, Invitrogen) that preserves and stabilizes the sample.

3   Methods

3.1   siRNA-Mediated Transfection

1. Plate HeLa cells at 600,000 cells in a 60 mm tissue culture dish in growth media (*see* **Note 2**).

2. After 24 h of growth, when the cells become approximately 50–60 % confluent, transfect the cells with the RAB7 siRNA or the control siRNA (siCon), as described by the manufacturer's protocol. For each dish of cells, add 2.5 μl of 20 μM siRNA stock to 22.5 μl of DMEM to dilute the siRNA to 2 μM. Mix 22 μl of 2 μM siRNA with 400 μl of DMEM and vortex well. Add 18 μl of Pulsin®, vortex and incubate at room temperature for 10 min. During that time, replace the media on the cells plated the day before with 4.0 ml of fresh growth media (37 °C). Add the siRNA/DMEM/Pulsin mixture dropwise to the dish of cells with constant rotation and mixing. The final siRNA concentration of this solution is 10 nM (*see* **Note 3**).

3. After 24 h of incubation, replate the cells for subsequent experiments. For the experiments described below, cells should be plated on NaOH-washed coverslips in each well of 24-well dishes (~50,000 cells/well), with at least two coverslips for each time point (*see* **Note 4**). Cells can also be plated in 35 mm dishes (200,000 cells/35 mm dish) for biochemical analysis such as radioligand binding or receptor degradation/activity assays. At a minimum, an additional 35 mm dish should be replated for immunoblot analysis of protein knock down (*see* **Notes 5** and **6**).

3.2   Determining Changes in the Steady-State EGFR Distribution

Many times when examining EGFR membrane trafficking, the focus is on the ligand-stimulated movement of the receptor through the endocytic pathway; the constitutive recycling, which shares much of the same endocytic machinery, is overlooked. Since full RAB7 knock down requires 72 h of siRNA incubation, the constitutive RAB7-dependent receptor trafficking is blocked to an increased extent over time. Accounting for the constitutive trafficking of the EGFR not only helps in understanding RAB7's

function, but also in interpreting ligand-stimulated endocytosis assays by allowing the investigator to account for decreases in cell surface EGFR expression. Using immunofluorescence to assess EGFR subcellular localization is the most efficient way to determine if a redistribution has occurred.

1. Seventy-two hours after introducing the siRNA, wash coverslips two times with ice cold PBS++++, and fix the cells in freshly made 4 % p-formaldehyde in PBS++. Incubate for 5 min at room temperature and an additional 15 min on ice.

2. Wash three times with PBS++ for 5 min (*see* **Note 7**). At this point, the coverslips can be stored in PBS++ at 4 °C for up to a week before progressing further.

3. To each well, add 500 µl of blocking buffer for 15 min at room temperature to permeabilize the cells. Wash three times with PBS++ for 5 min each time.

4. Incubate the coverslips with the mouse monoclonal EGFR antibody, Ab-1 and appropriate rabbit mono- or polyclonal antibodies for the endosomal markers, by diluting the antibodies appropriately (usually 1:500 to 1:2,500) in blocking buffer and centrifuging the solution for 5 min at ~20,000×*g* at room temperature to pellet any protein precipitates. Place 35 µl drops of the primary antibody on parafilm and place coverslips on top cell side down for 1 h at room temperature (*see* Fig. 4b).

5. Return coverslips (cell side up) to the 24-well dish with PBS++ and remove unbound antibody with 3×5 min washes in PBS++.

6. Prepare the Alexa 488-conjugated goat anti-mouse and Alexa 586-conjugated goat anti-rabbit secondary antibodies at a 1:250 dilution in blocking buffer. Centrifuge for 5 min at ~20,000×*g* at room temperature. Place 35 µl drops of the secondary antibody mixture on parafilm and place coverslips on top cell side down for 1 h at room temperature.

7. Return coverslips (cell side up) to the 24-well dish with PBS++ and remove unbound secondary antibody with six washes for 10 min each in PBS++.

8. Mount coverslips onto a slide by individually picking up the coverslip and dipping them into a beaker with ddH$_2$O to remove salts that may crystallize after mounting. Carefully touch the coverslip to a Kimwipe to remove excess fluid, and place cell side down on a ~7 µl drop of Prolong antifade on a standard microscope slide. With careful placement, four coverslips can be placed on each slide. Let the coverslips set for at least 16 h before viewing under a microscope (Fig. 1). For longer storage, keep at 4 °C.

9. Image cells under a fluorescence microscope.
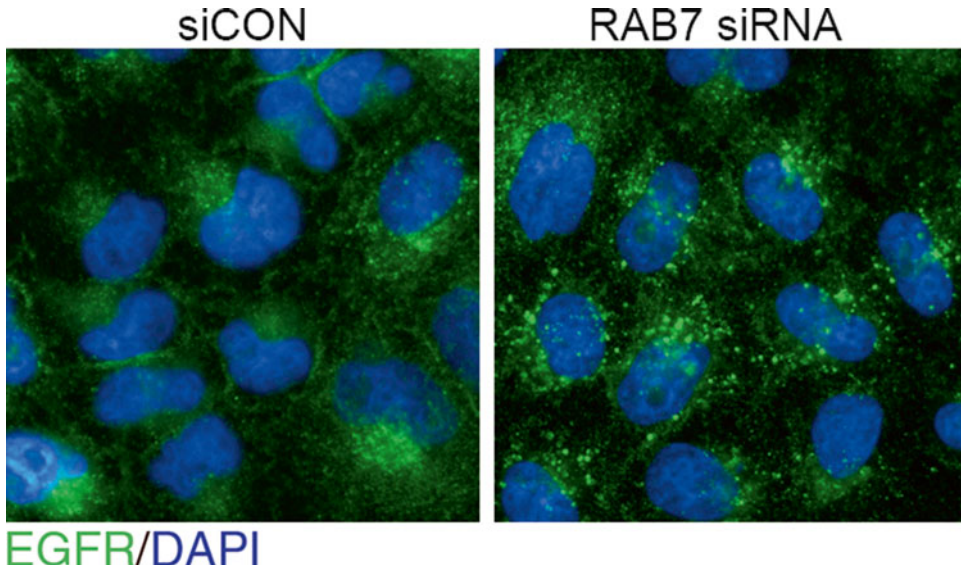
Fig. 1 Knock down of RAB7 alters the steady-state distribution of the EGFR. HeLa cells were transfected with either control (siCON) or RAB7-specific siRNA and incubated for 72 h in growth media. Cells were fixed and immunoblotted with an antibody against the EGFR (in *green*). Nuclei are stained with DAPI (*blue*)

3.3   Monitoring the Rate of Unliganded EGFR Endocytosis

This approach takes advantage of a commercially available antibody (Ab-1) that targets the EGFR and blocks ligand binding [6]. The high affinity antibody:receptor interaction will track the constitutively internalized EGFR and can easily be visualized using standard immunofluorescence techniques.

1. After cells have been replated on coverslips in 24-well dishes and been given sufficient time to settle down (~8 h, but this should be readily apparent by checking under the microscope), cells are incubated with 250 μl/well of a 1 μg/ml dilution of the mouse monoclonal antibody Ab-1 for an additional 48 h.

2. After 48 h of incubating the cells with the antibody, the protocol is similar to what is described earlier. Wash coverslips two times with ice cold PBS++, and fix the cells in 4 % p-formaldehyde in PBS++ (diluted from 16 % p-formaldehyde stock, immediately before using). Incubate for 5 min at room temperature and an additional 15 min on ice.

3. Wash three times with PBS++ for 5 min.

4. Permeabilize in 500 μl/well of blocking buffer for 15 min at room temp. Wash three times with PBS++ for 5 min.

5. Incubate the coverslips with primary rabbit mono- or polyclonal antibody for the endosomal marker (EEA1 or LAMP1/2), by diluting the antibody appropriately (usually 1:500 to 1:2,500) in blocking buffer and centrifuging the solution for 5 min at ~20,000×*g* at room temperature. Place 35 μl drops of the

primary antibody on parafilm and place coverslips on top cell side down for 1 h at room temperature (Fig. 4b).

6. Return coverslips (cell side up) to the 24-well dish with PBS++ and remove unbound antibody with 3×5 min washes in PBS++.

7. Prepare the Alexa 488-conjugated goat anti-mouse (to target the Ab-1) and Alexa 586-conjugated goat anti-rabbit (to target EEA1/LAMP1/2) secondary antibodies at a 1:250 dilution in blocking buffer. Centrifuge for 5 min at ~20,000 × g at room temperature to pellet protein precipitates. Place 35 µl drops of the primary antibody on parafilm and place coverslips on top cell side down for 1 h at room temperature.

8. Return coverslips (cell side up) to the 24-well dish with PBS++ and remove unbound secondary antibody with six washes for 10 min each in PBS++.

9. Mount coverslips onto a microscope slide by individually picking up the coverslip, dipping them into a beaker with ddH₂O, carefully blot dry on a Kimwipe, and place, cell side down, on a ~7 µl drop of Prolong. Allow the coverslip to cure overnight before imaging. Keep at 4 °C for long-term storage.

10. Image cells under a fluorescent microscope (Fig. 2).

3.4 Determine the Trafficking of Liganded Cell Surface EGFRs

Texas Red EGF (TxRed EGF) tracking of the EGFR is a great method for monitoring the movement of liganded receptors from the cell surface through the endocytic pathway in individual cells. By incubating cells with this fluorescent ligand for various
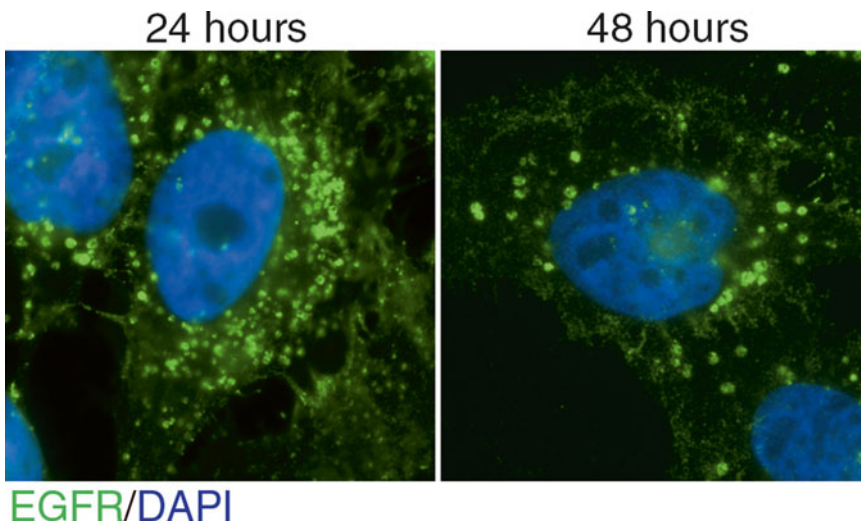
Fig. 2 Knock down of RAB7 prevents constitutive EGFR recycling. HeLa cells were transfected with either control (siCON) or RAB7-specific siRNA. After 24 h of recovery in growth media, cells were replated on coverslips and incubated with the anti-EGFR antibody (Ab-1) for an additional 24 or 48 h, as indicated. Cells were fixed, permeabilized, and incubated with an Alexa488 goat anti-mouse secondary antibody to localize the Ab-1 (*green*). Nuclei are stained with DAPI (*blue*)

amounts of time and costaining with endosomal markers, this strategy provides a quick and relatively easy estimation of the kinetics of the ligand:receptor complex's movements through the endocytic pathway.

1. Serum starve siRNA-transfected HeLa cells for 3 h by washing two times with PBS pH 7.4 and adding 500 μl DMEM (37 °C) to each well.

2. Incubate cells with Tx-Red EGF (4 ng/ml) that has been freshly diluted from a 50 μg/ml Tx-Red EGF stock (*see* **Note 8**). Place 35 μl drop of ligand on a piece of parafilm on a slide-warmer set to 37 °C. Place each coverslip on the fluorescent ligand drop, cell side down, and incubate 10 min at 37 °C.

3. Wash away free and cell surface Tx-Red EGF by transferring each coverslip (cell side up) to a 24-well dish on ice containing PBS pH 7.4. Continue to wash two times with ice cold PBS^{++++}, three times with ice cold citrate buffer, and reequilibrate to buffered conditions with two washes with ice cold PBS^{++++}. These washes do not require prolonged incubation; 15–30 s is enough. This procedure administers a "pulse" of Tx-Red EGF to the cell.

4. Chase the labeled EGF by incubating the cells in 37 °C DMEM (without EGF) for 0, 20, 50, 110, and 170 min, giving total incubation times of 10, 30, 60, 120, and 180 min. For HeLa cells, these time points reflect different stages of endocytic trafficking.

5. At each time point, wash coverslips two times with ice cold PBS^{++++}, and fix the cells in freshly dluted 4 % p-formaldehyde in PBS^{++}. Incubate for 5 min at room temperature and an additional 15 min on ice.

6. Wash three times with PBS^{++} for 5 min each. At this point, the coverslips can be stored in PBS^{++} at 4 °C for up to 1 week before progressing further.

7. Permeabilize the cells in 500 μl blocking buffer for 15 min at room temperature. Wash three times with PBS^{++} for 5 min each time.

8. Incubate the coverslips with primary antibody for the endosomal markers, by diluting the antibody appropriately (usually 1:500 to 1:2,500) in 500 μl blocking buffer and centrifuging the solution for 5 min at ~20,000 × g at room temperature. Place 35 μl drops of the primary antibody mixture on parafilm and place coverslips on top cell side down for 1 h at room temperature.

9. Return coverslips (cell side up) to the 24-well dish with PBS^{++} and remove unbound antibody with three 5 min washes in PBS^{++}.

10. Prepare the Alexa 488 secondary antibody at a 1:250 dilution in 500 µl blocking buffer. Centrifuge for 5 min at ~20,000×g at room temperature. Place 35 µl drops of the secondary antibody mixture on parafilm and place coverslips on top cell side down for 1 h at room temperature.

11. Return coverslips (cell side up) to the 24-well dish with PBS^{++} and remove unbound secondary antibody with six washes for 10 min each in PBS^{++}.

12. Mount coverslips on a slide by individually picking up the coverslip, dipping them into a beaker with ddH$_2$O, carefully blot dry on a Kimwipe, and place, cell side down, on a ~7 µl drop of Prolong. Allow the coverslip to cure overnight before imaging. Keep at 4 °C for long-term storage.

13. Image cells under a fluorescence microscope. By monitoring the colocalization of the Tx-Red EGF and the Alexa488 labeled endosomes, one can determine how the ligand:receptor complex traverses endocytic compartments (Fig. 3) (*see* **Notes 9** and **10**).

4   Notes

1. A number of commercially available EGFR antibodies exist. However, all do not function the same. Ab-1 is specifically used because it is excellent for immunofluorescence and it competes with ligand for binding to the EGFR [6, 9]. Using another amino terminal antibody that permits ligand binding may be problematic in interpreting data from constitutively internalized receptors.

2. HeLa cells are notorious for their heterogeneity, and certain "strains" may have subtly different growth properties, such as transfection or transduction efficiencies, etc. Therefore, the specific cell densities and plating conditions may need slight modification depending on which HeLa cells are being used.

3. An alternative approach to siRNA is to transfect plasmids encoding short hairpin RNA (shRNA). This would be more beneficial if stable cell lines were being created, although the use of an inducible construct (i.e., pSLIK—[7]) is highly recommended, as constitutive RAB7 knock down is likely to inhibit cell viability. Previously validated shRNA sequences can be found at www.codex.cshl.edu that will aid in rational plasmid design.

   Transfection of shRNA plasmids is performed like other gene transfers. The methodology will be largely dependent on the cell type, but these can range from liposomes to nucleofection to lentiviruses. Since these transfection techniques are not 100 % efficient, there may be an extra step to enrich in
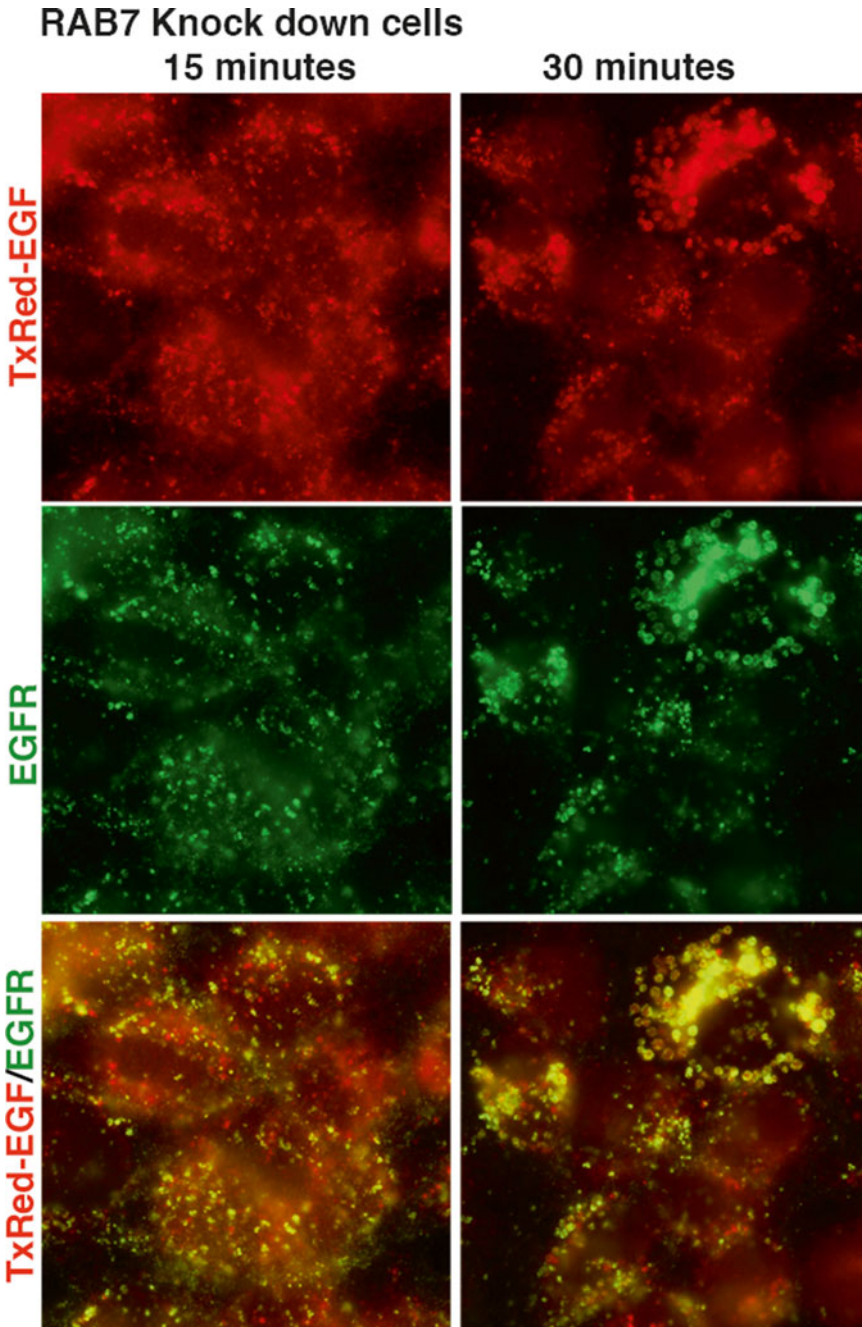
Fig. 3 EGFRs accumulate in endosomes when constitutive recycling has been blocked by RAB7 knock down. HeLa cells were transfected with RAB7-specific siRNA. After 24 h of recovery in growth media, cells were replated on coverslips and incubated with the anti-EGFR antibody (Ab-1) for an additional 48 h to mark preexisting EGFR-containing endosomes. Cells were incubated with TxRed-EGF for 15 or 30 min, as described in the text. Cells were fixed, permeabilized, and incubated with an Alexa488 goat anti-mouse secondary antibody to localize the Ab-1. Note at 15 min, there is little overlap of TxRed-EGF (*red*) and the EGFR (*green*); however, it is almost complete at the 30 min time point
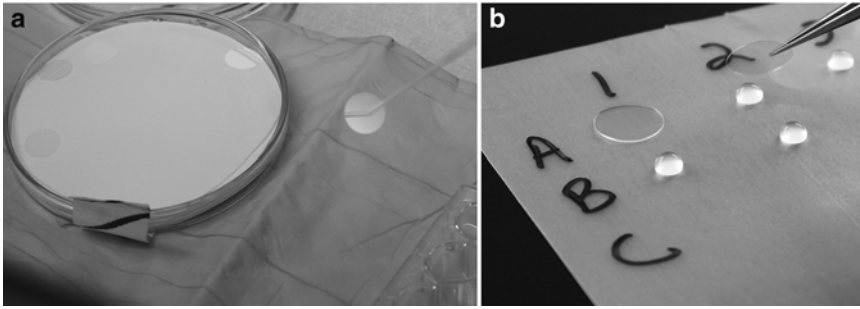
Fig. 4 Coverslip transfer. (**a**) Transfer of autoclaved, NaOH-treated coverslips from petri dish to the 24-well dish is facilitated by using a glass pipette attached to a vacuum line. This can only be done before the cells are plated onto the coverslip. (**b**) To minimize the amount of antibody used, 35 µl drops of antibody solution are placed on a labeled piece of parafilm. Coverslips are placed on top cell side down. Coverslips are typically incubated for 1 h at room temperature, before being carefully returned to a 24-well dish for washing

transfected cells, such as neomycin selection or FACS to enrich for cells with a coexpressed fluorescent protein.

4. Using a glass disposable glass pipette attached to a vacuum line is an easy way to transfer coverslips from the petri dishes to the 24-well dishes, before cells are plated on them (Fig. 4a).

5. Before any experimentation takes place, it is wise to verify the transfection technique and protein knock down. The investigator should perform a time course of protein knock down by harvesting cells at 24-h intervals, resolving equivalent amount of cell lysate by 10 % SDS-PAGE, and probing for RAB7 expression by immunoblot.

    An alternative approach to monitor gene silencing is to measure mRNA levels of the gene of interest. This may be useful when sample is in limited supply or there is no antibody available. However, it is important to keep in mind that only changes in protein levels will impact cell biology, so it is advisable to use a system that allows protein analysis.

6. It is important to get an accurate measure of RAB7 knock down. A useful technique to assess RAB7 knock down has been to run a SDS-PAGE gel with multiple protein concentrations of control and knock down cell lysates and immunoblot for RAB7 expression. By making sure the control lysates clearly show concentration-dependent RAB7 expression, one can get an accurate measure of any changes in RAB7 levels.

7. When washing coverslips, 500 µl of fluid is sufficient to cover the cells, but more will not hurt the cells. Buffers should be added slowly to the side of the dish, instead of directly onto the coverslip. Gently tilting the 24-well plate before aspirating will also help prevent the cells from lifting off the plate.

In addition, using a vacuum flask with a glass pipette covered with a P200 pipette tip will minimize breaking the glass pipette and slow aspiration of the fluid. It is recommended that scientists that are new to this technique should periodically check the cells on the coverslips under a light microscope to make sure that there are not an appreciable number of cells being dislodged during washes.

8. The EGF concentration can impact the route of internalization. Lower concentrations of EGF are associated with clathrin-mediated endocytosis, whereas higher (>50 ng/ml) are associated with non-clathrin-mediated endocytosis [8]. Therefore, one should be certain that the concentration of TxRed-EGF being used reflects the route of endocytosis that is being studied.

9. When following the uptake and trafficking of Tx-Red EGF, it is important to recognize that the ligand, and not the receptor, is being monitored. While the ligand:receptor complex is initially internalized, in principle, it could become dissociated and only the fluorescently labeled ligand would be monitored.

10. The assays presented here are designed to examine membrane trafficking on a cell-by-cell basis. It is important to complement these experiments with biochemical assays that examine the entire population of cells. Examples of this include receptor degradation, phosphorylation, and activation of downstream effectors or the use of radioligands to monitor receptor trafficking. By replating siRNA-transfected cells into 35 mm dishes, this protocol can be readily adapted to the appropriate biochemical assays.

Acknowledgments

References

1. Ceresa BP (2006) Regulation of EGFR endocytic trafficking by rab proteins. Histol Histopathol 21(9):987–993

2. Rush JS, Ceresa BP (2013) RAB7 and TSG101 are required for the constitutive recycling of unliganded EGFRs via distinct mechanisms. Mol Cell Endocrinol 381(1–2):188–197. doi:10.1016/j.mce.2013.07.029

3. Vanlandingham PA, Ceresa BP (2009) Rab7 regulates late endocytic trafficking downstream of multivesicular body biogenesis and cargo sequestration. J Biol Chem 284(18): 12110–12124

4. Herbst JJ, Opresko LK, Walsh BJ, Lauffenburger DA, Wiley HS (1994) Regulation of postendocytic trafficking of the epidermal growth factor

receptor through endosomal retention. J Biol Chem 269(17):12865–12873

5. Masui H, Castro L, Mendelsohn J (1993) Consumption of EGF by A431 cells: evidence for receptor recycling. J Cell Biol 120(1): 85–93

6. Kawamoto T, Sato JD, Le A, Polikoff J, Sato GH, Mendelsohn J (1983) Growth stimulation of A431 cells by epidermal growth factor: identification of high-affinity receptors for epidermal growth factor by an anti-receptor monoclonal antibody. Proc Natl Acad Sci U S A 80(5): 1337–1341

7. Shin KJ, Wall EA, Zavzavadjian JR, Santat LA, Liu J, Hwang JI, Rebres R, Roach T, Seaman W, Simon MI, Fraser ID (2006) A single lentiviral vector platform for microRNA-based conditional RNA interference and coordinated transgene expression. Proc Natl Acad Sci U S A 103(37):13759–13764. doi:10.1073/pnas. 0606179103

8. Sigismund S, Woelk T, Puri C, Maspero E, Tacchetti C, Transidico P, DiFiore PP, Polo S (2005) Clathrin-independent endocytosis of ubiquinated cargos. Proc Natl Acad Sci U S A 102(8):2760–2765

9. Dinneen JL, Ceresa BP (2004) Constitutive activation of rab5 results in a ligand independent redistribution of the EGFR and attenuates its ability to signal. Traffic 5(8):606–615

Chapter 27

Visualizing Directional Rab7 and TrkA Cotrafficking in Axons by pTIRF Microscopy

Kai Zhang, Praveen D. Chowdary, and Bianxiao Cui

Abstract

Rab7 GTPase is known to regulate protein degradation and intracellular signaling via endocytic sorting and is also known to be involved in peripheral neurodegeneration. Mutations in the GTP-binding pocket of Rab7 cause Charcot–Marie–Tooth type 2B (CMT-2B) neuropathy. It has been suggested that the CMT-2B-associated Rab7 mutants may disrupt retrograde survival signaling by degrading the signaling endosomes carrying the nerve growth factor (NGF) and its TrkA receptor. Studying the cotrafficking of Rab7 and retrograde-TrkA endosomes in axons is therefore important to understand how Rab7 mutants affect the NGF signaling in neurons. However, tracking the axonal transport of Rab7 and TrkA with conventional microscopy and assigning the transport directionality in mass neuronal cultures pose some practical challenges. In this chapter, we describe the combination of a single-molecule imaging technique, pseudo-total internal reflection fluorescence (pTIRF) microscopy, with microfluidic neuron cultures that enables the simultaneous tracking of fluorescently labeled Rab7- and TrkA-containing endosomes in axons.

Key words Pseudo-total internal reflection fluorescence (pTIRF) microscopy, Charcot–Marie–Tooth type 2B (CMT-2B), Rab7, Nerve growth factor (NGF), TrkA, Endosomes, Axonal transport, Dorsal root ganglion (DRG), Polydimethylsiloxane (PDMS), Compartmentalized microfluidic chamber

1 Introduction

1.1 Functionality of Rab7 GTPase and Its Mutants in Neurodegeneration

The Rab protein family belongs to the Ras superfamily of small GTPases. Most Rabs are involved in membrane trafficking pathways and play important roles in regulating vesicle formation, actin- and tubulin-dependent vesicle movement, and membrane fusion [1]. Rab7 GTPase mediates protein degradation by sorting early endosomes to late endosomes and lysosomes along the endocytic pathway. Missense mutations in Rab7 cause Charcot–Marie–Tooth type 2B (CMT-2B) disease, a length-dependent axonal neuropathy [2, 3]. The CMT-2B phenotype suggests that Rab7 mutants may cause neuropathy by interrupting the survival signals carried by NGF/TrkA endosomes in motor and sensory neurons [4, 5]. Therefore, besides functioning as an endosomal marker, Rab7 could also affect the properties and the trafficking of endosomes that it is associated with [6].

The influence of Rab7 on endosomal trafficking in neurons can be more significant than in nonpolarized cell types, where substrates and machinery are readily accessible by diffusion. In neurons, where the axons typically extend beyond hundreds of microns in length, robust long-distance axonal transport is required for efficient communication between the axon terminals and the cell bodies. For instance, anterogradely transported TrkA (from the cell body to the terminal) is targeted to the plasma membrane of axon terminals for seeking out target-derived growth factors [7]; retrogradely transported TrkA (from the axon terminal to the cell body) may carry NGF-survival signals to regulate gene expression in the cell bodies [8]. Therefore, for a better understanding of how Rab7 affects retrograde NGF/TrkA trafficking in neurons, it is imperative to study the colocalization and cotrafficking of Rab7 with NGF/TrkA-signaling endosomes in axons along with the accurate assignment of the endosomal transport directionality (anterograde versus retrograde).

1.2 Resolving Directional Axonal Transport by Compartmentalized Microfluidic Chambers

The directionality of axonal cargo transport is difficult to be assigned in conventional mass neuronal culture, due to the limited imaging field provided by high-magnification objectives (100× or 60×) and the imaging-sensor dimensions. The typical imaging area of ~100 μm × 100 μm cannot cover the millimeter-long axons that randomly grow along all directions in a mass culture, thus making it difficult to assign the transport directionality. One way to solve this problem is to compartmentalize the neuronal culture by spatially segregating the axon terminals from the cell bodies. First introduced by Campenot and colleagues [9], compartmentalized microfluidic cell-culture chambers segregate the chemical environments of cell bodies and axons. However, early design of Campenot chambers, made of nontransparent Teflon, was laborious to implement and not compatible with high-resolution optical imaging. Recent advances in microfluidics led to transparent and biocompatible polydimethylsiloxane (PDMS) microfluidic chambers that are compatible with neuronal culture and optical imaging [8, 10]. Custom-designed compartmentalized PDMS microfluidic cell culture chambers are now commercially available.

1.3 Pseudo-TIRF Microscopy for Tracking Axonal Transport with High Temporal Resolution

The colocalization and cotrafficking of axonal cargoes containing fluorescently labeled Rab7 and NGF/TrkA can be studied by multicolor live cell imaging. Conventional multicolor epi-illumination microscopy, where alternating fluorescence channels are often acquired sequentially, is not synchronous and typically limited to slow acquisition rates (~1 fps for two color imaging) due to the mechanical switching time of different filter cubes and weak signals. Such slow frame rates make it challenging to capture fast axonal transport, given the average speed of axonal endosome transport ~0.5–3.0 μm/s. Further, fluorescence signal from off-focal excitation degrades the signal-to-background (S/B) ratio (Fig. 1a)
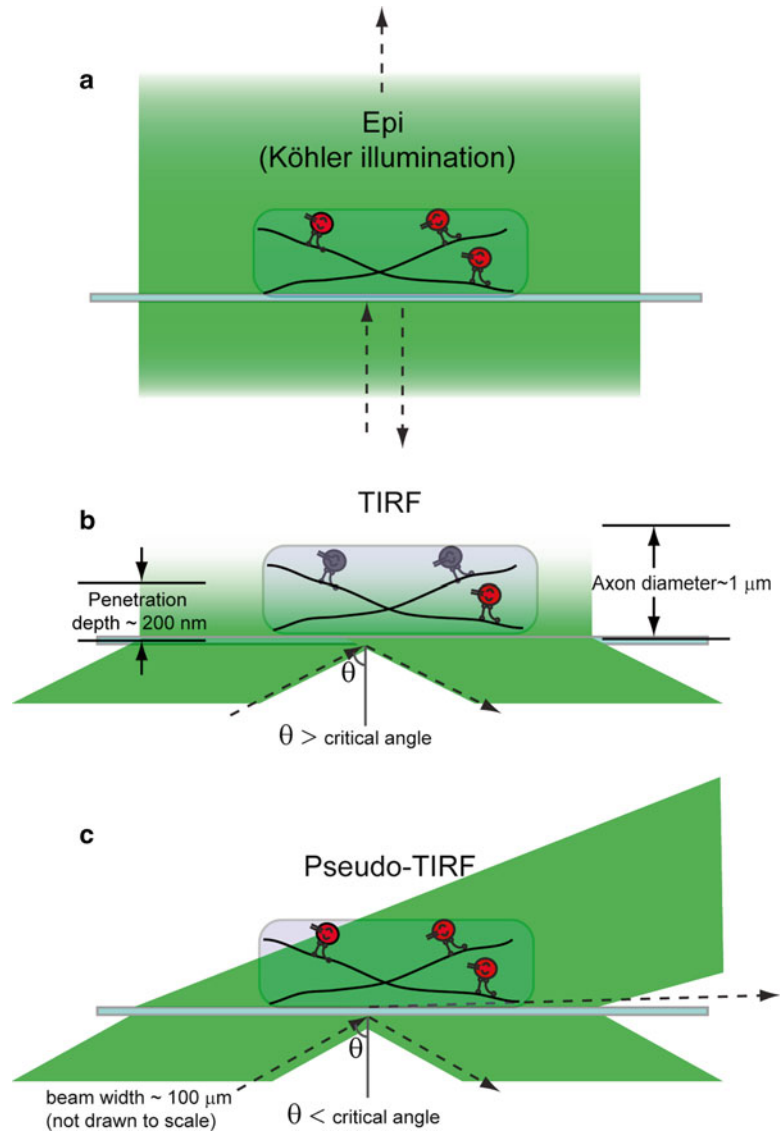
Fig. 1 Comparison of different illumination modes. (**a**) Epi-illumination (Köhler illumination) where a homogeneous excitation field passes the sample plane. Off-focal illumination and back reflection of the excitation light degrade the signal-to-background (S/B) ratio. (**b**) TIRF illumination where the incident angle of the excitation light is adjusted to the critical angle for total internal reflection. In such case, the penetration depth is about 200 nm and cannot cover the whole diameter of an axon. (**c**) pTIRF illumination where the incident angle of excitation light is adjusted to be slightly below the critical angle so that the penetrated beam depth of ~1–2 μm samples the whole volume of the axon

which limits the detection sensitivity of the fast-moving endosomes. Higher frame rates (>10 fps) can be achieved by using wide-field single-molecule fluorescence imaging such as total

internal reflection fluorescence microscopy (TIRFM), where a spatially confined evanescent field is used to excite fluorescent probes with efficient background rejection. Multicolor TIRFM can be used to simultaneously detect multiple fluorescently labeled targets instead of the sequential manner in conventional epi-illumination microscopy. However, the penetration depth of the evanescent field is only ~200 nm, about 20 % of the diameter of a single axon. Therefore, TIRF microscopy is not able to capture the axonal transport within the whole volume of an axon (Fig. 1b). To obviate this limitation, we developed pseudo-TIRF (pTIRF) microscopy, where the incident angle of excitation light beam is tuned to be just below the critical angle, so that the penetration depth can be raised to about 1–2 μm. pTIRF microscopy enabled us to image fluorescent probes within the whole volume of axons with simultaneous multicolor imaging capability and single-molecule detection sensitivity (Fig. 1c).

In this chapter, we describe the procedures for setting up a pTIRF microscope, labeling Rab7 and TrkA with fluorescent proteins in DRG neurons, culturing DRG in PDMS microfluidic devices, imaging axonal transport with multicolor pseudo-TIRF microscopy, and kymograph data analysis.

2   Materials

2.1   Pseudo-TIRF Microscope

The pseudo-TIRF illumination can practically be achieved on any microscope system implementing TIRF illumination by tuning the angle of incidence. Depending on the application, fluorescent probes with different color can be chosen and filter sets should be adjusted accordingly. Here we selected the light sources and optics for simultaneous detection of fluorescence from GFP (emission 500–550 nm) and mCherry (emission 575–650 nm).

1. Microscope frame: inverted microscope.
2. Excitation laser sources (488-nm laser line for GFP excitation; 561-nm laser line for mCherry excitation).
3. Dichroic mirrors and filter sets (Table 1 and Fig. 2).
4. Detector: EMCCD camera.
5. Image acquisition and analysis software.

2.2   DRG Cell Culturing

1. Freshly dissociated DRG cell cultures. Detailed protocols for DRG dissociation from embryonic [11] or adult [12] rat have been reported.
2. Plating medium: DMEM (*see* **Note 1**), 10 % FBS, 100 U/ml Penicillin, 200 μg/ml Streptomycin, 50 ng/ml NGF.
3. Maintenance medium: Neurobasal, 1× B27 (*see* **Note 2**), 0.5 mM L-Glutamine, 100 U/ml Penicillin, 200 μg/ml Streptomycin, 50 ng/ml NGF (*see* **Note 3**).

Table 1
Specification of optics in the pTIRF microscopy setup

Optics	Specs	
Objective	Magnification/N.A.	100×/1.49
Dichroic mirror (DM1)	Reflection/transmission	488 nm/561 nm
Dichroic mirror (DM2)	Laser line reflection	488 nm, 561 nm
Dichroic mirror (DM3)	Reflection/transmission	<550 nm/>550 nm
Emission filter (EM1)	Transmission	525 ± 20 nm
Emission filter (EM2)	Transmission	605 ± 20 nm
Lens (L)	Focal length	40 cm
Lens (L1)	Focal length	20 cm
Lens (L2)	Focal length	20 cm
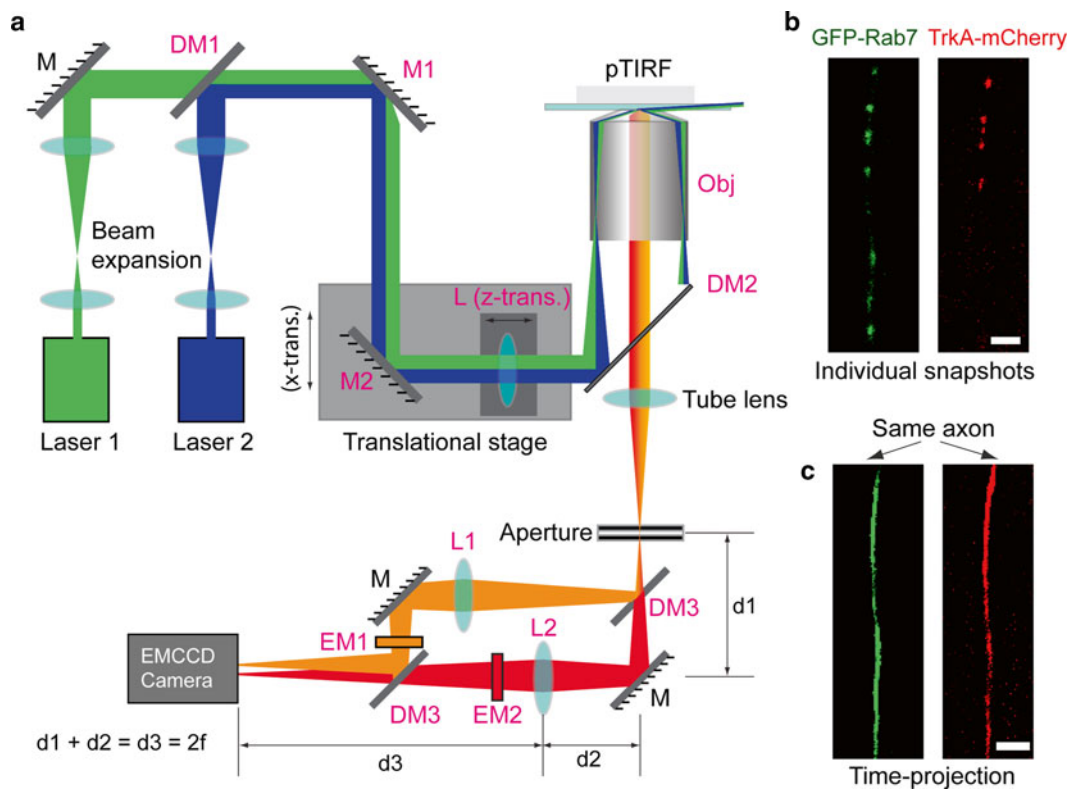
Fig. 2 (**a**) Experimental layout of multicolor single-molecule fluorescence microscopy with pTIRF configuration. (**b**) Representative snapshots of the axonal transport of GFP-Rab7 (*green*) and TrkA-mCherry (*red*) containing endosomes within a cotransfected DRG axon in a microfluidic channel. Endosomes appeared as individual fluorescent dots. (**c**) Time projection of the time-stamped image series in (**b**) generated an axon trace outlined by all the transported endosomes during the data acquisition time window. Such a trace was used to generate kymographs. Scale bar: 5 μm

4. Antimitotic medium: Neurobasal, 1× B27, 0.5 mM L-GLUTAMINE, 4 μM ARA-C, 100 U/ml Penicillin, 200 μg/ml Streptomycin, 50 ng/ml NGF.

5. Imaging medium: CO_2 independent medium (*see* **Note 4**).

6. Sterile poly-L-lysine coated 24 mm×40 mm cover slips.

7. Nucleofector system and nucleofection buffer (Lonza).

8. GFP-Rab7 and TrkA-mCherry DNA plasmids (*see* **Note 5**).

9. Compartmentalized PDMS microfluidic culture chamber. A detailed protocol of using this type of device has been reported in a previous chapter [13]. Alternatively, a fabrication protocol can be followed if custom-designed patterns are preferred [14]. The devices used in our current report are shown in Fig. 3a, b.
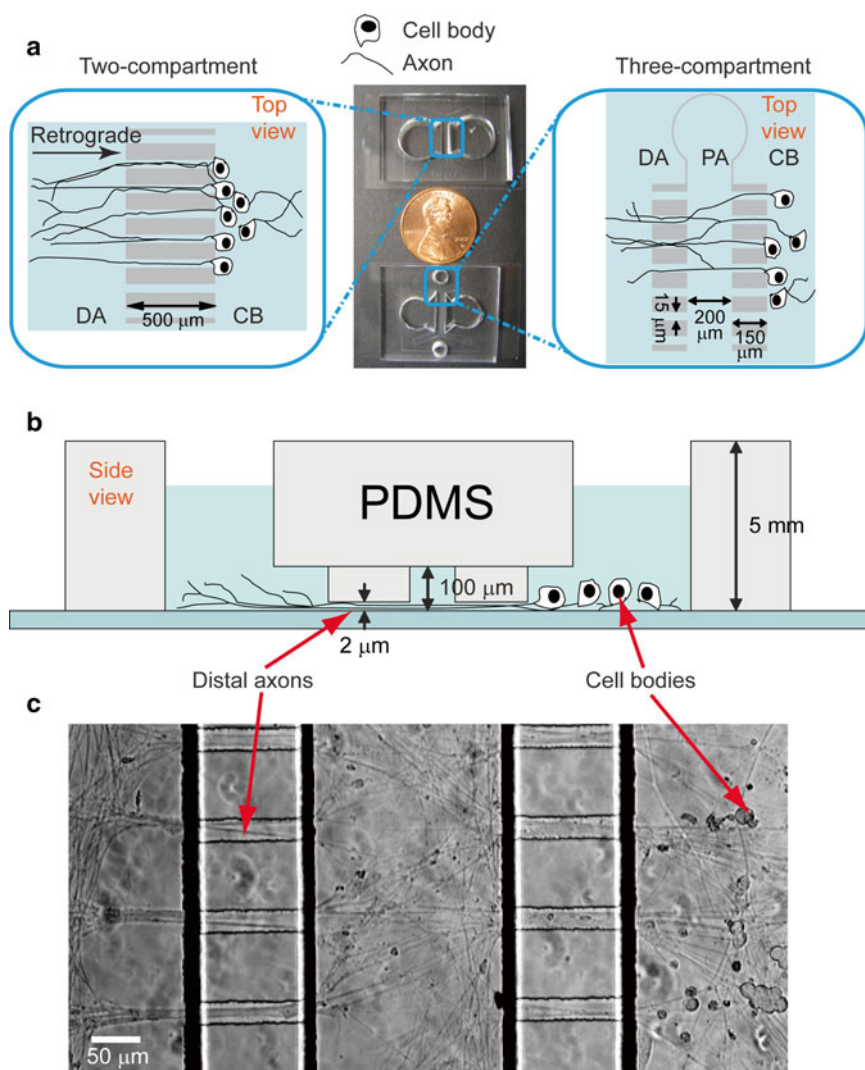
Fig. 3 Microfluidic chambers for culturing dorsal root ganglia neurons. Top view (**a**) and (**b**) side view of microfluidic chambers for DRG cell culture. (**c**) Bright-field image of a microfluidic DRG neuron culture 4 days after cell plating. Figures were adopted from ref. [15] reproduced by permission of the Royal Society of Chemistry

3   Methods

3.1   Setting Up a Pseudo-TIRF Microscope

1. Expand the excitation laser beams (488 nm and 561 nm) to about 3 cm in diameter and coalign the collimated beams through the standard epi-illumination port along the optical axis of the objective. Mount the mirror M2 on an *x*-translation mount so that the excitation beams can be horizontally displaced from the optical axis in a controlled manner.

2. Place a bare coverslip on the microscope stage and make contact with the microscope objective using immersion oil. Focus the objective on the top surface of the coverslip. The laser beams passing the objective form a large illumination region on the ceiling above the microscope.

3. Install an achromatic converging lens "L" on the same *x-translational* mount as M2 but with an independent *z-translational* control, roughly one focal length away from the back focal plane of the objective. Adjust the *z*-translation of the lens "L" to focus the excitation laser beams at the back focal plane of the objective, which then collimates the laser beams. Optimal position of this lens minimizes the size of the laser illumination spot on the ceiling (*see* **Note 6**).

4. The angle of incidence of the excitation laser beams at the coverslip can be systematically varied by horizontally displacing the laser beams (*x*-translation of M2 and L) from the optical axis to the edge of the back aperture of the objective (*see* **Note 7**). Gradually increase the angle of incidence till the laser illumination spot on the ceiling moves down along the wall and just disappears due to total internal reflection.

5. Now decrease the angle of incidence till the laser illumination spot just appears on the wall. At this point the angle of incidence is just below the critical angle and corresponds to the pTIRF illumination mode (*see* **Note 8**).

3.2   DRG Transfection and Culturing in a PDMS Compartmentalized Chamber

1. One nucleofection reaction uses ~200,000 DRG cells, 20 μl buffer, and 0.4 μg of DNA plasmids (*see* **Note 5**).

2. Add DNA plasmids into the freshly made nucleofection buffer immediately before transfection.

3. Measure ~200,000 DRG cells into a sterile 1.5 ml vial. Spin down the cells at $150 \times g$ for 3 min and resuspend the cell pellet in 20 μl of nucleofection buffer/DNA mixture (*see* **Note 9**).

4. Transfer the cell/buffer/DNA mixture into an electroporation cuvette.

5. Transfect with appropriate electroporation protocols for neurons.

6. After transfection, add 1 ml warm plating medium in the cuvette. Transfer the cell suspension into a sterile 1.5 ml vial. Spin down at $150 \times g$ for 3 min.

7. In the meantime, assemble the PDMS microfluidic chamber by placing a device with the microchannel pattern facing down on a PLL-coated coverslip. Gently push the edges of the device to ensure sealing (*see* **Note 10**).

8. After centrifugation, remove the supernatant and resuspend the cell pellet with 10 μl fresh plating medium. Plate all cells into a microfluidic chamber (*see* **Note 11**).

9. Add 200 μl plating medium into the cell body compartment; add 100 μl plating medium into the distal axon compartment (*see* **Note 12**).

10. Change the plating medium to maintenance medium 3 h after plating. All cells should attach by this time. Add 500 μl plating medium into the cell body compartment; add 300 μl plating medium into the distant axon compartment (*see* **Note 13**).

11. Change to the antimitotic medium 36 h after plating.

12. Change back to the maintenance medium after incubation of the antimitotic medium for 24 h (*see* **Note 14**).

13. Change half of the medium every other day (*see* **Note 15**).

3.3 Imaging Axonal Transport of Endosomes with Pseudo-TIRF Microscopy

1. Culture DRG cells in the microfluidic devices for 4–6 days, by when most axons should grow across the microchannels (Figs. 3c and 4a, b).

2. Warm the microscope stage and objective to 37 °C.

3. Immediately before imaging, change the culture medium to CO_2 independent medium (*see* **Note 4**).

4. Load the DRG culture on the heated microscope stage and wait for the temperature to equilibrate. Meanwhile, focus the objective to the surface of the coverslip (*see* **Note 16**).

5. Switch to laser light and move the microscope stage to a channel with fluorescently labeled axons. Fine tune the focus so that individual vesicles along axons can be seen (Fig. 2b). For healthy DRG cultures, most vesicles should be moving.

6. Find a region of interest (ROI) which displays one to three axons with a microchannel (*see* **Note 17**) and track the axonal transport of endosomes. Record the sides of cell body and distal axon so that the directionality of axonal transport can be assigned.

7. Start image acquisition and record the transport for a total of 600 frames with 100 ms exposure time per frame (10 fps). On average several tens of endosomes should be captured within this 1 min of imaging time.

8. Repeat image acquisition from a different ROI till the axons in different microfluidic channels are sampled (*see* **Note 18**).
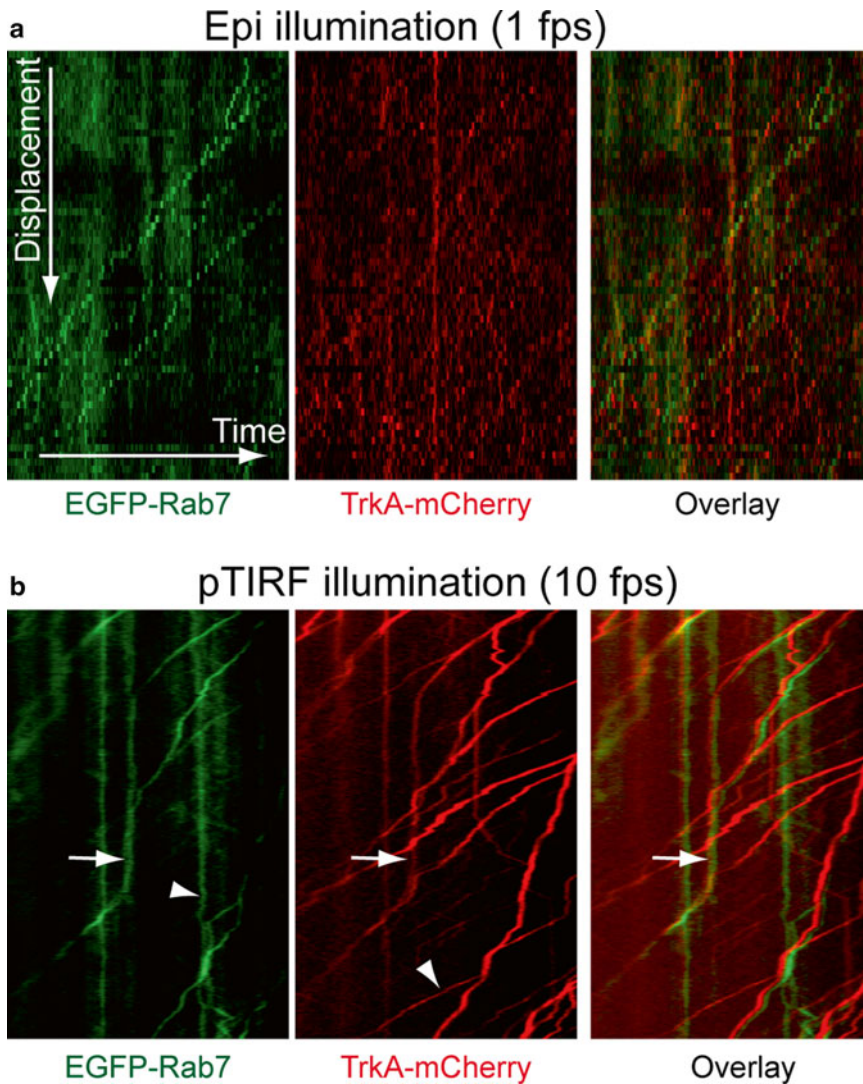
Fig. 4 Kymographs depicting the axonal transport of endosomes containing EGFP-Rab7 (*left*), TrkA-mCherry (*middle*), and overlay (*right*). (**a**) Epi-illumination imaging using a Leica DMI6000B microscope with a frame rate of 1 fps. The slow frame rate resulted in the apparent dotted lines for each trajectory in the kymograph. (**b**) pTIRF imaging with a frame rate of 10 fps. All the trajectories in the kymograph appeared much smoother. The *red* and *green* images were slightly shifted for clear visualization purpose in the overlay image to the right. Trajectories of endosomes with both Rab7 and TrkA were marked by arrow heads. Note that some endosomes did not contain both Rab7 and TrkA (*arrows*)

3.4 Kymograph Data Analysis

1. Export the time-stamped images of axonal transport to an image stack.

2. Use the "Kymograph" plug-in (J. Rietdorf and A. Seitz) in ImageJ to generate kymographs, which show the displacement of endosomes along an axon at different times. As each frame in a time-stamped image series is a snapshot of the position of

endosomes along axons (Fig. 2b), the maximum intensity of each frame can be projected on a time-projection image to display the axon traces (Fig. 2c). Movements of individual endosomes along each axon trace show up as individual trajectories on the kymograph (*see* **Note 19**).

3. A representative kymograph from the axonal transport of endosomes containing Rab7-GFP and TrkA-mCherry is shown in Fig. 4c, d. Notice that trajectories in the kymographs generated from epi-illumination show apparent dotted lines due to low frame rate (Fig. 4c) while high frame rate pTIRF microscopy gives smooth lines (Fig. 4d).

4   Notes

1. The L-glutamine component in DMEM will decay over time. Use before the expiration date.

2. Stock solution comes as 50×.

3. Store NGF aliquots in –80 °C freezer and thaw it only before preparing culture media. Repeated freeze–thaw of NGF will degrade its bioactivity.

4. Alternatively, an on-stage CO_2 chamber can be used for live cell imaging. In such a case, no CO_2 independent medium is required.

5. High-purity maxi-prep DNA plasmids are critical for successful transfection.

6. The beam diameter at the sample depends on the beam diameter at the lens L, the focal length of L, and the focal length of the objective. The variables are chosen so as to provide uniform illumination over the imaging field ~80–150 μm.

7. The center position corresponds to the epi-mode; the edge position corresponds to the TIRF mode.

8. Before each experiment with neuronal culture, fine tune the incident angle of excitation beam to maximize the signal-to-background ratio.

9. Pipette the cell pellet gently. Too much force is damaging to the cell.

10. Make sure both PDMS microfluidic device and the PLL-coated coverslip are sterile.

11. Plating low-density culture is not good for cell recovery and growth.

12. The pressure difference between the cell body and distal axon compartments facilitates axons to grow across the channel.

13. More medium provides enough nutrients to the cells.

14. Remove the antimitotic medium after 1 day. Long-time incubation of antimitotic medium will deteriorate the DRG cell health.

15. Make sure the medium does not dry out.

16. The edges of the microchannels can help locate the rough focal position under white light.

17. Try not to select ROIs with too dense axons or axons that cross over each other. Both cases will make it difficult to track the movement of single endosomes.

18. Make sure medium within the cell culture does not dry out during data acquisition on the heated stage.

19. We have developed a data acquisition software using MATLAB where kymographs can be generated with a batch mode operation.

References

1. Stenmark H, Olkkonen VM (2001) The Rab GTPase family. Genome Biol 2(5): REVIEWS3007

2. Spinosa MR, Progida C, De Luca A, Colucci AM, Alifano P, Bucci C (2008) Functional characterization of Rab7 mutant proteins associated with Charcot-Marie-Tooth type 2B disease. J Neurosci 28(7):1640–1648

3. Cogli L, Piro F, Bucci C (2009) Rab7 and the CMT2B disease. Biochem Soc Trans 37(Pt 5): 1027–1031

4. Saxena S, Bucci C, Weis J, Kruttgen A (2005) The small GTPase Rab7 controls the endosomal trafficking and neuritogenic signaling of the nerve growth factor receptor TrkA. J Neurosci 25(47):10930–10940

5. Deinhardt K, Salinas S, Verastegui C, Watson R, Worth D, Hanrahan S, Bucci C, Schiavo G (2006) Rab5 and Rab7 control endocytic sorting along the axonal retrograde transport pathway. Neuron 52(2):293–305

6. Zhang K, Fishel Ben Kenan R, Osakada Y, Xu W, Sinit RS, Chen L, Zhao X, Chen JY, Cui B, Wu C (2013) Defective axonal transport of Rab7 GTPase results in dysregulated trophic signaling. J Neurosci 33(17):7451–7462

7. Ascano M, Richmond A, Borden P, Kuruvilla R (2009) Axonal targeting of Trk receptors via transcytosis regulates sensitivity to neurotrophin responses. J Neurosci 29(37): 11674–11685

8. Cui B, Wu C, Chen L, Ramirez A, Bearer EL, Li WP, Mobley WC, Chu S (2007) One at a time, live tracking of NGF axonal transport using quantum dots. Proc Natl Acad Sci U S A 104(34):13666–13671

9. Ure DR, Campenot RB (1997) Retrograde transport and steady-state distribution of 125I-nerve growth factor in rat sympathetic neurons in compartmented cultures. J Neurosci 17(4):1282–1290

10. Taylor AM, Blurton-Jones M, Rhee SW, Cribbs DH, Cotman CW, Jeon NL (2005) A microfluidic culture platform for CNS axonal injury, regeneration and transport. Nat Methods 2(8):599–605

11. Moore SW, Lai Wing Sun K, Xie F, Barker PA, Conti M, Kennedy TE (2008) Soluble adenylyl cyclase is not required for axon guidance to netrin-1. J Neurosci 28(15):3920–3924

12. Owen DE, Egerton J (2012) Culture of dissociated sensory neurons from dorsal root ganglia of postnatal and adult rats. Methods Mol Biol 846:179–187

13. Darbinyan A, Pozniak P, Darbinian N, White MK, Khalili K (2013) Compartmentalized neuronal cultures. Methods Mol Biol 1078: 147–152

14. Park JW, Vahidi B, Taylor AM, Rhee SW, Jeon NL (2006) Microfluidic culture platform for neuroscience research. Nat Protoc 1(4): 2128–2136

15. Zhang K, Osakada Y, Vrljic M, Chen L, Mudrakola HV, Cui B (2010) Single-molecule imaging of NGF axonal transport in microfluidic devices. Lab Chip 10:2566–2573

Chapter 28

Quantitative Bead-Based Flow Cytometry for Assaying Rab7 GTPase Interaction with the Rab-Interacting Lysosomal Protein (RILP) Effector Protein

Jacob O. Agola, Daniel Sivalingam, Daniel F. Cimino, Peter C. Simons, Tione Buranda, Larry A. Sklar, and Angela Wandinger-Ness

Abstract

Rab7 facilitates vesicular transport and delivery from early endosomes to late endosomes as well as from late endosomes to lysosomes. The role of Rab7 in vesicular transport is dependent on its interactions with effector proteins, among them Rab-interacting lysosomal protein (RILP), which aids in the recruitment of active Rab7 (GTP-bound) onto dynein–dynactin motor complexes to facilitate late endosomal transport on the cytoskeleton. Here we detail a novel bead-based flow cytometry assay to measure Rab7 interaction with the Rab-interacting lysosomal protein (RILP) effector protein and demonstrate its utility for quantitative assessment and studying drug–target interactions. The specific binding of GTP-bound Rab7 to RILP is readily demonstrated and shown to be dose-dependent and saturable enabling K_d and B_{max} determinations. Furthermore, binding is nearly instantaneous and temperature-dependent. In a novel application of the assay method, a competitive small molecule inhibitor of Rab7 nucleotide binding (CID 1067700 or ML282) is shown to inhibit the Rab7–RILP interaction. Thus, the assay is able to distinguish that the small molecule, rather than incurring the active conformation, instead 'locks' the GTPase in the inactive conformation. Together, this work demonstrates the utility of using a flow cytometry assay to quantitatively characterize protein–protein interactions involving small GTPases and which has been adapted to high-throughput screening. Further, the method provides a platform for testing small molecule effects on protein–protein interactions, which can be relevant to drug discovery and development.

Key words Ras superfamily, Rab, Protein–protein interaction, Guanine nucleotide binding, GTP hydrolysis, GTPase effector, Quantitative flow cytometry, Glutathione-*S*-transferase (GST) assay, Drug discovery, HTS—High-throughput screening, Structure–activity relationship (SAR), G-Trap assay

1   Introduction

1.1 Rab7 and Its Effector Protein RILP Are Disease Relevant Proteins

Rab7 is a ubiquitously expressed Ras-superfamily GTPase, which functions in the endocytic pathway of mammalian cells to regulate vesicular traffic from early to late endosomes and then to lysosomes while playing a role in lysosome biogenesis [1–4]. Rab7 function is

pivotal for lysosome-mediated degradation of endocytosed signaling receptors, defective cell surface proteins, and excess internalized lipid [4, 5]. Under conditions of nutrient starvation, Rab7 mediates fusion of autophagic vacuoles with lysosomes to release key metabolites for cell survival [6, 7]. The homeostatic balance of these processes is crucial to cell growth and differentiation, with misregulation often resulting in human disease.

Rab7 is associated with inherited and acquired neurologic diseases, cancer, and infectious diseases. Typical examples include Charcot–Marie–Tooth type 2B (CMT2B) disease, which causes axonal degeneration and is linked to four Rab7 missense mutants [8], other neurodegenerative diseases and retinal degeneration associated with reduced Rab7 function in autophagy [9–13], and genetic lipid storage disorders such as Batten and Niemann–Pick Type C diseases that are in part caused by Rab7 inactivation due to the accumulation of cholesterol in late endosomes [14, 15]. Disease-causing pathogens also often hijack the endocytic machinery where Rab7 is pivotal to gain access to the cell interior for infection, replication, and long-term survival [16–18]. These representative examples of Rab7-associated diseases illustrate how alteration of the GTPase regulatory cycle, effector protein interactions, as well as vesicular trafficking and signal transduction processes can give rise to disease and thus, collectively calls for the need to explore diverse intervention approaches.

The 45 kDa Rab-interacting lysosomal protein (RILP) is one of several Rab7 effector proteins [19–23]. Recruitment of RILP by active (GTP-bound) Rab7 regulates endolysosomal morphogenesis and microtubule minus-end directed transport through the recruitment of the dynein–dynactin motor complex [23–25]. Recruitment of RILP is also vital for processes such as phagosome maturation and fusion with late endosomes and lysosomes [26, 27].

Biochemically, Rab7 interaction with RILP has been assessed primarily using glutathione beads and GST-RILP for pull-down assays followed by protein electrophoresis and immunodetection, which often do not provide quantitative information [28, 29]. The method described here uses glutathione flow cytometry beads and GST-RILP, followed by detection using a flow cytometer. Such, use of bead-based flow cytometry to measure protein–protein interactions is not only quantitative, but also provides an enabling environment for the application of high-throughput screening (HTS) approaches. For HTS, the bead-based method can be adapted to screening a protein of interest against protein libraries to identify potential interacting partners or screening libraries of small molecules that may modulate protein–protein interactions. Applying the latter case to Rab7, for instance, can help in identifying small molecules with the potential to regulate Rab7 activity that may be relevant to Rab7-associated diseases.

1.2 Rationale for a Bead-Based Flow Cytometry Assay for Quantitative Measurement of Rab7-Effector Protein Interactions

Use of the described bead-based flow cytometry approach to quantitatively characterize Rab7 interaction with RILP, as a model effector protein, is a viable alternative to the conventional glutathione-S-transferase (GST) pull-down method that is at best semiquantitative. We demonstrate that RILP interacts with active Rab7 only when bound to GTP, demonstrating specificity and that this specific binding is dose dependent and saturable, enabling B_{max} and K_d determination. Furthermore, the interaction is shown for the first time to be time and temperature dependent. When the small molecule 2-(benzoylcarbamothioylamino)-5, 5-dimethyl-4, 7-dihydrothieno[2,3-c]pyran-3-carboxylic acid (PubChem: CID 1067700 or ML282) was incorporated in the assay as a modulator of Rab7 activity, we obtained the novel result that this small molecule, previously characterized as a competitive inhibitor of Rab7 nucleotide binding [30], freezes Rab7 in a GDP-like conformation that does not bind RILP. The method has utility for quantitatively assaying effects of small molecules on Rab7 nucleotide bound status in cells, by using cell lysates in lieu of purified Rab7 in the assay. The experimental procedure is also readily adapted to investigating individual protein–protein interactions or identifying novel partners using HTS approaches [31, 32].

2 Materials

2.1 Reagent Sources

Reagents used in this report were obtained from various sources. Sephadex G-25, glutathione (GSH) Sepharose 4B, and Superdex (dextran/cross-linked agarose beads designed for peptide separation; 13 μm particle size with an exclusion limit of 7 kDa) are available from GE Healthcare (Piscataway, NJ). BODIPY (4,4-difluoro-4-bora-3a,4a-diaza-s-indacene or dipyrromethene boron difluoride) nucleotide analogs (BODIPY-GTP; 2′-(or 3′)-O-[N-(2-aminoethyl)urethane] G-35778 and BODIPY-GDP; 2′-(or-3′)-O-[N-(2-aminoethyl)urethane], G-22360) were from Invitrogen (merged with Life Technologies, Grand Island, NY). ProBond™ system for His-tagged protein purification was from Life Technologies (Grand Island, NY). GSH Sepharose 4B (GE Healthcare Bio-Sciences, Uppsala, Sweden). GFP-Rab7 was cloned into the pE-Sumo T7, amp vector from LifeSensors (Malvern, PA), which has a 6×His Tag for optimal bacterial expression of soluble protein and ease of purification [33]. Amicon Ultra Centrifugal Filters (30K MWCO) were obtained from Millipore Ireland Ltd. Protein concentrations were determined using a Bradford Colorimetric Assay from Bio-Rad (Hercules, CA) Unlabeled nucleotides (GDP, GTP, and GTP-γ-S) and buffer components were from Sigma (St. Louis, MO, USA). 2-(benzoylcarbamothioylamino)-5,5-dimethyl-4, 7-dihydrothieno[2,3-c]pyran-3-carboxylic acid (PubChem:

CID 1067700 or ML282) was from ChemDiv Inc. (San Diego, CA, USA) and is also available from Sigma-Aldrich and Cayman Chemical. Where applicable, a Becton Dickinson FACScan flow cytometer with a 488-nm excitation Argon (Ar) laser and standard detection optics was used for all assays [34]. Concentrations of BODIPY-linked nucleotides were based on absorbance measurements and an extinction coefficient value of 80,000 M^{-1} cm^{-1} at 488 nm. The major materials used in each relevant experimental procedure are further captured below.

2.2 Synthesis of GSH Beads for Flow Cytometry Assays

1. Superdex dextran/cross-linked agarose beads (13 μm, 7 kDa exclusion limit) in buffered suspension.
2. Reduced GSH solution.
3. Water soluble bis-epoxide, ethanol, sodium hydroxide, and 4-butanediol diglycidol ether.
4. 15 ml coarse sintered glass filter.
5. Sodium phosphate and EDTA solutions.
6. Appropriately supplemented HEPES (4-(2-hydroxyethyl)-1-piperazineethanesulfonic acid) based buffers as explained in Subheading 3.

2.3 Expression and Purification of GST, GST-RILP, GST-Rab7, His-Rab7, and His-SUMO-GFP-Rab7 in Bacterial Cells

1. Competent *E. coli* BL21 (DE3) cells.
2. LB agar plates and liquid broth supplemented with 100 μg/ml ampicillin.
3. pGEX vector for GST expression.
4. Plasmids encoding GST-Rab7 (pGEX Rab7), GST-RILP (pGEX RBD-RILP), His-Rab7 (pRSET Rab7), and His-SUMO-GFP-Rab7 (pE-Sumo T7 amp GFP-Rab7).
5. Isopropyl-beta-d-1-thiogalactopyranoside (IPTG).
6. Affinity purification resins (nickel resin—ProBond™ and GSH Sepharose 4B).
7. Appropriately supplemented phosphate-based buffers and other necessary chemicals.

2.4 Immobilization of GST, GST-Rab7, and GST-RILP on GSH Beads

1. 13 μm GSH-coated beads.
2. Purified GST, GST-Rab7, and GST-RILP.
3. Appropriately supplemented HEPES-based buffer as explained in Subheading 3.

2.5 Measurement of Specific Interaction Between Rab7 and RILP Effector Protein

1. 13 μm GSH coated beads.
2. Purified GST, GST-RILP, and His-Rab7.
3. Nucleotides: BODIPY-GTP dissolved in water.
4. Appropriately supplemented HEPES-based buffer as explained in Subheading 3.

2.6 Measurement of Time-Dependent Rab7 Interaction with RILP	1. 13 μm GSH-coated beads. 2. Purified GST, GST-RILP, His-Rab7, and GFP-Rab7. 3. Nucleotides: Unlabeled GDP, BODIPY-GTP, BODIPY-GDP, and GTP-γ-S in water. 4. Appropriately supplemented HEPES and phosphate-based buffers as explained in Subheading 3.
2.7 Measurement of Temperature-Dependent Rab7 Interaction with RILP	1. 13 μm GSH-coated beads. 2. Purified GST-RILP and His-Rab7. 3. Nucleotides: BODIPY-GTP in water. 4. Appropriately supplemented HEPES-based buffer as explained in Subheading 3.
2.8 Measurement of the Kinetics of BODIPY-GTP Displacement from Rab7 by Competitive Guanine Nucleotide-Binding Inhibitor (CID 1067700 or ML282)	1. 13 μm GSH-coated beads. 2. Purified GST-Rab7. 3. DMSO solvent. 4. Small molecule (PubChem: CID 1067700 or ML282) dissolved in DMSO. 5. Nucleotides: Unlabeled GDP and BODIPY-GTP in water. 6. HEPES-based buffers with appropriate supplementation as explained in Subheading 3.
2.9 Measurement of Rab7 Interaction with RILP in the Presence of a Competitive Guanine Nucleotide-Binding Inhibitor (CID 1067700 or ML282)	1. 13 μm GSH-coated beads. 2. Purified GST-RILP and GFP-Rab7. 3. Nucleotide: GTP-γ-S dissolved in water. 4. Small molecule: CID 1067700 or ML282. 5. HEPES-based buffers supplemented appropriately as explained in Subheading 3.

3 Methods

Subheading 3.1 provides an overview of a flow cytometric Rab7-effector binding assay with application to other Ras-superfamily GTPases. Subheadings 3.2–3.6 provide more detailed descriptions of methods and representative results for Rab7-effector protein binding measurements using RILP as a representative example; including determination of K_d and B_{max}, kinetic measurements, temperature dependence of binding, and the effect of a small molecule inhibitor of Rab7 nucleotide binding on effector interaction. Subheading 3.7 provides information on data analysis methods.

3.1 Experimental Design of a Bead-Based Flow Cytometry Assay and Its Application to Measurement of Protein–Protein Interactions

In biochemical assays, elucidation and characterization of protein–protein interactions often involves time-consuming preparation of cell lysates containing candidate proteins and then confirming evidence of interaction with antibody-based immunoblotting methods. The caveats of these approaches tend to be: (1) it is difficult to obtain quantitative information, (2) other proteins in the cell lysates can influence the assay outcome, and (3) assays are often subject to the quality and performance of the individual antibodies used for detection.

Sklar and colleagues pioneered the use of a bead-based flow cytometry approach to quantitatively measure protein–protein interactions associated with G-protein coupled receptors, initially taking advantage of streptavidin–biotin interactions [31, 32]. Further development of methodologies based on the use of GSH-beads and GST-fusion proteins led to the award of US patent 7,785,900 [35]. Nevertheless, traditional GST pull down and other nonquantitative or semiquantitative methods still remain in wide use [36, 37]. A bead-based flow cytometry assay for characterizing Rab GTPase and effector protein interactions can be set up in two ways using recombinant GST-fused RILP immobilized on GSH beads (Fig. 1a, b). In the first way, Rab7–RILP interaction is measured indirectly based on an increase in bead-associated fluorescence reflecting the binding of a Rab7-BODIPY-GTP complex to RILP (Fig. 1a). In the second way, Rab7–RILP interaction is measured directly based on the binding of GFP-Rab7 in the presence of nonhydrolyzable GTP-γ-S with GFP fluorescence measured by the flow cytometer (Fig. 1b). By applying these two approaches, the specificity of the protein–protein interaction between Rab7 and GSH bead-immobilized RILP is readily established.

3.2 Reagent Preparation for Quantitative Protein–Protein Interaction Measurements

*3.2.1 Synthesis of GSH Beads for Flow Cytometry Assays (see also **Note 1**)*

Superdex dextran/cross-linked agarose beads are extruded from a column, activated with a water-soluble bis-epoxide, and then coupled to reduced GSH purged with nitrogen or argon gas. One milliliter of 50 % slurry of beads in 20 % ethanol is reduced to a wet cake using a 15 ml coarse sintered glass filter, and washed three times with 15 ml water to remove the ethanol. The wet cake is transferred to a small screw-cap tube, and the filter is rinsed with 0.3 ml of water, which is added to the tube. The beads are suspended by vortexing, then 60 μl of 10 M NaOH and 300 μl of 1,4-butanediyl diglycidyl ether (formerly butanediol diglycidyl ether) are added, and the suspension is rocked gently at 40 °C for 4 h.

The epoxy-activated beads are rinsed four times on a coarse sintered-glass filter. For the preparation of high site density beads, 600 μl of 100 mM GSH in 100 mM sodium phosphate (pH is 7.5), 1 mM EDTA, is added to the epoxy-activated beads. The beads are kept in suspension for 16 h at 40 °C, then rinsed twice with 0.01 % dodecyl maltoside. Beads with about 40-fold less GSH derivatization are prepared using 20 mM GSH and reacted for 2 h. The remaining active sites are blocked with 1 % 2-mercaptoethanol
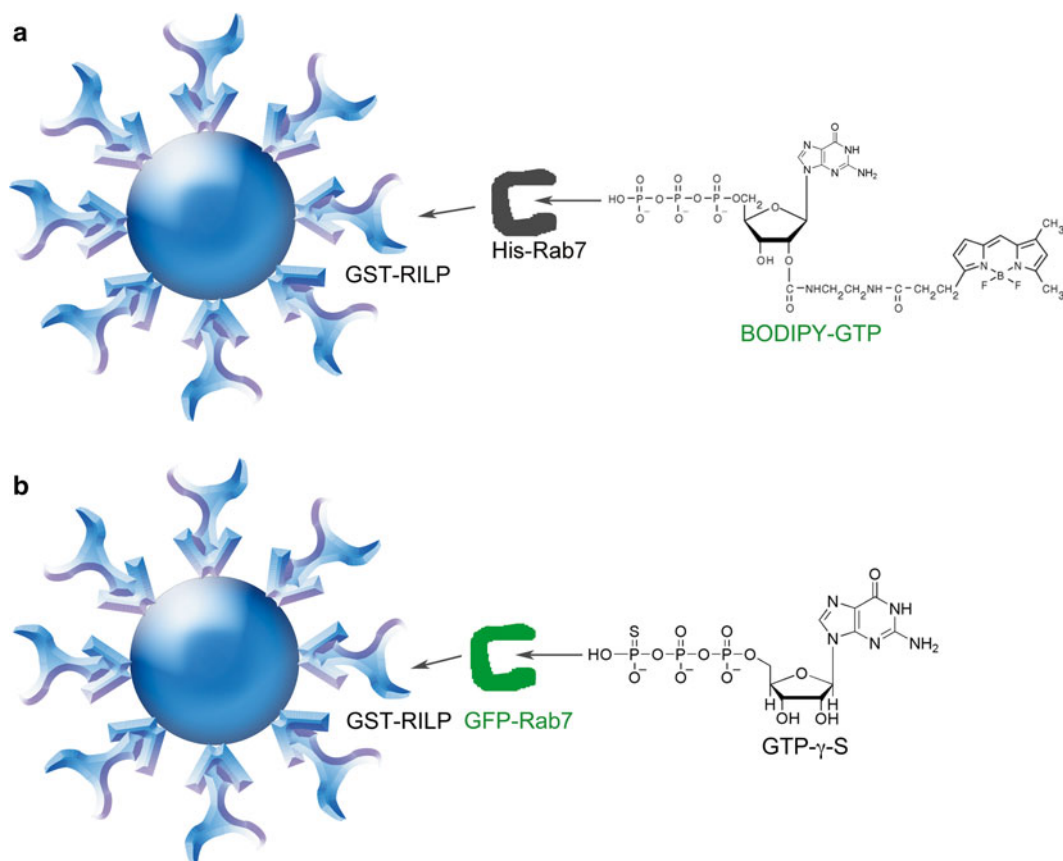
Fig. 1 GSH bead-based flow cytometry assay configurations for quantitative measurements of GTPase-effector protein binding. (**a**) Assay design for detecting Rab7 and Rab-interacting lysosomal protein (RILP) effector protein interaction based on detection of bound fluorescent BODIPY-GTP. GST-RILP (Rab binding domain of RILP only) is immobilized on 13 μm Superdex beads coated with GSH and incubated with purified His-tagged Rab7 complexed to fluorescent BODIPY-GTP. Flow cytometry detection is based on bead-associated fluorescence when His-Rab7-BODIPY-GTP binds to RILP. (**b**) Assay design for detecting Rab7 and Rab-interacting lysosomal protein (RILP) protein interaction based on detection of GFP-tagged Rab7. GST-RILP (Rab-binding domain of RILP only) is immobilized on 13 μm Superdex beads coated with GSH and incubated with GFP-tagged Rab7 complexed to nonhydrolyzable GTP-γ-S. Flow cytometry detection is based on bead-associated fluorescence when GFP-Rab7-GTP-γ-S binds to RILP

for 2 h. The beads are then rinsed twice followed by storage in 30 mM HEPES, pH 7.5, 100 mM KCl, 20 mM NaCl, 1 mM $MgCl_2$ with 0.01 % dodecyl maltoside and 0.02 % NaN_3 at 4 °C as a 50 % slurry, which corresponds to ~2.5×10^5 beads per microliter, or 25 assays of 10^4 beads each per microliter. High site density GSH derivatized beads have been successfully used for flow cytometry-based assays of GTPases and HTS of activators and inhibitors [38] (*see* also **Note 2**).

| 3.2.2 Expression and Purification of Recombinant Proteins | Competent *E. coli* (BL21) are used for transformation and expression of GST-Rab7, GST-Rab7-binding domain (RBD) of RILP (prepared as previously described by Dan Cimino [39]). Competent |

BL21(DE3)pLysS *E. coli* are used for transformation and expression of His-Rab7 or His-SUMO-GFP-Rab7. Transformants in all cases are selected on Luria–Broth (LB) agar plates containing 100 μg/ml ampicillin. Individual drug-resistant colonies (~20) are used to inoculate 100 ml of LB broth liquid cultures that are grown at 37 °C to a bacterial density of 0.5–0.7 absorbance units measured at 595 nm. Protein expression was induced by transfer to room temperature and addition of 0.2 mM isopropyl-beta-d-1-thio-galactopyranoside (IPTG) for 16–18 h to maximize yield of properly folded active fusion protein. (For pGEX vectors, IPTG induces gene expression directly under the control of a Ptac (hybrid trp/lac) promoter; for pRSET vectors, IPTG enables gene expression under the control of a T7 promoter via activation of LacZ-dependent T7 polymerase expression encoded by a lamba lysogen carried by the bacterial strain).

Purification of GST-Rab7 and GST-RILP is then performed according to standard published procedures [34, 38]. In brief, bacterial cells are snap frozen and thawed and lysed using a microtip sonicator (Misonix Inc., Newtown, CT, U.S.A.). Cell lysates are centrifuged at $8,000 \times g$ for 10 min to pellet the cellular debris. GST proteins are purified by batch purification method per GSH Sepharose 4B manufacturer's instructions (GE Healthcare) and eluted with 10 mM GSH. Eluted protein is concentrated using Amicon^R Ultra centrifugal filters (30K MWCO) and washed with three times with 10 volumes of HEPES buffer (30 mM HEPES, pH 7.5, 20 mM NaCl, and 100 mM KCl supplemented with 1 mM EDTA, 1 mM dithiothreitol (DTT)) to simultaneously remove excess GSH. Protein concentrations are determined using a BCA assay. Single-use aliquots are snap frozen and stored at –80 °C until used for experiments.

Purification of His-Rab7 or His-SUMO-GFP-Rab7 is performed by suspending the harvested bacterial cell pellets in cold native binding buffer for purification of His-tagged Rab7 proteins using the native protein purification method (manufacturer's instructions for protein isolation via nickel affinity resin, Life Technologies). Bacterial cells are lysed using lysozyme and a microtip sonicator (Misonix Inc., Newtown, CT, U.S.A.), and cell debris removed by centrifugation as earlier. The supernatant is mixed with freshly prepared ProBond™ nickel chelating resin and bound at room temperature for 45 min using gentle agitation to keep the resin suspended in the lysate solution. Resin with bound protein is settled using low speed centrifugation ($800 \times g$) followed by multiple washes before eluting the nickel bound His-tagged protein with imidazole-based native elution buffer. Imidazole is removed by dialysis and protein is concentrated using Amicon^R Ultra centrifugal filters (10K MWCO) followed by quantification using BCA protein assay. Single-use aliquots stored at –80 °C are used in the experiments.

3.2.3 Immobilization of GST, GST-Rab7, and GST-RILP on GSH Beads for Flow Cytometry	Purified GST, GST-Rab7 protein, or GST-RILP at 1 μM is incubated in 96-well plates or microfuge tubes at 4 °C overnight with 10^5 GSH beads in a total volume of 100 μl of HEPES buffer supplemented with 1 mM EDTA and freshly prepared 1 mM dithiothreitol (DTT). Beads in 96-well plates were kept suspended by rotation at ~300 rpm, while beads in microfuge tubes were kept suspended by slow end-over-end rotation. At the maximal concentration of protein, approximately 5×10^6 GST-Rab7 molecules are bound to each bead. This represents a concentration of ~8 nM bead-bound protein [38]. Unbound protein is removed by centrifugation twice at $800 \times g$ followed by resuspension of washed beads in fresh buffer (30 mM HEPES, pH 7.5, 20 mM NaCl and 100 mM KCl, 1 mM EDTA, 1 mM DTT, 0.1 % BSA).

3.2.4 Preparation of Nucleotide-Bound, Active Rab7	The assay requires exchanging endogenous nucleotide by preincubating purified Rab7 with excess BODIPY-GTP in the presence of ethylenediaminetetraacetic acid (EDTA) as metal cation chelator. Addition of exogenous magnesium cations to 'lock' bound BODIPY-GTP onto Rab7 prior to testing on immobilized RILP is also an important step in ensuring quantitative measurements. Increasing concentrations of His-Rab7 (purified on nickel beads as described under Subheading 3.2.2) are incubated with a fixed concentration of BODIPY-GTP (500 nM) in a buffer-promoting nucleotide exchange (30 mM HEPES, pH 7.5, 20 mM NaCl and 100 mM KCl, 5 mM EDTA, and 0.1 % BSA) for 20 min at room temperature. Bound nucleotide is 'locked-on' the GTPase with the addition of 20 mM $MgCl_2$ (final) and then the solutions are transferred to ice. The nucleotide must be kept cold to avoid GTP-hydrolysis and consequent conversion of the GTPase to the inactive conformation. Interaction measurements between Rab7 and RILP are initiated by mixing BODIPY-GTP-bound Rab7 with thoroughly washed GST-RILP immobilized on GSH beads. BODIPY-GTP-bound Rab7 mixed with GSH beads without bound protein and GST-coated GSH beads serve as negative controls. The mixtures are allowed to incubate for 15 min at room temperature before making fluorescence measurements on a FACScan flow cytometer using the fluorescein filter set (FL1). For GTPases with rapid hydrolysis rates, use non-hydrolyzable GTP-γ-S in lieu of GTP. His-SUMO-GFP-Rab7 is loaded with GTP-γ-S as detailed in 3.4.1.

3.2.5 Flow Cytometry Measurement of Bead-Associated Fluorescence	Recorded parameters of each event are based on light scattering and fluorescent properties. On the FACScan flow cytometer, GSH beads are first identified based on forward and side scattering. Fluorescence measurements from 1,000 events (beads) are averaged to mean channel fluorescence (MCF). Tubes suitable (Product No. 352008, BD Bioscience, San Jose, California, U.S.A.) for flow cytometry are used and reactions are diluted at least tenfold in HPSM buffer (30 mM HEPES, pH 7.5, 20 mM NaCl, 100 mM

KCl, 1 mM DTT, 1 mM EDTA, 0.1 % BSA, and 20 mM MgCl$_2$). This dilution step is necessary to ensure discrimination between bead-associated fluorescence and background fluorescence of soluble proteins as well as to ensure sufficient sample volume for the measurement.

3.3 Quantitative Measurement of the Specific Interaction Between Rab7 and RILP

GST-RILP-coated beads (10E5 beads/100 μl buffer) are incubated with increasing concentrations of His-Rab7 prebound to BODIPY-GTP for 30 min with mild agitation at 4 °C as described in 3.2.4 and the bead-associated fluorescence is compared to that obtained with GST-coated or naked GSH beads. Rab7 is able to specifically bind to GSH beads coated with GST-RILP in a dose-dependent saturable manner with minimal interaction with either immobilized GST or naked GSH beads (Fig. 2a, b). The specificity of the observed interaction agrees with studies that have used techniques other than flow cytometry to show that RILP is a protein–protein interaction partner of Rab7 [28, 29, 40]. The Rab7–RILP interaction measured using the described bead-based flow cytometry approach, yielded a B_{max} value of $(506.20 \pm 28.66) \times 10^3$ Rab7-BODIPY-GTP bound molecules per bead and equilibrium dissociation constant (K_d) of 1.87 ± 0.25 μM,
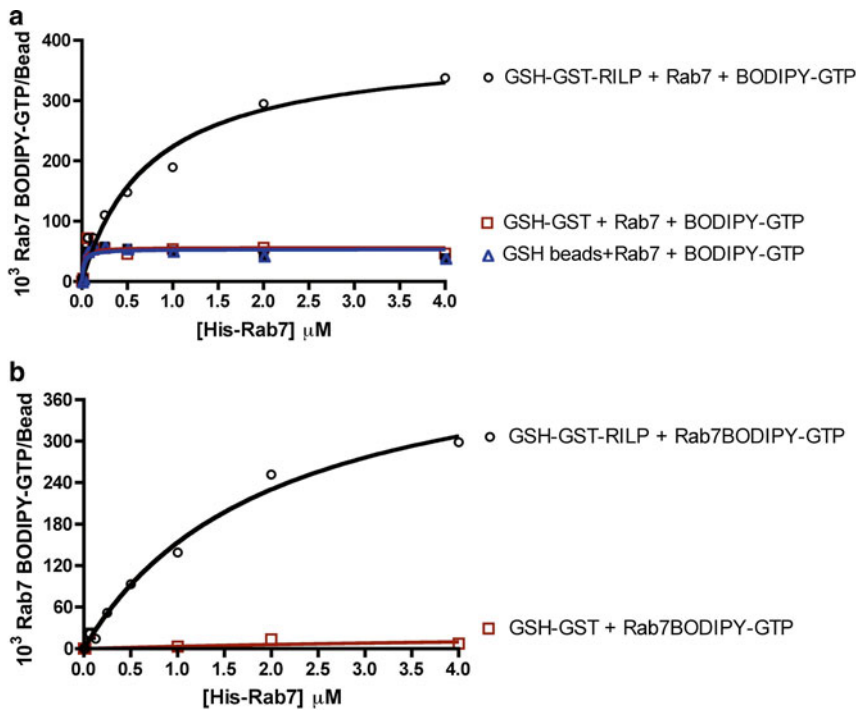
Fig. 2 Quantitative measurements of GTPase-effector protein binding. (**a**) Flow cytometry-based measurement of total Rab7 binding to RILP by detecting fluorescent BODIPY-GTP shows binding is saturable, quantitative, and specific. Rab7 binding to GSH beads coated with GST alone or without any protein coating was minimal. (**b**) Specific binding of Rab7-RILP with unwanted nonspecific background binding subtracted

calculated assuming one binding site per immobilized RILP for every Rab7 molecule. These results show that the interaction of Rab7 with RILP can be quantitatively measured by flow cytometry using small amounts of pure protein.

3.4 Measurement of the Time-Dependent Rab7 and RILP Interaction

3.4.1 Methods for Long-Term and Rapid Kinetic Measurements Using Flow Cytometry

For long-term kinetic measurements, purified GST or GST-RILP is incubated with 13 μm GSH beads as already described. One micromolar His-Rab7 'locked-on' with 500 nM BODIPY-GTP or BODIPY-GDP is then incubated with bead immobilized GST or GST-RILP for increasing time intervals (0–150) min. Mean channel fluorescence (MCF) is then obtained on the FACScan flow cytometer by diluting the bead mixture 10-fold in HPSM buffer (see Section 3.2.6) based on BODIPY fluorescence.

Early time point protein–protein association kinetic measurement is used to assay Rab7 interaction with RILP. GST-RILP is first incubated with 13 μm GSH beads overnight as already described. Nucleotide-bound Rab7 is then prepared by incubating 1 μM GFP-Rab7 purified on nickel beads with 1 μM GTP-γ-S or 1 μM unlabeled GDP in a nucleotide exchange buffer (30 mM HEPES, pH 7.5, 20 mM NaCl and 100 mM KCl, 5 mM EDTA, 0.1 % BSA, and 1 mM DTT) at room temperature for 20 min. Bound nucleotide is 'locked-on' with 20 mM MgCl$_2$ (final) and then put on ice. Real-time interaction between Rab7 and RILP is then initiated by mixing thoroughly washed GSH mobilized GST-RILP with nucleotide 'locked-on' GFP-Rab7. Mean channel fluorescence (MCF) is then obtained in HPSM buffer (30 mM HEPES pH 7.5, 20 mM NaCl, 100 mM KCl, 1 mM DTT, 1 mM EDTA and 0.1 % BSA, 20 mM MgCl$_2$) on the FACScan flow cytometer based on GFP fluorescence.

3.4.2 Representative Kinetic Measurements of Rab7–RILP Interaction

Traditional GST pull-down assay procedures are not suited for kinetic measurements. In contrast, the described bead-based flow cytometry method for protein–protein interaction measurement provides a robust and economical way of quantitatively measuring the time dependence of the interaction with only minor modification of the procedures.

To measure the time-dependent interaction of Rab7 with RILP, the binding of purified GFP-Rab7 to immobilized RILP is measured by monitoring bead-associated changes in GFP fluorescence. Concentrations of GST-RILP, GFP-Rab7, unlabeled GDP, and GTP-γ-S are held fixed in this case. GFP-Rab7 interaction with GSH bead-immobilized GST-RILP is found to occur within sample mixing time and with almost instantaneous kinetics both in long term (Fig. 3a), and in early time point assessments of binding kinetics (Fig. 3b)—seen as a rapid and saturable rise in bead-associated fluorescence. Further tests of the specificity and validity of flow cytometry-based Rab7-RILP binding measurement using unlabeled GDP show no binding to RILP by GFP-Rab7 prebound to unlabeled GDP (Fig. 3a), confirming that Rab7 has to be in the
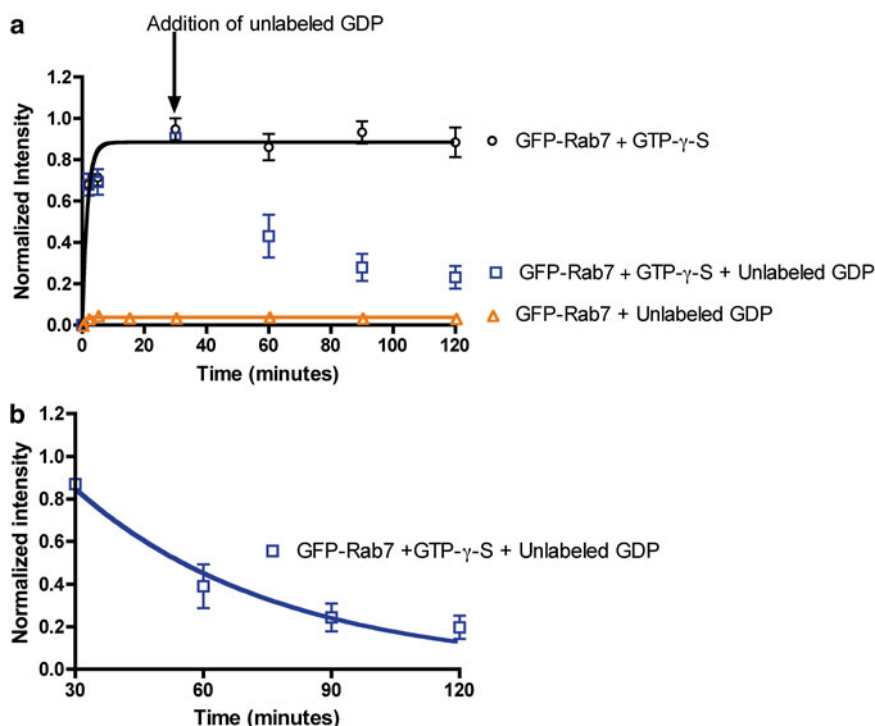
Fig. 3 Quantitative measurements of Rab7 GTPase-RILP effector binding is rapid and nucleotide specific. (**a**) Flow cytometry-based measurement of the long-term kinetics of Rab7 binding to RILP by detecting fluorescent GFP-Rab7 shows binding is rapid and dependent on Rab7 being GTP bound. GFP-Rab7 prebound to nonhydrolyzable GTP-γ-S is nearly instantaneous and stable over 120 min. Addition of GDP results in displacement of GTP-γ-S from Rab7 and dissociation of GFP-Rab7GDP complex detected as a loss of bead-associated fluorescence. There is no binding of GFP-Rab7 in the GDP-bound state to RILP. (**b**) Data from panel (**a**) were replotted starting at the 30 min time point to allow determination of the dissociation rate of GFP-Rab7-GDP from RILP. Data was fitted to single-phase exponential decay function using PRISM software yielding a dissociation rate of 0.020 ± 0.003 min^{-1}

GTP-bound state for interaction with the RILP effector protein to take place as previously observed [28, 29, 40]. Addition of unlabeled GDP is also able to competitively displace GTP-γ-S from the Rab7 nucleotide-binding pocket and cause the dissociation of GFP-Rab7 from the GST-RILP beads (Fig. 3a). When the rate of GFP-Rab7-GDP dissociation (Fig. 3b) is fitted to a single-phase exponential decay function using PRISM software, a calculated value of 0.020 ± 0.004 min^{-1} is deduced. Taken together, bead-based flow cytometry measurements are highly specific with only Rab7 in the GTP-bound nucleotide being able to bind RILP and further illuminate that Rab7 binding to RILP is very fast. Moreover, the use of GFP-Rab7 does not compromise RILP binding and is a useful tool for defining the equilibrium and kinetic parameters of the Rab7-RILP protein–protein interaction.

3.5 Measurement of the Temperature Dependence of Rab7 and RILP Interaction

3.5.1 Methods for Measuring Temperature-Dependent Protein–Protein Interaction

For the measurement of protein–protein interaction at varying temperatures (4–37 °C), GST-RILP (1 μM) is incubated with 13 μm GSH beads overnight at 4 °C in HPSM buffer (see Section 3.2.6). The following day, increasing concentrations of His-Rab7 are incubated with fixed concentrations of 500 nM BODIPY-GTP in a nucleotide exchange buffer (30 mM HEPES, pH 7.5, 20 mM NaCl and 100 mM KCl, 5 mM EDTA, 0.1 % BSA, and 1 mM DTT) for 20 min before adding 20 mM $MgCl_2$ (final) to 'lock' the bound nucleotide. Bead-immobilized GST-RILP is washed thoroughly with the same buffer system and then in cubated with nucleotide-bound Rab7 for 15 min at temperatures of 4, 22, and 37 °C. Fluorescence measurements are then obtained on Flow Cytometer using HPSM buffer as outlined in Section 3.4.1.

For temperature-shift experiments, purified 1 μM GST-RILP is first bound to beads in HPSM buffer. BODIPY-GTP-bound Rab7 is prepared as described in 3.2.4. To initiate the protein–protein interaction, BODIPY-GTP-bound Rab7 and thoroughly washed bead-immobilized GST-RILP are first mixed together on ice and then progressively shifted to 4 °C, 22 °C, and finally to 37 °C. On the FACScan flow cytometer, fluorescence measurements or MCF are made of Rab7-BODIPY-GTP bound to the RILP beads as a function of time following each temperature shift. All measurements are obtained in HPSM buffer as outlined in Section 3.4.1.

3.5.2 Representative Temperature-Dependent Rab7 and RILP Interaction Measurements

Temperature is an important determinant of protein–protein interactions because of its ability to affect the rate of protein conformation changes and molecular collisions. Typically, the rate of protein–protein interaction is favored at elevated temperatures due to enhanced frequency of molecular collisions at elevated temperatures. The bead-based flow cytometry assay was used for testing the impact of varying temperatures at 4 °C, 22 °C, and 37 °C on Rab7 and RILP interactions. The experiment is carried out with increasing concentrations of His-Rab7 against fixed concentrations of bead-immobilized RILP and BODIPY-GTP. His-Rab7 binding to RILP increases as the temperature is raised from 4 °C to 22 °C (Fig. 4a). Not surprisingly, when the assay is conducted at 37 °C, the fluorescence intensities—used as the measure of BODIPY-GTP-His-Rab7 bound to the RILP beads—are substantially lower across all concentrations of His-Rab7. In a kinetic temperature-shift experiment, His-Rab7, BODIPY-GTP, and bead-immobilized RILP are first mixed on ice and then progressively shifted to 4 °C, 22 °C and finally to 37 °C. Fluorescence measurements are made of Rab7-BODIPY-GTP bound to the RILP beads as a function of time following each temperature shift. A steady increase in binding is observed for temperature shifts from 0 °C through 22 °C, but again a sudden drop in fluorescence is observed as the reaction mixture is shifted from 22 °C to 37 °C (Fig. 4b). Estimation of the

rate of temperature-induced fluorescence loss is made by fitting the 37 °C time points (Fig. 4c) to a two-phase exponential decay function. The rate constants of 0.0436 ± 0.053 and 0.014 ± 0.003 min^{-1} for the fast and slow phases of fluorescence loss, respectively, are deduced, where the rate constant value calculated for the fast phase of fluorescence loss is statistically close to that measured for the dissociation of GFP-Rab7-GDP from RILP (Fig. 3a). The sudden drop in fluorescence at 37 °C is most likely due to Rab7-mediated hydrolysis of BODIPY-GTP to BODIPY-GDP resulting in a Rab7 conformational change which leads to Rab7 dissociation from RILP. The lack of fluorescent GTP-γ-S availability from commercial vendors precluded further testing of this significant observation though it remains of interest. The ability to rapidly measure nucleotide hydrolysis in real time helps mechanistic analyses and is a simple alternative to radioisotope-based filter-binding measurements of nucleotide hydrolysis.

3.6 Measurement of the Effect of a Novel Guanine Nucleotide-Binding Inhibitor on Rab7 and RILP Interaction

As a general note, direct fluorescent nucleotide displacement measurements are performed in HEPES buffer at nonequilibrium nucleotide-binding conditions. In brief, 1 µM GST-Rab7 is immobilized on GSH-beads as described in 3.2.3. Following GSH-bead immobilization of GST-Rab7, fluorescence baseline measurements are first obtained on the FACScan flow cytometer by measuring the fluorescence of thoroughly washed GSH bead-immobilized GST-Rab7 (2×10^3 GSH beads) before adding BODIPY-GTP (100 nM: K_d concentration for BODIPY-GTP binding to Rab7). After ~150 s, competition is initiated in situ against binding/loading BODIPY-GTP using either DMSO (1 % final) or CID 1067700 (10 µM final). As a negative control for all measurements, GST-Rab7 is prebound to GDP (500 µM) prior to adding BODIPY-GTP at the above concentration and the low level nonspecific bead-associated fluorescence is subtracted from fluorescence obtained from the DMSO or CID 1067700 treated samples to ensure that only specific nucleotide binding is finally considered.

3.6.1 Measuring the Kinetics of Direct BODIPY-GTP Nucleotide Displacement by a Competitive Guanine Nucleotide-Binding Inhibitor (CID 1067700)

3.6.2 Assessment of Rab7 Interaction with RILP in the Presence of Competitive Guanine Nucleotide-Binding Inhibitor (CID 1067700) Under Equilibrium Binding Conditions

GST-RILP at 1 µM is first immobilized on 13 µM GSH beads as described in Section 3.2.3. GFP-Rab7 (1 µM) purified on nickel beads is incubated with increasing concentrations of GTP-γ-S (1 % DMSO final treated), unlabeled GDP or CID 1067700 (dissolved in DMSO) hereby referred to as ligands in nucleotide exchange buffer for 20 min at room temperature. Bound nucleotide is 'locked-on' with 20 mM MgCl$_2$ (final) and then all sample sets are put on ice. The samples are then incubated with thoroughly washed GSH mobilized GST-RILP for 15 min at room temperature before obtaining fluorescence measurements in an HPSM buffer as outlined in Section 3.4.1. Mean channel fluorescence (MCF) as a measure of bead-associated GFP fluorescence is determined on a FACScan flow cytometer.
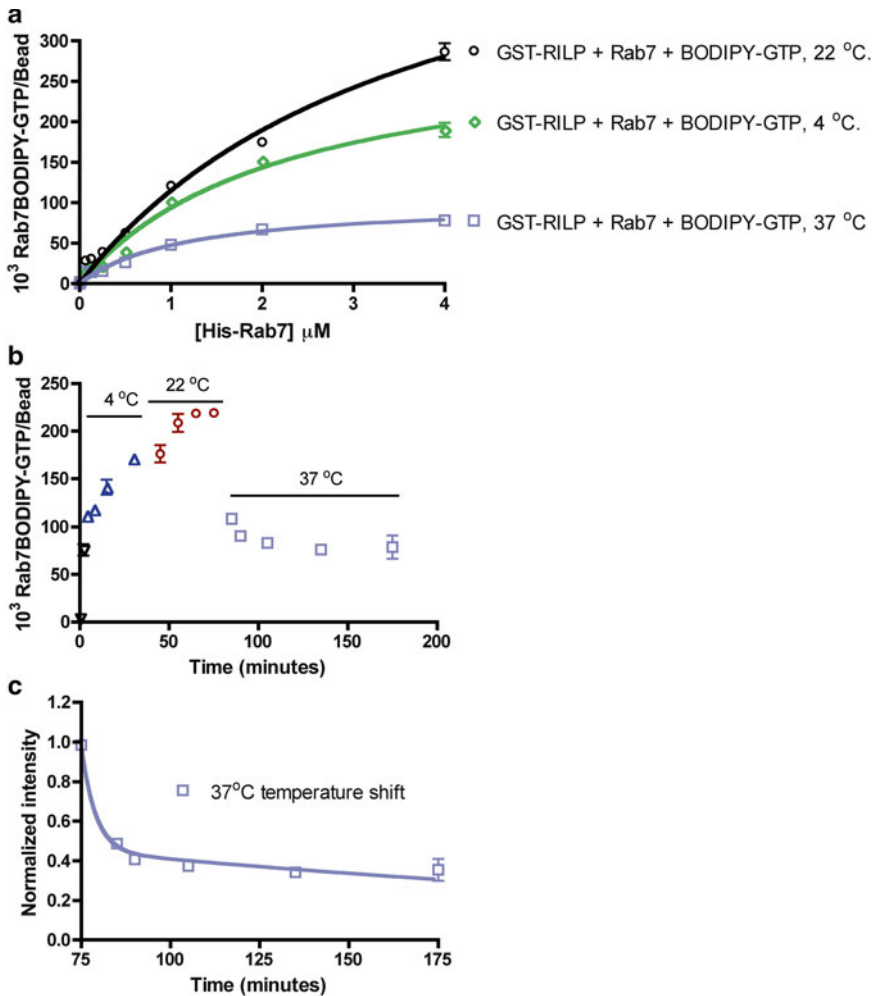
Fig. 4 Flow cytometry-based measurements show Rab7 GTPase-RILP effector binding is temperature dependent and sensitive to nucleotide hydrolysis. (**a**–**c**) Flow cytometry-based measurement of His-Rab7 binding to RILP by detecting fluorescent BODIPY-GTP. (**a**) Dose-dependent His-Rab7 binding is temperature dependent and negatively affected by GTP hydrolysis at higher temperature (**b** and **c**). (**b**) A kinetic temperature-shift experiment shows His-Rab7 binding to RILP increases steadily at 4 and 22 °C, but decreases rapidly upon shift to 37 °C, likely due to GTP hydrolysis and dissociation of Rab7 from RILP. (**c**) Data in (**b**) were replotted starting at the 75 min time point to allow determination of the dissociation rate. Data were fitted to a two-phase exponential decay function using PRISM software yielding a dissociation rate of 0.014 ± 0.003 min^{-1} for the slow phase and 0.0436 ± 0.053 min^{-1} for the fast phase. The rate constant value deduced for the fast phase is statistically close to that measured for the dissociation of GFP-Rab7-GDP from RILP in Fig. 2a, supporting the conclusion that 37 °C stimulates Rab7 GTPase hydrolysis of BODIPY-GTP and consequent dissociation from RILP

3.6.3 Measurement of the Effect of a Competitive Guanine Nucleotide-Binding Inhibitor on the Interaction Between Rab7 and RILP

We previously identified a first-in-class competitive guanine nucleotide-binding inhibitor (PubChem: CID 1067700 or ML282) with activity against Rab7 in vitro [30] and in cell-based assays [41]. The importance of the compound is recognized through the award of a US patent [42]. In the published work, GST-Rab7 was immobilized on GSH beads and BODIPY-nucleotide binding to Rab7 was measured as an increase in bead-associated fluorescence by flow cytometry and used to mechanistically characterize the small molecule competitor, as illustrated in cartoon form (Fig. 5a). The same assay setup is also useful to measure nucleotide-binding kinetics and changes induced by small molecule addition. For example, addition of CID 1067700 in such an assay results in a rapid decrease in bead-associated fluorescence as a function of time (Fig. 5b). This is due to displacement of BODIPY-GTP from Rab7 and disruption of further fluorescent nucleotide loading. One question that could not be resolved by the flow cytometry-based nucleotide-binding assay is whether or not CID 1067700 binding to Rab7 promotes the active conformation of Rab7 (normally induced by GTP) or instead retains Rab7 in the inactive conformation (normally induced by GDP).

The RILP-binding assay detailed here is able to discriminate Rab7 in the active conformation from the inactive conformation and hence is ideally suited for testing the impact of CID 1067700 on Rab7 conformational status. We monitored the interaction of bead-immobilized RILP with GFP-Rab7 in the presence of increasing concentrations of: (1) GTP-γ-S, (2) CID 1067700, or (3) GDP. CID1067700 and nucleotide stocks for this experiment are prepared in DMSO and diluted 1000x in the assay. In the presence of CID 1067700 alone, Rab7 is unable to adopt the 'active' like conformation and fails to bind to the RILP effector protein, analogous to the GDP negative control (Fig. 6a). In contrast, GFP-Rab7 is able to bind RILP in a saturable manner in the presence of GTP-γ-S. From this, one can conclude that the presence of CID 1067700 most likely freezes Rab7 in an inactive conformational state that does not support interaction with RILP (Fig. 6b). Together, this evidence supports the conclusion that CID 1067700 is a competitive inhibitor of Rab7 nucleotide binding, which does not induce Rab7 to adopt the active conformation, and thus also precludes interaction with downstream effector proteins. Such information is critical in the assessment of small molecule GTPase inhibitor suitability for in vivo utility.

3.6.4 Broader applications: Probing Other GTPases and Performing High Throughput Screens

The described effector binding assay can be extended to the study of other Ras-related GTPases andthe analyses of active GTPase status in cell lysates (*see* **Note 3**). Using multiplexing approaches requiring differentially labeled bead sets the assay can be adapted for high throughput screening assays (*see* **Note 4**).
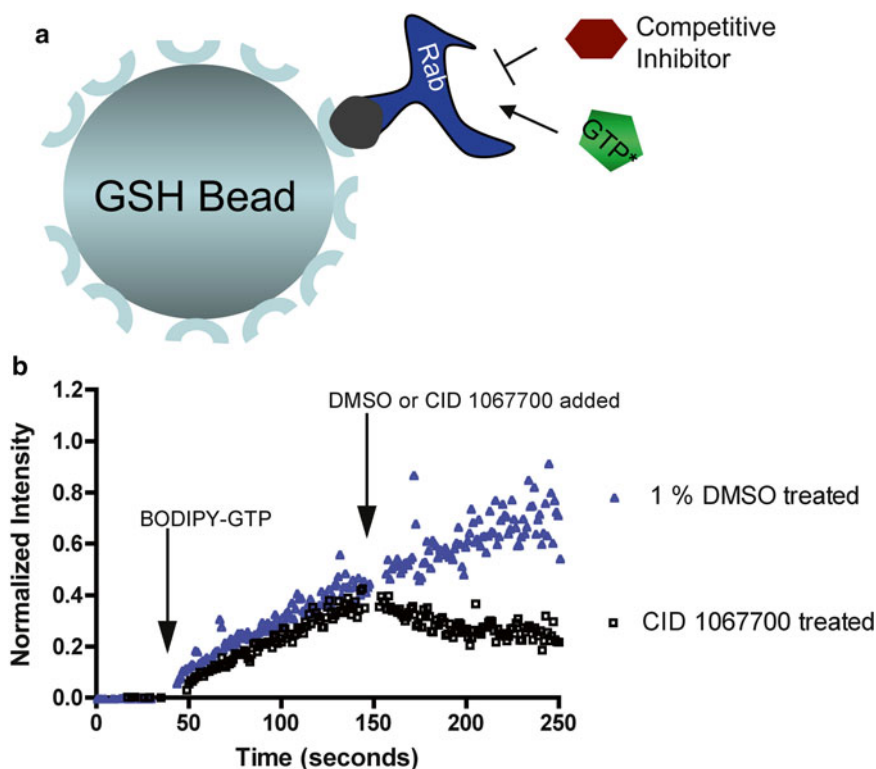
Fig. 5 GSH bead-based flow cytometry assays for quantitative measurements of Rab7 guanine nucleotide binding and dissociation kinetics. (**a**) Assay design for detecting nucleotide binding and dissociation kinetics on Rab7 based on detection of bound fluorescent BODIPY-GTP. GST-Rab7 is immobilized on 13 μm Superdex beads coated with GSH and detection is based on fluorescent BODIPY-GTP binding. (**b**) BODIPY-GTP (100 nM final) was added to GST-Rab7 immobilized on GSH beads suspended in 300 μl of buffer (*first arrow*). The ligand was allowed to bind for 100 s and then DMSO (1 % final) or CID 1067700 (10 μM final) was added at 150 s (*second arrow*). While the addition of a competitive guanine nucleotide-binding inhibitor (CID 1067700) causes dissociation of BODIPY-GTP, addition of DMSO has no effect on BODIPY-GTP-binding kinetics

Advantages of the assay over conventional methods are summarized in **Notes 5–6**.

3.7   Data Analyses   All data processing and analyses presented in this report employed GraphPad Prism software (GraphPad Software). For kinetic experiments, raw data acquired were first processed using IDLE query software (obtained from University of New Mexico Center for Molecular Discovery, UNM CMD) before further analysis using GraphPad Prism. All experiments are representative of at least three independent trials.

4   Notes

The following notes provide helpful tips and expand assay applications.

1. *GSH Bead Synthesis and Alternatives.* GSH prepared in phosphate buffer can reduce the pH of the solution. It is crucial to readjust the pH to 7.5 prior to incubation with the epoxy-activated Superdex beads for the coupling reaction to be effective.

   As an alternative, polystyrene beads (6–8 μm) precoated with GSH may be purchased (GSHP-60-5) from Spherotech (Lake Forest, IL). However, it should be noted that the polystyrene beads exhibit higher nonspecific binding than GSH cross-linked to dextran/cross-linked agarose beads as described here. Therefore, the substitution of GSH-polystyrene beads must be carefully optimized using relevant controls. For example, an irrelevant GST-fusion protein is best used as a negative control instead of beads coated with GST, which gives higher than expected background signal. Additionally, when using beads of a smaller diameter, the conditions for saturating with GST-tagged proteins and maximal binding of ligand must be optimized accordingly [34, 38], *see* also **Note 2**.

2. *Calculating Bead-Binding Sites and Assuring Saturation Binding of GST-Fusion Proteins to GSH Beads.* Utilizing the previously determined kinetic and equilibrium-binding constants for GST fused to green fluorescent protein (GST–GFP) binding to GSH beads is useful in establishing the optimal stoichiometric mixtures of GSH beads and individual GST-fusion proteins so as to achieve saturating site occupancies [34, 38]. The saturable site occupancy values for GST–GFP are a measure of the amount of bead-associated GSH. Based on a K_d for GST–GFP binding of approximately 80 nM, the optimal concentration of GST-fusion protein required to fully saturate the GSH sites on the beads is taken as $10 \times K_d$, giving 91 % saturation.

3. *Extrapolation to Different GTPases and Cell-Based Assays.* The effector binding assay described here can be extrapolated to different families of Ras-related GTPases and has utility for measuring GTPase activation status in cells. Examples of such applications include: determination of EC_{50} values of Rab and Rho GTPase-targeted small molecules in cell-based assays [41, 43]; for monitoring GTPase cascades in Sin nombre hantavirus infection [39], and responses of cancer patient samples to treatment with drugs that target GTPase activation [44]. Based on these examples, the assay has utility for monitoring host GTPase responses to viral, fungal, and bacterial pathogens and for studying changes in GTPase activation in
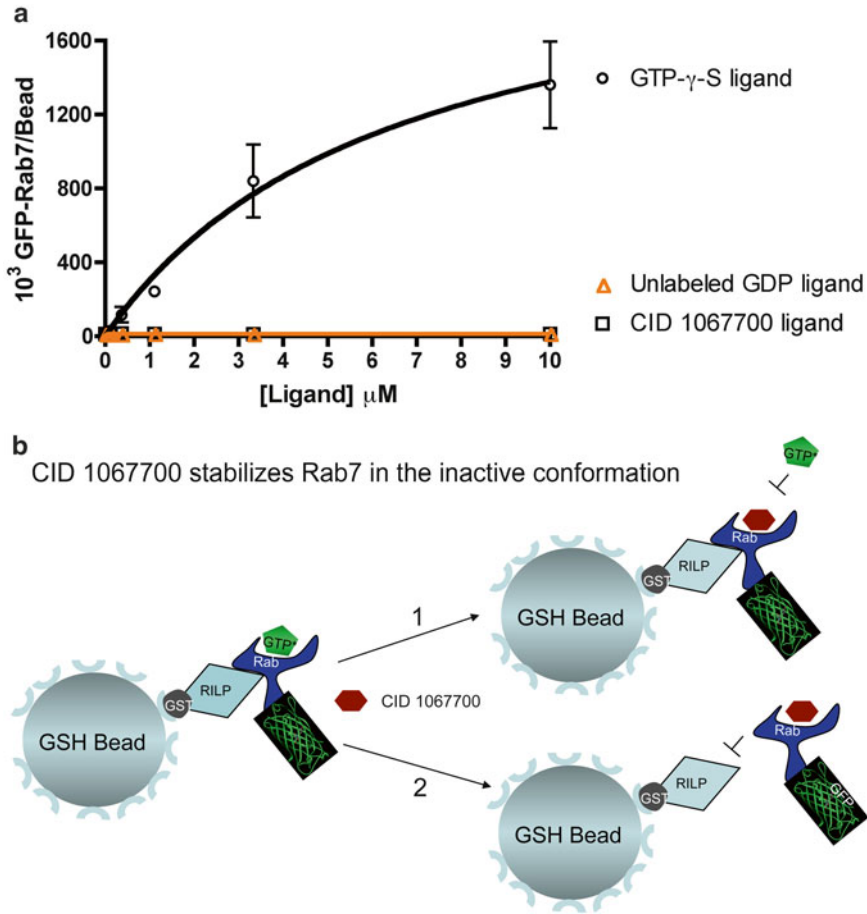
Fig. 6 GSH bead-based flow cytometry assay establishes that a competitive guanine nucleotide-binding inhibitor (CID 1067700) retains Rab7 in an inactive conformation. (**a**) Flow cytometry-based measurement of Rab7 binding to RILP by detecting fluorescent GFP-Rab7 in the presence of CID 1067700. GFP-Rab7 increasingly binds to RILP at increasing concentrations of nonhydrolyzable GTP-γ-S but fails to bind to RILP with increasing concentrations of GDP or CID 1067700. Rab7 does not adopt 'active' like conformation in the presence of CID 1067700 alone. (**b**) Graphical display of the two distinct possible scenarios that can result from competitive inhibitor (CID 1067700) binding to Rab7. In scenario 1, binding of the competitive inhibitor dissociates GTP from the nucleotide-binding pocket, but keeps Rab7 in the active conformation, which would still allow binding to the RILP effector. In scenario 2, binding of the competitive inhibitor to Rab7 causes the GTPase to assume or remain in the inactive conformation, which does not favor interaction with RILP. The data we have presented support scenario 2 and suggest that the guanine nucleotide-binding inhibitor should functionally inhibit Rab7 in cell-based assays

response to specific disease processes, growth factors, cytokines, toxins, among other extracellular stimuli.

In lieu of using BODIPY nucleotides or GFP-tagged GTPases for detection, effector binding can also be efficaciously measured using antibodies to detect bound GTPases (e.g., using a fluorescently conjugated primary antibody directed against the GTPase of interest or using an nonfluorescent primary antibody

followed by a fluorescent secondary antibody). Key negative controls include use of a control GST-effector protein to which the GTPase of interest is not expected to bind and omission of the primary antibody.

4. *Adapting the Assay to Multiplex and HTS Applications.* For multiplex analyses, 4 μm diameter, polystyrene GSH-beads with 1.2×10^6 GSH sites per bead and labeled with differing intensities of red fluorescent dye have been successfully used [45]. Up to seven different bead sets with varying emission magnitudes at 665 ± 10 nm can be uniformly excited at 635 nm and readily discriminated by flow cytometry. To capitalize on such beads for multiplex, HTS applications, GST-fusion proteins are individually coated onto different bead sets and the red fluorescence intensity serves as a 'zipcode' in the multiplex measurement for identifying sets of bound GST-proteins. Briefly, bead sets (at a concentration of 1.4×10^5 beads/μl and total volume of 240–250 μl) are first blocked with 0.1 % bovine serum albumin in 30 mM HEPES pH 7.5, 100 mM KCl, 20 mM NaCl containing 0.01 % (v/v) NP-40, and 1 mM EDTA for 30 min at room temperature. GST-fusion protein binding is conducted overnight at 4 °C with 1 μM GST-fusion protein in 100 μl of buffer (30 mM HEPES pH 7.5, 100 mM KCl, 20 mM NaCl containing 0.01 % (v/v) NP-40, and 1 mM EDTA). Protein-coupled beads are washed two times with 30 mM HEPES pH 7.5, 100 mM KCl, 20 mM NaCl, 0.01 % (v/v) NP-40, 1 mM EDTA buffer supplemented with 0.1 % BSA and 1 mM DTT. Bead sets are subsequently pooled for multiplex analyses and individual assays are conducted in 384-well plates. The described assay configuration has been used for HTS, multiplex measurement of small molecule interference with nucleotide binding to families of bead-immobilized GST-GTPases in compound library screens [45, 46], as well as for characterization of small molecules and their chemical optimization through structure–activity analyses [41, 43, 47–50]. The effector-binding assay described here is also suited for multiplex analyses and has been shown to have utility for quantitative, spatiotemporal resolution of GTPase cascades that are activated in response to hantavirus infection of cells [39] and growth factor stimulation [39, 41]. Further potential applications include screens for small molecule inhibitors of GTPase-effector protein interactions and parallel analyses of GTPase responses to diverse stimuli.

5. *Highlights of Comparative Advantages of Bead-Based Flow Cytometry Measurements.* The bead-based flow cytometry technique we have presented offers a more robust approach for quantitatively assaying equilibrium binding and kinetic parameters in comparison to some of the methods commonly used to

achieve the same [36, 37, 51–53]. The assays are simple to set up on account of the following realities: (1) it is easy to generate GST tagged protein, (2) tagging of interacting partners with flow cytometry-suited fluorophores does not require elaborate work, and (3) in the case of nucleotide-binding proteins, both labeled and unlabeled nucleotides can easily be obtained commercially. With respect to addressing specificity questions, a bead-based flow cytometry assay is also not susceptible to challenges inherent in cell-based assays such as difficulties in telling if the interaction between two proteins of interest is a direct process or occurs via a protein complex involving intermediaries. Elucidation of this question more often tends to involve time-consuming experiments that can lead to false-positive results. Moreover, it is also easy to assay the impact of other confounding factors on the interaction between two proteins. One can assess whether the interaction between two proteins is influenced by kinetics of protein–protein association or thermodynamics of the system, solution viscosity, pH, and/or salt concentrations [54].

6. *Conclusions.* Much as our current report centered primarily on Rab7 interaction with RILP as model system for method and protocol illustration, the design of the GSH bead-based flow cytometry assay can also be extended to some of the well-characterized Rab7 regulatory protein partners such as hVps39 [55], TBC1D15 [55, 56], ORPIL [25, 57], Rabring7 [58, 59], and an α-subunit of the proteasome–XAPC7 [60, 61]. Rab7 interaction with regulatory proteins is an important physiological process and controls important physiological processes that can result into human disease states when misregulated. Taken together, our findings present GSH bead-based flow cytometry as a simpler method for quantitatively measuring Rab7 interactions with guanine nucleotides and with regulatory proteins. Based on our evidence with CID 1067700, bead-based flow cytometry can also be used for HTS of small molecule modulators of Rab7 protein–protein interactions that may be pertinent for identifying activator and inhibitor small molecules that may have relevance in the long-term development of new therapeutics for Rab7-associated diseases.

Acknowledgements

References

1. Feng Y, Press B, Wandinger-Ness A (1995) Rab 7: an important regulator of late endocytic membrane traffic. J Cell Biol 131:1435–1452

2. Meresse S, Gorvel JP, Chavrier P (1995) The rab7 GTPase resides on a vesicular compartment connected to lysosomes. J Cell Sci 108:3349–3358

3. Press B, Feng Y, Hoflack B et al (1998) Mutant Rab7 causes the accumulation of cathepsin D and cation-independent mannose 6-phosphate receptor in an early endocytic compartment. J Cell Biol 140:1075–1089

4. Bucci C, Thomsen P, Nicoziani P et al (2000) Rab7: a key to lysosome biogenesis. Mol Biol Cell 11:467–480

5. Saxena S, Bucci C, Weis J et al (2005) The small GTPase Rab7 controls the endosomal trafficking and neuritogenic signaling of the nerve growth factor receptor TrkA. J Neurosci 25:10930–10940

6. Gutierrez MG, Munafó DB, Berón W et al (2004) Rab7 is required for the normal progression of the autophagic pathway in mammalian cells. J Cell Sci 117:2687–2697

7. Jager S, Bucci C, Tanida I et al (2004) Role for Rab7 in maturation of late autophagic vacuoles. J Cell Sci 117:4837–4848

8. Spinosa MR, Progida C, De Luca A et al (2008) Functional characterization of Rab7 mutant proteins associated with Charcot-Marie-Tooth type 2B disease. J Neurosci 28:1640–1648

9. Castino R, Lazzeri G, Lenzi P et al (2008) Suppression of autophagy precipitates neuronal cell death following low doses of methamphetamine. J Neurochem 106:1426–1439

10. Bains M, Zaegel V, Mize-Berge J et al (2011) IGF-I stimulates Rab7–RILP interaction during neuronal autophagy. Neurosci Lett 488:112–117

11. Chan CC, Epstein D, Hiesinger PR (2011) Intracellular trafficking in Drosophila visual system development: a basis for pattern formation through simple mechanisms. Dev Neurobiol 71:1227–1245

12. Midorikawa R, Yamamoto-Hino M, Awano W et al (2010) Autophagy-dependent rhodopsin degradation prevents retinal degeneration in Drosophila. J Neurosci 30:10703–10719

13. Takacs-Vellai K, Bayci A, Vellai T (2006) Autophagy in neuronal cell loss: a road to death. Bioessays 28:1126–1131

14. Choudhury A, Dominguez M, Puri V et al (2002) Rab proteins mediate Golgi transport of caveola-internalized glycosphingolipids and correct lipid trafficking in Niemann-Pick C cells. J Clin Invest 109:1541–1550

15. Haskell RE, Carr CJ, Pearce DA et al (2000) Batten disease: evaluation of CLN3 mutations on protein localization and function. Hum Mol Genet 9:735–744

16. Seabra MC, Mules EH, Hume AN (2002) Rab GTPases, intracellular traffic and disease. Trends Mol Med 8:23–30

17. Zhang M, Chen L, Wang S et al (2009) Rab7: roles in membrane trafficking and disease. Biosci Rep 29:193–209

18. Vonderheit A, Helenius A (2005) Rab7 associates with early endosomes to mediate sorting and transport of Semliki forest virus to late endosomes. PLoS Biol 3:e233

19. Agola JO, Jim PA, Ward HH et al (2011) Rab GTPases as regulators of endocytosis, targets of disease and therapeutic opportunities. Clin Genet 80:305–318

20. Bucci C, De Gregorio L, Bruni CB (2001) Expression analysis and chromosomal assignment of PRA1 and RILP genes. Biochem Biophys Res Commun 286:815–819

21. Cantalupo G, Alifano P, Roberti V et al (2001) Rab-interacting lysosomal protein (RILP): the Rab7 effector required for transport to lysosomes. EMBO J 20:683–693

22. Cogli L, Piro F, Bucci C (2009) Rab7 and the CMT2B disease. Biochem Soc Trans 37:1027–1031

23. Jordens I, Fernandez-Borja M, Marsman M et al (2001) The Rab7 effector protein RILP controls lysosomal transport by inducing the recruitment of dynein-dynactin motors. Curr Biol 11:1680–1685

24. Johansson M, Lehto M, Tanhuanpaa K et al (2005) The oxysterol-binding protein homologue ORP1L interacts with Rab7 and alters functional properties of late endocytic compartments. Mol Biol Cell 16:5480–5492

25. Johansson M, Rocha N, Zwart W et al (2007) Activation of endosomal dynein motors by stepwise assembly of Rab7-RILP-p150Glued, ORP1L, and the receptor betaIII spectrin. J Cell Biol 176:459–471

26. Harrison RE, Brumell JH, Khandani A et al (2004) Salmonella impairs RILP recruitment to Rab7 during maturation of invasion vacuoles. Mol Biol Cell 15:3146–3154

27. Marsman M, Jordens I, Kuijl C et al (2004) Dynein-mediated vesicle transport controls intracellular Salmonella replication. Mol Biol Cell 15:2954–2964

28. Sun J, Deghmane AE, Bucci C et al (2009) Detection of activated Rab7 GTPase with an immobilized RILP probe. Methods Mol Biol 531:57–69

29. Peralta ER, Martin BC, Edinger AL (2010) Differential effects of TBC1D15 and mammalian Vps39 on Rab7 activation state, lysosomal morphology, and growth factor dependence. J Biol Chem 285:16814

30. Agola JO, Hong L, Surviladze Z et al (2012) A competitive nucleotide binding inhibitor: in vitro characterization of Rab7 GTPase inhibition. ACS Chem Biol 7:1095–1108

31. Simons PC, Shi M, Foutz T et al (2003) Ligand-receptor-G-protein molecular assemblies on beads for mechanistic studies and screening by flow cytometry. Mol Pharmacol 64:1227–1238

32. Waller A, Simons PC, Biggs SM et al (2004) Techniques: GPCR assembly, pharmacology and screening by flow cytometry. Trends Pharmacol Sci 25:663–669

33. Butt TR, Edavettal SC, Hall JP et al (2005) Sumo fusion technology for difficult-to-express proteins. Protein Expr Purif 43:1–9

34. Tessema M, Simons PC, Cimino DF et al (2006) Glutathione-S-transferase-green fluorescent protein fusion protein reveals slow dissociation from high site density beads and measures free GSH. Cytometry A 69:326–334

35. Simons PC, Sklar LA, Prossnitz ER et al (2010) Glutathione beads and GST fusion proteins. STCUNM (Albuquerque, NM) Sanford-Burnham Medical Research Institute (La Jolla, CA), USA

36. Phizicky EM, Fields S (1995) Protein-protein interactions: methods for detection and analysis. Microbiol Rev 59:94–123

37. Nguyen TN, Goodrich JA (2006) Protein-protein interaction assays: eliminating false positive interactions. Nat Methods 3:135–139

38. Schwartz SL, Tessema M, Buranda T et al (2008) Flow cytometry for real-time measurement of guanine nucleotide binding and exchange by Ras-like GTPases. Anal Biochem 381:258–266

39. Buranda T, BasuRay S, Swanson S et al (2013) Rapid parallel flow cytometry assays of active GTPases using effector beads. Anal Biochem 442:149–157

40. Rosales KR, Peralta ER, Guenther GG et al (2009) Rab7 activation by growth factor withdrawal contributes to the induction of apoptosis. Mol Biol Cell 20:2831–2840

41. Hong L, Guo Y, BasuRay S et al. A Pan-GTPase inhibitor as a molecular probe. PLoS One under review

42. Wandinger-Ness A, Sklar LA, Agola JO et al (2014) Rab7 GTPase inhibitors and related methods of treatment. STCUNM (Albuquerque, NM) University of Kansas (Lawrence, KS), USA

43. Oprea TI, Sklar LA, Agola JO et al. Novel activities of select NSAID R-enantiomers against Rac1 and Cdc42 GTPases. PLoS One under review

44. Guo Y, Kenney SR, Cook L et al. Novel mechanism of therapeutic benefit through ketorolac usage in ovarian cancer patients. J Clin Oncol under review

45. Surviladze Z, Waller A, Wu Y et al (2010) Identification of a small GTPase inhibitor using a high-throughput flow cytometry bead-based multiplex assay. J Biomol Screen 15:10–20

46. Surviladze Z, Young SM, Sklar LA (2012) High-throughput flow cytometry bead-based multiplex assay for identification of Rho GTPase inhibitors. Methods Mol Biol 827:253–270

47. Surviladze Z, Ursu O, Miscioscia F et al (2010) Three small molecule pan activator families of Ras-related GTPases. Probe reports from the NIH Molecular Libraries Program

48. Surviladze Z, Waller A, Strouse JJ et al (2010) A potent and selective inhibitor of Cdc42 GTPase. Probe reports from the NIH Molecular Libraries Program

49. Hong L, Simons P, Waller A et al (2010) A small molecule pan-inhibitor of Ras-superfamily GTPases with high efficacy towards Rab7. Probe reports from the NIH Molecular Libraries Program

50. Hong L, Surviladze Z, Ursu O et al (2013) Characterization of a Cdc42 protein inhibitor and its use as a molecular probe. J Biol Chem 288:8531–8543

51. He L, Olson DP, Wu X et al (2003) A flow cytometric method to detect protein-protein interaction in living cells by directly visualizing donor fluorophore quenching during CFP → YFP fluorescence resonance energy transfer (FRET). Cytometry A 55:71–85

52. Dye BT, Schell K, Miller DJ et al (2005) Detecting protein-protein interaction in live yeast by flow cytometry. Cytometry A 63:77–86

53. Chen J, Carter MB, Edwards BS et al (2012) High throughput flow cytometry based yeast two-hybrid array approach for large-scale analysis of protein-protein interactions. Cytometry A 81:90–98

54. Schreiber G (2002) Kinetic studies of protein-protein interactions. Curr Opin Struct Biol 12:41–47

55. Flinn RJ, Yan Y, Goswami S et al (2010) The late endosome is essential for mTORC1 signaling. Mol Biol Cell 21:833–841

56. Zhang XM, Walsh B, Mitchell CA et al (2005) TBC domain family, member 15 is a novel mammalian Rab GTPase-activating protein with substrate preference for Rab7. Biochem Biophys Res Commun 335:154–161

57. Rocha N, Kuijl C, van der Kant R et al (2009) Cholesterol sensor ORP1L contacts the ER protein VAP to control Rab7-RILP-p150 Glued and late endosome positioning. J Cell Biol 185:1209–1225

58. Mizuno K, Kitamura A, Sasaki T (2003) Rabring7, a novel Rab7 target protein with a RING finger motif. Mol Biol Cell 14:3741–3752

59. Mizuno K, Sakane A, Sasaki T (2005) Rabring7: a target protein for rab7 small g protein. Methods Enzymol 403:687–696

60. Dong J, Chen W, Welford A et al (2004) The proteasome alpha-subunit XAPC7 interacts specifically with Rab7 and late endosomes. J Biol Chem 279:21334–21342

61. Mukherjee S, Dong J, Heincelman C et al (2005) Functional analyses and interaction of the XAPC7 proteasome subunit with Rab7. Methods Enzymol 403:650–663

ERRATUM TO

Methods for Analysis of AP-3/Rabin4′ in Regulation of Lysosome Distribution

Viorica Ivan and Peter van der Sluijs

"A protein name was incorrectly noted as Rabin4' in Chapter 21 and TOC. The correct name for the protein is Rabip4'."

The online version of the original chapter can be found at
http://dx.doi.org/10.1007/978-1-4939-2569-8_21

E1

INDEX